12
11/27/95 JS (1)

DOE/METC-95/1018, Vol. 1
(DE95009732)
CONF-9506163--Vol.1

# Proceedings of the Advanced Coal-Fired Power Systems '95 Review Meeting Volume I

Heather M. McDaniel
Darren J. Mollot
Venkat K. Venkataraman

June 1995

U.S. Department of Energy
Office of Fossil Energy
Morgantown Energy Technology Center
Morgantown, West Virginia

DISTRIBUTION OF THIS DOCUMENT IS UNLIMITED

# Disclaimer

This report was prepared as an account of work sponsored by an agency of the United States Government. Neither the United States Government nor any agency thereof, nor any of their employees, makes any warranty, express or implied, or assumes any legal liability or responsibility for the accuracy, completeness, or usefulness of any information, apparatus, product, or process disclosed, or represents that its use would not infringe privately owned rights. Reference herein to any specific commercial product, process, or service by trade name, trademark, manufacturer, or otherwise does not necessarily constitute or imply its endorsement, recommendation, or favoring by the United States Government or any agency thereof. The views and opinions of authors expressed herein do not necessarily state or reflect those of the United States Government or any agency thereof.

This report has been reproduced directly from the best available copy.

Available to DOE and DOE contractors from the Office of Scientific and Technical Information, 175 Oak Ridge Turnpike, Oak Ridge, TN 37831; prices available at (615) 576-8401.

Available to the public from the National Technical Information Service, U.S. Department of Commerce, 5285 Port Royal Road, Springfield, VA 22161; phone orders accepted at (703) 487-4650.

DOE/METC-95/1018, Vol. 1
(CONF-9506162)--Vol.1
(DE95009732)
Distribution Category UC-103
UC-106
UC-111

# Proceedings of the Advanced Coal-Fired Power Systems '95 Review Meeting Volume I

Editors
Heather M. McDaniel
Darren J. Mollot
Venkat K. Venkataraman

Sponsored by

U.S. Department of Energy
Office of Fossil Energy
Morgantown Energy Technology Center
P.O. Box 880
Morgantown, WV 26507-0880
(304) 285-4764
(304) 285-4403/4469

June 27-29, 1995

MASTER

DISTRIBUTION OF THIS DOCUMENT IS UNLIMITED

# Foreword

The Advanced Coal-Fired Power Systems '95 Review Meeting was held June 27-29, 1995, at the Morgantown Energy Technology Center (METC) in Morgantown, West Virginia. This meeting was sponsored and hosted by METC, the Office of Fossil Energy, U.S. Department of Energy (DOE).

METC annually sponsors this conference for energy executives, engineers, scientists, and other interested parties to review the results of research and development projects, to discuss the status of advanced coal-fired power systems and future plans with the industrial contractors, and to discuss cooperative industrial-government research opportunities with METC's in-house engineers and scientists. Presentations included industrial contractors and METC in-house technology developments related to the production of power via coal-fired Integrated Gasification Combined Cycle (IGCC), Pressurized Fluidized Bed Combustion (PFBC)systems, Externally Fired Combined Cycles (EFCC), the summary status of clean coal technologies, and developments and advancements in advanced technology subsystems such as advanced turbine systems and hot gas cleanup. A keynote speaker and other representatives from the electric power industry also gave their assessment of advanced power systems.

This meeting contained 9 formal sessions and two poster sessions, and included 49 presentations and 33 poster presentations. The papers printed in this document have been produced from camera-ready manuscripts provided by the authors. They have not been extensively edited.

Heather M. McDaniel
Darren J. Mollot
Venkat K. Venkataraman
Conference Technical Coordinators

# Contents

## Volume I

### Session 1 — Perspectives on the Future of Power Generation Industry


**1.1** And Deregulation Shall Lead Me to Lie Down in Green Pastures — Gary Weidinger ..... 3

**1.2** World Market: A Survey of Opportunities for Advanced Coal-Fired Systems — Neville A.H. Holt ..... 4

**1.3** METC Clean Coal Technology Status -- 1995 Update — Larry K. Carpenter ..... 19


### Session 2 — Advanced Power Systems


**2.1** Power Systems Development Facility Progress Report — Randall E. Rush, Howard L. Hendrix, Darrell L. Moore, Timothy E. Pinkston, P. Vimalchand, and John M. Wheeldon ..... 23

**2.2** Pilot Plant Becomes Demonstration Plant Design — Archie Robertson, James Van Hook, Frank Burkhard, Giovanni Carli, Rich Conn, Paul Crooker, Dave Kulcsar, Chongqing Lu, Anthony Mack, Aydemir Nehrozoglu, Mark Torpey, and Frank Zoldak ..... 32

**2.3** Gasification Product Improvement Facility Status — R. Don Carson, Vijay B. Dixit, Richard S. Sadowski, P. Thamaraichelvan, and H. Culberson ..... 47

**2.4** Externally Fired Combined Cycle Demonstration — Nelson J. Orozco, Stephen Young, Paul G. LaHaye, John Strom-Olsen, John L. Seger, and Helen Pickup ..... 55

**2.5** Advanced Gas Turbine Systems Program — Charles M. Zeh ..... 65

## Poster Session A — METC CRADA Opportunities


**PA.1** Dynamic Analysis of Process Reactors — Lawrence J. Shadle, Larry O. Lawson, and Stephen D. Noel ..... 69

**PA.2** CRADA Opportunities With METC's Gasification and Hot Gas Cleanup Facility — Edwin N. Galloway, John M. Rockey, and Mark S. Tucker ..... 70

**PA.4** CRADA Opportunities in Pressurized Combustion Research — Daniel J. Maloney, Thomas S. Norton, and Kent H. Casleton ..... 71

**PA.5** Pressure-Gain Combustion for Gas Turbines — Randall S. Gemmen, George A. Richards, and Michael C. Janus ..... 79

**PA.6** Hot-Gas Filter Testing With the Transport Reactor Demonstration Unit — Michael D. Mann, Michael L. Swanson, Robert O. Ness, and Jay S. Haley ..... 87

**PA.7** High-Temperature Gas Stream Cleanup Test Facility — John S. Ontko and Ta-Kuan Chiang ..... 98

**PA.8** Cooperative Research and Development Agreements at METC — J. Christopher Ludlow, Lisa A. Jarr, and Rodney J. Anderson ..... 104

**PA.9** High Pressure Optical Combustion Probe — Steven D. Woodruff and George A. Richards ..... 105

**PA.10** METC CFD Simulations of Hot Gas Filtration — Thomas J. O'Brien ..... 107

**PA.11** CRADA Opportunities in the Removal of Particulates From Hot-Gas Streams by Filtration — Duane H. Smith ..... 108

**PA.12** Dynamic Modeling of Power Systems — Michael E. Reed and Jay S. White ..... 109


## Session 3 — Hot Gas Particle Control


**3.1** Westinghouse Advanced Particle Filter System — Thomas E. Lippert, Gerald J. Bruck, Zal N. Sanjana, and Richard A. Newby ..... 123

**3.2** Lightweight Ceramic Filter Components: Evaluation and Application — Paul M. Eggerstedt ..... 140

3.3 Status of Granular Bed Filter Development Program — Keith B. Wilson, John C. Haas, and Jeff Prudhomme ..... 150

3.4 Pulsed Combustion and Hot Gas Cleanup Island — Ravi R. Chandran, Momtaz N. Mansour, S. Yavuzkurt, Gary H. Koopmann, and John L. Loth ..... 158

3.5 Filter Component Assessment — Mary Anne Alvin, Thomas E. Lippert, Edward S. Diaz, and Eugene E. Smeltzer ..... 160

3.6 Application of CFCC Technology to Hot Gas Filtration Applications — Scott Richlen ..... 183

## Session 4 — Hot Gas Desulfurization

4.1 Integrated Operation of a Pressurized Fixed Bed Gasifier, Hot Gas Desulfurization System and Turbine Simulator — Steve Bevan, David Najewicz, Raul E. Ayala, Alan Feitelberg, and Anthony Furman ..... 187

4.2 Pilot Scale Experience on IGCC Hot Gas Cleanup — Reza Ghazanfari, Gabor Feher, Jukka Konttinen, Arto Lehtovaara, and Wahab Mojtahedi ..... 202

4.3 Zinc Titanate Tests in Transport Reactor — Santosh K. Gangwal, William M. Campbell, Raghubir P. Gupta, and Gunnar B. Henningsen ..... 215

4.4 Slipstream Testing of Hot-Gas Desulfurization With Sulfur Recovery — Santosh K. Gangwal and Jeffrey W. Portzer ..... 220

4.5 Bench-Scale Testing of Fluidized-Bed Sorbents — ZT-4 — Santosh K. Gangwal and Raghubir P. Gupta ..... 229

4.6 Pilot Plant Tests of Z-Sorb™ Sorbent — G.J. Greenwood, G.P. Khare, D.H. Kubicek, G.A. Delzer, and D.L. Kinsinger ..... 241

## Session 5 — Fuel Gas Combustion

5.1 Fuel Gas Combustion Research at METC — Thomas S. Norton ..... 249

5.2 Performance of Low Btu Fuel Gas Turbine Combustors — Stephen Bevan, John H. Bowen, Alan S. Feitelberg, Stephen L. Hung, Michael A. Lacey, and Kenneth S. Manning ..... 250

**5.3** Development of a Topping Combustor for Advanced Concept Pressurized Fluidized-Bed Combustion Systems — William F. Domeracki, Thomas E. Dowdy, and Dennis Bachovchin ..... 263

**5.4** Development and Demonstration of a Solid Fuel-Fired Gas Turbine System — James G. Speight and Vijay K. Sethi ..... 275

## Poster Session B — Filters and Sorbents

**PB.1** Assessment of Ceramic Membrane Filters — Rajesh K. Ahluwalia, Howard K. Geyer, Kwan H. Im, Chao Zhu, David Shelleman, and Richard E. Tressler ..... 279

**PB.2** Carbon Formation and Metal Dusting in Hot-Gas Cleanup Systems of Coal Gasifiers — Roddie R. Judkins, Peter F. Tortorelli, Jackson H. DeVan, and Ian G. Wright ..... 292

**PB.3** Development of a Monolithic Ceramic Cross Flow Filter — David A. Larsen ..... 302

**PB.4** Properties of Ceramic Candle Filters — Duane H. Pontius and H. Stuart Starret ..... 318

**PB.5** Nitride-Bonded Silicon Carbide Composite Filter — Bruce N. Thomson and Stephen G. DiPietro ..... 320

**PB.6** 3-D Woven, Mullite Matrix, Composite Filter — Jay E. Lane, Carol J. Painter, Kenneth C. Radford, and Jean-Francois LeCostaouec ..... 329

**PB.7** Hot Particulate Removal and Desulfurization Results From the METC Integrated Gasification and Hot Gas Cleanup Facility — John M. Rockey ..... 340

**PB.8** Simultaneous Hot Desulfurization and Improved Filtration in Coal Utilization Processes — Paul M. Eggerstedt ..... 342

**PB.9a** Liming Efficacy and Transport in Soil of a Dry PFBC By-Product — Warren A. Dick ..... 356

**PB.9b** Characterization and Laboratory Weathering Studies — Joel H. Beeghly, Warren A. Dick, R.K. Fowler, U.I. Soto, and J.M. Bigham ..... 358

**PB.10** Disposal of Fluidized-Bed Combustion Ash in an Underground Mine to Control Acid Mine Drainage and Subsidence — Paul F. Ziemkiewicz, D. Courtney Black, William J. Head, Donald D. Gray, Hema J. Siriwardane, and William A. Sack ..... 360

**PB.11** Use of FBC Ash to Stabilize Dairy Barn Feedlots, Minimize Nutrient Pollution, and Develop New Utilization Outlets — Ronald F. Korcak and William L. Stout ..... 362

**PB.12** Hot Coal Gas Desulfurization With Manganese-Based Sorbents — Malcolm T. Hepworth and Rachid Ben-Slimane ..... 367

**PB.13** High-Temperature $H_2S$ Removal Using Limestones — Elton J. Cairns and Scott Lynn ..... 382

**PB.14** A Long Life ZnO - $TiO_2$ Sorbent — Michael E. Karpuk, Robert J. Copeland, Mike Cesario, Margarita Dubovik, Dan Feinberg, and Brian Windecker ..... 394

**PB.15** Development of Advanced Hot-Gas Desulfurization Sorbents — K. Jothimurugesan, Adeyinka A. Adeyiga, and Santosh K. Gangwal ..... 402

**PB.16** Advanced Low-Temperature Sorbents — Raúl E. Ayala, Venkat S. Venkataramani, Javad Abbasian, and Andy H. Hill ..... 407

**PB.17** Spectral Methods Applied to Fluidized Bed Combustors — Robert C. Brown, Thomas S. Raines, and Theodore D. Thiede ..... 417

**PB.18** Fossil Fuel Conversion – Measurement and Modeling — Peter R. Solomon, L. Douglas Smoot, Michael A. Serio, B. Scott Brewster, David G. Hamblen, and Predrag T. Radulovic ..... 425

**PB.19** Development of Methods to Predict Agglomeration and Deposition in FBCs — Michael D. Mann, Ann K. Henderson, Michael L. Swanson, and Thomas A. Erickson ..... 440

**PB.20** Evaluation of Options for $CO_2$ Capture/Utilization/Disposal — David K. Schmalzer and Richard D. Doctor ..... 448

**PB.21** Hot-Gas Filter Ash Characterization — John P. Hurley, Tina M. Strobel, and Bruce A. Dockter ..... 449

# Volume II

## Session 6A — Hot Gas Filter Issues


**6A.1** Development and Testing of PRD-66 Hot Gas Filters — Jeffrey A. Chambers ..... 467

**6A.2** Filter Systems for IGCC Applications — Stephen Bevan, Robert Gieger, Nelson Sobel, and Dale Johnson ..... 472

**6A.3** Thermal and Chemical Stability of Ceramic Candle Filters — Mary Anne Alvin, Thomas E. Lippert, Edward S. Diaz, and Eugene E. Smeltzer ..... 485

**6A.4** Novel Oxide-Oxide Fiber Reinforced Hot Gas Filter Development — Richard A.Wagner ..... 510

**6A.5** Filter Cake Characterization Studies — Richard A. Newby, Eugene E. Smeltzer, Mary Anne Alvin, and Thomas E. Lippert ..... 517

**6A.6** Hot Gas Filtration Technical Issues — Duane H. Pontius ..... 531


## Session 6B — Hazardous Air Pollutants (HAPS)


**6B.2** Comparison of HAPs From Advanced and Conventional Power Systems: Tidd Versus Cardinal — Steven A. Benson, Thomas A. Erickson, and David W. Brekke ..... 549

**6B.3** Trace Metal Transformations in Gasification — Steven A. Benson, Thomas A. Erickson , Christopher J. Zygarlicke, Cathy A. O'Keefe, Karen A. Katrinak, Sean E. Allan, David J. Hassett, and William B. Hauserman ..... 559

**6B.4** Hazardous Air Pollutant Testing at the LGTI Coal Gasification Plant — Robert G. Wetherold, W. Al Williams, David P. Maxwell, and Robert M. Mann ..... 573

**6B.5** Development of Mercury and Chloride Monitors for Coal Gasifiers — William H. Buttermore, Glenn A. Norton, Colin D. Chriswell, Dave E. Eckels, and Rachel E. Peters ..... 574

**6B.6** On-Line Elemental Analysis of Fossil Fuel Process Streams by Inductively Coupled Plasma Spectrometry — William P. Chisholm ..... 587

## Session 7A — Sorbent Development and Processes

**7A.1** Moving-Bed Sorbents — Raúl E. Ayala, Timothy Chuck, and Raghubir P. Gupta ..... 591

**7A.2** Spray-Dried Fluid-Bed Sorbent Tests – CMP-5 — Santosh K. Gangwal and Raghubir P. Gupta ..... 601

**7A.3** Desulfurization Sorbent Development Activities at METC — Ranjani V. Siriwardane ..... 609

**7A.4** Advanced Sulfur Control Concepts — Douglas P. Harrison, Alejandro Lopez-Ortiz, Julie D. White, and Frank R. Groves ..... 610

**7A.5** Advanced Sulfur Control Concepts — Santosh K. Gangwal, Brian S. Turk, and Raghubir P. Gupta ..... 622

**7A.6** Development of Disposable Sorbents for Chloride Removal From High-Temperature Coal-Derived Gases — Gopala N. Krishnan, B.J. Wood, A. Canizales, R. Gupta, S.D. Shelukar, and R. Ayala ..... 631

## Session 7B — Separation Technologies

**7B.1** Advanced Metal-Membrane Technology - Commercialization — David J. Edlund ..... 645

**7B.2** Separation of Hydrogen Using Thin Film Palladium-Ceramic Composite Membrane — Shamsuddin Ilias, Franklin G. King, Nan Su, and Uduak I. Udo-Aka ..... 646

**7B.3** A Calcium Oxide Sorbent Process for Bulk Separation of Carbon Dioxide — Douglas P. Harrison, Chun Han, and George Lee ..... 655

**7B.4** Thermal/Chemical Degradation of Inorganic Membrane Materials — Gopala N. Krishnan, Ashok S. Damle, Angel Sanjurjo, Bernard J. Wood, Kai-Hung Lau ..... 667

**7B.5** Electrochemical Polishing of Hydrogen Sulfide From Coal Synthesis Gas — E. Faith Gleason and Jack Winnick ..... 678

## Appendices

Agenda ..... 709

Meeting Participants ..... 721

Author Index ..... 747

Organization Index ..... 750

HMCDAN\1:951632

# Session 1

*Perspectives on the Future of Power Generation Industry*

## 1.1 And Deregulation Shall Lead Me to Lie Down in Green Pastures

Gary Weidinger
U.S. Generating Company

**ABSTRACT**

This presentation briefly reviews the history of the IPP industry, the current state of competition, and potential opportunities for IPPs in a deregulated environment.

Since the beginning of the PURPA created IPP industry, we have experienced many market phases. These began with "beat avoided cost," followed by "find a need and fill it," followed by "the bid fest," to today's "anything goes." During this time, market clearing prices have declined from over 8¢/KwHr to 2-4¢/KwHr.

Today's partially deregulated electric market includes fierce competition and several new players in the game. Where surplus capacity exists, IPPs must compete with subsidized power. Long-term contracts are no longer widely available. Access to markets is constrained by less than open transmission.

Even with these challenges, opportunities remain for the IPP supplier. Opportunities for advanced coal-fired power systems will be explored.

# 1.2 World Market: A Survey of Opportunities for Advanced Coal-Fired Systems

Neville A. H. Holt
Electric Power Research Institute

## ABSTRACT

Although there is a wide range of forecasts for the future of World energy demand and consumption over the next 25 years, all forecasts show marked increases being required for all forms of fossil fuels even when optimistic projections are made for the future adoption of Nuclear and Renewable energy. It is also generally expected that coal usage will in this period experience its greatest growth (a doubling) in the Asia-Pacific region dominated demographically by China and India.

In this paper, energy projections and the extent and nature of the coal reserves available worldwide are examined. While most coal technologies can handle a variety of feedstocks, there are often economic factors that will determine the preferred selection. The matching of technology to coal type and other factors is examined with particular reference to the Asia Pacific region.

Oil usage is similarly forecast to experience a comparable growth in this region. Over 70% of the World's oil reserves are heavy oils and refinery crudes are increasing in gravity and sulfur content. The clean coal technologies of gasification and fluid bed combustion can also use low value petroleum residuals as feedstocks. There is therefore a nearer term market opportunity to incorporate such technologies into cogeneration and coproduction schemes adjacent to refineries resulting in extremely efficient use of these resources.

## POPULATION GROWTH, ECONOMIC GROWTH AND ENERGY INTENSITY

In 1993 the World Energy Council's (WEC) Commission published the report, "Energy for Tomorrow's World - the Realities, the Real Options and the Agenda for Achievement". The Commission developed four energy cases, each representing different assumptions in terms of economic development, energy efficiencies, technology transfer and the financing of development around the world. In all four cases population growth was assumed to be the same and is taken from the current UN prediction as shown in Table 1. An increase is forecast from 5.3 billion in 1990 to 8.1 billion in 2020 with 90% of the increase coming from the developing world. The other major factors influencing energy demand, besides population growth, are economic growth and energy efficiency.

**Table 1. Global and Regional Population (millions)**

| | 1980 | 1990 | 2020 |
|---|---|---|---|
| North America | 251.9 | 275.9 | 326.4 |
| Latin America | 362.7 | 448.1 | 716.3 |
| Western Europe | 433.5 | 454.1 | 489.2 |
| Central & Eastern Europe | 95.3 | 100.2 | 111.0 |
| CIS | 265.5 | 288.6 | 343.9 |
| Middle East & North Africa | 200.3 | 271.0 | 543.3 |
| Sub-Saharan Africa | 370.0 | 501.6 | 1195.3 |
| Pacific | 1559.2 | 1806.9 | 2428.4 |
| (includes CPA) | (1084.7) | (1248.4) | (1652.5) |
| South Asia | 909.5 | 1146.0 | 1937.9 |
| WORLD | 4447.9 | 5292.4 | 8091.7 |

Since 1960, electricity has doubled its share of total energy consumption on a world wide basis and has increased in all groups of countries: OECD, CEE/CIS, and the developing countries. This has occurred even although energy usage per unit of GDP has declined. There is also a strong positive correlation of electrical usage per capita with the GDP per capita. The extension of electricity availability provides an important means of improving the quality of life in the developing countries. It is projected that world wide electricity usage will probably increase more than primary energy demand.

## FOUR ENERGY SUPPLY SCENARIOS

The key characteristics of the four WEC cases are given in Table 2. In each case, 2020 is adopted as the horizon year. The Reference Case B is an update of that developed by the WEC in 1989. This case reflects modest energy demand growth in developing countries and some reductions in energy/GDP intensity. Global energy demand rises over 50% between 1990 and 2020; Case $B_1$ assumes slower (less) reduction (improvement) in energy/GDP intensity in CEE/CIS and developing countries so that global energy demand in 2020 is projected to rise over 80% from 1990. Case A assumes a higher economic growth in developing countries and improvements in energy intensity are lower than Case B resulting in almost a doubling of global energy demand over the same period. Case C assumes a greater improvement of energy intensity than Case B, and a large contribution from 'new' renewable energy sources, and a smaller contribution from all other sources, particularly coal.

**Table 2. Description of the four WEC Energy Cases**

| Case | A | $B_1$ | B | C |
|---|---|---|---|---|
| Name | High Growth | Modified Reference | Reference | Ecologically Driven |
| Economic Growth % p.a. | High | Moderate | Moderate | Moderate |
| OECD | 2.4 | 2.4 | 2.4 | 2.4 |
| CEE/CIS | 2.4 | 2.4 | 2.4 | 2.4 |
| DCs | 5.6 | 4.6 | 4.6 | 4.6 |
| World | 3.8 | 3.3 | 3.3 | 3.3 |
| Energy Intensity Reduction % p.a. | High | Moderate | High | Very High |
| OECD | -1.8 | -1.9 | -1.9 | -2.8 |
| CEE/CIS | -1.7 | -1.2 | -2.1 | -2.7 |
| DCs | -1.3 | -0.8 | -1.7 | -2.1 |
| World | -1.6 | -1.3 | -1.9 | -2.4 |
| Technology Transfer | High | Moderate | High | Very high |
| Institutional Improvements (World) | High | Moderate | High | Very high |
| Possible Total Demand (Gtoe) | Very high 17.2 | High 16.0 | Moderate 13.4 | Low 11.3 |

**Table 3. Energy Mix - Annual Past and Future Global Fuel Use (Gtoe)**

| | 1960 | 1990 | in 2020 | | | |
|---|---|---|---|---|---|---|
| | | | A | $B_1$ | B | C |
| **Coal** | 1.4 | 2.3 | 4.9 | 3.8 | 3.0 | 2.1 |
| **Oil** | 1.0 | 2.8 | 4.6 | 4.5 | 3.8 | 2.9 |
| **Natural Gas** | 0.4 | 1.7 | 3.6 | 3.6 | 3.0 | 2.5 |
| **Nuclear** | – | 0.4 | 1.0 | 1.0 | 0.8 | 0.7 |
| **Large Hydro** | 0.15 | 0.5 | 1.0 | 1.0 | 0.9 | 0.7 |
| **"Traditional"** | 0.5 | 0.9 | 1.3 | 1.3 | 1.3 | 1.1 |
| **"New" Renewables** | – | 0.2 | 0.8 | 0.8 | 0.6 | 1.3 |
| **TOTAL** | 3.3 | 8.8 | 17.2 | 16.0 | 13.4 | 11.3 |

**Table 4. Fuel Mix in 1990 (Mtoe)**

| | Fossil Fuels | | | Renewables | | | | Total |
|---|---|---|---|---|---|---|---|---|
| | Coal | Oil | Natural Gas | Nuclear Energy | Hydro | Traditional | "New" | |
| North America | 508 | 809 | 497 | 145 | 127 | 38 | 34 | 2158 |
| Latin America | 22 | 218 | 80 | 3 | 80 | 125 | 50 | 578 |
| Western Europe | 333 | 568 | 254 | 169 | 99 | 20 | 19 | 1462 |
| Central & Eastern Europe | 156 | 49 | 64 | 11 | 5 | 4 | 4 | 293 |
| CIS | 365 | 378 | 569 | 47 | 50 | 26 | 11 | 1446 |
| Middle East & N.Africa | 7 | 167 | 117 | 0 | 5 | 21 | 1 | 318 |
| Sub-Saharan Africa | 68 | 38 | 4 | 1 | 9 | 141 | 6 | 267 |
| Pacific | 734 | 486 | 108 | 64 | 69 | 351 | 31 | 1843 |
| (includes CPA) | (575) | (100) | (14) | (0) | (30) | (218) | (13) | (949) |
| South Asia | 126 | 60 | 25 | 1 | 20 | 204 | 10 | 446 |
| WORLD | 2319 | 2773 | 1718 | 441 | 464 | 930 | 166 | 8811 |

The forecasted energy mix for Annual Past and Future Global Fuel Use is shown for the four cases in Table 3, and the breakdown of the global use by region for the reference Case B is shown in Table 4 for 1990 and in Table 5 for 2020.

**Table 5. Fuel Mix in 2020 for Case B (Mtoe)**

| | Fossil Fuels | | | Renewables | | | | Total |
|---|---|---|---|---|---|---|---|---|
| | Coal | Oil | Natural Gas | Nuclear Energy | Hydro | Tradi-tional | "New" | |
| North America | 400 | 793 | 601 | 188 | 162 | 46 | 147 | 2337 |
| Latin America | 79 | 483 | 296 | 26 | 235 | 179 | 99 | 1397 |
| Western Europe | 352 | 534 | 354 | 244 | 149 | 20 | 73 | 1726 |
| Central & Eastern Europe | 98 | 67 | 105 | 27 | 6 | 5 | 11 | 319 |
| CIS | 236 | 355 | 744 | 69 | 58 | 31 | 36 | 1529 |
| Middle East & N.Africa | 17 | 368 | 412 | 0 | 18 | 38 | 11 | 864 |
| Sub-Saharan Africa | 141 | 165 | 29 | 6 | 31 | 299 | 19 | 690 |
| Pacific | 1423 | 797 | 342 | 203 | 191 | 414 | 112 | 3482 |
| (includes CPA) | (1154) | (273) | (126) | (40) | (105) | (257) | (54) | (2009) |
| South Asia | 289 | 207 | 94 | 30 | 70 | 291 | 34 | 1015 |
| WORLD | 3035 | 3769 | 2977 | 793 | 920 | 1323 | 542 | 13359 |

Case A requires marked increases in coal, natural gas, and oil in the developing countries, dominated by China and India where major expansion of coal output would be required. Natural gas would be supplied long distance in Asia, and the transportation sector would require a large increase in oil supply.

Case B1 also requires substantial increased energy supply due to demand growth in the developing countries. Natural gas and oil are preferred for many, but China and India would continue to expand exploitation of their coal resources.

Case B reflects a more modest growth in energy demand of developing countries, but still a requirement for increased natural gas, oil, and coal supplies with China accounting for the bulk of the increased coal supply.

Case C by contrast relies on expanded supplies of new renewables and natural gas with some modest expansion of nuclear and hydro. Specific actions are implied in this case to curb the consumption of coal and oil.

The 2020 WEC forecasts with regard to coal are lower than others such as the U.S. EIA and some IEA forecasts. For example, under all four WEC scenarios, coal usage in North America and CEE/CIS declines and for Western Europe is generally flat. However, coal usage in Latin America, Sub Saharan Africa, Pacific and South Asia still rises under all WEC scenarios particularly in China and India. In Case B, oil usage is flat in North America, Western Europe and CEE/CIS but doubles for the rest of the world (as does coal). However, natural gas increases by about 30% in North America, Western Europe and CEE/CIS and in the rest of the world increases to 350% of the 1990 consumption.

In all cases, substantially increased and more widely spread gas finds would be required and associated large investments in transportation which will affect price and lengthen lead times. Increased coal production is probably less capital intensive given the location of the huge resource base. Constraints on coal use are more likely to come from emission regulations and whether potential climate change becomes a sufficiently significant issue.

All four cases assume an expansion of nuclear power availability by 2020. However, this is by no means certain given the current public perceptions and lack of political acceptability, except in France and Japan.

## FOSSIL FUEL RESOURCES

Current estimates of proven recoverable reserves of fossil fuels and the ratios of these reserves to current world use are shown in Table 6. The World Energy Council's estimate of the world's ultimately recoverable resources are shown in Table 7. The basis for resource estimates varies from country to country and for this reason comparisons are difficult.

There is no physical resource constraint on further expansion of nuclear power, but this will require renewed public confidence in the safety of such plants, the satisfactory disposal of nuclear waste, and substantial financial and technical resources. It has also been estimated that only a quarter of the world's hydro-electric potential (10,000 Twh) has so far been developed, although this too is controversial from an environmental point of view.

**Table 6. Proved Fossil Fuel Reserves and Reserves/Production Ratios**

| | Estimate of Cumulative Production to 1990 (Gtoe) | Estimate of Proven Reserves in 1990 (Gtoe) | Estimate of 1990 Reserves to Production Ratio (Years) |
|---|---|---|---|
| Coal (Excluding Lignite) | n/a | 496 | 197 |
| Lignite | n/a | 110 | 293 |
| Oil | 86 | 137 | 40 |
| Natural Gas | 40 | 108 | 56 |

Source: WEC Survey of Energy Resources

**Table 7. Ultimately Recoverable Fossil Fuel Resources**

| | Gtoe | % |
|---|---|---|
| Coal and Lignite | 3400 | 76 |
| Conventional Oil | 200 | 5 |
| Unconventional Oils: | | |
| Heavy Crude | 75 | 2 |
| Natural Bitumen | 70 | 2 |
| Oil Shale | 450 | 10 |
| Natural Gas | 220 | 5 |
| Total (approx.) | 4400 | 100 |

Source: WEC, 1992 Survey of Energy Resources; WEC 1989 World Energy Horizons 2000-2020; Masters C.D. et al, World Resources of Crude Oil and Natural Gas, 13th World Petroleum COngress, 1991; Masters C.D. et al, World Reserves of Crude Oil, Natural Gas, Natural Bitumen and Shale Oils, 12th World Petroleum Congress, 1987

Traditional biomass - fuel wood, crop residues, dung - account for 60% of total renewable energy available in 1990 and large scale hydro a further 30%. Even under a very optimistic scenario for 'new' forms of renewable energy - solar, wind, geothermal, modern biomass, ocean and small hydro -the traditional renewables are expected to account for over half of renewable energy in 2020.

The main realities of global energy are that for many decades fossil fuels (natural gas, oil, and coal) will continue to provide most of the supply. However, fossil fuel resources are unevenly distributed around the world. In 1990, it was estimated that the Middle East had 67% of the proved recoverable oil reserves, and Latin America 12%. The 1990 natural gas figures are 48% for CEE/CIS and 29% for the Middle East.

Coal is the most widely distributed fossil resource with USA, CIS, China, and India having the largest deposits. A number of other developing countries have large coal resources (Indonesia, North Korea, Vietnam, Philippines, etc.). The pressures to develop these are very strong and seen locally as high priority.

## COAL CHARACTERISTICS AND UTILIZATION TECHNOLOGIES

Coal composition and properties, and knowledge of the conditions at the time of formation can be used to identify behavior during utilization and indicate suitable end uses. The study of the organic constituents of coal (macerals) provides information about the coal origin.

The Laurasian (northern hemisphere - Illinois, Appalachia, Central Europe) carboniferous coals are rich in the vitrinite group of macerals. They tend to have relatively high sulfur contents with low ash and high rank.

In contrast, most Gondwanan (southern hemisphere - including South Africa, Australian, and Indian coals) are rich in the inertinite group of macerals. They tend to have lower sulfur contents, higher ash, and lower ranks.

In the later Jurassic, Cretaceous and Tertiary periods, plants were rapidly evolving and were therefore more diverse. This resulted in a greater range of coal type. The deposits of much of the Western USA, Western Canada, and China coal deposits are from the Cretaceous period. The later Tertiary period produced the deposits of Columbia/Venezuela, Indonesia, and additional deposits in Western USA and Canada.

Rank and coal type are not purely a result of age, and the coalification process can be accelerated by post-depositional heating through igneous activity. For example, Indonesian coals have far higher rank that would be expected for their geologic age.

Anthracite, the highest coal rank, is typified by very low volatile and inherent moisture contents. Coals with somewhat higher volatile content, bituminous coals, often have good caking characteristics suitable for coke manufacture. High volatile coals may or may not have caking properties and a higher inherent moisture content. 'Low rank' coals such as sub-bituminous coals, lignites, and brown coals are typified by very high inherent moisture contents, high volatile contents, and lower carbon contents.

Conventional Pulverized Coal (PC) boilers can successfully fire a very wide range of ranks and types of coal; however, the use of coal with poor properties usually incurs financial penalties. Ideally the moisture content should be less than 15%. The boiler design is very much affected by coal rank. Most conventional coal-fired power plants are designed to use low to medium-rank coals with over 20% volatile matter. High rank coals, or anthracites, can be used but require special designs. Some coal fired stations can use up to 30% ash contents without severe difficulties. Thermal coals are usually only washed or pretreated when ash contents are excessive, whereas coking coals are normally washed and beneficiated. High ash coals also present significant ash disposal problems. Finely disseminated minerals in the coal influence hardness and grindability, and mills must be designed accordingly. The slagging and fouling characteristics of coal ash are also important. Ash fusion temperatures should be not less than 1200° C in an oxidizing atmosphere. To minimize sulfur oxide emissions, the sulfur content of the coal should preferably not exceed 1%.

In most OECD countries, coals with sulfur contents over 1% will usually require flue gas desulfurization to meet emission

standards. Although the developing nations of the Asia Pacific region do not currently have sulfur oxide emission regulations, there is a possibility that they will be enacted in the future. However, most coals of this region are less than 1% sulfur and such regulations may not be of high priority.

If flue gas desulfurization is required, the capital cost is increased. Limestone (typically) must be mined, purchased, and delivered to site, and substantial costs incurred for the disposal of the calcium sulfate/sulfite sludge byproduct.

Conventional PC boilers raised steam and generate power by the Rankine cycle. Supercritical pressure steam can be generated to improve the overall efficiency. Low cooling water temperatures enable lower condenser vacuum pressures and higher efficiencies. Once through ocean cooling, water can reduce capital and operating costs by eliminating cooling water towers.

Overall, conventional PC plants are favored by the following conditions:

Low sulfur coal
High ash fusion temperature coal
Lower cooling water temperatures
Ocean water cooling
Modest emission regulations.

The PC power plant is a proven technology for small or large capacities up to 1300 MW using a single-shaft steam turbine.

Atmospheric Fluidized Bed Combustion (AFBC) is now a fully commercial technology with ten vendors, four of whom offer units as large as 250 MW. This technology is cost competitive with PC plants particularly in the small to moderate size ranges and may find applications for cogeneration in urban locations.

SOx is controlled by limestone addition to the fluid bed and with the lower combustion temperatures relative to a PC boiler NOx emissions are low. If appropriately designed, the AFBC can handle a wide range of coal feedstocks.

As with PC plants, AFBC is most competitive when used with low sulfur coals so that the limestone costs and solids disposal are minimized. Since it is still based on the Rankine cycle, the availability of low temperature cooling water and once through cooling water is similarly beneficial as for PC plants.

Pressurized Fluidized Bed Combustion (PFBC) has the advantage of smaller size and the potential for higher thermal efficiency (> 40%) than AFBC. The operating experience base is more limited for PFBC. Five units have been built of the 70 - 80 MW size. The U.S. unit at Tidd has just shut down; two units in Sweden and one in Spain are in operation and a unit in Japan was started up at the end of 1994. Japanese companies are planning PFBC scale up to the 250 - 320 MW size, which should be operational by 1998.

Power output from PFBC is still mostly from the Rankine cycle. Accordingly, PFBC is similarly favored by low sulfur coals and low cooling water temperatures and once through cooling.

The smaller size of PFBC is expected to provide an advantage over PC particularly in certain repowering applications at constrained existing sites and where the large incremental power additions (such as would be provided by natural gas or IGCC repowering) are not needed.

Gasification based systems, such as Integrated Gasification Combined Cycle (IGCC) can meet extremely stringent emission standards, since the emission forming constituents are removed prior to combustion. In most schemes, the coal sulfur is produced as elemental sulfur for sale, and thereby represents another revenue stream rather than a disposal problem. However, some fluid bed

gasification technologies such as KRW, IGT'U' Gas, British Coal, Kellogg transport and Foster Wheeler Hybrid gasification Technologies currently propose to effect sulfur control by limestone addition with attendant solid waste disposal.

Single train IGCC plants based on each of the major entrained flow gasification processes (Texaco, Destec, Shell, and Prenflo) using 1260° C firing temperature gas turbines will be demonstrated in the U.S. and Europe in 1995 - 8. The results from these demonstration plants will provide the basis for commercial IGCC plants anticipated to be deployed in the 2000+ time frame. The IGCC technology will also benefit greatly from other advances being made in gas turbine technology such as the currently offered ABB GT24, Siemens V84.3A, Westinghouse 501G and GE 7G and H machines, and further advances from the DOE ATS program - all of which will be available in this same time frame.

These larger, more efficient gas turbines will provide substantial capital and operating cost reductions for IGCC over those projected based on the demonstration plants about to be commissioned.

Gasification processes can generally handle a wide range of coals; however, each of the process has certain characteristics which affect the cost and efficiency of using various coals as shown in Table 8.

Entrained flow processes (Texaco, Destec, Shell, and Prenflo) operate in the slagging region. Their performance is best with low ash, lower ash fusion temperature bituminous coals. High ash fusion coals require flux addition (usually limestone). The slurry fed processes such as Texaco and Destec are adversely affected by coal characteristics that affect the energy density of the slurry such as high inherent moisture and ash contents. While such coals can be processed the oxygen usage required is usually prohibitive economically.

Fluid bed gasification (HT Winkler, IGT'U' gas, KRW, British Coal, Kellogg transport, and Foster Wheeler) can handle a wider range of coals and since they operate at temperatures lower than the slagging temperatures can handle high ash and high ash fusion coals. Those that rely on the addition of limestone for sulfur capture will prefer low sulfur coals. Fluid bed gasification is generally not as well developed as the entrained flow processes. However, the HT Winkler is operated commercially at 10 bar pressure in Germany on brown coal and on peat in Finland. Ten IGT'U' gas gasifiers at 4 bar pressure are being started up in Shanghai.

The entrained flow processes are currently only offered as oxygen blown systems. Fluid bed systems can be either oxygen or air blown. Currently most fluid bed schemes for IGCC power production are planned for air blown operation. A 95 MW air blown KRW IGCC is under construction for Sierra Pacific near Reno, NV and is scheduled for a late 1996 startup.

**Table 8. Gasification Technologies - Preferred Coal Feed Characteristics**

| | Texaco | Destec | Shell/ Prenflo | BGL | HT Winkler | KRW/ IGT'U' Gas/ Brit.Coal/ Kellogg Trans/FW |
|---|---|---|---|---|---|---|
| Bituminous | √ | √ | √ | √ | some | √ |
| Subbituminous/ Lignite | | √ | √ | some | √ | √ |
| High S | √ | √ | √ | √ | √ | |
| Low S | √ | √ | √ | √ | √ | √ |
| High Ash | | | | | <------OK- | ---------> |
| High Ash Fusion | <--------- | needs flux (usually limestone) | --------- | --------> | | |

**Table 9. Typical Asia-Pacific Coals**

| | Australia | India | China | | Indonesia | |
|---|---|---|---|---|---|---|
| | Newlands | Dakra | Shanxi | Shandong | Kaltim Prima | Air Laya |
| % Ash | 13.6 | 38.8 | 25.0 | 10.0 | 4.5 | 6 |
| % Moisture | 8.3 | 18.0-6.0 | 10.0 | 0.7 | 10.0 | 21.0 |
| MAF - % Vol. Mtr. | 31.6 | 44.6 | 40.0 | 30.0 | 40.0 | 43.0 |
| MAF- % S | 0.5 | 0.4 | 0.7 | 4.0 | 0.5 | 0.3 |
| MAF - HHV MJ/Kg | 34.2 | 32.3 | 32.1 | 36.1 | 34.0 | 33.5 |
| Ash Fusion Fluid Temp.°F | 2700+ | 2700+ | 2700+ | 2500 | -- | -- |

## ASIA PACIFIC COALS

Some key characteristics of typical coals available in the Asia Pacific region are shown in Table 9. As discussed previously the Gondwanan coals of Australia and India are low sulfur, high ash fusion and particularly in the case of India are of high ash content. Indonesian coals are generally of low sulfur content. Chinese coals have the widest range of properties and all ranks of coals can be found. Over half of the recoverable reserves of Chinese coal are bituminous coal or anthracite, and in 1991 the average sulfur and ash content was 1.1% and 30% respectively.

## INDIA - COAL

The most important coal deposits are found in the Raniganj and Jharia basins of North Eastern India and the states of Madya - Pradesh, Bihar, West Bengal and Orissa. The Jharia field is India's only source of prime coking coal. Some lignite is used at Neyveli in Tamil-Nadu. The 1991 production of Indian coal was 222 million metric tons, over half of it

for power generation. The bulk of the reserve consists of low grade coal with high ash content. It is projected that the coal for future power generation in India will generally have > 35% ash as compared to 10 - 15% in U.S. or other OECD countries.

The ash in Indian coal is generally refractory in nature. It consists mainly of silica, alumina, iron, and has a very low content of calcium, magnesium, sodium, and potassium. The ash is very abrasive and has a very high ash fusion temperature. The coal generally contains < 1% sulfur.

At this time, India does not have stringent SOx or NOx emissions regulations and with the relatively low sulfur content of the coal, it is by no means certain that such legislation will be a high priority.

Huge increases in power demand are generally forecast for India from about 80 GW of capacity in 1992 to 200 GW in 2010 with coal increasing from 52 to 118 GW. GE forecasts 70 GW for India in the next 10 years. However, without some essential tariff reform, leading to full cost pricing, it is doubtful if the financing for such expansion can be obtained.

Essentially, all coal power plants in India are PC plants, and despite the severe equipment erosion and low availability experienced in these plants, the majority of new power plants with probably be PC plants without FGD. However, some of the International banks are requiring that their loans be for more environmentally benign technologies. In the immediate future this would probably mean the addition of FGD (probably dry) for large power plants. AFBC will also find application for smaller plants and industrial cogeneration application.

India has shown considerable interest in IGCC and a small 40 MW IGCC unit is planned for Ahmedabad in Gujarat Province probably based on a fluid bed gasification process. However, the high ash nature of Indian coal is not a very suitable feedstock to the more developed entrained flow gasification technologies such as Texaco or Shell. The results of an IGCC study conducted by Bechtel and an Indian team in 1989 - 90 are shown in Table 10. Although the gas turbine and other assumptions are out of date and do not reflect current offerings; nevertheless the overall conclusion is probably still valid. Particularly in the absence of $SO_2$ emission legislation, entrained flow IGCC is unlikely to be cost competitive based on Indian coals. The fluid bed IGCC technology such as KRW or IGT'U' gas with the newer gas turbines could potentially be cost competitive particularly if sulfur removal is not required, or if it is found by successful demonstration that in-situ sulfur capture is sufficient , and that external desulfurization is not required.

PFBC and hybrid gasification schemes such as British Coal and Foster Wheeler may also prove competitive in similar circumstances. PFBC may be demonstrated at 320 MW by about the year 2000, and the KRW IGCC should be proven at the 95 MW size in a similar time frame. However, most of the fluid bed technologies are at an earlier stage of development and are unlikely to be candidates for commercial introduction until after 2005.

In the absence of sulfur emission regulation and even if higher quality imported coals such as Australian or Indonesian are considered, the coal technology will probably still primarily be PC and AFBC for the immediate future. This is also likely to be the case in most of South Asia because of the availability of low sulfur coal.

**Table 10. U.S. AID/Bechtel - Indian Coal Study (1990)**
**IGCC - PC Comparison (4thQ1989$)**

| IGCC Cases | Total Capital $M | Capital Cost $/kW | COE (1) ¢/kWh | Thermal Efficiency % HHV Basis |
|---|---|---|---|---|
| Shell | 1209 | 2143 | 7.9 | 35.1 |
| Texaco | 1211 | 2442 | 9.3 | 24.4 |
| KRW | 859 | 1488 | 5.6 | 40.2 |
| Moving Bed | 899 | 1535 | 6.2 | 32.9 |
| PC | 626 | 1122 | 4.8 | 31.8 |
| PC & FGD | 752 | 1357 | 5.5 | 31.6 |

(1) Based on 6000 hr/yr operation

REF: EPRI TR-100466 - R. Iyengar, S. Rao (CSIR India), T. P. Chen (Bechtel) pp. 28- (1-21)

## CHINA - COAL

Although China has coal resources in most provinces, over 75% of the recoverable reserves are in north and northwest China, and two-thirds of the reserves occur in the three provinces of Shanxi, Shaanxi, and Inner Mongolia. The IEA projects the electrical generating capacity to increase from 138 GW in 1990 to 310 GW in 2000 and 632 GW in 2010. Coal is projected to supply the majority of such growth increasing from 100 GW in 1990 to 210 GW in 2000 and 452 GW in 2010. Problems associated with the Chinese transport infrastructure, and especially its railways, have worsened in recent years. Although many new investments are planned including a coal-water slurry pipeline, it is judged that much of the new coal fired capacity will have to be mine mouth with consequent investment in power transmission facilities (and some attendant losses). Tariff reform in power, mining, and transportation sectors, again are essential to achieve the financing for such growth.

The average coal is still fairly low sulfur and although $SO_2$ emissions regulations have been suggested, most of the additional coal fired power plants will be PC plants with ESPs, while AFBCs will find application with smaller sizes and particularly in industrial cogeneration. Any constraints leveled by international banks with regard to emissions will probably be met in the immediate future by the addition of FGD. However, the above mentioned constraints on transportation also mean that China is reluctant to take up scarce transport capacity with limestone delivery and the consequent solid waste disposal. For this reason, plus the efficiency gain, IGCC has been a technology of great long term interest for China and a commercial sized demonstration plant is planned. PFBC design studies are also being conducted by ABB for potential Chinese clients. Major application of these technologies (IGCC, PFBC, etc.) in China will generally depend on the successful completion of the commercial sized demonstrations in the U.S., Europe, and Japan [A possible exception is the Texaco gasification technology which has been widely adopted in China (20 licenses) for ammonia, chemicals and towns gas manufacture, and which could be used for IGCC.]

Coal bed methane extraction for industrial use is also an excellent near term technology warranting wide application in China.

## COGENERATION AND COPRODUCTION OPPORTUNITIES

An alternative and perhaps a major opportunity for earlier introduction of clean coal technologies in the Asia - Pacific region is

suggested by an examination of coal usage in China as shown in Table 11. In 1990 coal usage for power was only 27% of total coal consumption; 13.5% used for iron and steel, 9% for chemicals, and 22% for other industries. Fully 16% or 118 million tons a year is used residentially for heating and cooking.

As any visitor to the major Chinese cities can attest, urban pollution is a real problem In the case of China, the major cause is the use of coal residentially and for small industries. The solution must be sought in increased electrification and expansion of gas supplies. The available natural gas supplies are mainly in the Southeast and Towns gas systems supply the major northern cities.

AFBC has been widely applied in China in small plants, with over 3000 in operation; however, these generally do not use limestone for sulfur control, have short stacks, and often no particulate removal beyond cyclones.

**Table 11. Chinese Coal Demand by Sector, Mtce**

| | 1980 | 1990 | 2000 | 2010 |
|---|---|---|---|---|
| Electricity Generation | 83 | 197 | 389 | 920 |
| Own Use, Losses, etc. | 30 | 44 | 5 | 50 |
| Iron & Steel | 71 | 100 | 120 | 140 |
| Other Industry | 141 | 222 | 314 | 320 |
| Residential, Commercial, & Other | 117 | 170 | 197 | 202 |
| TOTAL | 442 | 734 | 1075 | 1632 |

Source: Chinese coal prospects to 2010. M. Daniel IEAPER/11 JUNE 1994

Some of the cogeneration and coproduction opportunities suggested by these observations and from Table 11 include:

- Use of AFBC or PFBC for combined heat and power in urban locations. With district heating by hot water mains supplanting the use of direct open fire coal burning for home heating.

- Use of Coal Gasification to provide both fuel gas for gas turbine combined cycle power plants, and syngas for fertilizer (ammonia, urea) and other chemicals manufacture. The combined cycle can supply power and steam for industrial use.

- Use of Coal Gasification in urban centers to provide fuel gas for towns gas distribution and combined cycles providing power and steam or hot water for urban residential demand and domestic heating.

- Use of Coal Gasification and technologies such as COREX within the Iron and Steel industry, providing reducing gas and through combined cycle satisfying power and steam demands.

The uses mentioned above are also potentially applicable in India. However, for reasons previously discussed, due to the nature of Indian coals, they will be more limited most likely to FBC and fluid bed gasification technologies.

Some Chinese gasification coproduction projects have already been undertaken. At Shanghai Coking and Chemical Corporation, the eight air blown IGT'U' Gas gasifiers produce a low Btu gas which is used to underfire the coke ovens. This enables the portion of the higher heating value coke oven gas which was formerly used to underfire the ovens, to be added to the towns gas distribution system. A 70 - 80 MW gas turbine is to be added at the site to provide power and steam. There is also a Texaco gasifier at Shanghai Coking and Chemical supplying syngas for chemicals manufacture and blending into towns gas. Another Texaco gasifier at Shougang supplies syngas for use as fuel gas and reducing gas in iron and steel production.

## OIL REFINING

Examination of Tables 4 and 5 show that the WEC projects oil consumption in the Pacific region (including China itself) and South Asia to increase at an even higher percentage rate than coal. (The U.S. EIA forecasts are more conservative.) Just as economic aspirations and demographics will drive the demand for increased electrification and power usage, so will the demand for clean transportation fuels grow.

Crude oil refining capacities for China and India are currently 2.9 and 1.1 million barrels per day (MBPD) (compare to 15.3 MBPD in the U.S.). The number of people per car is about 680 in China and 122 in India compared to 2.5 in OECD and 1.7 in North America. Many new refineries and major expansions are already planned for these regions.

Over 70% of the World's known crude oil reserves are classified as heavy oils of high sulfur content. Over the past 15 years, refinery crude slates have steadily increased in gravity and sulfur contents. Legislation has been adopted in many OECD countries limiting the permissible sulfur content of #6 fuel oil for direct burning to < 1%. These changes plus the demand for cleaner transportation fuels has lead to the need to add heavy oil conversion such as hydrotreaters, hydrocrackers, and coking units to refineries with their attendant increased demands for hydrogen, steam, and power.

China and India are likely to have to rely mainly on imported heavy crudes for their refinery expansions. Clean coal technologies, particularly gasification, can also use petroleum residuals (vacuum residual oil, petroleum coke, etc.) to provide the steam and power needs of the refinery. In the case of gasification, hydrogen and syngas for methanol and other oxygenates manufacture can also be supplied. Several such projects are underway in Europe using Texaco or Shell-Lurgi heavy oil gasification with gas turbine combined cycles. These projects represent an extremely efficient use of these low value resources. An overall effective efficiency of 85 - 90% can be achieved.

## SUMMARY - PROSPECTS FOR COAL TECHNOLOGY MARKETS

The largest market for coal technology will be in the developing countries particularly the Asia Pacific region and primarily in China and India. Much of the current electric power production in these regions is from inefficient coal fired plants with minimal environmental controls. Major expansions in coal fired generation are expected in the next 25 years. However, the pacing issue will probably be tariff reform and realistic pricing leading to the development of financing capabilities and infrastructure. The selected technologies will primarily be those that can be implemented at relatively low cost and where there is an established extensive operational database.

- Modern higher efficiency PC plants will dominate the near term capacity expansion for large central stations.
- AFBC will compete effectively in the small to medium scale and especially in cogeneration applications.
- PFBC is a longer term option which requires demonstration at the larger sizes (300 MW) prior to its full commercial adoption. Some niche opportunities for the 80 MW units may be found.
- Coal gasification based systems such as IGCC, are also longer term options that will increase in importance as technology advances (e.g. gas turbines) and as environmental priorities increase.

- In certain developing countries such as China and India, with large coal reserves and industries, there are additional opportunities for the early application of coal gasification in cogeneration and coproduction of power, steam, towns gas, fertilizers, and chemicals.

- There is also a nearer term opportunity for the introduction of FBC and particularly gasification adjacent to oil refineries using petroleum residuals such as vacuum resid or petroleum coke as feedstocks and providing the refinery with power, steam, hydrogen, and syngas for oxygenates and chemicals.

New coal fired generating technologies are capital intensive and in today's competitive business environment, the traditional assumed 30 year book life is becoming increasingly irrelevant. They must compete with less capital intensive technologies with shorter capital recovery schedules. Wherever, natural gas is available at low cost, gas turbine combined cycles provide low capital cost, smaller size power plants which can be deployed quickly. Such plants will often be preferred in the rapid growth developing countries because of their ability to attract global investments and shorter capital recovery schedules.

The new coal technologies now entering commercial demonstration in the developed countries must focus on further reducing capital cost to better compete with lower cost gas turbine combined cycles and traditional PC plants either with or without emissions control. The new coal technologies are very much at the beginning of the learning curve and improvements in almost all aspects can be confidently expected to occur e.g. coal feeders, hot gas clean up, high firing temperature gas turbines, new cycles which can take advantage of lower cost gasifiers (e.g. quench), hybrid gasification/FBC cycles. Recent studies suggest that capital costs of about $1000/kW (U.S. basis) should be attainable.

Although it is projected that most added U.S. power generation will be gas turbines over the next 10 - 20 years, this will mean that the existing coal plants will mostly be at the end of their life in the 2010+ time frame. Similar situations may also occur elsewhere in the OECD countries. It is therefore very likely that coal based technologies will have to return to replace the aging U.S. coal fleet. The repowering of existing plants with PFBC or IGCC can enable the continued use of valuable existing generating sites and equipment with considerable capital cost savings over Greenfield sites. Repowering therefore represents the best opportunity for the commercial introduction of these technologies. Gasification will also provide the technology to ensure the continued operation of the very considerable industry investment in gas turbine combined cycles in the event that natural gas is no longer economically available. Even if the repowering of existing steam plants is initially conducted with natural gas fired gas turbines the later addition of gasification can provide a smooth transition to coal when that is economical and strategically necessary.

**References:**

"Energy for Tomorrow's World - the Realities, the Real Options and the Agenda for Achievement", World Energy Council, 1993.

"Major Coalfields of the World", S.Walker, IEA CR/51, January 1993, IEA Coal Research.

"Use of High Ash Indian Coal for IGCC Plant", R.K.Iyengar, S.K.Rao (CSIR - India), T.P.Chen (Bechtel) EPRI TR-100466 Proceedings: Ninth EPRI Conference on Gasification Power Plants, pp. 28 - 1ff.

"Chinese Coal Prospects to 2010", M. Daniel, IEA PER/11, 1994 IEA Coal Research.

"international Focus: China", Coal Magazine, May 1995.

"World Wide Activity in IGCC", EPRI Journal, July/August, 1994.

*Fossil Power Generation and Sustainable Development*, G.T. Preston (VP Generation - EPRI) Presentation to the Royal Society, London, UK, March 16, 1994.

*GE Forecast*, (D.L.Williamson - GEPS Asia) Presented at 1995 Asia Pacific Energy and Power Conference 11.

## 1.3 METC Clean Coal Technology Status -- 1995 Update

Larry K. Carpenter
Morgantown Energy Technology Center

### ABSTRACT

The Department of Energy (DOE) Clean Coal Technology (CCT) Program is assisting the private sector by funding demonstration programs to validate that CCT technologies are a low-risk, environmentally attractive, cost-competitive option for utility and industrial users. Since 1987, DOE has awarded 45 CCT projects worth a total value of $7 billion (including more than $2.3 billion of DOE funding). Within the CCT Program, the Morgantown Energy Technology Center (METC) is responsible for 17 advanced power generation systems and major industrial applications.

METC is an active partner in advancement of these technologies via direct CCT funding and via close cooperation and coordination of internal and external research and development activities. By their nature, METC projects are typically 6-10 years in duration and, in some cases, very complex in nature. However, as a result of strong commercial partnerships, progress in the development and commercialization of major utility and industrial projects has, and will continue to occur. It is believed that advanced power generation systems and industrial applications are on the brink of commercial deployment.

A status of METC CCT activities will be presented. Two projects have completed their operational phase, operations are underway at one project (two others are in the latter stages of construction/shakedown), four projects are in construction, six restructured. Also, present a snapshot of development activities that are an integral part of the advancement of these CCT initiatives will be presented.

# Session 2

*Advanced Power Systems*

## 2.1 Power Systems Development Facility Progress Report

### CONTRACT INFORMATION

**Cooperative Agreement** DE-FC21-90MC25140

**Contractor**
Southern Company Services, Inc.
P.O. Box 1069
Wilsonville, AL 35186
(205) 669-5840

**Other Funding Sources**
Electric Power Research Institute
Southern Company Services, Inc.
The M. W. Kellogg Company
Foster Wheeler
Westinghouse Electric Corporation
Industrial Filter and Pump Manufacturing Co.
Combustion Power Company
Nolan Multimedia

**Contractor Project Manager** Randall E. Rush

**Principal Investigators**
Howard L. Hendrix
Darrell L. Moore
Timothy E. Pinkston
P. Vimalchand
John M. Wheeldon, EPRI

**METC Project Manager** James R. Longanbach

**Period of Performance** June 7, 1994 to June 12, 1995

**Schedule and Milestones**

**FY95 and FY96 Program Schedule**

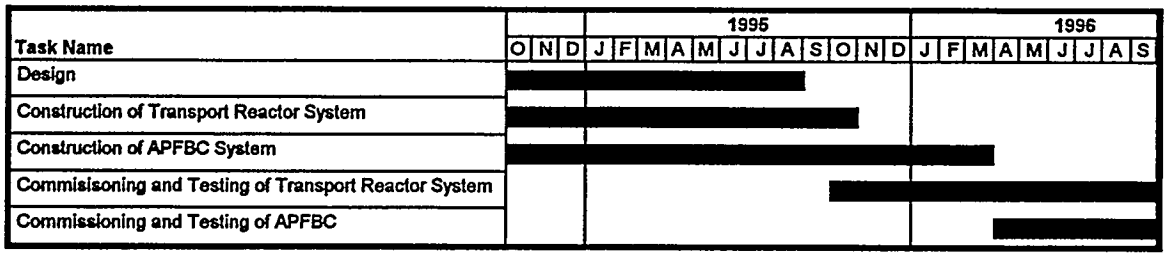

## OBJECTIVES

The objectives of the Power Systems Development Facility (PSDF) are to develop advanced coal-fired power generation technologies through the testing and evaluation of hot gas cleanup systems and other major components at the pilot scale and to assess and demonstrate the performance of the components in an integrated mode of operation and at a component size readily scaleable to commercial systems.

The primary focus of the PSDF project is to demonstrate and evaluate high temperature Particulate Control Devices (PCDs) which are the single most important component required for successful development of advanced power generation systems. High temperature PCDs are a common component of advanced gasification and Advanced Pressurized Fluidized Bed Combustion (APFBC) technologies, both of which will be evaluated at the facility. Successful high temperature gas cleanup will increase the efficiency and reduce the capital and operating costs of coal gasification processes by avoiding cooling and reheating of the syngas as is required in current technology. APFBC processes also benefit from the use of high-temperature PCDs which allow the use of modern high efficiency gas turbines instead of ruggedized expander turbines. A recent engineering and economic evaluation by the Electric Power Research Institute indicates that the capital cost of ABB-Carbon's bubbling PFBC can be reduced by as much as 9% when a PCD is used in conjunction with a non-ruggedized gas turbine.[1]

## BACKGROUND INFORMATION

The PSDF located at Wilsonville, Alabama will be the focal point for much of the Nation's advanced coal-fired electric power technology development in the latter 1990s and into the 21st century. Coal will supply at least half the Nation's electricity well into the 21st century (it currently accounts for 56%). Yet, future coal systems will have to be increasingly cleaner and more efficient if the United States is to use its most abundant fossil fuel to sustain economic growth.

Jointly sponsored by the Department of Energy and many of the Nation's most forward-looking power equipment developers, the PSDF will be a highly flexible modular test center. Equipment developers will be able to test innovative electric power system components--new combustors, improved cleanup systems, and advanced turbines and fuel cells--at a central location, saving the time and expense of building separate test facilities.

Plans call for the facility to contain five modules initially: (1) an advanced pressurized fluidized-bed combustion system, (2) a transport reactor gasifier and combustor, (3) a particulate control module, (4) an advanced burner-gas turbine module, and (5) a fuel cell. Combining these modules into a single structure has saved more than $32 million when compared to the cost of building stand-alone facilities.

Hardware systems can first be evaluated separately, then linked together in an integrated power system. Filters can be tested with a pressurized fluidized-bed combustor or with a coal gasifier. Advanced turbines and fuel cells can be tied into the process path in a variety of ways. The facility will be capable of operating at pilot to near-demonstration scales, large enough to give industry real-life data for scaleup to commercial size, yet small enough to be cost-effective and adaptable to a variety of industry needs.

## PROJECT DESCRIPTION

Initially, the five modules at the PSDF will be configured into two separate test trains as shown in the process schematic in Figure 1. The transport reactor train will be used to produce a particle-laden gas for testing of two of the PCDs. The APFBC module will be integrated with the topping combustor and gas turbine for long term testing of the PCDs in an integrated system and assessment of the control and integration issues associated with the APFBC system.

### Advanced Gasifier

The M.W. Kellogg transport reactor technology under development at the PSDF at a scale of 2 tons/ hour of coal can operate either as a gasifier or as a PFBC unit. A simplified process flow diagram for the transport reactor system is shown in Figure 2. Tests will be conducted in both configurations. In the gasifier mode, coal is introduced and fired substoichiometrically. The coal devolatilizes, the volatiles pyrolize and the residual char is steam gasified. This staging of the gasification reaction forces oxygen to react with char rather than volatiles, as is characteristic in fluid bed gasifiers. As a result, the size of the gasifier (and the capital cost) is reduced because the amount of char to be gasified by reaction with steam (which is quite slow) is reduced substantially. Operation in the circulating PFBC mode is similar, but the reactor is fired with excess air.[2]

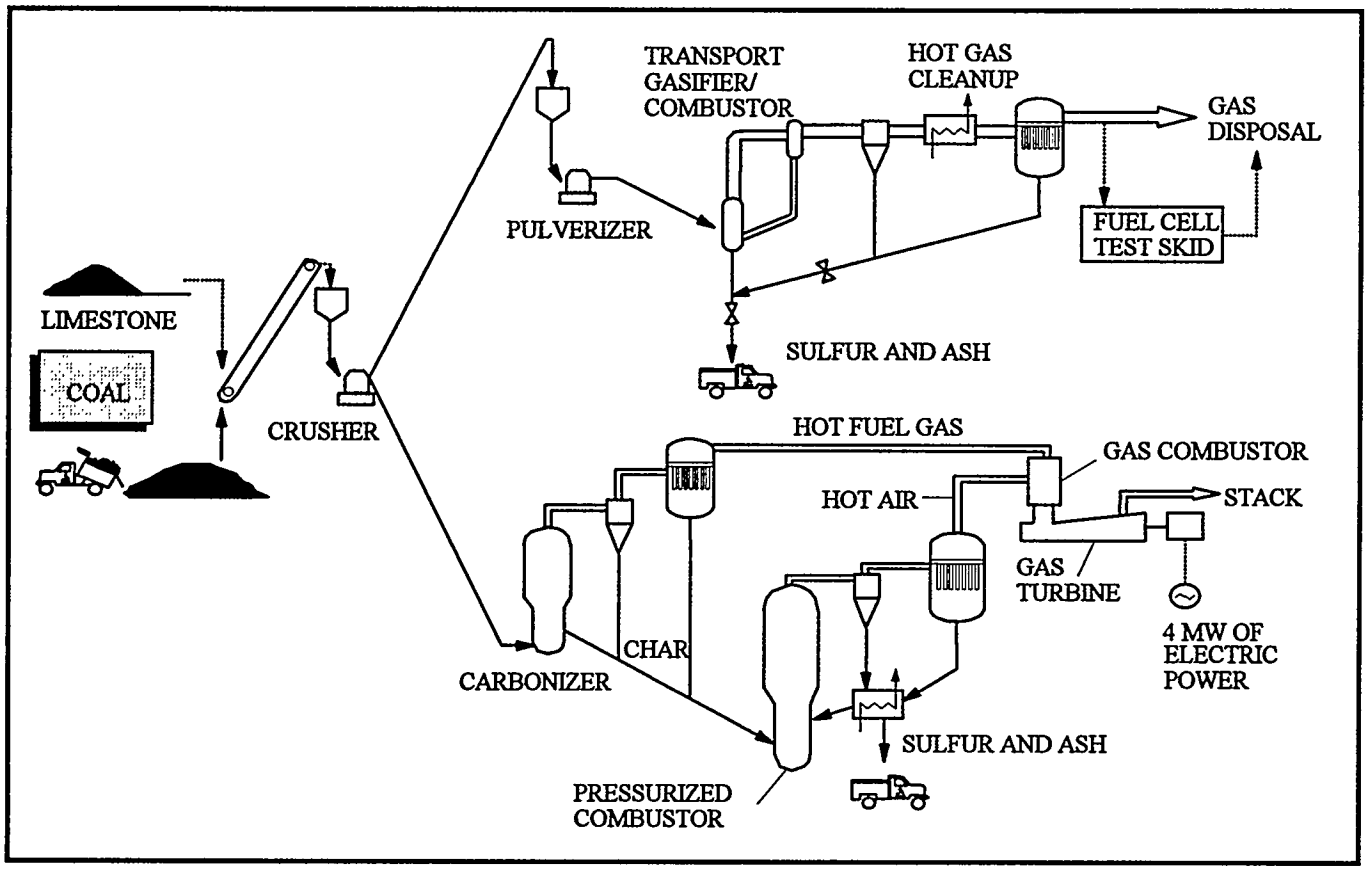


**Figure 1. Simplified Process Diagram of the PSDF**

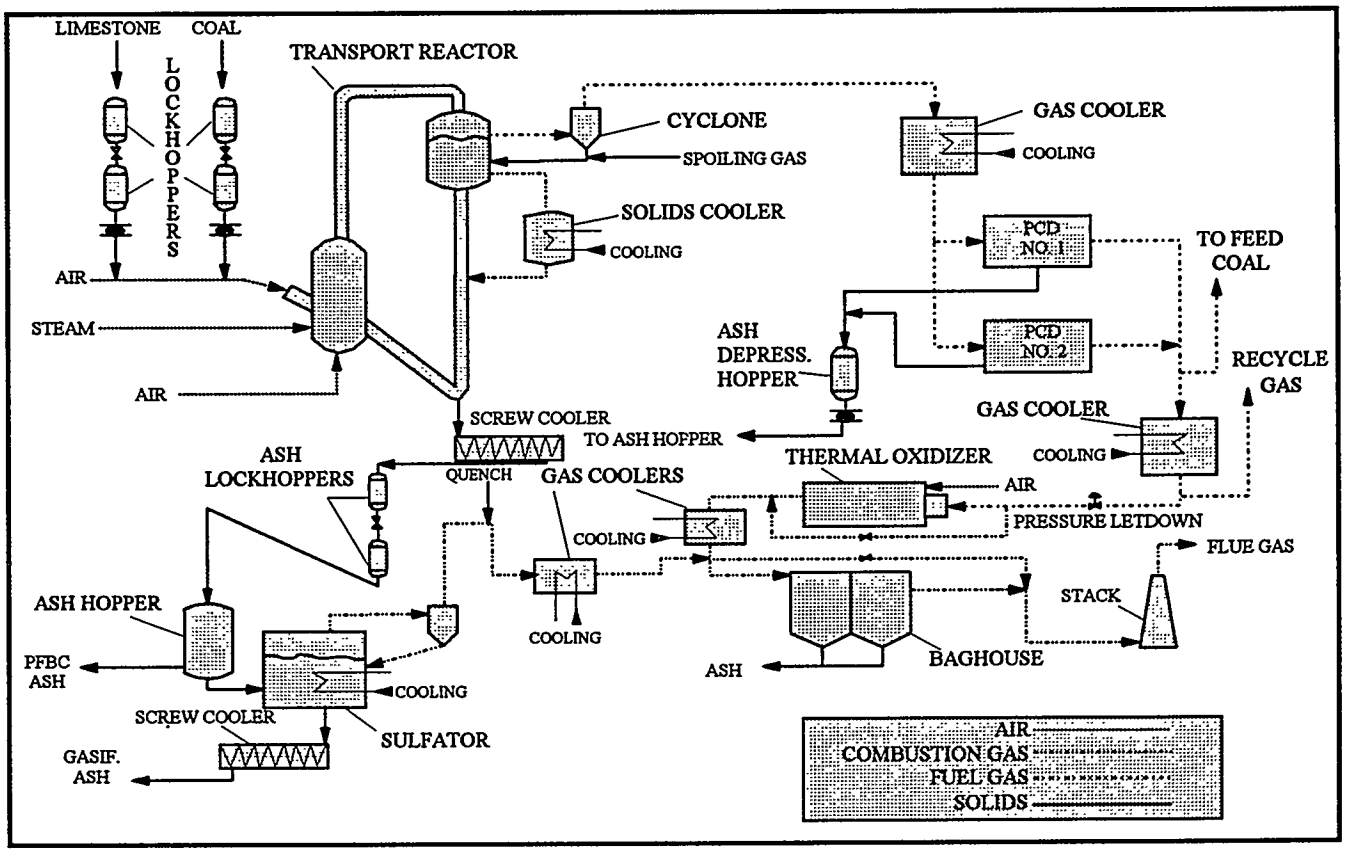


**Figure 2. M.W. Kellogg Advanced Gasifier Train**

## Advanced PFBC

APFBC continues to emerge as a viable coal-based advanced power generation technology in the utility industry for both repowering and new plants. First generation PFBC technology offers the advantages of being more compact and efficient, compared to pulverized coal units, and has a simpler design than most advanced power generation systems. However, first generation PFBC systems have limited efficiency due to low temperature operation and the use of ruggedized turbines. To improve efficiency, PFBC systems must employ hot particulate removal and a topping cycle in order to use advanced turbine designs. These second-generation APFBC designs are expected to be capable of achieving 45% net plant efficiency. Advancing the development of APFBC systems is one of the primary goals of the PSDF.

The Foster Wheeler APFBC system under development at the PSDF (see Figure 3) at a scale of 3 tons/hour utilizes a topping cycle. It is a hybrid system that combines partial gasification with PFBC. Coal is first fed to a pressurized carbonizer, where it is converted to a low-Btu fuel gas and char. The char produced in the carbonizer is transferred to a circulating PFBC (CPFBC) where it is subsequently burned. Sulfur is removed in the process by the addition of limestone into the carbonizer and CPFBC. The carbonizer fuel gas and CPFBC flue gas are cleaned of particulates in separate ceramic filters, after which the fuel gas is fired in a specially designed topping combustor outside a high-

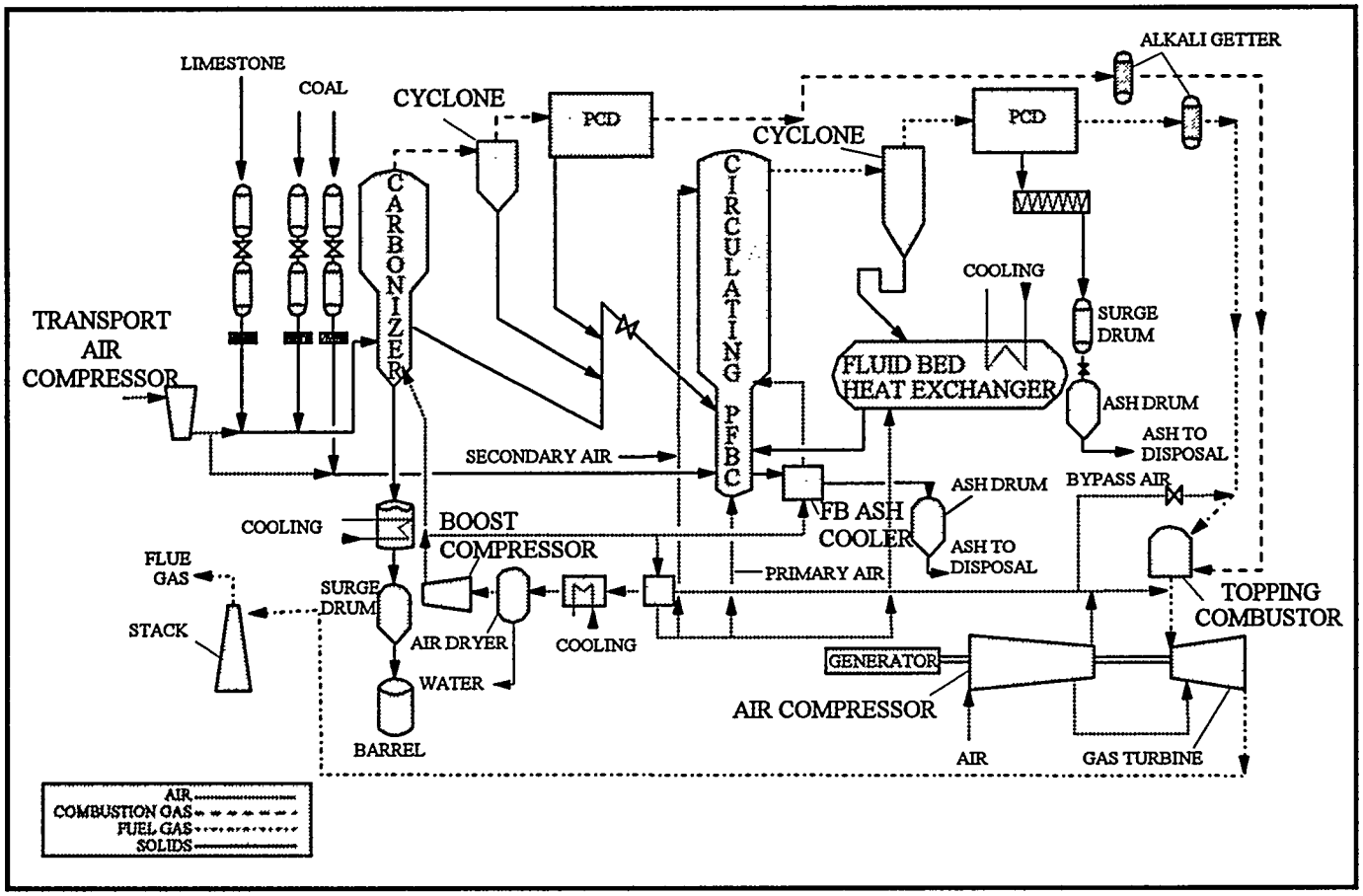


**Figure 3. Foster Wheeler APFBC Train**

temperature gas turbine using the CPFBC flue gas as the oxidant.

The APFBC plant at the PSDF will provide the first operation of a gas turbine and topping combustor with hot pressurized fuel gas from the carbonizer and hot pressurized flue gas from the APFBC. Periodic examination of the gas turbine will allow the merits of hot gas cleanup for APFBC systems to be evaluated.

## Particulate Control Devices

At the PSDF, four different PCDs will be evaluated initially. Industrial Filter & Pump Mfg. Co. (IF&P) will supply one PCD that will be tested initially on the Carbonizer fuel gas from the Foster Wheeler APFBC train. The IF&P device will contain ceramic (Fibrosic) candles and a ceramic tubesheet, but the design is flexible to allow the use of alternate elements as backup. The IF&P PCD is sized to match the gas flow requirements from the M.W. Kellogg transport reactor and can be moved to the transport reactor for testing at a later date.

Westinghouse will provide two PCDs. One will initially be tested on the M.W. Kellogg transport reactor and is interchangeable with the IF&P device on the Foster Wheeler APFBC process. This Westinghouse PCD will be capable of operating with several types of filter elements, but the initial configuration will use candle filters.

The Foster Wheeler APFBC system requires two PCDs. The second Westinghouse PCD for the combustor in the APFBC system will use mullite candle filter elements, but will not be interchangeable with other PCDs at the facility.

The fourth PCD is a moving, granular bed filter to be supplied by Combustion Power Company. This PCD is sized to be interchangeable with the IF&P PCD installed on the APFBC system, but because of its substantially different configuration, is not expected to be tested on the Foster Wheeler unit.

### Fuel Cell

A fuel cell is scheduled for integration with the advanced gasifier during the second year of operation after stable operation of the system is assured. The fuel cell will be connected to the advanced gasifier downstream of the PCD and the secondary gas cooler. This Integrated Gasification/Fuel Cell (IG/FC) system will be the first to operate with a hot gas cleanup system. IG/FC systems have the potential of achieving system efficiencies above 55% with extremely low emissions.

## RESULTS

The major activities during the past year have been the final stages of design, procurement of major equipment and bulk items, construction of the facility, and the preparation by the O&M staff for operation of the facility in late 1995.

### Design

The process design was predominantly completed in the previous reporting period and the design activities for the current period had little impact on the process flow sheets. A detailed description of the process design was presented in two previous papers at the Advanced Coal-Fired Power Systems Conference[3 4] and a detailed description of the PCDs also appears elsewhere[5]. M.W. Kellogg completed the design for the transport reactor system in December 1994 and Foster Wheeler is scheduled to complete the design of the Advanced PFBC system in July of 1995. The balance-of-plant (BOP) design is scheduled for completion by Southern Company Services in August of 1995.

One design item of note for the reporting period was the completion of a Design Hazard Review (DHR) for the APFBC and PCDs. A DHR was completed for the transport reactor system in May of 1994. The DHR for the BOP has been completed for that portion of the design prepared by Southern Company Services. The remainder of the BOP DHR will be completed in July after all final equipment vendor drawings are received.

The objective of the DHR was a qualitative assessment of the design using a structured format and methodology. The specific methodology for the reviews conducted used the "What-if" technique augmented by a guide-word checklist and was performed in accordance with the guidelines published by the American Institute of Chemical Engineers Center for Chemical Plant Safety. The review systematically examined design documentation in order to identify potential hazards and major operability problems in the facility which could compromise the ability of the systems and equipment to safely handle start-up and credible operating deviations from the design intent. The findings of the DHR were reviewed in detail and incorporated into the design as necessary.

## Construction

Site preparation was completed in the last reporting period. Installation of underground pipes and conduits began in July 1994 and was complete except for some miscellaneous connections by November 1994.

Erection of structural steel began in November of 1994 when work began on the structure to house the coal and limestone storage bins and mills for sizing the coal and limestone. Erection of the main process structure began in December 1994. The main process structure is five bays wide by three bays deep with the two outside bays on one side housing the APFBC system and the two outside bays on the other side housing the transport reactor system; the center bays between the two systems provide a buffer and access for maintenance. Erection of the steel for the transport reactor bays and the center bays has been completed to the top elevation of 190 feet above grade and the two bays for the APFBC system have been erected to 52 feet with equipment placement as the structure is built.

All of the major equipment for the transport reactor system has been placed in the structure and installation of all the large refractory-lined pipe is scheduled to be completed by the end of July. Installation of smaller diameter pipe has begun within the transport reactor process area and installation of instrument and power cables will begin soon with mechanical completion of the system expected in November 1995. Commissioning will begin in October and these activities will proceed in parallel with the final construction activities. The first coal feed is targeted for December 1995.

The erection of steel and installation of the major equipment and refractory-lined pipe for the AFPBC system is scheduled for completion in October. Installation of smaller diameter pipe and instrument and power cables will continue through March of 1996. Commissioning activities for the gas island will continue from March until the arrival of the Westinghouse topping combustor in June of 1996. After commissioning the topping combustor, the first coal feed to the APFBC system will occur.

Buildings housing the warehouse, maintenance shop, on-site laboratory, offices and control room are complete, and the O&M and the research staff moved to the site in April.

## Preparation for Operation

Southern Company Services personnel will be responsible for operation of the PSDF. The operations manager and maintenance supervisor were assigned to the project in the last quarter of 1994. Operations shift coordinators and the remainder of O&M supervisory personnel were assigned to the project beginning in March. The O&M staff is currently developing detailed operating manuals and maintenance procedures, setting up the maintenance shop, and preparing training materials in preparation for assignment of the first operators to the project in July of 1995. Alabama Power Company, a subsidiary of the Southern Company, will provide the PSDF well-trained and experienced operators and mechanics. Once trained on the specifics of the PSDF technologies, the operators and maintenance technicians will assist in final preparation of the operating and maintenance manuals and begin commissioning activities on the transport reactor system and balance-of-plant equipment.

Work started in the Fall of 1994 on developing a commissioning sequence that would logically order the equipment start-up testing and commissioning to allow significant pre-operational milestone tests and activities to occur before construction was complete on the entire process

train and balance-of-plant equipment. The commissioning schedule identified required components that need to be operational to complete each milestone activity. The commissioning schedule was integrated with the existing project engineering and construction schedule.

Electrical equipment (breakers, relays, motor starters) is being tested by construction and engineering personnel as it is installed and this process has already identified several bad relays that have been replaced by the vendor. All testing is being completed as early as possible to identify and correct any problem associated with equipment, before it could impact the process start-up date. Commissioning of the fire water system has also been completed.

**PSDF Experimental Test Program**

The critical issues to be addressed include the integration of PCDs into coal utilization systems, on-line cleaning techniques, chemical and thermal degradation of components, fatigue or structural failures, blinding, collection efficiency as a function of particle size, and scale-up to commercial-size systems. To facilitate the assessment of the PCDs, it is critical that the test conditions, such as gas temperature and particle loading, be variable over a range of values. Long-term endurance tests will involve about 1000 hours of continuous PCD operation at nominally constant operating conditions. The goals of these tests are to demonstrate integration of the PCDs into advanced power generation systems, assess the long-term durability of the PCDs, demonstrate durable candle materials, and evaluate load cycling effects on the PCDs.

In addition to being a resource for performance assessment of hot stream cleanup devices, the PSDF has been designed as a flexible test facility that will be used to test and optimize the operation of advanced power system components, such as the transport gasifier/combustor, and advanced topping combustor and turbine as well as fuel cell system configurations. Testing plan for PSDF will also focus on issues related to integration of several advanced power system components as part of an entire power generation train. The M.W. Kellogg transport reactor for the PSDF represents a novel design for a gas source, and the test plan will address the operation and characterization of the reactor as well as the behavior of the PCDs selected for testing with the transport reactor. Similarly, the test plan will also address the control issues associated with the operation of the Foster Wheeler APFBC train with PCDs integrated into the system.

An outline of the test plan for the transport reactor system has been developed and a detailed test plan and schedule will be completed in July. Most of the parametric testing will be done using the transport reactor system, since the APFBC system is integrated with a gas turbine and is less flexible in terms of the PCD operating conditions. The transport reactor will be operated as both a combustor and a gasifier to allow PCD testing in both modes of operation. Shakedown of the transport reactor system and the PCDs will begin in October 1995, and the test program will begin in January 1996. The transport reactor will be operated in the combustion mode first before proceeding with the gasification tests.

The initial operation, shakedown, characterization testing, and the first three months of performance testing, will be in the combustion mode. The temperature of the gases leaving the transport reactor can be lowered using a gas cooler, allowing for a range of PCD inlet temperatures. In view of reported problems with the thermal shock of the ceramic filter elements, the initial PCD testing will be

done at 1,000-1,200°F, and then gradually increased as experienced is gained in operating the PCDs.

The design of the transport reactor was based on Illinois #6 high sulfur, bituminous coal, but locally available bituminous coal will be used during initial operation. This will be followed by Illinois #6 and a Powder River Basin subbituminous coal. In the design specification limestone was specified as the sulfur sorbent. Both dolomite and limestone will be used, but the primary sorbent will depend on its effectiveness in lessening candle-cleaning difficulties.

The granular bed filter performance will be assessed by gathering inlet and outlet dust loading data at full- and part-load test conditions to determine the effect of reactor process variables (filtration gas velocity, inlet dust loading and size distribution, depth of filter media, media circulation rates, and media sizes) upon dust collection efficiency. The performance data will be compared with tests conducted previously at New York University to assess the effect of scale-up. The Westinghouse filter performance will similarly be assessed by determining how dust collection efficiency and filter cake removal is influenced by filtration gas velocity, inlet dust loading, inlet dust size distribution, load change and pulse parameters including pulse gas pressure and pulse frequency.

As tests with the filters are being performed, the transport reactor performance will be determined as a function of process variables and at full- and part-load conditions. The reactor performance indicators to be monitored include combustion and sulfur retention efficiencies, heat transfer rates to all cooling surfaces, alkali emissions before and after the flue gas cooler, $NO_x$ emissions, CO emissions, flue gas dust loadings leaving the cyclone, and the dynamic response rate of the reactor to changes in temperature, Ca/S molar ratio, and to simulated load changes. The combustion test program with the transport reactor and the filters will be followed by operating the reactor as a gasifier and subjecting the filters to tests with fuel gas. The range of operating conditions for parametric and long-term testing of the PCDs for both the M.W. Kellogg transport reactor and Foster Wheeler APFBC trains is given in Table 1.

An outline of the test plan for the APFBC will be completed in July and the detailed test plan and schedule will be completed in September of 1995.

## FUTURE WORK

Construction of the transport reactor system will be completed in November of 1995 at which time commissioning and testing activities will follow. The first coal feed to the system is targeted for December of 1995.

Construction of the APFBC system will be completed in March 1995 except for the topping combustor which is expected to be delivered in June 1996.

**Table 1. Test Parameter**

| Test Parameter | M.W. Kellogg Combustor | M.W. Kellogg Gasifier | Foster Wheeler Carbonizer | Foster Wheeler Combustor |
|---|---|---|---|---|
| Gas flow rate, acfm | 1,000 | 1,000 | 1,475 to 1,700 | 6,200 |
| Pressure, psia | 216 to 305 | 197 to 305 | 170 | 150 |
| Temperature, °F | 1,000 to 1,600 | 1,000 to 1,800 | 1,500 to 1,800 | 1,600 |
| Particulate load, ppmw | 4,000 to 10,000 | 4,000 to 16,000 | 11,000 | 8,000 |
| Mean particle size, μm | 3 to 16 | 3 to 16 | 15 | 5 |

## 2.2 Pilot Plant Becomes Demonstration Plant Design

**CONTRACT INFORMATION:**

| | |
|---|---|
| Contract Number: | DE-AC21-86MC21023 |
| Contractor: | Foster Wheeler Development Corporation<br>12 Peach Tree Hill Road<br>Livingston, NJ 07039<br>(201) 535-2328 |
| Contractor Program/Project Manager: | Archie Robertson |
| Contractor Project Engineer: | James Van Hook |
| Principal Investigators: | Frank Burkhard<br>Giovanni Carli<br>Rich Conn<br>Paul Crooker<br>Dave Kulcsar<br>Chongqing Lu<br>Anthony Mack<br>Aydemir Nehrozoglu<br>Mark Torpey<br>Frank Zoldak |
| METC Project Manager: | Donald Bonk |
| Period of Performance: | November, 1990 through January, 1996 |

**OBJECTIVES - PHASE 3**

The three major objectives of Phase 3 are: ▪ Test a 1.2-MWe equivalent carbonizer and Circulating Pressurized Fluidized Bed Combustor (CPFBC) with their associated ceramic candle filters as an integrated subsystem. ▪ Evaluate the effect of coal-water paste feed on carbonizer performance. ▪ Revise the commercial plant performance and economic predictions where necessary.

**BACKGROUND INFORMATION**

Advanced or second-generation pressurized fluidized bed combustion plants (APFBC) that generate electricity offer utilities the potential for significantly increased efficiencies with reduced costs of electricity and lower emissions while burning the nation's abundant supply of high-sulfur coal. Figure 1 is a simplified process block diagram of a second-generation PFB combustion plant.

In the plant, coal is fed to a pressurized carbonizer that produces a low-Btu fuel gas and char. After passing through a cyclone and ceramic barrier filter to remove gas-entrained particulates and a packed bed of emathelite pellets to remove alkali vapors, the fuel gas is burned in a topping combustor to produce the energy required to drive a gas turbine. The gas turbine drives a generator and a compressor that feeds air to the carbonizer, a CPFBC, and a fluidized bed heat exchanger (FBHE). The carbonizer char is burned in the CPFBC with high excess air. The vitiated air from the CPFBC supports combustion of the fuel gas in the topping combustor. Steam generated in a heat-recovery steam generator (HRSG) downstream of the gas turbine and in the FBHE associated with the CPFBC drives the steam turbine generator that furnishes the balance of electric power delivered by the plant.

The low-Btu gas is produced in the carbonizer by pyrolysis/mild devolatilization of coal in a fluidized bed reactor. Because this unit operates at temperatures much lower than gasifiers currently under development, it also produces a char residue. Left untreated, the fuel gas will contain hydrogen sulfide and sulfur-containing tar/light oil vapors; therefore, lime-based sorbents are injected into the carbonizer to catalytically enhance tar cracking and to capture sulfur as calcium sulfide. Sulfur is captured in situ, and the raw fuel gas is fired hot. Thus the expensive, complex, fuel gas heat exchangers and chemical or sulfur-capturing bed cleanup systems that are part of the coal gasification combined-cycle plants now being developed are eliminated.

The char and calcium sulfide produced in the carbonizer and contained in the fuel gas as elutriated particles are captured by high-temperature filters, rendering the fuel gas essentially particulate free and able to meet New Source Performance Standards (NSPS). The captured material, with carbonizer bed drains, is collected in a central hopper and injected into the CPFBC through a nitrogen-aerated nonmechanical valve. The high excess air in the combustor transforms the calcium sulfide to sulfate, allowing its disposal with the normal CPFBC spent sorbent.

In the CPFBC, the burning char heats the high-excess-air flue gas to 1600°F; any surplus heat is transferred to the FBHE by the recirculation of solids (sorbent and coal fly ash) between the units. Controlled recirculation is accomplished with cyclone separators and nonmechanical valves. The FBHE contains tube surfaces that cool the circulating solids. Because of the low fluidizing velocity in the FBHE (≤½ ft/s), the risk of tube erosion is virtually eliminated.

The exhaust gases leaving the carbonizer and the CPFBC contain sorbent and fly ash particles—both of which can erode and foul downtream equipment. A hot gas cleanup (HGCU) system, consisting of ceramic barrier filters preceded by cyclone separators, cleans the gases to <20 ppm solids loading before they enter the fuel gas topping combustor and the gas turbine, thus preventing erosion and fouling. Ceramic cross-flow filters, screenless granular-bed filters and others are candidate alternatives for the candle filters, should their performance and economics be found superior. All these devices are currently under development for first-generation PFB combustion plants. They should also be applicable to the second-generation plant.

The topping combustor, which consists of metallic-wall multiannular swirl burners (MASBs), will be provided in two external combustion assemblies (topping combustors) on opposite sides of the gas turbine. Each MASB contains a series of swirlers that aerodynamically create fuel-rich, quick-quench and fuel-lean zones to minimize $NO_x$ formation during the topping combustion process. The swirlers also

provide a thick layer of air at the wall boundary to control the temperature of the metallic walls.

A team of companies—led by Foster Wheeler Development Corporation (FWDC) with Foster Wheeler Energy Corporation and Foster Wheeler USA, Gilbert/Commonwealth, Inc., Institute of Gas Technology, Westinghouse Power Generation Business Unit (PGBU) and Science & Technology Center (STC)—has embarked upon a DOE funded three-phase program to develop the technology for this new type of plant. A conceptual design of a 3-percent-sulfur Pittsburgh No. 8 coal-fired second-generation PFB plant with a conventional 2400 psig/1000°F/1000°F/2-½ in. Hg steam cycle was prepared, and its economics were determined [1]. In 1987 we estimated that, when operated with a 14-atm/1600°F carbonizer, the plant efficiency would be 44.9 percent (based on the higher heating value of the coal) and its cost of electricity would be 21.8 percent lower than that of a conventional pulverized coal-fired plant. Tests conducted in our Phase 2 pilot-scale carbonizer yielded performance superior to that estimated in 1987. As a result, we now expect a more energetic fuel gas and a plant efficiency of 46.2 percent with a 1600 °F carbonizer [2].

## PROJECT DESCRIPTION

The second-generation PFB combustion plant development effort is divided into three phases, the first of which has already been completed and documented in a series of reports available through the National Technical Information Service.

The first phase of the DOE program was aimed at plant conceptualization and optimization and identification of plant R&D needs. The second phase, involving laboratory-scale tests of the key plant components is near completion.

The R&D needs of this new type plant were presented in the Phase 1 Task 2 Report issued under this contract [3]; an integrated program plan for meeting these needs was presented in the Task 3 Report [4].

The move to commercialization of this new type of plant involves the five steps shown in Figure 2. Starting from the left and moving to the right, each succeeding step involves increased integration of components and increased plant size/complexity. In the first step—Phase 2 of our DOE contract—the key components of this new type of plant were tested separately to ascertain their individual performance characteristics. These Phase 2 tests involved testing (1) a 10-in.-diameter carbonizer (Figure 3) with a cyclone and ceramic barrier filter, (2) an 8-in.-diameter CPFBC (Figure 4) with a cyclone and ceramic barrier filter and (3) 12-in., 14-in. and 18-in.-(Figure 5) diameter MASBs. The first two test programs were conducted by FWDC at its John Blizard Research Center in Livingston, New Jersey. These programs were successful and test reports have been released to the NTIS for publication. The MASB tests were conducted at the University of Tennessee Space Institute at Tullahoma, Tennessee, under the direction of Westinghouse PGBU. Although a final report has not yet been issued (two additional tests are planned), test results have been presented at previous meetings [5][6][7].

In the second step to commercialization—Phase 3 of our DOE contract—a carbonizer and CPFBC with their respective cyclones and ceramic candle filters are being interconnected and operated as an integrated subsystem. The FWDC PFB pilot plant in Livingston, New Jersey was expanded in 1994 to permit this integrated operation. The new and previously tested units are compared in Figures 3 and 4. The new CPFBC is 13 inches in diameter by 38.3 feet tall and operates at a 2 1/2 times higher throughput than the previous Phase 2 unit. The new

carbonizer is actually the previous unit lengthened by a 5-foot-tall spool piece that allows operation with a commercial-scale, 24-foot-deep bed height. The hot shakedown of the expanded/integrated carbonizer-CPFBC pilot plant is underway.

In step three of Figure 2, an MASB and a gas turbine will be integrated with a carbonizer and CPFBC. This will be the first either has operated with carbonizer fuel gas as all previous MASB tests utilized gas mixtures synthesized to the composition predicted by FWDC for a commercial plant. This integration will occur at the Southern Company Services Power Systems Development Facility (PSDF) at Wilsonville, Alabama. This facility is being funded by the US DOE, the Electric Power Research Institute, and Industry for advanced coal-based power system R&D.

The APFBC process will be tested at the PSDF and a process flow diagram is presented in Figure 6. The plant will incorporate a 37-inch-ID CPFBC, an FBHE with two tube-bundle-containing fluidized beds, cyclones and ceramic candle filters, an 18-inch MASB, and a ≈3-MWe gas turbine. For cost savings a steam turbine will not be provided and the FBHE heat absorption will be exhausted to atmosphere via cooling towers. The 18-in. MASB will combust ≈1700°F carbonizer fuel gas to raise the ≈1600°F CPFBC flue gas/vitiated air to 2300°F. The gas turbine, being a relatively small unit, operates with a 1975°F turbine inlet temperature. Compressor discharge air will be injected into the 2300°F MASB exhaust to cool it to 1975°F, thereby allowing commercial plant MASB operation to be demonstrated.

The PSDF will be operated with Illinois No. 6 bituminous and Eagle Butte subbituminous coals. Limestone from Longview, Alabama will be injected into the APFBC fluidized beds to capture sulfur in situ. Each of these feedstocks has already been successfully tested in the Livingston Phase 2 carbonizer and CPFBC pilot plants. Based on these tests the 1700°F Wilsonville carbonizer is expected to produce a fuel gas with a 124-Btu/SCF heating value when operating with Illinois No. 6 coal. A gas yield of 3.2 lb/lb of coal is expected and the limestone sulfur capture efficiency is projected to be 94 percent at a calcium to sulfur molar feed ration of 1.75. The detailed performance of the carbonizer is presented in Figure 7. The char-sorbent residue from the carbonizer will be transferred to and burned in the CPFBC. Livingston pilot plant test data shown in Figures 8 and 9 indicate the CPFBC will operate with at least a 99-percent combustion and a 97-percent sulfur capture efficiency, respectively. The Phase 2 CPFBC was operated with a 12 ft/s gas velocity, and the effectiveness of staged combustion for controlling $NO_X$ emissions was investigated. Because of the low height of the unit (28.5 feet) the gas residence time in the oxidizing zone was less than 1 1/2 seconds. The Phase 3 CPFBC is 38.3 feet tall and, with its higher oxidizing zone residence time, we anticipate $NO_X$ emissions will be substantially less than the levels shown in Figure 10.

The Wilsonville APTBC will be commissioned in stages. Beginning in early 1996 the plant will be operated as a first generation PFB (no carbonizer or topping combustion) with coal being fired in the CPFBC. Then when the topping combustor is delivered in second quarter 1996 integrated carbonizer-CPFBC operation will begin. With proposed feedstocks and operating conditions having already been tested in Phase 2 and with Wilsonville personnel having witnessed Phase 2 testing and Phase 3 integrated carbonizer-CPFBC pilot plant commissioning runs, we anticipate a successful two-year test program.

## REFERENCES


1. A. Robertson, et al. 1988. Second-Generation PFB Combustion Plant Performance and Economics. *1988 Seminar on Fluidized-bed Combustion Technology for Utility Applications*, Palo Alto, CA.

2. A. Robertson, et al. 1993. Second-Generation PFBC Systems Research and Development—Phase 2, Best Efficiency Approach in Light of Current Data. *Proceedings of the Coal-Fired Power Systems 93—Advances in IGCC and PFBC Review Meeting*, Don Bonk (ed.), DOE/METC 93/6131.

3. A. Robertson, et al. 1989. Second-Generation Pressurized Fluidized Bed Combustion Plant: Research and Development Needs. Foster Wheeler Development Corporation, Livingston, NJ. Phase 1 Task 2 Report FWC/FWDC-TR-89/06 to the U.S. DOE under Contract DE-AC21-86MC21023.

4. A. Robertson, et al. 1989. Second-Generation Pressurized Fluidized Bed Combustion Plant Integrated R&D Program Plan. Foster Wheeler Development Corporation, Livingston, NJ. Phase 1 Task 3 Report FWC/FWDC TR-89/08 to the U.S. DOE under contract DE-AC21-86M21023.

5. W. Domeracki, et al. 1994. Development of Topping Combustor for Advanced Concept Pressurized Fluidized Bed Combustion. *Proceedings of the Coal-Fired Power Systems 94*, M. McDaniel, R. Staubly and V. Venkataraman, (ed.), DOE/METC 94/1008.

6. W. Domeracki, et al. 1993. Second-Generation PFBC Systems Research and Development. *Proceedings of the Coal-Fired Power Systems 93*, Don Bonk (ed.), DOE/METC 93/6131.

7. W. Domeracki, et al. 1992. Second-Generation PFBC Systems Research and Development. *Proceedings of the Ninth Annual Coal-Fueled Heat Engines, Advanced Pressurized Fluidized ed Combustion and Gas Stream Cleanup Systems Contractors Review Meeting*, DOE/METC 93/6129.

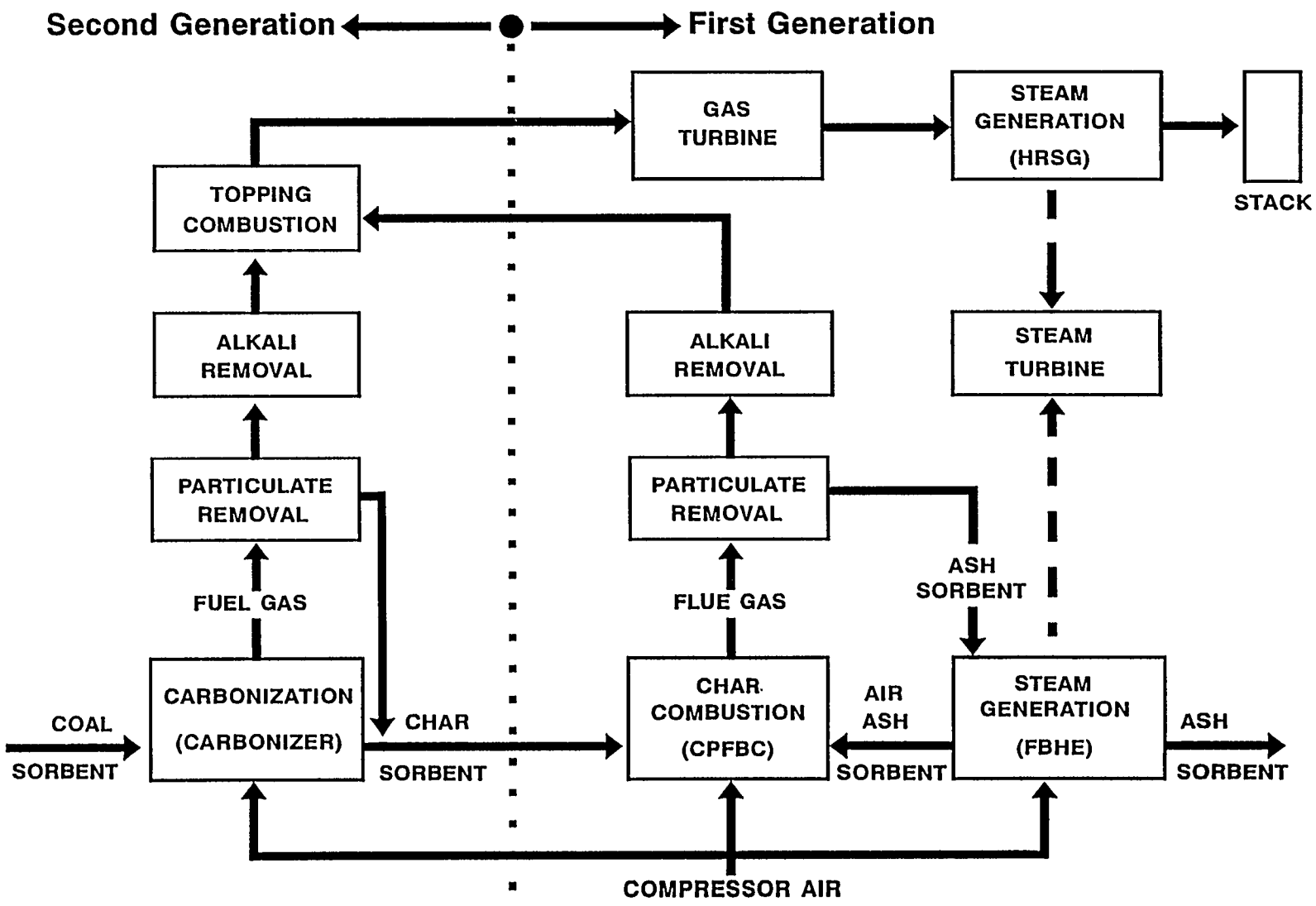


Figure 1. Simplified Process Block Diagram—Second-generation PFB Combustion Plant

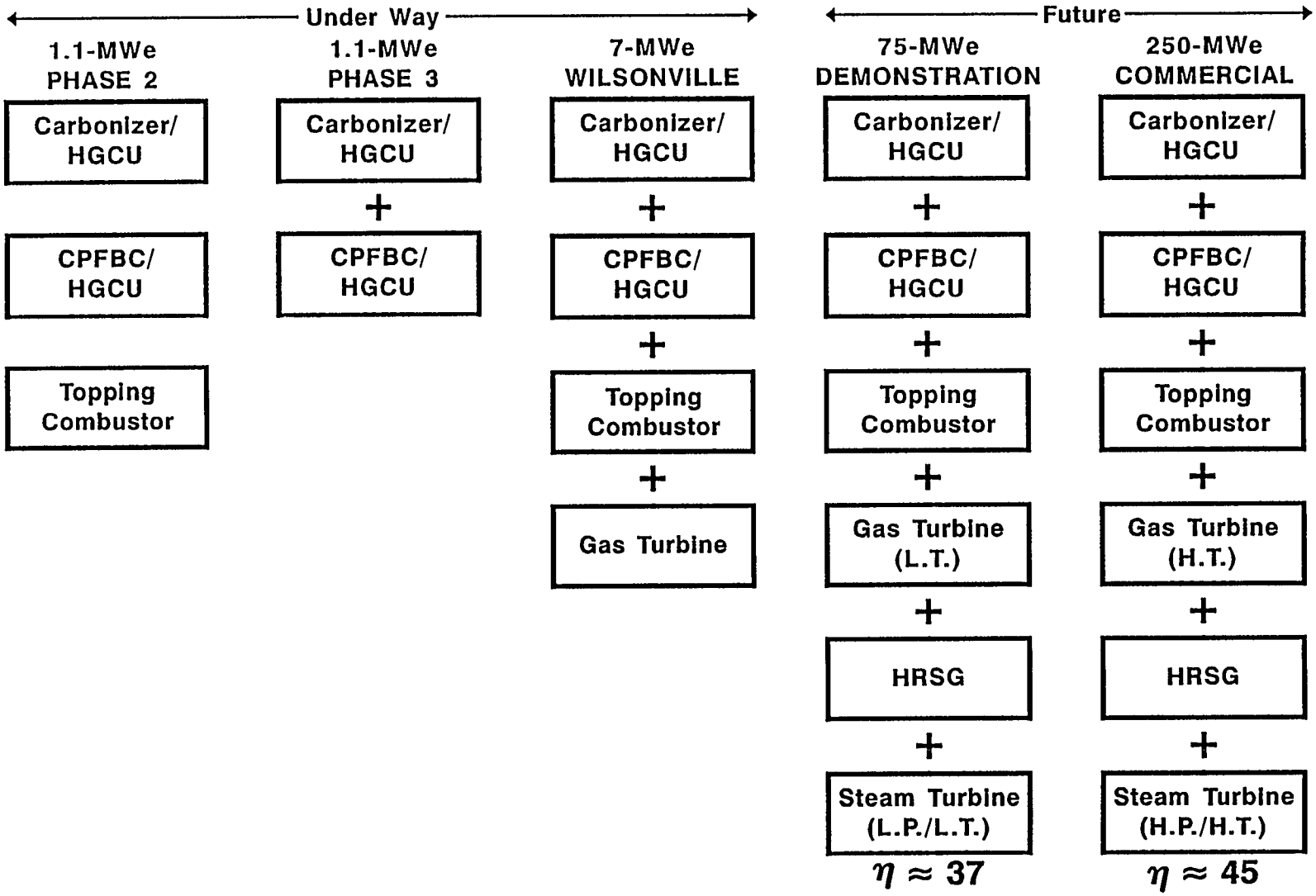


Figure 2. Second-generation PFB Plant Development Plan

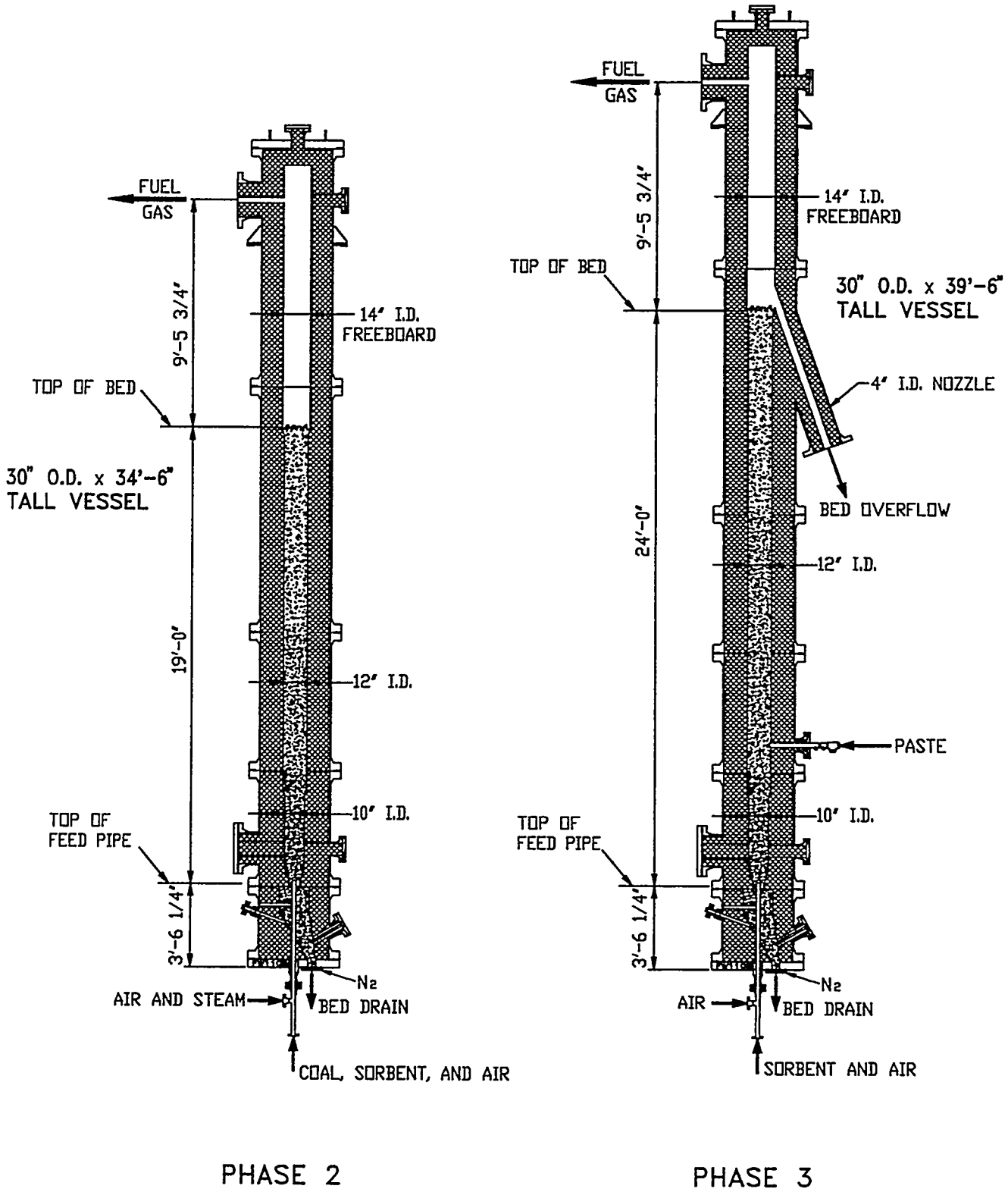


**Figure 3. Carbonizer Comparison**

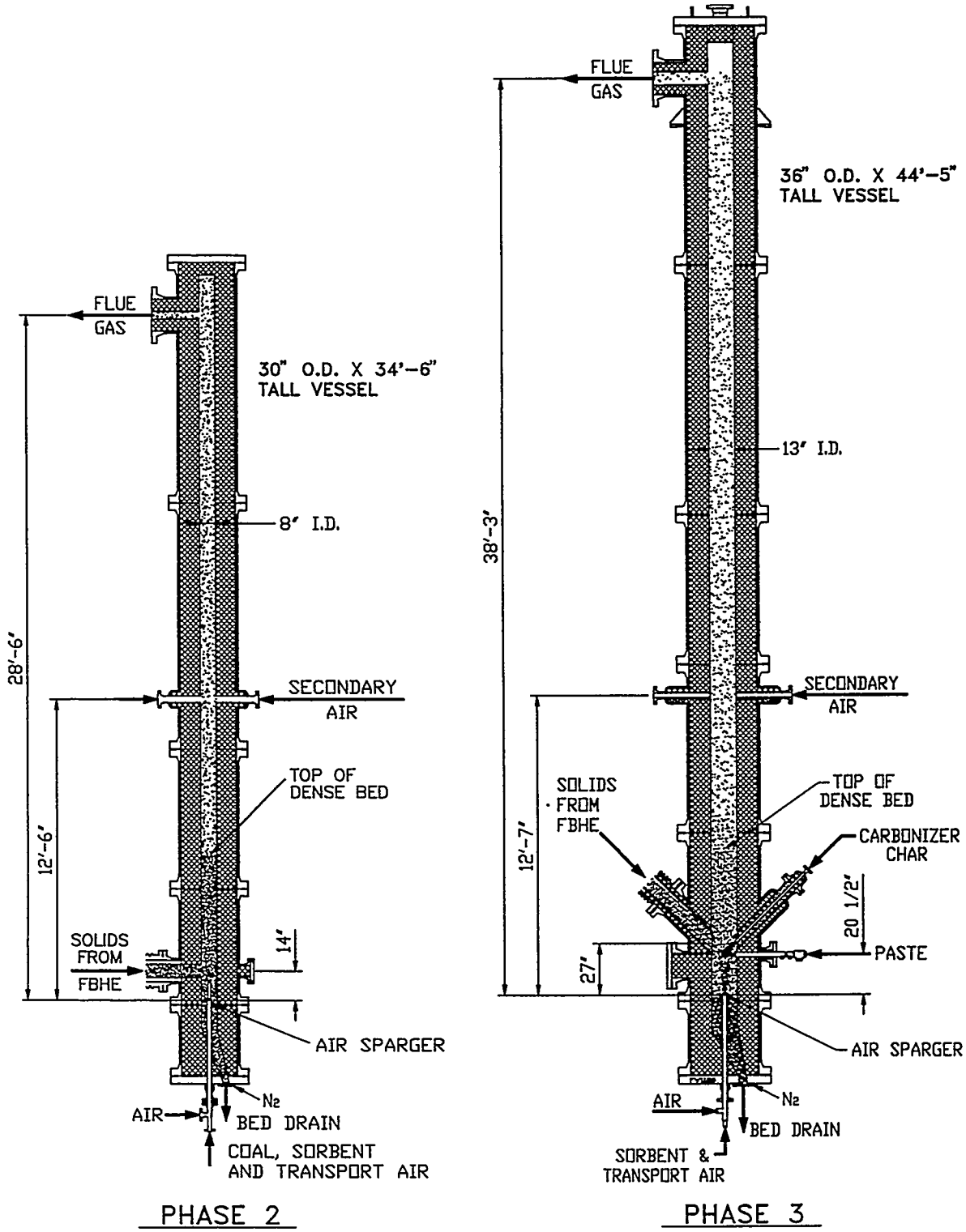


**Figure 4. CPFBC Comparison**

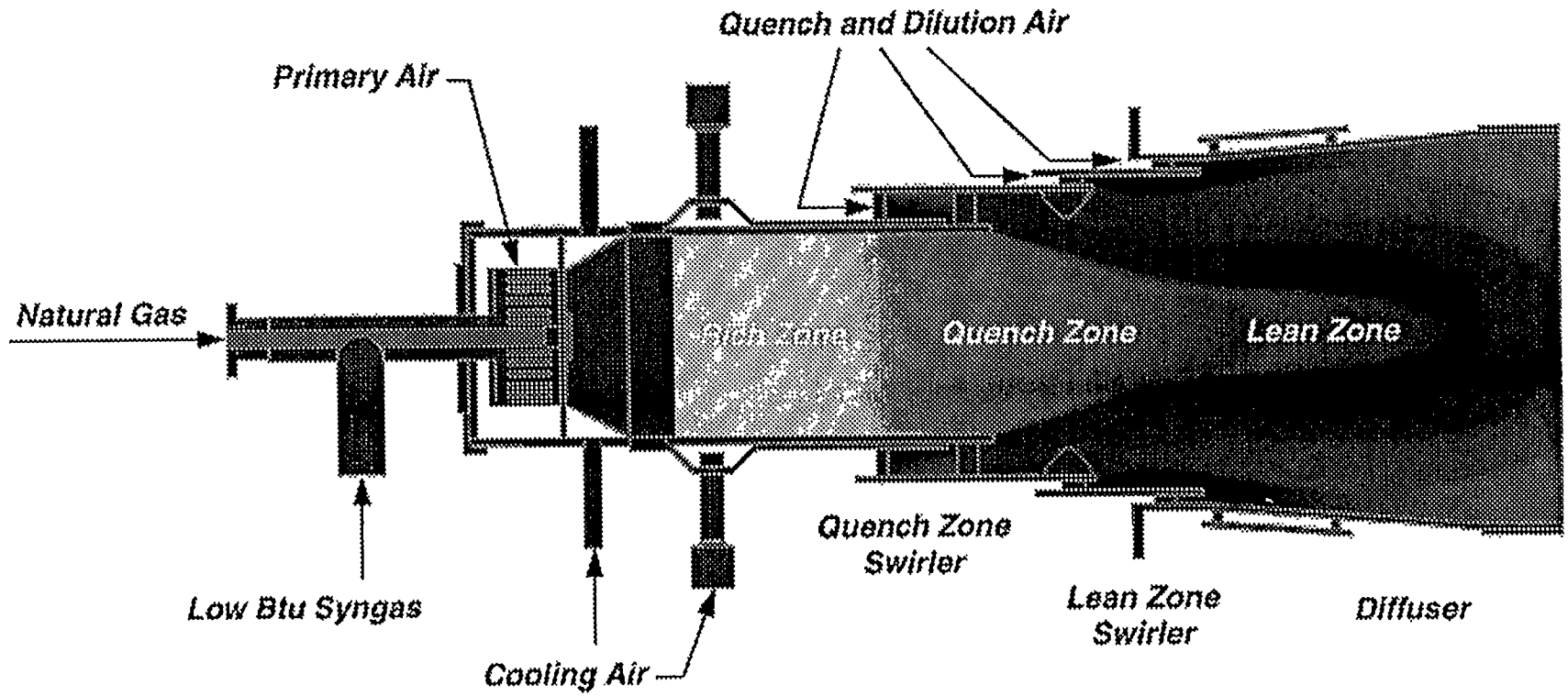


**Figure 5. 18-inch-diameter Westinghouse MASB Test Unit**

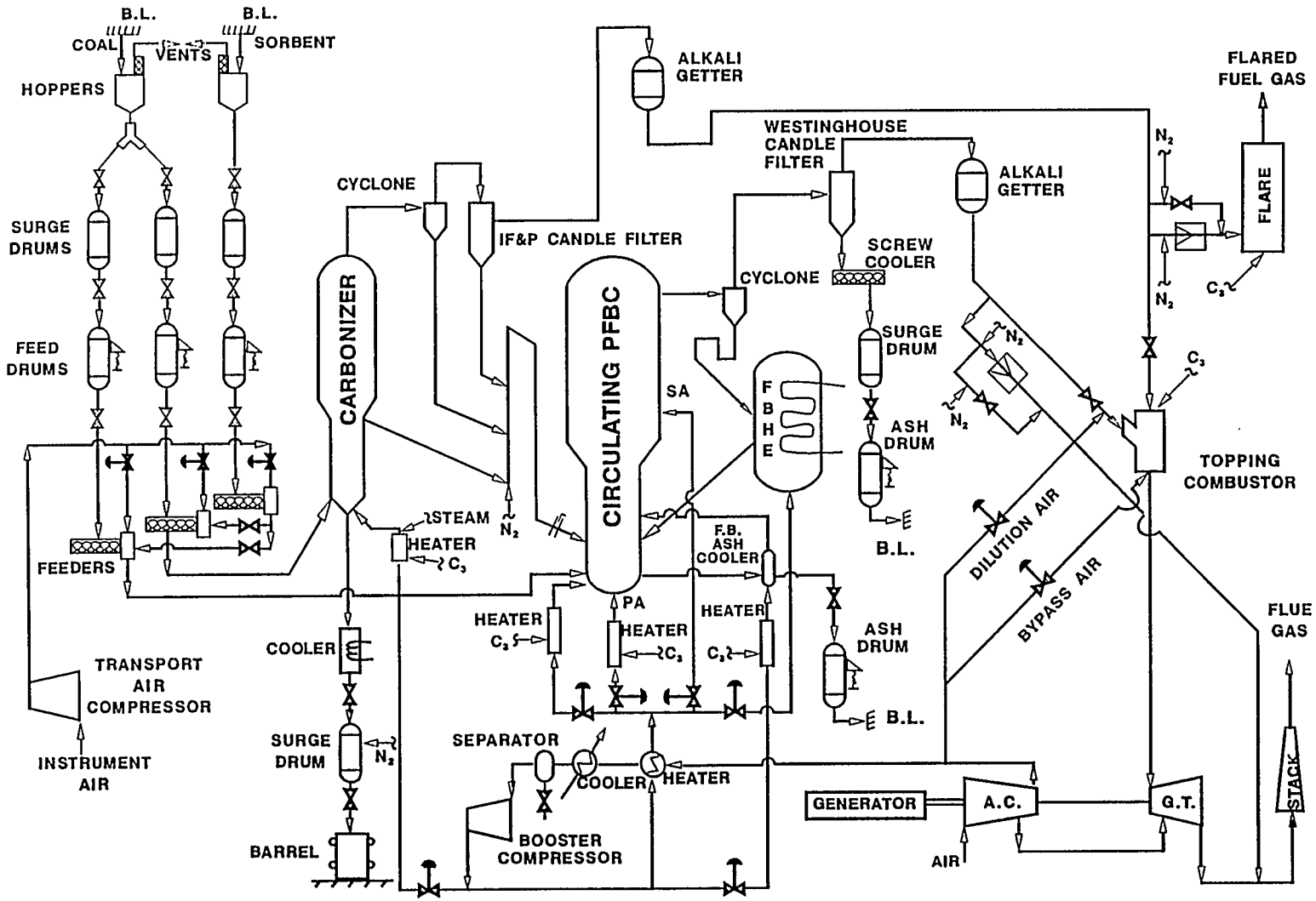


Figure 6. Wilsonville APFBC PFD

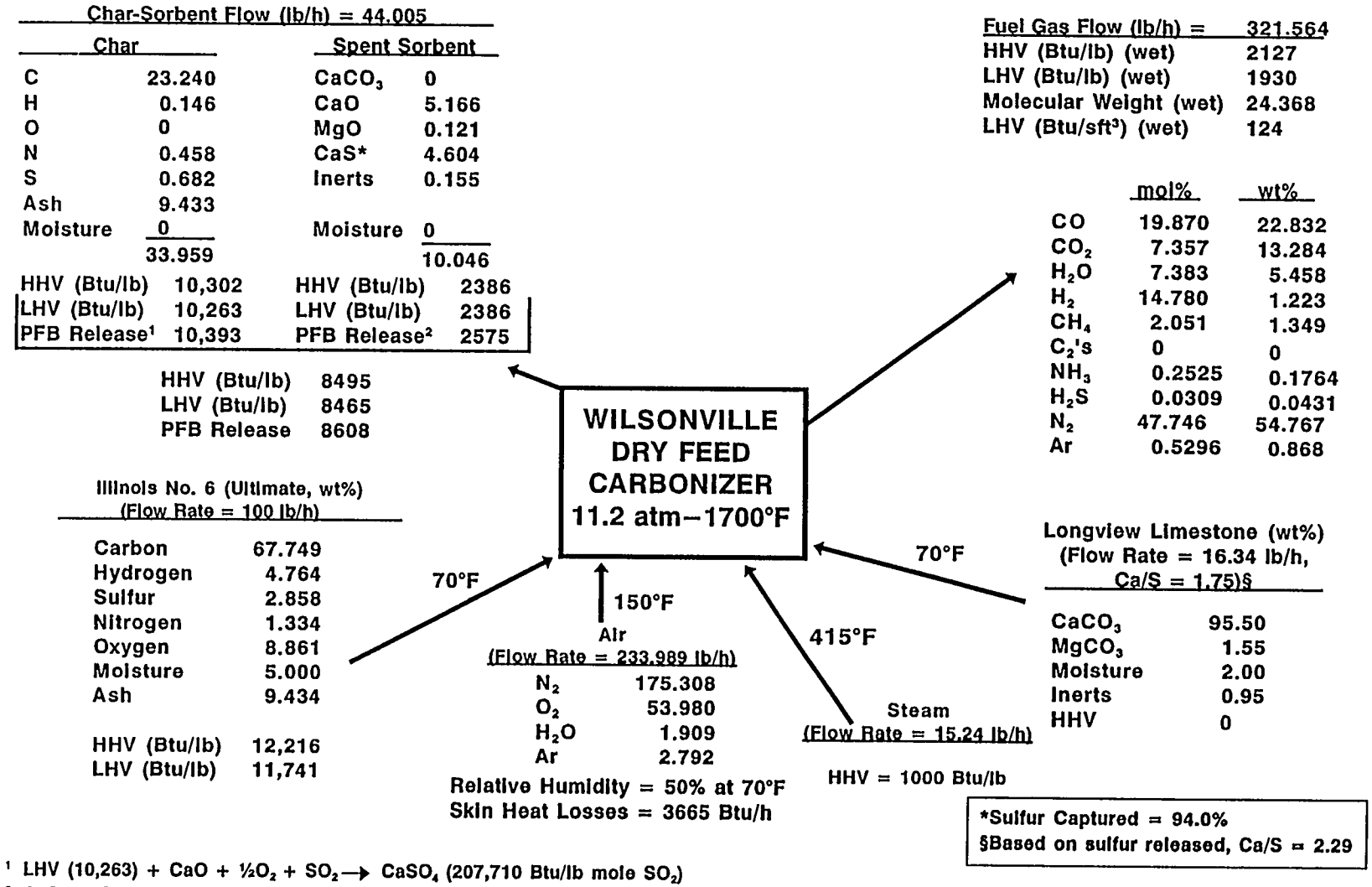


[1] LHV (10,263) + CaO + ½$O_2$ + $SO_2$ → $CaSO_4$ (207,710 Btu/lb mole $SO_2$)

[2] CaS + 2$O_2$ → $CaSO_4$(404,350 Btu/lb mole CaS) - $CaCO_3$ → CaO + $CO_2$ (-72,240 Btu/lb mole $CaCO_3$)

Figure 7. Wilsonville 1700°F Carbonizer Performance with Illinois No. 6 Coal

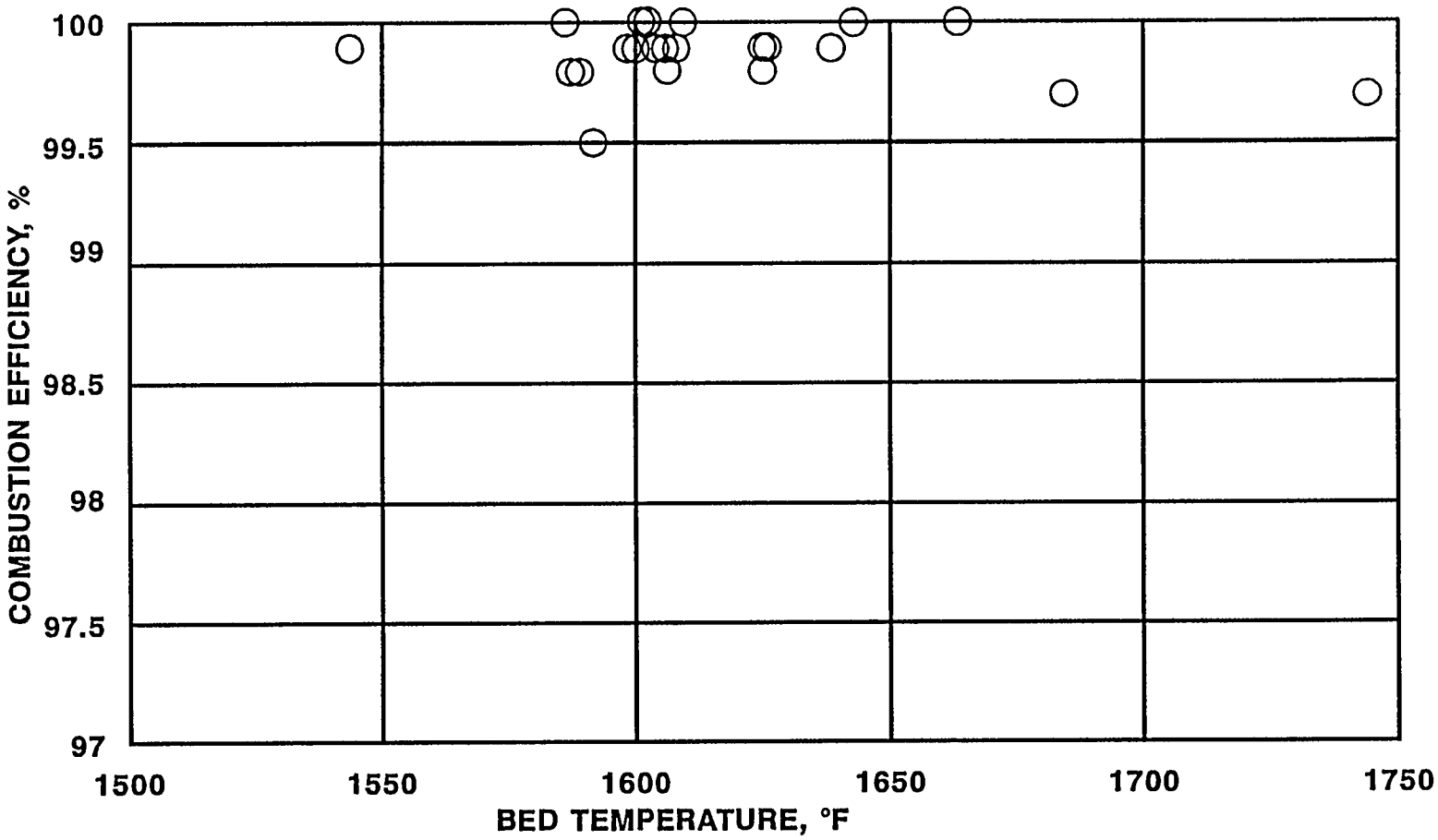


**Figure 8. Phase 2 CPFBC Combustion Efficiencies**

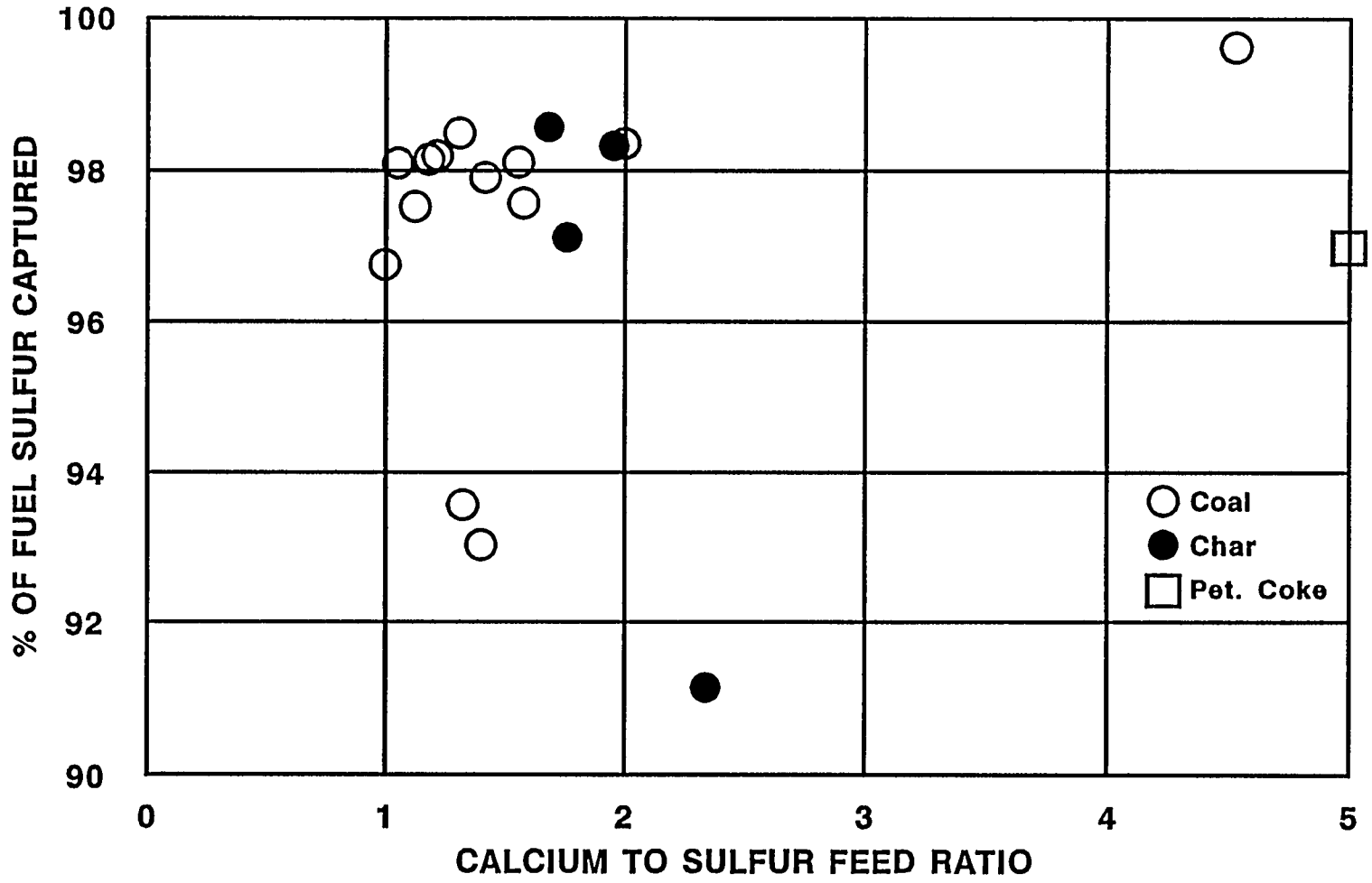


Figure 9. Phase 2 CPFBC Sulfur Capture Efficiencies

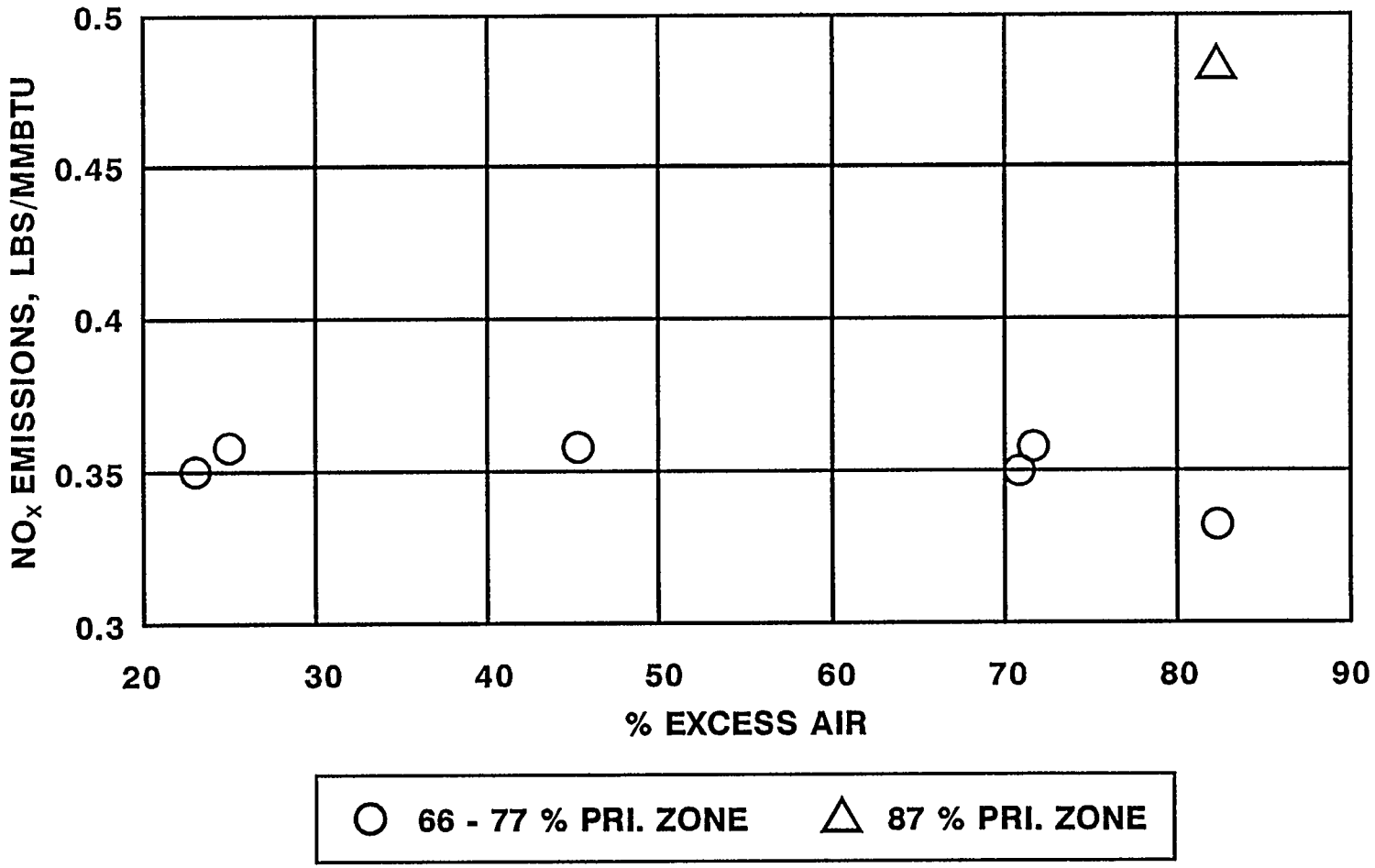


Figure 10. Phase 2 CPFBC $NO_x$ Levels

## 2.3 Gasification Product Improvement Facility Status

### CONTRACT INFORMATION

| | |
|---|---|
| **Contract Number** | DE-RP21-91MC28202 |
| **Contractor** | Jacobs-Sirrine Engineers, Inc.<br>1041 East Butler Road<br>P. O. Box 5456<br>Greenville, South Carolina 29606-5456<br>(803) 676-5037 |
| **Contractor Project Managers** | R. Don Carson, Jacobs-Sirrine Engineers, Inc.<br>Vijay B. Dixit, DB Riley, Inc. |
| **Principal Investigators** | Richard S. Sadowski, CRS Sirrine Engineers, Inc.<br>P.Thamaraichelvan, DB Riley, Inc.<br>H. Culberson, DB Riley, Inc. |
| **METC Project Manager** | Kanwal Mahajan |
| **Period of Performance** | October 1, 1992 to March 31, 1996 |

**Gasification Product Improvement Facility**
**Project Schedule**

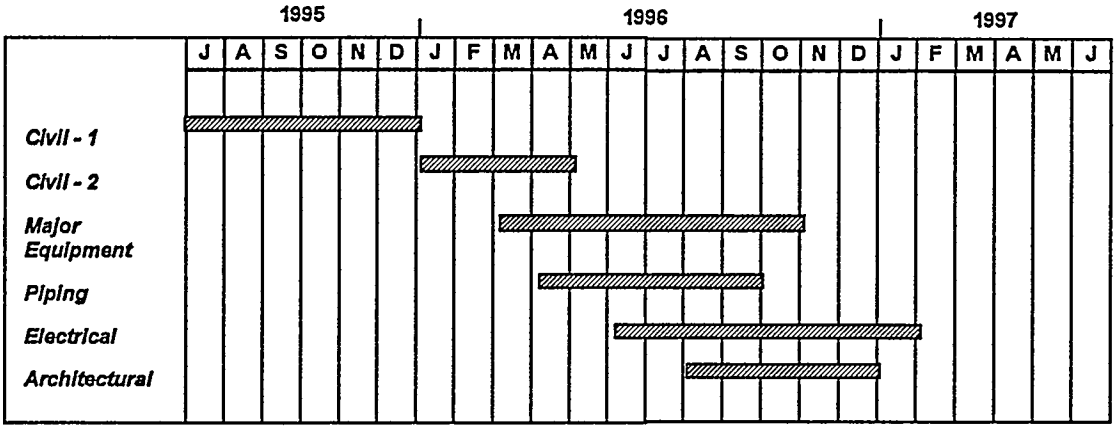


### OBJECTIVE

Department of Energy (DOE) has awarded a two phase contract for the construction of a Gasification Product Improvement Facility (GPIF) to develop an innovative air blown, dry bottom, pressurized fixed bed gasifier based on the patented PyGas™ fixed bed process (1,2). The objective of the project is to provide a test site to support early commercialization of the Integrated Gasification Combined Cycle (IGCC) technology. The GPIF will be capable of processing run of mine high swelling coals that comprise 87% of all Eastern U.S. coals. This program will generate useful scale up data that will be utilized to develop commercial size designs.

The project will also support the development of a hot gas clean up subsystem and the gasifier

infrastructure consisting of controls, special instrumentation and interconnects with Allegheny Power System's host power plant, Fort Martin Station in Maidesville, West Virginia.

This paper presents the status of the GPIF project. It describes the work performed in the past year on the PyGas™ process development, gasifier design, plant engineering/layout, tie in with the existing Fort Martin facility, procurement, site permitting and project scheduling.

## PROJECT ORGANIZATION AND GOALS

The project is an example of the partnership between the Government and industry. On the industry side, the project team consists of JSE, DB Riley, PSI Power Serv and Allegheny Power Systems (APS). JSE is the prime contractor responsible for the overall plant design. DB-Riley, as original equipment manufacturer (OEM), will supply the gasifier and the heat recovery steam generator (HRSG) and as the general contractor will be responsible for the plant construction and construction management. PSI PowerServ will supply special temperature and emission measurement equipment for the gasifier. The APS's Fort Martin facility represents the utility industry and is the end user of the steam product generated. Figure 1 depicts this partnership schematically. The partnering arrangement will combine the collective experience of the partners in the area of gasification, engineering, design, controls, fabrication, and field construction.

As the owner of the PyGas™ technology, DB Riley granted the technology rights to JSE for the GPIF project.

**Figure 1**
**GPIF - A Government, Utility, and Industry Partnership**

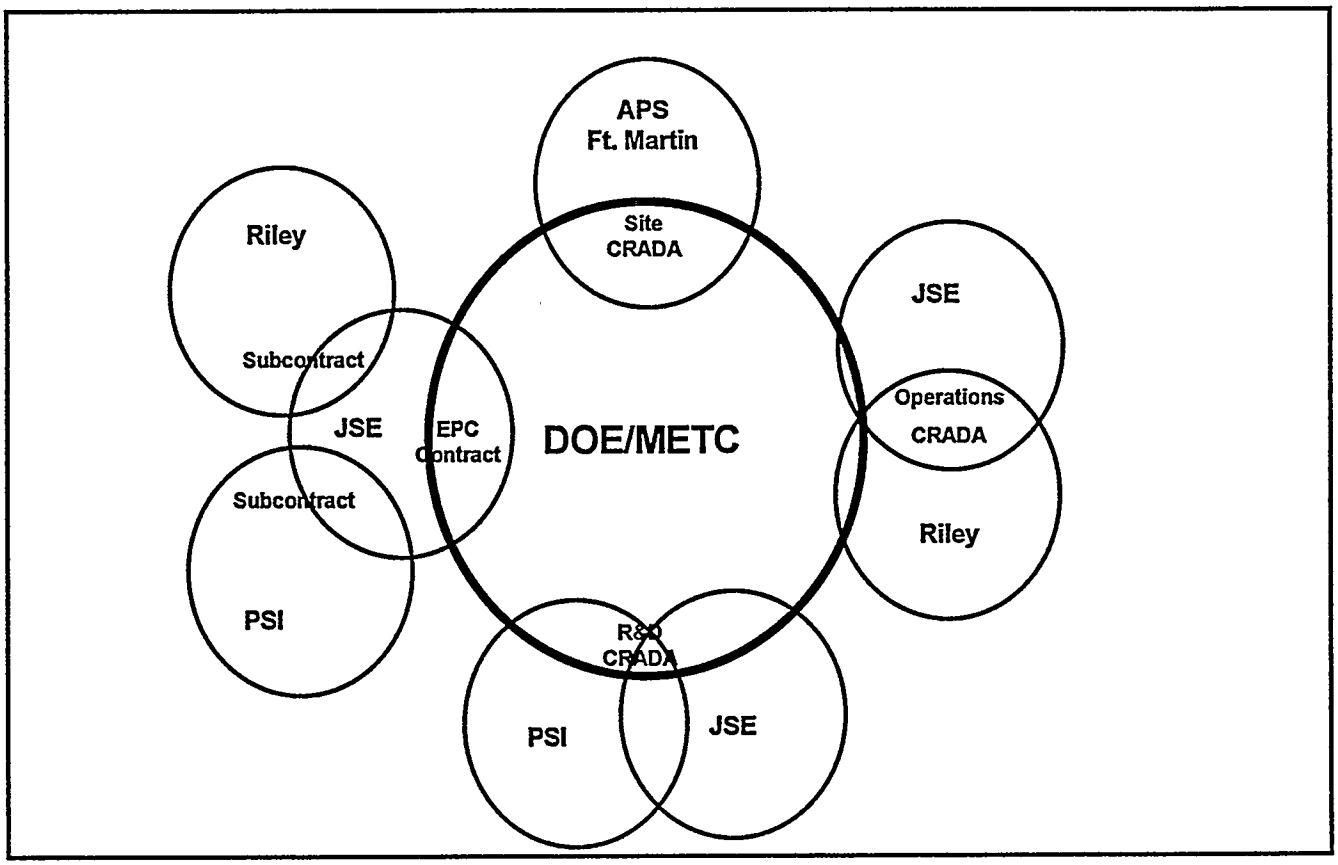

## PYGAS™ PROCESS DESCRIPTION

The PyGas™ process integrates both fixed and fluidized bed gasification technologies in a single vessel (1,2). The process gasifies coal in an air blown sysytem to produce low BTU gas for power generation. It is designed to handle high swelling coals, crack tars, and reduce ammonia and trace metal emissions in the gasifier. Sticky coal agglomerates can form during the heating process in a fixed bed gasifier using highly swelling coals. The PyGas™ process deals with this situation by carrying out the devolatilization by rapid heating and gasification at two separate locations in a single vessel.

Figure 2 schematically describes the steps in the PyGas™ process. Coal is pneumatically injected into the pyrolyzer section of the gasifier vessel. Steam can also be added to the pyrolyzer bottom if needed. The temperature in the pyrolyzer is maintained between 1500-1800°F. The intent is to decake the coal and maximize devolatilization in this region with some tar cracking.

**Figure 2**
**PyGas™ Process**

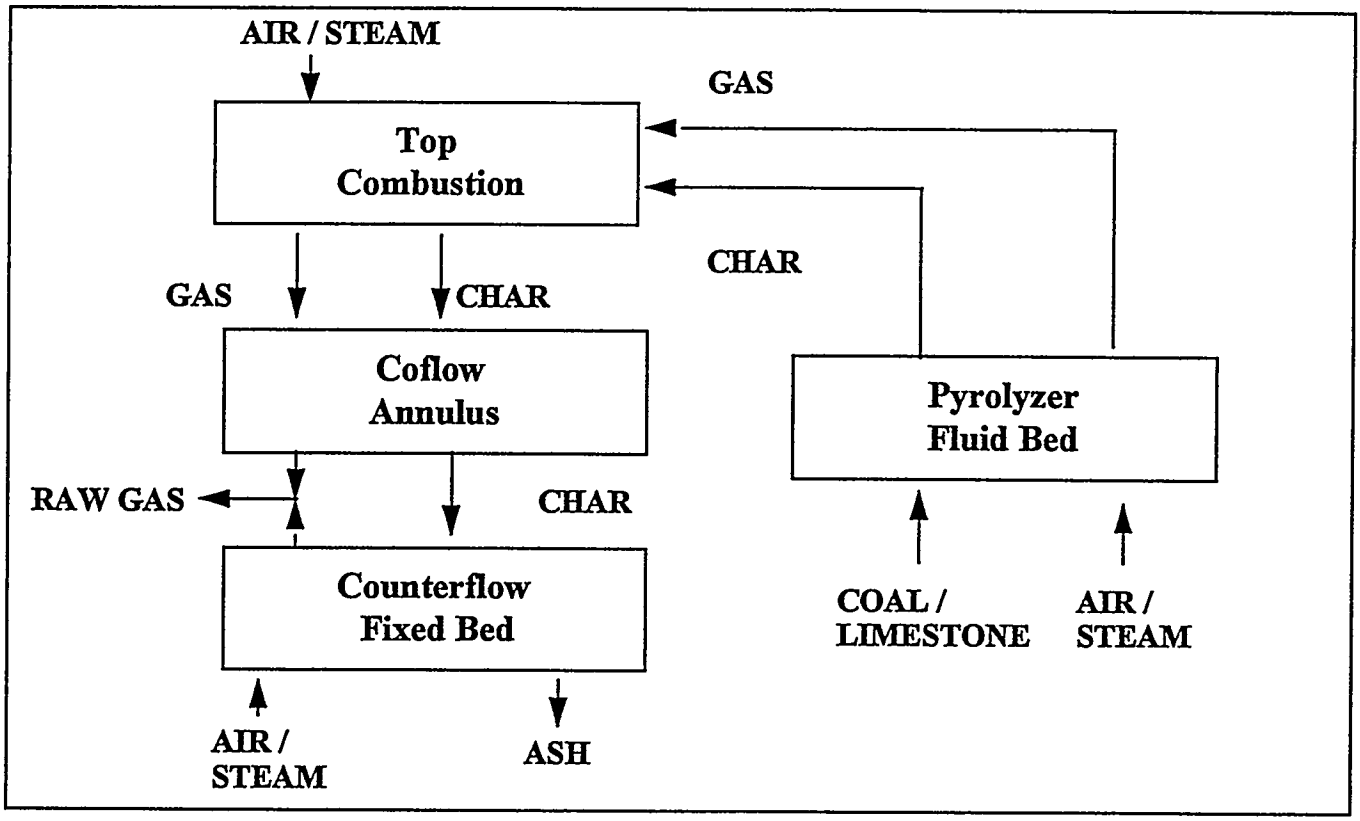


The remaining tars are cracked in the tar cracking zone down stream of the pyrolyzer. The gases and char then move down a co-flow annular section and to the top of the fixed bed where the final gasification of char takes place.

The combined gasification products from the fixed bed and the co-flow region exit the gasifier at approximately 1150°F and enter a cyclone for removal of particulates. The clean gases go through pressure reduction and enter the

combustion chamber of a Heat Recovery Steam Generator (HRSG) to produce steam for the process.

In a fully implemented IGCC system, the gas generated will be combusted in a combustion turbine to generate power and the HRSG will be located down stream of the combustion turbine.

## THE FORT MARTIN PROJECT SITE

Construction of the GPIF at the Fort Martin station provided the benefit of utilizing the existing infrastructure at the site for steam and other utility tie-ins. The 1100 $MW_e$ pulverized coal-fired electric utility facility is providing several key utility interfaces which would otherwise become added project costs. Also, the close vicinity to Morgantown Energy Technology Center (METC) would allow the METC personnel to be part of the operating crew.

The following utilities have been combined with the main site to minimize both the capital and operating costs:

- High and medium voltage power interconnects
- Backup steam for startup
- Cooling water
- Wastewater treatment
- Potable water supply
- Flue gas breaching tie to the existing electrostatic precipitator
- Coal sourcing
- Permitted ash disposal site
- Utilization of the steam byproduct

The integration of the PyGas™ process at Fort Martin alleviated several process and environmentally related concerns, which led to an approval of the required National Environmental Protection Act (NEPA) permit. After receiving the NEPA approval the DOE determined that it was also necessary to obtain an air permit for the GPIF from the West Virginia Environmental Protection Agency.

## PROJECT STATUS

Following is a summary of the major events during the past year:

- Conceptual design completed
- Operating pressure established at 400 psig
- Flue gas desulfurization system added to scope
- Air permit application submitted to State of West Virginia
- Initial process design basis completed
- Process analysis for the cold flow model submitted to DOE
- Work packages prepared
- 25% design review presented

Activities during the past year related to the development of the detailed design for the gasifier, HRSG and the major GPIF sub-systems. Design review and analyses of the pyrolyzer, gasifier and the vessel cooling was also conducted (3-11). Issues such as safety considerations, adherence to governing codes, start-up and operating procedures were examined. The balance of plant (BOP) equipment selection criteria was also developed

These activities allowed the contract to move to the next phase, construction. A comprehensive design, manufacturing and construction schedule was prepared in support of testing this technology.

The total GPIF system is schematically presented in Figure 3. It includes the following major components:

- Air Compressor
- Day Silo/Coal Dryer/Crusher
- Coal Pressure Lock
- PyGas™ Coal Gasifier
- Hot Gas Cyclones
- Pressure Reducing Station
- Emergency Flare Stack
- Heat Recovery Steam Generator (HRSG)
- Ash Depressurization Lock
  Wet Sulfation Tank/Pumps/Vacuum Filter
- Enclosed Ash Temporary Storage Slab
- Tarpaulin Covered Test Coal Pile Slab
- Caustic Scrubber
- Natural Gas Fired Reheater
- Limestone Storage Silo
- Administration Buildings/Facilities

**Figure 3**
**GPIF Systems Schematic**

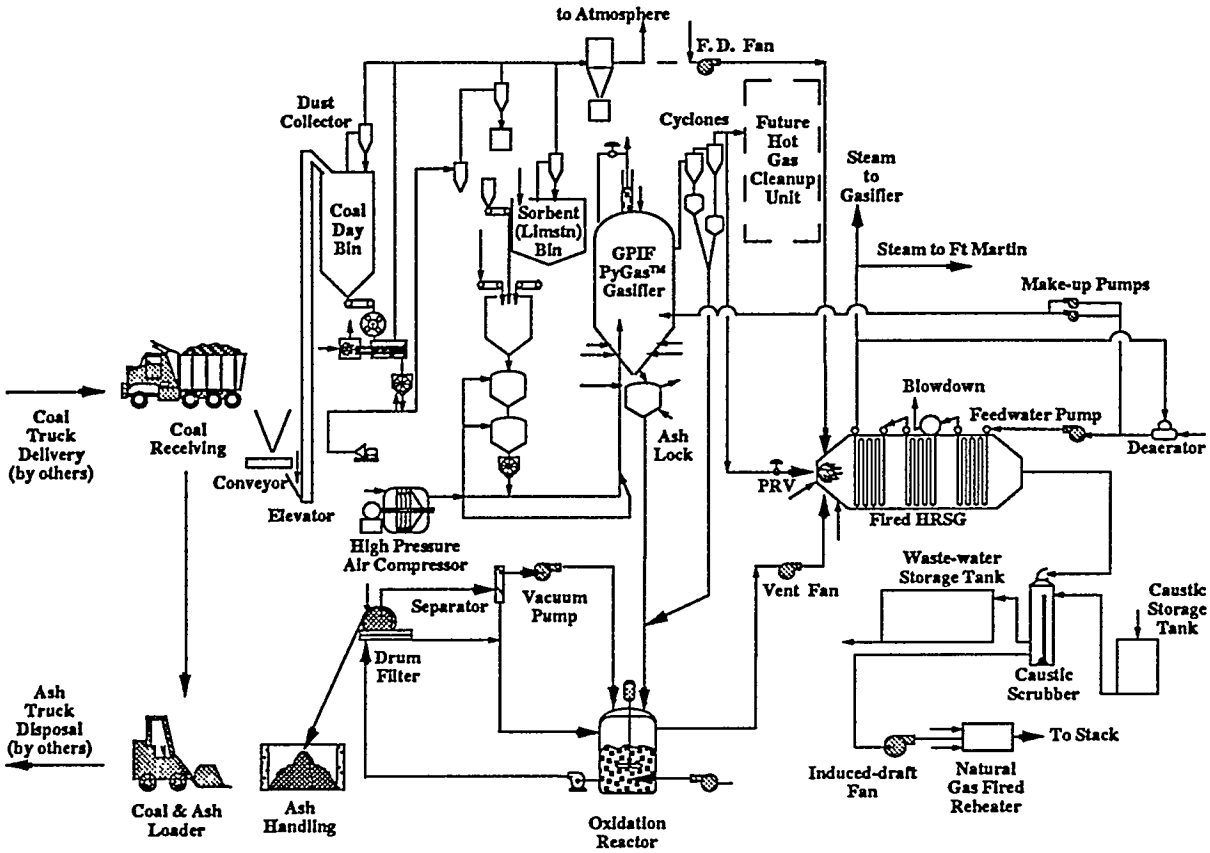


Discussion of the work related to the above activities is presented as follows:

## 1. Conceptual Design

Process analysis was performed on the pyrolyzer to evaluate its performance under various pressure and load conditions. The fuel feed system design was also examined to determine how it would influence the pyrolyzer performance and operation. Start up options for the pyrolyzer and various means of integrating them into the mechanical design were studied. Preheating requirements for the gasifier were established. The start up of the gasifier at partial and full operating pressure was examined.

## 2. Process Design

The major focus of the conceptual design effort was to develop a thorough understanding of the processes occurring in significant zones of the gasifier. To examine these areas independently, the gasifier was divided into four major sections as shown in Figure 2. This allowed us to study how individual parameters operate within these blocks to influence the overall performance.

During the course of the year the DOE asked that the design operating pressure for the gasifier be reduced from 600 to 400 psig. In the conceptual design phase of the project, many of the equipment suppliers noted that they would have to conduct considerable developemnt work to offer equipment for meeting the high GPIF operating pressure requirements. Same suppliers were able to offer equipment for the 400 psig operation. Therefore, to avoid this development step it was decided to design the gasifier for a maximum operating pressure of 400 psig.

Heat and mass balance data were developed for the new pressure condition. A process design package entitled Process Design Basis-Revision 0 was prepared for three operating conditions shown in Table 1. This package included the design criteria for the gasifier, HRSG and all the BOP equipment. Process flow diagrams for the primary and all auxiliary systems were also included in the Rev-0 document.

**Table 1**
**Process Design Basis Conditions**

| Description | Design Case | High Temp Case | Low Temp Case |
|---|---|---|---|
| Coal Flow, lb/hr | 8,000 | 8,000 | 4,000 |
| Operating pressure, psig | 400 | 400 | 200 |
| Pyrolyzer Exit Temp., °F | 1690 | 1856 | 1500 |

## 3. Mechanical Design

The gasifier arrangement is shown in Figure 4. The gasifier consists of two connected vessels. The upper vessel houses the central pyrolyzer tube, the upper shroud and the grate which supports the fixed bed. The grate is a reversing/ rotating grate with provision for breaking large agglomerates. It also has a water cooled ledge at the bottom that restricts the uncontrolled flow of fine ash from the gasifier. The vessel is of a double wall arrangement designed for water-cooling. Steam generated in the cooling circuit is used as process steam for the gasification process. The unused steam is condensed and re-circulted through the cooling jacket.

The upper section of the vessel is configured with two bolted sections for maintenance of the pyrolyzer internals. The lower vessel houses the ash discharge and the lower portion of the pyrolyzer.

The overall vessel has openings for gasification process inlet and/or outlet flows including coal and limestone, air, nitrogen, steam, coal gas, char and ash. Apart from the process design, openings for main vessel access, the rotating grate drive shaft, cooling water circuits, pressure relief mechanism along with numerous instrument connections are also included.

**Figure 4**
**Gasifier Arrangement**

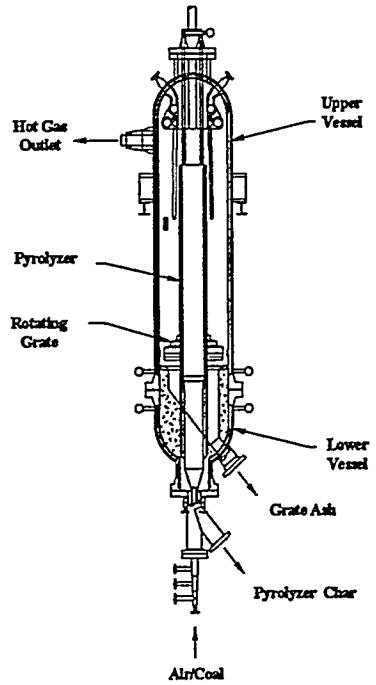


The cooling circuits for the pyrolyzer and the inner annulus were simplified by using water jackets rather than membrane walls as proposed earlier. It was also decided to cool the gasifier outlet duct to counter thermal stresses thus permitting the use of less expensive material. Because of the need to minimize heat losses and maintain pyrolysis temperature, the inner walls of the pyrolyzer are lined with insulating and high density refractory. The refractory will also protect the tube against abrasion.

The design approach employed for the gasifier focused on building sufficient mechanical flexibility to carry out development work for the PyGas™ process. Also, the pyrolyzer bottom and the inlet nozzels were arranged in gasifier vessel for ease of access.

The ASME codes were reviewed to determine the applicable code for the design and fabrication of the gasifier vessel. The pressure relief options for the gasifier were also studied. Preliminary stress analysis was performed to start work on selecting material thickness for

the inner and outer walls of the water jacket and the flanges.

The design pressure of the gasifier vessel was calculated based on the maximum operating gasification pressure, the pressure differential between the vessel cooling jacket and the gas side, maximum air/nitrogen/steam inlet pressure, and design margins placed on various pressure relief devices.

## 4. Production and construction

In preparation for starting the site work an organization was put in place at Riley for equipment procurement and construction. Participating in planning of this activity were representatives from purchasing, scheduling and construction areas.

The approach Riley is taking in the construction of the facility is to generate the least number of work sub-contract work packages while maximizing the activities required within them. The following equipment and construction work packages were prepared:

1. Major equipment
   - Gasifier
   - Heat Recovery Steam generator
   - Flue gas desulfurization system
   - Coal Preparation
   - Ash Handling
   - Air Compressor
2. Civil 1
3. Civil 2
4. Piping
5. Electrical
6. Architectural

The GPIF plot plan is schematically shown in Figure 5.

**Figure 5**
**GPIF Plot Plan**

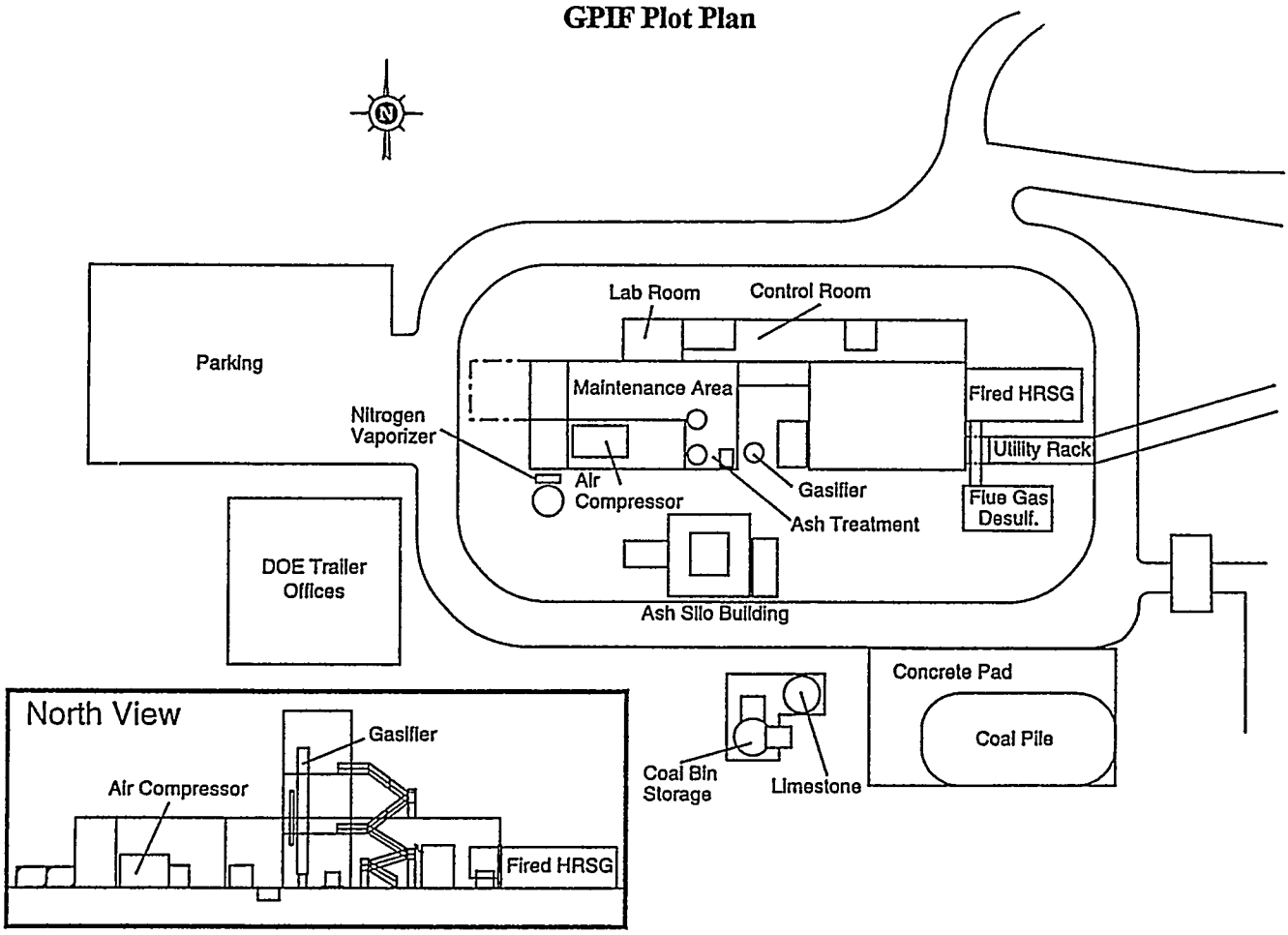

While this activity was proceeding the DOE determined that an air permit was required from the West Virginia State Department of Environmental Protection. Prior to the receipt of this permit no site related activity could begin. The permit is expected by October 15, 1995 which has delayed the construction of the GPIF. This situation led to the consideration that some of the construction activity may have to be carried out in the winter months. The other option was to stop during the winter months while fabrication continues on the longer lead items such as the gasifier, air compressor and heat recovery steam generator. With deliveries expected in early April of '96, the site will be re-mobilized in March 1996.

As part of the host site agreement, a new warehouse will be constructed in place of the old warehouse which will be the site of the GPIF. This work will begin by mid summer of '95, prior to the release of the air permit, which the construction of the GPIF is predicated.

The construction activities of the project will end in early 1997. At this time equipment commissioning and startup of the facility will begin and will initiate the operating CRADA, the next phase of the project.

## FUTURE WORK

The activities planned for the next fiscal year are:

- Finalize the gasifier design
- Complete the auxiliary system design
- Order long lead equipment
- Select subcontractors related to different work packages
- Install warehouse at the new location
- Complete site work
- Complete plant construction
- Negotiate the operating CRADA

The majority of construction is expected to be completed in the fiscal year 1996. Some of the work related to equipment installation, electrical and architectural will continue into the next year. The plant will be ready for pre-operational testing by the end of January 1997.

## REFERENCES


1. Gasification Product Improvement Facility (GPIF)-Project Status, 1992 DOE/METC Annual Contractors Meeting.
2. Gasification Product Improvement Facility Project Status, 1994 DOE/METC Annual Contractors Meeting.
3. Solids Circulation Patterns and Particles Mixing on a Large Jetting Fluidized Bed, W, Yang, et. al., AIChE Journal, December 1986.
4. Cold Flow Scale Up Facility Experimental Results and Comparison of Performance at Different Bed Configurations, DOE Contract DE-AC21-82MC19122, Vol 1, Topical Report, Jan-Dec 1983.
5. Fluidization, Second Edition, Davidson, J. F., et. al, Academic Press, 1995
6. Fluidization Engineering, Second Edition, Kunni, D. & Levenspiel, O., Butterworth-Heinemann, 1991
7. The Theory of Turbulent Jets, Abramovich, G. N., MIT Press, 1983
8. Heat Transfer between Gas Fluidized Beds of Solid Particles and the Surface of Immersed Heat Exchanger Elements, Part I, Chem. Eng. Proces., 18 (1984)
9. Entrained Bed Carbonization of Highly Fluid Bituminous Coals, Gomes, M, et. al., Bureau of Mines Report #7141
10. GPIF Analysis, David Archer, Carnegie Mellon University, Feb 1994
11. Chemistry of Coal Utilization, Second Supplementary Volume, Wiley-Interscience, 1981

## 2.4 Externally Fired Combined Cycle Demonstration

### CONTRACT INFORMATION

| | |
|---|---|
| **Contract Number** | DE-AC21-94MC31327 |
| **Contractor** | Hague International<br>3 Adams Street<br>South Portland, Maine 04106<br>(207) 799-7346 |
| **Contractor Project Manager** | Nelson J. Orozco |
| **Program Manager** | Stephen Young |
| **Principal Investigators** | Paul G. LaHaye<br>John Strom-Olsen<br>John L. Seger<br>Helen Pickup |
| **METC Program Manager** | Lee Paulson |
| **Period of Performance** | May 10, 1994 to June 26, 1995 |

## OBJECTIVES

Externally Fired Combined Cycles (EFCCs) can increase the amount of electricity produced from ash bearing fuels up to 40%, with overall powerplant efficiencies in excess of 45%. Achieving such high efficiencies requires high temperature - high pressure air heaters capable of driving modern gas turbines from gas streams containing the products of coal combustion.

A pilot plant has been constructed in Kennebunk, Maine to provide proof of concept and evaluation of system components. Tests using pulverized Western Pennsylvania bituminous coal have been carried out since April, 1995.

The ceramic air heater extracts energy from the products of coal combustion to power a gas turbine. This air heater has operated at gas inlet temperatures over 1095°C (2000°F) and pressures over 7.0 atm (100 PSI) without damage to the ceramic tube string components. Stable gas turbine operation has been achieved with energy input from the air heater and a supplementary gas fired combustor.

Efforts are underway to fire the cycle on coal only, and to increase the duration of the test runs. Air heater improvements are being implemented and evaluated. These improvements include installation of a second pass of ceramic tubes and evaluation of corrosion resistant coatings on the ceramic tubes.

## BACKGROUND INFORMATION

The Externally Fired Combined Cycle (EFCC) is an old concept. Essentially, an air heater fired on an ash bearing fuel that cannot be burned directly in the gas turbine energizes the cycle.

Use of the air heater means that the gas turbine does not come in contact with the products of combustion. In other words, the air heater protects the gas turbine from corrosion and erosion by chemicals and particulate produced by the combustion of the fuel.

The gas turbine compressor provides pressurized air to the tube-side of the ceramic air heater. Heat transferred from the hot combustion gases flowing through the shell-side of the air heater raises the temperature of the air to the desired gas turbine inlet temperature.

High pressure piping conducts this heated air to the turbine, where it expands, providing power to drive the electric generator and the gas turbine compressor.

The hot exhaust air from the turbine is used as combustion air in the coal burner.

The air heater's shell-side exit gas generates steam for a bottoming cycle.

EFCC studies have been performed since the 1930s, and there is a history of applications using low rank fuels and metallic heat exchangers dating to the 1950s [1, 2, 3].

A state of the art gas turbine, however, requires inlet temperatures in excess of the temperatures that can be achieved with metallic heat exchangers.

In 1971, Hague International began a series of experiments with ceramic materials that resulted in the construction of a ceramic tubular heat exchanger of novel design.

Hague's ceramic tubular heat exchangers have been in commercial operation since June, 1978. Gas inlet temperatures have ranged up to 1540°C (2800°F) at tube-side pressures averaging 0.3 atm (4 psi).

Such low pressure units have been installed in ferrous and non-ferrous secondary metals industries in North America and Japan, accumulating several million hours of successful operation in a variety of corrosive high temperature environments [4, 5, 6, 7, 8, 9].

In addition, low pressure ceramic tubular heat exchangers were exposed to the products of combustion of coal slurries to investigate the effects of ash.

These preliminary investigations indicated the need for an upstream ash collection system. Further and ongoing evaluation of the available ceramic materials for use in the air heater dictates that special consideration be given to corrosion resistance when operating on coal [10, 11, 12].

## PROJECT DESCRIPTION

Phase 1 of the project, beginning in 1987, investigated whether the ceramic materials then available for use in the air heater would withstand the corrosive environment produced by the combustion of coal up to the desired temperature of 1200°C (2200°F). Phase 1 of the project also evaluated, in a preliminary way, means of preventing the fouling of the air heater by fly ash. This experimental work was deemed successful by Stone & Webster Engineering Company [6, 13, 14].

Phase 2 of the program, initiated in 1990, built a 7MW thermal input pilot plant under the auspices of a cooperative agreement with the U.S. Department of Energy Morgantown Energy Technology Center (DOE METC). This work was funded by a consortium of electric utilities, utility organizations, industrial organizations, state agencies, international entities, and DOE METC.

During 1995 the pilot plant is intended to function as a proof of concept facility operating under conditions that simulate the conditions intended for the DOE Clean Coal Technology Round V demonstration plant [6, 15].

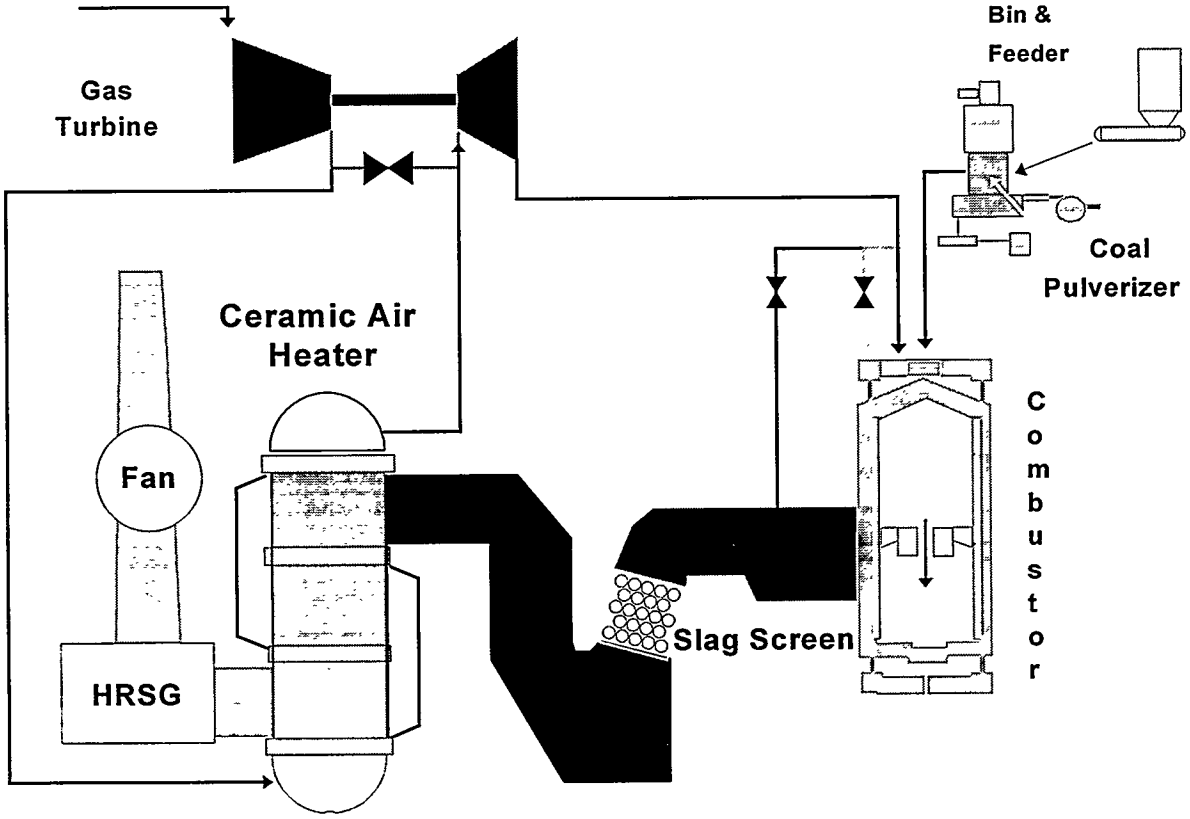


**Figure 1: Kennebunk Test Facility (KTF) Schematic**

## RESULTS

Construction of the Kennebunk Test Facility has been completed. This facility now incorporates all the major elements of an EFCC plant, with the exception of a steam turbine, omitted for reasons of economy. The steam generated is simply discharged to atmosphere.

Pennsylvania bituminous coal is fed through a weigh belt and a pulverizer before delivery to the combustor. The products of combustion pass through a slag screen before introduction to the air heater. The air heater is a three pass shell and tube heat exchanger that accepts high pressure tube-side air from the gas turbine compressor.

Pressurized heated air is delivered to the gas turbine. Gas turbine exhaust is used as combustion air to burn the coal. Heat exchanger shell-side exit flows to a steam generator.

A Garrett IE31-800 gas turbine with a rating of 500 KW has been installed. The test facility can accommodate gas turbines rated up to 2 MW with some modifications.

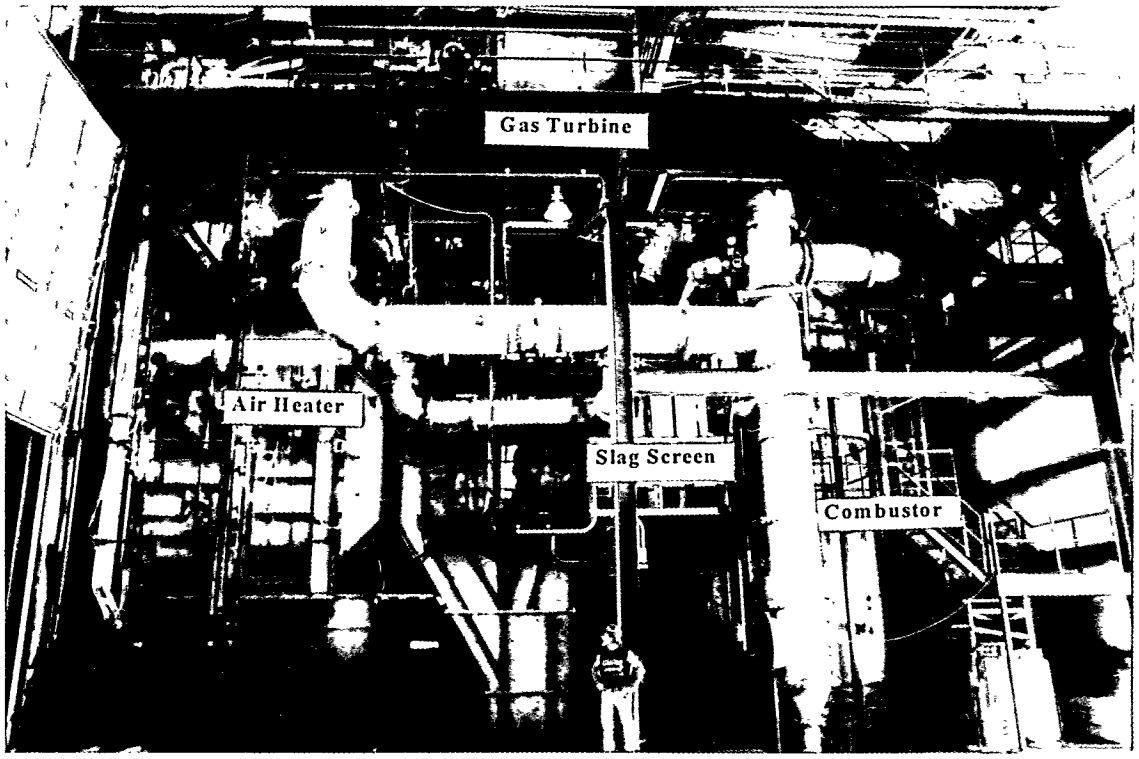


**Figure 2: KTF Combustor, Slag Screen, Ceramic Air Heater, Gas Turbine**

The coal combustor is staged to reduce $NO_x$ emissions. A Foster Wheeler Controlled Flow/Split Flame low $NO_x$ burner downfires into a cylindrical combustion chamber with the primary stage directly atop the secondary stage.

The total height of the combustor, including the burner, is approximately 12.1 meters (40 feet), and the outer diameter of the cylindrical casing is approximately 3.96 meters (13 feet). A slag tap is located at the base of the combustor.

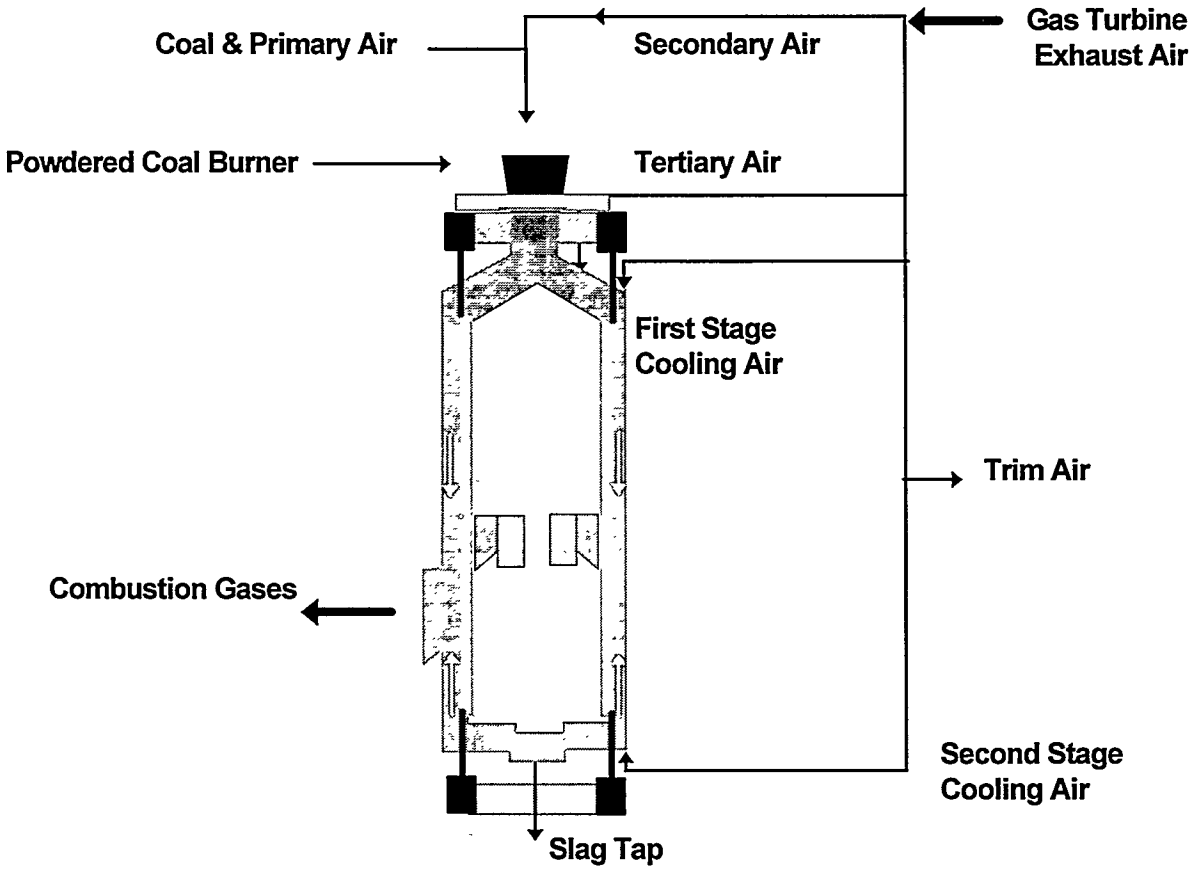


**Figure 3: Combustor Schematic**

Products of combustion exit the combustor and enter the slag screen at a high velocity.

The slag screen is an impact separator made up of ceramic rods. The slag screen is designed to be self cleaning.

After exiting the slag screen, the products of combustion flow to the air heater, passing over the air heater tubes at velocities approximately half the velocities in the slag screen. This assures minimal particle accumulation on the air heater tubes. These deposits can be removed by conventional means, such as soot blowers.

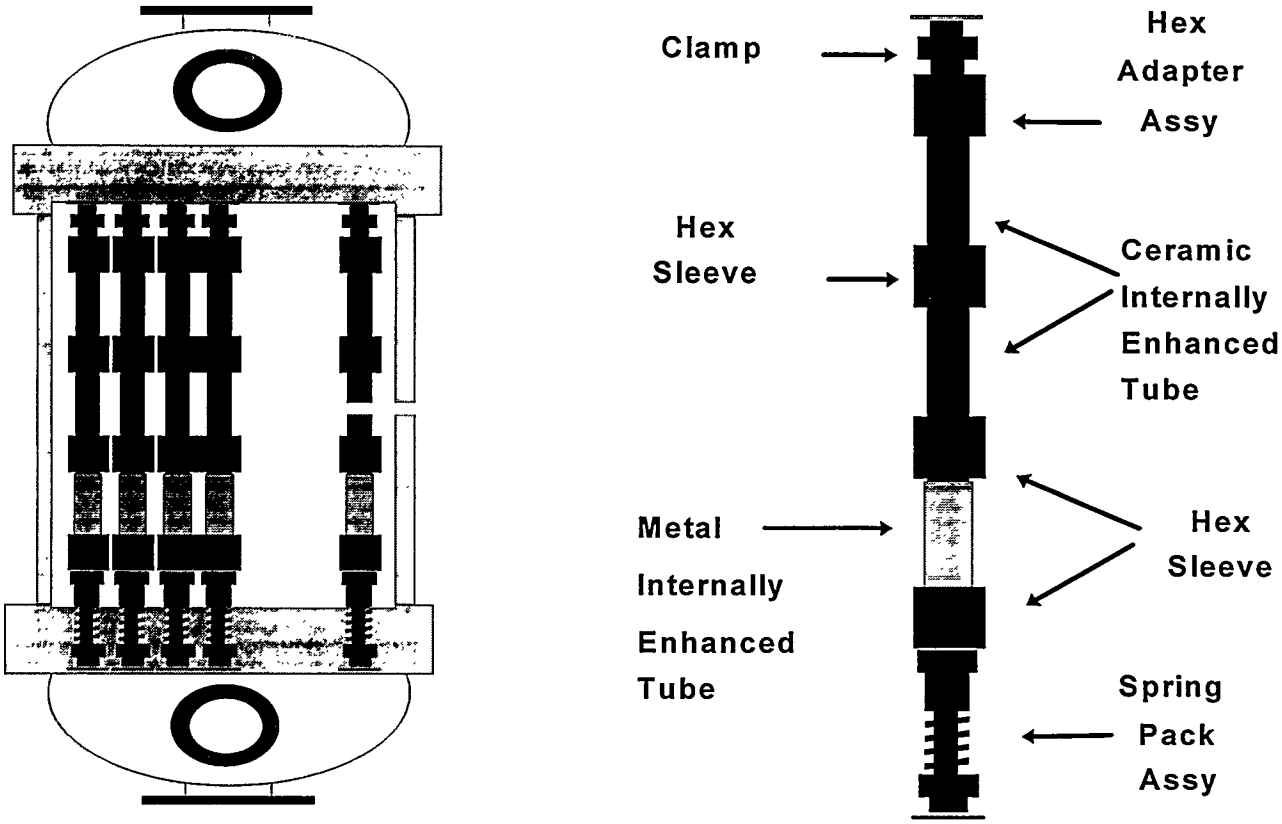


**Figure 4: Air Heater Schematic**

The air heater is the enabling technology for Externally Fired Combined Cycles [6, 16, 17]. The air heater at the Kennebunk Test Facility is made up of three passes of tubes, with 72 tubes in each pass.

Compressor discharge from the gas turbine flows inside the tube strings. The tubes are held in place by spring pack assemblies and hexagonal adapters.

Gasketed ball and socket joints allow independent movement of each component in the tube string as may be required to accommodate thermal distortion of the assembly. The ball and socket joints allow a relatively high degree of angular misalignment without leakage.

The spring pack assemblies hold the tube strings under compression. The spring pack assemblies are located on the cold end of the tube string, outside of the combustion gas path,

so that these components are not exposed to temperatures above 205°C (400°F).

Hexagonal adapters hold tube strings in place, and allow for differences in thermal expansion of individual tube strings.

These hexagonal pieces fit together in honeycomb fashion to form thermal barriers separating the shell-side flow of one pass from another pass, and provide refractory walls to protect the metal components of the air heater's plena.

Several types of silicon carbide ceramic tubes have been successfully used in the high pressure air heater at the Kennebunk Test Facility. Hague International has developed proprietary methods to prevent the sequential failure of brittle ceramic tubes.

In its present configuration, the heat exchanger has one pass of ceramic tubes, for exposure to the hottest combustion gases, and two passes of metallic tubes. A second pass of ceramic tubes is to be installed to increase the delivery temperature to the gas turbine during late summer, 1995.

Metal alloys can be used in the low temperature end of the heat exchanger (<760°C, <1400°F) for cost effectiveness.

The first coal-fired demonstration was to check out the coal handling and coal combustion systems, pressurize the air heater, and evaluate the performance of a partial pass of ceramic tubes. This was completed in March, 1995.

The second coal-fired demonstration at the Kennebunk Test Facility took place April 25-30, 1995. The first pass of the air heater consisted of 72 ceramic tubes. The remainder of the air heater was fitted with metal tubes. The goal of this demonstration was to extend coal-fired operations, run in EFCC mode without preheat to the combustor, and to integrate turbine controls. This demonstration was cut short when leaks developed in gaskets outside of the combustion gas path. These gaskets were replaced, and the facility is to be back on line in July, 1995.

Gas inlet temperatures to the air heater in excess of 1095°C (2000°F) and tube-side pressures in excess of 7.0 atm (100 psi) have been demonstrated.

Post demonstration analysis indicates that there has been no damage to the ceramic tubes during operation to date.

Slag screen performance has been as expected, even at low combustion gas velocities. Minor deposits of friable ash have been found in low gas velocity sections of the air heater. Previous experience with low pressure ceramic tubular heat exchangers indicates that such friable deposits can be removed with conventional sootblowers [7, 8, 10, 12].

Preliminary emissions testing has been encouraging, but more extended testing will be required before reliable data can be published.

## FUTURE WORK

Future work includes further EFCC demonstrations at the Kennebunk Test Facility. Demonstrations of up to 100 hours of continuous coal-fired turbine operation, without supplementary fuel, are planned for early fall. Longer runs are necessary to confirm, among other things, measurements of slag screen performance and $NO_x$ emissions.

To increase the air temperature to the turbine, two ceramic passes will be installed in the air heater.

Component evaluation will be performed after each run, with component and system improvements being made on the basis of post run analyses. Special attention will be paid to heat transfer, deposit accumulation, and corrosion resistance.

Ceramic materials continue to be evaluated. Promising tube joining techniques that would permit the fabrication of tubes 4.2m (14 feet) and longer are being pursued with government laboratories, independent laboratories, and vendors of ceramic components. The Idaho National Engineering Laboratory has provided samples of joined SiC tubing of the diameter to be used in a full scale ceramic air heater. Tests performed with flat samples indicated that the joint is at least as strong as the bulk silicon carbide. In principle there is no limit to the length of tubes which can be joined.

To reduce tube corrosion, tube coating technologies are being investigated with government laboratories, independent laboratories, and commercial vendors. The long term goal is to obtain a coating that will withstand 20,000 hours of operation in an environment of coal combustion products at 1370°C (2700°F). Ceramic oxide coatings applied to SiC tubes have been repeatedly cycled to 1100°C (2020°F) without adverse effect to the coating. There are no signs of spalling or lamination, and X-ray diffraction analyses of tested coatings indicate no change in the phase composition of the coatings or the substrate. It remains to be evaluated how resistant coatings are to coal combustion products for prolonged periods of time at operating temperature.

The United States Department of Energy has estimated a commercial potential for EFCC technology of 24GWe by 2010 [15].

Successful commercialization of EFCC technology will require demonstration of the technology in a commercial power generating environment, which is currently planned [6, 15].

EFCCs offer technical and economic advantages: no hot gas cleanup or novel chemical processes are required; and repowering and upgrading existing steam turbine power plants with EFCC technology makes maximum use of existing facilities.

Competition for EFCC is now and is expected to remain gas-fired combined cycles, as long as natural gas is readily available at low prices.

Repowering is an attractive initial focus of commercialization because there are approximately 500 coal-fired steam installations that are EFCC candidates in the United States. The EFCC concept is expected to have a major impact on repowering of existing coal-fired steam turbine power plants well into the next century.

## REFERENCES


1. Keller, C., *The Escher Wyss-AK Closed Cycle Turbine, Its Actual Development and Future Prospects*, ***Trans. ASME,*** Vol. 68, pp. 791-882, 1946

2. Keller, C. and Gaehler, W., *Coal-Burning Gas Turbine*, ASME Paper 61-GTP-2, presented at the Gas Turbine Power Conference, Washington, DC, March 5-9, 1961

3. Mordell, D.L. *The Exhaust-Heated Gas Turbine Cycle*, ***Trans. ASME***, Vol. 72, pp. 323-329, 1950

4. LaHaye, P.G. *High Temperature Heat Exchanger for Closed-Cycle Coal-Fired Gas Turbines*, presented at the National Coal Association Technical Sales Conference and Bituminous Coal Research Annual Meeting, Pittsburgh PA, September 14, 1966

5. Most, I.G. and Hagen, K.G., *A Ceramic Heat Exchanger for Exhaust Fired Gas Turbine Power Cycles*, ***Proceedings of the 12th Intersociety Energy Conversion Engineering Conference,*** 1977

6. LaHaye, P.G. and Bary, M.R, *Externally Fired Combustion Cycle (EFCC): A DOE Clean Coal V Project - Effective Means of Rejuvenation for Older Coal-Fired Stations*, ASME 94-GT-483, 1994

7. Young, S.B., *High Temperature Waste Heat Recovery Systems Using Ceramic Recuperators*, ***Proceedings of the 7th Energy Technology Conference & Exposition,*** 1980

8. Young, S.B. and Bjerklie, J.W., *High Temperature Ceramic Tube Recuperators*, ***Aluminum Industry Energy Conservation Workshop V Papers***, The Aluminum Association Incorporated, 1980

9. Orozco, N.J. *High Pressure Ceramic Air Heater for Indirectly-Fired Gas Turbine Applications*, ***Proceedings of the Joint Contractors Meeting: FE/EE Advanced Turbine Systems Conference FE Fuel Cells and Coal-Fired Heat Engines Conference***, Donald W. Geiling, ed., U.S. Department of Energy, Office of Fossil Energy, METC, August 3-5, 1993

10. Bjerklie, J.W. and Curtis, R.H., *Demonstration of Fuel Conservation in High Temperature Industrial Furnaces,* ASME Paper 78-WA/Ener-8, 1978

11. Bjerklie, J.W. and Penty, R.A., ***Demonstration and Testing of Coal/Oil Mixture as a Fuel for a Slot Furnace***, NTIS, U.S. Department of Commerce, C00-4237-T1, 1979

12. Bjerklie, J.W. , Green, C.P., Penty, R.A., and Young, S.B., *Forging with Coal/Oil Mixture Metallurgical and Environmental Effects*, ***Proceedings of the Third International Symposium on Coal Oil Mixture Combustion***, 1981

13. LaHaye, P.G. and Zabolotny, E., *Externally-Fired Combined Cycle (EFCC),* Presented at the ASME COGEN-TURBO Meeting, August 30 - September 2, 1989

14. Vandervort, C.L., *Factors Influencing Ash Particle Deposition in an Impact Separator at High Velocities and Temperatures*, ***Proceedings of the Engineering Foundation Conference on Inorganic Transformations and Ash Deposition During Combustion***. pp. 815-827, March, 1991

15. U.S. DOE, Assistant Secretary for Fossil Energy, Washington, DC. ***Clean Coal Technology Demonstration Program***, Program Update 1994, April, 1995

16. Eidenstein, L., Rosén, P., Sverdberg, G., Torisson, T. and Yan, J., *Analysis of Small Scale Evaporative Gas Turbines Part II: Externally Fired Gas Turbine with Solid Biomass*, ***Flowers 94: Proceedings of the Florence World Energy Research Symposium***, Florence, Italy, 6-8 July, 1994

17. Eidenstein, L., Yan, J. and Svedberg, G., *Biomass Externally Fired Gas Turbine Cogeneration*, ASME 94-GT-345, Presented at the International Gas Turbine and Aeroengine Congress and Exposition, The Hague, Netherlands, June 13-16, 1994


## ACKNOWLEDGMENTS


Support for the EFCC program is provided by the United States Department of Energy - Morgantown Energy Technology Center and the EFCC Consortium of government agencies, electric utilities, and both foreign and domestic industrial organizations. Their contributions are gratefully acknowledged.

## 2.5 Advanced Gas Turbine Systems Program

Charles M. Zeh
Morgantown Energy Technology Center

**ABSTRACT**

The U.S. Department of Energy (DOE) is sponsoring a program to develop fuel-efficient gas turbine-based power systems with low emissions. DOE's Office of Fossil Energy (DOE/FE) and Office of Energy Efficiency and Renewable Energy (DOE/EE) have initiated an 8-year program to develop high-efficiency, natural gas-fired advanced gas turbine power systems. The Advanced Turbine Systems (ATS) Program will support full-scale prototype demonstration of both industrial- and utility-scale systems that will provide commercial marketplace entries by the year 2000.

When the program targets are met, power system emissions will be lower than from the best technology in use today. Efficiency of the utility-scale units will be greater than 60 percent on a lower heating value basis, and emissions of carbon dioxide will be reduced inversely with this increase. Industrial systems will also see an improvement of at least 15 percent in efficiency. Nitrogen oxides will be reduced by at least 10 percent, and carbon monoxide and hydrocarbon emissions will each be kept below 20 parts per million, for both utility and industrial systems.

The program is highly cost shared by industry and is structured to support the development and commercial introduction of next-generation gas turbine technology. All major U.S. turbine manufacturers have participated in the program. Currently, General Electric Corporation, Westinghouse Electric Corporation, Asea Brown Boveri, Allison Engine Company, and Solar Turbines, Inc., are completing system studies and concept development for their ATS designs. Major turbine manufacturers are supported by a unique industry/university consortium managed by the South Carolina Energy Research and Development Center. The consortium currently sponsors 23 research projects within its membership of 73 universities located in 35 states.

This paper will discuss the status of the ATS Program and the current programmatic issues facing the ATS Program.

# Poster Session A

*METC CRADA Opportunities*

# PA.1 Dynamic Analysis of Process Reactors

Lawrence J. Shadle, Larry O. Lawson, and
Stephen D. Noel
Morgantown Energy Technology Center

## ABSTRACT

The approach and methodology of conducting a dynamic analysis is presented in this poster session in order to describe how this type of analysis can be used to evaluate the operation and control of process reactors. Dynamic analysis of the PyGas™ gasification process is used to illustrate the utility of this approach. PyGas™ is the gasifier being developed for the Gasification Product Improvement Facility (GPIF) by Jacobs-Sirrine Engineering and Riley Stoker. In the first step of the analysis, process models are used to calculate the steady-state conditions and associated sensitivities for the process. For the PyGas™ gasifier, the process models are non-linear mechanistic models of the jetting fluidized-bed pyrolyzer and the fixed-bed gasifier. These process sensitivities are key input, in the form of gain parameters or transfer functions, to the dynamic engineering models.

The dynamic models are developed from the global process phenomena as described by simple chemical, physical, and thermodynamic properties. These models will predict the dynamic interactions of reactions, component capacitance, and systems resistances in processes such as GPIF. Validation of both the steady-state models and the dynamic models will be accomplished by performing tests at the Morgantown Energy Technology Center in experimental rigs including a one-third scale, plastic, cold-flow model; a 10-inch fluidized-bed coal gasifier; and the pressurized gasification pot.

This type of dynamic analysis is used to investigate and validate alternative control strategies and operational scenarios. Added utility includes investigating unanticipated operational scenarios, instrument placement, and process design prior to construction and operation of GPIF. Expected results include operational control and safety analysis of transients caused by operational disturbances, changes in load variables, and changes in inlet conditions. The dynamic model can be readily adapted to the form of a computerized process simulator. This process simulator can further be used off-line to train operators for nominal process testing and unanticipated process disturbances.

## PA.2 CRADA Opportunities With METC's Gasification and Hot Gas Cleanup Facility

Edwin N. Galloway
John M. Rockey
Mark S. Tucker
Morgantown Energy Technology Center

### ABSTRACT

Opportunities exist for Cooperative Research and Development Agreements (CRADA) at the Morgantown Energy Technology Center (METC) to support commercialization of IGCC power systems. METC operates an integrated gasifier and hot gas cleanup facility for the development of gasification and hot gas cleanup technologies.

The objective of our program is to gather performance data on gasifier operation, particulate removal, desulfurization and regeneration technologies. Additionally, slip streams are provided for developing various technologies such as; alkali monitoring, particulate measuring, chloride removal, and contaminate recovery processes.

METC's 10-inch diameter air blown Fluid Bed Gasifier (FBG) provides 300 lb/hr of coal gas at 1100°F and 425 psig. The particulate laden gas is transported to METC's Modular Gas Cleanup Rig (MGCR). The gas pressure is reduced to 285 psig before being fed into a candle filter vessel. The candle filter vessel houses four candle filters and multiple test coupons. The particulate free gas is then desulfurized in a sorbent reactor. Starting in 1996 the MGCR system will be able to regenerate the sorbent in the same vessel.

The FBG and MGCR projects offer CRADA opportunities in the following areas:

- Advanced gasifier testing
- Particulate filter design and operation
- Candle filter and material testing
- Desulfurization and regeneration sorbent cycle testing
- Pollutant and corrosive specie abatement technologies
- Hazardous Air Pollutants (HAP) monitoring

The FBG and MGCR offer distinct advantages for CRADA opportunities:

- Synthesis gas produced by coal gasification
- Gasifier process conditions: 1700°F, 425 psig
- Hot gas cleanup process conditions: 1000°F, 285 psig

PA.4

# CRADA Opportunities in Pressurized Combustion Research

Daniel J. Maloney
Thomas S. Norton
Kent H. Casleton
Morgantown Energy Technology Center

## OBJECTIVES

The Morgantown Energy Technology Center recently began operation of a Low Emissions Combustor Test and Research (LECTR) Facility. This facility was built to support the development of Advanced Gas Turbine Systems (ATS) by providing test facilities and engineering support to METC customers through the ATS University-Industry Consortium and through CRADA participation with industrial partners.

## BACKGROUND INFORMATION

The ATS program is a major DOE initiative to develop more efficient gas turbine systems for base load utility and industrial electric power generation. The program goals include electric generating efficiency in excess of 60 percent, reductions in $NO_x$, CO, and unburned hydrocarbon (UHC) emissions, and 10 percent lower cost of electricity compared to existing technology. The strategy of the program is to fund teams led by U.S. turbine manufacturers to develop ATS systems while at the same time developing a technology base to address key technical issues. A university/ industry consortium administered by the South Carolina Energy Research and Development Center was established to provide cross-cutting technical support for the ATS program. The METC combustion facilities will play a key role in this technology base development by providing facilities and resources for concept testing and demonstration.

A major thrust of the METC program is in the area of low emissions combustor development. $NO_x$ formation and removal will be critical issues for selection of future power generation systems. Commercial vendors offer "ultra-low $NO_x$" (< 9 ppmvd) burners for gas turbine combustion systems fired with clean fuel gases (natural gas), but the demand for more efficient and cost effective power systems poses the challenge of increasing operating temperatures and pressures while burning lower quality "dirty" fuel gases. Meeting these demands is particularly important for Integrated Gasification Combined Cycle (IGCC) and Advanced Pressurized Fluidized-Bed Combustion (PFBC) Systems that burn coal-derived fuel gas in turbine combustors. The METC LECTR facility is designed to support the development of coal-derived, gas-fired combustors as well as the natural gas-fired combustion systems of primary interest for the ATS program.

## PROJECT DESCRIPTION

The LECTR is a versatile test facility with capabilities for evaluating a variety of low emissions combustion concepts at temperatures and pressures representative of gas turbine applications. The LECTR was constructed as a mid-scale test platform to support DOE's ATS program and utilizes the full range of high

pressure (up to 30 atm), high temperature (1000 °F air preheat, 3300 °F combustor wall), and mass flows (3.5 lb/s combustion air) available in METC's Advanced Combustion Facility. Figure 1 illustrates how the LECTR design incorporates a set of flanged sections or modules including an inlet plenum, combustor test sections, a gas sampling section, and an afterburner/quench section. Combustor test sections can be custom designed to meet a specific application by varying the internal refractory dimensions. This modular design approach offers the flexibility to test multiple concepts with rapid turnaround thus maximizing operating time while reducing the time and cost associated with building new inlet, sampling, and quench systems for each application. These features are illustrated in Figures 2 through 5. The high pressure and mass flow capabilities of the LECTR facility make it well suited for evaluation of advanced combustion concepts at combustion scales up to 3 $MW_{th}$ (10 MM Btu/h).

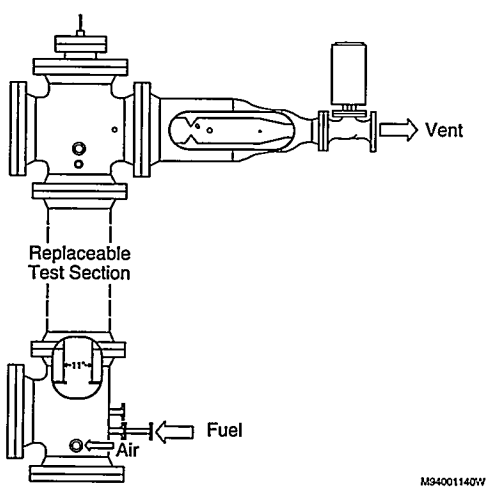


**Figure 1. Low Emissions Combustion Test and Research Facility**

The LECTR facility test modules are configured with multiple access ports for application of both intrusive probe measurements as well as optically based diagnostic systems. METC has the facilities and expertise for performing a range of diagnostic methods including extractive gas sampling and analysis, radiation pyrometry, video and high-speed imaging, and laser-based diagnostics for flow visualization, velocity, and species measurement. To complement these capabilities, METC has state-of-the-art, high-speed data acquisition capabilities to directly support our customer needs. This mix of test facilities, diagnostic capabilities, expertise, and mission enables METC to provide critical test data that otherwise would not be available to the customer.

In its current configuration, the LECTR employs an extractive gas sample probe supported by a number of on-line gas analyzers. Analysis capabilities include major combustion exhaust species such as $O_2$, $CO_2$, and $H_2O$ as well as CO, NO, and total $NO_x$, $N_2O$, and UHC. Details regarding specific analyzers, including analysis method and detection sensitivity, are provided in Table 1. Results of emissions measurements from recent combustion tests are illustrated in Figures 6 and 7. The saw tooth profiles observed in these figures are due to fluctuations in the air/fuel ratio (A/F) during the tests. As one might expect, when the A/F changes, resulting changes in the $O_2$ and $CO_2$ levels in the exhaust gas mirror each other. These figures are included to provide examples of the diagnostic capabilities and to illustrate the response and sensitivity of the analyzer train. A further illustration of the LECTR diagnostic capabilities is shown in Figure 8. This figure demonstrates results of radiation pyrometry measurements, indicating changes in burner surface temperature as a function of changing A/F. These data were taken during execution of a recent CRADA with a small industrial burner manufacturer.

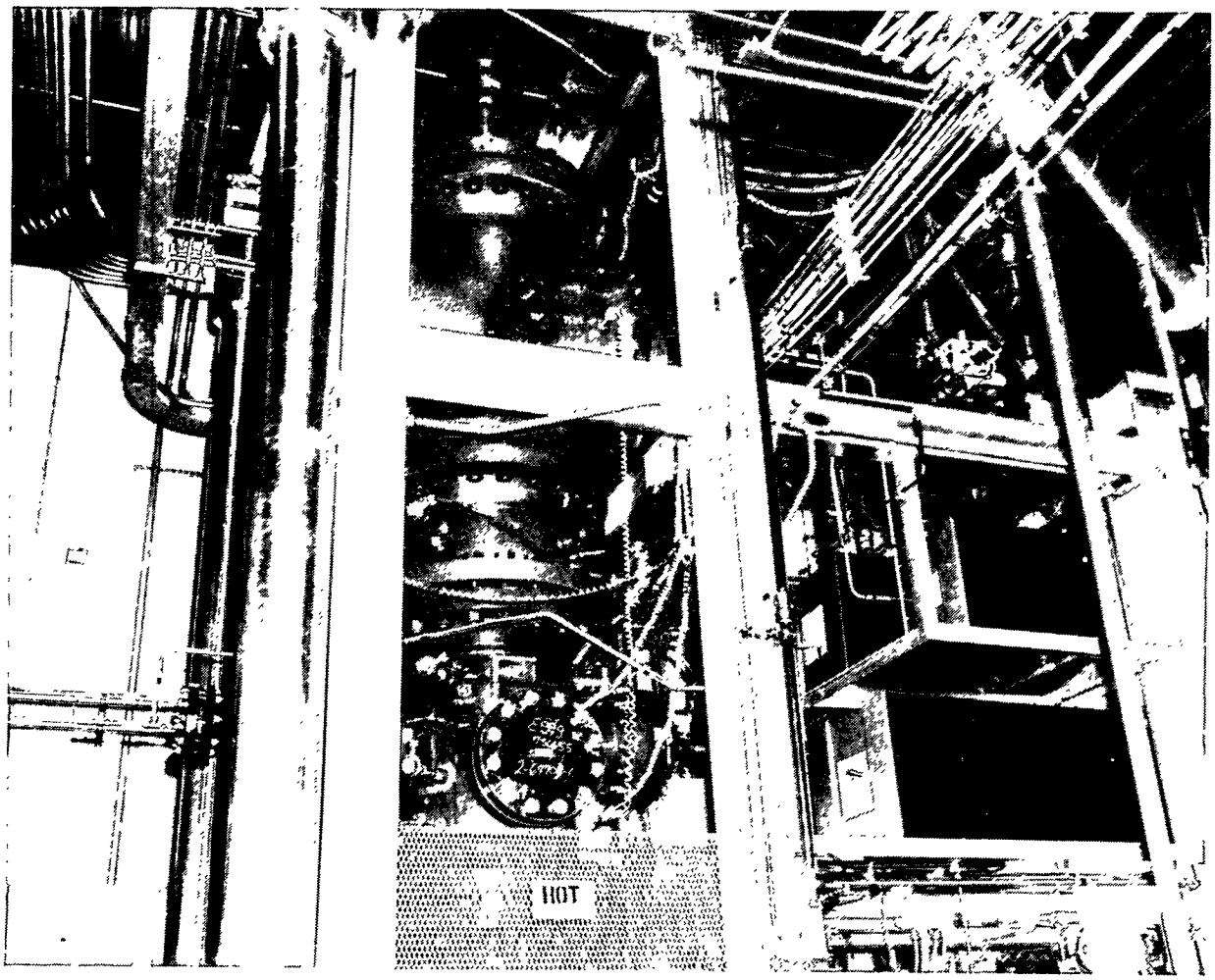


**Figure 2. LECTR Facility With Modules for Air/Fuel Inlet, Combustor Tests, Sampling, Gas Quench, and Pressure Letdown**

In the near future, METC plans to construct a gasification/cleanup Process Development Unit that will include a high volume output Syn-Gas Generator (SGG). Site development plans include integration of this SGG into METC's Advanced Combustion Facility (projected start-up date fall of 1996). When the SGG is integrated with the LECTR facility, METC will have unique test capabilities for evaluating combustion system integration issues associated with utilizing advanced gas turbine systems in IGCC and Advanced PFBC applications.

## FUTURE WORK

The LECTR is now operational and has most recently been employed to characterize the operating and emissions characteristics of an industrial-scale, lean premixed gas burner at elevated pressures for potential gas turbine

**Figure 3. Modular Design Offers Rapid, Cost-Effective Test Configuration Changes**

applications. This work was conducted as part of a CRADA arrangement with an industrial partner. At present, LECTR test modules are being configured to prepare for collaborative combustion tests with Vanderbilt University. These tests are part of METC's commitment to the ATS University-Industry Consortium discussed above and are expected to run through December of 1995. Discussions are in progress with several other potential partners for subsequent use of the LECTR facility. The facility is available for use by METC customers through CRADAs or other arrangements, and all interested parties should contact one of the authors for more details.

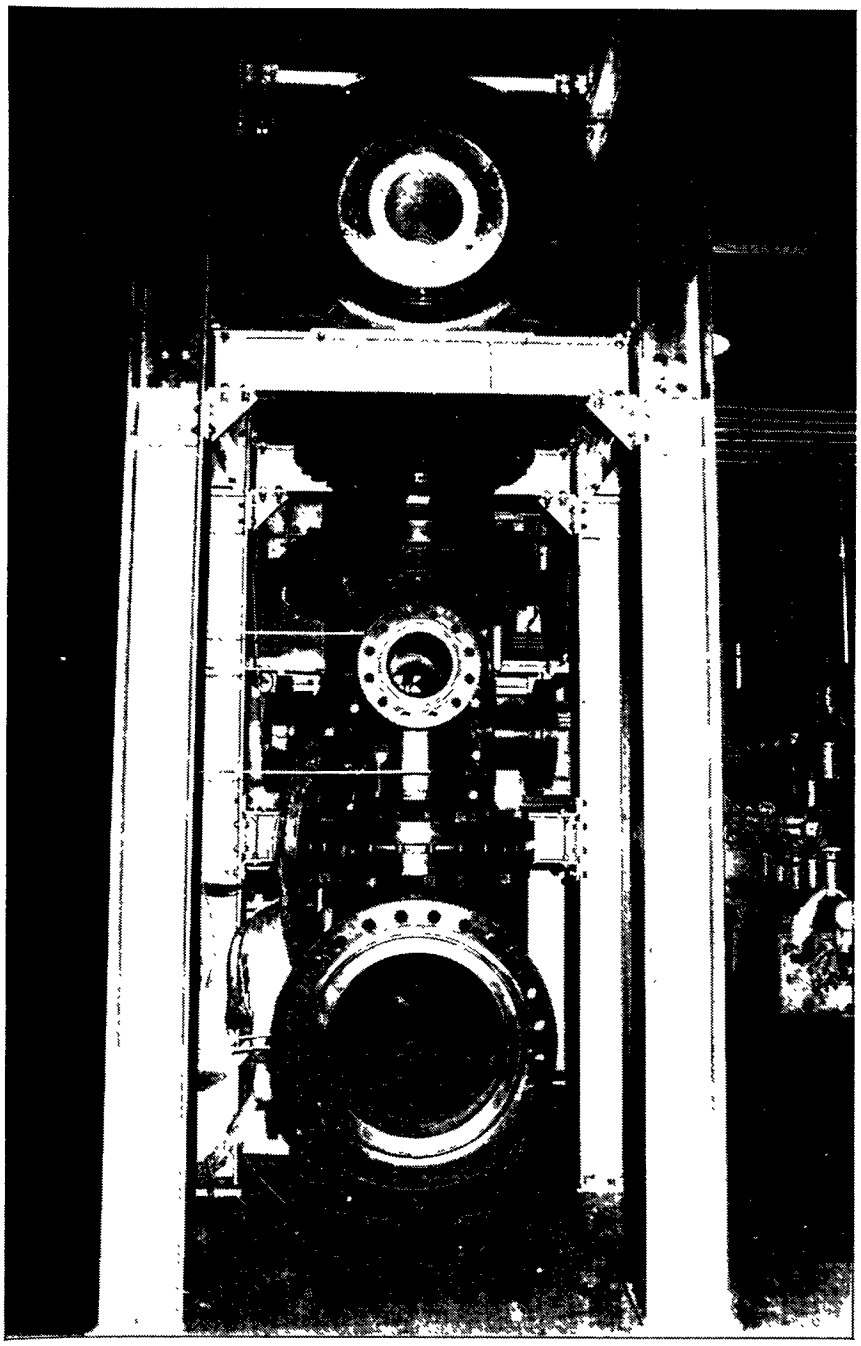

**Figure 4. Refractory-Lined Test Modules With Multiple Ports for Temperature and Pressure Measurements As Well As Optical Diagnostics**

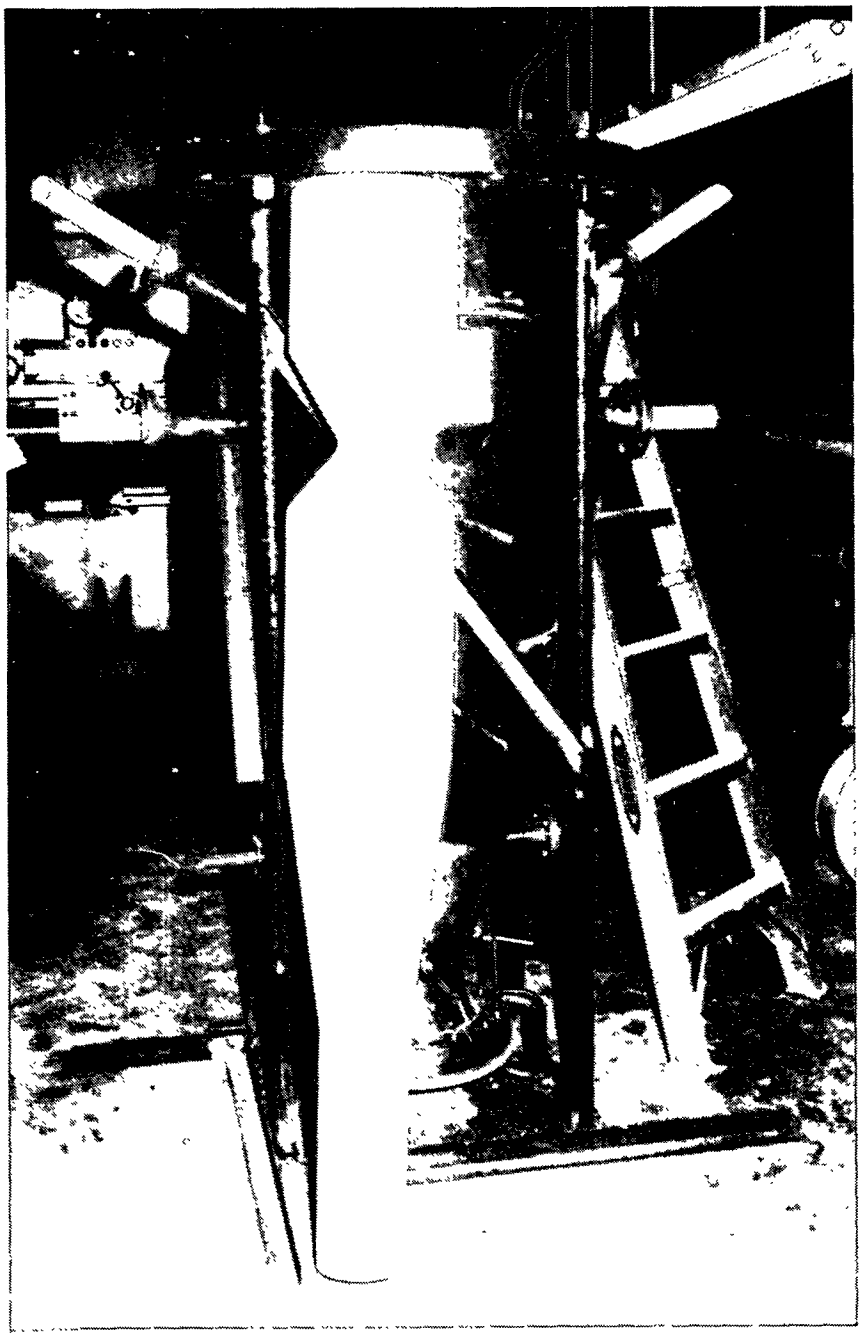

**Figure 5. Afterburner/Quench Module With Refractory Mold Shown; Refractory Can Be Cast to Meet the Application**

## Table 1. METC Gas Analyzers

| Analyzer | Manufacturer | Method | Ranges | Sensitivity |
|---|---|---|---|---|
| $O_2$ | Horiba | Paramagnetic | 0-10%<br>0-25% | 0.1% |
| $CO_2$ | Horiba | NDIR | 0-20% | 0.2% |
| CO | Horiba | NDIR | 0-500 ppm<br>0-1500 ppm<br>0-2500 ppm | 5 ppm |
| Total Hydrocarbons | Backman | FID | 0-40%<br>Continuously adjustable | ~ 1 ppm ? |
| $NO/NO_X$ | Horiba | Chemiluminescence | 20, 50, 100, 200, 500, 1000, 2,000 ppm | 0.2 ppm |
| $N_2O$ | Horiba | NDIR | 0-50 ppm<br>0-250 ppm | 0.5 ppm |
| $N_2O$ | Protimeter | Chilled mirror Dewpoint | DP -40 to 70 C<br>RH 0-100% | DP ± .03 C |
| Mass Spectrometer | VG/Fisons | Scanning Magnetic Sector | Variable | Variable |

M95002220W

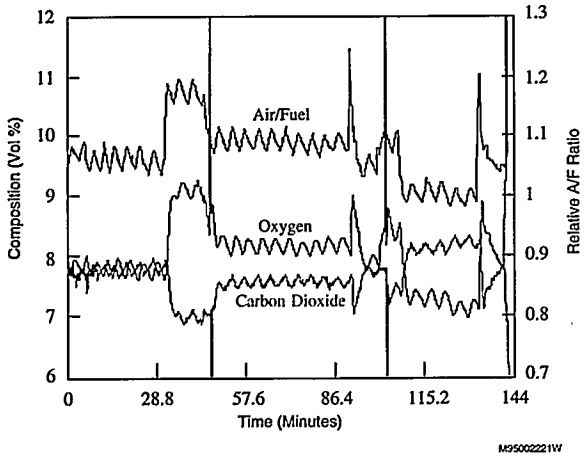


**Figure 6. Product Gas Compositions From Run 031695**

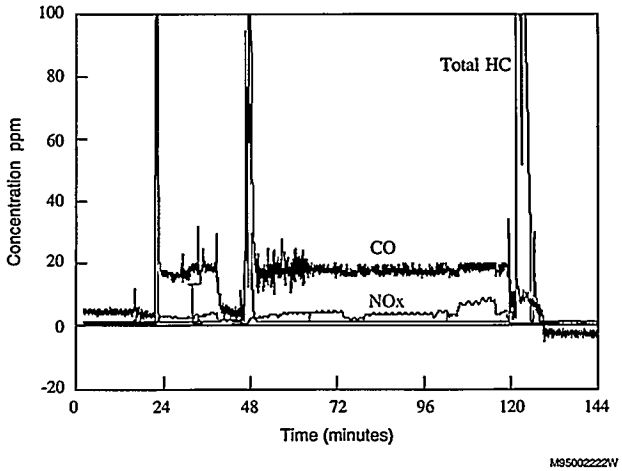


**Figure 7. Emissions Data From LECTR Run 031695**

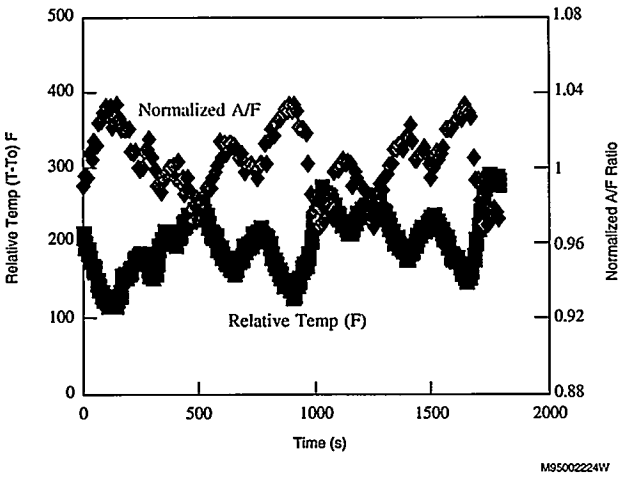


**Figure 8. Burner Surface T and A/F Ratio Variation**

DMALON\1:951374

PA.5

# Pressure-Gain Combustion for Gas Turbines

Randall S. Gemmen
George A. Richards
Michael C. Janus
Morgantown Energy Technology Center

## ABSTRACT

As part of the Department of Energy's *Advanced Gas Turbine Systems Program*, an investigation has been performed to evaluate "pressure-gain" combustion systems for gas turbine applications. Results from the investigation have shown that, due to the oscillatory combustion process, a pressure boost can be achieved for suitable combustor geometries. The pressure gains achieved thus far have been as high as 1 percent. It has also been shown that for some combustor designs operating under typical gas turbine conditions, $NO_x$ and CO emissions are about 30 ppmv and 8 ppmv, respectively. It is believed that with optimized designs, further improvements in both pressure gain and emissions may be possible. We have concluded that this technology remains a candidate for improving the efficiency of a gas turbine while reducing pollutant emissions.

## OBJECTIVES

This research supports the Department of Energy's *Advanced Gas Turbine Systems Program.* The goal of this program is to increase cycle efficiencies and to reduce pollutant emissions of utility and industrial gas turbine power generating systems. The objectives of the work reported here are to (1) determine how pressure gain can be achieved in combustion systems; (2) determine pressure effects for pressure-gain systems; and (3) evaluate their pollutant performance. Since such pressure-gain systems necessarily impose unsteadiness to the gas flow through a gas turbine, the ability to minimize such unsteadiness outside the combustor is also assessed.

## BACKGROUND

Several investigators have studied combustion systems capable of producing pressure gain: Thring (1961), Porter (1958), and Kentfield (1988), to name a few. Designs have varied from piston-cylinder arrangements to those supporting a fluid mechanic resonance. In all cases, the fundamental feature that enables pressure gain to be achieved is the ability to burn fuel in a constant-volume manner. The closer a system imitates a constant-volume combustion process, the greater will be the achieved pressure gain during the combustion event. Hence, piston-cylinder combustion geometries can usually be expected to produce a greater pressure gain given their more constant volume combustion process, as compared to acoustic devices that experience greater volumetric expansion.

Figure 1 shows how the efficiency of a simple-cycle gas turbine can be increased with pressure gain. For a detailed theoretical analysis, see Gemmen et al. (1992). Here, the pressure gain is shown as percent increase from compressor exit stagnation pressure to turbine inlet stagnation pressure: $(P_c-P_t)/P_c*100$, where $P_c$ is the compressor exit pressure, and $P_t$ is the turbine inlet pressure. The figure is based on an analysis assuming thermodynamically ideal conditions for all components and a specific heat ratio of 1.4.

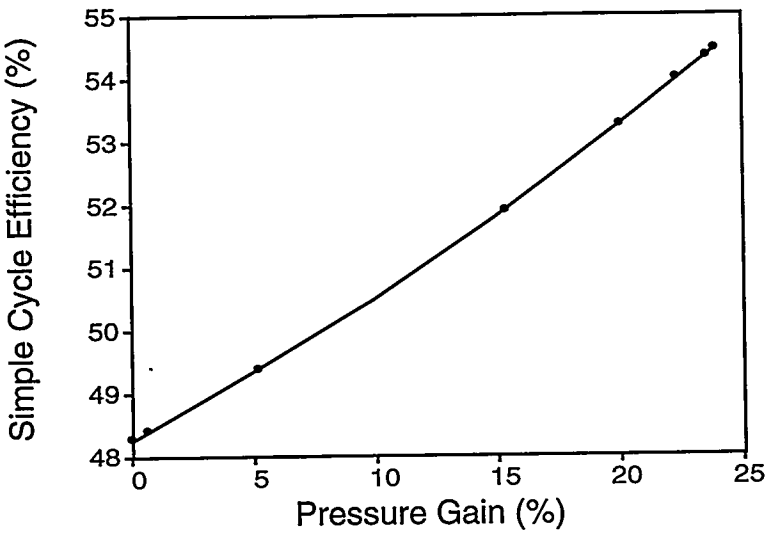


**Figure 1. Efficiency of a Simple-Cycle Gas Turbine Versus Pressure Gain**

The pressure ratio of the compressor stage was assumed to be 10, and the temperature ratio from the compressor inlet temperature to the end of the combustion process was assumed to be 4.5. Figure 1 shows that at the maximum pressure gain achieved (about 25 percent), the efficiency is more than 54 percent as compared to the ideal constant pressure cycle efficiency of about 48 percent. Hence, if the maximum pressure gain can be achieved, then a boost of nearly 6 percent can be obtained. Such a boost in efficiency can reduce fuel consumption by more than 12 percent for comparable systems. Such beneficial performance increases provide the motivation for this work.

## EXPERIMENTAL SETUP

Because resonating combustion systems can be designed without mechanically moving parts, our research has focused exclusively on these systems. Specifically, we have worked with aerovalve pulse combustors. These systems have been shown in prior work to support as great as 4 percent pressure increase (Kentfield and Fernandes 1990). The experimental research employed an atmospheric combustion rig as well as a pressurized combustion rig. Both systems have similar features, so only the atmospheric rig will be discussed here. A more detailed description of the pressurized rig has been reported (Gemmen et al. 1994). Figure 2 shows a typical configuration used for the atmospheric rig. Combustion air and fuel enter on the left at the inlet plenum. The combustion air enters directly into the inlet plenum, while the fuel is delivered to the combustor with typically a 1/8-inch diameter stainless steel tube. The combustion air and natural gas fuel mix inside the combustion chamber and ignite with the previous cycle's exhaust products. (No ignition source is required except for start-up.) The exhaust products exit out of the combustor through a tailpipe and enter the dilution plenum where they mix with dilution air. From the dilution plenum, the gas passes out through an 8-meter exhaust duct to the atmosphere. Thermocouples are used for temperature measurement at several locations over the combustor for wall and gas temperatures. The dynamic pressure inside the combustor is measured using a Kistler model #206 transducer. For the atmospheric rig, mean pressure differences across the combustor (pressure gain) and from inlet plenum into the combustion chamber are measured using either a water manometer or a Setra model #226 low-differential pressure gage.

## PRESSURE GAIN

The geometry that has produced the maximum pressure gain thus far in this work employs a flow rectification device taken after Kentfield and Fernandes (1990) and is shown in Figure 3. This geometry includes a by-pass tube that captures the reverse flow exiting out through the inlet. (Other geometries studied in our research that did not take advantage of the reverse flow energy showed poorer pressure-gain performance.) The by-pass tube included

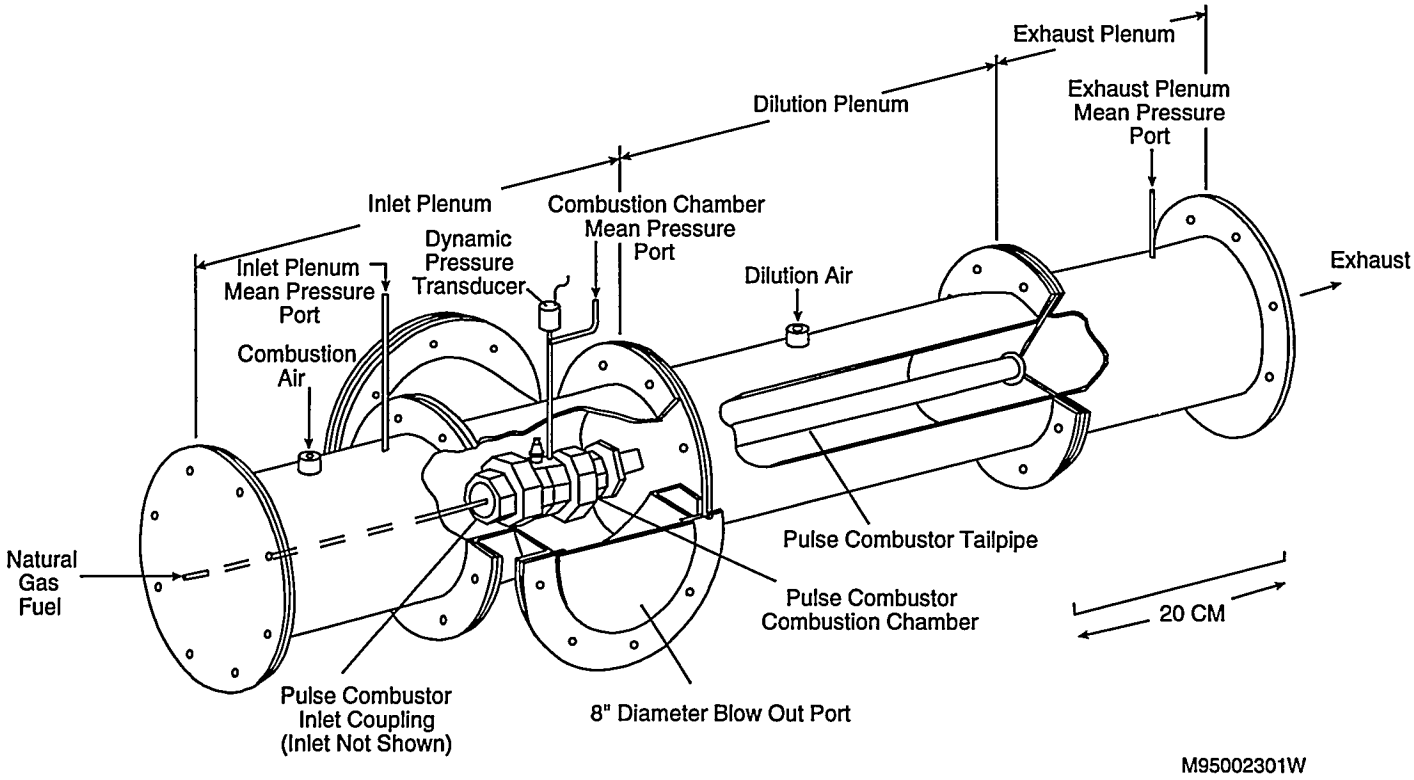


**Figure 2. Atmospheric Rig**

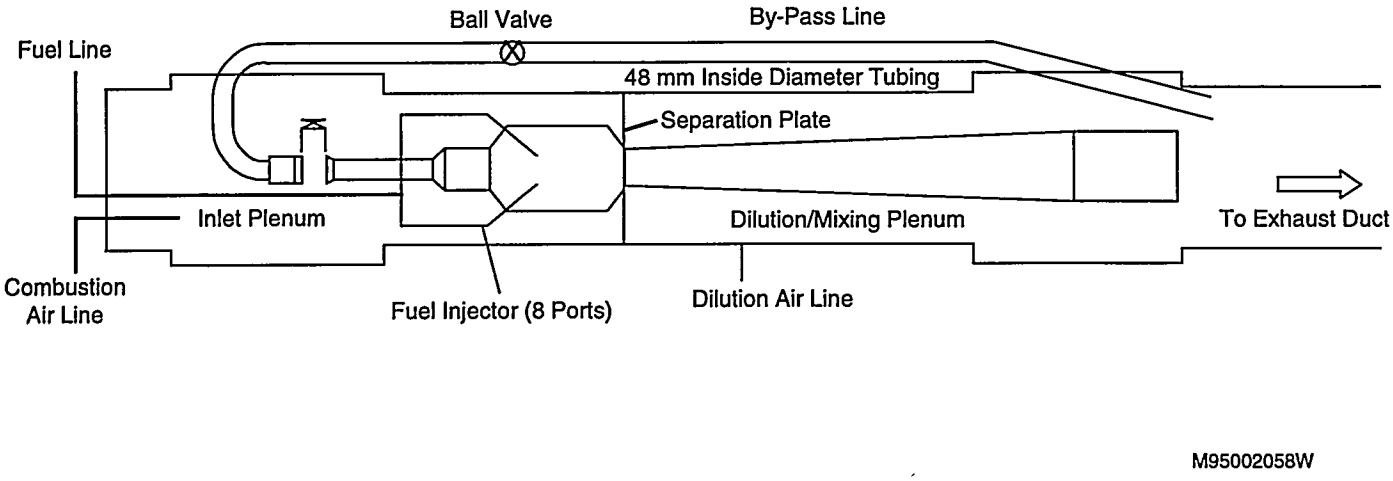


**Figure 3. Geometry With By-Pass Tube Producing 1 Percent Pressure Gain (After Kentfield and Fernandes 1990)**

a ball valve to control the flow rate of fluid through the by-pass. The separation between the by-pass tube and the inlet to the combustor was adjustable with a tube that slid over the by-pass tube. Some results from the experiments using this (somewhat crude) mode of rectification are shown in Figure 4. From other tests, it was determined that nearly 1 percent could be achieved. For this later case, the total air flow through the combustor and by-pass was 23 g/s and the fuel flow rate was 1.1 g/s. Through the use of gas sample data, it was determined that 33 percent of the air was passing through the by-pass, which produced a time average equivalence ratio inside the combustion chamber of 0.44.

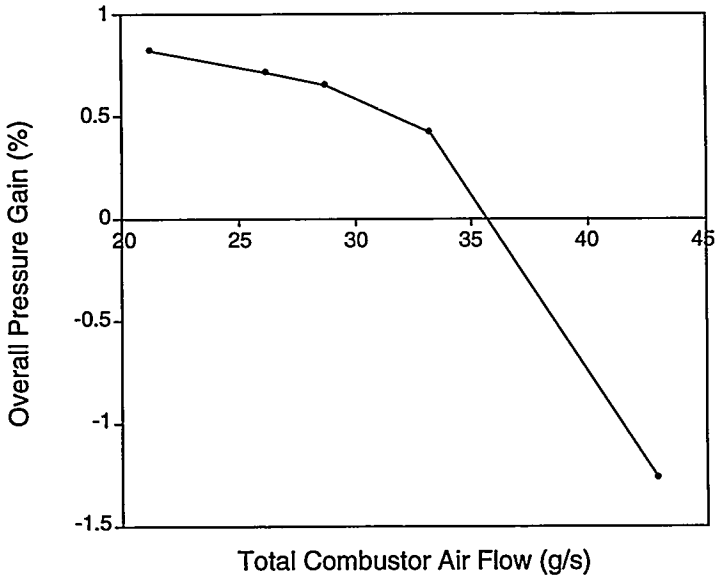


**Figure 4. Pressure Gain Versus Flow Rate for the Geometry Shown in Figure 3**

## POLLUTANT EMISSIONS

Not surprisingly, measurements of pollutant emissions depended strongly on combustor geometry. For geometries that did not use a by-pass tube, reasonable emissions of about 6 ppmv $NO_x$ and 50 ppmv CO could be

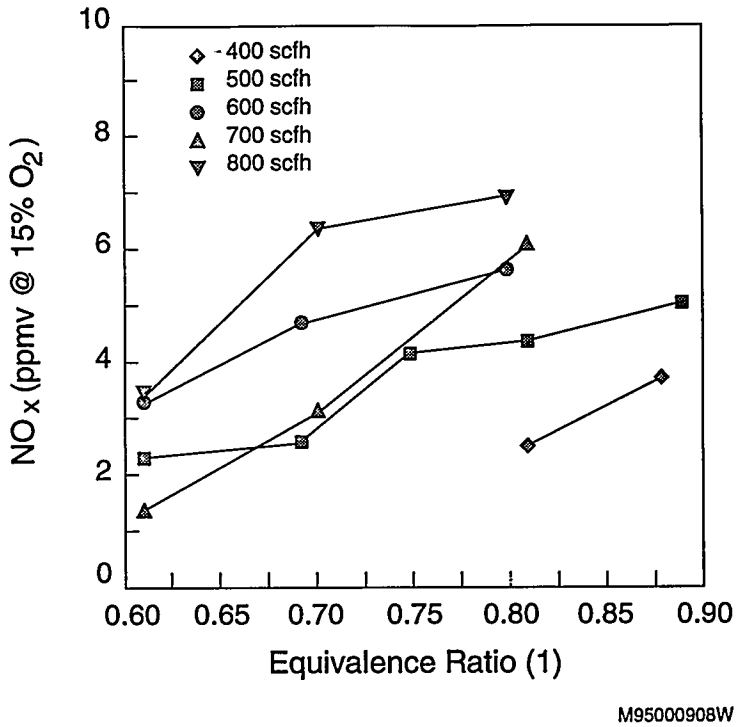


**Figure 5. $NO_x$ Versus Equivalence Ratio for a Combustor Operated at Atmospheric Pressure Without a By-Pass Tube**

expected for our atmospheric rig tests. (See Figures 5 and 6.) For the geometry shown in Figure 3, however, it was found that unburnt hydrocarbon (UHC) and CO emissions could be high in both tailpipe and by-pass flows -- about 175 ppmv and 1200 ppmv, respectively. $NO_x$ emissions were about 15 ppmv. Because the geometry of Figure 3 has not been optimized, these preliminary results should not be accepted as typical for this technology. Improvements discussed in the **Future Work** section explain the direction that needs to be taken.

## PRESSURE EFFECTS

The effect of mean operating pressure on overall pressure gain can be determined by extending the work reported in Gemmen et al.

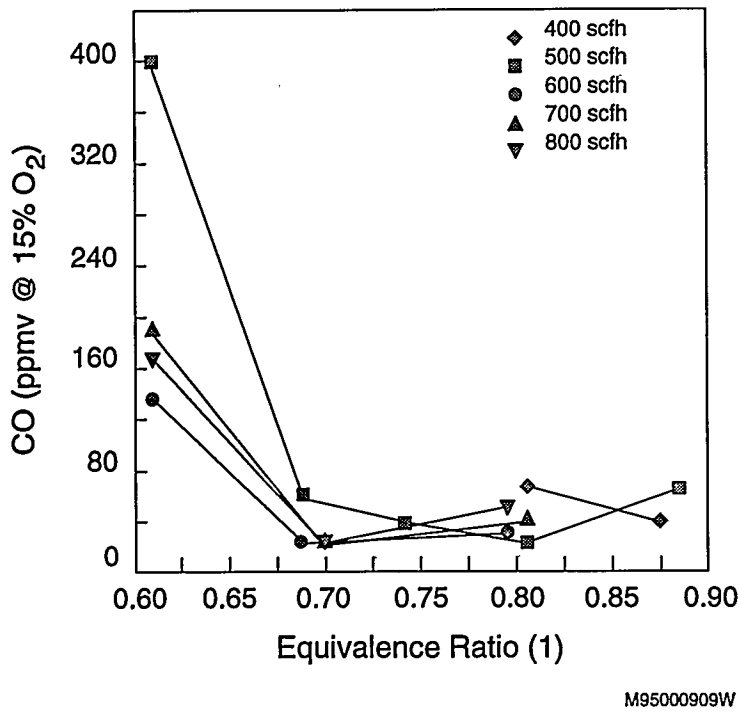


**Figure 6. CO Versus Equivalence Ratio for a Combustor Operated at Atmospheric Pressure Without a By-Pass Tube**

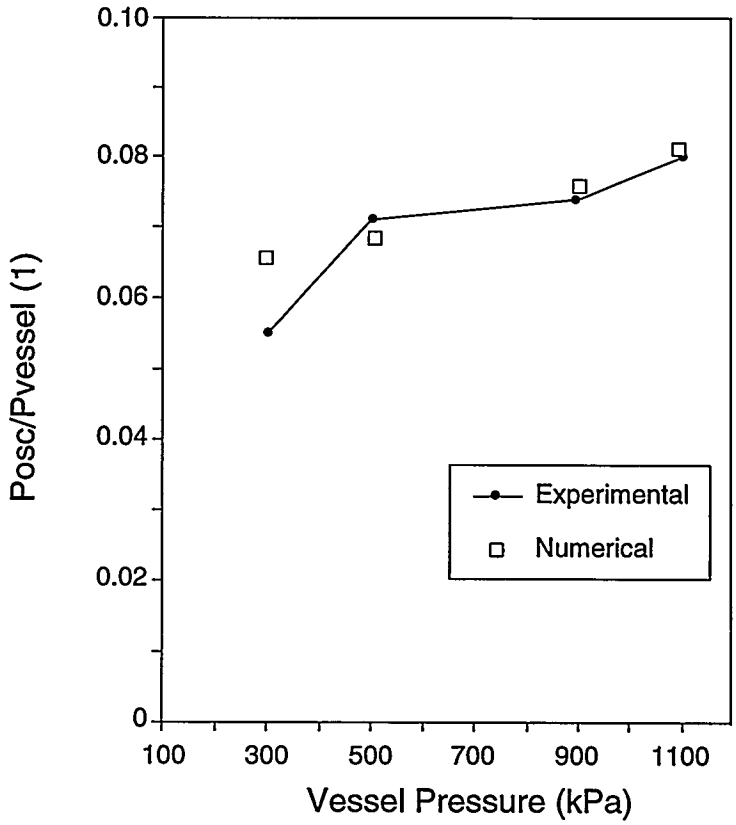


**Figure 7. Normalized Pressure Gain Achieved Across the Inlet to the Combustor Versus Operating Pressure**

(1994). In this work, single, non-rectified, combustor geometries were studied. There it was reported that the pressure gain achieved across the inlet to the combustor (normalized by operating pressure) increases slightly as operating pressure increased. (See Figure 7.) Such results can be predicted from the work of Narayanaswami and Richards (1994). They show that when the governing equations are suitably normalized, combustion operation (including pressure gain) is nearly insensitive to operating pressure. This result is especially true at high pressure where surface effects (friction and heat transfer) are of less significance.

Gemmen et al. (1994) prove that pollutant emissions for these highly unsteady combustion systems scale with pressure in the same manner as steady constant pressure combustion systems. In particular, $NO_x$ shows a $P^{0.28}$ effect and CO shows a $P^{-1.17}$ effect. This is similar to the results reported by Rizk and Mongia (1993). Such results are beneficial for extending aerovalve pulse combustor results at low pressure to any other operating pressure.

## WAVE ATTENUATION

As mentioned previously, all pressure-gain combustion systems necessarily require unsteady flow processes. It is important for purposes of reliability that any unsteadiness

caused by such combustion systems does not adversely affect the gas turbine system. Current steady flow gas turbine systems show about a 0.1 to 0.5 psi oscillation (Brandt and Wesorick 1994). To determine what might be expected for pressure-gain systems, the FLUENT computational fluid dynamics code was used for the problem shown in Figure 8. For this problem, FLUENT predicted the oscillation that could occur for a dual combustion system operating in-phase and anti-phase. It was shown that nearly a 90 percent reduction in pressure oscillation may be possible. Preliminary experimental data taken with two combustion systems operating anti-phase confirm that significant attenuation can be achieved. The magnitude of oscillation that remained downstream of the two combustors was about 0.024 psi for the atmospheric test. If scaled to 10 atmospheres, the expected oscillation amplitude would be about 0.24 psi. Hence, a negative impact to reliability can be avoided.

## FUTURE WORK

Overall, we have been encouraged by the magnitude of pressure gain that these systems are capable of producing (1 percent gain versus 4 percent pressure loss in current designs). Such pressure-gain capability can be expected to produce a 1 percent boost in cycle efficiency compared to current systems. Based on our overall research program, we are confident that further increases in pressure gain are possible as well as reduced pollutant emissions. To achieve this performance, a dual combustion system such as that shown in Figure 9 is proposed. In this design, all fuel is converted inside a high-temperature flow path, thereby significantly reducing the pollutant formation produced by the by-pass design of Figure 3. In addition, since both flow paths experience a pressure boost, increased pressure gain above the design shown in Figure 3 can be expected. Furthermore, when operating anti-phase, minimal wave energy will exist outside the combustion system.

To further progress in this area, the Morgantown Energy Technology Center is looking for an industrial gas turbine partner to supply a low-pressure ratio turbine and to mutually investigate the actual benefits possible with this technology.

## REFERENCES


Brandt, D.E., and R.R. Wesorick, 1994, "GE Gas Turbine Design Philosophy," GER-3434D.

Gemmen, R.S., S.D. Woodruff, G.A. Richards, and W.A. Rogers, 1992, "Pressure Gain Combustion," DOE/METC Report C-93/7050.

Gemmen, R.S., G.A. Richards, and M.C. Janus, 1994, "Development of a Pressure Gain Combustor for Improved Cycle Efficiency," DOE/METC Report C-94/7141, also presented at the ASME COGEN Turbo Power '94 Congress and Exposition, IGTI-Vol.

Gemmen, R.S., M.C. Janus, G.A. Richards, T.S. Norton, and W.A. Rogers, 1995, "Achieving Improved Cycle Efficiency Via Pressure Gain Combustors," DOE/METC Report C-95/7183, also to be presented at the ASME '95 Turbo Expo Power Conference and Exposition.

Kentfield, J.A.C., 1988, "The Feasibility, from an Installation Viewpoint, of Gas Turbine Pressure-Gain Combustors," ASME paper 88-GT-181.

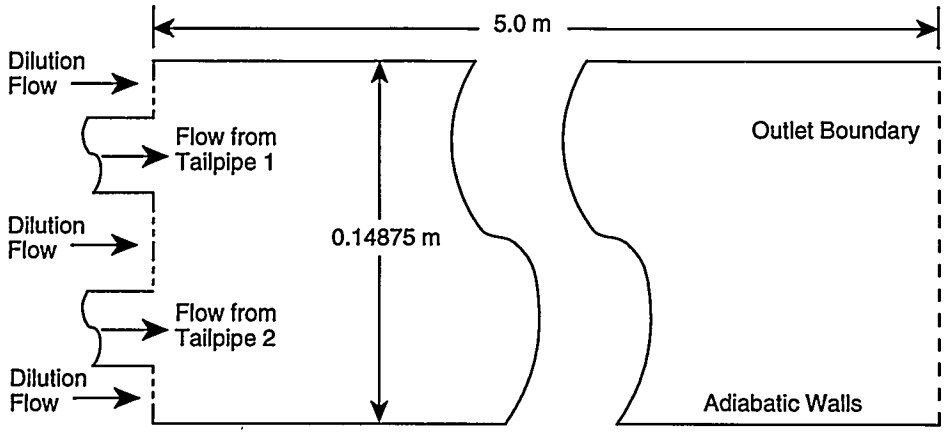


Operating Pressure: 10 atm
Dilution Flow : Steady, Velocity = 30 m/s, Temperature = 600K
Flow from Tailpipe 1: Velocity = 100 + 50sin ($\omega t + \phi$) m/s; Temperature = 1400 K
Flow from Tailpipe 2: Velocity = 100 + 50sin ($\omega t$) m/s; Temperature = 1400 K
Tailpipe Height = 0.04 m
Grid: 202 cells x-direction x 30 cells y-direction

M95002054W

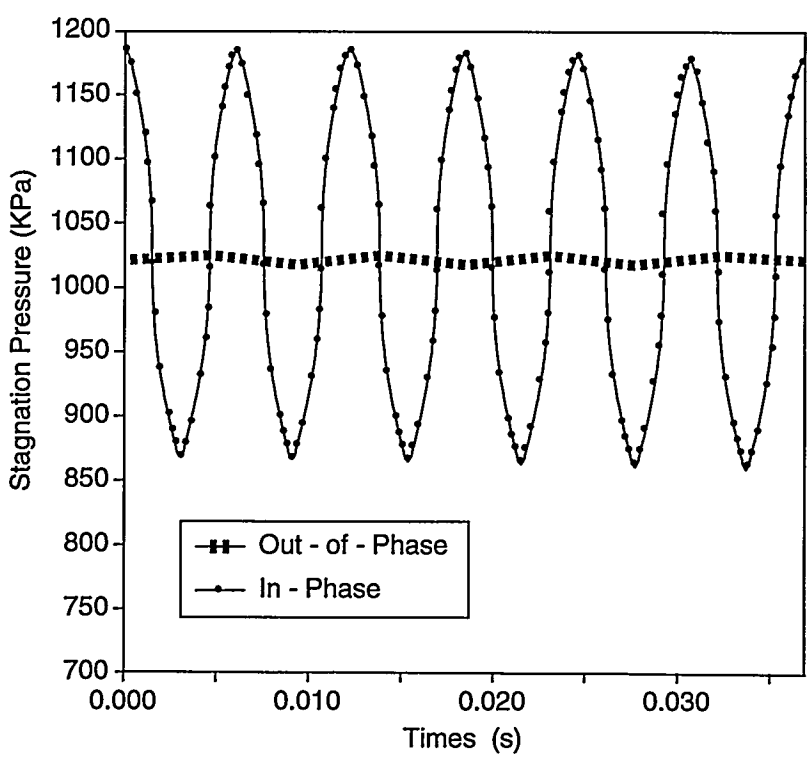


M95002308W

**Figure 8. FLUENT Simulation of a Dual Combustor for Wave Attenuation**

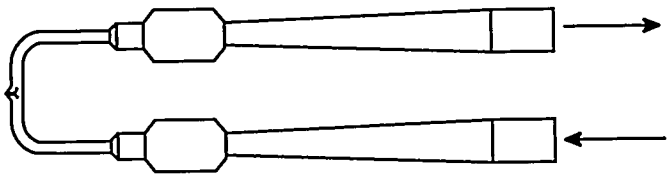

**Figure 9. Example Dual Combustion System Proposed for Future Work to Achieve Maximum Pressure Gain and Reduced Pollutant Emissions**


Kentfield, J.A.C., and L.C.V. Fernandes, 1990, "Improvements to the Performance of a Prototype Pulse, Pressure-Gain, Gas Turbine Combustor," J. Eng. for Gas Turbines and Power, 112, pp. 67-72.

Narayanaswami, L.L., and G.A. Richards, 1994, "Pressure-Gain Combustion. Part 1: Model Development," Submitted to ASME J. Engineering for Gas Turbines and Power.

Porter, C.D., 1958, "Valveless-Gas-Turbine Combustors with Pressure Gain," ASME paper 58-GTP-11.

Rizk, N.K., and H.C. Mongia, 1993, "Semianalytical Correlations for $NO_x$, CO, and UHC Emissions," J. Eng. for Gas Turbines and Power, 115, pp. 612-619.

Thring, M.W. (Ed.), 1961, *Pulsating Combustion--The Collected Works of F. H. Reynst,* Pergamon Press, Oxford.


RGEMME\1:951269

PA.6

# Hot-Gas Filter Testing With the Transport Reactor Demonstration Unit

## CONTRACT INFORMATION

**Cooperative Agreement No.** DE-FC21-93MC30097

**Contractor** University of North Dakota
Energy & Environmental Research Center
Box 9018, University Station
Grand Forks, North Dakota 58202
(701) 777-5000

**Contractor Program Manager** Michael D. Mann

**Principal Investigators** Michael L. Swanson
Robert O. Ness
Jay S. Haley

**METC Project Manager** Rich Dennis

**Period of Performance** January 1, 1995 to December 31, 1996

**Schedule and Milestones**

**FY95/96 Program Schedule**

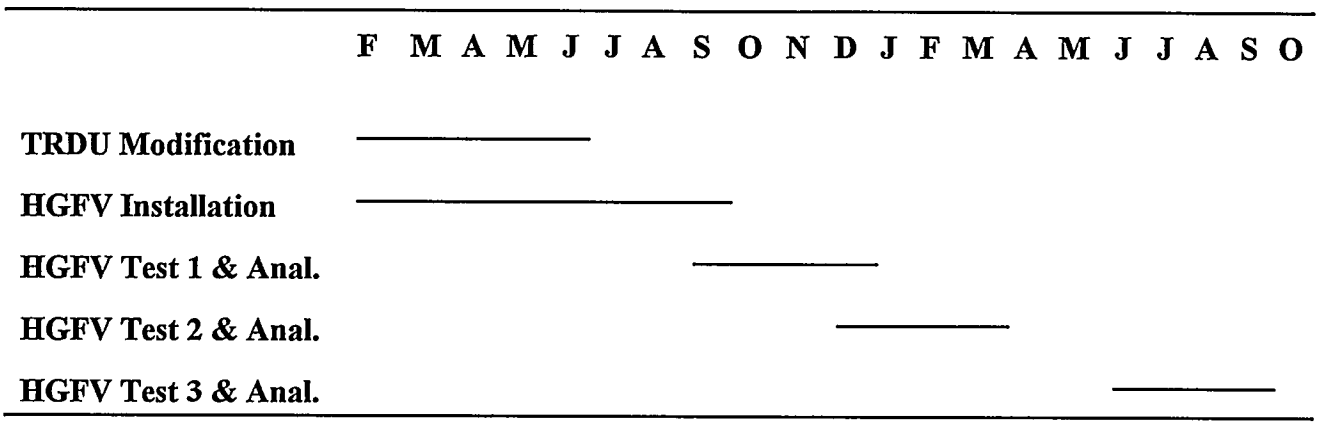


## OBJECTIVES

The objectives of the hot-gas cleanup (HGC) work on the transport reactor demonstration unit (TRDU) located at the Energy & Environmental Research Center (EERC) is to demonstrate acceptable performance of hot-gas filter elements in a pilot-scale system prior to long-term

demonstration tests. The primary focus of the experimental effort in the 2-year project will be the testing of hot-gas filter element performance (particulate collection efficiency, filter pressure differential, filter cleanability, and durability) as a function of temperature and filter face velocity during short-term operation (100–200 hours). This filter vessel will be utilized in combination with the TRDU to evaluate the performance of selected hot-gas filter elements under gasification operating conditions. This work will directly support the power systems development facility (PSDF) utilizing the M.W. Kellogg transport reactor located at Wilsonville, Alabama (1) and, indirectly, the Foster Wheeler advanced pressurized fluid-bed combustor, also located at Wilsonville (2, 3).

## BACKGROUND INFORMATION

The U.S. Department of Energy (DOE) Morgantown Energy Technology Center (METC) has a HGC program intended to develop and demonstrate gas stream cleanup options for use in combustion- or gasification-based advanced power systems. One objective of the METC HGC program is to support the development and demonstration of barrier filters to control particulate matter. The goal is not simply to meet current New Source Performance Standards (NSPS) with respect to particulate emissions, but also to protect high-efficiency gas turbines and control particulate emissions to low enough levels to meet more stringent regulatory requirements anticipated in the future. DOE-METC is investing significant resources in the PSDF under a Cooperative Agreement with Southern Company Services, Inc. (SCS). The Wilsonville facility will include five modules, including an advanced gasifier module and a hot-gas cleanup module. The gasifier module involves the M.W. Kellogg transport reactor technology for both gasification and combustion (4, 5). Several other demonstration-scale advanced power systems that will also utilize hot-gas particulate cleanup technology will benefit indirectly from this research. These systems include the Clean Coal IV Piñon Pine IGCC Power Project located at the Sierra Pacific Power Company's Tracy Station near Reno, Nevada.

The TRDU was built and operated at the EERC under Contract No. C-92-000276 with Southern Company Services, Inc. The M.W. Kellogg Company designed and procured the reactor and provided valuable on-site personnel for start-up and during operation. The Electric Power Research Institute (EPRI) was involved in establishing the program and operating objectives with the EERC project team.

The purpose of the previous program was to build a reactor system larger than the transport reactor test unit (TRTU) located in Houston, Texas, in support of the Wilsonville PSDF transport reactor train. The program was to address design and operation issues for the Wilsonville unit and also help develop information on the operation of the unit to decrease start-up costs.

The TRDU (200-lb/hr coal–limestone feed rate) now provides an intermediate scale to the TRTU (up to 10-lb/hr coal–limestone feed rate) and the Wilsonville Transport Reactor (3400-lb/hr feed rate). Some of the design, construction, start-up, and operational issues for the Wilsonville transport train were addressed during this project.

Five test periods were completed in the TRDU using Wyodak subbituminous coal. These were shakedown tests, which included cold and hot solids circulation, coal combustion, and coal gasification. The TRDU operated under solids circulation for a period of 256 hr, coal combustion for 46.5 hr, and coal gasification for 34 hr. Data

from four steady-state gasification periods (a total of approximately 18 hr) were analyzed (6, 7).

The four major design criteria that were established by EPRI were met. These included coal feed rate, operating pressure, carbon conversion, and high heating value of the product gas. Major accomplishments included showing that the TRDU performed well hydrodynamically, that it had the ability to switch from combustion mode to gasification mode easily and safely, that solids could be fed to and removed from the system, and the J-leg/standpipe and cyclone performed according to their design specifications. The staged char combustion mixing zone design was not verified because of the lack of nonvolatile char and a reduced operational schedule. This resulted in oxygen breakthrough from the mixing section into the riser as a result of insufficient carbon inventory in the circulating solids.

## PROJECT DESCRIPTION

This program has a phased approach involving modification and upgrades to the TRDU and the fabrication, assembly, and operation of a hot-gas filter vessel capable of operating at the outlet design conditions of the TRDU. The TRDU is a 200–300-lb/hr pressurized circulating fluid-bed gasifier similar to the gasifier being tested at the Wilsonville facility. The TRDU has an exit gas temperature of up to 980°C (1800°F), a gas flow rate of 300 scfm, and an operating pressure of 120–150 psig. Phase I will include upgrading the TRDU based upon past operating experiences. Additions will include a nitrogen supply system upgrade, upgraded LASH (lime ash) auger and coal feed lines, adding a second pressurized coal feed hopper, and a dipleg ash hopper, and modifications to spoil the performance of the primary cyclone.

The TRDU system can be divided into three sections: the coal feed section, the TRDU, and the product recovery section. The TRDU proper, as shown in Figure 1, consists of a riser reactor with an expanded mixing zone at the bottom, a disengager, and a primary cyclone and standpipe. The standpipe is connected to the mixing section of the riser by a J-leg transfer line. All of the components in the system are refractory-lined and designed mechanically for 150 psig and an internal temperature of 1090°C (2000°F). Table 1 summarizes the operational performance for the TRDU under the previous contract (6).

The premixed coal and limestone feed to the transport reactor can be admitted through three nozzles, which are at varying elevations. Two of these nozzles are located near the top of the mixing zone (gasification), and the remaining one is near the bottom of the mixing zone (combustion). During operation of the TRDU, feed is admitted through only one nozzle at a time. The coal feed is measured by an rpm-metering auger. Oxidant is fed to the reactor through two pairs of nozzles at varying elevations within the mixing zone. For the combustion mode of operation, additional nozzles are provided in the riser for feeding secondary air. Hot solids from the standpipe are circulated into the mixing zone where they come into contact with the oxidant and the steam, which is injected into the J-leg. This feature enables spent char to contact oxidant and steam prior to the fresh coal feed. This staged gasification process is expected to enhance the process efficiency. Gasification or combustion and desulfurization reactions are carried out in the riser, as coal, sorbent, and oxidant (with steam for gasification) flow up the tube. The solids circulation into the mixing zone is controlled by the solids level in the standpipe.

The riser, disengager, standpipe, and cyclones are equipped with several internal and skin

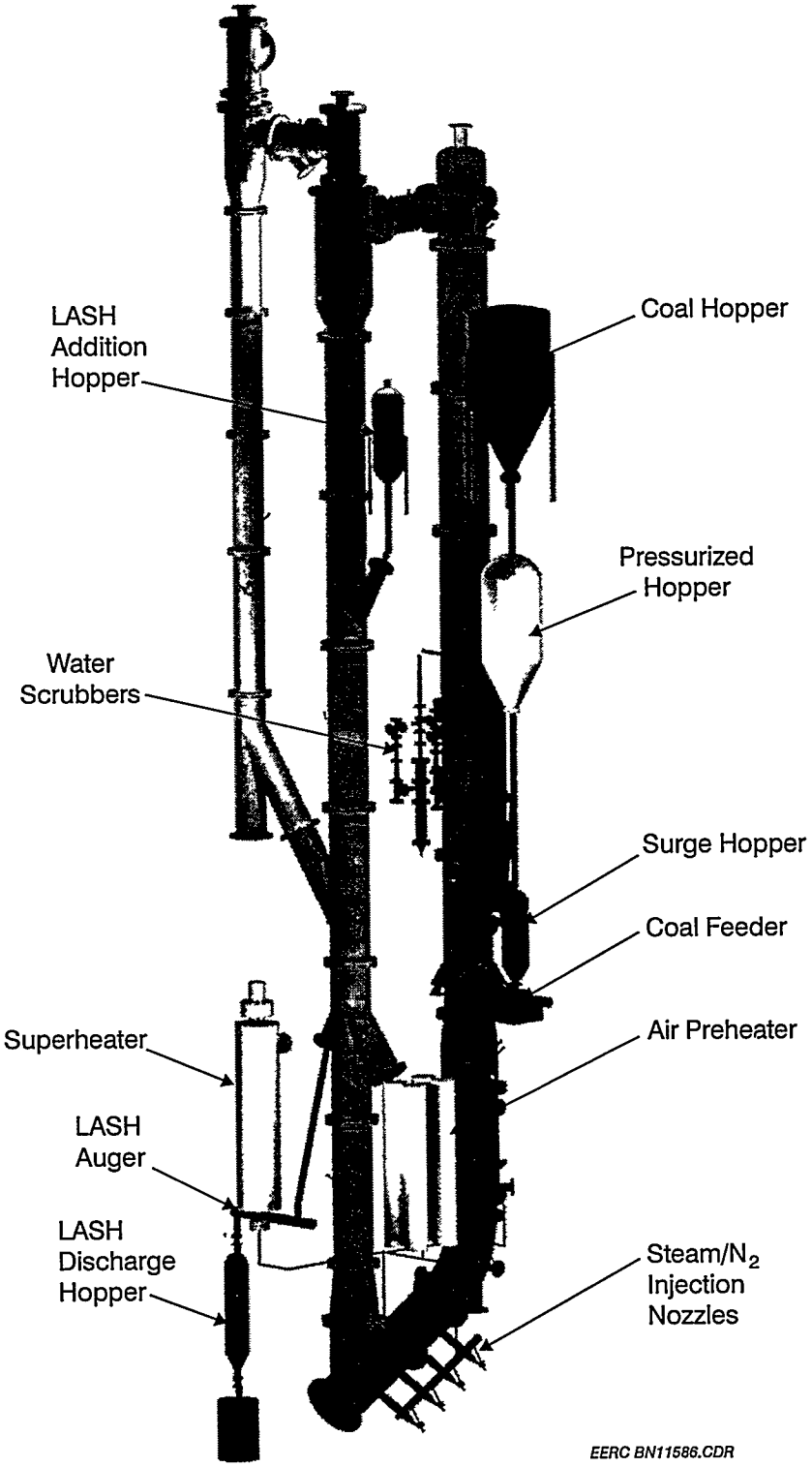


**Figure 1. TRDU in EERC Gasification Tower**

**Table 1. TRDU Operational Parameters**

| Parameter | Actual Operating Condition[1] |
|---|---|
| Coal | Wyodak |
| Moisture Content, % | 20 |
| Pressure, psig | 117–122 |
| Steam:Coal Ratio | 0.38 |
| Air:Coal Ratio | 3.5–4.7 |
| Ca:S Ratio, mole | 1.5 |
| Air Inlet Temperature, °C | 425 |
| Steam Preheat, °C | 390 |
| Coal Feed Rate, lb/hr | 173 |
| Gasifier Temperature, maximum °C | 850 |
| ΔT, maximum °C | 121 |
| Conversion, % | 96 |
| High Heating Value of Fuel Gas, Btu/scf | 104 |
| Heat Loss as Coal Feed, % | 27 |
| Riser Velocity, ft/sec | 28–30 |
| Heat Loss, Btu/hr | 420,000[2] |
| Standpipe Superficial Velocity, ft/sec | 0.4–0.54 |

[1] Steady-state conditions were not achieved.
[2] Estimated heat loss; steady-state conditions were not achieved.

thermocouples. Nitrogen-purged pressure taps are also provided to record differential pressure across the riser, disengager, and the cyclones. The bulk of entrained solids leaving the riser is separated from the gas stream in the disengager and circulated back to the riser via the standpipe. A solids stream is withdrawn from the standpipe via an auger to maintain the system's solids inventory. Gas exiting the disengager enters a primary cyclone that has been modified to provide variable particulate collection performance. Solids from diplegs of the primary cyclone are collected in a lock hopper. Gas exiting this cyclone enters a jacketed pipe heat exchanger before entering the HGC filter vessel. The cleaned gases leaving the HGC filter vessel enter a quench system before being depressurized and vented to a flare.

The quench system uses a sieve tower and two direct-contact water scrubbers to act as heat sinks and to remove impurities. All water and organic vapors are condensed in the first scrubber, with the second scrubber capturing entrained material and serving as a backup. The condensed liquid is separated from the gas stream in a cyclone that also serves as a reservoir. Liquid is pumped either

to the shell-and-tube heat exchanger for reinjection into the scrubber or down to the product receiver barrels.

**Hot-Gas Filter Vessel (HGFV)**

A new hot-gas filter program was started in January 1995 as an addition to the METC Cooperative Agreement entitled Subtask 3.13 – Hot-Gas Filter Testing. This new subtask has also supported upgrades to the TRDU and will support three 200-hour filter tests in the next 21 months. First-year funding was made available in March 1995 and has supported upgrades to the TRDU, installation of the new filter vessel and new inlet–outlet piping requirements, and will support one 200-hour filter test if initial shakedown of the TRDU demonstrates acceptable performance after the upgrades have been completed. The preliminary filter design criteria are summarized in Table 2.

This vessel is designed to handle all of the gas flow from the TRDU at its expected operating conditions. The vessel will be approximately 48 in. ID and 185 in. long and would be designed to handle gas flows of approximately 325 scfm at temperatures up to 980°C (1800°F) and 130 psig. The refractory will have a 28-in. ID with a shroud diameter of approximately 24 in. The shroud diameter might change, depending on the results from some computational fluid dynamic calculations that are currently being performed, but is not expected to change significantly. The vessel is sized such that it could handle candle filters up to 1.5 m long; however, 1-m candles are expected to be utilized in the initial 540°C (1000°F) gasification tests. Candle filters are projected to be 2.375 in. OD and would have a minimum 4 in. center line-to-center line spacing. It has been recommended to go with an even larger candle spacing. The total amount of 1-m candles that could be mounted in the current geometry of the HGFV tubesheet is 19. With this number of candles, it would be possible to go to a candle spacing as large 4.25 in. in our filter vessel.

This would enable filter face velocities as low as 2.5 ft/min to be tested. Phases III through V consist of 200-hr hot-gas filter tests under gasification conditions using the TRDU with the HGC operating at temperatures of 540°–650°C (1000°–1200°F), 120 psig, and increasing face velocities for each test. Higher face velocities would be achieved by using fewer candles. The preliminary test matrix would be to perform the first test at 540°–650°C (1000°–1200°F), 120 psig, 2.7 ft/min face velocity for the first test. The second test would remove six candles to increase the face velocity to approximately 4.0 ft/min at the same operating temperature and pressure. The openings for the six removed candles would simply be blanked off. If this test were successful, the third test would remove another six candles, seal off the candle openings, and repeat the procedure. The filter face velocity would increase up to 7.5 ft/min It has been proposed to look at seven Industrial Filter & Pump (IF&P) Fibrosic candles along with their ceramic tubesheet. Six ceramic fiber candles from the 3M company would also be tested, along with six metal candles from Pall Advanced Separation Systems Corporation.

Because an existing vessel could not meet our cost limitations or the size constraints dictated by the gasification tower space, a new filter vessel was purchased. The design specifications were for a metal temperature of 425°C (800°F) and operating pressures of up to 150 psi. A drawing of the new vessel design is presented in Figure 2. The anticipated delivery date for the new vessel is late June 1995. Installation of filter vessel and piping runs to and from the hot-gas filter vessel are expected to be completed by September 1, 1995, with leak checking and shakedown testing of components occurring in the first few weeks of

**Table 2. Design Criteria for the Pilot-Scale Hot-Gas Filter Vessel**

| | |
|---|---|
| Range of Operating Conditions | |
| Inlet Gas Temperature | 540°–980°C (1000°–1800°F) |
| Operating Pressure | 120–150 psig |
| Volumetric Gas Flow | 325 scfm |
| Number of Candles | 19 (1 or 1.5 m) |
| Candle Spacing | 4.25 in. ℄ to ℄ |
| Filter Face Velocity | 2.5–10 ft/min |
| Particulate Loading | <10,000 ppm |
| Temperature Drop Across HGFV | < 30°C (50°F) |
| Nitrogen Backpulse System | Unheated |

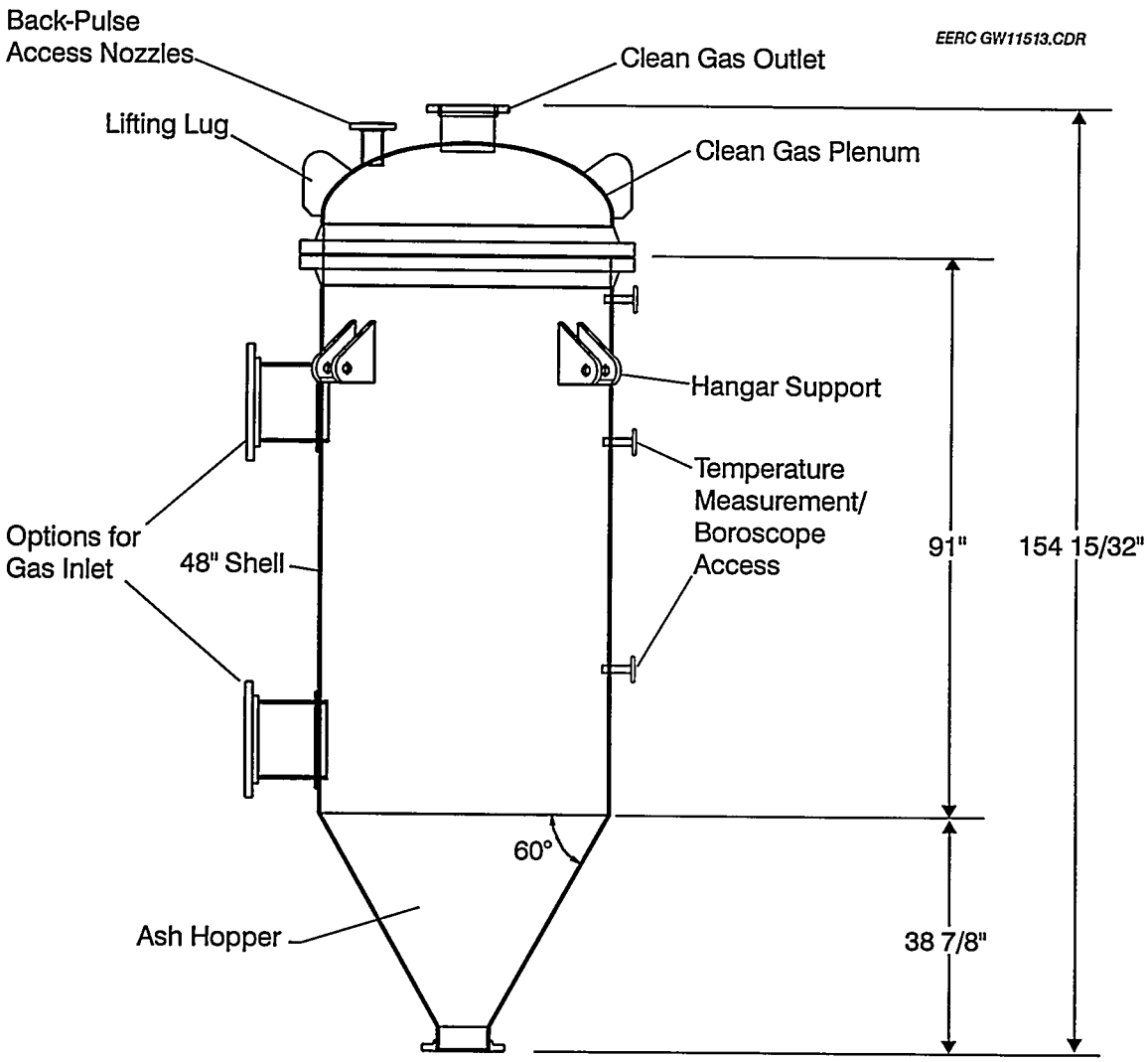


**Figure 2. Schematic of the New Filter Vessel Design**

September, followed by an 200-hr gasification test on Wyodak subbituminous coal with operation of the filter vessel by the end of September.

Ports have been added in the filter vessel for allowing temperature and pressure measurements to be obtained and for the insertion of a water-cooled boroscope probe for inspecting candle filters on-line. The ash letdown system consists of two sets of alternating high-temperature valves with a cylindrical pressure vessel to act as a lock hopper. Additionally, a preheat natural gas burner will be required to prevent condensation from collecting in the vessel while the gasifier is starting up. The hot gas from the burner will enter the vessel via a nozzle inlet separate from the dirty gas.

The nitrogen backpulse system will be constructed to backpulse up to four sets of four or five candle filters in a time-controlled sequence. Because of cost limitations, the backpulse nitrogen will not be capable of being heated to more than ambient temperatures. The pulse length and volume of nitrogen displaced into the filter vessel is controlled by the regulated pressure (up to 800 psig) of the nitrogen reservoir and the solenoid valves used to control the timing of the gas pulse. Figure 3 depicts the preliminary filter vessel location in the gasifier tower and piping requirements for its future use in conjunction with the TRDU. Since the first series of gasification tests are to be completed in the 540°–650°C (1000°–1200°F) range, a length of heat exchanger is utilized to drop the gas temperature to the desired range. Inserting an existing set of high-temperature valves in the fuel gas heat exchanger will allow bypassing the filter vessel during start-up and shakedown of the TRDU and enable switching to the preheated filter vessel when steady-state conditions are achieved. In addition, sample ports for obtaining particulate and hazardous air pollutant (HAP) samples have been added.

TRDU operation and filter element testing will benefit other ongoing projects at the EERC. The first sampling and analysis activities will be conducted to generate HAPs data concerning trace metal transformations, speciation of mercury, and metal concentrations at selected points within the TRDU and HGC in support of a project entitled "Trace Element Emissions" funded by METC. In addition, materials and ash data concerning the high-temperature filter media and ash interactions will be collected in support of a project entitled "Hot-Gas Filter Ash Characterization" jointly funded by METC and EPRI. While the cost of this specific data collection will be covered by the individual projects, the synergy that results from the integration of these projects will minimize the cost for collecting this information for all involved projects.

**High-Pressure and High-Temperature Sampling System**

The high-pressure and high-temperature sampling system (HPHTSS) was designed to extract dust-laden flue gas isokinetically from either an oxidizing or reducing environment. The maximum design temperature of the gas stream is specified as 980°C (1800°F) for the HPHTSS. The maximum working pressure of the gas stream for the HPHTSS is specified as 150 psig.

The probe for the HP is a 3/8-in.-OD and 1/8- in.-ID 304 stainless steel tube. The probe is used for only one sampling test and then discarded. The key to the sampling system is the use of a vessel, designed to withstand high-pressure and high-temperature conditions, to enclose the low- pressure sampling devices.

The vessel was constructed of 5-in. Schedule 80 pipe and fitted with raised face 300-lb flanges. The material used for the HPHTSS pressure vessel was 316L stainless steel. The HPHTSS was

designed to house both multicyclone assemblies with backup filter and a backup filter alone.

The principle of operation is to pressurize the outside of the sampling device (i.e., multicyclone assembly or backup filter) with nitrogen at a slightly higher gas pressure then the system pressure of the flue gas. The pressure differential between the nitrogen gas within the pressure vessel and the flue gas within the sampling device will be maintained at less than 5 psig.

If the HPHTSS is operating in a reducing environment where the presence of organic vapors is a possibility, the pressure vessel is capable of operating at temperatures as high as 540°C (1000°F) and maintaining nitrogen gas pressures up to 150 psig. This will prevent the heavier organic vapors from condensing while passing through the particulate sampling assembly. Electric resistance heaters of sufficient wattage will be used to heat pressure vessel to specified temperatures.

Once the process gas exits the sampling assembly, the gas pressure is reduced through a throttling valve to approximately 50 psig. The throttling valve will also act as the flow control valve for the sampling system. A second valve

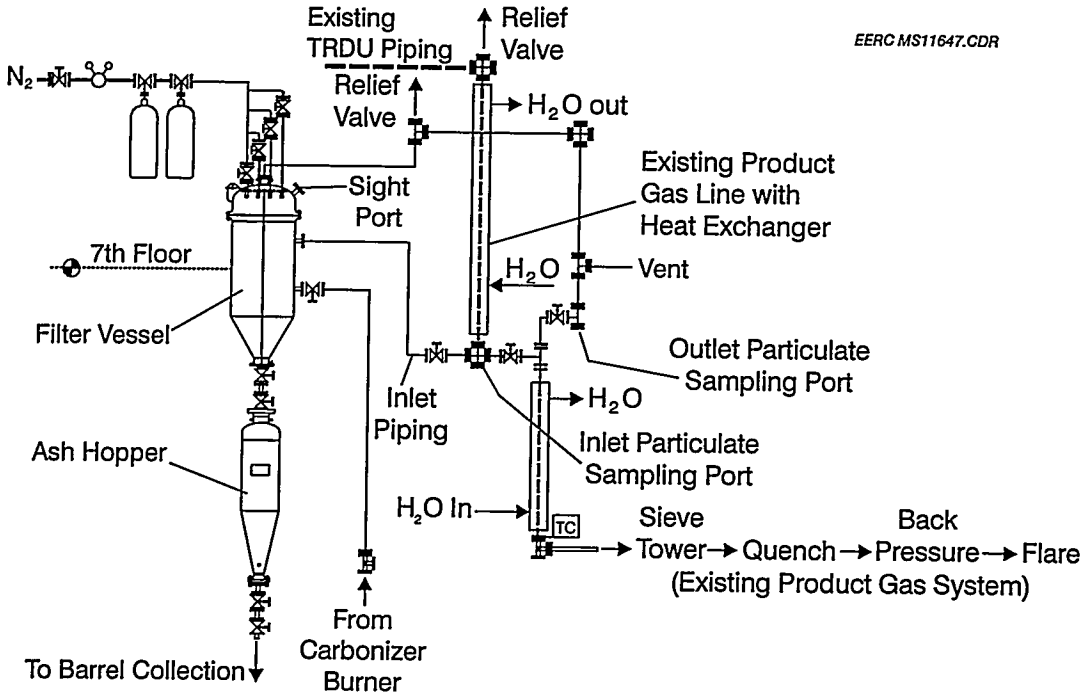


**Figure 3. Schematic Showing Additional High-Temperature, High-Pressure Piping Needed for Moderate-Temperature (540°–650°C) Filter Testing**

was installed in series in the event that the primary throttling valve failed to close.

After the throttling valve, the process gas is cooled through a set of impingers to remove moisture and organic vapors if present. A set of up to six impingers may be used in this sampling system. These impingers are rated for 200 psig at 120°C (250°F) maximum operating conditions. The impingers are made of 304 stainless steel, with the interior surfaces coated with teflon. The teflon-coated surfaces allow the HPHTSS to be used for trace metal sampling.

The dry gas is then throttled to atmospheric pressure and metered through a rotometer and orifice in order to measure total flow. The process gas then reenters the main gas stream for cleanup and disposal.

## FUTURE WORK

Future plans include some piping modifications to allow higher-temperature filter tests (at temperatures up to 980°C [1800°F]). With additional future funding, the design and installation of a waste heat recovery boiler would also allow the operation of the TRDU in a combustion mode.

## REFERENCES


1. Ness, R.O. "Transport Reactor Demonstration Unit," *In* Proceedings of the Coal-Fired Power Systems 93 – Advances in IGCC and PFBC Review Meeting; DOE/METC-93/6131 (DE93000289), June 1993; pp 357–358.

2. Sears, R.E.; Griswald, G.H.; Boyd, T.J.; Fankhanel, M.O.; Crumm, C.J.; Pontius, D.H. "Power Systems Development Facility, PFBC System Perspectives," *In* Proceedings of the Coal-Fired Power Systems 93 – Advances in IGCC, and PFBC Review Meeting; DOE/METC-93/6131 (DE93000289), June 1993; pp 121–128.

3. Rush, R.E.; Moore, D.L.; Haq, Z.U.; Pinkston, T.E.; Vimalchand, P.; McClung, J.D.; and Quandt, M.T. "Status of the Advanced PFBC at the Power Systems Development Facility," *In* Proceedings of the Coal-Fired Power Systems 94 – Advances in IGCC and PFBC Review Meeting; DOE/METC-94/1008 (DE94012252), June 1994; Vol. 1, pp 127–137.

4. Sears, R.E.; Griswald, G.H.; Kastner, C.E.; Pontius, D.H. "Hot Gas Cleanup Test Facility for Gasification and Pressurized Combustion," *In* Proceedings of the Twelfth Annual Gasification and Gas Stream Cleanup Systems Contractors Review Meeting; DOE/METC-92/6128, (DE93000228), Sept. 1992; Vol. 1, pp 53–63.

5. Dahlin, R.S.; Pontius, D.H.; Haq, Z.U.; Vimalchand, P.; Brown, R.; Wheeldon, J. "Plans for Hot Gas Cleanup Testing at the Power Systems Development Facility," *In* Proceedings of the 13th International Conference on Fluidized Bed Combustion; May 1995; Vol. 1, pp 449–459.

6. Rush, R.E.; Fankhanel, M.O.; Campbell, W.M. "Transport Reactor Development Status," *In* Proceedings of the Coal-Fired Power Systems 94 – Advances in IGCC and PFBC Review Meeting; DOE/METC-94/1008 (DE94012252), June 1994; Vol. 1, pp 73–82.

7. Ness, R.O. "Transport Reactor Demonstration Unit, Volume 1 – Final Report," EERC Publication No. 95-EERC-02-06, May 1995; 150 p.

PA.7

# High-Temperature Gas Stream Cleanup Test Facility

John S. Ontko
Ta-Kuan Chiang
Morgantown Energy Technology Center

## OBJECTIVES

The High-Temperature Gas Stream Cleanup Test Facility (HTGSCTF) at the Morgantown Energy Technology Center (METC) will, when completed, provide a versatile platform for testing novel hot gas filtration concepts. Its flexible modular design can provide filter developers with data to characterize filter behavior under statistically controlled conditions. With one module currently in shakedown and components of a second on site, ready for construction, the facility will soon be available for joint ventures with Cooperative Research and Development Agreement (CRADA) partners.

## BACKGROUND INFORMATION

Effective and economical hot gas particulate cleanup systems are essential to commercialization of advanced coal-fueled technologies. Pressurized Fluidized-Bed Combustion (PFBC) and the Integrated Gasification Combined Cycle (IGCC) require reliable particulate filtration both to ensure regulatory compliance and to protect expensive downstream components. To fully realize their inherent high thermal efficiencies, PFBC and IGCC filtration must be accomplished at elevated temperatures and pressures in an aggressive chemical environment. In addition, the pressure drop expended for filtration must not be excessive and the filters must have an acceptable life span. Thus aerodynamic, materials, and economic issues are all important to a successful design.

To aid in this effort, METC has undertaken the design and construction of a HTGSCTF. The facility's hardware and its capabilities are briefly described, followed by a discussion of the experimental methodology to be used.

## PROJECT DESCRIPTION

The HTGSCTF consists of two modules capable of independent or parallel operation. They may also be cross-connected, if desired, if both are operating under combustion conditions. Consideration is also being given to operating one module under reducing conditions with synthesized gasifier product gas (Syngas). Modules may be operated at any pressure from atmospheric to the 550 kPa (80 psia) design pressure.

Both modules are controlled by two computer systems: one handles process monitoring and control, and the other is dedicated to high-speed data acquisition and control of the back pulse filter cleaning system. Process control may also be effected manually from the control room. Figure 1 is a schematic diagram showing

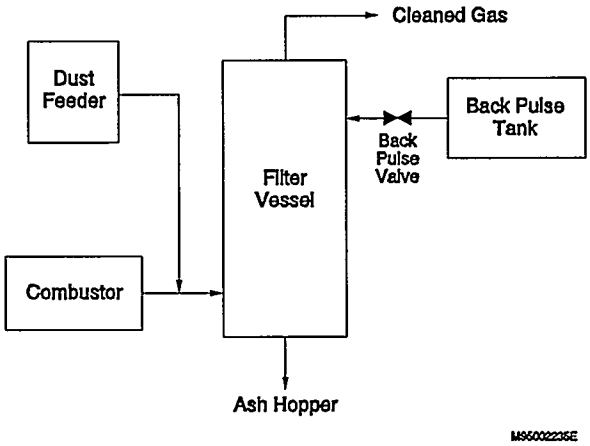


**Figure 1. HTGSCTF Module Schematic Diagram**

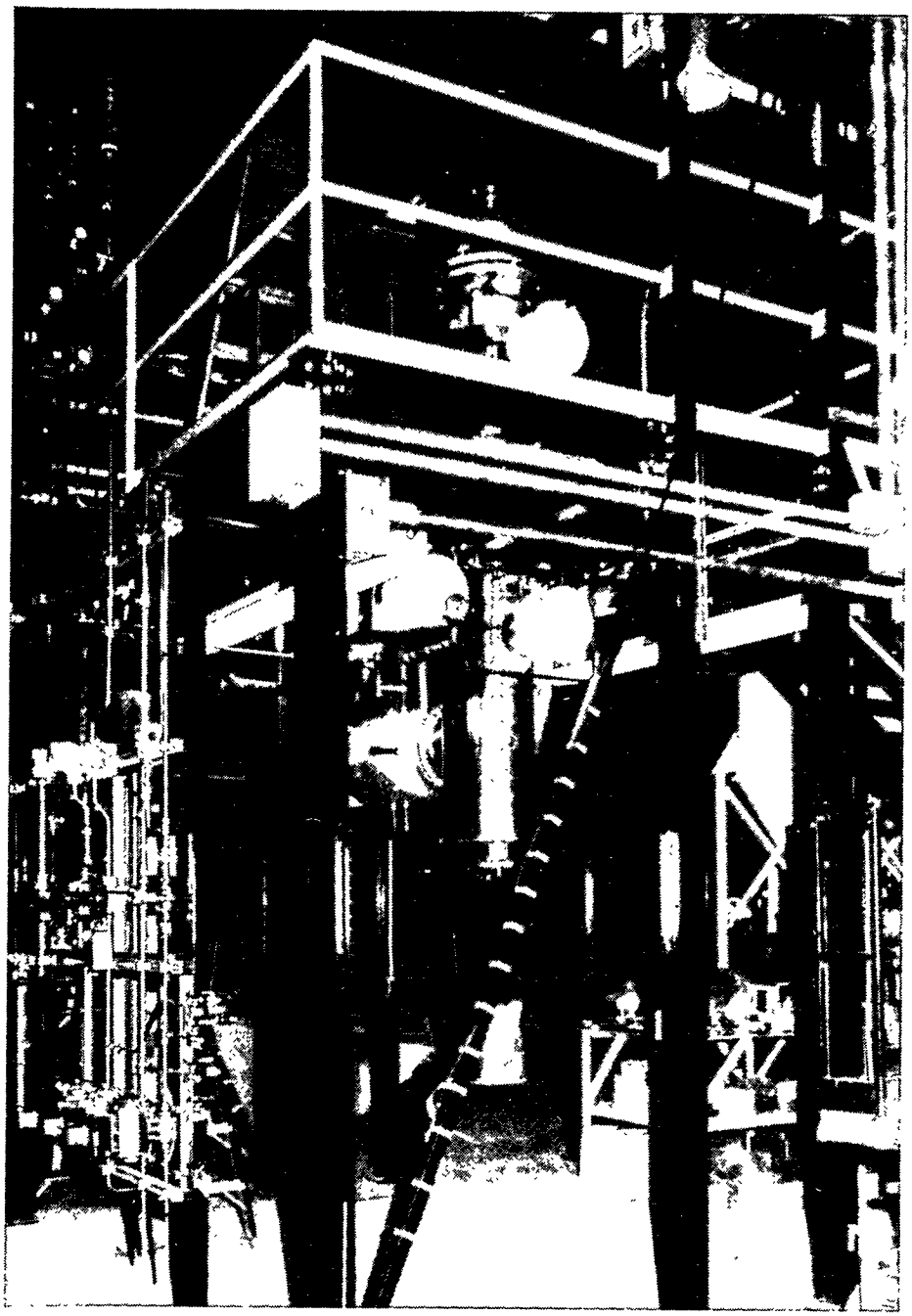

**Figure 2. Module Under Construction**

the major components of a module, and Figure 2 is a general view of a module under construction.

## Combustor

The combustor consists of a refractory-lined pressure vessel, a burner nozzle, and the associated piping and instrumentation. Natural gas,

primary air, and dilution air may be supplied up to the design pressure for a maximum throughput of 320 kg·hr$^{-1}$ (700 lb$_m$/hr), or a maximum firing rate of 140 kW (480 × 10$^3$ Btu/hr). The combustion product temperature is adjustable by controlled heat loss and dilution air injection. A port is provided at the combustor discharge for introducing particulate material. The burner is a concentric tube axial flow swirl generator [1] (swirl number $N_{sw}$ = 0.78) discharging into a diverging refractory nozzle. Combustion air mixes with fuel from radial ports in the annulus upstream of the swirl vanes. Testing at atmospheric pressure indicates the burner is capable of 8:1 turndown at stoichiometric conditions with good flame stabilization. A performance map over the entire range of pressure and equivalence ratio will be obtained during shakedown.

## Filter Vessel

Figure 3 shows the filter vessel (without the head) in cross section. The vessel is mounted vertically and is refractory lined, providing a test volume 203 mm (8 in) in diameter by 3 m (10 ft) in length. The supporting structure has a stairway, deck, and an integral hoist to simplify filter change-out and maintenance. Filter mounting is provided by a water-cooled tube sheet that may be custom fabricated to accommodate the filter design under test. Eight ports are available for cooling water, back pulse jets, and instrumentation. Two flanges provided on one side of the vessel offer a choice of combustor mounting positions. Three nitrogen-purged viewing ports are furnished for remote observation via closed circuit TV; one of these may be sacrificed for additional instrumentation, if required. The dust hopper (not shown) is bolted to the lower flange and may be interchanged with a spare to provide substantially continuous testing.

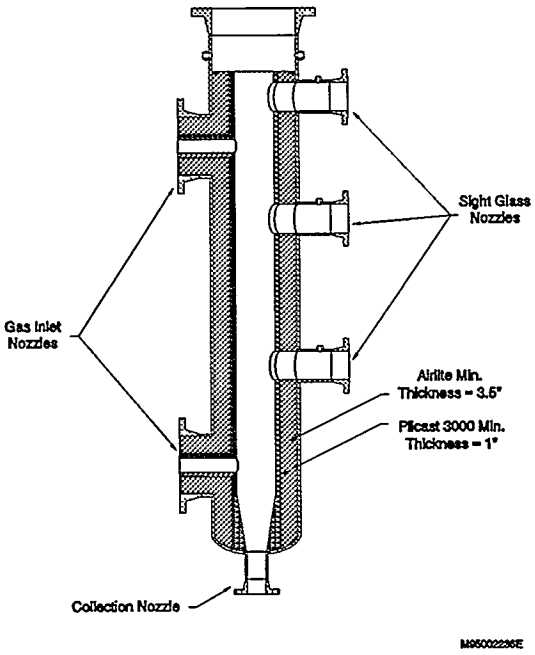


**Figure 3. Filter Vessel Cross Section**

## Dust Feeder

The combustion product stream is seeded with particulate material by a loss-in-weight, twin-screw feeder mounted in its own pressurized vessel. Dust may be fed at rates of 23 kg·hr$^{-1}$ (50 lb$_m$/hr) or more, depending on dust properties and the feed screws selected; the complete feed screw set range is available. Tests indicate that feed rate error is typically ± 4 percent full scale at the 95 percent confidence level. The feeder vessel is pressurized by nitrogen at 1.3 MPa (185 psia), which provides the motive power for conveying particulate material to the combustor dust port. The dust feeder supply hopper may be replenished while the vessel is pressurized. METC has a stock of fly ashes from various sources. Dust supplied by CRADA partners can also be used, if desired.

## Back Pulse Cleaning System

The back pulse cleaning system consists of a nitrogen back pulse surge tank, four fast-acting back pulse valves, and a dedicated high-speed data acquisition and control computer. The system may be pressurized up to 3.1 MPa (450 psia), which gives a 5.6:1 back pulse to process pressure ratio when the system is operating at design pressure. Back pulse valve firing

time and sequencing parameters are selected by the operator. The mass of nitrogen injected during each back pulse event is inferred thermodynamically from temperature and pressure traces from instrumentation in the back pulse surge tank. The tank is isolated from the high-pressure nitrogen header that supplies it, except while charging.

## Experimental Methodology

The HTGSCTF has been designed to produce high-quality data. To extract the maximum information the precision of the instrumentation will allow, statistical experimental techniques will be used. It is expected that factorial experiments, response surface methodology, and times series analysis will be the mainstays of the project [2,3]. The best method to use will depend on the problem at hand, and will be worked out in consultation with the CRADA partner on a case-by-case basis.

## Particle Capture

The overall particle capture efficiency, $\eta$, may be defined as the fraction of the incoming particulate mass that is captured. As was mentioned previously, the dust feed rate error is on the order of $\pm$ 4 percent full scale, so determinations of $\eta$ will be of commensurate accuracy. Short of filter breaching, we expect $\eta > 0.99$ as a matter of course.

Study of the deposited dust cake should yield valuable insights into filter performance. METC has considerable expertise in particle technology, surface science, and gas-solid computational fluid dynamics (CFD). A new Particulate Control Technology Laboratory provides facilities for the evaluation of dust cake mechanical properties. Surface science services include, but are not limited to, particle size and distribution measurements, surface property evaluation, and chemical analysis. METC's two-phase CFD expertise [4] has been of proven value to filter system designers and software developers. While not dedicated solely to this project, CRADA partners have these capabilities at their disposal should they be required.

## Pressure Drop

Figure 4 shows, in idealized form, the filter system conditioning process. The pressure drop, $\Delta p$, increases during time interval, $\Delta t_1$, from

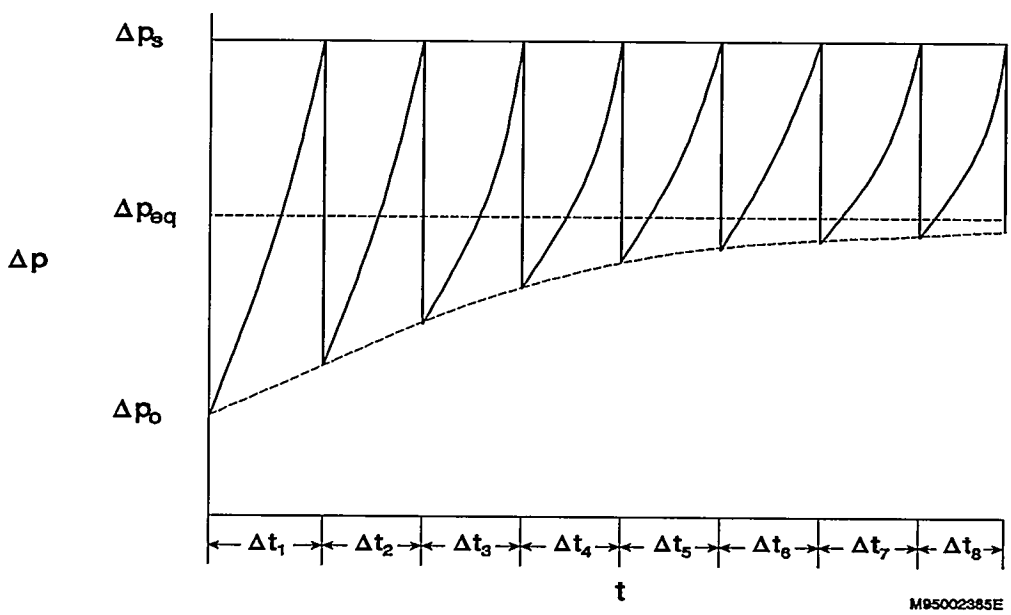


**Figure 4. Idealized Filter System Pressure Drop History During Conditioning**

$\Delta p_0$, the pressure drop associated with the virgin filter elements, to $\Delta p_s$, the back pulse trigger setpoint. The filters are then cleaned, reducing the pressure drop to a new minimum value $\Delta p_1 > \Delta p_0$. This process continues with $\Delta p_{n+1} > \Delta p_n$; eventually, it is hoped, a stable minimum equilibrium pressure, $\Delta p_{eq}$, is attained. Evidently, the pressure drop, $\Delta p$, at time, $t$, may be expressed as

$$\Delta p = \Delta p_0 + \Delta p_c \ , \qquad (1)$$

where $\Delta p_c$ is a function of time attributed to dust cake growth. By dividing Equation (1) by the superficial or face velocity $v_s = Q/A_s$, where $Q$ is the gas volumetric flow rate and $A_s$ the total filtration area, Williams, Hatch, and Greenburg [5] obtained

$$S = S_0 + K_2 W \ . \qquad (2)$$

The use of Equation (2) is customary in fabric filtration; the specific resistance coefficient, $K_2 = \Delta p_c / v_s W$, where $W$ is the so-called areal cake density, i.e., the mass of the filter cake divided by $A_s$. Assuming a constant inlet solids loading and $\eta \approx 1$, if $K_2$ were constant, $S$ (or $\Delta p$) would increase linearly with time. Rather than being a constant, $K_2$ has been found to depend, among other things, on the dust cake porosity $\varepsilon$, the particle density $\rho_p$, the inlet cumulative particulate mass distribution $\Phi$, the inlet dust loading, and the operational history of the filter system [6,7]. With rigid ceramic filters, there is some question whether a true $\Delta p_{eq}$ is ever attained.

Let $\delta$ be the average bed (cake plus filter) thickness, $\kappa$ the effective Darcy permeability, $\rho_g$ the gas density, and $\mu$ the gas viscosity. For a Darcy's Law medium, it may readily be shown that

$$N_p = \frac{\delta A_s^{1/2}}{\kappa} N_{Re}^{-1} \ , \qquad (3)$$

where the pressure coefficient $N_p = \Delta p \, A_s^2 / \rho_g Q^2$ and the Reynolds number $N_{Re} = \rho_g Q / \mu \, A_s^{1/2}$.

Equation (3) represents a generalization of Equation (2); both $\delta$ and $\kappa$ may vary in complicated ways, as indicated in the previous paragraph. There may also be departure from Darcy's Law. Then Equation (3) no longer holds, though it still supplies two dimensionless variables useful for designing experiments. If we fix the inlet particulate mass distribution and its properties, but consider the inlet particle mass flow rate m and time, dimensional analysis and Equation (3) yield

$$N_p = f(N_{Re}^{-1}, N_L, \tau) \ , \qquad (4)$$

where $f$ is an unknown function to be estimated, $N_L = m/\rho_g Q$ is the loading number, and $\tau = tQ/A_s^{3/2}$ is the dimensionless time. Equation (4) provides a compact framework for the process control variables. Subtler effects involving $\Phi$ and operational history require careful consideration when designing a complete experiment.

## FUTURE WORK

Upon completion of shakedown, one module of the HTGSCTF will be available for CRADA work. As scheduling permits, the second module will be constructed and put into operation. Interested potential CRADA partners are encouraged to contact the authors for further information.

## REFERENCES


1. Beér, J. M., and N. A. Chigier. 1972. *Combustion Aerodynamics*, pp. 110-111. London: Applied Science Publishers.

2. Box, G. E. P., W. G. Hunter, and J. S. Hunter. 1978. *Statistics for Experimenters*. New York: John Wiley & Sons.

3. Box, G. E. P., and N. R. Draper. 1987. *Empirical Model-Building and Response Surfaces*. New York: John Wiley & Sons.

4. Syamlal, M., W. Rogers, and T. J. O'Brien. 1993. *MFIX Documentation Theory Guide*. DOE/METC-94/1004. NTIS/DE94000087. Springfield, VA: National Technical Information Service.

5. Williams, C. E., T. Hatch, and L. Greenburg. 1940. Determination of Cloth Area for Industrial Air Filters. *Heating, Piping, and Air Conditioning* 12:259-263.

6. Rudnick, S. N. 1978. *Fundamental Factors Governing Specific Resistance of Filter Dust Cakes*. Thesis. Boston: Harvard School of Public Health.

7. Dennis, R., and J. A. Dirgo. 1981. Comparison of Laboratory and Field Derived $K_2$ Values for Dust Collected on Fabric Filters. *Filtration & Separation* 18(5):394-396.

JONTKO\1:951270

PA.8

# Cooperative Research and Development Agreements at METC

J. Christopher Ludlow
Lisa A. Jarr
Rodney J. Anderson
Morgantown Energy Technology Center

**ABSTRACT**

The Federal Technology Transfer Act of 1986 (P.L. 99-502) provided a new mechanism for joint research between private parties and the Morgantown Energy Technology Center (METC). Joint projects under this law are called Cooperative Research And Development Agreements (CRADAs) and are simply agreements between METC and the private sector to work together on a mutually beneficial project. Of primary interest to METC is the development and deployment of:

- clean, efficient power generation technologies,
- technologies for the characterization and exploitation of the Nation's natural gas resource,
- environmental remediation technologies.

For power generation, METC's primary focus is on integrated gasification combined cycle (IGCC) systems, advanced pressurized fluidized-bed combustion (PFBC) systems, advanced turbine systems (ATS), externally fired combined-cycle power systems, and fuel cell systems. In natural gas, it is resource characterization, exploration, production, processing, and storage. METC's environmental remediation interests focus on the development of high-payoff technologies to clean up the inventory of DOE nuclear component manufacturing sites and to manage waste generated by advanced power generation technologies faster, and more cheaply than currently available technologies allow. Potential partners for these joint projects include private industry, educational institutions, and other research organizations. In a CRADA, both the Government and the participating partner(s) may contribute personnel, equipment, or facilities to the project but no funds may be supplied by the Government to the CRADA partner as part of the CRADA. One of the advantages of a CRADA is the fact that METC's Director is able to negotiate directly with the partners on issues, including the allocation of rights to patents developed during the CRADA, protection of information generated under the CRADA, and exclusive or non-exclusive licensing of METC inventions. Since the enactment of the law, METC has entered into 29 CRADAs.

## PA.9 High Pressure Optical Combustion Probe

Steven D. Woodruff
George A. Richards
Morgantown Energy Technology Center

### ABSTRACT

The Department of Energy's Morgantown Energy Technology Center has developed a combustion probe for monitoring flame presense and heat release. The technology involved is a compact optical detector of the OH radical's UV fluorescence. The OH Monitor/Probe is designed to determine the flame presence and provide a qualitative signal proportional to the flame intensity. The probe can be adjusted to monitor a specific volume in the combustion zone to track spatial fluctuations in the flame. The probe is capable of nanosecond time response and is usually slowed electronically to fit the flame characteristics.

The probe is a sapphire rod in a stainless steel tube which may be inserted into the combustion chamber and pointed at the flame zone. The end of the sapphire rod is retracted into the SS tube to define a narrow optical collection cone. The collection cone may be adjusted to fit the experiment. The fluorescence signal is collected by the sapphire rod and transmitted through a UV transmitting, fused silica, fiber optic to the detector assembly. The detector is a side window photomultiplier (PMT) with a 310 nm line filter. A Hamamatsu photomultiplier base combined with a integral high voltage power supply permits this to be a low voltage device. Electronic connections include: a power lead from a modular DC power supply for 15 VDC; a control lead for 0-1 volts to control the high voltage level (and therefore gain); and a lead out for the actual signal. All low voltage connections make this a safe and easy to use device while still delivering the sensitivity required.

The detector may be contolled and monitored remotely from any data acquisition and control system using DC signal conversion. A ±10 volt ADC card is used to monitor the detector signal. A 0-1 volt DAC may be used to automatically control the gain or a precision voltage supply may be use to control the gain manually. An oscilloscope or computer display of the ADC signal is used to monitor the signal in real time.

The system may be modified to monitor other chemical species by changing the line filter on the PMT to another wavelength. An example would be to monitor the CH radical in the blue portion of the spectrum, another good flame indicator. By using multiple probes at selected locations on the combustor, flame motions may be correlated spatially and temporally between the probes or to other monitors such as a pressure probe.

Potential Commercial Uses:

* Any combustion system exhibiting motion of the flame front which must be monitored or eliminated

* Research, analysis, and development of engines operating at pressure

* Monitoring instaneous heat release

Benefits
:

* OH fluorescence is a measure of heat release

* OH fluorescence is concentrated in the flame front

* Probe can withstand high pressures

* Simple design, low cost

Key Words

OH Fluorescence
Flame monitor

# PA.10 METC CFD Simulations of Hot Gas Filtration

Thomas J. O'Brien
Morgantown Energy Technology Center

## ABSTRACT

Computational Fluid Dynamic (CFD) simulations of the fluid/particle flow in several hot gas filtration vessels will be presented. These simulations have been useful in designing filtration vessels and in diagnosing problems with filter operation. The simulations were performed using the commercial code FLUENT and the METC-developed code MFIX.

Simulations of the initial configuration of the Karhula facility indicated that the dirty gas flow over the filter assemblage was very non-uniform. The force of the dirty gas inlet flow was inducing a large circulation pattern that caused flow around the candles to be in opposite directions on opposite sides of the vessel. By introducing a system of baffles, a more uniform flow pattern was developed. This modification may have contributed to the success of the project.

Several simulations of configurations proposed by Industrial Filter and Pump were performed, varying the position of the inlet. A detailed resolution of the geometry of the candles allowed determination of the flow between the individual candles.

Recent simulations in support of the METC/CeraMem Cooperative Research and Development Agreement have analyzed the flow in the vessel during the cleaning back-pulse. Visualization of experiments at the CeraMem cold-flow facility provided confidence in the use of CFD. Extensive simulations were then performed to assist in the design of the hot test facility being built by Ahlstrom/Pyropower. These tests are intended to demonstrate the CeraMem technology.

# PA.11 CRADA Opportunities in the Removal of Particulates From Hot-Gas Streams by Filtration

Duane H. Smith
Morgantown Energy Technology Center

## ABSTRACT

Our analyses of samples and operating data from the Pressurized Fluidized Bed Combustion (PFBC), cyclone, and filtration units of the Tidd Clean Coal demonstration facility show that calcined dolomitic sorbent reacted with $SO_2$ (and $O_2$) to form sulfates ($CaSO_4$ and CaMgn $[SO_4]$n+1) not only in the PFBC bed, but also in the filtration vessel. Analyses of limited data from the journal literature suggest that the filter-vessel reactions may have produced sulfate "necks," which bonded the particles together, thus substantially increasing the critical angle of repose and shear tensile strengths of the filtered powders. This proposed mechanism rationalizes the "bridging" and other particle-accumulation problems that caused filter breakage. Engineering services potentially available to resolve these problems include elucidation and modeling of ex-situ and in-situ filter-vessel chemistry, measurement and modeling of particulate materials properties, and measurement and modeling of cleaning back-pulse aerodynamics and cleaning efficiencies.

PA.12

# Dynamic Modeling of Power Systems

Michael E. Reed
Morgantown Energy Technology Center

Jay S. White
Gilbert/Commonwealth, Inc.

## ABSTRACT

Morgantown Energy Technology Center's (METC) Process and Project Engineering (P&PE) personnel continue to refine and modify dynamic modeling or simulations for advanced power systems. P&PE, supported by Gilbert/ Commonwealth, Inc. (G/C), has adapted PC/ TRAX commercial dynamic software to include equipment found in advanced power systems. PC/TRAX's software contains the equations that describe the operation of standard power plant equipment such as gas turbines, feedwater pumps, and steam turbines. The METC team has incorporated customized dynamic models using Advanced Continuous Simulation Language (ACSL) code for pressurized circulating fluidized-bed combustors, carbonizers, and other components that are found in Advanced Pressurized Fluidized-Bed Combustion (APFBC) systems.

A dynamic model of a commercial-size APFBC power plant was constructed in order to determine representative operating characteristics of the plant and to gain some insight into the best type of control system design. The dynamic model contains both process and control model components. This presentation covers development of a model used to describe the commercial APFBC power plant. Results of exercising the model to simulate plant performance are described and illustrated. Information gained during the APFBC study was applied to a dynamic model of a 1-1/2 generation PFBC system. Some initial results from this study are also presented.

With input from commercial vendors, METC now has the tools to simulate a number of the advanced power systems approaching commercial size. These tools are important because the dynamics of each individual component affects neighboring components due to the highly integrated nature of advanced combined-cycle concepts. The effects of primary interest include: thermal inertias, process time constants, and the transport lag associated with large gas/solid volumes. METC has the capability to investigate these effects for various gasifiers, gas turbines, particulate and sorbent subsystems, and other advanced combine-cycle components before startup of the first commercial-size plant.

## INTRODUCTION

Figure 1 shows a simplified schematic of a APFBC power plant. As can be seen in the schematic, the process is highly integrated. The primary components that make up the APFBC concept include a carbonizer, pressurized fluidized-bed combustor (PFBC), fluidized-bed heat exchanger (FBHE), gas turbine (GT), waste heat recovery, and a steam turbine bottoming cycle. Electrical power is produced by both the gas and steam turbines.

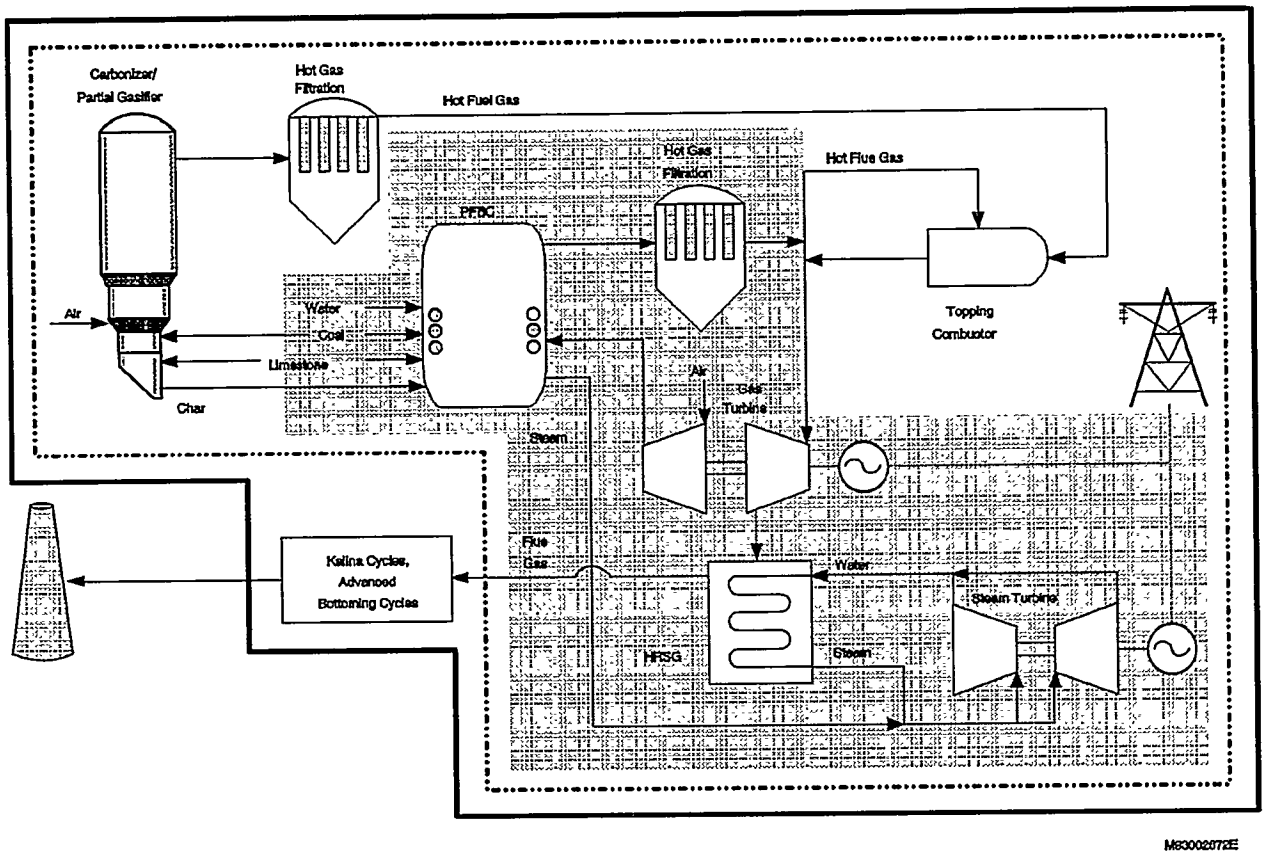


**Figure 1. APFBC Schematic**

The carbonizer is a bubbling bed reactor that operates at approximately 14 atmospheres and 1,600 °F. In the carbonizer, coal is converted into a low-Btu gas and char. Air is used to combust a small portion of the coal that provides the energy required by the carbonization reactions. For the 1,600 °F carbonizer condition, the fuel gas has an LHV of 2,247 Btu/lb while that of the char is 11,700 Btu/lb. A calcium-based sorbent is used to capture gaseous sulfur species such as $H_2S$. Char and sorbent not entrained in the fuel gas steam exits the bottom of the vessel. The fuel gas is cleaned of particulate material and routed to the topping combustor.

Char and sorbent removed from the carbonizer is routed to the PFBC. The PFBC is a fluidized bed that operates at approximately 14 atmospheres and 1,600 °F. A large amount of excess air is used to combust the char. Excess air values are typically above 200 percent. Calcium present in the char/sorbent mixture removed from the carbonizer is used to remove $SO_2$ from the flue gas. The hot flue gas from the PFBC is cleaned of particulate matter and routed to the topping combustor.

Fuel gas generated in the carbonizer is combusted and expanded in a Westinghouse 501F GT. The turbine inlet temperature of the GT is 2,350 °F. Hot combustion air from the PFBC helps maintain this high firing temperature. The 501F GT is a single shaft machine. The GT compressor provides all of the air required by the process. The GT produces approximately 140 $MW_e$ of electrical power

when firing the fuel gas generated in the carbonizer.

Excess heat from the PFBC and heat recovery steam generator (HRSG) is recovered and used to generate 2,400 psig/1,000 °F steam that is utilized in the steam turbine bottoming cycle. The steam bottoming cycle consists of heat recovery components and a condensing steam turbine. Two steam drums are used to recover heat and generate steam. Heat transfer surface in the FBHE is used to provide heat duty needed to maintain superheat and reheat steam temperatures of 1,000 °F. The steam turbine exhausts into a condenser with a back pressure of 2.5 inches of Hg absolute. Deaeration is provided through I/P steam extraction.

To produce worthwhile results, a dynamic model of a commercial-sized APFBC power plant must provide all of the mathematical statements necessary to reflect the power cycle as described above. Each primary component must be described in sufficient detail so that it may successfully interact with the other components. Otherwise, model results would be of little use.

The model developed in this study describes all of the primary variables associated with the APFBC concept. To accomplish this, mathematical models of advanced concept components were developed and interfaced with a commercial software product. A control scheme has been interfaced with the process model. The control scheme is of sufficient detail to provide usable results.

## DYNAMIC MODEL DEVELOPMENT

A PC/TRAX based dynamic model was developed to investigate commercial APFBC power plant performance under transient conditions. The power plant model contains the necessary process and control parameters required to produce realistic component responses. This section describes the model and software used and developed in this study.

### Dynamic Model Software

PC/TRAX is a commercial software tool that allows for the dynamic analysis of fossil-based power plants. PC/TRAX was chosen because it contains standard modules appropriate for describing the dynamic behavior and control of much of the components that make up the APFBC concept. Standard PC/TRAX modules were used to model all of the plant control hardware, the GT, most of the steam turbine bottoming cycle, as well as all of the plant valving and piping.

Because the APFBC power plant is an advanced technology concept, some component models are not available in PC/TRAX's library of standardized dynamic modules. These advanced components include the carbonizer, char hopper, PFBC, FBHE, topping combustor, and ash cooler. Therefore, customized dynamic modules were developed to describe the dynamic behavior of these components.

The customized dynamic models were coded in Advanced Continuous Simulation Language (ACSL). ACSL is a general computer language designed to dynamically model continuous time-dependent systems and is commercially available from Mitchell and Gauthier Associates. The customized ACSL models were then dynamically interfaced with the standard PC/TRAX modules. The customized ACSL modules are supported by FORTRAN subroutines that are utilized to perform non-dynamic algorithms. PC/TRAX provides an easy method for the interface of the ACSL modules and standard TRAX code. Table 1 lists the model type associated with each component.

**Table 1. Model Components and Types**

| SUBSYSTEM | MODEL TYPE |
|---|---|
| Carbonizer | Custom ACSL |
| PFBC | Custom ACSL |
| FBHE | Custom ACSL |
| Char Hopper | Custom ACSL |
| Ash Cooler | Custom ACSL |
| Topping Combustor | PC/TRAX |
| Compressors | PC/TRAX |
| Gas Turbine | PC/TRAX |
| HRSG | PC/TRAX |
| Steam Turbines | PC/TRAX |
| Condenser | PC/TRAX |
| Piping | PC/TRAX |
| Control Valves | PC/TRAX |

## Process Model

The process model must incorporate the thermodynamics, hydrodynamics, and chemistry in sufficient detail to provide accurate performance results during steady-state and transient operation. This detail must be balanced to yield an effective yet uncumbersome model. The dynamic model developed in this study provides mass and energy balances, appropriate chemistry, pressure-flow relationships, and velocity affects.

The process model consists of two distinct parts. One model contains the customized ACSL code while the other contains standard PC/TRAX modules. The standard PC/TRAX modules are described in the documentation provided by the TRAX corporation. The customized modules contained in the ACSL code are described next.

Carbonizer chemistry is based on work recently completed by FWDC. Carbon conversion is an algebraic expression based on stoichiometry. Reaction modes include pyrolysis, carbonization/gasification, and complete combustion. For substoichiometric performance, the fuel gas is assumed to be in water-gas shift equilibrium. $CaCO_3$ calcination is a function of temperature. Sulfur is preferentially captured by incoming sorbent feed, but may also react with solid material in the bed.

Carbonizer hydrodynamics account for solids elutriation, pressure drop across the vessel, and absolute vessel pressure. Elutriation is dependent upon the current solids particle size distribution (PSD) and superficial gas velocity. The carbonizer's solid bed PSD is constantly updated. Pressure drop is determined for either a fluidized or packed bed, depending on the values of the superficial and minimum fluidization gas velocities. Absolute pressure is determined from a differential gas phase material balance, temperature differential, and volume affects.

Solids from the char hopper flow into the PFBC. The char hopper model provides a consistent material balance and accounts for volume affects. The PFBC chemistry accounts for both oxidized and reduced modes of operation. For reduced mode operation, the chemistry is identical to that of the carbonizer. $CaCO_3$ calcination is a function of the partial pressure of $CO_2$. Sulfur capture and sorbent oxidation reactions are accounted.

The principal hydrodynamic feature of the PFBC is the solids circulation rate, which is dependent on the solid PSD and secondary zone

superficial gas velocity. A nonlinear relationship is used to describe changes in solid circulation with gas velocity. Pressure drop and absolute pressure determinations are identical to that described above for the carbonizer.

The FBHE is divided into seven individual cells. Six of these cells contain heat transfer surface area. Convection is the predominant mode of heat transfer for the submerged tube bundles and submerged enclosure wall surface. Radiation predominates in the FBHE freeboard, where enclosure wall surface areas are above the solid bed. It is assumed that there are no solid-gas reactions in the FBHE. Pressure drop and absolute pressure determinations are identical to that described above for the carbonizer and PFBC. Air is used as the fluidizing agent.

A differential energy balance accounting for energy entering, exiting, liberated, required, lost, and stored is used in the carbonizer, PFBC, and FBHE to determine vessel temperature. In the FBHE, a differential energy balance is used in each of the seven cells. Differential mass balance equations are used to describe the flow of solids from each vessel. The hard refractory of the carbonizer and PFBC are treated as a lumped parameter system, with constant heat loss to ambient.

The topping combustor was modeled to account for reducing as well as oxidizing conditions. PC/TRAX has a combustor model that can accommodate two fuels, steam, and an air stream. A specific composition vector is used to describe all inlet streams. Ideally, the carbonizer fuel gas would be connected to one of the fuel ports while the PFBC vitiated air stream would be connected to the air inlet. This scheme would work as long as the carbonizer remained in a reduced mode and the PFBC remained in an oxidized mode. As the custom ACSL model provided for either reducing or oxidizing operation in both the carbonizer and PFBC, it was expected that the GT must accommodate this. It would be cumbersome to use the standard PC/TRAX combustor module in this service, and, it was expected that multiple air streams would be required, so a customized topping combustor model was developed.

The customized topping combustor model can operate in either reducing or oxidizing mode. There is no set composition vector for the inlet streams. Additional ports for supplemental fuel, steam, and bypass process air are available. The energy balance accounts for losses to ambient as well as losses to the metal during temperature transients. Absolute pressure is based on temperature and mass balance differentials. Component pressure drop is a function of total flow and gas density.

The ash cooler model utilizes the NTU-effectiveness method to determine solids and water outlet temperatures. It is assumed that there is no energy storage. Water flow through the ash coolers is based on pressure differences between inlet and outlet.

**Control Model**

All process control and instrumentation model components utilize standard PC/TRAX modules. Module types that were used included transmitters, various mathematical operators, function generators, three mode controllers (also known as Proportional-Integral-Derivative controllers [PID]), three element controllers, auto-manual stations, and lead-lag elements. The remainder of this section contains a summary of the control scheme investigated in this study.

TRAX control models are built by linking several modules to produce a given block of logic and hardware. Figure 2 contains a

schematic of a Scientific Apparatus Manufacturers Association (SAMA) diagram for the HRSG steam drum level control. This diagram contains the logic and hardware that is required of the controller. Figure 3 shows the TRAX blocks needed to represent the drum level controller and associated hardware.

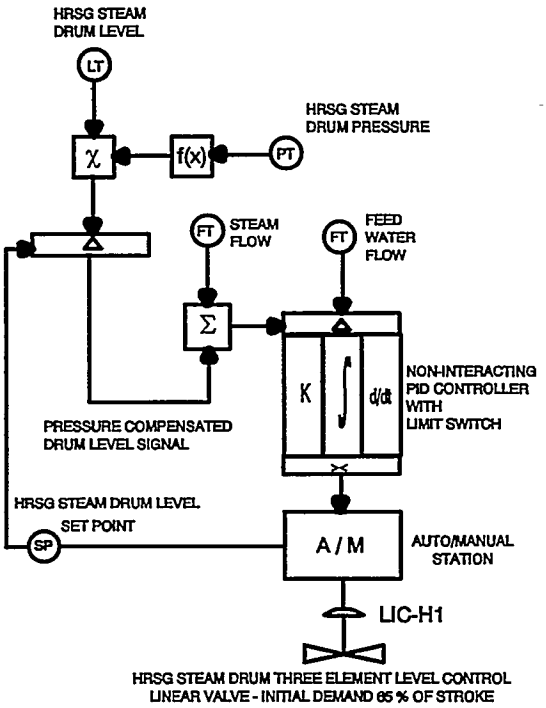


**Figure 2. SAMA Diagram of HRSG Steam Drum Level Control**

Sorbent and steam flow to the carbonizer is maintained as a linear ratio of coal flow. Solids transport air is maintained at a set superficial gas velocity to prevent saltation of the solids. Primary air flow to the carbonizer is established as a function of coal flow. The ratio is modified to maintain carbonizer temperature. Primary and transport air flows are controlled by inlet guide vanes (IGV's) on their respective boost compressors. Steam flow is controlled by modulating the carbonizer steam control valve.

Solids level in the char hopper is set at a constant height. Therefore a change in coal flow will be followed by a change in char feed to the PFBC. The PFBC primary zone superficial gas velocity is maintained by controlling primary zone air flow. Secondary air flow is established and maintained by a PID controller as a function of coal flow and corrected to maintain a set PFBC bed temperature. This correction is very similar to that used for the carbonizer primary air flow. Air flow to the FBHE is controlled by seven PID controllers to maintain a constant superficial gas velocity through each of the seven heat transfer compartments.

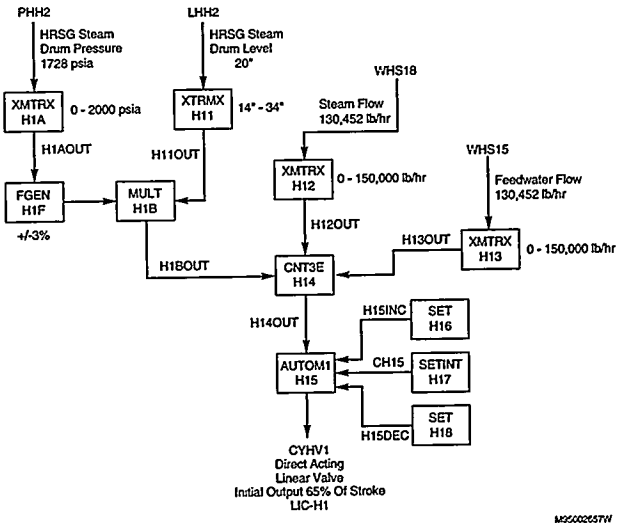


**Figure 3. TRAX Block Diagram of HRSG Steam Drum Level Control**

Control valves are used to control the PFBC primary air and FBHE fluidizing air flows. PFBC secondary air flow is controlled by split ranging the secondary air flow control valve and GT compressor IGV's. The secondary air flow control valve and GT IGV's are direct acting and operate over a controller signal range of 0 to 50 percent and 50 to 100 percent respectively. This split range arrangement was used so that additional process air could be made

available if an upset were to occur at 100 percent operating condition.

The GT compressor is a constant volume machine and therefore delivers a constant mass flow given constant ambient conditions. With the present design, at 100 percent load, all of the GT compressor air is utilized. During a turndown in plant coal feed, less air is required by the carbonizer and PFBC. The surplus air is bypassed from the air header into the topping combustor. A PID controller is used to regulate the bypass valve. The GT combustor pressure is determined by upstream conditions. The GT combustor temperature is a function of the fuel and flue gas compositions and temperatures. Emergency stop valves on the fuel stream are provided for combustor over-temperature protection.

Steam drum levels in the HRSG and FBHE are maintained by three element controllers. Control valves downstream of the HRSG economizer maintain flow. Steam flow into the H/P steam turbine is regulated by a PID controller to maintain a constant steam header pressure. Superheat and reheat steam temperatures are maintained by controlling solids distribution in the FBHE, in which solids diverters are used to distribute solids to superheater and reheater steam passes.

Condenser hotwell level is maintained at set point by a three element controller. The controller's output regulates two valves -- the spillover valve to the condensate storage tank and the makeup valve from the condensate storage tank. These valves are split ranged and opposite acting.

## MODEL ANALYSIS

Following development of the model containing the customized ACSL modules and the model containing the standard PC/TRAX modules, the models were interfaced so information could be communicated from one model to the next. Shared variables are passed between the interface and the two models are executed simultaneously. The process control schemes were then added on top of the process model platform.

### Steady-State Model Performance

Following completion of the dynamic model, steady-state results generated by the PC/TRAX based model at 100 percent of design load were compared to results generated with the steady-state software tool ASPEN™ (Advanced System for Process ENgineering). The ASPEN™ model is based on work completed by G/C and FWDC in an on-going study. The steady-state ASPEN™ model was the template for the dynamic model.

Comparison of the steady-state models showed relatively good agreement among all of the process variables. The model was sufficiently stable to run a half hour uncontrolled. Following comparison of the steady-state model values, the controls were built on top of the process model. Each control loop was individually tuned to determine appropriate gains and constants. The fully integrated and controlled model results were then compared to the steady-state ASPEN™ results. Good agreement was found. Table 2 compares various primary process values generated by each model.

Table 2 shows that there is good agreement between most of the process variables. Carbonizer and PFBC temperatures, pressures, and flowrates show very little variance. The gas and steam turbine power outputs also compare favorably. The most striking difference in model variables is the HRSG exhaust temperature that differs by 29 °F. This difference is due to small differences in thermodynamic methods of the two codes. Both codes use the ASME steam tables but differ in the gas side calculation.

**Table 2. Steady-State Variable Comparison**

| Model Variable | ASPEN Model | PC/TRAX Model |
|---|---|---|
| Dry Coal Flow | 151,061 lb/hr | 151,061 lb/hr |
| Carbonizer Temp | 1,600 °F | 1,600 °F |
| Carbonizer Pres | 209.4 psia | 209.7 psia |
| Fuel Gas Flow | 325,727 lb/hr | 326,000 lb/hr |
| Char Flow | 112,754 lb/hr | 112,550 lb/hr |
| PFBC Temp | 1,600 °F | 1,600 °F |
| PFBC Pres | 173.8 psia | 173.8 psia |
| Vitiated Air Flow | 2,702,371 lb/hr | 2,700,100 lb/hr |
| Topping Comb Temp | 2,350 °F | 2,350 °F |
| GT Exhaust Flow | 3,564,850 lb/hr | 3,567,200 lb/hr |
| GT Exhaust Temp | 1,141 °F | 1,141 °F |
| HRSG Exit Temp | 280 °F | 309 °F |
| Throttle Steam Flow | 1,597,900 lb/hr | 1,589,800 lb/hr |
| Deaerator Steam | 86,498 lb/hr | 80,665 lb/hr |
| GT Power | 140 $MW_e$ | 138 $MW_e$ |
| ST Power | 280 $MW_e$ | 282 $MW_e$ |

Figure 4 shows plots for the carbonizer, PFBC, and topping combustor temperatures. The time scale of the plot is 50 minutes. The plot shows steady, stable plant performance.

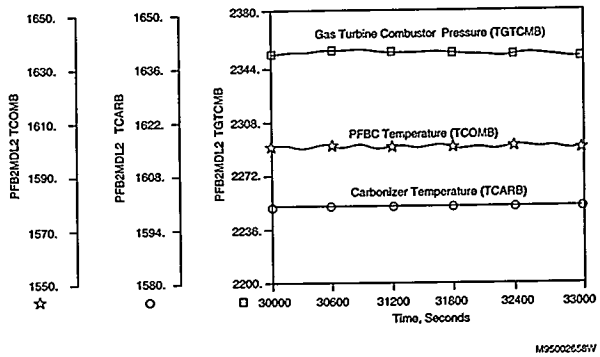


**Figure 4. Steady-State Temperatures**

Figure 5 shows the pressure in the carbonizer, FBHE freeboard, PFBC, and topping combustor. Again, the time span of the plot is 50 minutes. Stable performance is observed. Following favorable steady-state results, the model was subjected to several transients.

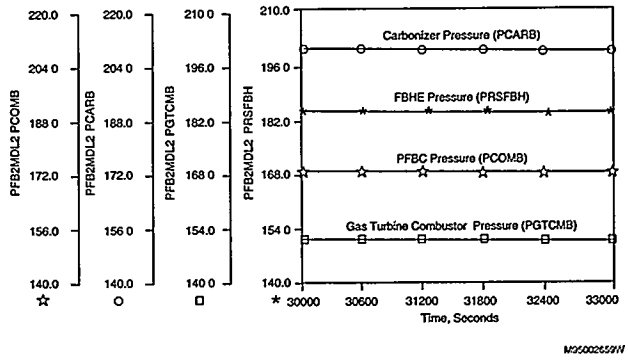


**Figure 5. Steady-State Pressures**

## Transient Model Performance

It was desired to bring the plant from 100 percent design load down to 90 percent, and from 100 percent design load down to 50 percent of design. Significant interaction between the PFBC/FBHE and steam bottoming cycle adversely affected plant stability following the load changes.

With the present control scheme, total plant power output is varied by ramping coal flow. During a model test run, the analyst manually inputs a ramp rate and final value. Figure 6 shows coal flow, carbonizer temperature, and carbonizer pressure for a 10-percent decrease in coal flow at a rate of 1 percent a minute. For the first 10 minutes of the ramping period, carbonizer temperature is maintained at 1,600 °F and the pressure slowly starts to decrease. The decrease in pressure reflects decreased gas flow through the carbonizer. After 10 minutes of ramp, the carbonizer temperature and pressure begin to show disfavorable responses. This phenomena is caused by downstream conditions as will be discussed next.

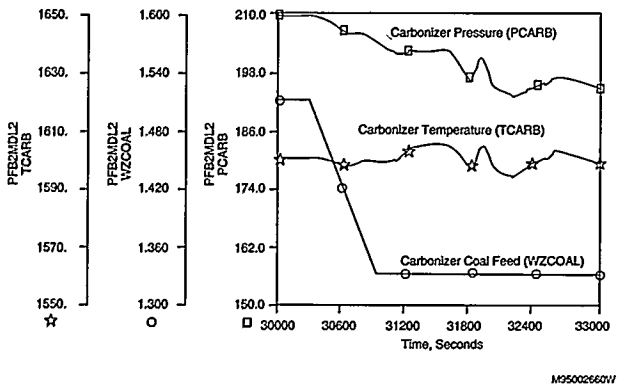


**Figure 6. Transient Response (10 Percent Decrease in Coal at 1 Percent/min)**

Figure 7 shows plots of the PFBC temperature and solids flow through the reheater pass of the FBHE for the same ramp. For the first 10 minutes of the ramp period, the PFBC temperature is fairly stable but wanders about 8 °F from 1,600 °F. The initial dip in PFBC temperature is caused by a decrease in the char flow that closely follows the coal ramp. As the valves on the secondary air flow close, the PFBC temperature rises back to 1,600 °F. Following this, the PFBC temperature experiences several large temperature excursions. The apex of the PFBC temperature excursion occurs during the nadir of the solids flow through the FBHE heat exchange passes. Decreased flow through the heat exchange passes prohibits the removal of heat from the PFBC, which is manifest in increased PFBC temperature. This is evident in Figure 7.

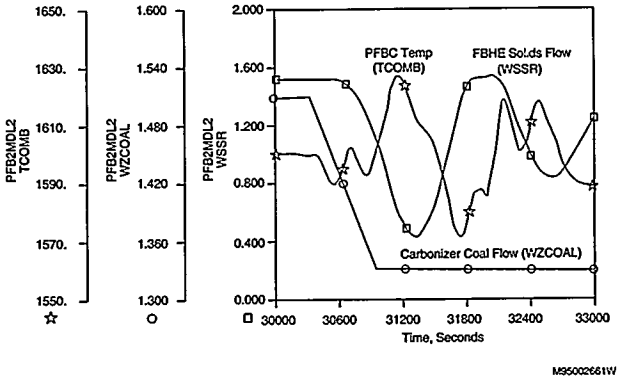


**Figure 7. Transient Response (10 Percent Decrease in Coal at 1 Percent/min)**

Figure 8 shows the air bypass valve position and steam turbine throttle flow. The air bypass valve opens in response to decreased air

requirements in the carbonizer and PFBC. The bypassed air flows into the gas turbine combustor directly decreasing turbine inlet temperature and indirectly causing decreased steaming in the HRSG steam drum. Decreased steaming causes a decrease in the steam turbine throttle flow. Lower steam flow means less heat is removed from the PFBC/FBHE arrangement, causing the PFBC temperature to increase as shown in Figure 7.

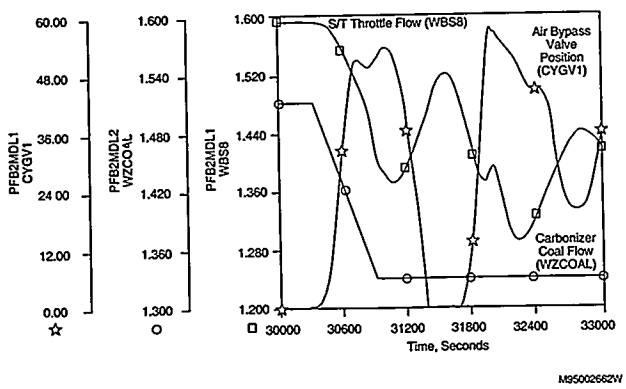


**Figure 8. Transient Response (10 Percent Decrease in Coal at 1 Percent/min)**

As evident in Figures 7 and 8, a chain reaction of large excursions between the PFBC/FBHE arrangement and steam turbine bottoming cycle are too large and lengthy for adequate control of a power plant. Large excursions were found with both faster and slower ramp speeds. A decrease to 50 percent of design flow showed the same oscillatory behavior. This oscillatory behavior inhibited the current control scheme from delivering adequate plant responses to changes in load.

To obtain adequate plant response, the control scheme must be changed. Several variations of the theme were tried, but none were successful. Each control scheme involved the bypassing of compressor air from the air header into the topping combustor in response to decreased air requirements due to decreased coal flow. Various alternative control schemes have been proposed that attempt to make the PFBC/FBHE arrangement and steam bottoming cycle less interactive by introducing new control parameters, such as attemperation in the reheater and superheater passes, or the inclusion of coal feed to the PFBC during transients. These alternatives will be investigated in the future.

## 1-1/2 GENERATION PFBC PLANT MODELING

The 1-1/2 generation PFBC power plant concept is an intermediate step from 1st Generation PFBC to APFBC. It is similar to APFBC except there is no carbonizer and associated fuel-gas generating equipment. The GT fires natural gas instead. The shaded portion of the schematic in Figure 1 corresponds to the 1-1/2 generation PFBC power plant concept.

A TRAX model of a 110 $MW_e$ 1-1/2 generation PFBC power plant was developed using the APFBC TRAX model as a starting point. The process model is similar to the APFBC process model in approach, with the only significant changes being geometry and configuration. The control model, however, is fundamentally different. The FBHE and PFBC components are decoupled from a control standpoint. Coal flow is a function of PFBC temperature, rather than air, and solids distribution in the FBHE is a function of heat input to the PFBC.

Figure 9 shows GT, ST, and total power output for a plant turndown from 100 percent to

64 percent of design load. Turndown was initiated by a ramp on natural gas flow from a 100 percent of design flow to zero. Figure 10 shows coal, natural gas, and sorbent flows corresponding to the transient in Figure 9. Figure 11 shows steam turbine throttle pressure control output.

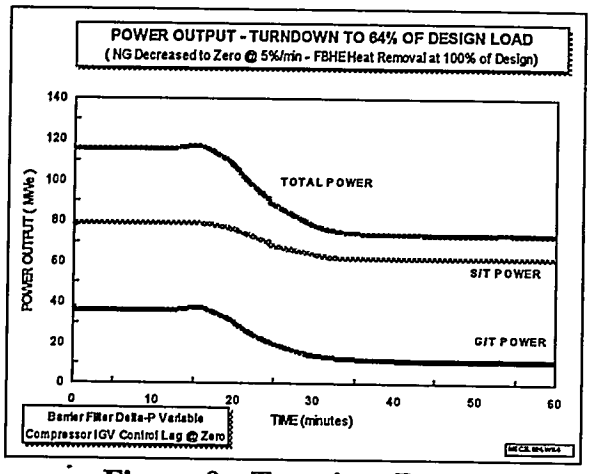


**Figure 9. Transient Response (100 Percent Decrease in NG at 5 Percent/min)**

The transient in Figure 9 shows plant response from operation at 100 percent of design turned down to 64 percent of design. As can be seen in the plots, plant response is stable. The control changes, described previously, helped provide a more stable plant response.

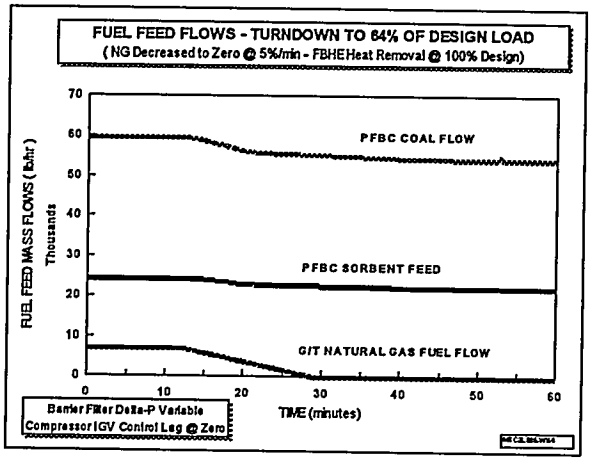


**Figure 10. Transient Response (100 Percent Decrease in NG at 5 Percent/min)**

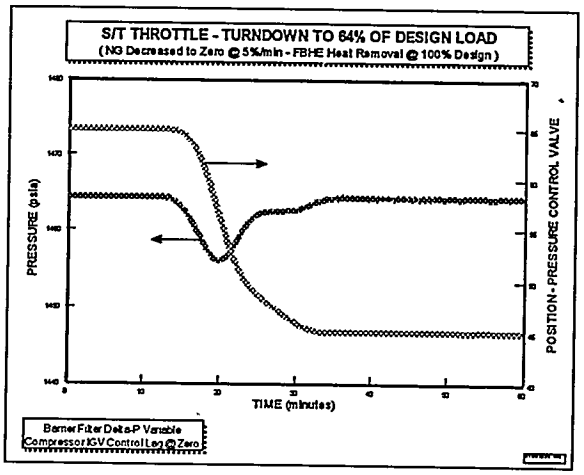


**Figure 11. Transient Response (100 Percent Decrease in Gas at 5 Percent/min)**

## CONCLUSIONS

Dynamic models of an APFBC and a 1-1/2 PFBC generation combined-cycle power plant were described. The models included both process and control descriptions. The process models describe the appropriate thermodynamics, hydrodynamics, chemistry, and pressure flow relationship. The control models account for and describe basic instrumentation, control logic, and hardware.

The models developed in this study are useful tools with which APFBC combined cycle can be studied. Lessons learned during the APFBC study were applied to a 1-1/2 generation PFBC combined-cycle power plant model. Stable plant response was shown to be significantly sensitive to the solids distribution in the FBHE at part load.

The models and knowledge gained during this study could easily be applied to other advanced combined cycles that are nearing commercialization. Application of the TRAX software to other power cycles is aided by the generic nature of the software. An additional plus is the ability of easily augmenting the existing software package with user-supplied dynamic models. The model will soon be applied to the Wilsonville APFBC project.

METC has developed a considerable knowledge base of TRAX-based dynamic models. METC hopes to use this information and expertise as a basis in the formation of cooperative agreements with interested industry partners that share a need for dynamic analysis. The application of dynamic models to emerging technologies offers the ability to examine control issues early in the design process. This advantage should greatly reduce the time and expense of control and process design.

MREED\951301

# Session 3

## *Hot Gas Particle Control*

## 3.1 Westinghouse Advanced Particle Filter System

### CONTRACT INFORMATION

| | |
|---|---|
| **Contract Number** | DE-FC21-89MC21023<br>DE-FC21-89MC26042<br>DE-FC21-90MC25140 |
| **Contractor** | Westinghouse Electric Corporation<br>Science & Technology Center<br>1310 Beulah Road<br>Pittsburgh, PA 15235<br>(412) 256-2440 |
| **Other Funding Source** | Westinghouse Electric Corporation |
| **Contractor Project Manager** | Thomas E. Lippert |
| **Principal Investigators** | Gerald J. Bruck<br>Zal N. Sanjana<br>Richard A. Newby |
| **METC Project Manager** | Richard A. Dennis<br>Donald L. Bonk<br>James R. Longanbach |
| **Period of Performance** | October 1992 thru September 1997 |

**Schedule and Milestones**

**Schedule and Milestones by Quarter**

| | FY 95 | | | | FY 96 | | | |
|---|---|---|---|---|---|---|---|---|
| Pilot Plant Testing | 1st | 2nd | 3rd | 4th | 1st | 2nd | 3rd | 4th |
| Tidd/APF - PFBC | | | Δ | | | | | |
| Karhula - PCFB | | | | | | | Δ | |
| FW/Livingston | | | | | | | | |
| Phase II | | Δ | | | | | | |
| Phase III | | | | | Δ | | | |
| SCS/PSDF | | | | | | | | Δ |

## OBJECTIVES

Integrated Gasification Combined Cycles (IGCC), Pressurized Fluidized Bed Combustion (PFBC) and Advanced PFBC (APFB) are being developed and demonstrated for commercial power generation application. Hot gas particulate filters are key components for the successful implementation of IGCC, PFBC and APFB in power generation gas turbine cycles. The objective of this work is to develop and qualify through analysis and testing a practical hot gas ceramic barrier filter system that meets the performance and operational requirements of these advanced, solid fuel power generation cycles.

## BACKGROUND INFORMATION

High temperature particulate filters are a key component in advanced, coal based gas turbine cycles (IGCC and PFBC) that are currently under development by DOE/METC for clean coal demonstration. In these applications the hot gas particulate filter protects the downstream heat exchanger and gas turbine components from particle fouling and erosion effects and cleans the gas to meet particulate emission requirements. Both PFBC and IGCC plants benefit because of lower cost downstream components, improved energy efficiency, lower maintenance and the elimination of additional and expensive flue gas treatment systems.

In IGCC systems, the hot gas particulate filter must operated in reducing gas conditions (i.e., presence of $H_2$, $CH_4$, CO), high system pressure (150 psi to 350 psi) and at operating temperatures usually determined by the method of sulfur removal, i.e., in bed, external or by cold gas scrubbing, Figure 1. Typically, these temperatures range around 1650°F (in bed), 900

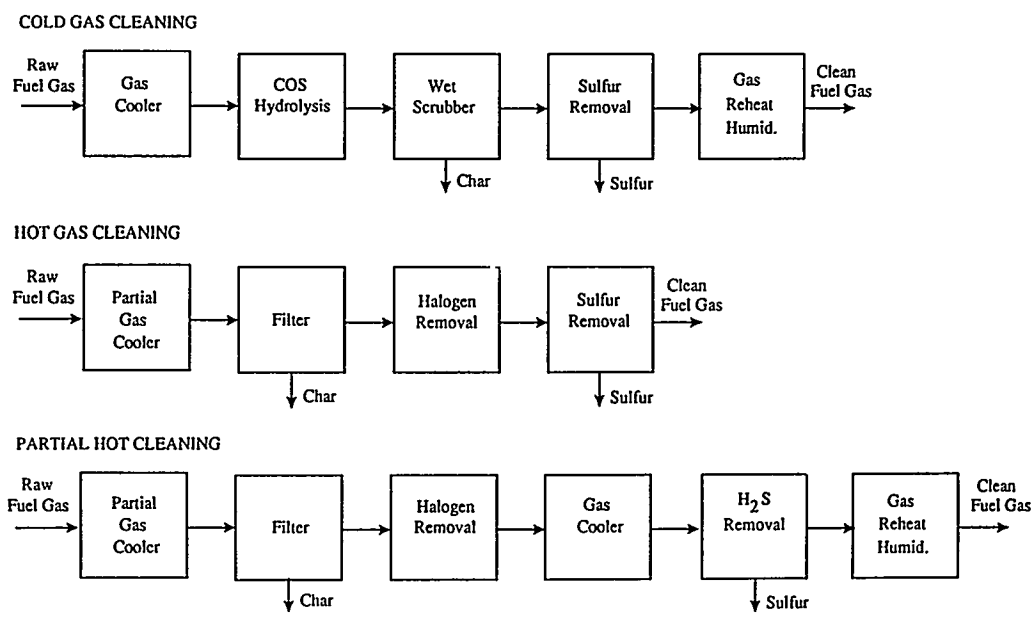


**Figure 1. IGCC - Fuel Gas Cleaning Options**

to 1200°F (external) and 1000°F to 500°F (cold scrubbing).

In gasification applications, cold scrubbing of the fuel gas has been demonstrated as effective in cleaning the fuel gas to meet turbine and environmental requirements. However, with this process, plant energy efficiency is reduced, and higher capital costs are incurred. Incorporating a hot particulate filter upstream of the scrubbing unit reduces heat exchanger costs and provides for dry ash handling (partial hot gas cleaning).

Hot fuel gas cleaning concepts (in bed and external) have also been proposed that utilize reactive solid sorbents to remove gas phase sulfur and hot gas filters to collect the ash and sorbent particles. This approach in IGCC provides for highest energy efficiency and lowest cost of electricity.

IGCC systems may utilize air or oxygen blown entrained or fluid bed gasifiers. Specific operating conditions of the hot gas particulate filter will vary depending on these choices. In general, hot gas filter pilot plant test experience suggests that gasifier ash/char is noncohesive with relatively high flow resistance. Thus, the potential for fines reentrainment and high filter pressure drop are reduced by selecting a relatively low design filter operating face velocity (<5 ft/min). Since the filter treats only the fuel gas component of the total gas flow, the choice of a low filter face velocity does not adversely impact economics. Typically, for a 100 $MW_e$ IGCC system, the filter is required to treat only 6000 to 12,000 acfm, depending if the gasifier is oxygen or air blown. Inlet dust loadings may also vary widely, ranging from <1000 ppmw to 10,000 ppmw.

Bubbling bed PFBC technology is currently being demonstrated at commercial scale. Two PFBC units are located in Sweden (Stockholm Energi, Vartan Plant), another one at the Endesa's Escatron Plant in Spain and one in the United States at the American Electric Power's (AEP Tidd Plant located in Brilliant, Ohio. The Tidd PFBC is a 70 $MW_e$ demonstration plant awarded through the Round 1 of U.S. DOE Clean Coal Technology Demonstration Program. Currently, all four plants utilize high efficiency cyclones to remove greater than 95% of the ash and a ruggedized gas turbine to tolerate ash carried over from the upstream cyclones. Economic and performance improvements in these first generation type PFBC plants can be realized with the application of hot gas particulate filters. Both the secondary cyclone(s) and stack gas ESP(s) could be eliminated saving costs and providing lower system pressure losses. The cleaner gas (basically ash free) provided with the hot gas filter, also permits a wider selection of gas turbines with potentially higher performance.

For these bubbling bed PFBC applications, the hot gas filter must operate at temperatures of 1580°F and system pressures of 175 psia (conditions typical of the Tidd PFBC plant). Inlet dust loadings to the filter are estimated to be about 500 to 1000 ppm with mass mean particle diameters ranging from 1.5 to 3 μm. For commercial applications typical of the 70 $MW_e$ Tidd PFBC demonstration unit, the filter must treat up to 56,600 acfm of gas flow. Scaleup to about 310 $MW_e$ would require filtering over 160,000 acfm gas flow. For these commercial scale systems, multiple filter vessels are required. Thus, the filter design should be modular for scaling.

An alternative to the bubbling bed PFBC is the circulating bed concept. In this process the hot gas filter will in general be exposed to higher operating temperatures (1650°F) and higher (factor of 10 or more) particle loading. Although the inlet particle loading is high, it

contains a significantly coarser fraction (mass mean generally >15 μm) which helps mitigate the effect of the higher mass loading. For a 75 $MW_e$ commercial scale circulating bed PFBC plant, gas flow to the filter is approximately 70,000 acfm. At this scale, multiple vessels with modular filter subassemblies are required.

Second generation or topping PFBC is being developed and planned for demonstration and commercialization. In this plant, higher (than first generation PFBC) turbine inlet temperatures are achieved by partially devolatilizing the coal in a carbonizer unit producing a fuel gas. The char produced is transferred and burned in a circulating PFBC unit with high excess air. The hot (1600°F) vitiated air produced is used to combust the hot fuel gas to raise the combustion gas temperature to as high as 2350°F (Robertson, et al., 1989). With second generation PFBC, two hot gas filters are required. One filter is used to collect the ash and char material carried over from the carbonizer unit with the hot fuel gas. The second filter is used to remove ash and sorbent particles carried over with the hot vitiated air leaving the circulating pressurized fluidized bed combustor (CPFBC). Both filter units are required to operate at high temperatures (1200 to 1600°F) and high particle loading. The fuel gas filter will operate in reducing gas while the CPFBC filter operates in oxidizing conditions. A 95 $MW_e$ second generation PFBC demonstration plant requires a hot fuel gas flow to its filter of about 8000 acfm and hot vitiated air flow to its filter of approximately 64,000 acfm.

In advanced coal based gas turbine cycles, the hot gas filter must meet the application requirements summarized in Table 1. The hot gas filter must remove sufficient particulate to protect the gas turbine from erosion damage, corrosion and particle deposition and meet power plant environmental emission standards (NSPS). Turbine tolerance estimates and current NSPS requirements are shown in Figure 2. Also shown are ceramic barrier filter outlet particle loading data from subpilot and pilot plant test facilities. This data shows the high performance potential of hot gas ceramic filter devices relative to application requirements. Candle, cross flow and tube filters are examples of ceramic barrier filter devices being developed for high temperature particle filtration. These filter devices are basically absolute filters on ash material, can be operated at high gas throughput and can be cleaned by simple pulse jet methods.

**Table 1. Hot Gas Filter Application Requirements**

- Effective Filter
  - Meet NSPS
  - Protect Downstream Equipment
- Operate Reliably
  - Cleanable
  - Stable Pressure Drop Characteristics
- Robust
  - Oxidizing/Reducing Environments
  - Alkali/Acid Gas
  - Thermal Cycling

## PROJECT DESCRIPTION

Westinghouse is developing a high temperature particulate filter system for application in IGCC and PFBC, advanced power generation systems.

### Hot Gas Filter System

The Westinghouse hot gas filter design, shown in Figure 3, consists of stacked arrays of filter elements supported from a common tubesheet structure. In this design, the arrays are

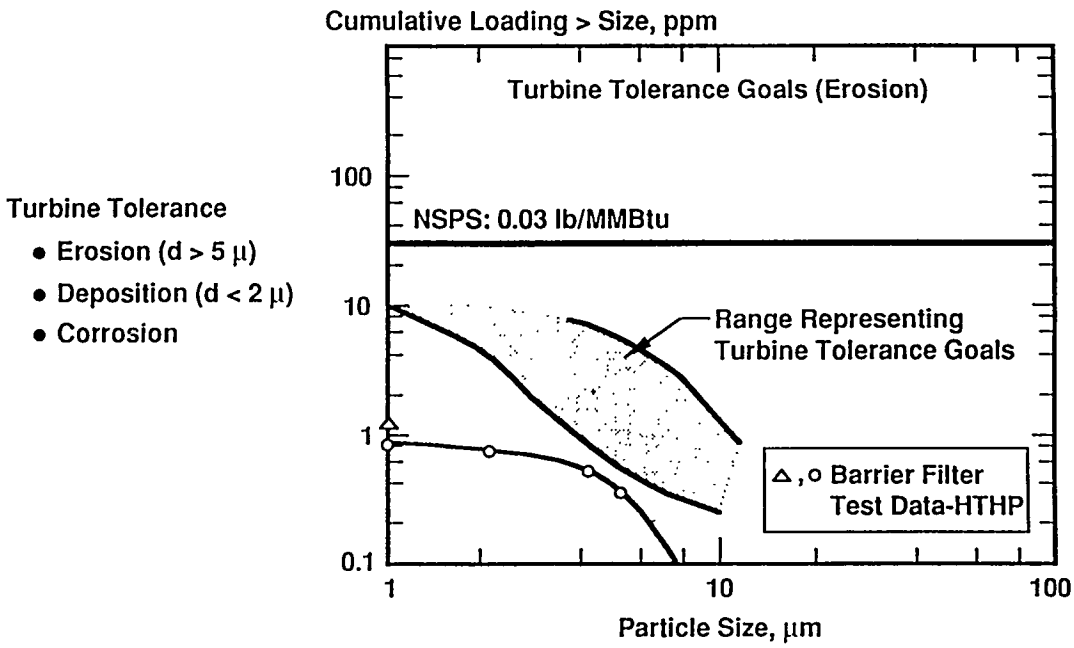


**Figure 2. Turbine Tolerance and Particulate Emission Requirements in Coal Fueled Gas Turbine Applications**

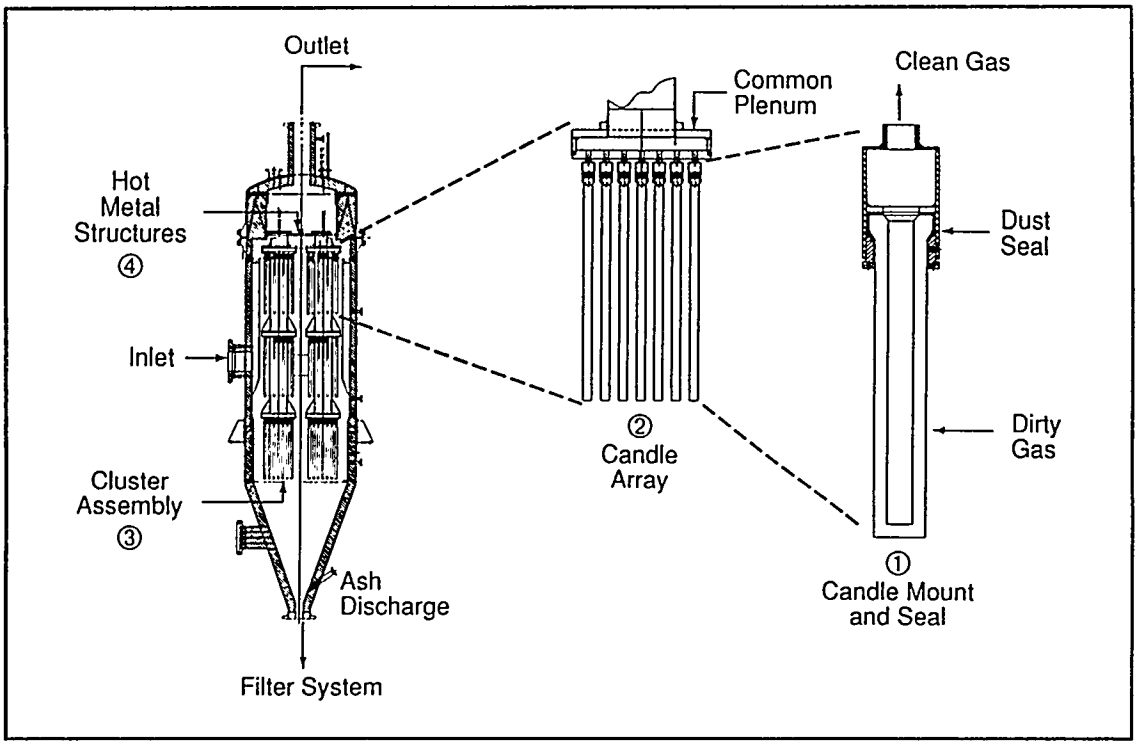


**Figure 3. Hot Gas Cleaning Systems - Westinghouse Candle Filter System**

formed by attaching individual candle elements (Item 1) to a common plenum section (Item 2). All the dirty gas filtered through the candles comprising this single array is collected in the common plenum section and discharged through a pipe to the clean side of the tubesheet structure. Each array of filter elements is cleaned from a single pulse nozzle source. The individual plenum assemblies (or arrays) are stacked vertically from a common support structure (pipe), forming a filter cluster (Item 3). The individual clusters are supported from a common, high alloy tubesheet structure and expansion assembly (Item 4) that spans the pressure vessel and divides the vessel into its "clean" and "dirty" gas sides. Each cluster attaches to the tubesheet structure by a specially designed split ring assembly. The cluster is free to grow down at temperatures. The plenum discharge pipes ducting the filtered gas to the clean gas side of the tubesheet structure are contained within the cluster support pipe and terminate at the tubesheet. Each discharge pipe contains an eductor section. Separate pulse nozzles are positioned over each eductor section. The eductors assist pulse cleaning. During cleaning, the pulse gas is contained within and ducted down the discharge pipe and pressurizes the respective plenum section.

The plenum assembly and cluster (stacked plenums) form the basic modules needed for constructing large filter systems indicative of PFBC requirements. The scaleup approach is:

- Increasing plenum diameter (more filter elements per array)
- Increasing the number of plenums per cluster
- Increasing the vessel diameter to hold more clusters

In general, vessel diameter will be limited by the tubesheet structure and desire to shop fabricate the vessel. Larger PFBC plants would utilize multiple vessels.

**Filter Technology**

Ceramic barrier filter devices, such as candles and cross flow filters, are under development for hot gas filter application. These devices have been shown to be basically absolute filters on ash material, can be operated at relatively high gas throughput with acceptable pressure drop and cleanable by simple reverse pulse jet methods. Clay bonded silicon carbide (SiC) candle filters are commercially available. The structure of these elements is mainly a coarse-grained SiC bonded by a clay-based binder. Each element is provided with a fine grained SiC or aluminosilicate fiber outer skin that serves as the filtration surface. Alternate, oxide-based ceramic materials are also being developed for ceramic barrier filter application. Both first generation, full-scale cross flow and candle filter elements have been constructed using a homogeneous structure that is an alumina/mullite (A/M) matrix containing a small percentage of amorphous (glass) phase. Laboratory and field evaluation of these and other materials are being conducted to identify, characterize and compare their respective chemical and thermal stability for IGCC and PFBC applications (Alvin et al., 1993).

This paper updates the assessment of the Westinghouse hot gas filter design based on ongoing testing and analysis.

An important aspect of the filter system development includes the selection and qualification of the ceramic filter element and the implementation and integrated operation of these filters in pilot plant facilities (Lippert et al., 1993).

The qualification and commercialization of the Westinghouse hot gas filter system is being supported through key subpilot, pilot and demonstration programs.

This paper provides a summary of Westinghouse test experience to date focusing on key technology areas. Table 2 provides a summary of Westinghouse subpilot and pilot plant IGCC and PFBC hot gas filter testing experience. Westinghouse currently has accumulated over 2400 hours of ceramic barrier HGF operating experience in gasification environments, both fluidized bed gasification and entrained gasification. In PFBC environments, Westinghouse has accumulated over 8700 hours of experience. In addition to this field experience, over 25,000 hours of test experience has been compiled in Westinghouse HGF, high temperature high pressure simulators.

## RESULTS

### Entrained Gasification

In this program, a subpilot scale hot gas filter was integrated with the 15 tpd (570 kg/hr) Texaco entrained gasification facility located in Montebello California and operated from April 1989 through August 1992. Filter testing was in support of a base program that was focused on evaluating hot desulfurization technologies. In this testing, the filter was used to protect the external sulfur sorbent beds from ash plugging. Initially, cross flow filters were utilized (Lippert et al., 1993). The filter unit was later backfitted with a 19-element candle array. The candles were implemented to provide data on an alternate filter element geometry, thus providing a basis to directly compare and assess operating characteristics. Seventeen (17) of the candles were the Schumacher 1.5-m (5 ft) long clay bonded SiC F40's; two (2) candles were 1-m long prototype designs of the Coors alumina/mullite.

In the candle filter testing, approximately 300 hours of operation on coal were achieved in four separate test runs, Table 3. In this testing, operating face velocities were maintained at relatively low values necessitated by high ash flow resistance and probable occurrence of fines reentrainment. The performance of the unit was determined by inspection between test runs. In general, these inspections (Test Runs 1 thru 3) confirmed candle integrity and absence of dust leaks. At the end of Test Run 4, a greater than 1800°F temperature excursion occurred. Subsequent inspection showed that three candle elements had failed (one of the SiC and the two, 1.0-m long alumina/mullite prototype elements).

Test results show that in the entrained gasification application stable pressure drop operation can be achieved but the ceramic barrier filter system must be sized and designed for relatively low face velocity (<4 ft/min) and high operating pressure drop. No significant differences between the operating characteristics of the cross flow and candle could be identified.

### Pressurized Fluidized Bed Combustion

Westinghouse is conducting hot gas filter testing at two different PFBC facilities: at the American Electric Power (AEP) 70 $MW_e$ Tidd-PFBC demonstration plant located in Brilliant Ohio, and in the Ahlstrom 10 $MW_t$ circulating PFBC facility located in Karhula Finland.

In August 1989 a cooperative agreement was signed between Ohio Power Company, through its agent, the American Electric Power (AEP) Service Corporation and the U.S. DOE to

## Table 2. Westinghouse IGCC and PFBC Hot Gas Cleaning Testing Experience

| Facility | Pressure (psi) | Temperature Range (°F) | Flow (ACFM) | Dust Load (ppmw) | Test Hours |
|---|---|---|---|---|---|
| Texaco Gasifier<br>- Cross-flow<br>- Candle | 350 | 1000 - 1400 | 50 - 110 | 300 - 25,000 | 700 |
| KRW Gasifier<br>- Candle | 131 - 231 | 1050 | 50 - 300 | 1,000 - 25,000 | 1300 |
| Foster Wheeler Carbonizer<br>- Cross-flow<br>- Candle | 150 - 200 | 1100 - 1500 | 100 | 5,000 - 35,000 | 400 |
| Foster Wheeler Combustor<br>- Cross-flow<br>- Candle | 150 - 200 | 1100 - 1500 | 100 | 5,000 - 35,000 | 900 |
| AEP Tidd PFBC<br>- Candle | 135 | 1200 - 1550 | 7,500 | 600 - 10,000 | 5,800 |
| Ahlstrom Karhula PCFB<br>- Candle | 160 | 1550 - 1650 | 3,070 | 4,000 - 18,000 | 2,056 |
| SCS Wilsonville<br>(Kellogg, Foster Wheeler)<br>- Candle<br>- Cross-flow<br>- Bag<br>- Parallel Channel | 200 - 350 | 1200 - 1900 | 1,000 - 1,700 | 4,000 - 40,000 | Startup Late 1995 |
| SPPC, Pinon Pine IGCC Project<br>- Candle | 260 | 1000 | 13,391 | 18,000 | Design Phase Startup Late 1996 |

## Table 3. Hot Gas Filter Test Experience

### Entrained Gasification (Texaco/Montebello)

| Operating Parameters | Candles (SiC/Alumina Mullite) | Cross Flow (Alumina Mullite) |
|---|---|---|
| Scale (Pilot), acfm | 70 to 110 | 50 to 110 |
| Pressure, psig | 350 | 350 |
| Temperature, °F | 1300 - 1500 | 1000 - 1400 (Excursion 1800) |
| Face Velocity, ft/min | 1.5 - 2.5 | 1 - 3.5 |
| No. of Filter Elements | 17 | 4 and 8 |
| Inlet Dust Loading, ppmw | 650 - 12,350 | 250 - 22,500 |
| Hours of Operation | 300 | 400 |
| Status | Completed | Completed |

(DE-AC21-88MC24021)

assess the readiness and economic viability of high temperature and high pressure particulate filter systems for PFBC. The hot gas test facility (see Mudd et al., 1992) is a one seventh (1/7) slipstream taken from the Tidd 70 $MW_e$ PFBC Clean Coal Demonstration Plant. The HGF slipstream replaces one of the seven secondary cyclones by taking 100,000 lb/hr of gas from the discharge of one of the primary cyclones, to outside of the combustor vessel, and into the Westinghouse Advanced Particle Filter (W-APF). The gas flows through a backup cyclone, and then is returned to the combustor vessel and rejoins the gas flow exiting the six cyclone strings. The combined gas flow is then expanded through the gas turbine system.

In the slipstream, ash laden gas at 165 psia, 1550°F flows into the W-APF, Figure 3. The W-APF is designed to use up to 384, 1.5-m long candle elements. Ash collected in the filter is discharged to a screw cooler and into a lockhopper which feeds a vacuum pneumatic ash transport system.

The W-APF unit was commissioned in October 1992 utilizing a full complement of Dia Schumalith F40 candle elements. There have been five (5) test periods since initial operation with over 5800 accumulated test hours, Table 4. In test period 4 and 5, several advanced candle filter elements have been tested in limited numbers, Table 5.

In the early operation of the AEP/APF unit (Test Periods 1 and 2) a relatively high efficient, primary cyclone was utilized in front of the hot gas filter unit. Ash inlet loading was relatively low with an ash mass mean diameter of only 1 to 3 μm. This ash was extremely chemically active with the $SO_2$ and $CO_2$ and showed a high tendency to sinter to from an extremely hard dust cake. Under these conditions, stable filter pressure drops could not be achieved above about 1450°F. In addition, at operating temperatures between about 1300°F to 1450°F, stable pressure drop could be achieved over long operating periods (hundreds of hours) but ash cake would tend to accumulate on the metal dust sheds and between candles. This would eventually cause candle damage or failure, particularly during cooldown events. Below about 1300°F, the ash reactivity and flow characteristics appeared to improve significantly and the filter unit could be operated without issue.

In Test Periods 3 and 4, the primary cyclone was detuned by injecting air up through its discharge leg. This increased the mass loading and mass mean particle diameter of the ash entering the filter unit. The ash reactivity and flow characteristics, however, did not improve significantly. Visual inspection of the filter showed ash bridging and ash collected on the metal dust sheds.

In Test Period 5, the primary cyclone was taken out of service, dramatically increasing mass loading and the mass mean particle size. Figure 4 compares the particle size distribution for the three cyclone conditions (in-service, detuned, out of service). The APF unit was successfully operated with the primary cyclone out of service even with higher face velocities (see Table 4). Following the 1100 hr test period, visual inspection confirmed that no ash bridging was evident and the dust shed completely clean of ash buildup.

During Test Period 3, key filter outlet sampling was conducted. Particle outlet loading was measured and $SO_2$ data obtained upstream and downstream of the hot gas filter unit. The sampling was conducted by Radian and reported in DCN94-633-021-03. The outlet total particle mass loading was measured at less than 1 ppm.

## Table 4. Summary of Westinghouse PFBC Hot Gas Filter Testing - Tidd/AEP

| Test Period | 1 (10/92 - 12/92) | 2 (7/93 - 9/93) | 3 (1/94 - 4/94) | 4 (7/94 - 10/94) | 5 (1/95 - 3/95) |
|---|---|---|---|---|---|
| No. of Candles | 384 | 384 | 384 | 288 | 288 |
| Primary Cyclone | In Service | In Service | Detuned | Detuned | Out |
| Test Period, Hours | 464 | 1295 | 1279 | 1705 | 1110 |
| Operating Temperature, °F | 1345 - 1450 | 1150 - 1450 | 1200 - 1435 | 1220 - 1400 | 1400 - 1550 |
| Nominal Face Velocity, ft/min | 4.8 - 6.6 | 4.8 - 6.6 | 4.6 - 6.6 | 6 - 8.8 | 9.5 |
| Inlet Dust Loading, ppmw | 600 | 600 | 3200 | 3200 | 18000 |
| Ash Mass Mean, µm | 1 - 3 | 1 - 3 | 5 - 7 | 5 - 7 | 27 |
| Measured APF Outlet Loading* | | | <1.0 | | |

* By Radian (DCN 94-633-021-03)

## Table 5. Advanced Filter Elements Under PFBC Testing

| Designation | Supplier | Matrix |
|---|---|---|
| Vitropore 442T | Pall | Clay Bonded SiC |
| FT20 | Schumacher | Clay Bonded SiC |
| SiC-Composite | 3M | CVI Infiltrated |
| P-100A | Coors | Alumina/Mullite |
| PRD-66 | DuPont | Filament Wound Oxide |

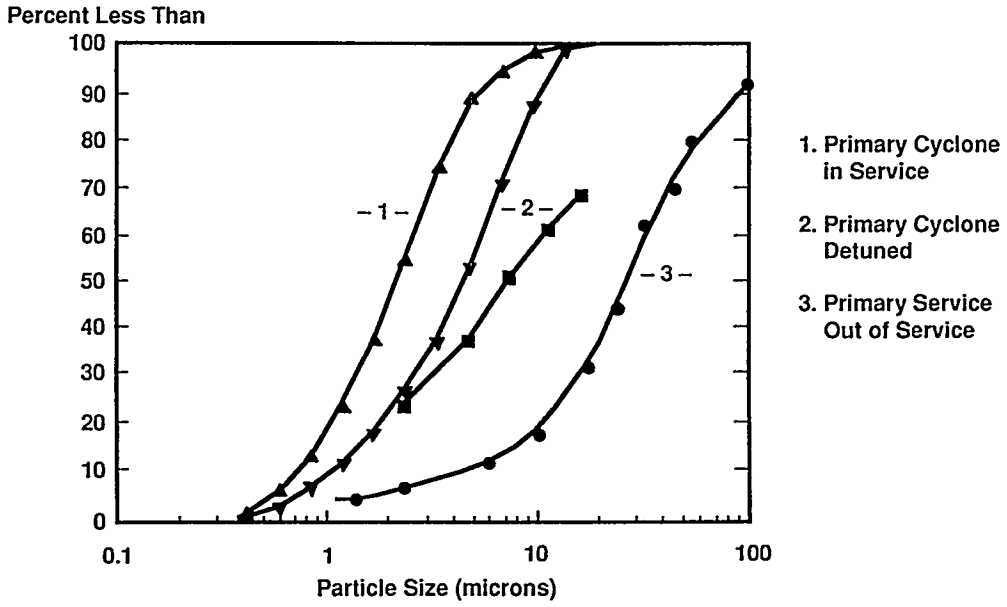


**Figure 4. Ash Particle Size Distribution in PFBC/Tidd APF Testing**

Results of the $SO_2$ sampling is given in Table 6. Results showed that across the filter unit an additional 40 to 45% $SO_2$ removal was achieved.

Through the AEP-PFBC hot gas cleanup cooperative agreement, the U.S.DOE, AEP, Ahlstrom/Pyropower, EPRI and Westinghouse have embarked on a program to also test the W-APF under Pressurized Circulating Fluid Bed (PCFB) conditions. This testing is being conducted at the Ahlstrom 10 MWt PCFB facility located in Karhula Finland, see Lippert et al., 1994. The Westinghouse candle filter installed at Ahlstrom facility consisted of a single 3-array cluster identical to the clusters installed at Tidd, Figure 5. Filter operation was initiated in late October 1992 utilizing a full compliment of 128 alumina/mullite candle filter elements. Operation has included three test segments, achieving approximately 2046 hours of operation, Tables 7 and 8. This testing has included a wide range of coal types and operation to temperatures of 1650°F (900°C). Also, in Test Segments 2 and 3, the alumina/mullite candles were replaced with clay bonded Vitropore 442T SiC elements.

Stable filter pressure drop has also been achieved in the Ahlstrom facility while operating over a wide range of coal/sorbent types and gas temperature to 1650°F (900°C). Figure 6 compares the pressure drop characteristics for the different coal types used in this test program. The stable filter operating conditions in this facility are attributed to the relatively large fraction of ash particles above 10 microns, characteristic of circulating fluid beds. In general, the ash was free flowing and did not accumulate on the metal structures or plenum dust shields. Figure 7 shows the baseline pressure drop for the different coal types over the range of flow conditions tested.

Following the various test runs in both the Ahlstrom and Tidd and PFBC facilities the respective filter units were inspected. In general, these inspections confirmed the effectiveness of the dust seals and integrity of the metal structures. In both test programs extended, trouble-free operating periods have been achieved in which the candle filter units have demonstrated excellent particle collection efficiency.

**Topping PFBC**

Development of the Topping PFBC (second generation PFBC) is taking place at the Foster Wheeler Development Corporation (FWDC) pilot plant facility located at the John Blizard Research Center in Livingston, New Jersey. The program is in three phases. Phase 1, already completed, developed a conceptual design of the commercial scale plant and identified R&D needs (Robertson et al., 1989). The second phase, also completed, involved separate subscale pilot tests of the carbonizer/filter and combustor/filter. Carbonizer/filter testing occurred in 1992. Combustor/filter testing was completed in 1993. Results of this testing are summarized in Table 9. In 1994 the facility was converted for integrated operation.

During the carbonizer/filter testing, the carbonizer was operated as a jetting fluidized bed unit. Approximately 150 hours of filter operation was achieved. This testing used cross flow filter elements for about 100 hours . Stable filter operation was demonstrated. The carbonizer char showed relatively high flow permeability compared to earlier entrained gasification experience. The char was free flowing and no difficulty was experienced draining the filter vessel.

**Table 6. Tidd/PFBC - Hot Gas Filter Sulfur Retention (PPMV $SO_2$)**

| | APF | | ESP | |
|---|---|---|---|---|
| | Inlet | Outlet | Inlet | Outlet |
| Sample 1 | - - - - | 119 | 202 | 202 |
| Sample 2 | 243 | 135 | 193 | 192 |
| Sample 3 | 201 | 114 | 185 | - - - - |

Measurements Show 40 to 45% $SO_2$ Removal Across Hot Gas Particulate Filter

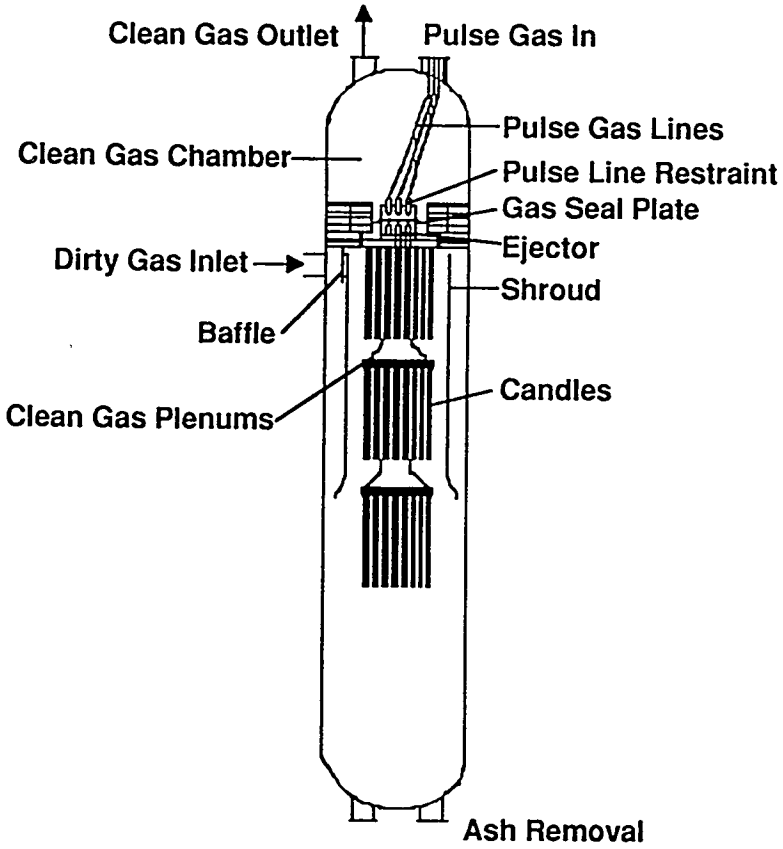


**Figure 5. Schematic of PCFB Hot Gas Candle Filter**

| Table 7. Summary of Westinghouse Hot Gas Filter Operation at the Ahlstrom PCFB Facility - Karhula, Finland | | | | |
|---|---|---|---|---|
| Coal | Segment 1 (Hours) | Segment 2 (Hours) | Segment 3 (Hours) | Total |
| Illinois No. 6 | 85 | 221 | -- | 306 |
| Iowa Rawhide | 61 | -- | -- | 61 |
| Newland | 300 | -- | -- | 300 |
| Kentucky | 270 | -- | -- | 270 |
| Bituminous | -- | -- | 170 | 170 |
| Pennsylvania | -- | -- | 135 | 135 |
| Black Thunder | -- | 291 | 513 | 804 |
| Total Coal | 716 | 512 | 818 | 2046 |

| Table 8. Summary of Karhula PCFB Testing | | | |
|---|---|---|---|
| | Test Segment 1 | Test Segment 2 | Test Segment 3 |
| Type of Candles | Alumina/Mullite | SiC-442T | SiC-442T |
| Operating Temperature, °C | 870-900 | 720-830 | 690-850 |
| Nominal Face Velocity, cm/s | 2.9-4.0 | 1.7-3.3 | 1.5-4.0 |
| Inlet Dust Loading, ppm | 4,460-13,000 | 2060-12,300 | 3000-10,000 |
| Operating Hours | 716 | 512 | 818 |

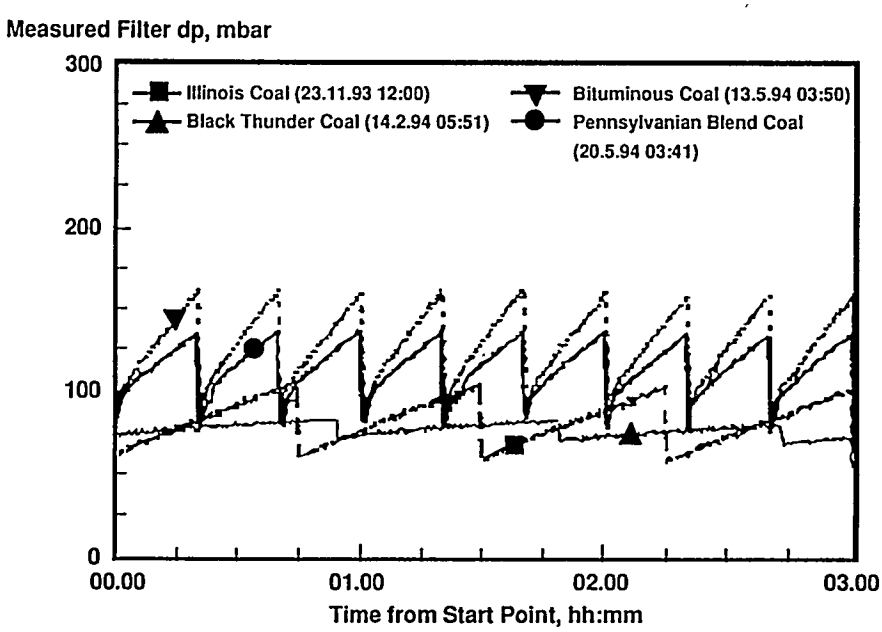


**Figure 6. Typical Hot Gas Candle Filter Pressure Drop Characteristics in PCFB Pilot Plant - Test Segments 2 and 3**

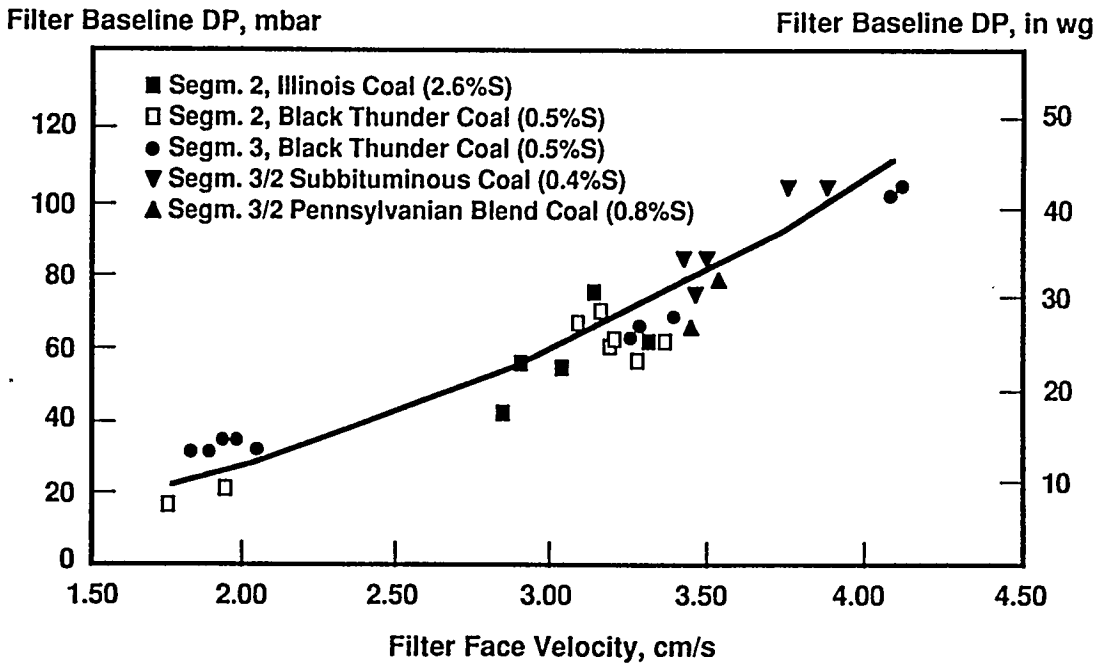


**Figure 7. Hot Gas Candle Filter Pressure Drop Characteristics in PCFB Pilot Plant - Test Segments 2 and 3**

**Table 9. Hot Gas Filter Test Experience**

Foster Wheeler - APFB

| Operating Parameters | Carbonizer | Combustor |
|---|---|---|
| Scale (Pilot) | 120 acfm | 400 acfm |
| Type Filters | Cross Flow Candles (SiC) | Candles (A/M) Candles (SiC) |
| Pressure, psig | 100 - 200 | 100 - 200 |
| Temperature, °F | 1100 - 1500 | 1400 - 1700 |
| Face Velocity, ft/min | 1.5 | 4 - 8 |
| Dust Loading, ppmw | 4,000 - 30,000 | 2,000 - 35,000 |
| Hours of Operation (thru 1994) | 150 | 700 |
| No. Test Runs | 3 | 12 |
| Status | Phase III | Phase III |

Following carbonizer testing, the facility was modified to operate in the pressurized circulating fluidized bed combustion mode. The filter unit was configured to a 22-element candle array. Approximately 700 operating hours were accumulated. The PCFB testing included a significant shakedown period (approximately 400 hours) to evaluate PCFB operation and control. During this period the PCFB was tested on both coke and coal and the filter was exposed to severe upset conditions. Candle breakage was incurred in some of the shakedown runs.

The final PCFB test run following shakedown included a 180 hour continuous test period in which the PCFB and filter operated under char and coal fired conditions. In this test, the filter was configured with a 14 candle elements to operate at a face velocity of about 8 ft/min. The PCFB operated smoothly and without major upset. Filter operating pressure drop was stable throughout the test run. Inspection of the filter following completion of the test run showed the 14 candle elements to be undamaged. There was no indication of dust leaks to the clean side. Phase III operation is currently in progress. In this testing, the carbonizer and combustor are integrated. The carbonizer filter is the 22-element candle array previously utilized in the Phase II testing. A second candle filter unit was designed and supplied for the combustor leg. This filter contains 45 candle elements in a two plenum array.

**Candle Material Surveillance.** Material surveillance programs have been implemented to recover and characterize selected filter elements from the various field test programs. The objectives are to identify the potential long term thermal/chemical effects that advanced coal based power generating systems have on the stability of porous ceramic filter materials and assess the influence of these effects on filter operating performance and life. Most of the current operating experience has been with first generation monolithic porous ceramic candles. The Coors alumina/mullite and clay bonded silicon carbide Pall Vitropore 442T and Schumacher Dia Schumalith F40 candle filters have typically operated between temperatures of 1000°F to 1650°F (540°C and 900°C) in both oxidizing and reducing gas environments representative of advanced coal-fired process applications. Surveillance candles recovered from the pilot plant testing have been destructively evaluated for strength and characterized using SEM/EDAX analytical techniques, (Alvin et al., 1994). A companion paper updates the Westinghouse filter materials development work.

**SCS/PSDF - Hot Gas Filters.** Westinghouse is designing two hot gas particle control devices (PCD) for installation at the Southern Company Services Power System Development Facility located in Wilsonville, Alabama. Table 10 summarizes the basis for the two PCD designs. PCD 352 will be installed and integrated with the Foster Wheeler circulating PFBC unit. The filter is designed to utilize candle filter elements. Operating experience gained from the Karhula PCFB and Tidd PFBC filter testing have been factored into the PCD 352 design. Improvements include increased spacing between the candle elements and plenum pipe support structure, redesign of the plenum dust shields to enlarge and improve the path for ash discharge; recessing the candle filter holders into the clean gas plenum sections thus eliminating the region where dust can bridge and form clumps that ultimately can break off and get trapped between the candle elements. A steeper cone angle and large outlet flange are also employed in the vessel ash hopper region to promote ash discharge.

**Table 10. SCS/PSDF - Westinghouse Hot Gas Filter**

| HGF Design/Operating Parameters | FW/APFB Combustor | FW/APFB Carbonizer and MWK Transport Reactor |
|---|---|---|
| Gas Flow, acfm | 2000 to 8800 | 1000 to 2000 |
| Design Pressure, psig | 350 | 350 |
| Operating Temperature, °F | 1200 to 1650 | 1000 to 1800 |
| Inlet Dust Loading, ppmw | 15,000 | 4,000 to 16,000 |
| Filter Elements | Candles | Candles (Initial)* |
| No. Elements (Max) | 273 | 91 |
| Face Velocity, ft/min | 8 @ 6200 acfm | 4.2 @ 1000 acfm |
| *Options | | Cross Flow<br>CeraMem<br>Ceramic Bags |

The PCD 301 unit will be initially installed and operated on the M. W. Kellogg transport reactor test module. The PCD 301 is designed to interchange the test cluster to accommodate a variety of filter types including:

- Advanced Candles
- Cross Flow
- CeraMem Axial Cross Flow
- Ceramic Bags

## FUTURE WORK

Continued testing of Westinghouse hot gas filter system is planned this summer at the Foster Wheeler APFBC pilot plant facility. Testing of the advanced design PCD 301 and 352 at the SCS/PSDF is scheduled to be initiated in the third quarter in 1995. Results of these and other ongoing filter testing will be utilized to demonstrate and qualify the Westinghouse Advanced Particle Filter for Clean Coal and commercial application.

## REFERENCES


Alvin, M. A., T. E. Lippert, E. S. Diaz, and E. E. Smeltzer, 1994, "Durability of Ceramic Filters," *Proceedings of the Coal-Fired Power Systems 94 - Advances in IGCC and PFBC Review Meeting,* Volume II, pp. 545-571.

Alvin, M. A., et al., 1993. "Hot Gas Cleanup and Gas Turbine Aspects of an Advanced PFBC Power Plant," *Proceedings of the Ninth Annual Coal-Fueled Heat Engines, Advanced Pressurized Fluidized-Bed Combustion (PFBC) and Gas Stream Cleanup Systems Contractors Review Meeting*, p. 168, DOE/METC-93/6129.

Lippert, T. E., G. J. Bruck, and J. Isaksson, 1994, "Karhula Hot Gas Cleanup Test Results," *Proceedings of the Coal-Fired Power Systems 94 - Advances in IGCC and PFBC Review Meeting,* Volume II, 1994, pp. 535-544.

Lippert, T. E., M. A. Alvin, E. E. Smeltzer, D. M. Bachovchin, and J. H. Meyer, 1993, "Subpilot Scale Gasifier Evaluation of Ceramic Cross Flow Filter - Final Report," DOE/METC Contract No. DE-AC21-88MC24021, August.

Mudd, M. J. et al., 1992, "Initial Operation of the Tidd PFBC HGCU Test Facility," *Proceedings of the Ninth Annual Coal-Fueled Heat Engines, Advanced Pressurized Fluidized-Bed Combustion (PFBC), and Gas Stream Cleanup Systems Contractors Review Meeting*, p. 27, DOE/METC-93/6129.

Robertson, A., et al., 1989, "Second-Generation Pressurized Fluidized Bed combustion Plant: Research and Development Needs," Foster Wheeler Development Corporation, Livingston, NJ. Phase 1, Task 2 Report FWC/FWDC-TR-89/06 to the U.S. DOE under contract DE-AC21-86MC21023.

## 3.2 Lightweight Ceramic Filter Components: Evaluation and Application

### CONTRACT INFORMATION

**Contract Number** DE-FG02-92ER81349

**Contractor** Industrial Filter & Pump Mfg. Co., Inc.
5900 Ogden Avenue
Cicero, IL 60650
(708)656-7800

**Contract Project Manager** Paul M. Eggerstedt

**Principal Investigator** Paul M. Eggerstedt

**METC Project Manager** Norman T. Holcombe

**Period of Performance** July 27, 1992 to February 17, 1995 (extended to October 15, 1995)

**Schedule of Milestones**

**Program Schedule**

| | 1992 | 1993 | 1994 | 1995 |
|---|---|---|---|---|
| **Phase 1** | ********** | | | |
| **Phase 2** | ********** | ********** | ********** | ********** |
| **Candle Strength Testing** | ********** | ********** | ********** | |
| **Tubesheet Strength Testing** | ********** | ********** | ********** | |
| **Corrosion Studies** | | | ********** | ********** |

### OBJECTIVES

The primary objective of this SBIR research program is to increase the performance, durability, and corrosion resistance of lightweight filter candles and filter tubesheet components (Fibrosic™), fabricated from vacuum formed chopped ceramic fiber (VFCCF), for use in advanced coal utilization applications. Phase I results[1] proved that significant gains in material strength and particle retentivity are possible by treatment of VFCCF materials with colloidal ceramic oxides. Phase II efforts will show how these treated materials tolerate high temperature and vapor-phase alkali species, on a long-term basis. With good durability and corrosion resistance, high temperature capability, and a low installed and replacement cost, these novel materials will help promote commercial acceptance of ceramic candle filter technology, as well as

increase the efficiency and reliability of coal utilization processes in general.

## BACKGROUND INFORMATION

Ceramic candle filtration is an attractive technology for particulate removal at high temperatures. Due to their simple and cost effective design, temperature capability, and high filtration efficiency, ceramic candles are one of the few clean-up technologies which can consistently meet gas turbine manufacturer's inlet particulate requirements and Clean Air Act mandates. Unfortunately, traditional ceramic candles, made from granular silicon carbide, etc., can be prone to failure from physical and thermal shock as well as chemical attack. These candles also tend to be expensive and, owing to their weight, present internal filter design problems.

### VFCCF Filter Materials

Unlike traditional filter candles, VFCCF filter candles offer unique properties for use in HGCU applications, as shown below:

<u>VFCCF Filter Candle Properties:</u>

- Formed from stable ceramic oxides
- Lightweight
- High temperature capability
- Fibers & binder share similar thermochemical properties
- "Knitted" pore matrix

Typically, VFCCF filter candles are formed from commercially available fibers and binders, using existing vacuum forming technology, resulting in a low cost product with excellent manufacturing uniformity and quality control. Because the fibers and binders are essentially a blend of stable, pure ceramic oxides, such as alumina and aluminosilicate materials, the amount of contaminants, organics, etc. which might be reactive in certain applications is negligible.

With apparent density values in the range of 17-22 lbs/ft$^3$, VFCCF candles are much lighter in weight than their granular ceramic counterparts. This low density, which translates into a weight savings of 70-80% over isostatically pressed silicon carbide filter elements, results in a highly permeable filter with roughly twice the pore volume as granular filter candles. Additionally, as a direct result of the weight savings, the design and construction of the tubesheet and supporting hardware becomes a much easier task, not to mention the reduced stress on the filter candle flange.

VFCCF fibers and binders are typically rated for a maximum temperature of 2600°F to 2800°F, and do not exhibit significant physical changes, such as shrinkage, until a temperature of about 2300°F. is reached. As a result, they are suitable for use in nearly all IGCC and PFBC applications, where temperatures are generally 2000°F. or lower.

Because VFCCF binders are nearly identical in chemical composition to that of the fibers, differences in thermochemical properties between the binder and fiber are negligible, resulting in excellent thermal shock and thermal spalling resistance, as well as resistance to microcracking caused by differences in the thermal expansion coefficients of the fiber and binder. As a consequence of the fiber geometry within the VFCCF matrix, these candles also have an inherently high crack resistance, due to the "knitting" tendency of the fibers during fabrication, and their random orientation which tends to blunt microcrack propagation. Table 1 summarizes these important properties of VFCCF materials.

In the course of fabrication of VFCCF candles, it was found that such materials respond extremely

well to treatment with colloidal ceramic oxide materials, which can increase strength, add corrosion resistance to suit a given application, and allow for the particle retention of the filter element to be controlled, all of which have led to the research effort discussed in this report. With their combined high temperature capability, low thermal expansion, corrosion resistance, and resistance to catastrophic failure, VFCCF materials show promise for use as filter candles and other internal filter hardware, such as a tubesheet, with proper colloidal treatment.

**Table 1. VFCCF Material Properties**

| | |
|---|---|
| Typical Chemistry | 35-60% $Al_2O_3$<br>40-65% $SiO_2$ |
| Apparent Density | 17-22 lbs/ft$^3$ |
| Maximum Use Temperature | 2800°F |
| Thermal Conductivity (1500°F) | 1.26 BTU-in/ft$^2$-°F-hr |
| Permanent Lineal Shrinkage (2000°F) | less than 0.8% |
| Coefficient of Thermal Expansion | 2.8 x $10^{-6}$ in/in-°F |

## PROJECT DESCRIPTION

### Phase 1 Efforts

The overall objective of the Phase 1 effort was to determine which colloidal ceramic oxides of those tested exhibited the greatest increase in the strength of VFCCF filter candle and tubesheet specimens. In the case of VFCCF filter candles, strength increases were valued as important, but not at the expense of acceptable permeability. A total of five different colloidal ceramic oxides, applied using two distinctly different methods, were investigated as shown in Table 2.

**Table 2. Colloidal Ceramic Oxide Tests**

| Materials Tested | Application Methods |
|---|---|
| Silica<br>Alumina<br>Zirconia<br>Yttria<br>Ceria | Spray<br>Infusion |

The materials above were selected on the basis of their temperature capability, corrosion resistance, thermal expansion compatability with VFCCF materials, commercial availability, and cost. Application methods were approached from the standpoints of reproducibility of results, relative cost, and minimal complexity. In both application methods, variations in the colloidal material concentrations as well as the total amount of material applied to the candle and tubesheet test specimens were evaluated in an effort to optimize a technique for producing filtration components with superior performance characteristics.

### Phase 2 Efforts

Several goals of the Phase 2 effort are expected to be met as a result of this ongoing research, namely:

- Selection of the most suitable colloidal ceramic oxide material for use in increasing VFCCF material strength and corrosion resistance, without greatly sacrificing permeability (in the case of filter candle applications);
- Development and optimization of the most promising colloidal ceramic oxide

application methods, suitable for mass production of VFCCF components;

- Development and refinement of other means of increasing strength and durability of VFCCF materials, including such techniques as:

  -Filter candle flange, end-cap, and forming die modifications;
  -Investigating the effect of varying fiber type and fiber length on VFCCF material strength;
  -Investigation of lamination and joining techniques for structural VFCCF uses.

Descriptions of each of the above aspects of this research effort follow.

**Colloidal Ceramic Oxide Material Selection.** In addition to the colloidal oxide materials cited earlier, Phase 2 tests involving colloidal mullite were performed. Colloidal mullite has good thermochemical properties and corrosion resistance, adds strength, and tends to form a desirable divergent, acicular pore structure within the VFCCF candle matrix after infusion and subsequent curing. Several VFCCF filter candle specimens prepared in this manner were tested in a PFBC application at Argonne National Laboratory, through funding from the Illinois Clean Coal Institute (ICCI), with excellent results[2]; other similarly prepared candles have been tested for permeability decay and durability at Acurex Corp. in Mountain View, CA.[3]

**Colloidal Ceramic Oxide Treatment of VFCCF Materials; Spray Application Trials.** In continuation of the Phase 1 effort, colloidal ceramic oxides have been applied to aluminosilicate VFCCF matrices, both singularly and in combination, by spraying and immersion application techniques in the Phase 2 effort. In the case of application of colloidal oxides by spraying directly onto VFCCF specimens, a number of problems were encountered, including clogging of the spray nozzles due to drying of the ceramic oxide solids within the nozzle during application. Another problem noted during spraying was a gradual but evident dimensional change of the spray nozzle, presumably due to erosion caused by the ceramic oxide's high velocity through the nozzle orifice. This resulted in an increase in deposited material on subsequent samples, over time.

A third problem noted with the spraying technique was that it provided only a very superficial coating of ceramic oxide material onto the sample. This was alleviated partially by the use of a slight amount of vacuum on the downstream side of the specimen, but the additional amount of ceramic oxide coating observed on each specimen was very small. Efforts were made to produce very fine spray patterns for greater penetration of the colloidal oxides into the VFCCF matrices, but this was found to be troublesome and produced substantial amounts of "overspray" due to the fineness of the spray droplets.

**Immersion (Infusion) Application Trials.** By comparison, application of the colloidal ceramic oxides by means of simple immersion (infusion) was much more successful and easier to control. Limited to only a few variables, namely the concentration of the ceramic oxide material and the infusion duration, the application from one specimen to the next was found to be much more uniform and predictable than application by spraying techniques.

**VFCCF Filter Candle Development Program**. In addition to the work involving colloidal ceramic oxides, other means of increasing the durability of VFCCF filter candles has been ongoing, as part of this research grant. Geometry changes in the critical flange and end cap zones

has been one successful approach. A female vacuum forming die was constructed to permit forming of an integral candle flange, in order to eliminate the original bonded flange design, which subjected the flange joint to shear when positioned in a tubesheet. In so doing, it was believed that the filter element would be inherently stronger in the flange area, by the complete elimination of the ceramic adhesive joint. Several dozen filter candles were made using the new forming die, but it was found that in every case, the tapered flange section of the filter candles did not form sufficiently thick to permit machining to the traditional (rectangular or hemispherical) flange shapes which are accepted commercially. In spite of repeated attempts using different vacuum forming pressures, flowrates, and slurry concentrations, a wall thickness of only 7-10mm resulted in the tapered (flange) section of the die.

In view of the above, the approach whereby the outside flange taper would simply be machined to the desired flange geometry was modified. Numerous designs and procedures were tested, but the most promising approach involved fabrication of full length (1500mm) filter candles using a male forming mandrel, followed by machining both the filtering surface and filter flange using a tracer lathe. Doing so results in a reasonably smooth final product, with excellent concentricity and dimensional tolerances.

End cap failures have been virtually eliminated using the procedure developed in the Phase 2 effort. By rewetting the open filter candle end temporarily, it became possible to insert a conical VFCCF plug into the softened end to serve as an end cap, much like a stopper in a flask. By inserting the plug backwards (i.e., widest end first), however, the softened cylinder could then be drawn or "puckered" around the conical taper of the plug, after which it would reharden upon drying.

## RESULTS

### Phase 1 Efforts

Phase 1 test results showed that the bending strength characteristics of VFCCF materials can increase substantially as a result of the infusion of colloidal ceramic oxide suspensions. In some instances, strength of typical VFCCF tubesheet specimens increased eight-fold, in comparison to the strength of untreated specimens. By variation in colloidal solution application techniques and curing methods, it was also possible to greatly increase VFCCF filter candle strength in critical flange and end cap areas, with a minimal decrease in overall candle permeability. Table 3 provides the highlights of some of the infusion trials, which were quite successful.

**Table 3. Results of Phase 1 Testing**
Aluminosilicate VFCCF Tubesheet Specimen Strength Test Results After Colloidal Ceramic Oxide Infusions

| Infusion Description | Apparent Density (lbs./ft.$^3$) | Modulus of Rupture (lbs./in$^2$) |
|---|---|---|
| Untreated Aluminosilicate | 17.02 | 52.68 |
| Single Immersion, $SiO_2$ | 36.83 | 274.11 |
| Single Immersion, $Al_2O_3$ | 32.67 | 127.84 |
| Double Immersion, $SiO_2$, then $Al_2O_3$ | 47.06 | 440.45 |
| Single Immersion, $ZrO_2$ | 32.08 | 61.79 |
| Single Immersion, $Y_2O_3$ | 28.81 | 168.15 |
| Single Immersion, $CeO_2$ | 30.84 | 86.1 |

**Phase 2 Efforts**

**Single Infusion Studies.** Because of the problems cited earlier with the application of colloidal ceramic oxides by means of spraying, Phase 2 efforts focused primarily on infusion (immersion) as the method of application. Numerous single infusions of VFCCF (aluminosilicate) fiber specimens were made; in each case, the solids concentration of the various colloidal suspensions used was as follows:

- Silica 40% w/w
- Mullite 28% w/w
- Yttria 14% w/w
- Alumina 20% w/w

While it would have been desirable to test using identical concentrations of each suspension, the number and significance of other variables (e.g., pH, viscosity, particle size distribution, etc.), combined with the relative instability of the suspensions, made this an impossible task. Also, unlike Phase 1 testing, ceria and zirconia colloidal ceramic oxides were eliminated in the Phase 2 tests, due to their relatively small resultant strength enhancement of VFCCF matrices.

In the case of silica, a single immersion appeared to increase weight and also strength of the aluminosilicate fiber matrix considerably more than any other material, but at the same time appeared to "seal" the outer pores of each specimen so as to prevent further penetration of colloidal oxides after a subsequent immersion. Although silica is known to increase VFCCF material strength dramatically, because of its susceptibility to corrosion in high temperature environments (from steam, alkali and other corrosive attack mechanisms), it became apparent that another additional ceramic oxide must be applied over the silica layer to produce a durable product. Because of the sealing tendency of the silica, however, it became questionable if suitable penetration by a subsequent corrosion resistant material would in fact take place.

Another material which was tested in a single treatment immersion application was that of colloidal mullite. While the mullite applications did not see the rather dramatic weight or strength increases observed with the silica treatment, it was noted that the mullite treatment penetrated very uniformly in each specimen tested, and did not have the tendency to seal or "blind" the pores, as was noted in the silica immersion trials. This observation seems to indicate that subsequent immersions in colloidal mullite, or other colloidal ceramic oxides might lead to greater overall penetration than was noted in the silica trials. Given the advantage mullite has over silica in terms of corrosion resistance, (particularly against vapor phase alkali species in a hot gas environment), combined with good thermal shock resistance and low thermal expansion, mullite is considered to be a choice colloidal material for VFCCF treatment. In each test case involving mullite, a weight increase of 45-85% was noted.

Still another material which was tested in a single treatment immersion study was that of alumina. Alumina has a very high corrosion resistance with regard to vapor phase alkali species, but it was noted that the amount of alumina infused into the VFCCF specimens resulted in a weight increase less than that of mullite, in the range of 45-65%. Based on Phase 1 bending strength test data, alumina did not significantly increase strength, so it was concluded that the use of colloidal alumina for VFCCF materials would be limited to that of a final corrosion resistant treatment only.

The last colloidal ceramic oxide material which was applied by means of single immersion techniques in the Phase 2 effort was that of yttria. Yttria has high thermal stability, good corrosion resistance, and has been found to increase the

strength of VFCCF materials without nearly as much weight increase or permeability loss as silica, mullite, or alumina. In spite of the somewhat higher cost of colloidal yttria in contrast to the other materials tested, it can be used successfully even after 3:1 dilution with water.

In summary then, the strength of structural VFCCF aluminosilicate materials can be substantially increased by a single immersion in silica, whereas strength and corrosion resistance may be increased by immersions using mullite, or more preferably, yttria colloidal ceramic oxide materials.

**VFCCF Fiber Length Variation; Mullite and High Alumina Fiber Testing.** Efforts involving variations in VFCCF fiber length, as well as forming of filter components using mullite fiber and alumina fiber, rather than aluminosilicate fiber, were performed to see what effect these changes might have on VFCCF material strength. The comparative testing was limited to three-point modulus of rupture (M.O.R.) bend tests, performed on specimens having dimensions of 3" x 2" x 12" (span). The average strength values from these tests are shown in Tables 4 and 5.

**Table 4. VFCCF Fiber Length vs. Strength**

| Nominal Fiber Length (mm) | Modulus of Rupture (psi) |
|---|---|
| 30 | 55.35 |
| 15* | 55.65 |
| 7.50 | 85.95 |

*This material is our VFCCF "standard" material.

**Table 5. VFCCF Fiber Type vs. Strength**

| Fiber Type (Nominal Length, mm) | Modulus of Rupture (psi) |
|---|---|
| Aluminosilicate, 15mm | 55.65 |
| Mullite, 15mm | 24.30 |
| High Alumina, 15mm | 48.15 |

The above results indicate that longer aluminosilicate fiber lengths, which produce a lower density product, do not increase strength in comparison to the standard (medium length) aluminosilicate fiber normally used. Shorter, high density aluminosilicate fibers, however, appear to increase strength substantially, by approximately 55%. In the case of the various fiber types tested, both the pure mullite fibers and high alumina fibers show lower strength values than the standard medium length aluminosilicate fiber.

**VFCCF Filter Candle Internal Reinforcement.** Two novel approaches for internal reinforcement of VFCCF filter candles are currently being developed, both of which involve imbedded reinforcing components within the VFCCF candle matrix. In one instance, a cylindrically woven coarse Nextel™ sock is vacuum formed within the VFCCF candle matrix to provide additional structural integrity and to alleviate the potential for filter candle rupture during high intensity jet pulse cleaning. In a second instance, a formed cylinder of continuous fiber ceramic composite (CFCC) material is used to act as a high performance "skeleton" within the VFCCF matrix. In the latter instance, both candle crush strength as well as candle burst (rupture) strength are readily increased.

Each of the above instances involves imbedding the structural reinforcement material intimately within the VFCCF matrix during vacuum forming of the candles. The chopped fibers knit through and around the coarse weave of the Nextel™ or

CFCC skeleton, permanently bonding to the skeleton. As both the Nextel™ and CFCC materials have thermal expansion coefficients nearly identical to the VFCCF material, no increased risk of failure due to thermal incompatibility is anticipated.

Prototypical specimens of both approaches have been formed and tested with a high degree of success. Figure 1 shows an example of the CFCC skeleton for one of the prototype candles prior to vacuum forming of the VFCCF matrix.

**Figure 1. CFCC Filter Candle Reinforcement**

**Ceramic Fiber Composite Materials (for structural applications).** Investigation of a commercially available pressure-laminated aluminosilicate fiber composite material has also been underway as a result of this research effort, for use as a suitable material for hot gas filter structural components. The composite material closely matches the chemical composition of VFCCF aluminosilicate boards, but has improved properties both in compression (up to10,000 psi strength) and tension (up to 8,000 psi strength).

Thicknesses are commercially available up to a maximum of 4", and sizes of up to 60" square can be obtained. Because of the size limitations, however, the joining of sections of this material is required to fabricate ceramic tubesheets, etc. in excess of the above dimensions. For filter applications involving large tubesheet designs, a joined tubesheet eliminates several drawbacks associated with monolithically formed tubesheets, namely:

- The tendency for formation of air pockets, poor fiber "knitting", etc. in VFCCF specimens thicker than about 2";
- Inability to vacuum form, dry, and cure large diameter specimens, due to existing equipment size limitations (tanks, dies, ovens, etc.);
- Inability to physically handle large specimens while wet, due to their fragility.

In view of the above, the concept of laminating and joining composite ceramic fiber board sections to create a larger final product is being pursued; an 18" x 30" laminated tubesheet specimen shown in Figure 2 has been tested for high temperature creep strength at Acurex Corp. of Mountain View, CA, without failure[3]. Moreover, in-house tests of laminated vs. monolithic tubesheet specimens show that a properly prepared laminated glue joint is as strong or stronger than a monolithic specimen in transverse shear.

In addition to high strength, advantages of laminated and joined composite ceramic tubeheets include:

- Utilization of "off-the-shelf" VFCCF and composite board materials for maximum product uniformity, tolerances, etc.;

- No special oversize dies, ovens, tankage, etc. required;
- Attractive cost;
- No special one-of-a-kind tooling required for each particular product design;
- Chemical stability, corrosion resistance, and thermal expansion properties similar to VFCCF materials;
- The need to stock only laminated boards and ceramic adhesive for virtually any tubesheet application.

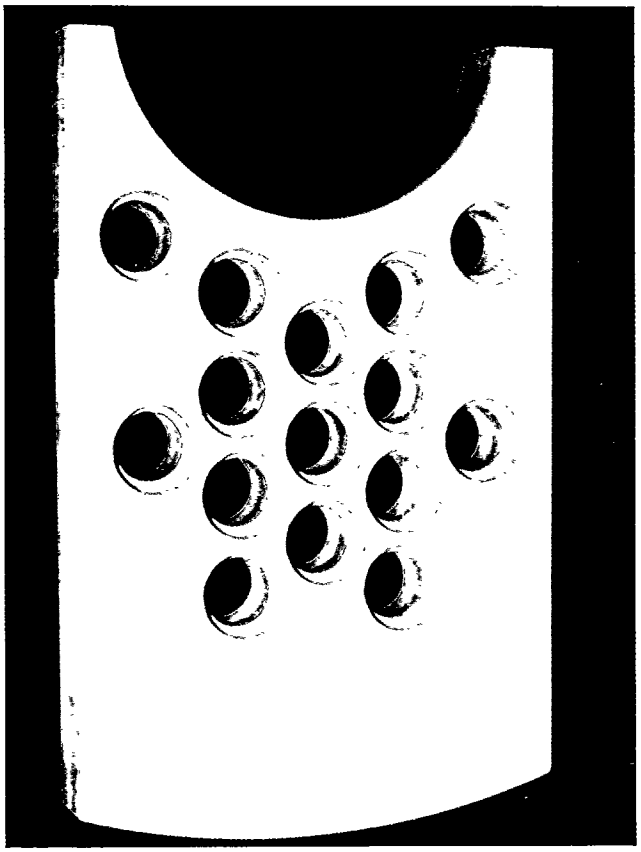

**Figure 2. Laminated Composite Ceramic Tubesheet Section**

**Conclusions**

As evidenced from the preceding sections, yttria appears to be the most promising colloidal ceramic oxide treatment material for VFCCF filter candle matrices. Colloidal yttria increases the strength of VFCCF filter candles without a significant decrease in candle permeability, and creates a desirable divergent, acicular pore geometry during high temperature curing.

Additional reinforcement of lightweight filter candles by means of Nextel™ or CFCC imbedded components appears very promising.

An integrally formed flange and plug end cap design appear to be highly successful.

Aluminosilicate fiber composite materials, for use as lightweight ceramic structural components, offer high strength and can be successfully laminated for even greater strength, using proper joining techniques and ceramic adhesives suited for VFCCF materials.

**FUTURE WORK**

Future VFCCF filter candle developmental efforts will consist of:

- Continued development of the Nextel™ and CFCC reinforced filter candle designs.

Regarding VFCCF and aluminosilicate composite materials, for structural (tubesheet) applications, future efforts will include:

- Development of the optimum lamination, joining, and curing procedures for maximum strength and thermal integrity of these critical components.

## REFERENCES


1) Eggerstedt, P. M., (1993) Final Technical Report of Phase 1 Project Entitled: "Durable, Low Cost Ceramic Materials for Use in Hot Gas Filtration Equipment"; USDOE SBIR Grant No. DE-FG02-92ER81349,Cicero, Illinois.

2) Lee, S.H.D., (1994), "Evaluate FIBROSIC™ Candle Filter for Particle Control In PFBC", Illinois Clean Coal Institute Final Technical Report for September 1, 1992 through December 31, 1993, Argonne National Laboratory, Argonne, IL.

3) Acurex Environmental Final Report 94-124 "Thermal/Chemical Degradation of Ceramic Candle Filter Materials" (1995); DOE Contract DE-AC21-88MC25203, Acurex Environmental Corp., Mountain View, CA.

## 3.3 Status of Granular Bed Filter Development Program

### CONTRACT INFORMATION

| | |
|---|---|
| **Contract Number** | DE-AC21-90MC27423 |
| **Contractor** | Combustion Power Company<br>2101 Webster Street #1700<br>Oakland, CA 94612<br>510-286-8820 |
| **Contractor Project Manager** | Keith B. Wilson |
| **Principal Investigators** | John C. Haas<br>Jeff Prudhomme |
| **METC Project Manager** | Heather M. McDaniel |
| **Period of Performance** | October 1992 to April 1995 |

**Schedule and Milestones**

**FY92-97 Program Schedule**

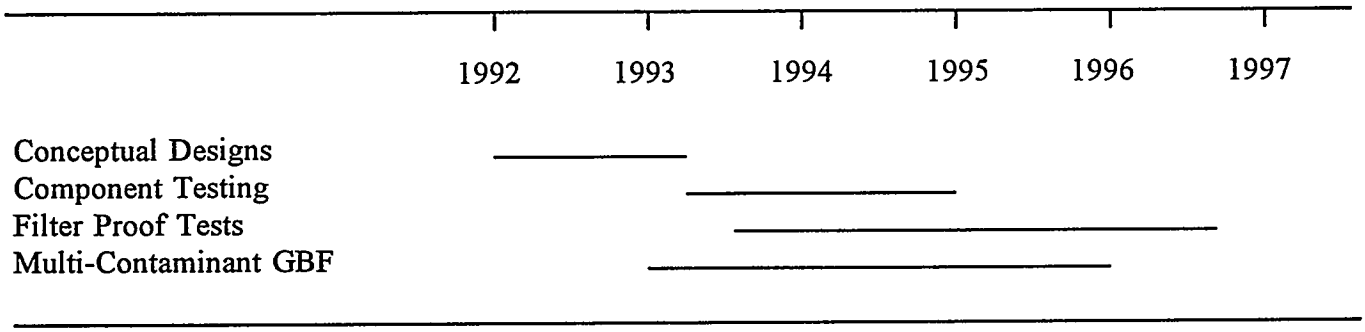


### OBJECTIVES

Efforts to design and operate coal-fired gas turbines plants in advanced gasification and combustion power cycles have been intensified in recent years. These efforts, such as those carried out by Combustion Power Company in the early 1970's, have been plagued by turbine problems due to ash-ladened combustion gases. It is generally recognized that a hot gas cleanup train must be used before the gas turbine to remove the major portion of the particulate. Advantages are also evident for a filter system that can remove other coal derived contaminants such as alkali, halogens and ammonia. With most particulate and other contaminants removed, erosion and corrosion of turbine materials, as well as deposition of particles within the turbine, are reduced to acceptable levels.

The contract is arranged as a base contract with three options. The objective of the base contract was to develop conceptual design(s) of moving granular bed filter (GBF) and ceramic candle filter technology for control of particles from integrated gasification combined cycle systems, pressurized fluidized-bed combustors (PFBC), and direct coal fueled turbine environments. The conceptual design(s) of these filter technologies were compared, primarily from an economic perspective.

Three program options follow the base contract as shown in the schedule above. The objective of Option I, Component Testing, is to identify and resolve technical issues regarding granular bed filter development for gasification and PFBC environments. The objective of Option 2, Filter Proof Tests, is being fulfilled by a separate contract to test and evaluate the moving granular bed filter system at a government-furnished test facility. This facility is at Southern Company Services, Wilsonville, Alabama. The objective of Option III, Multi-contaminant GBF, is to develop moving granular-bed filtration technology for control of particles and other coal-derived contaminants such as alkali, halogens and ammonia.

## BACKGROUND INFORMATION

The granular bed filter was developed through low pressure, high temperature (1600°F) testing in the late 1970's and early 1980's (Guillory, 1980). Collection efficiencies over 99% were obtained. In 1988, high pressure, high temperature testing was completed at New York University (NYU), Westbury, N.Y., utilizing a coal-fired pressurized, fluidized bed combustor. High particulate removal efficiencies were confirmed as it was shown that both New Source Performance Standards and turbine tolerance limits could be met (Wilson, 1989).

The early scale-up work of the granular bed filter indicated potential limitations due to size, cost, and mechanical complexity. These limitations were addressed in the base contract of the present program (Wilson, 1992). It is currently proposed to use large diameter filters with 6 mm spherical filter medium to increase filtration capacity and reduce system complexity. Figure 1 shows a granular bed filter designed for a 100 MWe KRW (air) gasifier. The filter

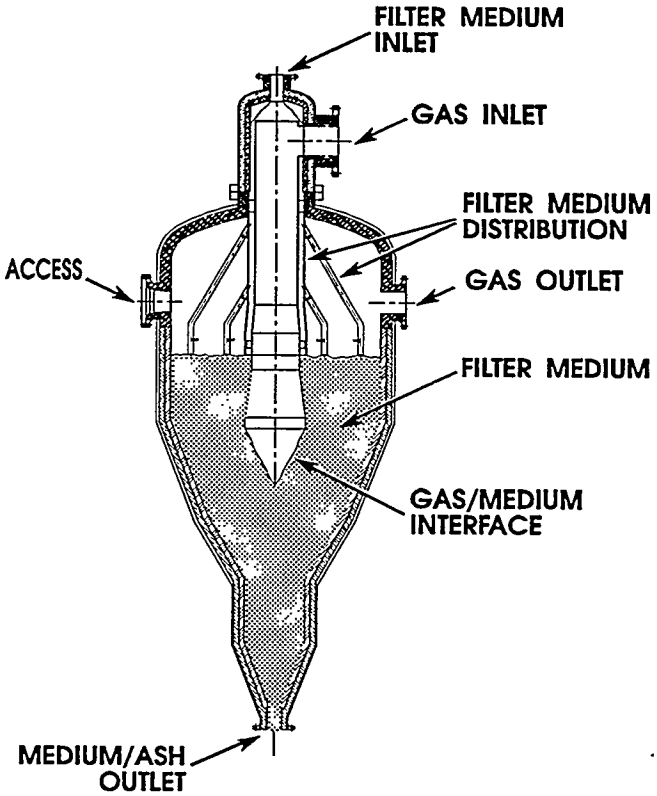


**Fig. 1 Granular Bed Filter for 100 MWe KRW (Air) Gasifier**

has an inside diameter of 14 ft with a nominal bed depth of 5 ft.

Dust laden gas enters the filter through an inlet duct which conveys the gas and dust into the filter medium. The gas initially flows downward, then turns and flows across the filter medium and then upward flow countercurrent to

the downward moving filter medium. As the gas and dust passes through the filter medium, dust is removed. Dust and filter medium are removed at the bottom cone of the filter. A pressurized pneumatic lift pipe moves the filter medium for return to the filter. The transport gas and dust, after separation of the filter medium, are cooled in a recuperative heat exchanger and passes through a pressurized bag house which removes the collected dust. The cleaned transport gas pressure is boosted 15 psi through a blower, is reheated in the recuperative heat exchanger and returned to the bottom of the lift pipe. The cleaned filter medium from the de-entrainment vessel at the top of the lift pipe flows by gravity back into the top of the filter.

## PROJECT DESCRIPTION

### GBF Component Development Program

Task 2 of the GBF development program identified technical issues which needed to be addressed. Some of the issues such as filter efficiency under different operating conditions are best resolved during testing at DOE's Power Systems Development Facility. Other issues such as filter scale-up are best addressed in a Component Test Facility. Besides scale-up, the following issues are being addressed in the Component Test Facility: 1) The overall height of the filter may be reduced by using a shallower cone angle at the bottom of the filter. 2) The affect of cone angle on the motion of the filter medium needs to be determined. 3) The maximum gas filtration rate needs to be determined; as well as, other variables which influence the filtration rate. 4) During the NYU tests, the refractory in the lift pipe experienced abnormal wear indicating a need to evaluate different refractories for abrasion resistance with GBF media. 5) Six mm diameter filter medium needs to be evaluated for durability and structural integrity. 6) Computational fluid dynamics (CFD) showed that the pressure drop through the filter could be reduced by enlarging the gas inlet duct at the gas filter medium interface. CFD results needs verification as well as determining its affect on the flow the filter medium.

The specific objectives of the GBF Component Test Facility are: 1) to determine filter dimensions to insure mass flow of the filter medium, 2) measure the spouting velocity of the filter medium, 3) confirm the suitability of the enlarged gas inlet, 4) measure the minimum fluidization velocity of the 6 mm filter medium, 5) determine the effect of surface roughness on filter medium flow, 6) confirm CFD model and scale-up factors, 7) evaluate wear resistance of candidate pipe liners, and 8) evaluate strain and deflection of the gas inlet pipe. To accomplish these objectives, several arrangements of equipment are used. The first tests were conducted in a 3.5 ft diameter spilt filter with a transparent cross section which allowed observation of the motion of filter medium. The split filter used surfaces with different roughness to simulate the effect of a refractory liner. Two cone angles were tested with the split filter. Two inlet geometries were also tested. One inlet configuration emulated the high velocity design used for the testing at NYU. The other design had a larger inlet area designed to reduce filter pressure drop. Following the tests with the split filter, tests will be run in a 3.5 ft diameter full circumference filter and in a 6.0 ft diameter filter. These tests will help evaluate scale-up. Pipe liner abrasion resistance tests are proposed in a rolling drum containing filter medium and refractory test specimens. Fluidization properties of the filter medium were evaluated in a 1 ft diameter fluidized bed.

### Multi-Contaminant Control

Besides particulate removal, a GBF may be able to capture other coal contaminants through the

use of chemically reactive filter material. Combustion Power Co. proposed to develop a reactive of filter material composed of limestone and clay for the removal of sulfur species and alkali (Wilson 1994). This approach was changed because of the well devolved alternative methods of sulfur removal, the thermodynamic limitations of limestone for the capture of $H_2S$, and the problems associated with the oxidation of calcium sulfide to sulfate. Combustion Power entered a teaming agreement with Research Triangle Institute (RTI) to investigate three types of reactive filter medium. The program is divided into four phases. The first phase will investigate clay based sorbents for control of alkali. Option 1 investigates clay based sorbents for the additional sorption of lead, cadmium, barium beryllium, and chromium. Option 2 investigates the sodium based sorbents for the sorption of halogens and metalloid, and Option 3 investigates ammonia decomposition catalysts.

The filter medium would continue to be 6 mm spheres as is used for particulate control. The following five clays have been identified as potential alkali sorbents: Emathlite (Bachovchin, 1986), Kaolin (Uberoi,1990), Bauxitic kaolin, Attapulgite (McLaughlin,1990), and Calcium montmorillonite (McLaughlin,1990). Thermal gravimetric analysis (TGA) reactivity tests will be used to screen the clays. Each clay will be mixed with NaCl and heated in a TGA apparatus in both a oxidizing and reducing gas. The mixture with the lowest weight loss will retain the most sodium. Three of the five clays will be selected for evaluation of sorption of lead, cadmium and chromium in a reducing gas. Two types of clay will be chosen for further evaluation. The selection process will be based on the reactivity of each clay with sodium chloride, with each of the heavy metals and the relative cost of the each of the clays.

Each clay will be pelletized, using an extrusion process, into 3 mm and 6 mm pellets and evaluated in terms of strength, attrition resistance and chemical reactivity.

The most promising of the two clays will be used in binder and pelletization studies. Five binders have been identified for evaluation with pelletization through extrusion with pellet rounding and by disk pelletization. The 20 formulations will be evaluated in terms of strength, attrition resistance and chemical reactivity. The reactivity tests will use a TGA to measure the weight gain of pellets over which passes a reducing gas containing 40 ppmv concentration of NaCl.

Based on the above screening tests, one clay formulation will be chosen for detailed characterization. Sodium saturation capacity of the sorbent will be evaluated with a TGA in which sodium chloride vapors pass over the sorbent. The test will continue until the reaction rate has decline to 5% of the initial rate. Test will be run with and without HCl a known inhibitor of alkali sorption (McLaughlin, 1990). Integral fixed-bed experiments will be run on a deep bed, 8 cm diameter by 30 cm, with the preferred formulation. Four integral tests are planned to evaluate the effects of gas composition and HCl concentration of the reaction kinetics. The strength of cured, calcined, and reacted pellets of the preferred formulation will be determined with crush and attrition tests.

The kinetic data from the integral reactor tests will be used to develop a kinetic expression for the reaction of alkali vapors with the clay sorbent. The kinetics will take into account the effect of alkali vapor concentration and the effect of HCl on reaction rates. The kinetic expression will be incorporated in an engineering model of the GBF.

## GBF Testing at the Power Systems Development Facility

Southern Company Services, Inc has entered into a cooperative agreement with the Department of Energy, Morgantown Energy Technology Center (DOE/METC) for the design, construction and operation of a hot gas cleanup test facility for gasification and pressurized combustion. This facility is being installed in Wilsonville, Alabama. Shakedown and testing will commence in late 1995.

The primary objective of the Power Systems Development Facility (PSDF) at Wilsonville is to carry out meaningful systems and component testing for advanced coal-based power development. The integration of the granular bed filter into the PSDF addresses the advanced power generation research and development need as identified by industry and DOE/METC.

The basic filter design is patterned after the test units from Combustion Power Company development in the 1980's and the successful tests at New York University. Filter design changes are based on principles determined by computational fluid dynamics. Dimensions of the filter are adjustable. The depth of the filter can be changed from 5' to 10' if it is determined that a deeper filtration bed is needed for ash collection efficiency. The filter diameter can be adjusted to allow operation at different capacities. System design of the granular-bed filter is the same as for a commercial unit.

## RESULTS

### GBF Component Development Program

The split filter was used for observation of gas and filter medium flow. Figure 2 shows a gas velocity profile at the top surface of the filter. The filter medium at the surface is contoured

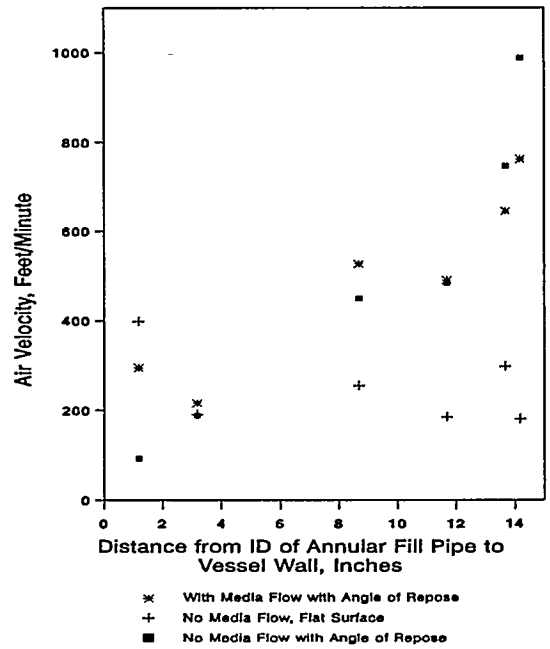


**Fig.2 Air Velocity Profile at Surface of GBF**

due to its angle of repose. As a result, the gas flow varies across the surface, being higher in the valleys and lower near the filter material inlets. The filter medium along the outside wall of the filter is a valley which has relatively high gas velocity. When the surface of the filter medium was leveled to eliminate the effect of changing filter medium depth, the gas velocity profile across the surface was relatively uniform. This result agrees with CFD modeling which predicted flow variation across the contoured surface but showed uniform flow about a foot below the lowest point on the filter. Within the scatter of the data, filter medium motion did not appear to effect the gas flow profile.

Figure 3 shows the velocity profile of the filter medium at the surface of the filter for different gas flows using the high gas velocity gas inlet. The filter material moves uniformly at all positions except very near the outside wall. Although the filter medium moves in mass flow with no stagnation areas it is not perfect plug flow. This observation was true for the split

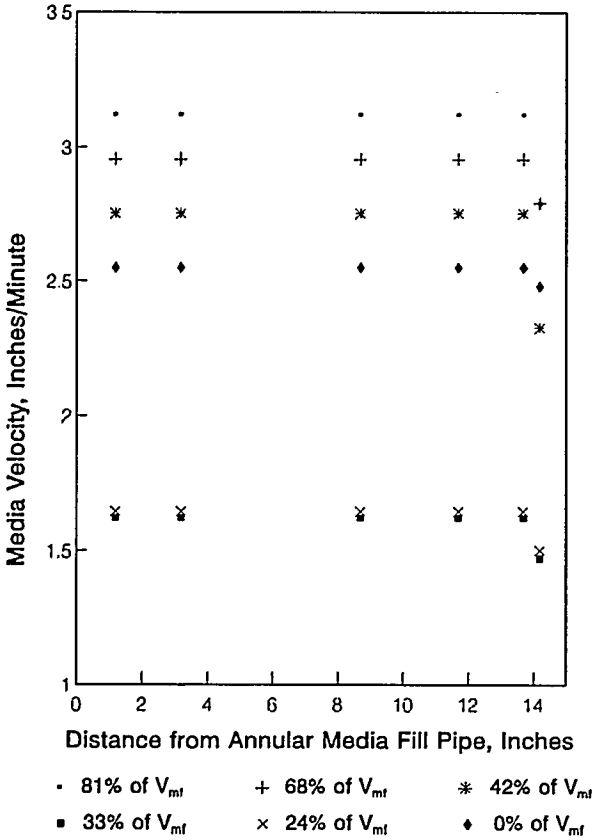


**Fig.3 Filter Medium Velocity Profile**

filter using the high velocity inlet with either a low friction wall surface or with a high friction surface. Filter material slip at the outer wall did not appear to adversely affect the filters tested at other locations.

The split filter allowed observation of the gas/filter medium interface below the gas inlet duct. With the high gas velocity inlet design , the interface appeared to be unstable at gas velocities approaching 50% of the minimum fluidization velocity. Some filter material was entrained in the gas flow and swirled in the gas space under the inlet pipe. At higher gas velocities, a gas bubble would form at the outer edge of the gas duct and begin to move up through the filter where it was absorbed into the filter medium. With the low velocity gas inlet having a larger cross sectional area, the filter medium was stable with a gas flow of 50% of minimum fluidization velocity. There was relatively little filter material motion and no bubble formation until higher gas flows.

Figure 4 shows velocity versus pressure drop for the high velocity gas inlet, for the low velocity inlet and for filter medium in a packed bed with a uniform gas distributor. The velocity is made non-dimensional by dividing by the minimum fluidization velocity, $V_{mf}$, , and the pressure drop is made non-dimensional by dividing by the weight of the bed per unit area. At a gas velocity of 50% of the minimum fluidization velocity, the pressure drop of the low velocity inlet is 36% lower than that of the high velocity gas inlet. The pressure drop of the low velocity

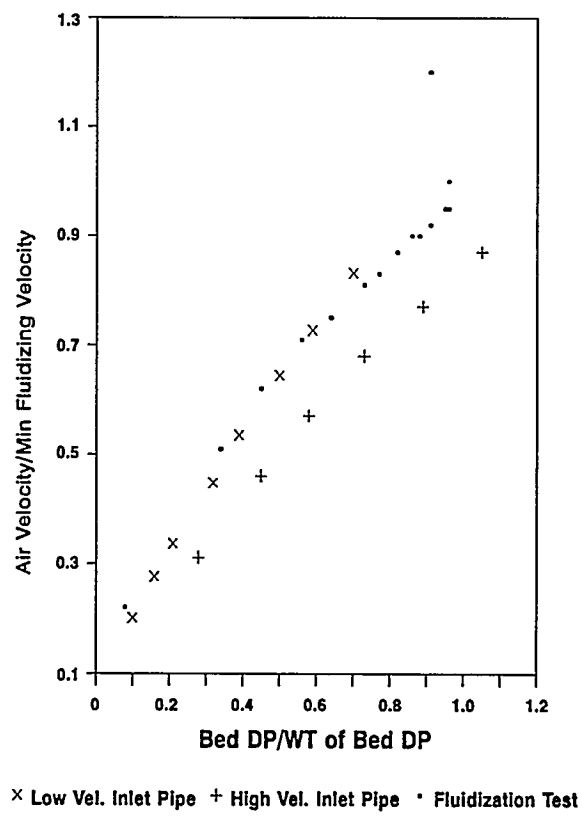


**Fig.4 GBF Pressure Drop**

gas inlet is similar to that of a packed bed with

uniform gas distribution.

All the testing with the split flow filter was without the presence of dust in the gas. When dust was used, there was dust by-pass in the corners of the filter formed by the intersection of the vertical face with the surfaces of the filter. With this caveat we have drawn the following conclusions: 1) The filter medium moves in mass flow with slip occurring at solid surfaces. 2) There is increased gas flow at the top surface near the outer wall of the 3.5 ft diameter filter due to the surface contour of the media. 3) Filter medium flow in the counterflow zone was not affected by change to a higher friction wall surface. 4) The larger gas inlet duct had a lower pressure drop and a more stable gas/filter medium interface than the high velocity gas inlet duct. 5) A change in filter cone angle from 70° to 60° did not change the flow profile of filter medium in the cylindrical section of the filter.

**Multi-Contaminant Control**

Table 1 shows the composition the clays to be evaluated as reported by the commercial suppliers. The GTA evaluation test are just getting underway.

## FUTURE WORK

Testing at the component test facility is expected to be completed by Oct. of '95. The first phase the multi-contaminant control investigation will be completed in May of '96. The latter 3 phases of multi-contaminant control would be completed by Dec of '96. Testing at the PSDF is scheduled to occur during 1996.

## REFERENCES


Bachovchin, D.M., M.A. Alvin, E.A. Dezubay and P.R. Mulik. 1986. "Study of High Temperature Removal of Alkali of a Pressurized Gasification System." Final Report DOE-MC-20050-2226.

Guillory, J. L. 1980 *High-Temperature Particulate Removal By Moving Bed Granular Filtration.* TR 80-3. Menlo Park CA: Combustion Power Company.

McLaughlin, J. 1990. "The Removal of Volatile Alkali Salt Vapors from Hot Coal-Derived Gases". PhD Thesis, Guildford, UK, Dept. of Chemical and Process Engineering, University of Surrey, 214 pp.


Table 1 Composition of Clays

| | Emathlite Mid Florida Mining | Kaolin Albion Kaolin | Bauxitic Kaolin CE Min. | Attapulgite Floridin | Ca Montmorillonite Floridin |
|---|---|---|---|---|---|
| $SiO_2$ | 72.3 | 52.3 | 37.8 | 66.2 | 62.3 |
| $Al_2O_3$ | 11.4 | 41.1 | 58.0 | 11.7 | 25.5 |
| $TiO_2$ | 0.5 | 2.3 | 2.2 | 0.6 | |
| $Fe_2O_3$ | 3.2 | 0.8 | 1.1 | 4.0 | 1.8 |
| CaO | 8.4 | 0.0 | 0.1 | 2.9 | 4.9 |
| MgO | 3.8 | 0.1 | 0.1 | 9.7 | 2.9 |
| $K_2O$ | 0.4 | 0.6 | 0.0 | 1.1 | 0.6 |
| $Na_2O$ | | 0.1 | 0.1 | | 2.0 |

Uberoi, M., W.A. Punjak and F. Shadman. 1990. "Kinetics and Mechanism of Alkali Removal from Flue Gases by Solid Sorbents." *Prog. Energy Combustion Science*, Vol. 16, No. 4, pp. 205-211.

Wilson, K.B., Haas, J.C. & Olivo, C.A. June, 1994. Multi-Contaminant Control Granular Bed Filter. In *Proceedings of the Coal-Fired Power Systems 94 -- Advances in IGCC and PFBC Review Meeting.* ed. H.M. McDaniel, R.K. Staubly, V.K. Venkataraman. 176-186. Doe/METC-94/1008, Vol. 1, (DE94012252), Morgantown, WV.

Wilson, K. B. March 1989. Performance Evaluation of a Screenless (Counter-Current) Granular Bed Filter on a Subpilot-Scale PFBC. In *Proceedings of the Sixth Annual Coal-Fueled Heat Engines and Gas Stream Cleanup Systems Contractors Review Meeting,* ed. R.C. Bedick, T.P. Dorchak, N.F. Rekos, H.A. Webb, 293-303. Doe/METC-89/6101 (DE89000952) Morgantown, West Virginia.

Wilson, K.B., J.C. Haas, and M.B. Eschelman, 1992. Moving Granular Bed Filter Development Program. In *Proceedings of the Twelve Annual Gasification and Gas Stream Cleanup Systems Contractors Review Meeting Vol 1,* ed. R.A. Johnson and S.C. Jain, 289-296. DOE/METC--92/6128 (DE93000228) Morgantown, West Virginia.

## 3.4 Pulsed Combustion and Hot Gas Cleanup Island

CONTRACT INFORMATION

| | |
|---|---|
| Contract Number | DE-AC21-89MC26288 |
| Contractor | Manufacturing and Technology Conversion International, Inc. (MTCI)<br>P.O. Box 21<br>Columbia, MD 21045<br>(410) 381-4200 |
| Contractor Project Manager | Ravi R. Chandran |
| Principal Investigators | Ravi R. Chandran<br>Momtaz N. Mansour<br>S. Yavuzkurt (Penn State U.)<br>Gary H. Koopmann (Penn State U.)<br>John L. Loth (West Virginia U.) |
| METC Project Manager | Darren J. Mollot |
| Period of Performance | June 15, 1989 to Dec. 1, 1995 |

ABSTRACT

The overall objective of this project is to demonstrate pulse combustion induced acoustic enhancement of coal ash agglomeration and sulfur capture at conditions typical of direct coal-fired turbines. The goal of the program is to support the mission of the Department of Energy (DOE) for developing coal-fired combustion gas turbines. MTCI has been focusing on hardware development and system demonstration, Penn State University (PSU) has been investigating and modeling acoustic agglomeration and sulfur capture, and West Virginia University (WVU) has been studying aerovalve fluid dynamics.

Experiments have been conducted in a process development unit (PDU) at MTCI. Twenty-seven tests have been performed at 3 atm pressure with a pulverized coal (Pittsburgh No. 8) and four different sorbents for sulfur capture. The combustion efficiency exceeded 99%, sulfur capture efficiency was as high as 98%, $NO_x$ emissions

were in the 0.3 to 0.6 lb/MMBtu range and the solids loading in cyclone exit flue-gas (analogous to turbine inlet solids loading) was as low as 23 ppmw. The solids loading result greatly surpassed the original target goal of 100-150 ppmw and is good enough to meet the current New Source Performance Standards (NSPS) for particulate emissions from power plants ($<0.03$ lb/MMBtu). These results are very encouraging and provide impetus for further development and commercialization of this technology.

Based on the success of the above program, MTCI has proposed an alternate advanced combustor island concept for development and demonstration. This advanced concept shows potential to meet DOE's mission-oriented criteria in such "critical" or "enabling" technology areas as hot gas filtration, cycle efficiency improvement and environmental performance ($SO_2$ and $NO_x$ emissions). This concept permits flexible system configurations suitable for repowering as well as greenfield applications. The target goals for this advanced system are high cycle efficiency ($\sim 45\%$), low emissions (one-tenth of NSPS) and lower cost of electricity ($\sim 20\%$ less than that for conventional coal plants).

MTCI has performed cycle analyses and is designing the components for a process development unit (PDU) based on the proposed advanced combustor island concept. PSU is continuing the work on the modification of the PCGC-2 code to simulate sulfur capture and agglomeration under pulse combustions conditions. WVU is continuing the development of advanced aerovalve.

## 3.5 Filter Component Assessment

### CONTRACT INFORMATION

| | |
|---|---|
| **Contract Number** | DE-AC21-94MC31147<br>DE-FC21-89MC26042 |
| **Contractor** | Westinghouse Electric Corporation<br>Science & Technology Center<br>1310 Beulah Road<br>Pittsburgh, PA 15235-5098<br>(412) 256-2066 (Telephone)<br>(412) 256-2121 (Telefax) |
| **Contractor Project Manager** | Mary Anne Alvin |
| **Principal Investigators** | Mary Anne Alvin<br>Thomas E. Lippert<br>Edward S. Diaz<br>Eugene E. Smeltzer |
| **METC Project Manager** | Richard A. Dennis |
| **Period of Performance** | September 15, 1994 - December 14, 1996 |

**Schedule and Milestones**

**FY 95 Program Schedule**

| TASK | S | O | N | D | J | F | M | A | M | J | J | A |
|---|---|---|---|---|---|---|---|---|---|---|---|---|
| Test Plan | ——— | | | | | | | | | | | |
| Filter Characterization | | | | ——— | ——— | ——— | ——— | ——— | ——— | ——— | | |
| Mechanical Durability | | | | | | | | | ——— | | | |
| Corrosion Resistance | | | | ——— | ——— | ——— | ——— | ——— | ——— | ——— | | |
| Additional Testing | | | | | | | | | | | ——— | ——— |

### OBJECTIVES

The objectives of this program are to provide a more "ruggedized" filter system that utilizes porous ceramic filters which have improved resistance to damage resulting from crack propagation, thermal fatigue and/or thermal excursions during plant or process transient conditions, and/or mechanical ash bridging events within the candle filter array.

## BACKGROUND INFORMATION

Characterization of the monolithic alumina/mullite and clay bonded silicon carbide candle filter materials after 716 and 1341 hours of operation in the Westinghouse Advanced Particulate Filtration (W-APF) system at the Ahlstrom pressurized circulating fluidized-bed combustion (PCFBC) test facility in Karhula, Finland, as well as after 5855 hours of operation at the pressurized fluidized-bed combustion (PFBC) test facility at the American Electric Power (AEP) Tidd Demonstration Plant in Brilliant, Ohio, indicated that the porous ceramic filters typically lose strength at process operating conditions until a "conditioned" state is achieved. These materials also experienced numerous phase changes within the bulk matrix or binder phases, which reflected a response to both process operating temperature and flue gas chemistry.[1,2] Microcrack formations have been identified frequently within the alumina/mullite filter matrix, and are also expected to occur within the binder phase and silicon carbide grains in the clay bonded filter materials.

In order to provide a more "ruggedized" filter system, development of porous ceramic filters has been undertaken to produce filters with improved creep resistance, fracture toughness, and oxidation or corrosion resistance for extended use in either advanced coal-fired combustion or gasification process applications. Several manufacturers have developed, or are in the process of developing, chemically vapor infiltrated (CVI) candle filters which are expected to have "improved" fracture toughness characteristics. Improved toughness characteristics are considered to mitigate crack propagation through the porous ceramic matrix, which ultimately minimizes catastrophic failure, particularly under thermal fatigue and/or shock conditions during process operation. CVI toughened materials typically include the use of both oxide and nonoxide continuous fiber ceramic composites (CFCCs).

In recent developmental and prototype CFCC filter manufacturing efforts which involve the use of nonoxide CFCCs, the stability and oxidation resistance of the fiber/matrix interface are considered to be potential issues limiting high temperature use. Although the nonoxide CFCCs exhibit nonbrittle failure characteristics and have sufficient room temperature mechanical proprieties, the mechanical properties of the nonoxide CFCCs may degrade as a result of oxidation of the interface layer during exposure to high temperature (>800°C) in an oxidizing environment. When this occurs, the CFCC matrix will exhibit brittle characteristics. In the development of an oxide-based CFCC matrix, key issues which remain to be resolved are the production of oxide fibers with improved high temperature capabilities, particularly under low stress (i.e., 5-15 ksi) loads, as well as the development of functional interface coatings which toughen the nonbrittle oxide CFCC matrix.

Alternate manufacturers have or are in the process of developing similar fracture toughened materials which utilize solgel and/or chemical vapor composite (CVC) techniques to form potentially less expensive fiber, felt or mat, whisker or particulate reinforced, oxide and nonoxide ceramic composites. The concept of utilizing a single phase matrix also has merit in the production of porous ceramic filter elements, since phase transformations frequently result during process operation which potentially lead to a mismatch in the thermal coefficient of expansion of the various resulting phases. Alternately the inclusion of conductive phases (i.e., SiC) within oxide-based ceramic matrices has been considered.

As with current filter materials, the advanced or second generation filter materials are required to achieve reliable long-term service use, as well as

be reproducibly manufactured during large volume production (i.e., 500-1000 filter elements). The criteria for reliable, long-term service operation conceivably includes a minimum of 10,000-25,000 hours of maintenance-free life; 10-20 emergency shutdowns during which time the ceramic filters may experience thermal shock conditions; >100 controlled process startups and shutdowns; temperature excursions of up to ~1000-1200°F; cleanability of adherent, "sticky" or adhesive ash cake layers; resistance to fracture and catastrophic failure during ash bridging events; and chemical and phase stability during exposure to corrosive alkali, sulfur, or chloride gas, liquid, or condensed phase species. In order to "design" and manufacture ceramics which are capable of withstanding the service operating criteria, material properties, crack resistance ($K_{1c}$), slow crack growth data, materials with a Weibull modulus of 20, and preferentially smooth, "nonstick" surface textures are needed. Similarly failure probability calculations, simulated thermal transient testing under steady state, accelerated pulse cycling, and process transient conditions, and corrosion testing, all form the basis of developing reliable, mechanically durable, and chemically stable porous ceramic filters for extended PFBC and/or integrated gasification combined cycle (IGCC) service use.

## PROJECT DESCRIPTION

As part of the current Phase 1, Task 1, effort of this program, Westinghouse is evaluating the filtration characteristics, mechanical integrity, and corrosion resistance of the following advanced or second generation candle filters for use in advanced coal-fired process applications:

- 3M CVI-SiC composite - chemical vapor infiltration of silicon carbide into an aluminosilicate Nextel™ 312 fiber preform
- DuPont PRD-66 - filament wound candle filter structure containing corundum, cordierite, cristobalite, and mullite
- DuPont SiC-SiC - chemical infiltration of silicon carbide into a silicon carbide Nicalon™ fiber mat or felt preform
- IF&P Fibrosic™ - vacuum infiltrated oxide-based chopped fibrous matrix.

In Task 1.1, Test Plan and Selection of Prototype Filters, candle filter dimensional tolerance specifications were provided to each filter supplier, identifying the candle filter length; OD dimensions of the flange and candle body; flange radius, geometry, and dimensions; and a preferred candle filter wall thickness along the flange for ease of installation and use with the existing Westinghouse holder/mount design. In addition, specifications relating to the candle filter linearity, concentricity, perpendicularity, as-manufactured pressure drop, and particle collection efficiency were provided to each supplier. Westinghouse similarly required that QA/QC procedures be implemented during the production of each filter batch or lot, in order to assure homogeneity not only among filters produced during a single production firing, but also between various filter production firings. Homogeneity is required not only for the raw materials utilized during the actual manufacturing process, but is also required in terms of resulting strength, porosity, membrane and/or bulk support matrix characteristics, absence of cracks and/or scratches, integrity of the flange and end cap, etc. The presence of patches and/or repairs which produce an out-of-spec body were not considered to be acceptable by the Westinghouse QA/QC dimensional tolerance criteria. Documentation and certification that the initial raw materials and manufacturing process were within the vendor's ISO-9000 standards, and that these had not changed or been modified since delivery of the initial set of filters. Destructive and non-destructive characterization data of the final

filter production batch(es) were requested to be submitted by each supplier.

As part of Task 1.2, Assessment of Prototype Filter Filtration Characteristics, Westinghouse has assessed the cold permeability and filter production uniformity of the as-manufactured 3M CVI-SiC composite, DuPont PRD-66, DuPont SiC-SiC, and IF&P Fibrosic™ candle filters. Additional high temperature permeability, filtration efficiency, cleanability, pressure drop characteristics, and fine particle penetration into the advanced candle filter matrices are being evaluated during conduct of steady state, high temperature, high pressure (HTHP) testing in one of Westinghouse's PFBC hot gas filtration systems in Pittsburgh, PA.

In order to assess the mechanical durability of the advanced or second generation candles, the elements were subjected to extended accelerated pulse cycling conditions in the Westinghouse HTHP PFBC test facility as part of Task 1.3, Assessment of Prototype Filter Mechanical Durability. By acquiring ~3500 simulated pulse cycles, the possible influence of thermal fatigue on the resulting bulk strength and fracture toughness of the ceramic matrices is identified. Additional HTHP PFBC testing included exposure of the advanced, second generation candle filters to a series of thermal transient events which represented either mild or severe process system temperature excursions that had previously been experienced in pilot plant testing. By monitoring the residual bulk strength, fracture toughness, and microstructure of the filter elements after exposure to the simulated PFBC process transient conditions, a defined process operating regime, as well as plant control requirements, may be identified for viable operation of the advanced, second generation filters.

Previous efforts at Westinghouse have indicated the potential susceptibility of the nonoxide filter matrices to oxidize and/or experience corrosive attack during operation at high temperature, particularly in a steam and/or steam/alkali-containing environment.[3-5] In order to identify the response of the advanced, second generation filter materials to possible gas phase reactions, flow-through testing was conducted in which either mini-candles or discs of the advanced, second generation candle filters were exposed for 400 hours at 870°C, to either a 5-7% steam/air or 20 ppm NaCl/5-7% steam/air gas phase environment, with pulse cycling (Task 1.4, Assessment of Prototype Filter Chemical Resistance). Post-test characterization of the exposed filter matrices has included determination of the residual bulk strength of the material. Additional analyses will include identification of the phase and/or morphology changes that have occurred as a result of exposure of the ceramic filter materials to the high temperature, steam/air and alkali/steam/air, flow-through test environment.

During conduct of the cold permeability, steady-state, corrosion, and/or thermal transient testing, modifications may become apparent which would improve the performance and operating life of the advanced, second generation candle filters. Pending that these modifications can be made to the advanced, second generation filters (i.e., alternate design or material composition, etc.), further testing or re-qualification of the modified filter elements will be undertaken in Task 1.5, Additional Testing of Improved Prototype Filters.

All results generated during conduct of Tasks 1 through 5 in this program will be summarized and presented in a Topical Report (Task 1.6).

## RESULTS

Since September 1994, efforts at Westinghouse have been focused on identifying the high temperature particulate filtration characteristics, as well as the thermal, mechanical and corrosion stability of four advanced, second generation filter elements. The following sections present a discussion of the filtration characteristics and materials evaluation which have been conducted after bench-scale exposure of the advanced filters at Westinghouse, as well as after 1110-1705 hours of hot gas filtration in the W-APF system at the AEP Power Demonstration Plant in Brilliant, Ohio.

### Permeability Measurements

Manufacture of 1.4-1.5 m advanced, second generation candle filters has been achieved within the past two years. The room temperature, gas flow resistance of the as-manufactured 3M CVI-SiC composite, DuPont PRD-66, DuPont SiC-SiC, and IF&P Fibrosic™ candle filters is shown in Figure 1 in conjunction with first generation, monolithic filter elements. These data indicate the relatively high initial permeability of the porous, light weight, second generation filter elements.

### As-Manufactured Filter Material Strength

All four candle filters were characterized in terms of their as-manufactured, compressive and tensile strengths via C-ring and/or O-ring testing at room temperature and at various elevated temperatures which reflect specific process operating conditions. For example, 732°C is representative of the nominal W-APF system operating temperature at AEP in Test Segment #4;[6] 843°C reflects the operating temperature of the Westinghouse HTHP PFBC test facility during accelerated pulse cycling and/or process transient testing; 870°C is representative of the Westinghouse flow-through alkali corrosion test temperature. Typically 15 or 25.4 mm samples are cut from each candle filter using a diamond wheel. The orientation of the C-ring sample notch is rotated around the filter body in order to eliminate any uniaxial processing or manufacturing effects.

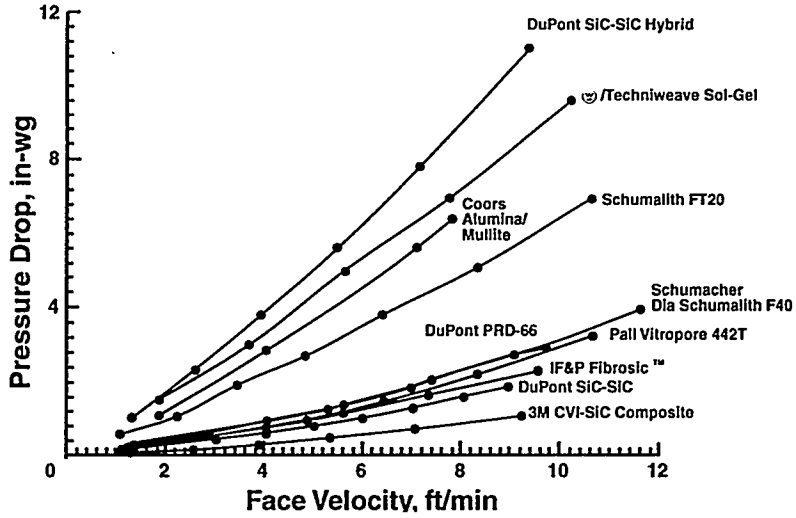


**Figure 1. Room Temperature Gas Flow Resistance of the First Generation Monolithic and Advanced Second Generation Candle Filters**

As shown in Table 1, the as-manufactured strengths of the advanced, second generation candle filters vary from being relatively low for the IF&P Fibrosic™ matrix, to moderately strong for the filament wound DuPont PRD-66 filter matrix, to extremely strong for the 3M CVI-SiC triaxial braid and DuPont SiC-SiC composite matrices. Both the applied load to failure and resulting calculated strength vary slightly depending on the whether the sample length is 15 or 25.4 mm, and whether C-ring or O-ring testing is conducted. By adopting a standard sample length (i.e., 15 or 25.4 mm) and test methodology, the as-manufactured and field-tested filter strength data can be compared, provided that the filter matrix can be cut as an integral unit. For this reason, Westinghouse has selected to continue testing 15 mm samples, utilizing predominantly C-ring compressive and tensile testing to monitor changes along the gas contacted outer surface and pulse cycled inner surface of the filter element, respectively, both at room temperature, as well as at process operating temperatures. This test methodology has been shown to be adequate for maintaining the integral nature of all four advanced, second generation filter materials. Limited additional testing is, however, conducted at Westinghouse utilizing either 15 or 25.4 mm O-rings.

Due to the relatively thin wall construction of the 3M CVI-SiC and DuPont SiC-SiC composite matrices (i.e., ~3.6 mm 3M composite thickness; ~1.3 mm 3M triaxial support braid thickness; and ~1.6 mm DuPont composite thickness), the resulting strength of these materials is calculated to be extremely high in comparison to the monolithic or first generation, and alternate advanced or second generation filter elements (Table 2). In contrast, however, the applied load required to fail the 3M CVI-SiC and DuPont SiC-SiC composite materials is substantially lower than the applied load required to fail the first generation monolithic materials, but is higher than the applied load needed to fail the IF&P Fibrosic™ matrix. Given the applied loads shown in Table 2, failure of either the first generation monolithic or advanced, second generation candles would be expected to result if ash bridging were to occur within a candle cluster or array during process operation.

As-manufactured bulk strength data as a function of temperature are currently being developed for each of the advanced, second generation filter materials. As shown in Table 3, the bulk strength of the DuPont PRD-66 matrix appears to increase as temperature increases. In addition, the resulting load vs deflection curves which are generated for each fiber reinforced filter material during bulk strength testing are being utilized to provide preliminary information regarding the fracture toughness of the various porous ceramic filter matrices.

## HTHP Testing

In order to develop the thermal shock and thermal fatigue characteristics of the advanced, second generation filter elements, testing was conducted in Westinghouse's high temperature, high pressure (HTHP), pressurized fluidized-bed combustion (PFBC) test facility, utilizing arrays which contained all four filter element types. A brief description of the test procedures that were used to evaluate or qualify the filter elements prior to use in field test operations, and general comments regarding the response of the various filter elements to simulated process transients and accelerated pulse cycle testing follow. Post-test residual bulk strength characterization (i.e., C-ring compressive and/or tensile testing at 25°C and 843°C; room temperature burst testing), and scanning electron microscopy/energy dispersive x-ray analysis (SEM/EDAX) are currently being performed on each exposed filter element. The results of these analyses will be reported at a later date.

## Table 1. Load and Ultimate Strength of the As-Manufactured Second Generation Candle Filters

| Sample ID No. | Room Temperature Load, lbs | Room Temperature Strength, psi | 843°C Load, lbs | 843°C Strength, psi | 870°C Load, lbs | 870°C Strength, psi |
|---|---|---|---|---|---|---|
| 3M CVI-SiC Composite | | | | | | |
| 43-1-2 C-Ring Compression (15 mm) | 2.5 | 1343 (13187) (a) | 2.6 (b) | 1352 (13444) (b) | TDB | TBD |
| 43-1-2 C-Ring Compression (25.4 mm) | 5.4 | 1635 (17012) | 5.1 (b) | 1425 (16857) (b) | | TBD |
| 43-1-2 O-Ring Compression (15 mm) | 7.7±0.84 | 1315±186 | 5.98±1.03(b) | 1104±350 (b) | TBD | TBD |
| | | (13276±1417) | | (11250±3595) (b) | | TBD |
| 43-1-2 O-Ring Compression (25.4 mm) | 13.61±1.90 | 1314±254 | 10.8±1.7 (b) | 1060±219 (b) | TBD | TBD |
| | | (14026±2012) | | 11012±1795 (b) | | TBD |
| DuPont PRD-66 | | | | | | |
| D-259 C-Ring Compression (15 mm) | 10.84±0.41 | 1325.01±71.11 | 12.69±1.72 | 1543.35±196.99 | 13.29±0.95 | 1629.41±142.14 |
| D-259 C-Ring Tension (15 mm) | 7.54±1.77 | 1195.95±280.56 | 7.53±0.58 | 1213.25±93.22 | 8.73±1.85 | 1393.56±280.96 |
| D-249 O-Ring Compression (15 mm) | 27.93±1.93 | 1064.89±84.21 | 30.21±4.02 | 1160.89±197.40 | 30.08±3.19 | 1144.78±139.90 |
| D-249 O-Ring Compression (20.4 mm) | 37.21±3.00 | 1040.44±106.19 | 37.48±4.75 | 1033.56±129.84 | 41.60±6.52 | 1148.56±173.54 |
| DuPont SiC-SiC | | | | | | |
| D/O C-Ring Compression (15 mm) | 4.12±0.38 | 11905±1556 | 5.90±0.80 | 18518±2378 | 5.53±140 | 16585±5220 |
| D/O C-Ring Tension (15 mm) | 6.48±0.84 | 20210±4139 | 5.80±0.86 | 18811±3617 | 6.48±1.67 | 20242±5560 |
| D/O O-Ring Compression (15 mm) | 18.57±2.18 | 16303±1249 | 19.73±2.57 | 18810±1374 | 21.37±1.12 | 18902±652 |
| D/O O-Ring Compression (25.4 mm) | 32.63±8.24 | 18064±2156 | 26.53±5.78 | 14887±271 | 33.70±6.61 | 16226±252 |
| IF&P Fibrosic™ | | | | | | |
| RX9502-1709 C-Ring Comp (15 mm) | 0.64±0.12 | 28.13±6.70 | 2.11±0.41 | 98.86±18.69 | 2.14±0.59 | 95.70±17.58 |
| RX9502-1709 C-Ring Tension (15 mm) | 0.71±0.15 | 50.90±11.96 | 1.03±0.16 | 70.70±11.71 | 1.04±0.36 | 74.45±25.59 |
| RX9502-1708 O-Ring Comp (15 mm) | 2.62±0.23 | 53.22±5.45 | 3.24±0.55 | 66.56±9.90 | 3.62±0.49 | 71.67±12.54 |
| RX9502-1708 O-Ring Comp (20.4 mm) | 4.03±0.24 | 59.33±7.11 | 4.74±0.90 | 67.56±15.70 | 5.36±0.42 | 78.67±9.64 |

(a) Three Layer Composite Strength; (Triaxial Braid Support).
(b) Strength Measured At 732°C; Strengths To Be Determined At Temperatures Of 843°C And 870°C.
TBD: To Be Determined.
Cross-Head Speed of 0.05 in/min Is Consistently Utilized During Conduct of C-Ring Compressive or Tensile Testing.

## Table 2. Comparison of the First and Second Generation As-Manufactured Candle Filter Material Properties

| Filter Matrix (15 mm) | 25°C C-Ring Strength, psi, | | 25°C C-Ring Ultimate Load, lbs | | Burst Pressure, psi | Ultimate Hoop Stress,psi | Elastic Modulus, psi x 10^6 | Poissons Ratio |
|---|---|---|---|---|---|---|---|---|
| | Compression | Tension | Compression | Tension | | | | |
| Coors Alumina/Mullite | 2575±182 | 2721±415 | 42.8±2.4 | 31.4±4.9 | 860 | 2317 | 5.7 | 0.23 |
| Pall Vitropore 442T | 2857±186 | 2574±177 | 60.5±5.9 | 35.3±1.8 | 513-970 | 1307-2499 | 5.25-6.67 | 0.14-0.19 |
| Schumacher Dia Schumalith F40 | 1300±213 (a)<br>1790±112 (b) | 1907±111<br>2308±275 | 74.5±14.2<br>102.1±9.4 | 53.4±3.7<br>63.8±8.2 | 1140-1370 | 1893-2267 | 5.89-6.26 | 0.25-0.31 |
| Schumacher Dia Schumalith FT20 | 2296±261 | 2268±167 | 44.2±4.8 | 29.2±2.9 | 665 | 1703 | 7.3 | 0.17 |
| 3M CVI-SiC Composite | 1343 (c)<br>13187 (d)<br>1315±186 (c) *<br>13276±1417 (d) * | | 2.5<br>2.5<br>7.7±0.84 *<br>7.7±0.84 * | | | 1.01 | 2.96-3.38 | 0.14-0.27 |
| DuPont SiC-SiC | 11905±1556<br>16303±1249 * | 20210±4139 | 4.12±0.38<br>18.57±2.18 * | 6.48±0.84 | | 2972 (e) | | |
| DuPont PRD-66 | 1219±162 | 1265±188 | 9.2±1.0 | 7.3±1.3 | 120 | 462 | 9.36 - 15.44 | 2.25 |
| IF&P Fibrosic™ | 28.1±6.7<br>53.2±5.5 * | 50.9±12.0 | 0.64±0.12<br>2.6±0.2 * | 0.71±0.15 | | 41 | 0.5 | 0.4 |

(a) 1991 Production Lot.
(b) 1992 Production Lot.
(c) Composite Strength (Containment Layer, Filtration Mat, And Triaxial Support Braid).
(d) Triaxial Support Braid.
(e) Seam Rupture.
* 15 mm O-Ring Diametral Compressive Strength Or Load.

## Table 3. Strength Characterization of the As-Manufactured DuPont PRD-66 Candle Filter Matrix

| Temperature, °C | C-Ring Compression, psi | C-Ring Tension, psi | O-Ring Compression, psi |
|---|---|---|---|
| 25 | 876±151 | 874± 79 | 990± 77 |
| 200 | 914±138 | 955±184 | 990±138 |
| 400 | 881±119 | 911±153 | 1004± 70 |
| 600 | 733± 49 | 826±133 | 1069± 69 |
| 800 | 1009±118 | 831±130 | 1205± 60 |
| 900 | 1086±178 | 878±143 | 1171± 97 |
| 1000 | 1092± 65 | 963±168 | 1251± 49 |

Sample Width: 15 mm.

**Simulated Process Transient Testing.** HTHP testing was completed in Westinghouse's PFBC simulator test facility in which a 1.5 m 3M CVI-SiC composite candle, a 1.5 m DuPont PRD-66 candle filter, a 1.4 m DuPont SiC-SiC candle filter, and a 1.5 m IF&P Fibrosic™ candle were subjected to seven process transients (i.e., increasing gas temperature excursions ranging from mild to severe), nine maximum severity process transients, ten accelerated pulse cycles, and a final maximum severity process transient. The HTHP PFBC test facility was operated at 843°C and 100 psig, and during conduct of the maximum severity transients, temperature along the outer surface of the filter elements decreased by 110°C and 240°C within the first 5 and 60 seconds, respectively, after initiation of the transient.[2] After each transient, a rapid reheat was conducted in order to return the process operating temperature to 843°C within one hour after transient initiation.

With the exception of the DuPont SiC-SiC candle, all filters remained intact. The seam which ran along the entire length of the DuPont SiC-SiC candle filter partially opened (i.e., <1 mm gap; ~40 cm rupture length), permitting fines to penetrate through, and to be released into the off-gas stream (Figure 2). During handling the candle fractured into two segments.

**Accelerated Pulse Cycling.** In order to identify the viability and thermal fatigue resistance of the advanced, second generation filter elements, all four filter element types (i.e., 3M CVI-SiC composite candle; DuPont PRD-66 candle; DuPont SiC-SiC candle; and IF&P Fibrosic™ candle) were subjected to accelerated pulse cycling. The pulse cycle that was delivered to the array was representative of the conditions which have commonly been used during field operation of W-APF systems.

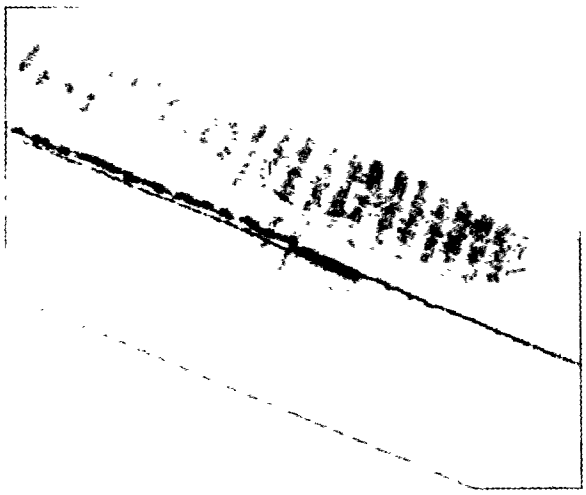

**Figure 2. Ruptured Seam of the DuPont SiC-SiC Composite Candle Filter After Process Transient Testing**

HTHP testing was conducted at temperatures of 843°C and pressures of 100 psig, with a pulse cycle delivered every 2.5 minutes. After 1645 pulse cycles, dust was detected in the off-gas, indicating that a breach had occurred within the filter system. Upon disassembly, the IF&P Fibrosic™ candle was observed to have fractured along the mid-body (Figure 3). A large hole (~75 mm long; ~40 mm wide) was evident below the flange, and a smaller through-wall hole (i.e., ~10 mm) was evident along the filter body. The longitudinal fractured surface of the Fibrosic™ matrix followed what appeared to be the "bark-like" or matrix texture lines that were apparent along the outer surface of the filter element. Striated layers of the chopped fiber matrix were evident throughout the fractured IF&P Fibrosic™ filter wall.

Gas flow "stream" lines were evident along the ID wall of the fractured IF&P Fibrosic™ candle. These lines which were approximately 180° from the large hole that resulted below the flange, were considered to have resulted from repeated pulse cycling. Further inspection of the ID surface near the flange indicated that the surface of the infiltrate

**Figure 3. Fractured IF&P Fibrosic™ Candle Filter After 1645 Accelerated Pulse Cycles Under HTHP Conditions**

that was used to provide additional strength along the flange had partially separated from the support matrix.

After removal of the failed IF&P Fibrosic™ filter element from the HTHP array, testing was reinitiated, and continued until 3514 pulse cycles had been delivered to the array. Subsequently ash was fed for an additional eight hours in order to develop a dust cake along the outer surface of each of the remaining filter elements. Post-test inspection indicated that with the exception of the 3M CVI-SiC composite filter, all of the remaining filter elements were intact. Failure at the base of the flange of the 3M CVI-SiC composite matrix resulted from extended pulse cycling which partially dislodged the primary gasket seal from its original position in the filter holder mount.

## Corrosion Testing

Westinghouse has previously demonstrated the relative thermal/chemical stability of the oxide-based alumina/mullite filter matrix during exposure to high temperature, oxidizing conditions which contain gas phase alkali and steam.[3-5] In order to demonstrate the stability of the oxide-based DuPont PRD-66 and IF&P Fibrosic™ materials, PRD-66 mini-candles which were manufactured with an ~75 mm section of open filtration area, and 70 mm diameter x 6.4 mm thick membrane coated IF&P discs were exposed for 400 hours at 870°C to 5-7% steam/air and 20 ppm NaCl/5-7% steam/air flow-through testing. During the 400 hour exposure, both the mini-candles and filter discs were subjected to pulse cycling at every 20 minute intervals.

High temperature, flow-through testing was similarly conducted for the nonoxide-based, advanced, second generation filters using mini-candles of the 3M CVI-SiC composite matrix, and discs of the DuPont SiC-SiC composite matrix. Post-test characterization of each material has included C-ring compression testing at 870°C of the as-manufactured and flow-through tested mini-

candles, and 4-point bend, 1/4-point flexural strength testing at 870°C of the as-manufactured and flow-through tested filter discs. SEM/EDAX analyses are also being performed. A description of the resulting exposed filter matrices, and currently available test results are presented in the following sections.

**3M CVI-SiC Composite Matrix.** The 3M CVI-SiC composite filter consists of three layers -- an outer open mesh confinement layer, a middle filtration mat, and an inner triaxial braided fabric layer which forms the structural support matrix of the filter element. Within the confinement and filtration mat layers, an ~1-2 μm layer of silicon carbide encapsulates Nextel™ 312 or alumina-based fibers, while an ~100 μm layer of silicon carbide is deposited along the Nextel™ 312 triaxial braid in the support matrix.

After exposure to either the high temperature steam/air or alkali/steam/air flow-through environment, the 3M mini-candles appeared to be intact, retaining their initial configuration. What was readily apparent, however, was the very brittle nature of the outer confinement layer along the alkali/steam/air-exposed 3M CVI-SiC composite matrix. In several locations, the fiber bundles of the confinement layer weave were broken or missing.

During preparation of the 3M CVI-SiC matrix for strength testing, two as-manufactured mini-candles were cut into 15 or 25.4 mm sections for high temperature C-ring compression testing. These sections were removed from the open filtration area of the mini-candle. Similarly, a 25.4 mm O-ring section was removed from the reinforced filter matrix directly below the flange. All three layers of the as-manufactured 3M CVI-SiC composite matrix remained bonded together during preparation of either the 15 and 25.4 mm C-ring, or 25.4 mm O-ring samples.

Similar C-ring and O-ring samples were removed from the steam/air and alkali/steam/air-exposed 3M CVI-SiC mini-candles. During sample preparation, the three composite layers of the steam/air-exposed 3M CVI-SiC matrix remained bonded together, while debonding occurred along both the 15 and 25.4 mm C-ring sections that were removed from the alkali/steam/air-exposed 3M filter matrix.

What was also apparent for both the steam/air and alkali/steam/air-exposed 3M mini-candles was the extreme difficulty that was encountered during cutting of the reinforced matrix directly below the flange. As shown in Table 4, the applied compressive load required to fail the flange reinforced O-ring sections, and the resulting diametral strength generally decreased after the 3M CVI-SiC composite matrix was exposed for 400 hours at temperatures of 870°C to either the steam/air or alkali/steam/air flow-through environment.

As shown in Table 5, the applied compressive load required to fail C-rings that were removed from the 3M CVI-SiC composite filtration area, and the resulting strength also decreased after 400 hours of exposure in the 870°C steam/air or alkali/steam/air flow-through environment. The resulting load vs deflection curves that were generated during C-ring compression testing tended to indicate that a reduction in the fracture toughness of the embrittled, 3M CVI-SiC composite matrix resulted after exposure at high temperature to the steam/air and alkali/steam/air test conditions.

Preliminary SEM/EDAX analyses of the steam/air and alkali/steam/air-exposed 3M CVI-SiC filter matrices indicated that the ~1-2 μm SiC layer which had been deposited within the outer confinement layer and triaxial braid support fiber bundles, and along the alumina-based filtration mat fibers, had generally been removed. The ~100 μm

**Table 4. Diametral Compressive Strength of the 3M CVI-SiC Composite Mini-Candle Reinforced Flange**

| Filter ID No. | Exposure | Time, Hrs | Temp., °C | Diametral Testing At 870°C | |
|---|---|---|---|---|---|
| | | | | Load, lbs | Strength, psi |
| 3M-453707 | As-Manufactured (25.4 mm) | --- | --- | 30.5 | 2247 |
| 3M-453715 | As-Manufactured (25.4 mm) | --- | --- | 32.7 | 1907 |
| 3M-453710 | Steam/Air (25.4 mm) | 400 | 870 | 19.9 | 1975 |
| 3M-453708 | Alkali/Steam/Air (25.4 mm) | 400 | 870 | 18.5 | 1375 |

**Table 5. Strength Characterization of the Steam/Air and Alkali/Steam/Air-Exposed 3M CVI-SiC Composite Mini-Candles**

| Filter ID No. | Exposure | Time, Hrs | Temp., °C | Compressive Load, lbs | C-Ring Compressive Strength at 870°C, psi | |
|---|---|---|---|---|---|---|
| | | | | | Composite Matrix | Triaxial Support Braid |
| 3M-453707 | As-Manufactured(15 mm) | --- | --- | 3.3±0.36 | 1739±259 | 11784±1476 (a) |
| 3M-453715 | As-Manufactured(25.4 mm) | --- | --- | 4.0±0.14 | 1183± 78 | 8561±463 (a) |
| 3M-453710 | Steam/Air(15 mm) | 400 | 870 | 2.10±0.62 | 987±250 | 8533±1546 (a) |
| 3M-453708 | Alkali/Steam/Air(15 mm) | 400 | 870 | 1.7 | 717 (a) | 6298 |
| 3M-453708 | Alkali/Steam/Air(25.4 mm) | 400 | 870 | 2.85±0.64 | 762±151 (a) | 5808±695 |

(a) Calculated Based On Either The Triaxial Support Braid Or Composite Matrix Wall Thickness.

CVI-SiC deposited layer which coated the triaxial support braid was intact, but was enriched with oxygen. Due to the very thin nature of the interface layer that initially coated the Nextel™ and alumina-based fibers, resolution and identification of its presence in either the as-manufactured or flow-through tested mini-candles could not be made using SEM/EDAX analytical techniques. Aluminum and silicon-rich, micron, nodular formations were evident along the Nextel™ and alumina-based fibers in all three composite layers of the steam/air-exposed 3M CVI-SiC composite matrix.

**DuPont PRD-66 Filament Wound Matrix.** The oxide-based, filament wound, DuPont PRD-66 matrix consists of a layered cordierite, mullite, cristobalite, and corundum microstructure. An amorphous phase is also present in the as-manufactured PRD-66 filter matrix. Due to the difference in the thermal coefficient of expansion of mullite, cordierite, and corundum which are present in the PRD-66 matrix, a microcracked structure is formed after high firing.

The "diamond" pattern weave of the polycrystalline refractory oxide-based fibers forms

the ~7 mm structural support layer of the DuPont PRD-66 filter matrix. A thin membrane layer is wrapped along the outer surface of the support matrix, producing a light weight, bulk filter element.

After 400 hours of exposure in the 870°C, steam/air and alkali/steam/air environment, the DuPont PRD-66 mini-candles generally remained intact. However, along the outer membrane surface of the filtration area of the alkali/steam/air-exposed mini-candle, numerous longitudinal cracks were evident (Figure 4). In addition, a 1 cm x 1.5 cm section of the membrane and several of the underlying structural support fibers had been removed along the alkali/steam/air-exposed mini-candle.

As shown in Table 6, the high temperature, C-ring compressive strength of the filtration area in the brittle PRD-66 filter matrix appeared to slightly increase after 400 hours of exposure to the steam/air flow-through environment, while a slight decrease in strength was observed after 400 hours of exposure in the alkali/steam/air environment. In contrast virtually no change in strength was observed along the slurry infiltrated flange or end cap areas of the PRD-66 mini-candles after exposure to either the high temperature steam/air or alkali/steam/air environment (Table 7).

**DuPont SiC-SiC Composite Matrix.** The DuPont SiC-SiC composite matrix consists of an ~10-20 μm silicon carbide layer which is chemically vapor infiltrated (CVI) along an ~2-5 μm interface coating layer which encapsulates ~15 μm Nicalon™ fibers. Several issues have been raised as to the oxidative stability of the dual single-ply felt or hybrid (i.e., single-ply felt; single-ply open mesh screen) DuPont SiC-SiC composite matrix, and in particular the stability of the interface coating and Nicalon™ fibers.

After 400 hours of exposure of the DuPont SiC-SiC matrix to either the 870°C, flow-through, steam/air or alkali/steam/air environment, depletion of the interface coating resulted (Figure 5). A mottled crystalline phase formed along the SiC-SiC surface which was identified by EDAX analysis to contain silicon and oxygen (i.e., on a 1:1 atomic percent basis). The Si-O phase formed a rather noncontinuous layer along the surface of the SiC-SiC matrix. The presence of gas phase sodium appeared to enhance surface oxidation of the SiC-SiC matrix, leading to areas that were enriched with $SiO_2$. Sorption of sodium into the $SiO_x$ or $SiO_2$ layer which covered the SiC-SiC matrix was not detectable by EDAX analysis after 400 hours of exposure of the DuPont composite matrix to the 870°C, 20 ppm NaCl/steam/air, flow-through environment. Continued exposure may be needed to promote sorption of alkali, and possibly formation of the sodium silicate eutectic phase. In this manner, the relatively inert SiC-SiC matrix appears to exhibit a slower oxidation or corrosion rate in comparison to the clay bonded silicon carbide filter materials.

In contrast, the fine grained SiC membrane coating of the DuPont matrix tended to form a glaze during the high temperature, alkali/steam/air exposure, which reduced gas flow permeability through the filter disc (Figure 6). The glazed surface which was enriched with sodium could conceivably serve as a potential site for collection and adherence of ash fines at process operating temperatures, which may ultimately cause blinding of the filter element surface.

The residual strength of the hybrid DuPont SiC-SiC matrix (i.e., single-ply felt; single-ply open mesh screen) was determined at 870°C via 4-point bend, 1/4-point flexural strength testing of bend bars that had been removed from the alkali-exposed filter disc. Approximately 60% of the as-manufactured strength remained along the surface of the matrix that had been subjected to pulse

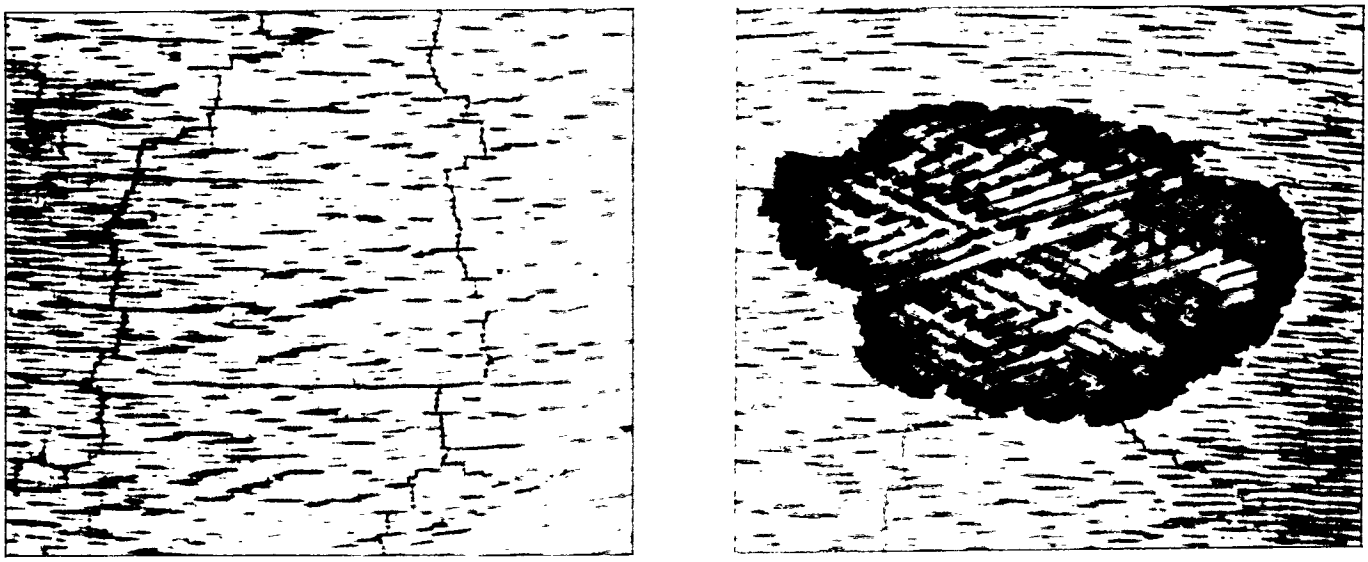

**Figure 4. Cracks and Spalled Areas of the OD Surface Membrane of the 400 Hour, 870°C, 20 ppm NaCl/5-7% Steam/Air-Exposed DuPont PRD-66 Filter Matrix**

**Table 6. Strength Characterization of the Steam/Air and Alkali/Steam/Air-Exposed DuPont PRD-66 Mini-Candles**

| Filter ID No. | Exposure | Time, Hrs | Temp., °C | C-Ring Compression At 870°C | |
|---|---|---|---|---|---|
| | | | | Load, lbs | Strength, psi |
| D-282 | As-Manufactured (15 mm) | --- | --- | 9.65±0.72 | 1352±135 |
| D-289 | Steam/Air (15 mm) | 400 | 870 | 11.88±0.71 | 1541±146 |
| D-288 | Alkali/Steam/Air (15 mm) | 400 | 870 | 8.58±1.70 | 1093±265 |

**Table 7. Strength of the Reinforced Flange and End Cap Sections of the DuPont PRD-66 Mini-Candles After Flow-Through Testing**

| Filter ID No. | Exposure | Time, Hrs | Temp., °C | Diametral O-Ring Compression | | | |
|---|---|---|---|---|---|---|---|
| | | | | Flange | | End Cap | |
| | | | | Load, lbs | Strength, psi | Load, lbs | Strength, psi |
| D-282 | As-Manufactured (25.4 mm) | --- | --- | 81.3 | 2341 | 56.3 | 1625 |
| D-289 | Steam/Air (25.4 mm) | 400 | 870 | 74 | 1997 | 60.5 | 1665 |
| D-288 | Alkali/Steam/Air (25.4 mm) | 400 | 870 | 84.2 | 1819 | 50.5 | 1619 |

(a) (b)

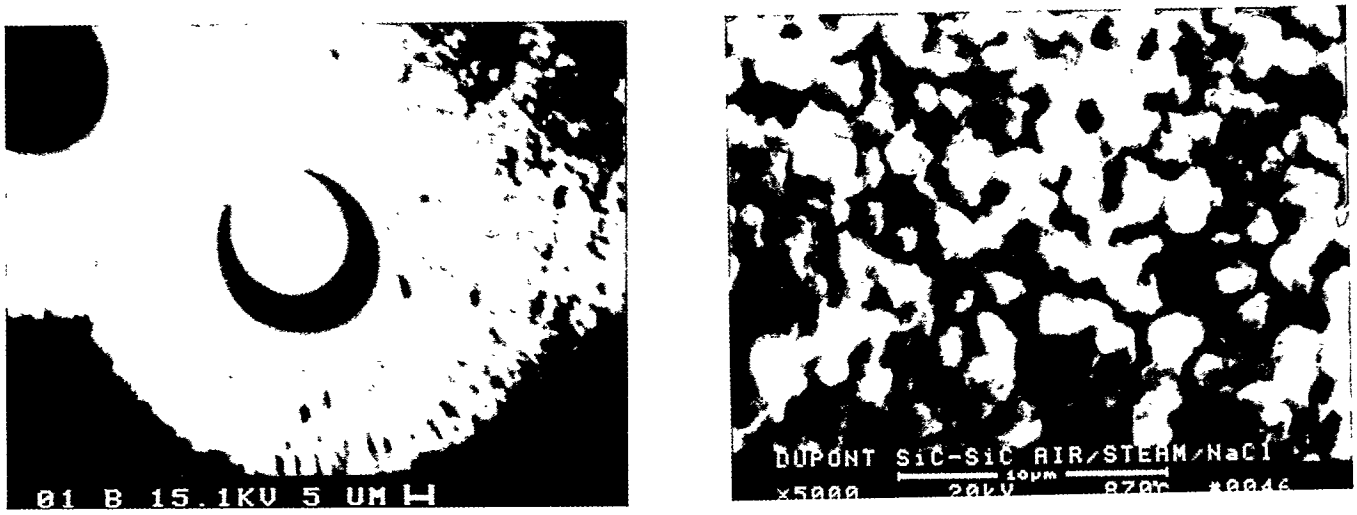


**Figure 5. DuPont SiC-SiC Composite Matrix After 400 Hours of Exposure at 870°C to the 20 ppm NaCl/5-7% Steam/Air Flow-Through Test Environment (a) Depletion of the Interface Coating; (b) Oxidation of the CVI-SiC Surface**

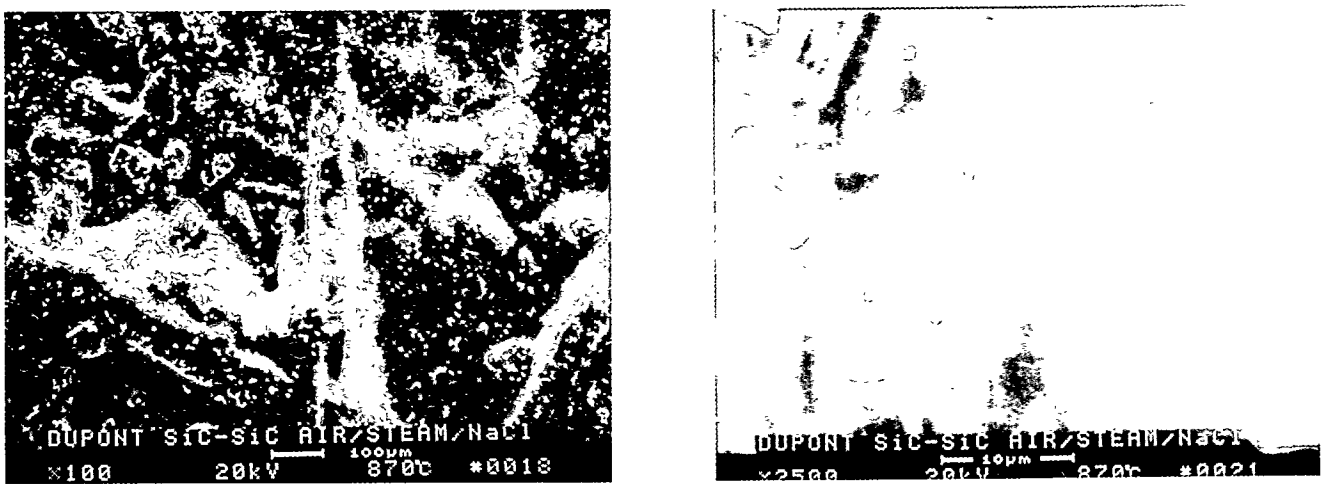


**Figure 6. Glazed Sodium-Enriched Surface Membrane of the DuPont SiC-SiC Composite Candle Filter Matrix After 400 Hours of Exposure to 870°C, 20 ppm NaCl/5-7% Steam/Air Flow-Through Test Environment**

cleaning, while only 42% of the as-manufactured strength remained along the membrane coated surface that sorbed alkali during the 400 hour alkali/steam/air, flow-through test exposure (Table 8). Based on the load vs deflection curves that were generated during high temperature, flexural strength testing, the fracture toughness of the low fiber volume, DuPont SiC-SiC filter matrix appeared to decrease after 400 hours of exposure in either the 870°C steam/air or alkali/steam/air environment.

**IF&P Fibrosic™ Filter Matrix.** The vacuum infiltrated alumina and aluminosilicate chopped fiber IF&P Fibrosic™ matrix was similarly subjected to 400 hours of flow-through testing at 870°C in both the steam/air and alkali/steam/air environment. After 400 hours of exposure in the 870°C steam/air environment, the membrane coated IF&P Fibrosic™ disc was torn as the result or repeated pulse cycling (Figure 7). In contrast, the IF&P Fibrosic™ disc which had been exposed for 400 hours at 870°C to the alkali/steam/air environment remained intact, and appeared to have rigidized. SEM/EDAX and XRD analyses will be utilized to differentiate between the resulting phases in the steam/air and alkali/steam/air - exposed IF&P Fibrosic™ discs.

Four-point bend, 1/4-point flexural testing of the IF&P filter matrix was intended to be conducted for strength evaluation of the as-manufactured and flow-through tested discs. In order to cut bend bars from the matrix, the as-manufactured filter disc was positioned along a metal support block with double-backed tape, and cut dry with a diamond wheel. Unfortunately during removal of the bend bars, tearing resulted, and further characterization of the as-manufactured and residual strength of the alkali/steam/air-exposed discs was suspended.

In both the flow-through and HTHP accelerated pulse cycle tests, tearing and/or failure of the IF&P Fibrosic™ vacuum infiltrated, chopped fiber body resulted. During flow-through testing, the pulse gas directly contacted the "non-membrane" coated surface of the IF&P Fibrosic™ matrix, while a baffled plenum prevented direct

**Table 8. 4-Point Bend, 1/4-Point Flexural Strength of the Steam/Sir and Alkali/Steam/Air-Exposed DuPont SiC-SiC Filter Matrix**

| | Membrane Tested In Compression, psi (a) | | Membrane Tested In Tension, psi (b) | |
|---|---|---|---|---|
| Filter Matrix | 25°C | 870°C | 25°C | 870°C |
| As-Manufactured | 13118±1697 (c) | 12068±3128 (c) | 7269±272 (c) | 4981±1801 (c) |
| Steam/Air | NA | 5427±749 (d) | NA | 4450±541 (d) |
| Alkali/Steam/Air | NA | 3953± 90 (d) | NA | 3092±304 (d) |
| Alkali/Steam/Air | NA | 7269±557 (c) | NA | 2106±454 (c) |

Span: 1.57 inch; Cross-Head Speed: 0.02 in/min.

(a) Pulse Cycled Surface Strength; (Open Mesh Screen).
(b) Membrane Coated Surface Strength; (Single-Ply Felt Mat).
(c) Bend Bars Were Cut Parallel To The Open Mesh Screen Ribs.
(d) Bend Bars Were Cut On A Diagonal To The Open Mesh Screen Ribs.
NA: Not Applicable.

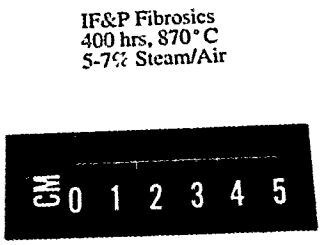


**Figure 7. IF&P Fibrosic™ Filter Disc After 400 Hours of Exposure at 870°C to the 5-7% Steam/Air Flow-Through Test Environment**

impingement of the pulse gas along the ID bore of the filter element during HTHP testing.

## Field Testing

Both 3M CVI-SiC composite and DuPont PRD-66 filament wound candles were installed in the W-APF system at AEP during operation of the 288 candle filter system in Test Segment #4 and Test Segment #5 (Table 9). A description of the 3M CVI-SiC and DuPont PRD-66 filter elements after each test segment, and currently available materials analyses are provided in the following sections. The materials characterization results of alternate candle filters (i.e., Schumacher Dia Schumalith F40; Schumacher Dia Schumalith FT20; Pall Vitropore 442T; and Coors alumina/mullite) that were also installed and operated in the W-APF at AEP are presented elsewhere.[2]

**3M CVI-SiC Composite Filters.** Three 3M CVI-SiC composite filters had been initially installed in a middle array in the W-APF in July 1994, and after 1015 hours of operation, two of the elements failed at the base of their flange. The third 3M filter element, which remained intact and achieved 1705 hours of PFBC test operation prior to termination of Test Segment #4 at AEP, was recovered for materials characterization.[6]

Post-test, room temperature, gas flow resistance measurements of the intact PFBC-exposed 3M filter indicted that the pressure drop across the element was ~220 in-wg at a gas face velocity of 10 ft/min. The room temperature pressure drop across the ash coated 3M filter was relatively high in comparison to alternate filter elements which were exposed to similar PFBC test conditions (i.e., Coors alumina/mullite: 50 in-wg at 10 ft/min). The high pressure drop across the 3M PFBC-exposed candle filter was attributed to the adherence of the dust cake layer along and within the confinement layer, as well as through the filtration mat, and triaxial support braid.

Characterization of the 3M CVI-SiC matrix via scanning electron microscopy/energy dispersive x-ray analysis indicated that minor changes in the morphology of the filter matrix had occurred after 1705 hours of operation in the 660-760°C, W-APF system at AEP (Figure 8). Due to deposition of the thin <1 μm interface coating, it was frequently difficult to discern whether the interface coating had remained intact. A gap or separation was considered to exist between the CVI-SiC coating and the underlying Nextel™ 312 fibers in several areas of the PFBC-exposed 3M composite filter matrix. In the high temperature

**Table 9. Summary of the W-PFBC Hot Gas Filter Testing at AEP**

| Test Segment | 1<br>10/92-12/92 | 2<br>7/93-9/93 | 3<br>1/94-4/94 | 4<br>7/94-10/94 | 5<br>1/95-3/95 |
|---|---|---|---|---|---|
| Number Of Candles | 384 | 384 | 384 | 288 | 288 |
| Primary Cyclone | In-Service | In-Service | Detuned | Detuned | Inactive |
| Operating Hours | 464.4 | 1295 | 1278.8 | 1705.8 | 1110.4 |
| Operating Temperature, °C | 730-790 | 620-790 | 650-780 | 660-760 | 760-845 |
| Nominal Face Velocity, cm/s | 2.4-3.3 | 2.3-3.3 | 2.3-3.3 | 3.0-4.4 | 4.5 |
| Inlet Dust Loading, ppmw | 600 | 600 | 3200 | 3200 | 18000 |
| Ash Mass Mean, µm | 1-3 | 1-3 | 5-7 | 5-7 | 27 |

(a) (b)

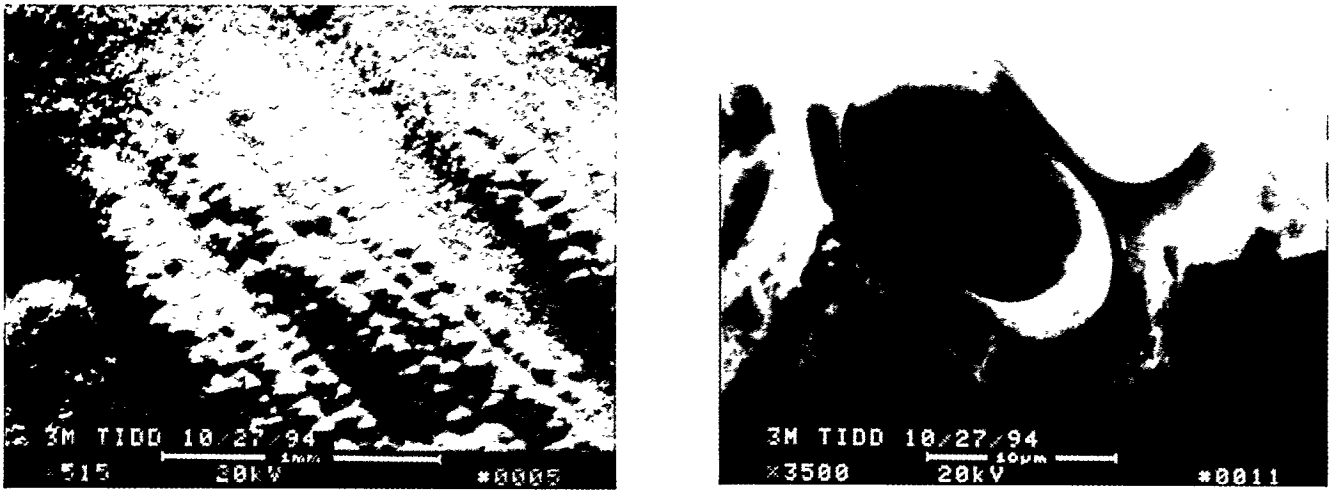


**Figure 8. Morphology of the 3M CVI-SiC Composite Matrix after 1705 Hours of Operation in the 660-760°C PFBC Environment**

PFBC environment, oxidation of the interface coating is expected to occur.

Post-test diametral compressive strength testing indicated that the strength of the PFBC-exposed 3M CVI-SiC composite matrix was greater than that of the as-manufactured filter matrix (Table 10). Crystallization of the amorphous phase which is initially expected to be present in the as-manufactured Nextel™ 312 fibers, may be responsible for strengthening of the filter matrix. Alternately, due to the accumulation of fines within the PFBC-exposed matrix, "wedging" of fines in between the SiC coated fibers may require a higher load to be applied to the matrix prior to failure, thus generating what appeared to be a strengthened composite matrix. During diametral compressive strength testing, the relatively low load bearing, 732°C (i.e., nominal operating temperature), PFBC-exposed, 3M CVI-SiC matrix generally retained the graceful fiber "pull-out" characteristics of the fracture toughened, as-manufactured matrix.

Testing was reinitiated at AEP in January 1995 during which time ten newly manufactured, 3M CVI-SIC composite filters were installed in the W-APF system. After 1110 hours of filter operation at temperatures ranging between 760 and 845°C, testing was terminated. Post-test inspection of the filter cluster indicated that all ten of the 3M CVI-SiC composite filter elements were intact. Further inspection of the 3M candles indicated that ash had been carried into the ID bore of the elements due to a breach within an alternate filter array. As a result, ash fines became tightly packed in the bottom of several of the filter elements. After cool-down of the W-APF, cracks were evident along the internally ash plugged section of at least one filter element (Figure 9). Along an alternate 3M filter element, a 25.4 mm diameter hole was evident along the outer confinement layer. The location of the removed confinement layer was ~75 mm below the flange.

Assuming that the strength of the as-manufactured 3M filters which were used for testing at Tidd in Test Segment #5 was equivalent to the strength of the as-manufactured filter elements which were used in Test Segment #4, strength characterization of the 1110 hour, Tidd-exposed 3M CVI-SiC composite filter elements

**Table 10. Residual Strength of the 3M CVI-SiC Composite Filter Matrix After Exposure in the W-APF at AEP**

| | | | | Diametral O-Ring Testing | | | | | |
|---|---|---|---|---|---|---|---|---|---|
| | | | | Room Temperature Strength, psi | | High Temperature (732°C) Strength, psi | | High Temperature (843°C) Strength, psi | |
| Filter ID No. | Candle Filter Location | Test Segment No. | Operating Time, Hrs | Composite | Triaxial Briad | Composite | Triaxial Braid | Composite | Triaxial Braid |
| 43-1-2 | --- | --- | --- | 1341±254 | 14026±2012 | 1060±219 | 11012±1795 | NA | NA |
| 43-1-6 | B/M-15 | 4 | 1705 | 1696±195 | 18220±1356 | 1429±159 | 15599±2246 | NA | NA |
| 45-18-02 | C/T-18 | 5 | 1110 | 2333±415 | 18975±3117 | 2225±361 | 18001±3745 | 1850±299 | 16173±2245 |

NA: Not Available.

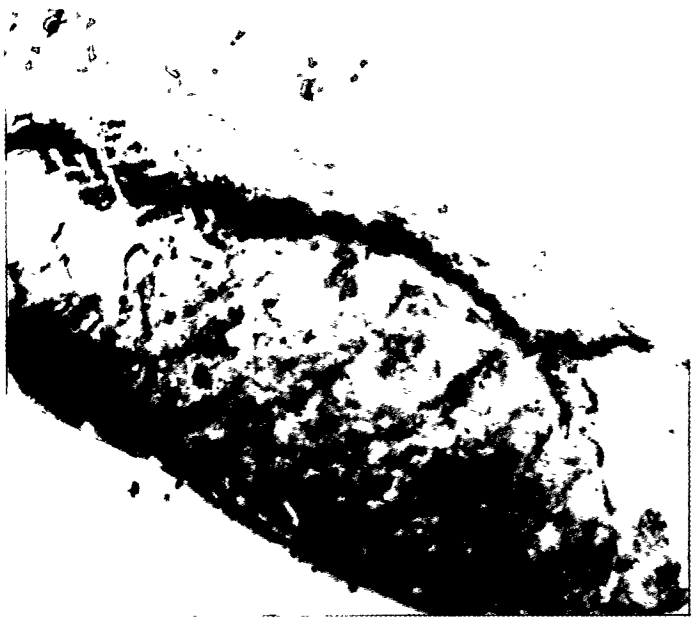

**Figure 9. Fractured 3M CVI-SiC Composite Filter End Cap After 1110 Hours of Operation in the W-APF System at AEP in Test Segment #5**

indicated that the ash-filled matrix once again appeared to increase. The shape of the load vs deflection curves generated during high temperature C-ring strength testing are being evaluated to determine the residual fracture toughness of the 3M CVI-SiC composite filter matrix after 1110 hours of exposure in the elevated temperature PFBC environment.

**DuPont PRD-66 Filament Wound Filters.** During operation of the W-APF system in Test Segment #4, three DuPont PRD-66 filter elements were installed in a middle array. After 1705 hours of operation, all three filters remained intact. During C-ring preparation of the Tidd-exposed PRD-66 filter element, magnesium sulfate recrystallized along the outer surface of the filter, as a result of leaching of the ash that was contained within the filter ID bore and wall during wet cutting with a diamond wheel. Post-test strength characterization of the PRD-66 matrix indicated that the bulk strength of the ash filled matrix tended to increase after 1705 hours of operation at AEP in Test Segment #4 (Table 11).

Twenty-two DuPont PRD-66 candle filters were installed in a top array for operation in Test Segment #5. After ~232 hours of operation, sections of the PRD-66 matrix were identified in the ash hopper discharge, implying that failure had occurred. Testing continued, and after ~775 hours of operation, additional sections of the PRD-66 filter matrix were evident in the ash hopper discharge.

Testing was terminated after 1110 hours of operation in Test Segment #5. Post-test inspection of the W-APF internals indicated that ash bridging had been eliminated as the result of completely detuning the primary cyclone.[7] Only two of the DuPont PRD-66 filter elements remained intact, four had suffered either mid-body fracture or failure at a location that was ~3/4 below the flange, and sixteen filters had fractured at the base of each flange. The outer surface of the intact and fractured filters was generally "ash free", particularly along the portion of the body that was adjacent to the plenum pipe, and to approximately mid-way down the length of the filter element. Alternately 1-2 mm of ash was deposited along the outer surface of the PRD-66 candles, near the bottom end cap. "Divot-like" formations resulted in lines which ran parallel down both sides of the remaining intact and fractured filter elements (Figure 10). Localized "divoting" was also observed underneath the outer protected gasket sleeve, as well as in alternate, isolated areas along the filter body. Currently the mechanisms leading to "divoting", flange fracture, and mid-body failure of the DuPont PRD-66 filter elements in Test Segment #5 are under investigation. Since the PRD-66 filter array had

**Table 11. Residual Strength of the DuPont PRD-66 Filter Matrix After Exposure in the W-APF at AEP**

| Filter ID No. | Filter Location | Test Segment No. | Operating Time, Hrs | C-Ring Testing: Room Temperature Strength, psi | | High Temperature (732°C) Strength, psi | | High Temperature (843°C) Strength, psi | |
|---|---|---|---|---|---|---|---|---|---|
| | | | | Compression | Tension | Compression | Tension | Compression | Tension |
| D-99 | --- | --- | --- | 1219±162 | 1265±188 | 1277±178 | 1304±327 | NA | NA |
| D-132 | B/M-7 | 4 | 1705 | 1830±238 | 1725±320 | 1884±142 | 1642±401 | NA | NA |
| D-237 | B/M-8 | 5 | 1110 | 1533±202 | 1380±188 | 1897±256 | 1356±104 | 1872±230 | 1460±197 |

**Figure 10. Aligned Divot-Like Formations Along the Surface of the DuPont PRD-66 Candle Filter OD Surface After 1110 Hours of Operation in the W-APF System at AEP in Test Segment #5**

suffered failure after ~232 hours of operation, ash filled the inside bore of the remaining PRD-66 candles (i.e., 120 mm and 350 mm) during pulse cycling. Failure of the ash-filled PRD-66 end cap region was not observed.

Assuming that the strength of the PRD-66 elements used in Test Segment #5 was equivalent to the strength of the PRD-66 elements used in Test Segment #4, post-test strength characterization of the 1110 hour Tidd-exposed PRD-66 filter matrix indicated that an increase in strength appeared to have occurred along the ash-filled OD surface, while virtually no change in strength was detected along the ID or pulse cycled surface of the filament wound matrix (Table 11).

## Comment

Corrosion and HTHP testing is viewed by Westinghouse as a means to "pre-qualify" a filter element, prior to implementing its use in field test applications. By this means, many of the failure mechanisms described above, can be minimized and/or eliminated.

Although a loss of bulk material strength in the advanced, second generation filter materials generally results during steam/air or alkali/steam/air testing, these results should be viewed solely as a material response which is not influenced by the presence of ash. To date, filter qualification testing has not been focused on demonstrating the impact of ash bridging within a filter array. Bridging may not only be dependent on the size of the ash particles which enter the filter vessel, but may also be dependent on the process operating temperatures which are encountered during field testing, as well as

system design. Similarly, the resulting dust cake thickness and mechanism of removal are considered to primarily depend on the process operating parameters, coal and sorbent feed,[8] and perhaps the outer surface roughness or finish of each filter element.

## FUTURE WORK

- Complete materials characterization of the filter elements that have been subjected to HTHP accelerated pulse cycling and process transient testing.

- Complete characterization of the mini-candles and filter discs that have been exposed to flow-through testing in the 870°C steam/air and alkali/steam/air environment.

- Initiate mechanical durability and corrosion testing of the various advanced, second generation filter elements after design, construction and/or compositional modifications have been made by each supplier which potentially reflect improved filter operating reliability and extended service life.

## ACKNOWLEDGMENTS

We wish to acknowledge Mr. Richard Dennis at DOE/METC, as well as Mr. Mike Mudd and Mr. John Hoffman at AEP, for their continued support.

We also wish to acknowledge the efforts of Mr. Bob Walko for performing the destructive strength testing; Mr. Richard Kunkle for conducting the flow-through corrosion tests; and Mr. Art Fellers, Mr. George Schneider, Mr. Joe Condle, Mr. Tony Gasparovic, and Mr. John Meyer for participating in the HTHP test program. We also wish to thank Mr. Bob Palmquist and Mr. Tom Mullen for performing the analytical microscopy efforts.

## REFERENCES

1. M. A. Alvin, R. E. Tressler, T. E. Lippert, E. S. Diaz, and E. E. Smeltzer, "Durability of Ceramic Filters," *Proceedings of Coal-Fired Power Systems 94 -- Advances in IGCC and PFBC Review Meeting*, June 21-23, 1994, Morgantown, WV.

2. M. A. Alvin, T. E. Lippert, E. S. Diaz, and E. E. Smelter, "Thermal and Chemical Stability of Ceramic Candle Filters," *Proceedings of Advanced Coal-Fired Power Systems '95 Review Meeting*, June 27-29, 1995, Morgantown, WV.

3. M. A. Alvin, R. E. Tressler, T. E. Lippert, E. S. Diaz, "Evaluation of Ceramic Filter Material, Selection for Application," *Proceedings of Coal-Fired Power Systems '93 - Contractors Review Meeting*, June 28-30, 1993, Morgantown, WV.

4. M. A. Alvin, D. M. Bachovchin, T. E. Lippert, R. E. Tressler, and K. B. McNerney, "Thermal/Chemical Stability of Ceramic Cross Flow Filter Materials," *Proceedings of Twelfth Annual Gasification and Gas Stream Cleanup Systems Contractors Review Meeting*, September 15-17, 1992, Morgantown, WV.

5. M. A. Alvin, T. E. Lippert, D. M. Bachovchin, and R. E. Tressler, "High Temperature Filter Materials," *Proceedings of Coal-Fired Heat Engines, PFBC, and Gas Stream Cleanup Systems Contractors Review Meeting*, October 27-29, 1992, Morgantown, WV.

6. T. E. Lippert and R. A. Newby, "Development and Commercialization of Hot Gas Filters for Power Generation Applications," *Proceedings of International Gas Turbine and Aeroengine Congress and Exposition*, June 5-8, 1995, Houston, TX.

7. T. E. Lippert, G. J. Bruck, Z. Sanjana, and R. A. Newby, "Westinghouse Advanced Particle Filter System," *Proceedings of Advanced Coal-Fired Power Systems '95 Review Meeting*, June 27-29, 1995, Morgantown, WV.

8. R. A. Newby, T. E. Lippert, M. A. Alvin, and E. E. Smeltzer, "Filter Cake Characterization Studies," *Proceedings of Advanced Coal-Fired Power Systems '95 Review Meeting*, June 27-29, 1995, Morgantown, WV.

## 3.6 Application of CFCC Technology to Hot Gas Filtration Applications

Scott Richlen
U.S. Department of Energy

### ABSTRACT

Discussion will feature high temperature filter development under the DOE's Office of Industrial Technologies' Continuous Fiber Ceramic Composite (CFCC) Program. Within the CFCC Program there are four industry projects and a national laboratory technology support project. Atlantic Research, Babcock & Wilcox, DuPont Lanxide Composites, and Textron are developing processing methods to produce CFCC Components with various types of matrices and composites, along with the manufacturing methods to produce industrial components, including high temperature gas filters. The Oak Ridge National Laboratory is leading a National Laboratory/University effort to increase knowledge of such generic and supportive technology areas as environmental degradation, measurement of mechanical properties, long-term performance, thermal shock and thermal cycling, creep and fatigue, and non-destructive characterization. Tasks include composite design, materials characterization, test methods, and performance-related phenomena, that will support the high temperature filter activities of industry and government.

# Session 4

*Hot Gas Desulfurization*

## 4.1 Integrated Operation of a Pressurized Fixed Bed Gasifier, Hot Gas Desulfurization System and Turbine Simulator

### CONTRACT INFORMATION

| | |
|---|---|
| **Contract Number** | DE-AC21-87MC23170 |
| **Contractor** | GE Environmental Services, Inc.<br>200 N. Seventh St.<br>Lebanon, PA 17046-5006<br>(717-274-7077) |
| **Contractor Project Manager** | Steve Bevan - GEESI, David Najewicz - GE-CRD |
| **Principal Investigators** | Raul E. Ayala<br>Alan Feitelberg<br>Anthony Furman |
| **METC Project Manager** | Justin Beeson |
| **Period of Performance** | September 30, 1987 to September 30, 1995 |

**Schedule and Milestones**

**Project Schedule**

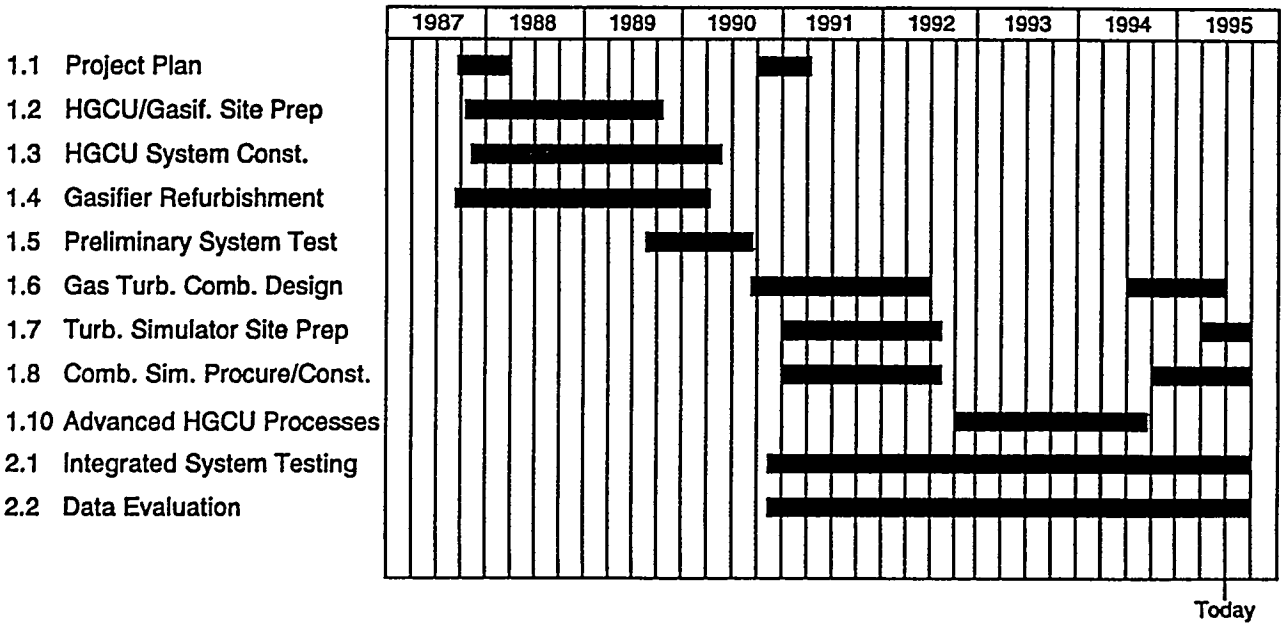

## OBJECTIVES

The overall objective of the General Electric Hot Gas Cleanup (HGCU) Program is to develop a commercially viable technology to remove sulfur, particulates, and halogens from a high-temperature fuel gas stream using a moving bed, regenerable mixed metal oxide sorbent based process. This technology will ultimately be incorporated into advanced Integrated Gasification Combined Cycle (IGCC) power generation systems. In IGCC applications, HGCU is projected to improve overall power generation cycle efficiencies by 1 to 2% compared with conventional low-temperature cleanup technologies, and will also offer the potential for reducing plant capital and operating costs.

The HGCU Program is based on the design and demonstration of the HGCU system in a test facility made up of a pilot-scale fixed bed gasifier, a HGCU system, and a turbine simulator in Schenectady, NY, at the General Electric Research and Development Center (GE-CRD). A modified GE MS6000 gas turbine combustor and a film-cooled, first-stage LM6000 nozzle assembly are incorporated into the turbine simulator.

The objectives of the turbine simulator testing are (1) to demonstrate the suitability of fuel gas processed by the HGCU system for use in state-of-the-art gas turbines firing at "F" conditions (2350°F rotor inlet temperature) and (2) to quantify the combustion characteristics and emissions on low-Btu (LBtu) fuel gas. The turbine simulator program also includes the development and operation of experimental combustors based on the rich-quench-lean concept (RQL) to minimize the conversion of ammonia and other fuel-bound nitrogen species to $NO_X$ during combustion.

The HGCU system and turbine simulator have been designed to process approximately 8000 lb/hr of low heating value fuel gas produced by the GE fixed bed gasifier. The raw fuel gas is provided to the HGCU and turbine simulator systems at 280 psig and 1000°F. The HGCU system has utilized several mixed metal oxide sorbents — including zinc ferrite, zinc titanate, and Z-Sorb (a proprietary zinc-based sorbent developed by Phillips Petroleum Company) — with the objective of demonstrating good sulfur removal and mechanical attrition resistance as well as economic cost characteristics. Demonstration of halogen removal and the characterization of alkali and trace metal concentrations in the fuel gas are subordinate objectives of the overall program.

## BACKGROUND INFORMATION

As a result of the availability of advanced gas turbine combined cycles that fire at temperatures of over 2350°F and the advent of integrated gasification/oxygen separation technology, IGCC plants now offer overall plant efficiencies of 42–44% with extremely low emissions of $SO_X$, $NO_X$, and particulate.

Although the capital cost of IGCC technology is higher than conventional coal-fired steam turbine plants, it is rapidly dropping to competitive levels. As IGCC power generation technology reaches the early stage of demonstration and commercialization, the first plants built will use conventional low-temperature gas-cleaning technology. However the goal of HGCU is that, when fully developed, it will represent a "second generation" cleanup technology offering further improvements in IGCC power generation efficiency and operation flexibility, as well as reduced capital and operating costs.

Fuel gas derived from coal by gasification processes contains sulfur in the form of $H_2S$ and COS at concentrations of up to several thousand parts per million (ppm). In order to comply with increasingly stringent environmental regulations and to meet the conditions required for the long life of gas turbine components, it is necessary to reduce both the sulfur and particulate in coal-derived fuel gas to low levels. In the temperature range of approximately 800–1200°F, mixed metal oxides, such as zinc oxide, react with these gaseous sulfur species, forming metal sulfides under reducing conditions. These metal sulfides can then be regenerated to their original oxide state, producing a sulfur-dioxide-rich off-gas suitable for conversion either to sulfuric acid or to elemental sulfur. GE Environmental Systems, Inc. (GEESI) has patented a moving bed process to utilize mixed metal oxide sorbents to remove sulfur from a high-temperature fuel gas stream and regenerate the sorbent for reuse while producing a byproduct stream suitable for the recovery of sulfur.

The history of this project and the concurrent development of high-temperature particulate removal systems based on cyclones has been documented by Smith et al. (1987), Cook et al. (1988, 1989, 1990, 1991, and 1992), and Bevan et al. (1994a and 1994b). In addition, the previous development of the mixed metal oxide sorbents and turbine simulator have been documented by Ayala et al. (1992, 1993, and 1994) and Feitelberg et al. (1993 and 1994).

## PROJECT DESCRIPTION

The HGCU Program is based on the design and demonstration of gas cleaning technologies at GE-CRD's Process Evaluation Facility (PEF) located in Schenectady, NY. This work is being carried out under a current DOE contract, with the most recent schedule shown in the Schedule section at the beginning of this paper. Construction of the basic facility was completed in late 1990, with continuing modifications and test operation taking place since that time. A summary of the test runs performed to date is shown in Table 1. These tests include 13 long duration runs (approximately 100 hours each), incorporating a variety of new hardware features and sorbents. Test 8 is scheduled for later in 1995.

**Table 1. Gasifier/HGCU/Turbine Simulator Test Operation — 20 atm, 1000°F**

| Run | Date | Run Hours | Coal Type | System Configuration |
|---|---|---|---|---|
| 1-2B | 12/90-4/92 | 230 | I6 | Gasifier/HGCU/GT Valve |
| 3 | 8/30/92 | 88 | I6 | Gasifier/HGCU/GT Valve/MS6000 Simulator |
| 3A | 2/7/93 | 120 | Anthracite | Gasifier/HGCU/GT Valve/MS6000 Simulator |
| 4 | 6/13/93 | 100 | I6, Crown II | Gasifier/HGCU/GT Valve/Simulator/Halogen |
| 5 | 11/1/93 | 103 | I6, Crown II | Gasifier/HGCU/GT Valve/Halogen/"F" Simulator 2300°F |
| 6 | 5/1/94 | 85 | I6 | Gasifier/Guard Bed/HGCU/GT Valve/Halogen/"F" Simulator 2500°F |
| 7A | 8/14/94 | 99 | I6 | Gasifier/HGCU/GT Valve/Halogen/"F" Simulator 2500°F |
| 4A | 11/13/94 | 115 | I6, Anthracite | Gasifier/HGCU/GT Valve/R-Q-L Sub-Scale |
| 7B-I, 7B-II | 3/5/95 3/26/95 | 190 | I6 | Gasifier/HGCU/GT Valve/CFB Halogen/Simulator 2500°F |
| 8 | 3Q95 | 100-200 | I6 | Gasifier/HGCU/GT Valve/CFB Halogen/RQL Full-Scale |

A schematic of the PEF facility, as configured at the conclusion of Test 7B, is shown in Figure 1. The GE-CRD fixed bed, pressurized air-/steam-blown gasifier is shown on the left. The gasifier includes a water-cooled bed stirrer, alternating pressurized coal feed lock-hoppers, and a rotating grate for ash removal. The LBtu coal gas is directed from the gasifier to the primary cyclone located immediately downstream of the gasifier, through the recently installed circulating fluidized bed (CFB) chloride removal vessel, then to the HGCU system, which consists of the absorber and associated upper and lower lock-hoppers, regenerator with recycle gas system, fines screen, and elevator. A secondary cyclone is located downstream of the HGCU system, and the cleaned fuel can be directed either to the MS6000 turbine simulator or to the system flare. Using analytical instrumentation in "real time" to allow process control, both the process fuel gas and the recycle gas are sampled continuously during the run. Solid flows are sampled periodically for later chemical analysis.

## RESULTS

Testing of the GE HGCU pilot system has been underway since December 1990. During this period, three sorbents and a variety of constantly improving system configurations have been tested, including zinc ferrite, zinc titanate and Z-Sorb sorbents, a single-/two-stage regenerator with mass flow bottom and annular reaction zones, alternate recycle blower configurations, and dedicated vessels for removing chlorides from the gas streams. Since the last contractor's report, three long duration tests have been completed in the following sequence: 7A, 4A, and 7B (7B was completed in two parts). In each test Z-Sorb sorbent was used for sulfur removal. Test 7A, completed in August 1994, was the second long duration test using Z-Sorb sorbent. Included in the run were operation of the chloride guard bed and the turbine simulator with a scaled fuel nozzle based on the nozzle design for the Tampa Electric Company project. During Test 4A, the sub-scale RQL combustor was operated for the first time on

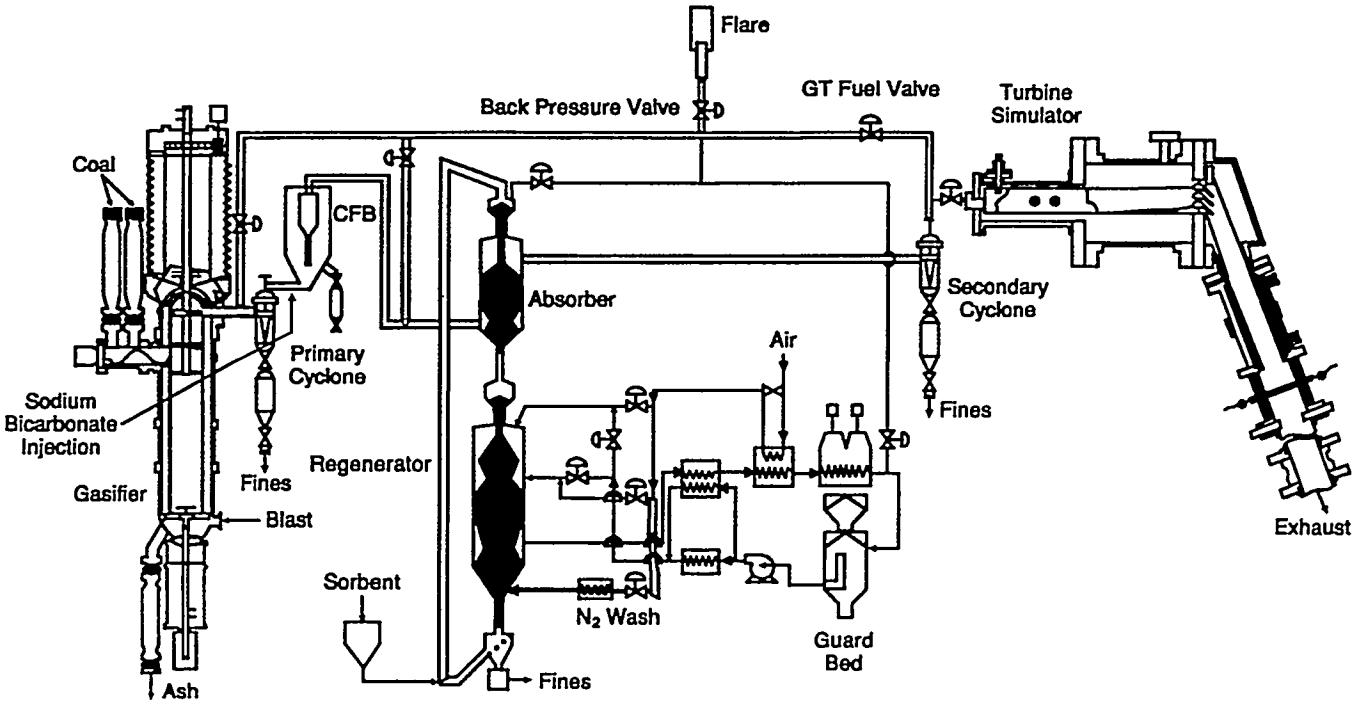


**Figure 1. GE Gasifier/Hot Gas Cleanup Process Flow Diagram**

coal gas to demonstrate the feasibility of applying the staged combustion concept to minimize conversion of fuel-bound nitrogen to $NO_X$. In this test the Z-Sorb sorbent used for Tests 6 and 7A was bolstered with fresh makeup to further evaluate its performance under pilot conditions. Tests 7B-I and 7B-II included initial operation of the CFB chloride removal system using sodium bicarbonate injection, in addition to testing of the HGCU on a fresh charge of Z-Sorb sorbent. The turbine simulator was operated with a modified fuel nozzle for improved part-load operation. The hardware modifications, operating conditions, and system performance for each test are discussed in detail in the following sections.

### Test 7A - Conditions and Hardware Configuration

Long Duration test 7A was performed at GE-CRD's pilot plant in August 1994 using Z-Sorb sorbent. This sorbent had been used previously for approximately 80 hours of integrated operation in Test 6 and demonstrated acceptable operation at the 25% sulfur loading tested, with sulfur removal efficiencies of 98-99% achieved at steady state. Illinois 6 coal, nominal 1.7% sulfur, was used as the test coal for Test 7A. Anthracite coal (0.5% sulfur) was used for startup and shutdown to minimize tar condensation from the fixed bed gasifier.

Because test data on absorber samples showed a significant range of sulfur loadings on sorbent sampled at the outlet, the absorber was modified between Tests 6 and 7A to incorporate a mass flow bottom to improve the uniformity of sorbent flow. A similar modification was tested successfully on the regenerator in Test 6 and significantly improved the uniformity of solids loading. The current regenerator configuration and the modified absorber are shown in Figure 2. Off-line testing with sorbent after the modification indicated uniform transfer of solids with little radial movement. The two-stage regenerator configuration

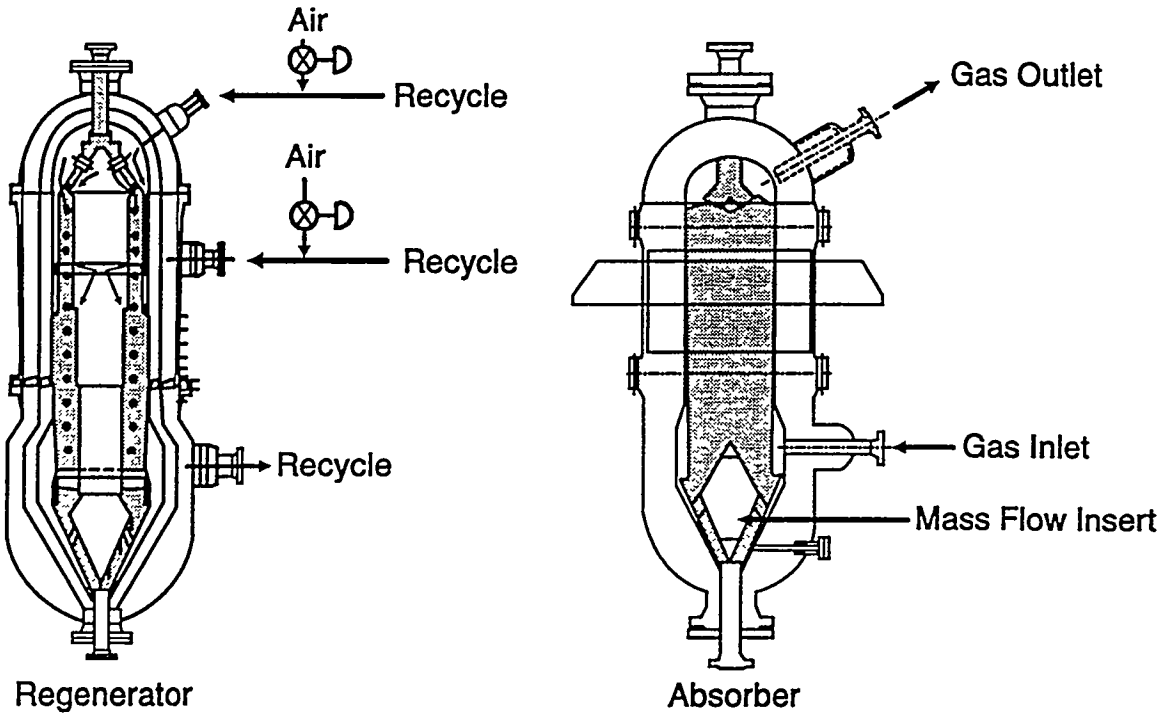


**Figure 2. Regenerator and Absorber Vessel Configurations - Test 7A**

with automatic control of temperatures to the first and second stages that was developed in previous testing was preserved for Test 7A.

The exotherm generated by the combustion of sulfur in the regenerator is controlled in the GE system by modulating the oxygen concentration to each stage and by controlling the recycle flowrate through the regenerator to provide convective cooling. Data from previous tests indicated that the throughput of the system was limited by the necessity for controlling regenerator temperatures to the 1400°F level anticipated for Z-Sorb sorbent. Modifications were made to the recycle compressor to upgrade the motor to a larger, higher speed drive prior to Test 7A. This upgrade resulted in a 20% increase in available recycle flow, which in turn provided for additional temperature modulation, higher throughput, and improved control of the regeneration process. During operation, a portion of the increased capacity is used to automatically modulate peak temperatures. A high-temperature third-stage nitrogen source was added to the regenerator for control of sulfate formation

As previously reported, chlorides in the coal gas stream cause problems to the HGCU system by absorbing on the sorbent in the absorber with subsequent release in the recycle gas during regeneration. In the regenerator the chlorides react with the sorbent and $SO_2$ to form zinc sulfate and zinc chloride deposits in the recycle loop heat exchangers, leading to blockage after several days of operation. In Test 6A, a combination of in-duct injection of sodium bicarbonate upstream of the gasifier primary cyclone and a guard bed using sodium bicarbonate pellets in the recycle loop had successfully controlled recycle loop deposits. For Test 7A, a zinc/calcium-based sorbent material manufactured by United Catalyst Inc. was substituted for the sodium bicarbonate pellets to reduce problems with moisture generation and handling.

Modifications to the MS6000 turbine simulator included a new fuel nozzle patterned after the nozzle being developed by GE Power Generation for the Tampa Electric Company's MS7000F gas turbine.

**Test 7A - Results**

Test 7A was conducted to obtain additional understanding of the operational characteristics of the Z-Sorb sorbent and, more specifically, to load the sorbent to the 50% of theoretical sulfur levels required for the Tampa Electric Company demonstration project. The gasifier and regenerator were operated for 100 hours, with 84 hours of integrated operation of the HGCU system achieved. The sulfur content of the coal gas ranged from 1000 ppmv $H_2S$ during startup on anthracite to 3500 ppmv on Illinois 6. As indicated in Figure 3, $H_2S$ levels in the fuel gas downstream of the absorber ranged from 50 ppmv during steady state to 700 ppmv during periods of interrupted sorbent transfer or off-design operation.

The HGCU system was started at a sorbent transfer rate equivalent to 25% sulfur loading, as successfully demonstrated in Test 6; then the transfer rate was lowered to increase the residence time and sulfur loading to the 50% target. Problems with a rotary feeder drive early in the test period led to excessively low transfer rates with resulting high outlet $H_2S$ concentrations. The problem was corrected approximately 18 hours into the run, and outlet sulfur levels returned to acceptable levels as sorbent transfer rates equivalent to 25% loading were achieved. As sorbent transfer rates were decreased to achieve higher loadings, however, the outlet $H_2S$ levels

increased, giving rise to the spikes in $H_2S$ levels seen in Figure 3.

Analysis of sorbent samples collected from the absorber and regenerator outlets during Test 7A indicated sulfur loadings of less than 25% of theoretical sulfur loading independent of sorbent transfer rate. This decrease indicates a loss of capacity of the sorbent and is consistent with the pilot data, which indicated good sulfur removal at low sorbent loadings but a decrease in performance as sorbent sulfur loadings were increased. Bench-scale testing confirmed the loss of reactivity. At the end of Test 7A, the relative capacity was around 40% of that of the fresh material. The source of the degradation was believed to be the presence of water vapor produced by oxidation of the tars deposited on the sorbent combined with the high-temperature in the regenerator.

Analysis of sorbent samples confirmed that good regeneration was achieved. Sorbent leaving the regenerator typically contained less than 0.5% residual sulfur and virtually no carbon. Temperature control in the regenerator was improved over previous runs through upgrades to the recycle compressor and tuning of the control parameters for first- and second-stage oxygen control. Some spikes were noted above the 1400°F target point, particularly in the first stage, as gasifier throughputs above 75% were attempted.

Effective chloride control was provided by the combination of in-duct injection of sodium bicarbonate upstream of the absorber and use of the zinc/calcium-based sorbent in the recycle loop guard bed. The zinc/calcium-based sorbent did not show any signs of clinkering or degradation over the course of the run. The guard bed material was changed once during the test. HCl levels in the recycle loop were generally under 200 ppmv, as compared to 1000–2000 ppmv without the guard bed. No plugging of the recycle loop heat exchanger was noted. However, since only 35% of the chlorides are being removed upstream of the absorber, chlorides were still being picked up by the sorbent, giving rise to concerns about long-term operability as well as plant emissions.

Performance of the HGCU valving and sorbent transfer equipment continued to be satisfactory. No problems were encountered with

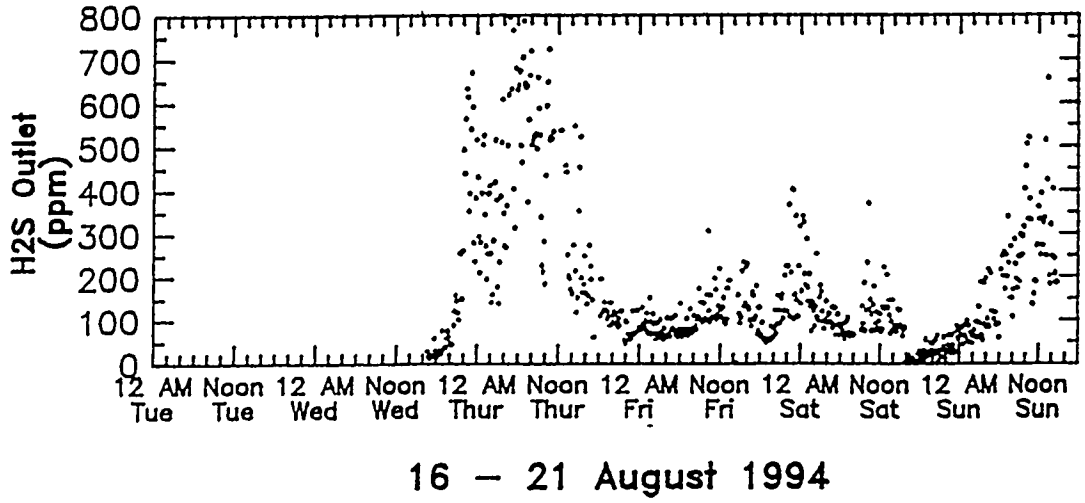


**Figure 3. Absorber Outlet $H_2S$ Concentrations - Test 7A. Inlet Conditions: P=280 psig, T=1020°F, Illinois 6 coal - 3500 ppm $H_2S$ Inlet**

transfer of Z-Sorb sorbent during the entire test. A total of 64,800 lb of sorbent was transferred, or slightly under 10 inventory turnovers, at a run-averaged attrition rate of 0.5%, based on a 12 mesh screen.

The turbine simulator was operated for 81 hours, including 50 hours at "F" class turbine conditions. Operation of the new fuel nozzle was satisfactory, with nozzle and liner temperatures within acceptable ranges. Stable combustion was achieved over a wide range of firing temperatures, although some instability was noted at part-load conditions.

**Test 4A - Conditions and System Modifications**

Long Duration test 4A was performed during the period of November 13 to November 18, 1994. The primary objective was to test the sub-scale RQL staged combustor on coal gas containing approximately 2000 ppmv of ammonia. The secondary objective was to obtain test data on the fresh Z-Sorb sorbent that was added to the existing charge in the ratio of 1 part new to 2 parts old. The existing material had been run in Tests 6 and 7A and was known to have lost significant capacity. Run conditions were modified to limit regenerator temperatures to 1350°F, compared with 1400°F in 7A, and operation was split between anthracite coal and Illinois 6. The low volatile anthracite was chosen to minimize tar production in order to (1) eliminate condensation in the piping at the low gas flowrates required by the RQL combustor and (2) minimize the introduction of water into the regenerator resulting from tar absorption on the sorbent. The second half of Test 4A was run with the MS6000 turbine simulator on-line using a modified version of the fuel nozzle tested in 7A. No sodium bicarbonate injection was performed during Test 4A. The chloride guard bed was operated in the recycle loop using the zinc/calcium-based sorbent tested successfully in 7A.

Samples of fresh sorbent were placed in a slipstream on the regenerator recycle loop. The samples were located in an oven capable of operating at temperatures from 1300°F to 1500°F to determine the effect of regeneration temperature on sorbent life. Prior to the start of the test, basket samples of fresh sorbent were also placed in the coal gas stream at the absorber inlet and outlet and at one location in the recycle loop. The basket samples were left in for the duration of Test 4A so that they were exposed to both anthracite and Illinois 6 fuel gas for a total of 100 hours.

A change in sorbent transfer procedure was implemented during Test 4A. Smaller increments of sorbent were moved more frequently through the absorber and regenerator to maintain the same hourly rate but provide a more continuous feed of fresh sorbent to the absorber and sulfided material to the regenerator.

**Test 4A - Results**

A total of 100 hours of uninterrupted HGCU operation was obtained: 52 hours on anthracite and 48 hours on Illinois 6. System throughputs were reduced to approximately 50% for anthracite during RQL testing and increased to 65–75% for Illinois 6. The $H_2S$ removal efficiency of the HGCU for Test 4A is shown in Figure 4. Inlet $H_2S$ concentrations averaged 1000 ppmv for anthracite and 3500 ppmv for Illinois 6. The outlet $H_2S$ during anthracite gasification was around 20 ppmv; during steady state operation on Illinois 6, it was around 50 ppmv. The higher peaks seen on Thursday occurred when sorbent transfer rates lagged the required value for 25% sulfur loading during the transition from 1000 ppmv to 3500 ppmv coal gas. A change in sorbent

transfer procedure was also implemented at this time. Sorbent was moved in smaller increments every 15 minutes through both the absorber and regenerator; previously a single but larger batch of sorbent was transferred once per hour through the absorber.

Sulfur levels in the sorbent samples taken at the absorber outlet were around 4% (22% of theoretical) for anthracite and 4.5% (25% of theoretical) for Illinois 6. Both were on target for the test conditions set. Achievement of 50% of theoretical sulfur loading on the sorbent was not an objective of this test since it was known that the sorbent sulfur capacity had deteriorated by the end of Test 7A. The sulfur levels measured in the regenerator samples averaged between 0.5 and 1.0%, slightly higher than the target of 0.5% but sufficient to meet the requirements for desulfurization at the sorbent duty selected. As a result of higher regenerator inlet temperatures, the level of regeneration was slightly better during Illinois 6 operation.

Both stages of regeneration were run under automatic temperature control. Continued tuning of the control parameters and lowering of the overall high temperature setpoint allowed maximum bed temperatures to be maintained below the prescribed absolute limit of 1400°F under fully automatic modulation of air and recycle flows. Table 2 summarizes the temperature control results. This represents an improvement over Test 7A where occasional spikes to 1500°F were noted at the inlet to the first stage.

Thermo Gravimetric Analysis (TGA) testing of slip stream sorbent samples run at 1300, 1400, and 1500°F for 10 hours indicated no loss in reactivity on the 1300°F sample even in the presence of 2% water in the recycle loop. Although very little change was noted at 1400°F, a significant loss in reactivity was observed at 1500°F, indicating that the combination of 2% $H_2O$ and 1400°F is the practical limit for Z-Sorb sorbent regeneration.

TGA analysis of the sorbent basket samples located at the absorber inlet and outlet indicated that after exposure to 100 hours of coal gas, the inlet samples retained a high sulfur capacity, 90% of theoretical, whereas the outlet samples had lost

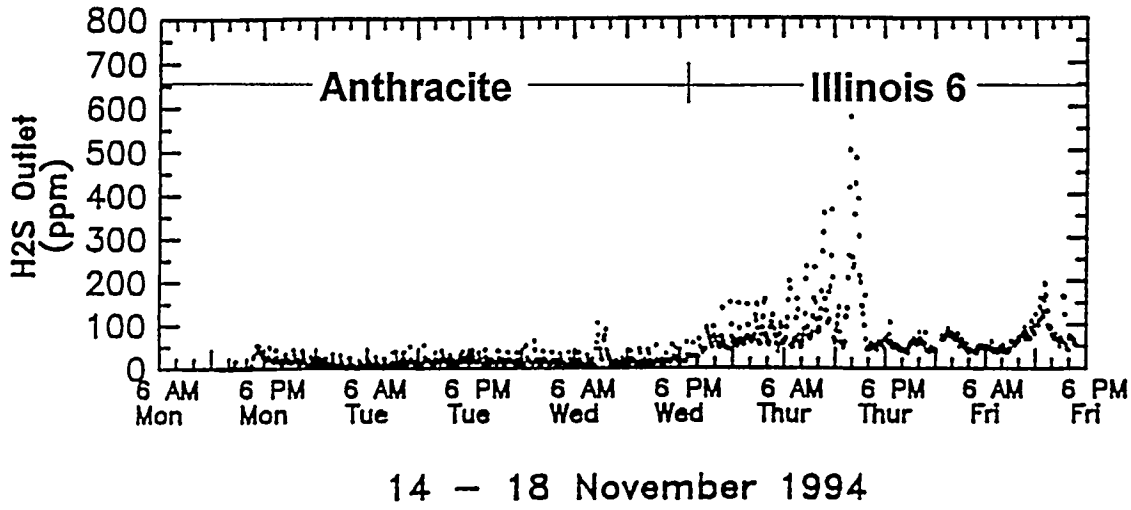


**Figure 4. Absorber Outlet $H_2S$ Concentrations - Test 4A. Inlet Conditions: P=280 psig, T=925–1020°F, Illinois 6 - 3500 ppm $H_2S$ Inlet, Anthracite - 1000 ppm $H_2S$**

**Table 2. Regenerator Temperature Control - Test 4A**

| | Anthracite | Illinois 6 |
|---|---|---|
| Absorption Temperature, °F | 900-1000 | 900-1000 |
| Regenerator Mean Maximum Temperature, °F | <1300 | <1300 |
| Peak Maximum Bed Temperatures, °F | 1380-1390 | 1390 |
| Range of Bulk Temperatures in Regenerator, °F | 800-1200 | 800-1300 |

**Table 3. Comparison of Sulfur Capacity on Sorbent Basket Samples Exposed to Coal Gas at Absorber Inlet and Outlet - Test 4A**

| | Absorber Inlet | Absorber Outlet |
|---|---|---|
| 2 hour TGA reactivity * | 91% of fresh | 71% of fresh |
| Sulfur loading, Wt % | 13.9 (77% of theoretical) | 3.8 (21% of theoretical) |
| Carbon loading, Wt % | 4.9 | 1.4 |

* After regeneration in the laboratory

almost 30% capacity. The data is summarized in Table 3. The reasons for this difference are not fully understood at present.

The actual sulfur loading on the basket sample sorbent pellets, as shown in Table 3, indicates that the loading achieved during Test 4A is dependent on the levels of $H_2S$ to which the pellets were exposed. Seventy-seven percent of theoretical sulfur loading was achieved on the absorber inlet samples at $H_2S$ levels of 1000–3500 ppmv, compared with only 21% of theoretical sulfur loading on the absorber outlet samples where $H_2S$ levels were much lower, averaging 50 ppmv. The exposure time of 100 hours was the same for both locations.

Conclusions from analysis of absorber and regenerator samples collected throughout the run indicated that little if any further degradation occurred in Z-Sorb sorbent reactivity beyond that measured at the end of Test 7A. At the conclusion of Test 4A, fresh sorbent that had been added at the start of the test retained about 70% of theoretical reactivity as measured in a TGA analysis, as compared to only 30–40% of fresh reactivity for samples taken at the end of Test 7A There were a number of differences in operating conditions for these two tests: In Test 4A peak regenerator temperatures were lower, there was more operational time on the low volatile, low tar anthracite fuel, and no sodium bicarbonate injection was used for chloride control.

## Tests 7B-I and 7B-II - Conditions and System Modifications

Long Duration tests 7B-I and 7B-II were performed in March 1995. Test 7B was scheduled as a single 100-hour test, but hardware problems prematurely halted operations after 70 hours. The test was continued as 7B-II during the last week of March. A major focus in Test 7B was the installation and operation of an enhanced circulating fluidized bed (CFB) chloride removal system. The CFB is designed to replace the induct injection of sodium bicarbonate with a system capable of high levels of removal efficiency upstream of the absorber. Chloride removal efficiency of the once-through sodium bicarbonate injection averaged about 35%. Modeling work supported by bench-scale experiments in the University of North Dakota Energy and Environmental Center's pressurized drop tube furnace demonstrated that removal rates of over 90% were possible using longer gas/solid residence times, finer powder, and increased stoichiometry. The CFB design incorporates these features in a single vessel.

The CFB, shown schematically in Figure 5, is located downstream of the primary cyclone. It consists of a recycle cyclone located in a pressure vessel sized to provide about a 10-second residence time for the coal gas. Powdered sodium bicarbonate is injected upstream with the LBtu coal gas and enters at the bottom of the CFB vessel. The sodium bicarbonate rapidly calcines to sodium carbonate in the 1000°F gas stream, forming highly porous particles that react with hydrogen chloride in the coal gas to form sodium chloride. Larger particles settle out at the lower CFB bed velocities to form a fluidized bed at the gas inlet while the smaller particles remain entrained with the gas for removal in the internal cyclone. The particulate is recycled to the bed via

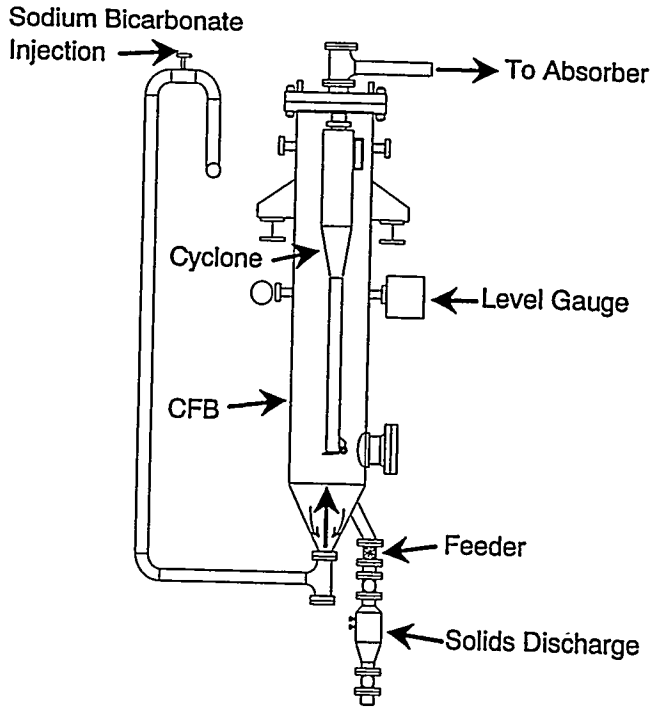


**Figure 5. Circulating Fluidized Bed Chloride Removal System**

a dipleg and foot valve below the cyclone for increased utilization of sorbent. Clean gas exits the top. Spent sorbent is removed through a solids off-take pipe and lock-hopper. A nuclear level gauge is provided on the internal dipleg to monitor performance.

A second major focus in Test 7B was the evaluation of system performance on a fresh charge of Z-Sorb sorbent. The material was similar in composition to that tested in Tests 6, 7A, and 4A, but with a slightly smaller, 3-mm average pellet size. Prior to the start of fired operation, sorbent was circulated through the system under dry nitrogen to measure background mechanical attrition. Less than 0.2% of <12 mesh material was obtained. The off-line sorbent attrition test also provided the opportunity to test and debug the automatic sorbent transfer software that was implemented for the first time in Test 7A.

Illinois 6 coal (1.8% sulfur) was used as the test coal, producing 3500–4000 ppmv $H_2S$ in the coal gas. The recycle loop guard bed utilized the zinc/calcium-based sorbent used successfully in Tests 4A and 7A.

Modifications to the turbine simulator included a modified version of the Tampa Electric Company fuel nozzle used in the second half of Test 4A.

**Test 7B - Results**

The HGCU was operated for approximately 70 hours in 7B before being shut down due to failure of the sorbent transfer elevator. Preliminary operation of the CFB during this time indicated elevated levels of chloride capture (75%) as bed inventory was increased. Problems were encountered with blockage of the solids discharge pipe that prevented attainment of steady state operation. The suspected cause of blockage was condensation of steam and tars from the coal gas in combination with the sodium carbonate powder. Chloride concentrations in the recycle loop were significantly lower than seen in the previous run.

Excellent sulfur removal was achieved in the HGCU at sorbent transfer rates equivalent to 30% of theoretical loading. During the first hours of operation on anthracite coal at 1000 ppmv $H_2S$ levels, the absorber outlet $H_2S$ concentrations were less than 10 ppmv. As the inlet coal gas $H_2S$ concentration increased to 3500 ppmv under Illinois 6, the outlet concentration remained under 50 ppmv. At 400–500 lb/hr sorbent transfer rate, the measured sulfur loading reached the target of 30% set for the first part of the test. Analysis of the regenerator samples indicated satisfactory regeneration of the sorbent, with residual sulfur levels dropping to 0.5% as steady state operation was achieved. Temperatures in the regenerator were successfully controlled to the target of 1350°F through two-stage automatic control of oxygen and recycle flowrates.

TGA analysis of sorbent samples collected at the 30 hour and 50 hour mark, however, indicated that the sorbent had lost significant reactivity in spite of the generally good performance of the HGCU system. This condition was not reflected as a loss in sulfur removal performance because the sorbent still had sufficient reactivity to perform at the 30% level targeted for the start of Test 7B.

Modifications were made to the CFB to remove the rotary feeder on the solids discharge pipe and add additional heat tracing to prevent condensation of tars and water. A coarser sodium bicarbonate feed stock was obtained to improve sorbent flowability during startup. Operating procedures for the CFB were modified to further reduce the chance of solids blockage in the discharge pipe.

Test 7B was continued March 26–April 1 using Illinois 6 coal and Z-Sorb sorbent. A total of 124 hours of additional operation was obtained, of which 80 were fully integrated. Performance of the CFB system was significantly improved during 7B-II. No problems were encountered with discharge of spent sorbent throughout the run. The CFB was started on a coarser USP #5 sodium bicarbonate, then switched to USP #2 (nominal 75-micron) after 40 hours. Chloride removal levels were approximately 50–75% at low CFB sorbent bed concentrations and coarser feed stock but increased to over 95% as sorbent inventory was increased to design levels on USP #2 material. HCl concentration as a function of run time is shown in Figure 6. The CFB was intentionally started at low inventories because of concerns over blockage, then run for up to one

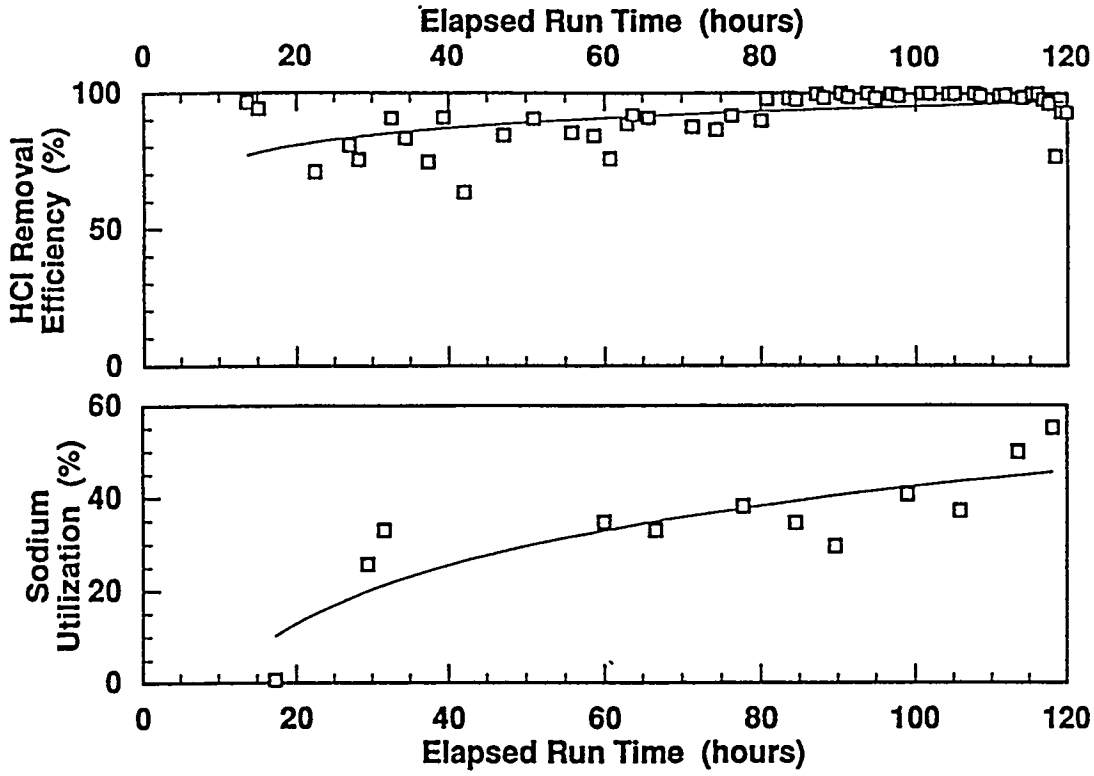


**Figure 6. Circulating Fluidized Bed HCL Removal Efficiency - Test 7B**

hour with the outlet lockhopper closed. Sorbent utilization approached 55% at the conclusion of the test. Chloride levels in the recycle loop were the lowest recorded to date. No fouling of the heat exchangers was observed.

Sulfur removal performance of the HGCU is shown in Figure 7. Outlet $H_2S$ levels ranged from baseline values of 50 ppmv at sorbent transfer rates equivalent to ≤30 % of theoretical sulfur loading, to several hundred ppmv $H_2S$ as sorbent

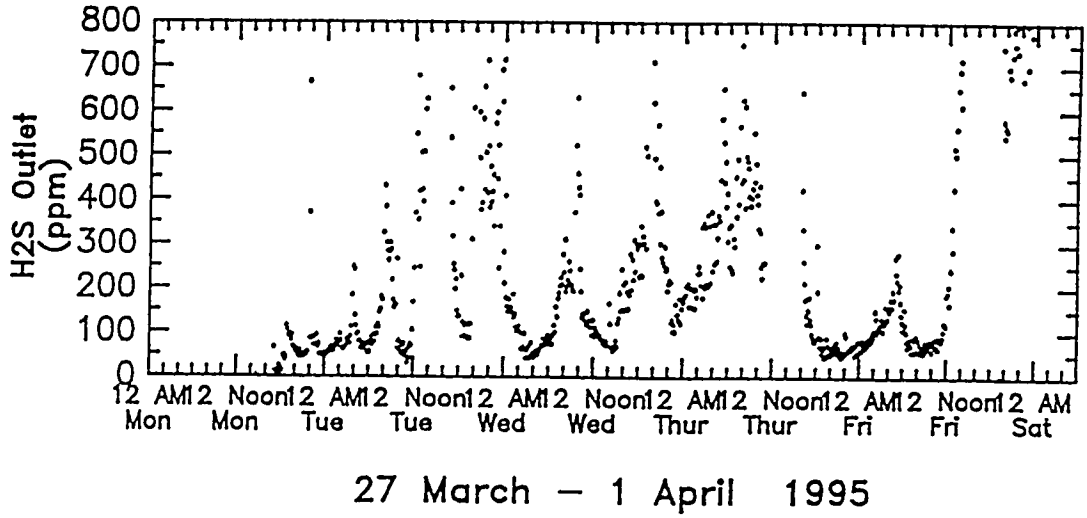


**Figure 7. Absorber Outlet $H_2S$ Concentrations - Test 7B. Inlet Conditions: P=280 psig, T=875–950°F, Illinois 6 coal - 3500 ppm $H_2S$ Inlet**

transfer rates were slowed, and the gasifier throughput rate was increased in an attempt to reach the target loading of 50%. Absorber operation was intentionally interrupted twice to permit off-line regeneration of the bed prior to attempting 40 and 50% sulfur loadings. The HGCU was run under automatic sorbent transfer and temperature control, with the upper limit on regenerator temperatures set to 1350°F. Temperature control in the regenerator was the best to date.

Post test analysis of sorbent samples collected during Test 7B indicated the sorbent retained approximately 25% to 30% of theoretical capacity. This level of capacity is consistent with the pilot plant data, which showed good performance at sorbent transfer rates equivalent to 30% loading but dropped off as higher sorbent loadings were attempted. The sorbent did not meet the demonstration target of 50% required for commercial operation at the pilot plant conditions.

## FUTURE WORK

One additional Long Duration test, Test 8, is included in the current contract for fiscal year 1995. A series of bench-scale tests will be performed to evaluate alternate sorbent candidates, the most promising of which will be selected for operation in the pilot plant during Test 8. The three candidates currently under evaluation include a modified zinc titanate, modified Z-sorb sorbent, and a proprietary sorbent under development by DOE-METC. Hardware modifications for Test 8 will include installation of a stainless steel liner in the upper portion of the absorber to minimize wall effects, modification to the CFB solids discharge to include the outlet rotary feeder, and installation of the full-scale RQL combustor.

## REFERENCES


Ayala, R., September 1992. "Enhanced Durability of High Temperature Desulfurization Sorbents for Moving-Bed Applications," Twelfth Annual Gasification and Gas Stream Cleanup Systems Contractors Review Meeting, Report DE/AC21-88C25003.

Ayala, R., E. Gal, and R.P. Gupta, 1993. "Testing of Zinc Titanate Sorbents for Moving Bed Applications." In Proceedings of the Coal Fired Power Systems 93 — Advances in IGCC and PFBC Review Meeting, DOE/METC-93/6131.

Ayala, R., T. Chuck, E. Gal, and R.P. Gupta, 1994. "Development of Sorbents for High-Temperature Desulfurization in Moving-Bed Systems," Proceedings of the Coal-Fired Power Systems 94 — Advances in IGCC and PFBC Review Meeting, DOE/METC-94/1008, Vol. 2.

Bevan, S., N. Abuaf, A. Feitelberg, S. Hung, M. Samuels, A. Tolpadi, June 1994a. "Development and Testing of Low Btu Fuel Gas Turbine Combustors," Proceedings of the Coal-Fired Power Systems 94 — Advances in IGCC and PFBC Review Meeting, DOE/METC-94/1008, Vol. 2.

Bevan, S., D. Najewicz, E. Gal, A. Furman, R. Ayala, A. Feitelberg, June 1994b. "Development of Sorbents for High-Temperature Desulfurization in Moving-Bed Systems," Proceedings of the Coal-Fired Power Systems 94 — Advances in IGCC and PFBC Review Meeting, DOE/METC-94/1008, Vol. 2.

Cook, C.S., E. Gal, A.H. Furman, R. Ayala, and R.M. Tucker, May 1988. "Integrated Operation of a Pressurized Fixed Bed Gasifier and Hot Gas Desulfurization System," Eighth Annual Gasification and Gas Stream Cleanup Systems Contractors Review Meeting, Report DOE/METC/88/6092.

Cook, C.S., E. Gal, A.H. Furman, R.M. Tucker, and B. Parekh, June 1989. "Integrated Operation of a Pressurized Fixed Bed Gasifier and Hot Gas Desulfurization System," Ninth Annual Gasification and Gas Stream Cleanup Systems Contractors Review Meeting, Report DOE/METC/89/6107, Vol. 1.

Cook, C.S., E. Gal, A.H. Furman, R.M. Tucker, and B. Parekh, August 1990. "Integrated Operation of a Pressurized Fixed Bed Gasifier and Hot Gas Desulfurization System," Tenth Annual Gasification and Gas Stream Cleanup Systems Contractors Review Meeting, Report DOE/METC/90/6115, Vol. 1.

Cook, C.S., E. Gal, A.H. Furman, and R. Ayala, August 1991. "Integrated Operation of a Pressurized Fixed Bed Gasifier and Hot Gas Desulfurization System," Tenth Annual Gasification and Gas Stream Cleanup Systems Contractors Review Meeting, Report DOE/METC/91/6123, Vol. 1.

Cook, C.S., E. Gal, A.H. Furman, and R. Ayala, September 1992. "Integrated Operation of a Pressurized Fixed Bed Gasifier and Hot Gas Desulfurization System," Twelfth Annual Gasification and Gas Stream Cleanup Systems Contractors Review Meeting, Report DOE/METC-92/6128, Vol. 1.

Feitelberg, A.S., C.S. Cook, N. Abuaf, S.L. Hung, M.S. Samuels, and D.J. Najewicz, 1993. "Combustion Tests of a Turbine Simulator Burning Low Btu Fuel and a Rich-Quench-Lean Combustor." In Proceedings of the Coal Fired Power Systems 93 — Advances in IGCC and PFBC Review Meeting,. DOE/METC-93/6131.

Feitelberg, A.S., N. Abuaf, S.L. Hung, M.S. Samuels, A. Tolpadi, and D.J. Najewicz, 1994. "Development and Testing of Low Btu Fuel Gas Turbine Combustors." In Proceedings of the Coal Fired Power Systems 94 — Advances in IGCC and PFBC Review Meeting, DOE/METC-94/1008, Vol. 1.

Smith, D.P., E. Gal, C.S. Cook, and A.H. Furman, June 1987. "Design Studies for Hot Gas Cleanup System in a Load Following Mode," Seventh Annual Gasification and Gas Stream Cleanup Systems Contractors Review Meeting, Report DOE/METC/87/6079.

## 4.2 Pilot Scale Experience on IGCC Hot Gas Cleanup

### CONTRACT INFORMATION

**Cooperative Research and Development Agreement Number:** 93-016

**Contractor:**

Enviropower Inc.
P.O. Box 35
33701 Tampere
Finland
+358-31-2413511

**Contractor Administrative Contact:** Kari Salo

**Contractor Technical Contact:**

Reza Ghazanfari
Gabor Feher

**Principal Investigators:**

Jukka Konttinen
Reza Ghazanfari
Arto Lehtovaara
Wahab Mojtahedi

**METC Project Manager:** Thomas P. Dorchak

**Period of Performance:** September 8, 1993 to December 31, 1995

**Scedule and milestones:**

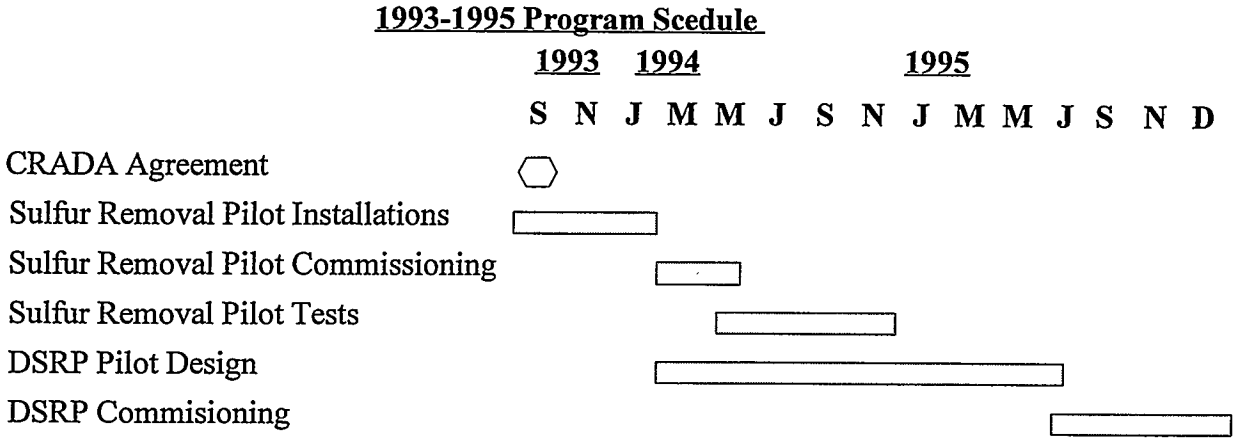

## OBJECTIVES

In September 1993 Enviropower Inc. entered into a Cooperative Research and Development Agreement (CRADA) with the Department of Energy in order to develop and demonstrate the major components of an IGCC process such as hot gas cleanup systems.

The objectives of the project are to develop and demonstrate 1) hydrogen sulfide removal using regenerable metal oxide sorbent in pressurized fluidized bed reactors, 2) recovery of elemental sulfur from the tail-gas of the sorbent regenerator and 3) hot gas particulate removal using ceramic candle filters.

## BACKGROUND INFORMATION

Enviropower Inc. is a subsidiary of Tampella Power Inc. which is the parent company of the Tampella Power Corporation in the U.S.A. Enviropower Inc. is actively involved in the development of the Integrated Gasification Combined Cycle (IGCC) process. Enviropower's IGCC concept incorporates pressurized fluidized bed gasification of different solid fuels, applying air-blown gasification and hot gas clean-up. The IGCC process and the demonstration activities have been described in detail elsewhere /1, 2/.

Enviropower's pressurized fluidized bed gasification pilot plant has a maximum thermal input of 10 MW (35 mtpd) for coal and 15 MW (100 mtpd) for biomass. The gasifier is an air blown U-gas system, which Enviropower has developed further. The pilot plant includes a complete hot gas cleanup train which operates at up to 30 bar (435 psia) and temperatures at up to 650°C (1200°F). The components of the pilot-process are presented in Figure 1.

Enviropower's IGCC hot gas cleanup concept is based on sulfur removal using different methods and particle filtration using ceramic candle filters. The bulk of fuel bound sulfur can be removed in the gasifier by means of a calcium based sorbent such as limestone or dolomite and the rest is removed externally in a fluidized bed system using a regenerable metal oxide sorbent such as zinc titanate. The sulfur removal options in Enviropower's IGCC process can be seen in Figure 2. Novel zinc titanate sorbents suitable for fluidized bed application have been tested and the plan is to use the regenerable sulfur removal system as the sole method of sulfur removal in the future. This will reduce the bulk of solid waste from the gasifier and improve the system performance and economy.

Cyclic sulfidation and regeneration tests with zinc titanate have been carried out in a 3-inch I.D. batch fluidized bed reactor which is located at the Institute of Gas Technology in Chicago. The reactor is capable of operating at temperatures up to 1000°C (1830°F) and pressures up to 30 bar (435 psia) with synthetic gas mixtures containing all the gaseous components for sulfidation and regeneration reactions. The 3-inch pressurized fluidized bed reactor assembly has been described in detail elsewhere /3/. The laboratory- and bench-scale test results have been reported earlier /3, 4, 5/.

## PROJECT DESCRIPTION

The CRADA-project consists of the following subtasks:

• Pilot-plant testing of the metal oxide sorbents is carried out in Envirpower's pilot plant, using a pressurized fluidized-bed absorber and regenerator. The sulfur removal efficiency and long term durability of the sorbent are evaluated in these tests. Sorbent samples from the pilot-plant tests are analyzed by Enviropower,

IGT and METC.

• Laboratory-scale tests are conducted on the sorbents used at the pilot-plant for removal of hydrogen sulfide. These tests are performed in a 3 inch pressurized fluidized bed under conditions simulating the real situation with respect to temperature, pressure and gas composition. Sorbents are evaluated for their physical, chemical and mechanical durability.

• The tail gas from the regeneration contains sulfur dioxide which can be converted to usable elemental sulfur. A technology called the Direct Sulfur Recovery Process (DSRP) has been developed at Research Triangle Institute (RTI) /6/ to achieve this objective. A skid-mounted DSRP unit is under construction by METC. This unit will be shipped to the pilot plant in Finland for installation and testing with a slipstream of the U-gas process coal gas. Suitability of the DSRP process and sulfur conversion efficiency will be examined during testing. Design data will also be obtained for scale-up for commercial-sized systems.

• The collection efficiency and operability of ceramic candle filters for removing particles from the hot gas have been examined in full scale pilot plant tests.

## RESULTS AND FUTURE WORK

### Pilot-scale sulfur removal tests

The sulfur removal pilot consists of high temperature and pressure (HTHP) fluidized-bed type sulfider and regenerator reactors and systems for fresh sorbent feeding, sorbent circulation between reactors and gas preheating/cooling for regenerator.

In 1994 two types of zinc titanate sorbents, designated as ZT-4-L and UCI-5, were tested at high pressure and temperature. ZT-4-L was manufactured by Contract Materials Processing, Inc. as a subcontractor to Research Triangle Institute (RTI) and UCI-5 was manufactured by United Catalysts Inc. The physical properties of the two sorbents, fresh and after reaction, are shown in Table 1.

UCI-5 was tested in two coal gasification test runs with 5-6 days of continuous operation in each test. The sulfur removal efficiency after reaching steady operation can be seen in Figure 3. Typical performance of sulfider and regenerator reactors in combined operation can be seen in Figures 4 and 5. Both reactors were operating at the same pressure level as the gasifier. As can be seen from Figure 4, satisfactorily high sulfur removal efficiency in the sulfider was achieved in combined operation.

ZT-4-L was used in a test run in November 1994. The sulfur removal efficiency in the beginning of the test (coke gasification start-up) can be seen in Figure 6. In comparison with Figure 3, the sulfur capture efficiency is higher than with UCI-5. This is most propably due to higher surface area, as shown in Table 1. The regenerator performance with ZT-4-L sorbent can be seen in Figure 7 with continuous production of $SO_2$-containing off-gas. The start-up of regeneration with ZT-4-L was more difficult than with UCI-5, as can be seen from the long (2-hour) period of increasing the bed temperature from about 520°C to 700°C (970 - 1300°F) (Figure 7). This may be partly due to a higher dependence of reaction rate on temperature.

Nitrogen or steam was used to dilute the air in the regenerator inlet gas. UCI-5 was tested with both diluents and ZT-4-L with $N_2$. According to the test data, steam was as effective as nitrogen, and did not show any detrimental effect on sorbent performance.

In the beginning of the test runs a small fraction of fines (5-10 μm) was created with both sorbents, which was then elutriated from the beds. This is partly due to the attritive effect of fluidization on fresh sorbent particles as already observed in bench-scale tests. The other reason might be a slight grinding effect of the screw feeder used in sorbent injection. This can be eliminated by using some other type of sorbent feeding. The tests also showed that the amount of fine dust at the sulfider exit increases during start-up after off-balance operation periods with used sorbent. However, during steady-state combined sulfider and regenerator operation periods, bed material attrition or elutriation was satisfactory.

In order to fully determine the long-term durability of the process and sorbents tested with real coal gas, test runs of longer duration than a week are needed, which tests have not been executed so far.

**Pilot Tests with Ceramic Filter**

During coal gasification test runs in 1994 the major emphasis in the development of hot gas cleanup was directed towards testing of the sulfur removal system. The ceramic filter testing was already in the category of routine operation. A schematic diagram of the filter unit is shown in Figure 8. The filter unit is completely intergrated with the control system of the pilot plant. The filter cleaning strategy was mainly based on a constant cycle time using on-line pulsing with pressurized nitrogen.

The test runs were carried out with two-layered, SiC-based, round shaped ceramic candle elements. The filter unit was operated at the temperature range of 450-600°C (840-1110°F), which will be used in the simplified IGCC applications. Figures 9, 10 and 11 show the typical filter operation and performance values. An example of the effect of the cycle time can be seen in Figure 9. The cycle time was decreased 25 % due to a slight increase in Δp-baseline at the beginning of the test period. After the change of the cycle time Δp-baseline decreased to about 9 kPa (0.13 psi) value and after that remained constant.

Dust loadings below 5 ppmw in product gas and vapour-phase alkali (Na+K) concentrations below 0.05 ppmw were measured after filtration. These values are below the levels generally required by gas turbine manufacturers and well below the environmental standards. During operation the filter pressure drop has generally stayed low and the filter permeance constant. It should be noted, however, that long gasification periods are needed to completely verify the long term development of the filter permeability and filtration reliability.

More information on the ceramic filter behavior during biomass gasification is presented in /2/.

**Laboratory-scale work**

The physical properties of the used ZT-4-L and UCI-5 sulfider and regenerator bed material samples (taken during pilot-tests) are shown in Table 1. It can be seen that for the used sorbents the particle density increases and porosity decreases. For ZT-4-L the surface area surprisingly increases, which was also observed in the laboratory tests. Figure 12 shows the sulfidation breakthrough curves for fresh and used UCI-5 samples obtained from the 3" batch fluidized bed. The most important observation is that the physical properties of the pilot-samples change the same way as in the bench-scale tests. The same goes for sulfidation and regeneration reactivity. This indicates that the conctact with real coal gas for 5-6 days has no detrimental effect on sorbent physical or chemical properties.

Table 1 also shows the sulfate sulfur analysis for the sorbents taken from the regenerator. These analyses as well as the pilot-test results indicate that undesirable zinc sulfate is not accumulated into the sorbent (if formed at all), when operating the fluidized-bed regenerator at temperatures of 600-750°C (1110-1380°F), 2-4 vol-% of $O_2$ and steam or nitrogen as diluent.

**Modelling efforts**

A steady-state kinetic model for hot gas desulfurization system has been developed based on laboratory- and bench-scale tests with zinc titanate sorbents. The model was used in the dimensioning of the pilot and commercial-scale sulfur removal systems. The results from the test runs in 1994 show that the model predictions are in good agreement with the test results. The pseudo first-order sulfidation reaction rate constants determined from pilot results indicate that the reactivity, as well as sulfur capacity of ZT-4-L is 1.5-2 times higher than of UCI-5. However, the sulfidation and regeneration performance of UCI-5 at the operating conditions tested was satisfactory for a real-scale unit.

By assuming that the regeneration reaction rate is first-order with respect to reactants (oxygen and zinc sulfide), it was possible to determine the activation energy of the reaction rate constant from the pilot-test data. The value of activation energy obtained for ZT-4-L was higher than for UCI-5, which means higher sensitivity of the rate of regeneration towards regenerator temperature.

A dynamic model for the pilot and commercial-scale post-bed sulfur removal system is under development. The objective is to use it for predicting the effects of the changes in regenerator inlet gases, sorbent transport velocity, fluidization velocities, etc., on the overall performance. This information can be used to adjust the control system of the process. The response of the regenerator dynamic model is shown in Figure 13, which should be compared with Figure 5. In the future the dynamic model will be added as a module into Enviropower's existing IGCC-plant dynamic simulator for design and training purposes.

**DSRP pilot design**

The DSRP skid-mounted pilot-unit is under construction by METC. The skid will be shipped to Finland by the end of September. The commissioning of the unit in connection with pilot-gasifier and sulfur removal unit will be performed towards the end of 1995.

## CONCLUSIONS

During coal gasification test runs in 1994 the major emphasis in development of hot gas cleanup was focused on testing of the sulfur removal system. The ceramic filter unit testing was already in the category of routine operation. The operating temperature was 450-600°C (840-1110°F) at gasifier pressures. These conditions will be used in commercial-scale simplified IGCC applications.

Three test runs with two types of zinc titanate sorbent was accomplished with the sulfur removal pilot; each of them with 5-6 days of continuous operaration. The results showed that high sulfidation efficiency as well as continuous production of $SO_2$-containing regenerator off-gas at design temperatures and pressures could be achieved. The observed difference in sulfidation reactivity between the two sorbents was related to the sorbent physical properties, like surface area. Regeneration reactivity was about the same for both sorbents and the formation of undesirable sulfate sulfur in regenerator could be avoided with steam or nitrogen as inlet diluent gases.

The change of sorbent properties when in contact with real coal gas was the same as observed in laboratory- and bench-scale tests with simulated gases after continuous sulfidation-regeneration cycling.

In the test with ceramic filter, the dust loadings below 5 ppmw solids in the product gas and vapour-phase alkali (Na+K) concentrations below 0.05 ppmw after the filter unit have been measured. These values are below the levels generally required by gas turbine manufacturers and well below the environmental standards. During operation the filter pressure drop has generally stayed low and the filter permeance constant.

Steady-state and dynamic models to predict and simulate the operation of sulfider and regenerator reactors have been developed. The results of pilot-scale tests are in good agreement with modelling results.

A pilot-scale process for the recovery of elemental sulfur, called DSRP, is under construction. It will be tested in combined operation with the sulfur removal pilot under the present CRADA project.

## REFERENCES


1. PATEL J.G.; The simplified IGCC Process - Clean Coal Technology for Power Generation. Paper presented at *Comparative Economics of Emerging Clean Coal Technologies III: Advanced Power & Environmental Control.* Washington, DC, USA, February 28 & March 1, 1994.

2. LIINANKI, L., HORVATH, A., LEHTOVAARA, A. AND LINDGREN, G.; The Development of a Biomass Based Simplified IGCC Process. In: *Thirteenth EPRI Conference on Gasification Power Plants*, San Francisco, USA, October 19-21, 1994.

3. ABBASIAN J., BACHTA R.P., WANGEROW J. R., MOJTAHEDI W., SALO K.; Advanced High-Pressure Bench-Scale Reactor for Testing with Hot Corrosive Gases. *Ind. Eng. Chem. Res.* 33(1994)1.

4. MOJTAHEDI W., SALO K., ABBASIAN J.; Desulfurization of hot coal gas in fluidized bed with regenerable zinc titanate sorbents. *Fuel Processing Technology* 37(1994) 53-65.

5. KONTTINEN J., MOJTAHEDI W.; Gasifier gas desulfurization at high temperature and pressure. *Kemia-Kemi (Finnish Chemistry)* (1993)11-12. (In English)

6. GANGWAL S.K., PORTZER, J.W., HOWE G.B., CHEN D.H., MCMILLIAN M.H.; Slipstream Testing of the Direct Sulfur Recovery Process. In: *Proceedings of the Coal-Fired Power Systems 94 -- Advances in IGCC and PFBC Review Meeting*, Volume 1. Morgantown, WV, USA, June 21-23, 1994.

**Table 1. The Physical Properties of the Fresh and Used Zinc Titanate Sorbents.**

| Property | Fresh UCI-5 | UCI-5, Sulfider sample *) | UCI-5, Regenerator sample *) | Fresh ZT-4-L | ZT-4-L Sulfider sample *) | ZT-4-L Regenerator sample *) |
|---|---|---|---|---|---|---|
| Particle Density [g/cm$^3$] | 2.26 | 2.51 | 2.44 | 2.14 | 2.46 | 2.38 |
| Pore volume [cm$^3$/g] | 0.26 | 0.128 | 0.172 | 0.22 | 0.12 | 0.17 |
| Surface Area [m$^2$/g] | 1.4 | 4.3 | 1.2 | 3.5 | 11.1 | 5.5 |
| Median pore diam. [Å] | - | 5000 | - | 2700 | 1600 | 2200 |
| S-sulfide [w-%] | 0.019 | 9.31 | 0.29 | 0.01 | 10.3 | 3.86 |
| S-sulfate [w-%] | 0.057 | 0.11 | 0.14 | 0.03 | 0.11 | 0.038 |
| Dp, Avg [µm] | 287 | 267 | 285 | 239 | 223 | 237 |

***) Samples were taken in the end of each test run.**

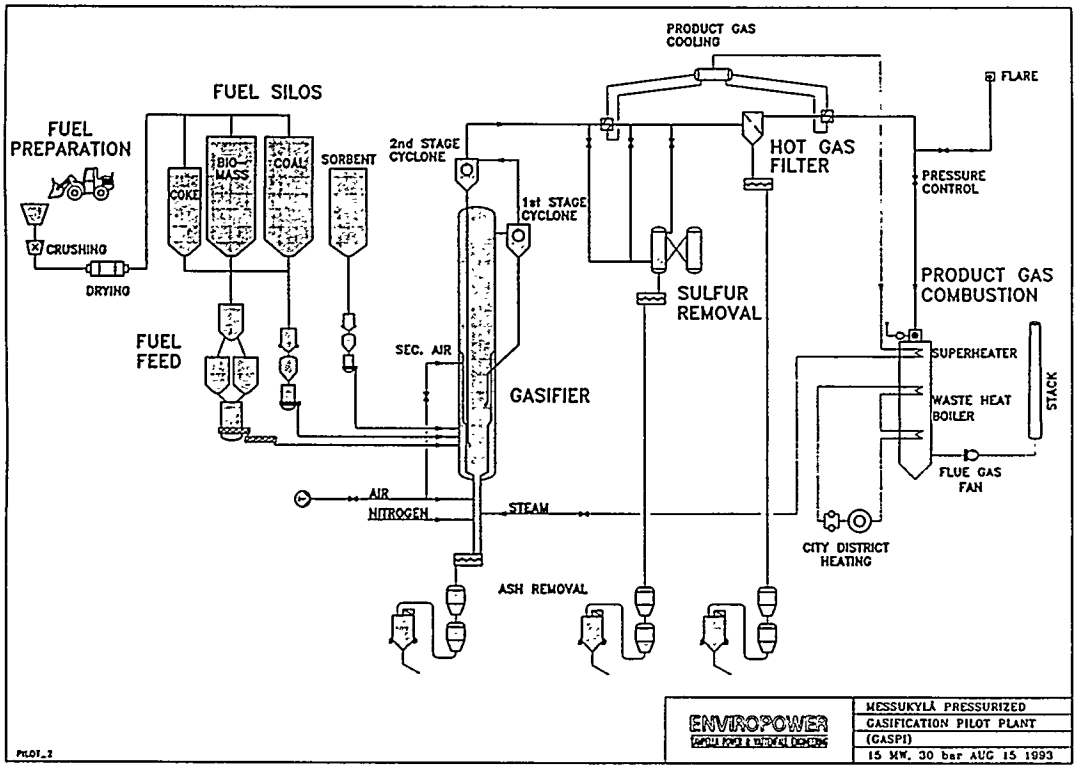


Figure 1. Enviropower's Pressurized Gasification Pilot Plant.

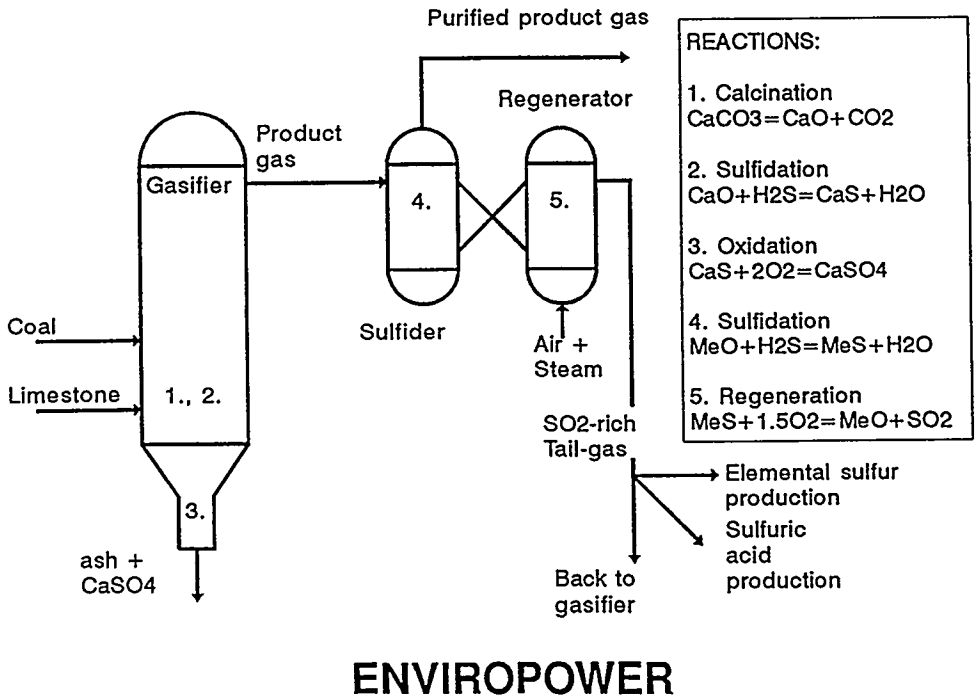


Figure 2. Tampella's Initial Concept for Sulfur Removal.

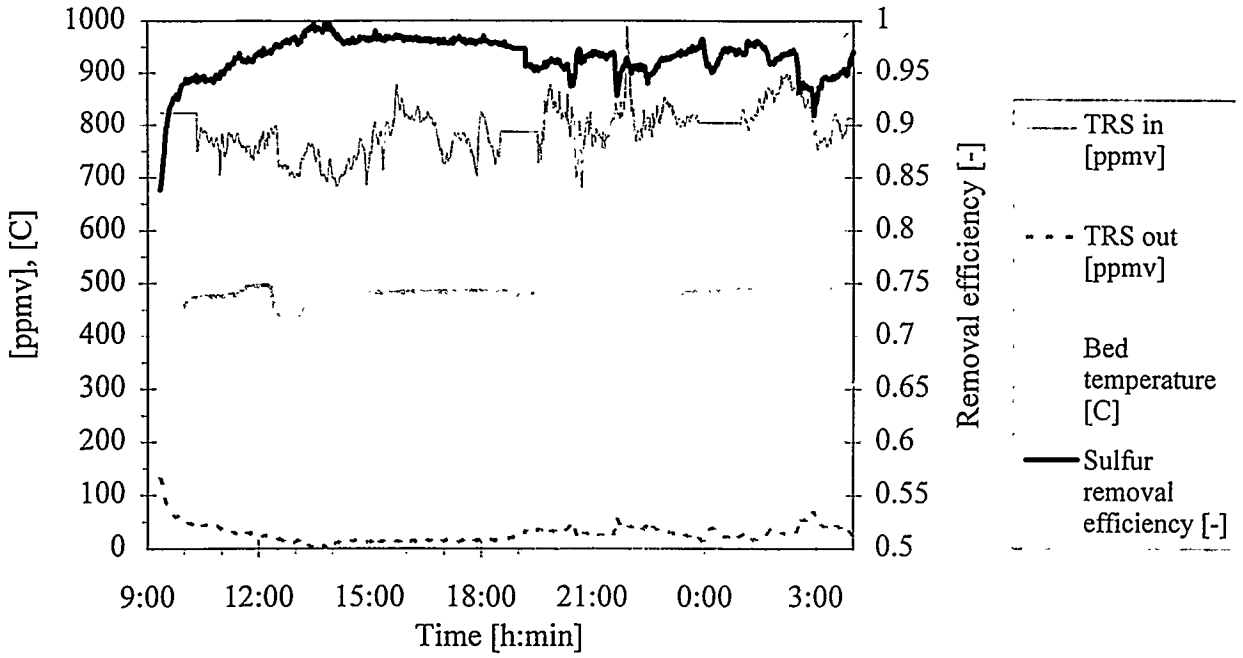


Figure 3. Sulfur Removal Efficiency with UCI-5-sorbent in the Beginning of Test Run. (TRS = Total Reduced Sulfur)

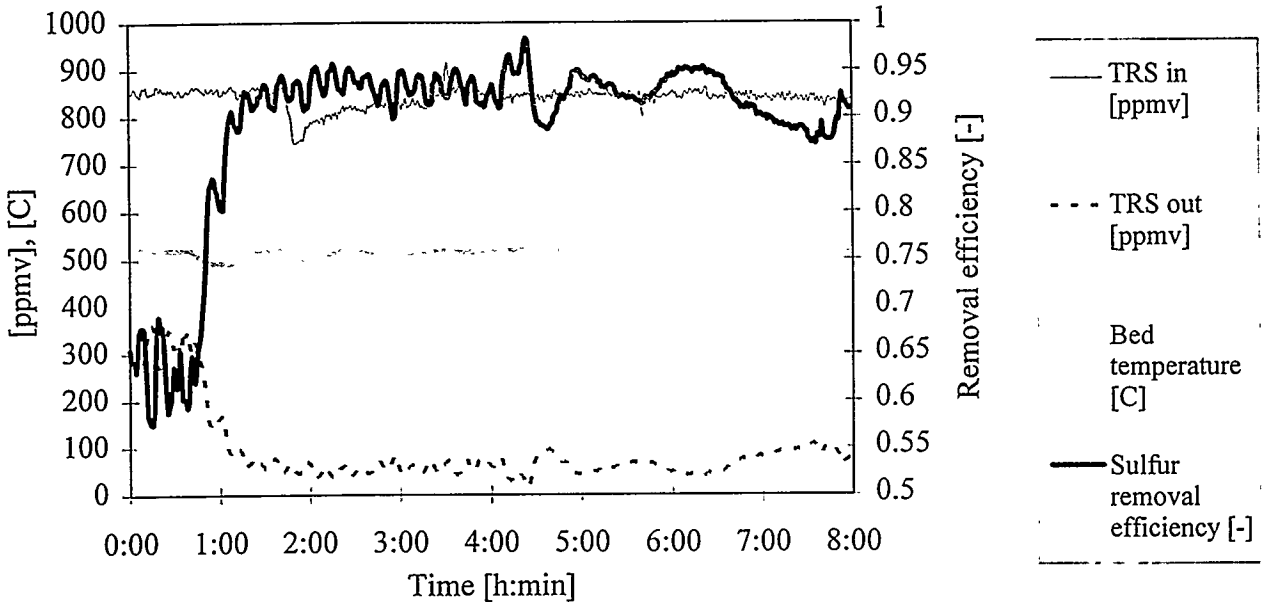


Figure 4. UCI-5 Sulfur Removal Efficiency when Both Sulfider and Regenerator On-Line.

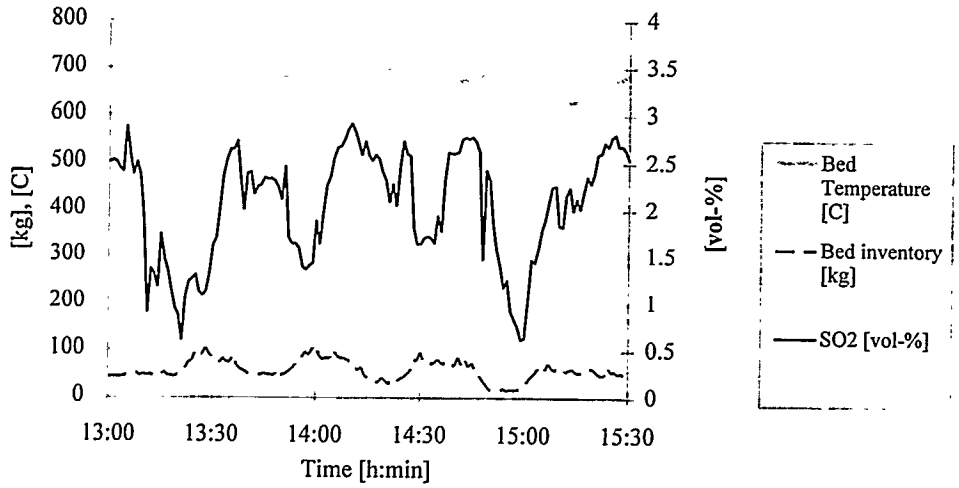


Figure 5. Regenerator Performance with UCI-5- Sorbent.

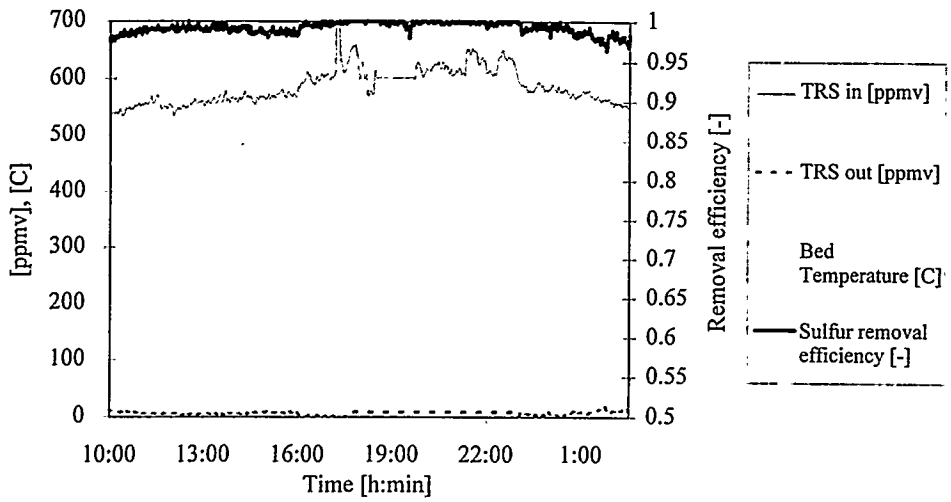


Figure 6. Sulfur Removal Efficiency with ZT-4-L-Sorbent.

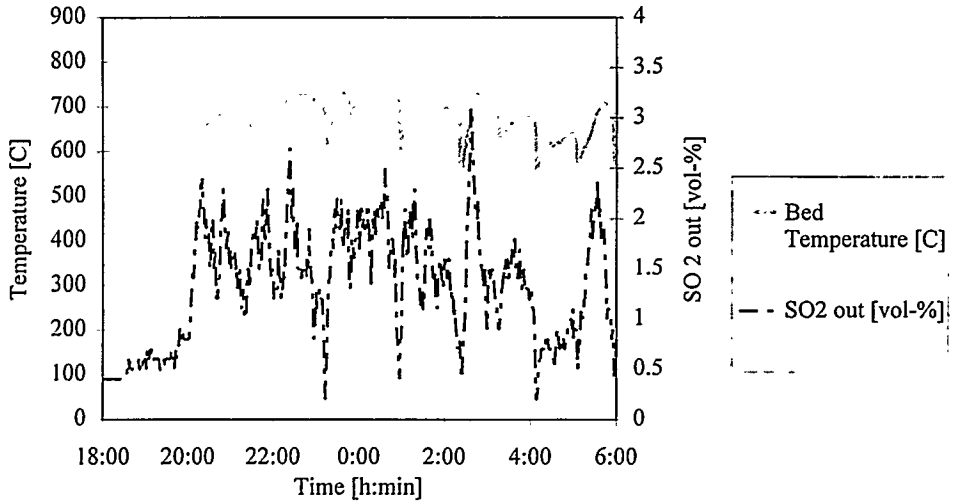


Figure 7. Regenerator Performance with ZT-4-L- Sorbent.

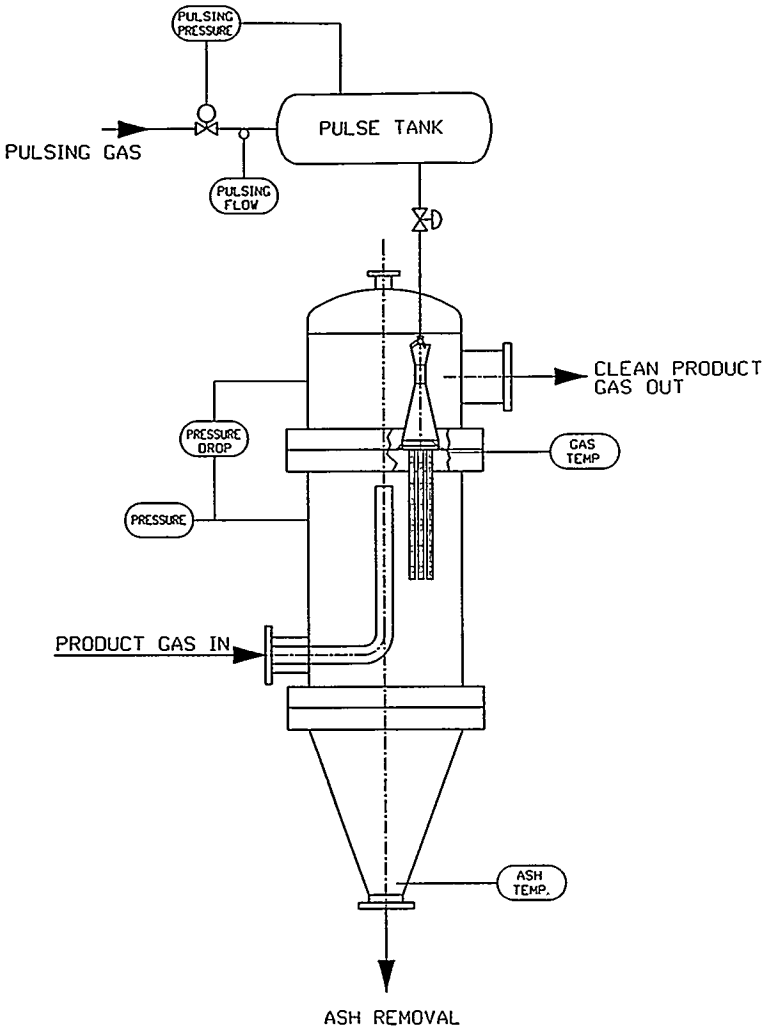


Figure 8. Pilot Filtration Unit.

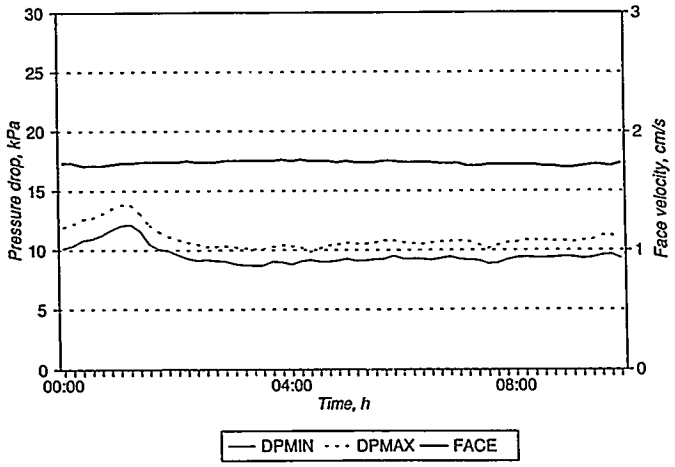


Figure 9. Filter Pressure Drop Across the Filter Elements and Face Velocity (dpmin and dpmax are minimum and maximum pressure drops, respectively).

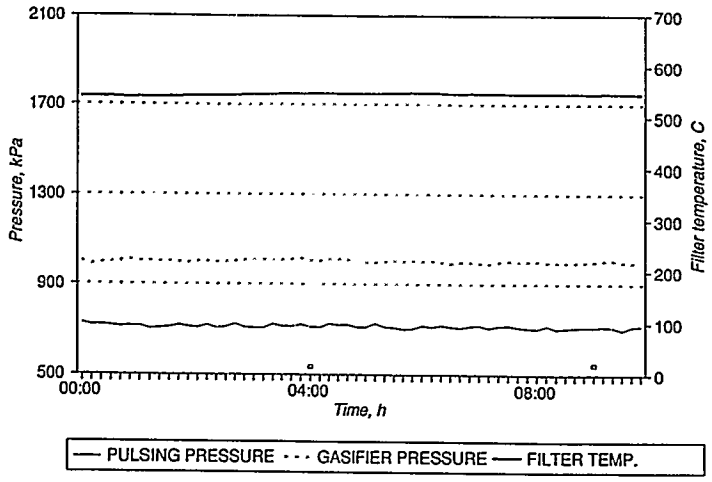


Figure 10. Filter Pulsing Pressure, Product Gas Pressure and Temperature.

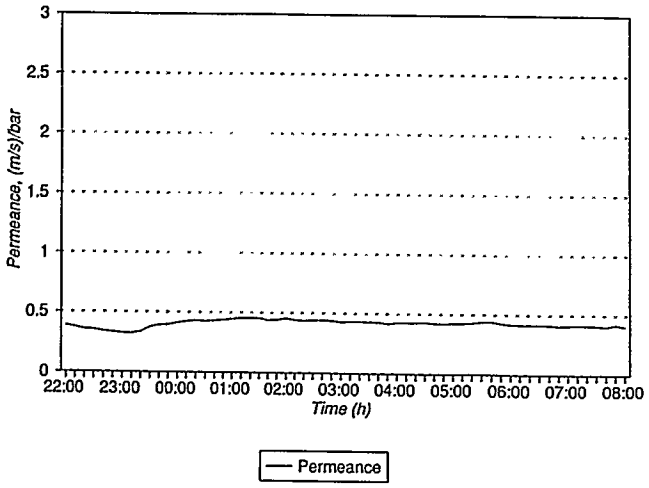


Figure 11. Filter Permeance.

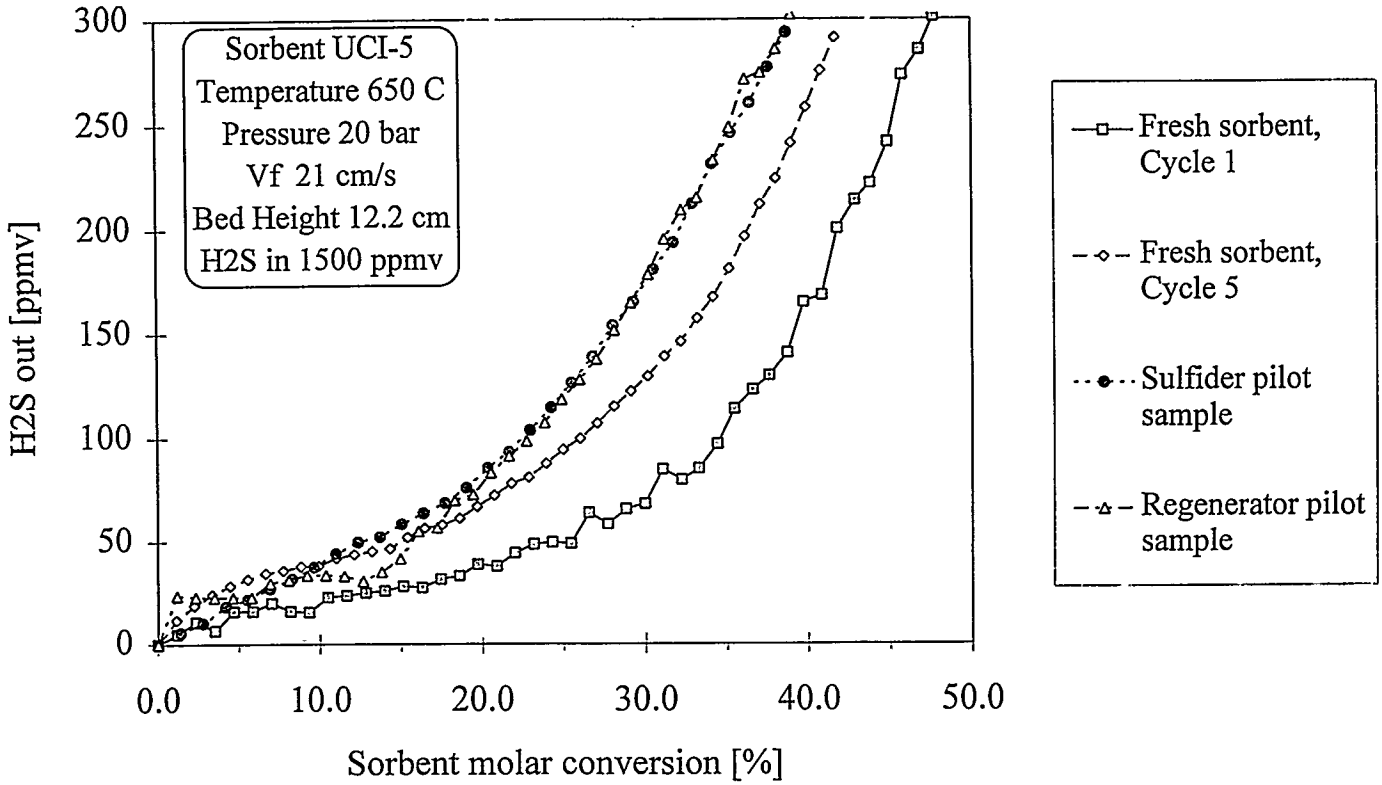


Figure 12. Comparison of Sulfidation Breakthrough Curves in 3" Batch BFB Reactor with UCI-5-Sorbent

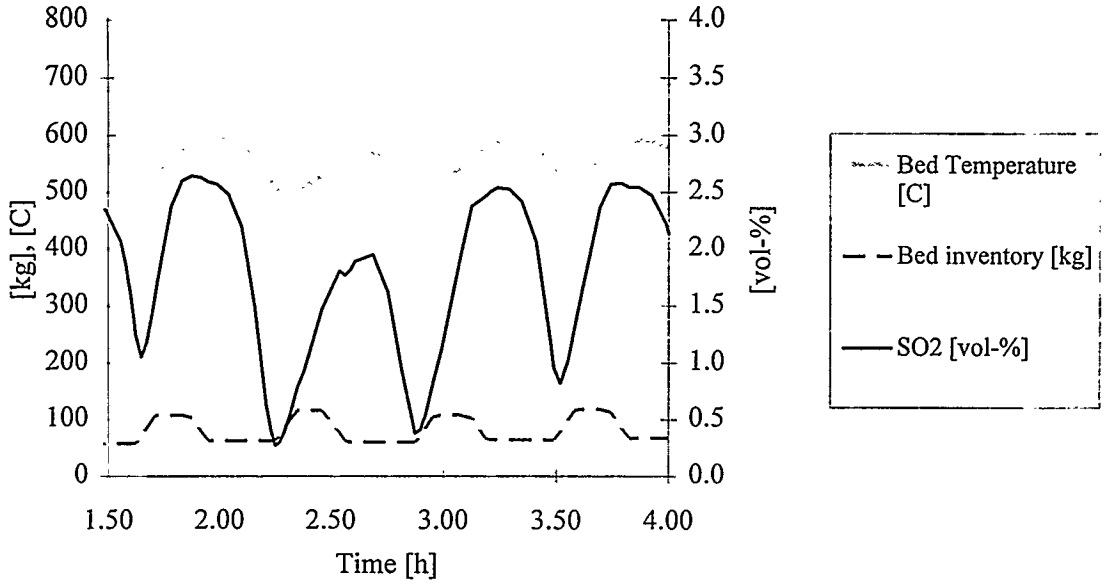


Figure 13. Regenerator Dynamic Model Response (in comparison with real situation in Figure 5).

## 4.3 Zinc Titanate Tests in Transport Reactor

### CONTRACT INFORMATION

| | |
|---|---|
| **Contract Number** | DE-AC21-88MC25006 |
| **Contractor** | Research Triangle Institute<br>P.O. Box 12194<br>Research Triangle Park, NC 27709-2194<br>919-541-8023 |
| **Contractor Project Manager** | Santosh K. Gangwal |
| **Subcontractor** | The M.W. Kellogg Company<br>P.O. Box 4557<br>Houston, TX 77210-4557<br>713-537-8534 |
| **Subcontractor Project Manager** | William M. Campbell |
| **Principal Investigator** | Raghubir P. Gupta (RTI)<br>GunnarB. Henningsen (MWK) |
| **METC Project Manager** | Daniel C. Cicero |
| **Period of Performance** | June 1995 - September 1995 |

### OBJECTIVES

The M.W. Kellogg Company is developing a Transport reactor process which promises to reduce the cost of the hot gas desulfurization system in IGCC power plants. Research Triangle Institute (RTI) has been developing proprietary fluidized-bed zinc titanate sorbents for hot gas desulfurization applications for the past five years with DOE/METC sponsorship. These sorbents are prepared using granulation and spray drying techniques. Recently, RTI and Contract Materials Processing (CMP), Inc. have teamed up to produce a spray-dried zinc titanate formulation, ZMP-5, in the 100-250 $\mu$m particle size range. This size range is preferred by Kellogg for the Transport reactor application.

Kellogg, in cooperation with RTI, will perform scoping and multi-cycle tests with ZMP-5 sorbent in its new bench-scale Transport Reactor Test Unit (TRTU-II). The objective of the test program is to establish an appropriate range of operating conditions for the use of this sorbent formulation in a Transport reactor system.

## BACKGROUND INFORMATION

A fixed-bed hot gas desulfurization (HGD) system was tested at the KRW, Waltz Mill, Pennsylvania, Process Development Unit. In this unit zinc ferrite was tested in both bulk and polishing modes of operation. When the Piñon Pine Power project was selected by the USDOE in Clean Coal Round IV, three zinc-based sorbents were tested at the Morgantown Energy Technology Center (METC) for the fixed-bed HGD application. In this testing, zinc ferrite and zinc titanate tended to decrepitate over extended multi-cycle testing. It was thought that this decrepitation was caused by the inherent high loading of sulfur on the sorbent in the fixed bed configuration. A third material, Z-Sorb sorbent, developed by Phillips Petroleum Company, showed no signs of decrepitation, but tended to lose capacity over time when regenerated in the presence of steam.

One way to avoid the high sulfur loading on the sorbent and to avoid using steam for heat dissipation during regeneration is to use a Transport reaction system. Kellogg first checked this idea in proof-of-concept tests in 1993. In these first tests, the Z-Sorb sorbent was used and there was no detectable leakage of sulfur from the Transport Absorber over a wide range of operating conditions. By limiting the amount of oxidant used during regeneration, such that only partial regeneration is accomplished, the sorbent acted as the heat sink and the oxidative exotherm was controlled. After a series of additional tests in 1994 in Kellogg's Transport Reactor Test Unit (TRTU) and a detailed technical review and comparison of both fixed-bed and Transport concepts, it was decided to include a Transport HGD system on the Piñon Pine Power project.

This paper reports on the results of recent HGD tests in Kellogg's new TRTU using spray-dried zinc titanate developed by RTI and supplied by CMP, Inc.

## PROJECT DESCRIPTION

Figure 1. is a sketch of Kellogg's new Transport Reactor Test Unit (TRTU-II). The TRTU-II was built for tests not related to this HGD test program but it was selected for this test program because the new design offers greater flexibility and is more like a commercial reactor configuration than the TRTU used in previous HGD testing.

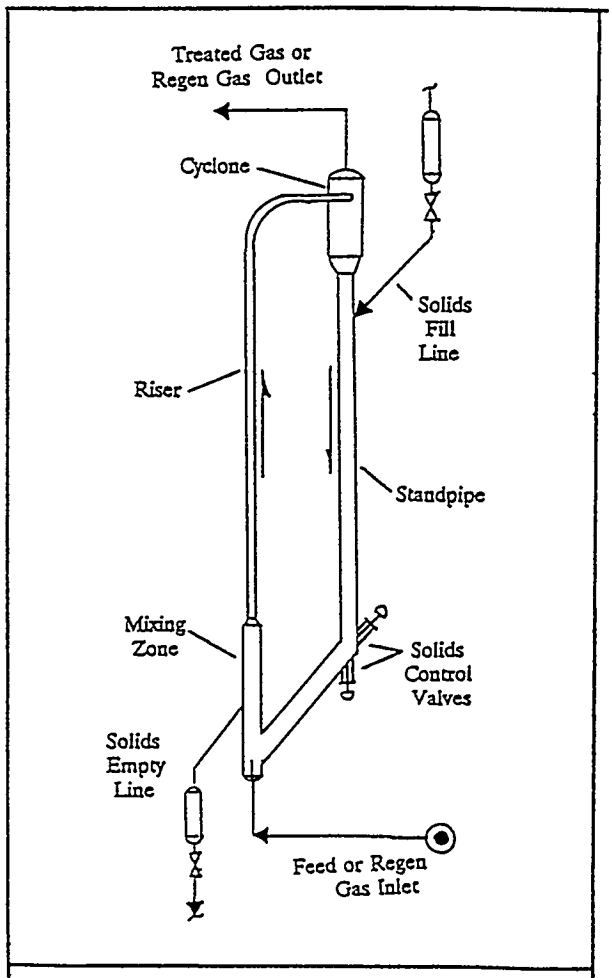


Figure 1.
Kellogg's Transport Reactor Test Unit

Transport reactors are devices that circulate fluidized solids at sufficiently high velocity to fully entrain the solid materials. The circulating solids are of substantially smaller diameter than those normally found in fixed-bed reactors, which results in improved reaction rates. The high circulation rates provide substantial gas-solid and solid-solid contact for excellent mass and heat transfer.

The TRTU-II consists of a 1-1/2 inch diameter Mixing Zone which is ten feet long, a Riser one inch in diameter and 32 feet long, a solids disengaging cyclone, and a 1-1/2 inch standpipe which returns the disengaged solids to the bottom of the Mixing Zone. The standpipe maintains an inventory of solids and includes a plug-like valve which permits controlling the rate of solids circulation in the reactor. The reactor is made of schedule 160 alloy piping materials which permits operation up to 1800°F and 100 psig. The reactor is heavily insulated and is heated by a number of electrical elements that permit accurate temperature control when determining yield data and kinetic reaction rates.

The TRTU is designed for proof-of-concept testing and data collection on gasification and combustion technologies as well as other gas-solid reaction systems where highly exothermic or endothermic reactions take place. The circulating solids provide a large heat sink to moderate temperature changes. The Mixing Zone of the reactor permits staging either gaseous reactants or solid, liquid and gas feeds. Staging is used on the oxidant during sorbent regeneration.

## TEST PROGRAM

There are a number of sorbent characteristics that are essential to successful operation of a Transport HGD system. Most important are the reactivity of the sorbent at operating conditions and its attrition resistance. High sulfur capacity is not of primary concern since the sorbant is regenerated continuously.

In the absorption mode two independent variables are of interest; process gas temperature and sorbent density in the Riser. Typically, the absorption reaction rate is very high and the effect of temperature is not great, indicating a diffusion-controlled reaction. The temperature range of interest is 1000-1200°F. Solid circulation rate can be varied to determine the effect on sulfur leakage of sorbent concentration in the Riser. Low circulation rate is desirable since sorbent attrition losses should be directionally lower.

Surprisingly, even though the regeneration reaction is highly exothermic, the reaction rate is relatively slow. The proper combination of temperature and oxygen and sulfur concentrations is important. Since zinc titanate tends to form sulfate in the presence of excess oxygen, the initial mode of operation will be to operate in the substoichiometric oxygen range. Sulfur concentration can be increased by raising the level in the spent sorbent or by increasing the circulation of sorbent in the regenerator. The exotherm is controlled by limiting the amount of air fed.

The temperature at which regeneration initiates is a key variable to be studied for any given sorbent formulation. If the regeneration initiation temperature or the temperature required for effective regeneration is significantly higher than the temperature in the Absorber, then the sorbent has to be heated and cooled on each regeneration pass. One purpose of the mixing zone in the Regenerator and of the staged oxidant introduction is to bring the sorbent up to an effective regeneration temperature before the sorbent enters the Riser where the highest temperature is experienced.

The ideal sorbent would operate at the same temperature in both absorption and regeneration modes. The effectiveness of any given sorbent formulation in a Transport reaction system depends upon finding an effective balance between the operating conditions of the Absorber and Regenerator. Multi-cycle (repeated absorption and regeneration) tests indicate whether these conditions vary as the sorbent ages.

## RESULTS

**At the time of publication the test program had not been initiated. A failure of several heating elments in theTRTU-II during reactor shakedown forced the test program to be delayed. Testing is expected to be completed in the next few months.**

**Anyone interested in receiving a copy of this paper, updated to reflect the results of the test program should write or FAX (713-753-7836) the author and a copy will be forwarded as soon as available.**

## FUTURE WORK

In addition to the testing in Kellogg's TRTU, METC is currently building a HGD Process Development Unit to support continued sorbent development. Figure xx is a schematic of METC's HGD-PDU. The unit is designed to process 150,000 SCFH of simulated gasifier fuel in either the fluid-bed or Transport mode of operation.

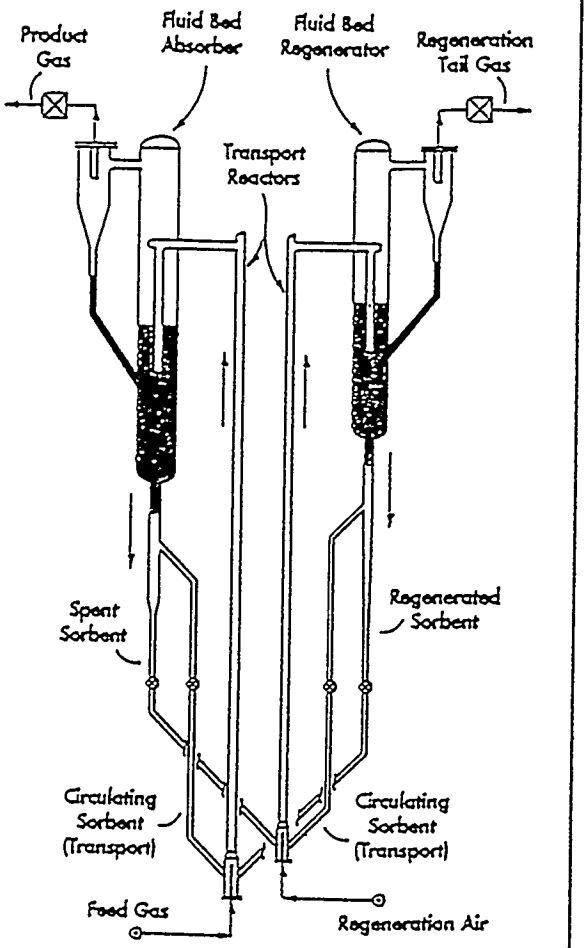


Figure xx
Schematic of METC's HGD-PDU

The diameters of the Transport Absorber and Regenerator are 6 inches and 2 inches respectively. This unit will be capable of testing a variety of sorbents over a range of operating conditions.

Figure yy is a sketch of the Transport HGD system for Sierra Pacific Power Company's 100 MWe Piñon Pine Power Poject. The Transport reactor for the Piñon Pine project has an Absorber diameter of 42 inches and a Regenerator diameter of 2-1/2 inches. The notable difference in reactor diameters is due to the large gas flow to the Absorber and the low level of sulfur in the gas.

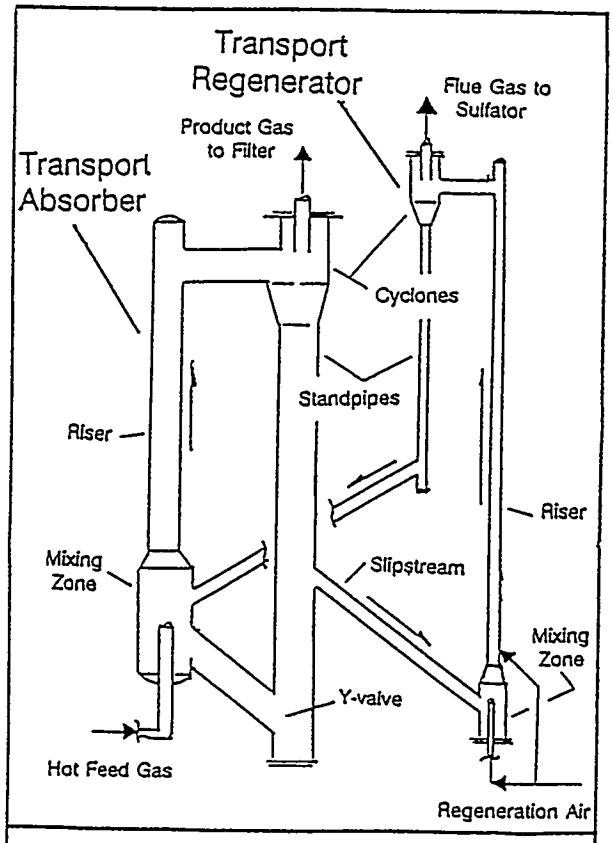


Figure yy
Piñon Pine Transport Desulfurizer

## 4.4 Slipstream Testing of Hot-Gas Desulfurization With Sulfur Recovery

### CONTRACT INFORMATION

| | |
|---|---|
| **Contract Number** | DE-AC21-93MC30010 |
| **Contractor** | Research Triangle Institute<br>P.O. Box 12194<br>Research Triangle Park, NC 27709-2194<br>Telephone: (919) 541-8033<br>Facsimile: (919) 541-8000 |
| **Other Funding Sources** | None |
| **Contractor Project Manager** | Santosh K. Gangwal |
| **Principal Investigators** | Jeffrey W. Portzer |
| **METC Project Manager** | Thomas P. Dorchak |
| **Period of Performance** | July 1, 1993 to December 31, 1995 |

**Schedule and Milestones**

**FY95-96 Program Schedule**

| | S | O | N | D | J | F | M | A | M | J | J | A | S | O | N | D |
|---|---|---|---|---|---|---|---|---|---|---|---|---|---|---|---|---|
| MET Field Test | | | | | | | | | | | | | | | | |
| Large-Scale System | | | | | | | | | | | | | | | | |

### OBJECTIVES

The objective of this work is to further the development of zinc titanate fluidized-bed desulfurization (ZTFBD), and the Direct Sulfur Recovery Process (DSRP) for hot-gas cleanup in integrated gasification combined cycle (IGCC) power generating systems. There are three main goals of this project:

- Development and testing of an integrated, skid-mounted, bench-scale ZTFBD/DSRP reactor system with a slipstream of actual coal gas;
- Testing the DSRP over an extended period with a slipstream of actual coal gas to quantify the degradation in performance, if any, caused by the trace contaminants present in coal gas (including heavy metals, chlorides, fluorides, and ammonia) and
- Design, fabrication, and shipment of a six-fold larger-scale DSRP reactor system for the Enviropower U-Gas 15-MW (thermal) pilot plant.

## BACKGROUND INFORMATION

Hot-gas desulfurization processes for IGCC and other advanced power applications utilize regenerable mixed metal-oxide sorbents to remove hydrogen sulfide ($H_2S$) from raw coal gas. Regeneration of these sorbents produces a tailgas typically containing 1 to 3 percent sulfur dioxide ($SO_2$). Reduction to elemental sulfur is a highly desirable option for the ultimate disposal of the $SO_2$ content of this offgas. Elemental sulfur, an essential industrial commodity, is easily stored and transported. The DSRP is a simple and attractive process for production of elemental sulfur from the regeneration offgases.

In the DSRP (Dorchak et al., 1991; Gangwal et al., 1993), the $SO_2$ tailgas is reacted with a slipstream of coal gas over a fixed bed of a selective catalyst to directly produce elemental sulfur at the high-temperature, high-pressure (HTHP) conditions of the tailgas and coal gas. Overall reactions involved are shown below:

$$2\ H_2 + SO_2 \rightarrow (1/n)\ S_n + 2\ H_2O$$

$$2\ CO + SO_2 \rightarrow (1/n)\ S_n + 2\ CO_2$$

$$H_2 + (1/n)\ S_n \rightarrow H_2S\ .$$

$$2\ H_2S + SO_2 \rightarrow (3/n)\ S_n + 2\ H_2O$$

The DSRP was initially developed as a two-stage process using simulated coal gas in the laboratory. The original process concept employed two catalytic reactors in series, each followed by a sulfur condenser. Hot regeneration tailgas was mixed with a hot coal gas slipstream (to act as the reducing gas) and fed to the first DSRP reactor. Approximately 95 percent of the combined sulfur in the inlet stream to the first reactor was converted to elemental sulfur. The outlet gas of the first reactor was then cooled, condensing out the sulfur. The cooled gas stream was reheated and sent to the second DSRP reactor where 80 to 90 percent of the remaining sulfur compounds were converted to elemental sulfur via the modified Claus reaction at high pressure. The total efficiency of the two reactors for the conversion of sulfur compounds to elemental sulfur was projected to be 99 percent.

However, based on the initial results, reported here, from the slipstream tests with actual coal gas, the second stage does not appear necessary. Greater than 99 percent sulfur recovery could be achieved in the first stage with careful control of the stoichiometric ratio of the gas input. The new simple single-stage process is shown in Figure 1 with a potential for "zero" sulfur emissions if the gas is recycled.

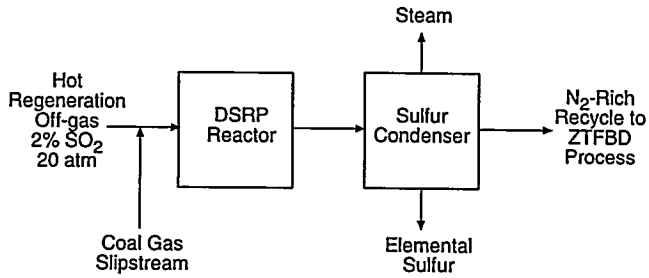


**Figure 1. New Single-Stage DSRP**

In addition to the patented DSRP, the Research Triangle Institute (RTI) under contract with the Morgantown Energy Technology Center (METC) has been developing zinc titanate sorbent technology since 1986 and has recently patented a fluidizable zinc titanate sorbent called ZT-4. The ZT-4 sorbent manufacture has been scaled up to pilot-scale quantities and the sorbent has been independently tested at a number of organizations including the Institute of Gas Technology, the Particulate Solids Research Institute; Enviropower, Inc. in Finland and the Coal Technology Development Division in England. Indeed, Enviropower (Konttinnen et al., 1995) has now successfully tested ZT-4 in a 33-inch fluidized bed at their 15-MW (thermal) pilot gasifier. However, the slipstream testing, reported here, supported the pilot testing of ZT-4.

## PROJECT DESCRIPTION

The slipstream testing activities are being conducted in two distinct phases. The first testing phase is being conducted at METC using a slipstream from a 10-in. experimental fluidized-bed gasifier. The second phase involves design and commissioning of a six-fold larger-scale DSRP unit that is to be tested at the Enviropower pilot plant employing a U-gas gasifier coupled to a ZTFBD system. Enviropower, a subsidiary of Tampella Power Corporation, is attempting to commercialize clean coal technologies in the United States and abroad.

The slipstream equipment, consisting of RTI's ZTFBD/DSRP mobile laboratory (trailer), for the testing at METC was described in detail in last year's contractor's meeting paper (Portzer and Gangwal, 1994). The METC coal gasifier is a fluidized-bed gasifier providing approximately 4,750 std $ft^3/h$ of low Btu coal gas from a nominal charge rate of 80 lb/h of coal. A heated slipstream, approximately 170 std $ft^3/h$ (80 std L/min), is directed to the RTI trailer. The process flow diagram of the trailer equipment is shown in Figure 2.

The trailer is divided into two sections—a high-pressure process section and a control section with a partition in between. The process is operated remotely from the control side to protect the operators from high pressure operation and potential toxic gas leaks. The design of the system has undergone extensive METC safety review, and permits have been obtained for its operation.

As shown in Figure 2, the hot-gas slipstream is first directed through a high-temperature filter. It then divides into two flows, one going to the 3-in. ZTFBD bench-scale reactor and the other to the DSRP system. The ZTFBD reactor system is

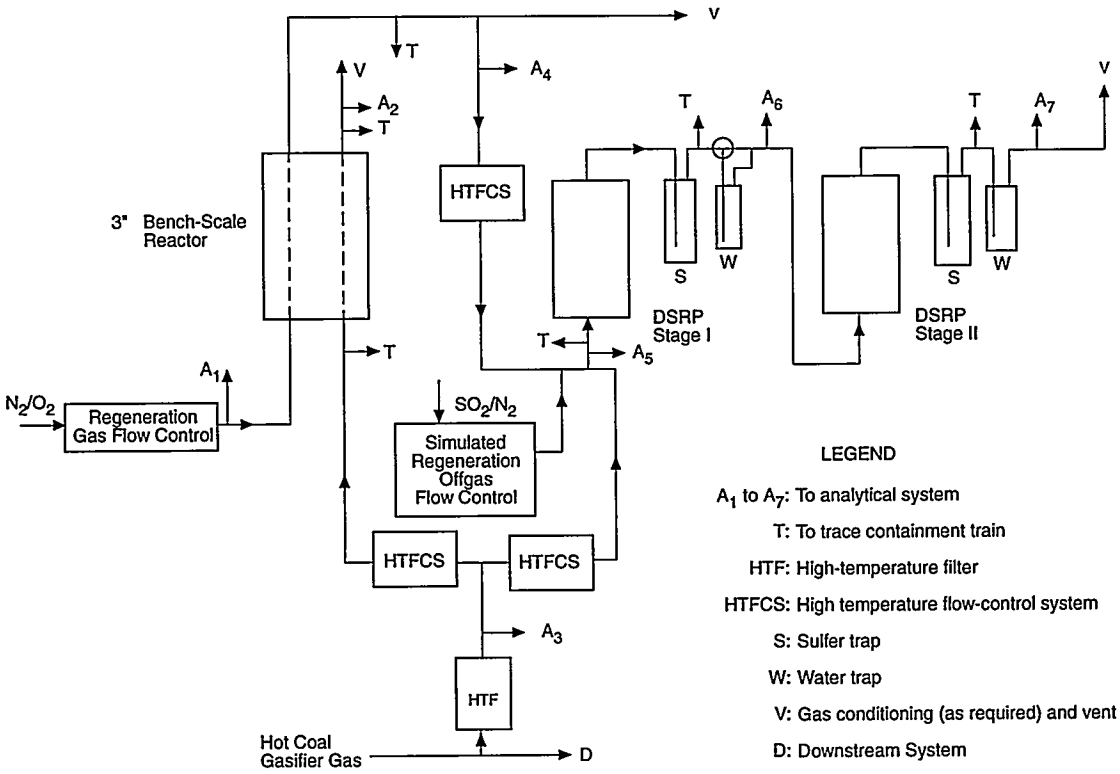


**Figure 2. Integrated Zinc Titanate and DSRP Reactor System**

operated batch-wise using cyclic sulfidation and regeneration. The regeneration tail gas is directed to the DSRP system. It mixes with the coal gas so that a molar ratio of 2 to 1, reducing gases to $SO_2$, is achieved after mixing. During the sulfidation portion of the cycle, the DSRP can also be run independently using simulated $SO_2$ (obtained using a liquid $SO_2$ pumping system) and actual coal gas. This provides the flexibility for extended operation of the DSRP with actual coal gas. As mentioned earlier, the DSRP, as originally installed, was a two-stage system with 3-in. fixed-bed 1-L catalytic reactors and a sulfur trap after each reactor.

A number of analytical and trace contaminant sampling points are installed throughout the system. The gases are analyzed using a number of gas chromatographs and continuous analyzers for all of the necessary key components ($H_2$, CO, $CO_2$, $H_2S$, COS, $SO_2$ $N_2$, $O_2$). Samples to enable trace contaminant measurements are collected using impinger trains. An EPA Method 29 multimetals train is used to test for volatile heavy metals including As, Se, and Hg. An acidic impinger train is used to test for $NH_3$ whereas a basic impinger train is used to test for halides (chloride and fluoride).

## RESULTS - SHAKEDOWN TESTING

After completing construction and preliminary checkout of the mobile laboratory unit (trailer) consisting of the ZTFBD and DSRP reactor systems, the trailer was transported to METC and parked during August 15-17, 1994. The trailer weighed about 16 tons with the equipment in place. A commercial crane company, assisted by METC personnel, lifted the trailer into place near the METC fluidized-bed gasifier (B-12) location. After the trailer was in position, intense activity followed to hook up the utilities (cooling water, city water, sewer, electricity, incinerator vent line, stack vent line) and the heated coal gas delivery line to the trailer. Preparations were made for shakedown testing of the RTI trailer in mid-September. Parallel to these preparations, the final application for the operating plan along with final design drawings was submitted. Pressure testing of the reactors at the operating temperature and 1.5 times the operating pressures was conducted on site.

The operating plan application was successfully defended on August 25, 1994. Comments provided by the safety committee were incorporated into the final operating plan. All indicated corrective actions to comply with the Occupational Safety and Health Administration (OSHA) and Environmental Safety and Health (ES&H) were successfully implemented in time for shakedown testing. METC personnel provided support to RTI throughout this critical period.

After obtaining an operating permit, the shakedown testing was ready to begin during the week of September 12, 1994. The ZTFBD reactor was loaded with 500 g of sorbent. The Stage I DSRP reactor was loaded with 1,000 $cm^3$ of catalyst and 1,500 $cm^3$ of catalyst was loaded in the Stage II DSRP reactor. Nitrogen flow was established through the coal gas line and the reactors at the desired set point. Heaters and furnaces were turned on and adjusted to obtain the desired temperature in each reactor, and backpressure regulators were used to control the reactor pressures.

Two cycles, each consisting of a sulfidation and a regeneration/integrated DSRP operation, were conducted during the shakedown test. Problems were experienced in the testing due to plugging of the coal gas control valves for both sulfidation and DSRP reactors. Later it was discovered that entrained particles from the gasifier cleanup system made their way to the RTI system through the 3/8-in. coal gas line. Also, the ceramic filter in the RTI trailer did not perform as well as expected and allowed some of these particles to get into the valves. Most likely the filter problem was due to differential thermal expansion of the alumina ceramic filter and the stainless steel housing.

The shakedown testing was successful in that promising results were demonstrated with the sorbent and DSRP even though the integrated regeneration-DSRP operation was carried out with erratic system pressure and coal gas flow. The objective of the testing was met since problems were identified that could be corrected prior to the formal test to be conducted.

## RESULTS - FORMAL TESTING

The formal 160-h slipstream test began on October 24, 1994, after correcting the problems found in the shakedown test. Although the run was curtailed due to mechanical problems with METC's gasifier, there was sufficient on-stream time to demonstrate highly successful operation of both the ZTFBD and the DSRP with actual coal gas. Also, the multimetals, $NH_3$ and HCl/HF impinger trains were successfully used during the run to determine the level of trace contaminants. No significant effect of the contaminants was detected on either the ZTFBD or DSRP over the 70 h of operation.

The process equipment in the ZTFBD unit worked extremely well in both the sulfidation and regeneration modes. The fluidizable zinc titanate formulation ZT-4L demonstrated 99+ percent removal of $H_2S$ from actual coal gas over three cycles and up to 20 lb sulfur per 100 lb sorbent loading capacity. It also demonstrated consistent, smooth regeneration behavior. For the most part, the DSRP unit also ran smoothly with actual coal gas. As planned, to obtain extended operation of the DSRP, provisions were made to produce simulated regeneration offgas using liquid sulfur dioxide which was successful. During periods of lined-out operation, the DSRP had concentrations of sulfur compounds in the exit gas corresponding to up to 99+ percent conversion in Stage 1 and 95 to 96 percent overall conversion for the two-stage system. This suggested problems of reverse Claus reactions in Stage 2:

$$2\ H_2O + (3/n)\ S_n \rightarrow 2\ H_2S + SO_2.$$

For a commercial system one stage may be sufficient, thus further improving the economics of the DSRP.

The DSRP unit was also successfully run in a fully integrated mode using actual regeneration tail gas. However, the ZTFBD run times in this mode were fairly short (due to a limited capacity to produce actual tail gas) and because of the longer response time of the DSRP unit, lined-out operation could not be achieved.

The DSRP unit experienced some plugging problems that resulted in unscheduled outages. At the high temperature, high pressure (HTHP) conditions, the flow of coal gas required by the DSRP was very small, requiring a fine orifice in the control valve. It tended to plug if there were any particulate matter in the coal gas. The high-temperature ceramic filter on the RTI equipment was apparently not completely effective and suggests that a stainless steel filter may be better for small equipment. There were also some problems with sulfur plugging in the cold end of the unit that required depressurization and disassembly to unblock. This suggests that the exit gases must be kept hot to prevent pluggage for continuous operation.

There was coal gas available at the RTI trailer for a total of 70 hours during the shortened October run. RTI was taking coal gas for 45.5 of those hours, for a utilization factor of 65 percent. Three sulfidation cycles (~25 h), two integrated DSRP tests (2.5 h) and four simulated DSRP tests (18 h) were conducted. Test conditions and main results of the testing are presented. A typical METC coal gas composition is shown in Table 1.

Points to note are that $H_2S$ and HCl vary due to coal's variability and at times doping of the coal with salt to increase the HCl level for a slipstream test on chloride removal. The ammonia analysis is an estimated value due to coal gas line plugging during the sampling. The trace

contaminant values were below or near the detection limit of our sampling system.

**Table 1. METC Gasifier Coal Gas Composition (vol%)**

| | |
|---|---|
| $CH_4$ | 1.97 |
| $H_2$ | 14.9 |
| $CO_2$ | 11.5 |
| CO | 9.87 |
| $H_2O$ | 11.0 |
| $H_2S$ | 0.1–0.75 |
| $N_2$ | Balance |
| HCl | 5–80 ppmv |
| As | <10 μg/m$^3$ |
| Se | 16 μg/m$^3$ |
| Hg | <2 μg/m$^3$ |
| $NH_3$ | ~800 ppmv |

Test conditions for sulfidation and regeneration of ZT-4L over the 2.5 cycles are shown in Table 2. Under these conditions, an $H_2S$ breakthrough curve during cycle 3 is shown in Figure 3.

**Table 2. ZT-4 Reactor Conditions**
(3.0-in. reactor; 600 g sorbent loaded)

| | Sulfidation | Regeneration |
|---|---|---|
| Temperature (°C) | 600 | 730 |
| Pressure (psig) | 260 | 260 |
| $U_s$ (cm/s) | 4.3 | 4.9 |
| Gas | Coal gas | 2.25% $O_2$ in $N_2$ |

The sorbent exhibited excellent removal efficiency and capacity even with the highly variable inlet $H_2S$ levels. Sorbent regeneration, which went very smoothly, is shown in Figure 4. Note that with 2.25 percent $O_2$ in the inlet, nearly two-thirds, i.e., ~1.5 percent, $SO_2$ is obtained in the offgas, indicating that sulfation did not occur. The properties of the fresh and three-cycle (sulfided) materials are compared in Table 3.

**Table 3. Properties of Fresh and Reacted ZT-4L**

| | Fresh | 3-Cycle Sulfidated |
|---|---|---|
| Exposure time (h) | 0 | Coal gas (25); temperature (>100) |
| Surface area (m$^2$/g) | 3.2 | 7.56 |
| Pore volume (cm$^3$/g) | 0.234 | 0.11 |
| Pore diameter (Å) | 2,500 | 1,800 |
| Particle size (μm) | 112 | 95 |
| Air-jet attrition (%) | | |
| 5-h loss | 16 | 1.4 |
| 20-h loss | 36 | 6.2 |
| Compacted density (lb/ft$^3$) | 91.6 | 107 |
| Zn/Ti | 1.35 ± 0.05 | 1.42 ± 0.05 |
| TGA capacity (g/100 g) | 21.0 | 20.5 |
| As (μg/g) | 0.7 | 8.4 |
| Se (μg/g) | <0.57 | 0.72 |
| Pb (μg/g) | <30 | 50 |
| Cl (μg/g) | NM | 38 |

NM = Not measured.

Note that the surface area of the sulfided material is higher and the pore volume is lower. The material significantly improved in attrition resistance over the three cycles. The thermogravimetric analysis (TGA) measured capacity did not

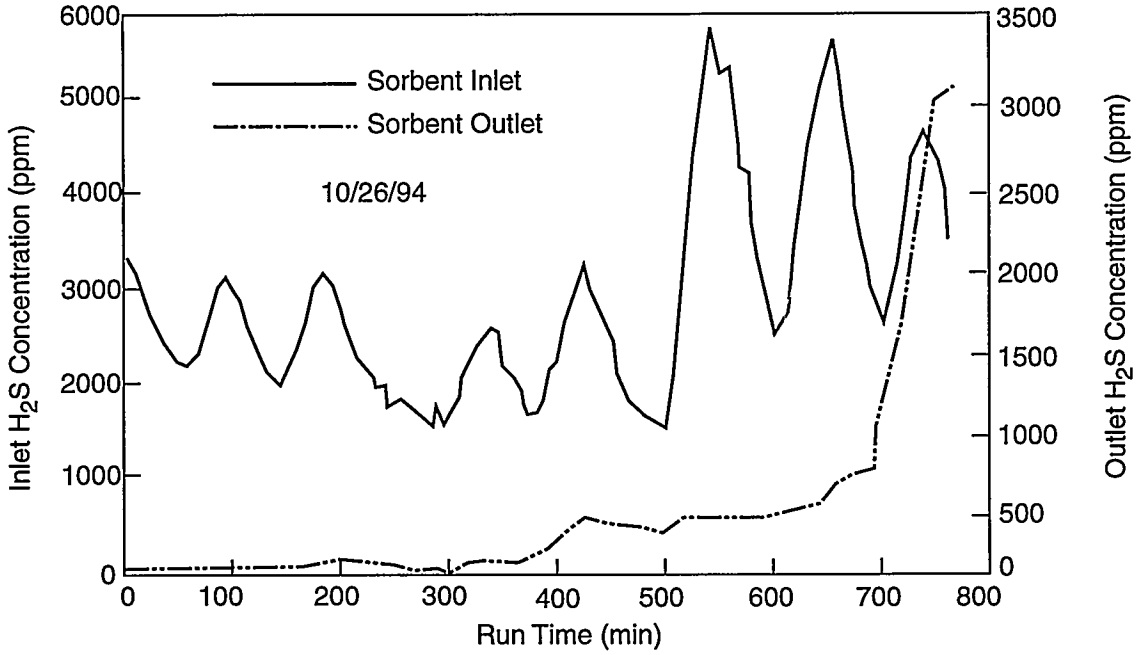


**Figure 3. Sorbent Sulfidation Curves**

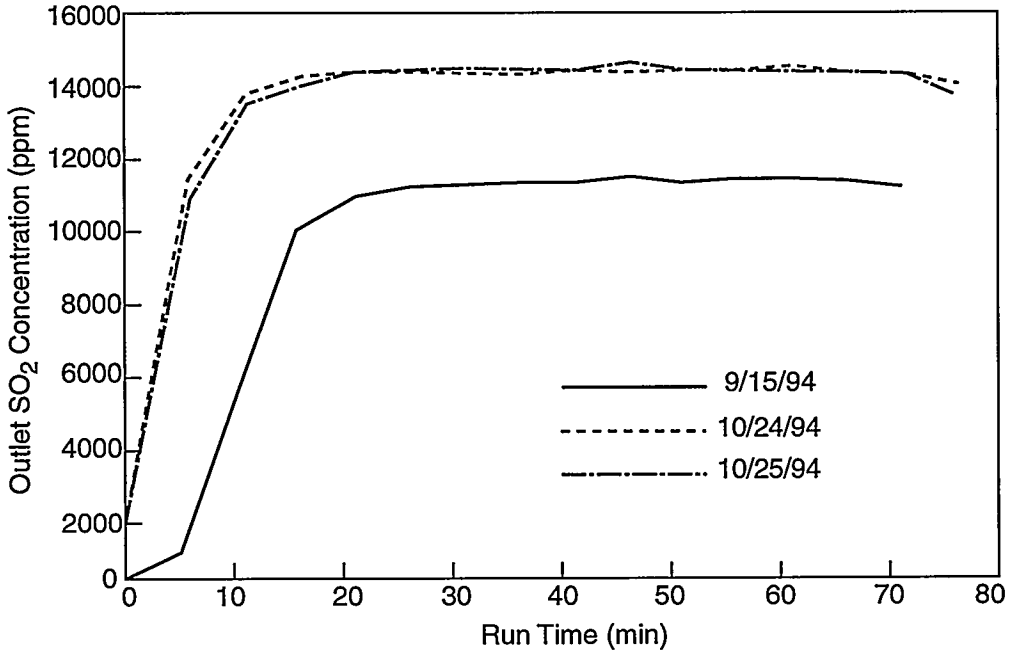


**Figure 4. Sorbent Regeneration Curves**

change from fresh to used material and was at 20 lb/100 lb sorbent.

Preliminary indications are that the actual coal gas-sulfided sorbent required somewhat higher temperature for regeneration than a sorbent sulfided with simulated coal gas. This may be due to reactions of one or more of the contaminants in coal gas with the sorbent. Analysis of trace contaminants in the sorbent indicated a buildup of As (from 0.7 to 8.4 ppm), Se (from <0.57 ppm to 0.72 ppm), Pb (from <30 ppm to 50 ppm), and Cl (up to 38 ppm). No Hg was detected in the gas or sorbent. The estimated gaseous concentrations of As and Se in the gas are ~100 and ~10 $\mu g/m^3$, respectively. The requirement for higher regeneration temperatures for the coal-gas exposed sorbent needs further validation.

The test conditions for the DSRP Stage I reactor are shown in Table 4. As indicated earlier, two integrated ZTFBD-DSRP and four simulated $SO_2$-DSRP tests were conducted using the METC gasifier coal gas. During the integrated tests, it was not possible to obtain lined-out operation in the short duration of regeneration due to a larger time constant (~2 h) of the DSRP. However, three of the simulated $SO_2$-DSRP tests were highly successful. One of the simulated $SO_2$-DSRP tests was not successful due to plugging of the coal gas line from METC's gasifier. The results of the successful DSRP tests are shown in Table 5. Note that in Run 1 (with fresh catalyst) extremely high sulfur conversion (up to 99.7 percent) is achieved. Some selectivity toward $H_2S$ is seen in later runs, probably due to a less than optimum stoichiometric ratio, although even in these tests a 96 percent sulfur conversion level is achieved. This is an excellent performance by the DSRP.

The fresh and used catalyst properties are shown in Table 6. The used catalyst showed better crush strength but a lower surface area. Also, chloride is picked up by the catalyst but does not appear to affect its activity significantly even at 300 ppmv level. No other trace contaminants are detected in the catalyst. DSRP sulfur purity was checked using a differential scanning calorimeter. It was found that the DSRP sulfur exhibited the same endotherms as pure sulfur.

**Table 4. DSRP Stage I Reactor Conditions**

| | |
|---|---|
| Temperature (°C) | 550–610 |
| Pressure (psig) | 260 |
| Space velocity (std $cm^3/cm^3 \cdot h$) | 4,560 |
| Reactor diameter (in.) | 3.0 |
| Inlet $SO_2$ (%) | 1.8 |

**Table 5. Stage 1 DSRP Results During Lined-out Operation with Simulated $SO_2$**

| Run Time (min) | $SO_2$ Conversion (%) | $SO_2$ Conversion to $H_2S$ (%) | $SO_2$ Conversion to Sulfur (%) |
|---|---|---|---|
| Run No. 1 | | | |
| 32 | 99.4 | 0.0 | 99.4 |
| 36 | 99.4 | 0.0 | 99.4 |
| 40 | 99.5 | 0.0 | 99.5 |
| 44 | 99.7 | 0.0 | 99.7 |
| 48 | 99.5 | 0.0 | 99.5 |
| 52 | 98.5 | 0.0 | 98.5 |
| 56 | 98.0 | 0.0 | 98.0 |
| Run No. 3 | | | |
| 117 | 99.6 | 1.2 | 98.4 |
| 121 | 100.0 | 4.1 | 95.9 |
| 125 | 100.0 | 4.9 | 95.1 |
| 129 | 100.0 | 2.4 | 97.6 |
| Run No. 4 | | | |
| 175 | 100.0 | 4.9 | 95.1 |
| 179 | 100.0 | 4.1 | 95.9 |
| 183 | 100.0 | 4.9 | 95.1 |
| 199 | 100.0 | 4.7 | 95.3 |

**Table 6. DSRP Stage I Catalyst**

| | Fresh | Used |
|---|---|---|
| Size (in.) | 1/8 | 1/8 |
| Crush strength (lbf/mm) | 2.0 | 2.5 |
| Surface area ($m^2/g$) | 208 | 158 |
| Exposure (h) | 0 | Coal gas (20); Temperature (>100) |
| Cl (ppmw) | 21 | 300 |
| As (ppmw) | <11 | <10 |
| Se (ppmw) | <10 | <10 |

To conclude, both ZT-4L and DSRP showed very promising results in short-term testing with actual coal gas. Based on the results of the slipstream testing, the new DSRP is envisioned as a single-stage process rather than a two-stage process. This further improves on the already attractive economics of the DSRP. The long-term test of 160 h needs to be completed to fully evaluate longer-term degradation effects.

## FUTURE PLANS

Since the October test was curtailed, a decision was made to conduct an additional slipstream test of 160 h to achieve a total 200 h of operation of the DSRP. This test is currently scheduled to begin on July 17, 1995, and will include:

- A 160-h test of single-stage DSRP with actual coal gas and simulated regeneration offgas, and due to a change in priority,

- A 100-h test of $NH_3$ decomposition at 850 °C and 150 psia.

The ZTFBD system will be modified for $NH_3$ decomposition testing. The two-stage DSRP system will be modified to a single stage with improved control of stoichiometric ratio of reducing gas to $SO_2$ entering the reactor. Coordination meetings for the test and $NH_3$ analysis have already been held at METC and the test is on schedule.

For the larger-scale DSRP system, two detailed meetings have been held, one on site in Finland and one at Tampella Power offices in Atlanta with METC and Enviropower. Significant progress has been made toward the goal of supplying the reactor system to Enviropower which is currently on schedule for delivery later this year.

## REFERENCES


Dorchak, T.P., S.K. Gangwal, and W.J. McMichael. 1991. "The Direct Sulfur Recovery Process." *Environmental Progress* 10(2):68.

Gangwal, S.K., W.J. McMichael, and T.P. Dorchak. 1992. "The Direct Sulfur Recovery Process for Refinery Gas Processing." AIChE Meeting, New Orleans, March.

Konttinen J., A. R. Ghazanfari 1995 "Pilot Scale Experience on IGCC Hot Gas Cleanup" *Proceedings of the Coal-Fired Power System 95 Review Meeting*, U.S. Department of Energy, Office of Fossil Energy, Morgantown Energy Technology Center, Morgantown, WV.

Portzer, J., and S.K. Gangwal. 1994. "Slipstream Testing of the Direct Sulfur Recovery Process," in *Proceedings of the Coal-Fired Power System 94—Advances in IGCC and PFBC Review Meeting*, Vol. I. U.S. Department of Energy, Office of Fossil Energy, Morgantown Energy Technology Center, Morgantown, WV.

## 4.5 Bench-Scale Testing of Fluidized-Bed Sorbents—ZT-4

### CONTRACT INFORMATION

| | |
|---|---|
| **Contract Number** | DE-AC21-88MC25006 |
| **Contractor** | Research Triangle Institute<br>P. O. Box 12194<br>Research Triangle Park, NC 27709-2194<br>(919) 541-8023 |
| **Contractor Project Manager** | Santosh K. Gangwal |
| **Principal Investigator** | Raghubir P. Gupta |
| **METC Project Managers** | Daniel C. Cicero |
| **Period of Performance** | September 21, 1988 to Setpember 30, 1995 |

**Schedule and Milestones**

**FY95 Program Schedule**

| | S | O | N | D | J | F | M | A | M | J | J | A | S |
|---|---|---|---|---|---|---|---|---|---|---|---|---|---|
| Life-Cycle Test with ZT-4 | — | — | — | — | | | | | | | | | |
| CMP-5 Sorbent Testing | | | | | — | — | — | — | — | | | | |
| CMP-5 Sorbent Production | | | | | | | — | — | — | — | — | | |
| TRTU Testing at M.W. Kellogg | | | | | | | | | | — | — | — | |
| Topical Report | | | | | | | | | | | | — | — |

### OBJECTIVES

The objectives of this project are to identify and demonstrate methods for enhancing long-term chemical reactivity and attrition resistance of zinc oxide-based mixed metal-oxide sorbents for desulfurization of hot coal-derived gases in a high-temperature, high-pressure (HTHP) fluidized-bed reactor. Specific objectives of this study are the following:

- Investigating various manufacturing methods to produce fluidizable zinc ferrite and zinc titanate sorbents in a particle size range of 50 to 400 µm;
- Characterizating and screening the formulations for chemical reactivity, attrition resistance, and structural properties;

- Testing selected formulations in an HTHP bench-scale fluidized-bed reactor to obtain an unbiased ranking of the promising sorbents;

- Investigating the effect of various process variables, such as temperature, nature of coal gas, gas velocity, and chemical composition of the sorbent, on the performance of the sorbent;

- Life-cycle testing of the superior zinc ferrite and zinc titanate formulations under HTHP conditions to determine their long-term chemical reactivity and mechanical strength;

- Addressing various reactor design issues;

- Generating a database on sorbent properties and performance (e.g., rates of reaction, attrition rate) to be used in the design and scaleup of future commercial hot-gas desulfurization systems;

- Transferring sorbent manufacturing technology to the private sector;

- Producing large batches (in tonnage quantities) of the sorbent to demonstrate commercial feasibility of the preparation method; and

- Coordinate testing of superior formulations in pilot plants with real and/or simulated coal gas.

## BACKGROUND INFORMATION

Research Triangle Institute (RTI) is assisting the U.S. Department of Energy/Morgantown Energy Technology Center (DOE/METC) in the development of a fluidized-bed hot-gas desulfurization system employing ZnO-based mixed metal-oxide sorbents for removal of sulfurous compounds (e.g., $H_2S$, COS, $CS_2$) at high-temperature (500 to 750 °C [932 to 1,382 °F]), high-pressure (15 to 20 atm) conditions. Desulfurization of hot coal gas in a fluidized-bed reactor offers a number of potential advantages over fixed beds. Although fixed-bed reactors are operationally simple and provide high sorbent sulfur capacity and zinc utilization and low sulfur breakthrough, they suffer from some serious problems including the need to use hot valves and poor ability to control the temperature during highly exothermic regeneration. Recently, severe spalling and decrepitation of zinc titanate sorbent pellets in fixed beds surfaced as a serious problem due to the formation of zinc sulfate and subsequent expansion in molar volume during regeneration (Mei et al., 1993). In contrast, fluidizable zinc titanate particles became stronger with cycling and do not suffer from sulfate formation problems (Gupta and Gangwal, 1993). Additionally, fluidized-bed reactors have a number of advantages including easier control of temperature during regeneration, use of small particles leading to faster overall kinetics, and nearly continuous steady-state operation. However, a highly reactive and attrition-resistant sorbent is required, and scaleup and turndown limitations exist for fluidized-bed systems.

## PROJECT DESCRIPTION

In this program, regenerable ZnO-based mixed metal-oxide sorbents, including zinc ferrite and zinc titanate are being developed and tested. A brief description of pertinent project accomplishments is provided below.

### Design and Construction of an HTHP Bench-Scale Sorbent Test Facility

During the first phase (1989) of this program, a 3-in. ID bench-scale HTHP semibatch fluidized-bed reactor system was designed and constructed. This reactor operates in a semibatch mode because the flow of gas phase is continuous while sorbent particles remain in the reactor. This system is capable of operation at up to 871 °C (1,600 °F) at 20 atm (294 psi). Any simulated coal gas can be generated in this system using a battery of eight mass flow controllers and three positive displacement pumps (for pumping liquid water to generate

steam). This system is equipped with a state-of-the-art computer controlled data acquisition system. A series of gas chromatographs (GCs) and continuous on-line analyzers measure the concentrations of various species in the reactor exit gas such as $H_2S$, COS, $SO_2$, $CO_2$, $H_2$, $CH_4$, $N_2$, CO, $O_2$. A complete description of this test facility is given elsewhere (Gupta and Gangwal, 1992; 1993).

## Development and Testing of Zinc Ferrite Sorbents

Earlier work in this program was focused on preparing fluidizable zinc ferrite particles in 50- to 300-µm particle diameter range. A number of sorbent preparation techniques were investigated including spray drying, impregnation, crushing the durable extrudates and screening, and granulation.

Of these techniques investigated, granulation proved to be the most successful and a number of zinc ferrite sorbent formulations were prepared using this technique. Testing of these sorbents in the HTHP bench reactor demonstrated that these sorbents possess sulfur capacity and attrition resistance as good as or better than sorbents prepared by crushing and screening. Results of bench-scale testing of selected sorbent formulations are described elsewhere (Gupta and Gangwal, 1991).

With zinc ferrite sorbents, excessive sorbent loss was observed at a sulfidation temperature of 625 °C (1,157 °F). It is thought that attrition of the sorbent in the reactor is primarily due to chemical transformations rather than mechanical forces. Possible chemical transformations responsible for attrition are excessive reduction of $ZnFe_2O_4$ and iron carbide formation (Gupta and Gangwal, 1991; Gupta et al., 1992).

The applicability of zinc ferrite as a hot-gas desulfurization sorbent, therefore, is conservatively limited to below 550 °C (1,022 °F) and to moderately reducing coal gases, such as low-Btu gas from an air-blown gasifier containing at least 15 percent water vapor. Higher temperatures, as shown in the study, led to excessive sorbent weakening.

## Development and Testing of Zinc Titanate Sorbents

To extend the operating temperature and desulfurize highly reducing coal gases, zinc titanate sorbent was developed for fluidized-bed reactors. Following the success of the granulation technique with zinc ferrite sorbents, it was used to prepare a series of zinc titanate formulations in the 50- to 400-µm particle diameter range. A number of sorbent formulations prepared using the granulation technique exhibited excellent durability, attrition resistance, and sulfur capacity during multicycle testing as described in an RTI topical report to METC (Gupta and Gangwal, 1992).

Based on screening tests, a series of promising sorbent formulations were identified. Further testing of these formulations indicated that ZT-4 sorbent had the best overall performance tested in terms of attrition resistance, chemical reactivity, regenerability, sulfur capacity, and other physical and structural properties. RTI was granted a U.S. Patent on manufacture of fluidizable zinc titanate sorbent (Gupta et al., 1993).

Ten HTHP runs were carried out, each involving 10 sulfidation-regeneration cycles in the bench unit. Bench-scale testing variables included sorbent type, temperature (550 to 750 °C [1,022 to 1,382 °F]), gas type (KRW or Texaco gasifier gas), steam content of coal gas, and fluidizing gas velocity (6 to 15 cm/sec). In all 10 multicycle tests, unlike zinc ferrite sorbents, the sulfur capacity utilization for zinc titanate sorbents at breakthrough was consistently between 40 and 60 percent with very little decline with cycling. The attrition resistance of 10-cycle regenerated sorbent was significantly better than the fresh sorbent in

all the runs. The detailed test results are described in an RTI topical report to METC (Gupta and Gangwal, 1992).

### 100-Cycle Test with ZT-4

Following the successful multicycle parametric testing of various zinc titanate formulations in the bench-scale fluidized-bed reactor, a life-cycle test consisting of 100 sulfidation-regeneration cycles was carried out to determine the long-term reactivity and mechanical strength of ZT-4 sorbent. This life-cycle test was carried out at 750 °C (1,382 °F) sulfidation temperature, 15 atm (220 psia) pressure with a medium Btu Texaco $O_2$-blown gasifier gas containing 11,400 ppmv of $H_2S$. These highly severe sulfidation conditions were purposely selected to provide possible worst-case results of long-term sorbent durability. Regeneration of the sulfided sorbent was performed using 2 to 2.5 percent $O_2$ in $N_2$ in a temperature range of 720 to 760 °C (1,328 to 1,400 °F). The amount of sorbent in the reactor was 500 g and a relatively high superficial gas velocity of 15 cm/s was used to ensure good fluidization and to more closely simulate commercial operation. This resulted in a superficial gas residence time of only about 1.24 seconds.

This life cycle test conducted under extremely severe operating conditions, and highly reducing nature of coal gas, demonstrated superior performance of the ZT-4 sorbent. The following were the pertinent findings of this life-cycle test:

- The ZT-4 sorbent consistently reduced the $H_2S$ content of coal gas from 11,400 ppmv to <20 ppmv in a semibatch bench-scale fluidized-bed at 750 °C (1,382 °F) and 15 atm.

- The sorbent was found to be fully regenerable, with negligible residual sulfate remaining. An oxygen concentration of 2 to 3 percent with $N_2$ diluent was found to result in adequate regeneration rates with no temperature control problems due to the exothermicity of the regeneration reaction.

- The sulfur capacity of the sorbent at breakthrough of 500 ppmv $H_2S$ ranged from 12.6 wt% in Cycle 1 to 5.8 wt% in Cycle 100 with an average of about 9 percent. Most of the decline in the sulfur capacity occurred during the first 50 cycles.

- The decline in sulfur capture capacity was found to correlate with a decrease in the BET surface area, pore volume, and internal porosity. The best correlation, as expected with small particles, was with the BET surface area.

- X-ray diffraction (XRD) analysis indicated the presence of zinc silicate in the sorbent, which is believed to result from the reaction of ZnO with free $SiO_2$ released from the distributor material. Zinc silicate is believed to be a potential cause of some of the reactivity loss.

- Attrition resistance measurements carried out in RTI's three-hole airjet attrition tester indicated that the attrition resistance of the sorbent after 100 cycles of testing was significantly higher (<3% 5-h loss) over that of the fresh sorbent (about 40% 5-h loss).

- No significant sorbent loss (<2%) from the reactor was detected over 100 cycles. The total zinc loss determined by chemical analysis was negligible.

Complete details of the test conditions and experimental results are reported in RTI's topical report to METC (Gupta and Gangwal, 1993).

### Scaleup of the Granulation Technique

As discussed previously, the fluidizable zinc titanate sorbents (e.g., ZT-4) prepared by granulation technique exhibited superior performance during long-term testing. These sorbents were pre-

pared in a laboratory-scale granulator of 2-L capacity. In order to prepare large sorbent batches for clean coal demonstration plants, the lab-scale granulator was replaced by a 35-L machine. A number of zinc titanate batches were prepared in this machine with the recipe used in preparation of ZT-4. The ZT-4 formulations prepared in the 35-L machine were designated as ZT-4L ('L' refers to the large machine). A comparison of physical and chemical properties indicated superior attrition resistance and chemical reactivity of ZT-4L sorbent compared to that of ZT-4, indicating successful scaleup as discussed in Gupta and Gangwal (1995).

After the successful scaleup of the granulation process from 2-L to 35-L batches, RTI entered into a subcontract agreement with Contract Materials Processing (CMP), Inc., Baltimore, MD, to produce about 5,000 lb of ZT-4L sorbent using this technique. CMP has extensive experience and facilities for manufacturing relatively large quantities of custom (toll) catalysts and adsorbents for variety of applications.

In the summer 1994, using the same 35-L granulator that was used in the demonstration runs for scaleup, CMP produced about 5,000 lb of ZT-4L at their Baltimore facility. The yield of the sorbent in 100- to 300-µm particle size range was not as good as was expected. Also the attrition resistance of the sorbent was somewhat poorer than the original material. The finer particle size and poor attrition resistance of the ZT-4L batch produced by CMP are attributed to high humidity levels in the summer months in the CMP plant in Baltimore. Humidity plays a vital role in formation of good sorbent particles in the granulator.

A qualitative comparison of physical and chemical properties of these two ZT-4L samples is provided in Table 1. As can be seen, the attrition resistance and yield in the 100- to 300-µm range of the production batch are significantly poor compared to the demonstration batch. However, no significant changes are evident in other physical or chemical properties. In fact, the TGA reactivity of the production batch is superior compared to the demo batch, perhaps due to its higher porosity.

**Table 1. Physical and Chemical Properties of ZT-4L Batches**

| | ZT-4L demonstration run | ZT-4L production run at CMP |
|---|---|---|
| Production time | Winter 1993 | Summer 1994 |
| Batch size | 35 L | 35 L |
| Chemical composition | | |
| $ZnO/TiO_2$ (molar) | 1.5 | 1.5 |
| Bentonite (wt%) | 5 | 5 |
| Presence of additives | No | Yes |
| Free ZnO (wt%) | <2 | <2 |
| Particle density (g/cm$^3$) | 2.06 | 2.30 |
| Bulk density (g/cm$^3$) | 1.37 | 1.36 |
| BET surface area (m$^2$/g) | 3.4 | 3.2 |
| Pore size distribution | | |
| Hg-pore volume (cm$^3$/g) | 0.20 | 0.23 |
| Median pore diameter (Å) | 1,734 | 2,485 |
| Porosity (%) | 40.6 | 54.0 |
| Chemical reactivity | | |
| TGA[a] sulfur capacity (wt%) | 22.5 | 23.2 |
| Regenerability | Good | Fair |
| Attrition resistance (wt%) | | |
| 5-h loss | 17.0 | 38.0 |
| 20-h loss | 51.0 | 84.0 |
| Particle size distribution | | |
| Yield in 100 to 300 µm | 60 | 40 |
| APS[b] determined using a prescreened sample in 100- to 300-µm range | 176 | 172 |
| Fines problem | No | Yes |

[a] TGA = thermogravimetric analysis.
[b] APS = average particle size.

A 2,000 kg (4,400 lb) batch of the production sample was shipped to Enviropower in Finland for testing in their 15-MW pilot plant with actual coal

gas. Also, CMP shipped 200 lb of this sorbent to DOE/METC for testing in the modular gas cleaning rig (MGCR) connected to the METC fluidized-bed gasifier. A 60-lb batch of this sorbent was shipped to Particulate Solids Research (PSRI), Inc., for a loop attrition test.

## Life Cycling Testing of ZT-4L Sorbent

The life cycle testing of the ZT-4L sorbent was carried out using the test conditions shown in Table 2 to demonstrate its long-term chemical reactivity and attrition resistance. The composition of simulated air-blown U-gasifier gas is included in Table 3. Testing was done in a 2-in. diameter reactor with 500 g sorbent. The detailed test procedure is described elsewhere (Gupta et al., 1994; Gupta and Gangwal, 1995). The sorbent was subjected to alternating periods of sulfidation and regeneration.

**Table 2. Nominal Test Conditions**

| | |
|---|---|
| **Sulfidation** | |
| Sorbent | ZT-4L |
| Temperature | 600 °C (1,112 °F) |
| Pressure | 20 atm (294 psia) |
| Particle size | 100 to 300 μm (APS = 172 μm)[a] |
| Sorbent inventory | 500 g |
| Total gas flow rate | 75 std L/min (159 std $ft^3/h$) |
| Superficial gas velocity | 9.86 cm/s (0.32 ft/s) |
| Sulfidation gas | Simulated U-Gas gasifier gas[b] |
| $H_2S$ content of coal gas | 5,000 ppmv (0.5 mol%) |
| Reactor tube diameter | 5.08 cm (2-in.) ID |
| **Regeneration** | |
| Initiation temperature | 650 to 700 °C (1,202 to 1,292 °F) |
| Pressure | 20 atm (294 psia) |
| Total gas flow rate | 75 std L/min (159 std $ft^3/h$) |
| Regeneration gas | 2 to 2.5 mol% $O_2$ in $N_2$ |

[a] Average particle size (APS) is calculated as harmonic mean.
[b] Gas composition is specified in Table 3.

**Table 3. Nominal Gas Composition of the Simulated U-Gas**

| Component | Vol% |
|---|---|
| $H_2$ | 14.2 |
| $CO_2$ | 5.8 |
| $H_2O$ | 6.6 |
| $H_2S$ | 0.5 (5,000 ppmv) |
| $N_2$ | 49.8 |
| CO | 23.1 |
| Total | 100.0 |

Initially 18 sulfidation-regeneration cycles were successfully completed. During startup for the 19th sulfidation, the pressure drop across the bed increased to 50-in. of $H_2O$ with very poor fluidization. At this point, the reactor was cooled down and opened up. The reacted sorbent removed from the reactor had formed agglomerates and was yellowish in color. About 21 g of the sorbent was stuck to the alumina distributor and was removed by scrapping. The Inconnel thermocouple underwent delapidation as its size increased from 1/8-in. to about 1/4-in. It is suspected that some metal compounds (presumably Ni compounds) in the Inconnel thermocouple used in the reactor reacted with the sorbent forming inert compounds in the pore structure, thus reducing the surface area and pore volume. This theory was corroborated with chemical analysis results of the particles that were scrapped from the thermocouple surface. it is quite plausible that the actual temperature was 50 to 100 °C higher than that detected by the thermocouple, which would explain excessive sintering of the sorbent. Details of the test results for this 18-cycle test are described in Gupta and Gangwal (1995).

## The 40-Cycle Test with ZT-4L

As noted above, the 18-cycle test that was carried out was repeated to obtain long-term chemical activity and mechanical strength data. The repeat test consisted of 40 sulfidation-regeneration cycles under the conditions listed in Tables 2 and 3. Additionally, to avoid temperature excursion problems, in addition to the two main thermocouples, additional thermocouples were inserted in the sorbent bed. The run was stopped after 25 cycles and the reactor was opened. A sample of 25-cycle reacted sorbent was removed for characterization. Cycles 26 to 40 were carried out with 400 g of sorbents in the cage. A detailed description of test results for this run is provided below.

Figure 1 shows the $H_2S$ breakthrough curves for selected cycles. As can be seen from Figure 2, during the first 10 cycles no change in sorbent activity is evident. However, in the subsequent cycles, chemical reactivity of the sorbent gradually declined.

From the breakthrough data, the sulfur capture capacity of the sorbent was calculated for Cycles 1 to 40. Figure 2 shows the actual sulfur picked up by the sorbent as a function of cycle number at breakthrough—500 ppmv $H_2S$ in the reactor outlet gas. During the first 10 cycles, the average sulfur capacity was 23.35 g S/100 g of the

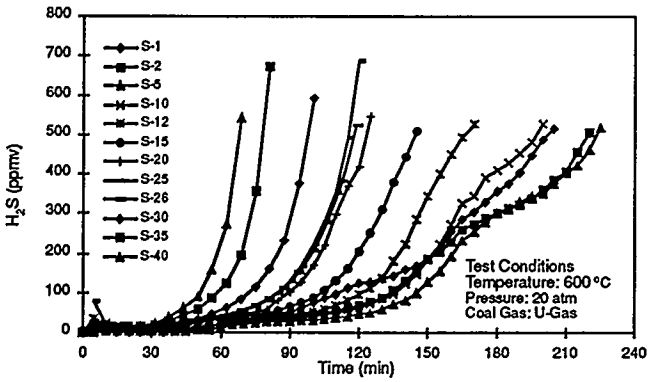


**Figure 1. Breakthrough behavior of ZT-4L sorbent during selected cycles.**

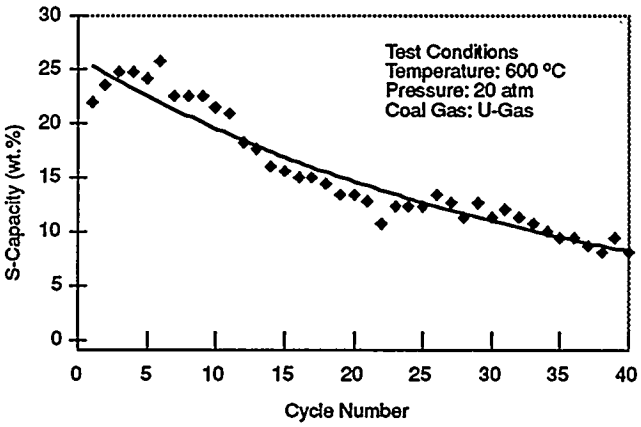


**Figure 2. Sulfur capacity of the ZT-4L sorbent for Cycles 1 to 40.**

fresh sorbent, indicating nearly complete capacity utilization. As noted previously, a gradual decline in the capacity was observed thereafter. The sulfur capacities of the sorbent during the 25th and 40th cycles were 12.32 and 8.03 g S/100 g fresh sorbent, respectively. The average capacities over the first 25 cycles and the entire 40 cycles were 18.14 and 15.31 g S/100 g of fresh sorbent, respectively.

Figure 3 shows the temperature profiles for selected regeneration cycles. As expected, similar to breakthrough curves, these temperature profiles shift to the left, indicating less time taken for regeneration resulting from gradual decline in sulfur pickup during sulfidation.

The $SO_2$ evolution profiles for selected cycles are shown in Figure 4. Similar to temperature profiles shown in Figure 3, $SO_2$ profiles also gradually shift toward the left, indicating gradual degradation in the sorbent performance. However, the shape of these curves remains unchanged, indicating good regenerability despite decline in the chemical reactivity.

Initially 500 g of the prescreened (in 100- to 300-μm particle size range) sorbent was loaded in the reactor. After the 25th regeneration, the

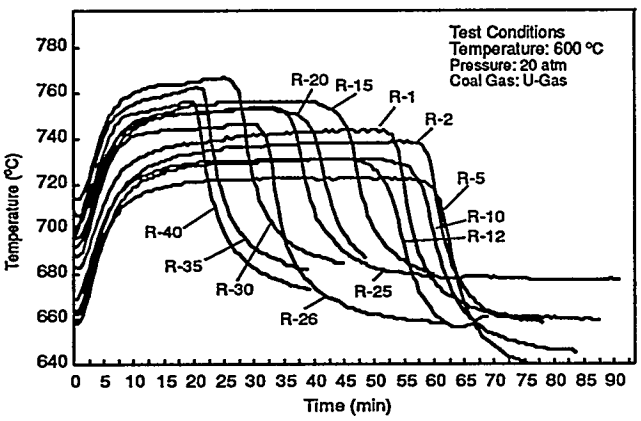


**Figure 3. Temperature profiles during selected regeneration cycles.**

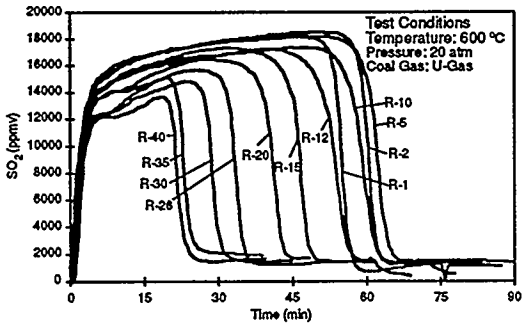


**Figure 4. $SO_2$ evolution profiles during selected regeneration cycles.**

reactor was cooled and dismantled to remove the sorbent. After removal of the sorbent, inside reactor walls, regeneration and sulfidation lines and filters, thermocouples, and distributor were examined for particle buildup. The primary thermocouple that was immersed in the sorbent bed had a considerable amount of deposit on the first 5-in. of the length from the tip. Visually these deposits appeared to be fine dust particles stuck together like a ceramic coating, presumably due to metal corrosion and interaction of thermocouple metals with the sorbent.

The weight of the sorbent removed from the reactor was 496.2 g. Some sorbent agglomeration did occur, but unlike the 18-cycle run, these agglomerates were fairly soft and broke during gentle screening through a 50-mesh screen. Out of 496.2 g of the sorbent, 481.5 g was below 50 mesh. Out of these, 400 g of the sorbent was loaded in the reactor and 81.5 g was kept for characterization. Sulfidation filter had a 2.2 g deposit, while the regeneration filter had 1.5 g of the particle deposits.

Cycles 26 to 40 were continued with 400 g of the sorbent. No change in coal gas flow rate was made; as a result, the breakthrough time reduced by 80 percent as noted previously. At the end of the 40th regeneration, the reactor was opened, and 395.1 g of the sorbent were recovered from the reactor. No agglomerates were found in the sorbent this time. The sulfidation filter had a 0.2 g deposit, while 5.0 g of sorbent deposited on the regeneration filter.

Table 4 shows the material balance of the sorbent over the 40 cycles. The net sorbent loss

**Table 4. Sorbent Material Balance for Cycles 1 to 40**

| | |
|---|---|
| **Initial** | |
| Initial sorbent charge | 500 g |
| **After 25 Cycles** | |
| Sorbent removed from the cage | 496.2 g |
| Collected from sulfidation filter | 2.2 g |
| Collected from regeneration filter | 1.5 g |
| Total accounted | 499.9 g |
| Net loss over 25 cycles | 0.1 g |
| Sorbent loaded | 400 g |
| **After 40 Cycles** | |
| Sorbent removed form the cage | 395.1 g |
| Sorbent collected from sulfidation filter | 0.2 g |
| Sorbent collected from regeneration filter | 5.0 g |
| Total accounted | 400.3 g |
| Net loss | (0.3) g |

from the reactor was zero. Excluding the sorbent deposited on the filters, the gross sorbent loss was about 2 percent, indicating good attrition resistance of this material.

Table 5 shows a comparison of various physical and chemical properties of the fresh, 25-cycle reacted and 40-cycle reacted sorbent. Over 40 cycles of testing, sorbent underwent significant changes in the properties corroborating the capacity decline. The average particle size reduced by 12 percent over 25 cycles and by 19 percent over 40 cycles, indicative of gradual shrinkage of the particles with cycling possibly associated with internal structural changes.

**Table 5. Physical and Chemical Characterization of Fresh, 25-Cycle Reacted and 40-Cycle Reacted ZT-4L Sorbent**

| | Fresh | 25-Cycle Reacted | 40-Cycle Reacted |
|---|---|---|---|
| Particle size distribution (wt%) | | | |
| MESH | | | |
| + 50 | 0.0 | 0.0 | 0.0 |
| - 50 + 60 | 20.0 | 2.7 | 0.0 |
| -60 + 80 | 34.9 | 37.7 | 32.5 |
| - 80 + 100 | 15.1 | 19.7 | 17.8 |
| - 100 + 120 | 18.7 | 20.0 | 18.1 |
| - 120 + 140 | 11.3 | 12.7 | 14.8 |
| - 140 | 0.0 | 7.3 | 16.8 |
| Total | 100.0 | 100.0 | 100.0 |
| Average particle size (μm) | 178 | 157 | 144 |
| BET surface area ($m^2/g$) | 3.2 | 2.33 | 2.02 |
| Pore size distribution | | | |
| Mercury pore volume ($cm^3/g$) | 0.2341 | 0.0961 | 0.0653 |
| Median pore diameter (Å) | 2,495 | 1,126 | 848 |
| Porosity (%) | 55 | 48 | 31 |
| Compacted bulk density ($lb/ft^3$) | 91.6 | 112.0 | 129.3 |
| Attrition resistance (%) | | | |
| 5-h loss | 38.0 | 0.6 | 0.4 |
| 20-h loss | 84.0 | 7.2 | 5.8 |
| XRD[a] phases | $Zn_2Ti_3O_8$, $Zn_2TiO_4$, and traces of $TiO_2$ and $ZnTiO_3$ | $Zn_2Ti_3O_8$ and $Zn_2TiO_4$ | $Zn_2Ti_3O_8$ |
| ICP[b] analysis (wt%) | | | |
| Zn | 42.7 | 41.6 | 41.6 |
| Ti | 23.0 | 22.6 | 20.6 |

[a] XRD = x-ray diffraction.
[b] ICP = inductively coupled plasma.

As expected, the BET surface area dropped by 37 percent over 40 cycles. However, this drop in surface area cannot explain the entire capacity decline. In RTI's previous study, it was found that BET surface area decline linearly correlates the capacity drop (Gupta and Gangwal, 1993). There had to be some other factors for such drastic decline in the capacity as will be discussed later. Comparison of the TGA reactivities of fresh and reacted sorbent samples confirmed the reactivity loss observed in the bench unit (Gupta and Gangwal, 1995).

The pore size distribution data indicated a rather unexpected drop in pore volume and median pore diameter. A good correlation was found between the drop in pore diameter and capacity decline. This indicates formation of inert unreactive species inside the pores of the sorbent.

Decline in the pore volume resulted in the decrease in sorbent's internal porosity and increase in compacted bulk density. As a result, the attrition resistance of the sorbent increased at least by an order of magnitude.

ICP analysis indicated very little, if any, changes in zinc and titanium content of the sorbent, showing no zinc loss due to ZnO reduction followed by vaporization despite the highly reducing nature of the coal gas.

The decrease in surface area did not completely explain the drop in sulfur capacity as discussed in the previous section. Furthermore, decline in median pore diameter and pore volume provided a good correlation with capacity decline. These two factors suggest formation of inert compounds inside the pores. XRD analysis of the 40-cycle reacted sorbent did not indicate any extraneous peaks, perhaps because of very small concentration of these inert compounds. To further investigate this, a complete inductively coupled plasma (ICP) scan was performed on the fresh, 25-cycle, and 50-cycle reacted zinc titanate sorbent samples. This completely automated ICP scan detects 16 elements in the sample as shown in Table 6.

A comparison of concentrations of various elements indicates a significant increase in the concentration of Ni and a modest increase in the Mo concentration. The Ni concentration increased from 10.3 to 523 ppmw after 25 cycles and 915 ppmw after 40 cycles. It is plausible that interaction of Ni with the zinc titanate sorbent is partially responsible for the capacity decline of the sorbent.

## Independent Testing of ZT-4L

The Institute of Gas Technology (IGT) tested the ZT-4 sorbent for 10 sulfidation-regeneration cycles. These test results released by IGT on this sorbent have been reported in RTI's topical report (Gupta and Gangwal, 1993). In general, this sorbent exhibited excellent performance, both in terms of chemical reactivity as well as attrition resistance at IGT.

**Table 6. ICP Scan of Fresh and Reacted Samples**

| Element | Fresh (ppmw) | 25-Cycle Reacted (ppmw) | 40-Cycle Reacted (ppmw) |
|---|---|---|---|
| Al | 16,600 | 16,600 | 19,100 |
| Ba | 12.7 | 23.0 | 20.2 |
| Be | 1.37 | 1.47 | 2.26 |
| Cd | 10.6 | <5.0 | <5.0 |
| Cr | <10.0 | 22.8 | <10.0 |
| Cu | <15 | <15 | <15 |
| Fe | 1,280 | 2,120 | 1,540 |
| Pb | <30 | 32.6 | <30 |
| Mg | 826 | 838 | 937 |
| Mn | 4.19 | 20.1 | 10.9 |
| Mo | 45.4 | 77.1 | 89.2 |
| Ni | 10.3 | 523 | 915 |
| Sr | 14.8 | 16.3 | 15.8 |
| V | 192 | 188 | 189 |

Testing of this sorbent in Enviropower's 15-MW pilot plant with actual coal gas indicated that the sorbent was able to remove the total sulfur content of coal gas from an inlet value of 500 to 550 ppmv to 5 to 40 ppmv over a 22-h stable operation at a temperature of 450 °C. Due to some problems in screening the sorbent at CMP, some fines were present in the sorbent which escaped during the operation at Enviropower. Besides this, the ZT-4 sorbent exhibited good performance with actual coal gas despite a low operating temperature.

This sorbent was also tested with actual coal gas from the METC fluidized-bed gasifier and Coal Technology Development Division (CTDD) in England. At METC, the ZT-4 consistently removed $H_2S$ from coal gas down to <20 ppmv at 600 °C (1,112 °F) and 1.89 MPa (260 psig) over three cycles of operation. Tests at CTDD showed that at 525 °C and 10 atm, this sorbent was able to reduce the $H_2S$ content of coal gas from 1,500 ppmv to <10 ppmv in an actual coal gas stream generated from a pilot-scale gasifier. The gas composition of the fuel gas in CTDD runs was similar to that of an air-blown fluidized-bed gasifier. Furthermore, CTDD could regenerate this sorbent at 600 °C using about 2 percent oxygen in nitrogen without any sulfate formation.

This sorbent was independently tested for its attrition properties at PSRI in a loop attrition test simulating an industrial fluidized-bed system. PSRI reported that the attrition resistance of this sorbent was better than a commercial fluid catalytic cracking (FCC) catalyst used in petroleum refineries (Gupta and Gangwal, 1995).

### Developments of Sorbents by Spray Drying

RTI and CMP are jointly developing zinc titanate sorbents by spray drying. One of the superior spray-dried formulation CMP-5 was tested in RTI's HTHP bench unit. This sorbent exhibited excellent performance in the bench-scale tests. Currently, RTI and CMP have successfully produced larger size (100 to 300 µm) zinc titanate particles by spray drying. This sorbent formulation is currently being tested at the M.W. Kellogg Company in their transport reactor test unit. The details of the development and testing of spray-dried sorbents are described in a separate paper entitled "Spray Dried Sorbents—CMP-5," included in this proceedings volume.

## FUTURE WORK

Future work in this contract is focussed on the testing of spray-dried sorbents at RTI and M.W. Kellogg.

## REFERENCES

Gupta, R., and S.K. Gangwal. 1991. "Enhanced Durability of Desulfurization Sorbents for Fluidized Bed Applications." Topical Report to DOE/METC. Report No. DOE/MC/25006-3011. U.S. Department of Energy/Morgantown Energy Technology Center. Morgantown, WV. NTIS/ DE91002090. June.

Gupta, R., S.K. Gangwal, and S.C. Jain. 1992. "Development of Zinc Ferrite Sorbents for Desulfurization of Hot Coal Gas in a Fluid-Bed Reactor." *Energy and Fuels* 6:21-27.

Gupta, R., and S.K. Gangwal. 1992. "Enhanced Durability of Desulfurization Sorbents for Fluidized-Bed Applications—Development and Testing of Zinc Titanate Sorbents." Topical Report to DOE/METC. Report No. DOE/MC/ 25006-3271. U.S. Department of Energy/Morgantown Energy Technology Center. Morgantown, WV. November.

Gupta, R., and S.K. Gangwal. 1993. "High-Temperature, High-Pressure Testing of Zinc Titanate in a Bench-Scale Fluidized-Bed Reactor for 100 Cycles." Topical Report to DOE/METC. Contract No. DE-AC21-88MC25006. June.

Gupta, R., and S.K. Gangwal. 1995. "Multicycle Testing of ZT-4L Sorbent." Topical Report to DOE/METC. Contract No. DE-AC21-88MC 25006. U.S. Department of Energy/Morgantown Energy Technology Center. Morgantown, WV. June.

Gupta, R. et al. 1993. "Fluidizable Zinc Titanate Materials With High Chemical Reactivity and Attrition Resistance." U.S. Patent No. 5,254,516. October 19.

Mei, J.S., L.D. Gasper-Galvin, C.E. Everitt, and S. Katta. 1993. Fixed Bed Testing of a Molybdenum-promoted Zinc Titanate Sorbent for Hot Gas Desulfurization. In *Proceedings of the Coal-fired Power Systems 93—Advances in IGCC and PFBC Review Meeting*. p. 315. DOE/METC–93/6131. NTIS/DE 93000289. Springfield, VA: National Technical Information Service.

## 4.6 Pilot Plant Tests of Z-Sorb™ Sorbent

### CONTRACT INFORMATION

| | |
|---|---|
| **Contract Number** | N/A |
| **Contractor** | Phillips Petroleum Company |
| **Other Funding Sources** | N/A |
| **Contractor Project Manager** | N/A |
| **Principal Investigators** | G. J. Greenwood<br>G. P. Khare<br>D. H. Kubicek<br>G. A. Delzer<br>D. L. Kinsinger |
| **METC Project Manager** | N/A |
| **Period of Performance** | N/A |

---

### OBJECTIVES:

The objective of this work is to determine the long-term chemical reactivity and mechanical durability of Phillips Petroleum Company's (PPCo's) proprietary Z-Sorb™ sorbent. Materials developed for fixed-, moving- and fluid bed desulfurization of coal derived gases at high pressure (5-20 atm) and moderate operating temperatures (600-1000°F) will be discussed.

### BACKGROUND:

Z-Sorb™ sorbent is a regenerable absorbent for hydrogen sulfide. It is based on zinc oxide supported in a porous matrix and contains a nickel oxide promoter. Originally, it was developed for tail gas cleanup (Brinkmeyer and Delzer, 1990), but recently it has been tested for removal of hydrogen sulfide from fuel gas that is generated in a clean coal process. For the latter technology, previous fixed-bed sorbents have shown poor mechanical stability due to spalling when absorbing hydrogen sulfide in reducing gas atmospheres or when being regenerated over many cycles (Mei et al., 1993).

In an ongoing sorbent research and development program, Phillips Petroleum Company has developed sorbents that would fulfill the requirements of long term sorbent reactivity, chemical/mechanical stability and attrition resistance. Sorbents developed to fulfill a variety of client needs will be the subject of this paper.

**PROJECT DESCRIPTION:**

Project participants working with Phillips in this study have been the M. W. Kellogg Company, General Electric (GE), Research Triangle Institute (RTI), Morgantown Energy Technology Center (METC) and members of the European Coal and Steel Community (ECSC). All of the materials used in this study were prepared at Phillips Petroleum Catalysts Development Center with the exception of materials used in the General Electric Moving Bed Pilot Plant which were manufactured by Calsicat.

Fixed bed testing of Z-Sorb™ sorbent at METC showed excellent desulfurization activity and durability (Campbell et al., 1993). Pressure drop readings across the bed were very low both for absorption and for regeneration. This showed that there was little swelling of the extrudate during its sulfided state, and that there was no break-up of the extrudate as it was being cycled. Over a wide range of experimental conditions there was no detectable loss of zinc from the sorbent. Break through curves were found to be independent of absorption temperatures in the range of 900-1100°F. High temperature steam regenerations (1400°F) caused a decrease in sulfur loading capacity.

The fluidized version of Phillips proprietary Z-Sorb™ III sorbent was prepared by Phillips Corporate Technology. The sorbent used in these studies had an average particle size of 175 $\mu$m, a particle size range of 50-300 $\mu$m and an apparent bulk density of 0.90-1.00 g/cc. The sorbent manufacturing process has been demonstrated for 100-lb batch sizes and has been scaled to provide commercial quantities.

For a moving-bed test, a spherical sorbent with average pellet diameter of 4.1 mm and bulk density of 0.96 g/cc was used. This sorbent was manufactured in commercial equipment and 24,000 lb have been prepared. The moving-bed and fluidizable sorbents are commercially available through Phillips licensed/certified manufacturers Calsicat and United Catalysts Inc. (UCI).

**RESULTS:**

Information obtained from fixed-, fluid and moving bed testing of Z-Sorb™ sorbent under a variety of simulated and authentic coal gases as well as various reactor configurations has revealed a number of facts concerning the sorbent. It is evident that this sorbent has a high chemical reactivity for sulfur capture at relatively low operating temperatures of 700-1000°F (370-450°C) (Gangwal et al. 1994; ECSC Progress Report, 1994; Khare et al., 1994). Experimental details for the 50 cycle (sulfidation and regeneration) long term testing of the sorbent are described elsewhere (Gupta and Gangwal, 1993; Gangwal et al. 1994. This gas composition for these tests was a simulated air-blower U gasifier gas, shown in Table 1. Results of the sulfidation runs, which were conducted at 294 psia and 1000°F (540°C) using 5000 ppm $H_2S$ in the feed are shown in Figure 1. The sulfur loading was constant for the first ten cycles with breakthrough occurring in 175 minutes (500 ppm $H_2S$ in effluent). Estimation of sorbent utilization indicated that essentially 100 percent of the sorbent theoretical loading capacity was utilized over the first 10 cycles. Another interesting feature for this sorbent was its high efficiency for sulfur removal manifested in complete removal of $H_2S$ (to nearly zero ppm) for the first 70 percent of each cycle prior to breakthrough.

## TABLE 1

Gas Composition for the Fluidized Bed Test at RTI

| Component | Vol % |
|---|---|
| $H_2$ | 14.2 |
| $H_2S$ | 0.5 (5000 ppmv) |
| CO | 23.1 |
| $CO_2$ | 5.8 |
| $N_2$ | 49.8 |
| $H_2O$ | 6.6 |

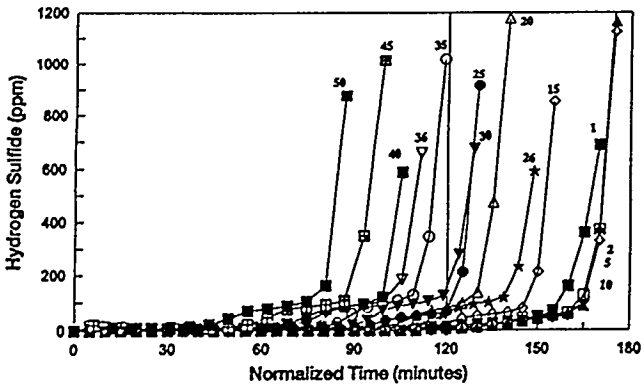


Figure 1. Breakthrough Behavior of Z-SORB III Sorbent U-Gas; 20 atm; 538 °C (1,000 °F)

The sulfided sorbent removed from the reactor after 25 cycles was reloaded in the reactor after being stored for about 6-7 weeks to complete necessary analyses. The amount of sorbent reloaded was 20 percent less than the initial start-of-the-run loading; therefore, the feed gas flow rate was reduced by 20 percent for cycles 26-35, i.e., from 75.0 to 60.0 slpm. The initial regeneration (No. 25) was successful and the sorbent reactivity in the 26th cycle was actually higher than what was observed prior to reactor unloading. After the next several cycles of operation, it became evident that the gas flow rate of 60 slpm was not quite enough to achieve a good quality fluidization of the reactor content; therefore, starting at cycle 36 the gas flow rate was restored to 75 slpm. This change resulted in smoother cycling. The sorbent performance remained quite high after 50 cycles of operation.

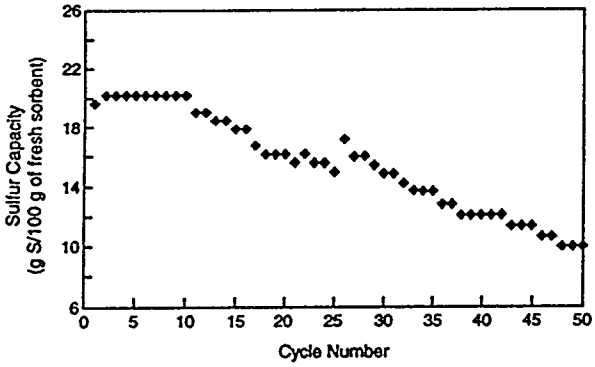


Figure 2. Sulfur Capacity of Z-SORB III Sorbent U-Gas; 538 °C (1,000 °F);20 atm; 500 ppm Breakthrough.

The sulfur capacities of the sorbent during cycles 1 and 50 were 20.2 and 10.0 g S/100 g of sorbent, respectively, indicating about a 50 percent capacity utilization even after 50 cycles. In Figure 2, the sulfur capacity (g of S pickup per 100 g of sorbent) is plotted as a function of cycle number. Sulfur capacity is calculated using the concentration of $H_2S$ in feed, breakthrough time and the amount of sorbent used. Actual sulfur chemical analyses after 25 and 50 cycles closely supported the calculated capacity.

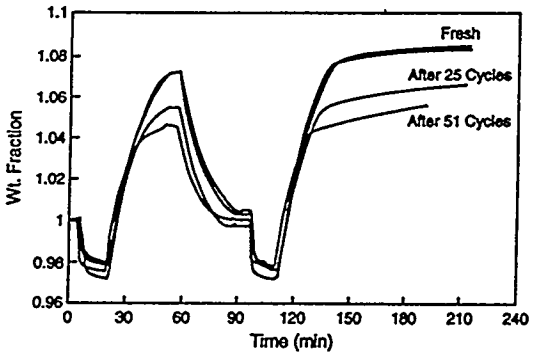


Figure 3. TGA Reactivity of Fresh and Reacted Z-SORB Sorbent

As mentioned previously, the sorbent for the desulfurization application must have high chemical reactivity. The chemical reactivity is measured by the total sulfur loading capacity as well as the rate of sulfur absorption. In order to measure the latter, standard 1.5-cycle TGA reactivity tests described in Gupta and Gangwal (1992) were carried out for fresh, and 25- and 50-

cycle used sorbent. Figure 3 depicts both the saturation (indicated by the maximum weight gain during the second cycle) and the rate of sulfur pickup (indicated by the slope of the sulfidation curve). While this figure shows that saturation sulfur pickup decreases with increasing number of cycles as expected and observed for conventional desulfurization sorbents, an unusual feature unique to Z-Sorb™ sorbent emerges in that the rate of sulfur pickup for 25- and 50-cycle used sorbent remained relatively constant even though the capacity has dropped. This observation has also been substantiated in single pellet TGA tests performed by GE on sample of Z-Sorb™ sorbent used in the moving bed reactor (Ayala).

**TABLE 2**

Lab A Gas Composition (Simulated Shell-Type Coal Gas)

| Component | Vol% |
|---|---|
| $H_2$ | 28.5 |
| CO | 58.9 |
| $CO_2$ | 2.2 |
| $H_2O$ | 5.0 |
| $N_2$ | 3.3 |
| $H_2S$ | 1.0 |

| Lab A Reactor Conditions | |
|---|---|
| Sulfidation Temperature | 750°F |
| Regeneration Temperature | 1112°F |
| Pressure | 20 atm (294 psia) |
| Sorbent Particle Size | 100-300 $\mu$m |
| Sorbent inventory | 40 g |
| Gas Flow | 560 ml/mm |
| Sorbent Bed Dimension | 10.2 mm x 50 mm |

Similar results have been obtained by fluid bed testing of Z-Sorb™ sorbent in Europe. Table 2 lists the simulated coal gas composition and reactor conditions for the test. Results of sulfur pickup at 750°F for eight cycles is shown in Table 3. The ninth cycle was run at 660°F to determine capacity roll off with lower sorption temperature. This data appears to be consistent with performance observed at RTI. It should be noted that both tests were run at 20 atm.

**TABLE 3**

Lab A Absorptions with Simulated Shell-Type Coal Gas

| Absorption | Temp (°F) | S-Pickup (wt%) |
|---|---|---|
| 1 | 750 | 20.3 |
| 2 | 750 | 16.6 |
| 3 | 750 | 17.8 |
| 4 | 750 | 18.1 |
| 5 | 750 | 17.8 |
| 6 | 750 | 16.8 |
| 7 | 750 | 17.8 |
| 8 | 750 | 17.6 |
| 9 | 660 | 15.4 |

Pilot plant testing of Z-Sorb™ sorbent in GE's moving bed pilot plant was conducted from May 1994 to May 1995. Detailed discussions of test conditions have been presented previously (Bevan et al. 1994). Three long duration tests (280 hours) at GE have confirmed the high activity of Z-Sorb™ sorbents for hot gas desulfurization. Pilot plant data also shows high sulfur removal efficiency of 98-99 percent, leading to consistent $H_2S$ levels of less than 50 ppm in the outlet stream for loadings of 20-30%, very low levels of sulfate accumulation (<0.5 percent) and very low attrition losses. Testing at GE has provided insight into the effects of tars, steam, sodium and temperature on the performance of the sorbent.

Fixed bed testing of Z-Sorb™ sorbent in Europe, Table 4, with authentic coal gas at 10 atm using both high and low sulfur loadings suggest Z-Sorb™ sorbent to be more steam stable than data obtained under GE pilot plant conditions.

**TABLE 4**

Lab B Gas Composition

| Component | Vol % |
|---|---|
| $H_2$ | 12.2 - 13.3 |
| CO | 12.9 - 13.6 |
| $CO_2$ | 8.2 - 9.3 |
| $H_2O$ | 8.5 - 20.2 |
| $N_2$ | 56.8 - 41.9 |
| $CH_4$ | 1.4 - 1.7 |

| Conditions | Run 1 | Run 2 |
|---|---|---|
| Inlet Temp. (°F) | 995 | 995 |
| Bed Temp. (°F) | 986-1256 | 986-1256 |
| Pressure (atm) | 10.5 | 10.5 |
| Space Velocity ($h^{-1}$) | 3300 | 3300 |
| Inlet $H_2S$ (ppm) | 1700-1900 | 200-400 |
| Outlet $H_2S$ (ppm) | <10 | N/D |
| Sulfur Capacity | 10.5 | 10.5[1] |

| | |
|---|---|
| Regeneration Temp. (°F) | 1076-1346 |
| Pressure (atm) | 7 |
| Oxygen Concentration | 1.4 |

a. Calculated by extrapolating final bed S profile to breakthrough.

## FUTURE WORK

We have earlier noted the adverse effect of steam regenerations at high temperatures (1400°F) on Z-Sorb™ III sorbent. Phillips has undertaken an R&D program to develop enhanced steam resistant sorbents. The bench scale test results of one new fluid bed formulation at atmospheric pressure and 1000°F temperature are shown in Figure 4. The activity of a new formulation, Z-Sorb™ IV, and Z-Sorb™ III sorbent are compared. It is evident from this data that Z-Sorb™ IV sorbent does not show any sulfur loading capacity loss when regenerated in air diluted with 42 vol% steam at 1200°F. At 1400°F, however, there is a 30% loss in capacity, but the residual capacity is still very high, estimated to be 16-17 wt% sulfur, in contrast to the Z-Sorb™ III where a similar treatment resulted in a capacity of only about 6 wt%.

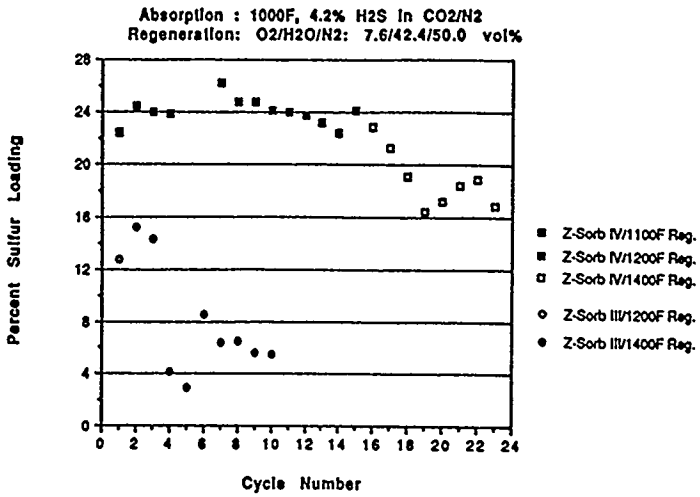


FIGURE 4. Sulfur Loading of Fluidized Bed Z-Sorb™ IV Sorbent

Efforts are in progress to pelletize the formulation for applications in fixed and moving bed reactor systems.


## ACKNOWLEDGMENTS:

The authors would like to thank researchers at M. W. Kellogg, Research Triangle Institute and General Electric for many helpful discussions and the support and encouragement of METC.


## REFERENCES


F.M. Brinkmeyer and G.A. Delzer. Z-Sorb - A New Sulfur Removal Process, National Meeting of the AIChE, Session 28, Tail Gas Treatment, Paper 28d, San Diego, August 1990.

J.S. Mei, L.D. Gasper-Galvin, C.E. Everitt, and S. Katta, 1993. Fixed Bed Testing of a Molybdenum - promoted Zinc Titanate Sorbentfor Hot Gas Desulfurization. In Proceedings of the Coal-fired Power Systems 93 -- Advances in IGCC and PFBC Review Meeting, p. 315. DOE/METC - 93/6131.NTIS/DE 93000289. Springfield, VA: National Technical Information Service.

W.M. Campbell, J.J. O'Donnell, S. Katta, T. Grindley, G.A. Delzer, and G.P Khare, 1993. Desulfurization of Hot Fuel Gas with Z-Sorb III Sorbent. In Proceedings of the Coal-fired Power Systems 93 -- Advances in IGCC and PFBC Review Meeting, p. 79. DOE/METC - 93/6131. NTIS/DE 93000289. Springfield, VA: National Technical Information Service.

G.A. Delzer, G.P. Khare, and G.J. Greenwood, 1993. Z-Sorb Absorbent for Hot Gas Desulfurization, AIChE Annual Meeting, Symposium on Gas Purification, Session 130; St. Louis, Missouri, November 7-12.

S.K. Gangwal, R.P. Gupta, G.P. Khare, G.A. Delzer and D.H. Kubicek, 1994. Fluidization Studies Using Phillips Z-Sorb Sorbent. In Proceedings of the Coal-fired Power Systems 94 -- Advances in IGCC and PFBC Review Meeting, p. 654, DOE/METC-94/1008. NTIS/DE94012252. Springfield, VA: National Technical Service.

European Coal and Steel Community, Annual Meeting June 1994, Cheltenham, England. Private Communication.

G.P. Khare, G.A. Delzer, D.H. Kubicek and G.J. Greenwood. 1994. Hot Gas Desuflurization with Phillips Z-Sorb Sorbents, Presented at the AIChE Annual Meeting, Symposium on Gas Purification, No. 247e. San Francisco, California November 13-18.

R.P. Gupta and S.K. Gangwal, 1993. High Tempertaure, High-Pressure Testing of Zinc Titanate in a Bench-Scale Fluidized-Bed Reactor for 100 Cycles. Topical Report to DOE/METC. Contract No. DE-AC21-88MC 25006. June.

R. Ayala unpublished data.

S. Bevan, D. Najewicz, E. Gal, A.H. Furman, R. Ayala and A. Feitelberg, 1994. Integrated Operation of a Pressurized Gasifier, Hot Gas Desulfurization System and Turbine Simulator. In Proceedings of the Coal-Fired Power Systems 94 -- Advances in IGCC and PFBC Review Meeting. p. 222, DOE/METC - 94/1008. NTIS/DE 94012252. Springfield, VA: National Technical Service.

# Session 5

## *Fuel Gas Combustion*

# 5.1 Fuel Gas Combustion Research at METC

Thomas S. Norton
Morgantown Energy Technology Center

**ABSTRACT**

The in-house combustion research program at METC is an integral part of many METC activities, providing support to METC product teams, project managers, and external industrial and university partners. While the majority of in-house combustion research in recent years has been focussed on the lean premixed combustion of natural gas fuel for Advanced Turbine Systems (ATS) applications, increasing emphasis is being placed on issues of syngas combustion, as the time approaches when the ATS and coal-fired power systems programs will reach convergence.

When the METC syngas generator is built in 1996, METC will have the unique combination of mid-scale pressurized experimental facilities, a continuous syngas supply with variable ammonia loading, and a team of people with expertise in low-emissions combustion, chemical kinetics, combustion modeling, combustion diagnostics, and the control of combustion instabilities. These will enable us to investigate such issues as the effects of pressure, temperature, and fuel gas composition on the rate of conversion of fuel nitrogen to NOx, and on combustion instabilities in a variety of combustor designs.

In this paper, several achievements from recent combustion research activities at METC will be presented, including:

- construction and shakedown of a combustor test rig capable of operating at pressures up to 30 atm and firing rates up to 3 MWth (10 MMBTU/hr).
- testing of pressure effects on a novel dry low-NOx combustor, as part of a Cooperative Research and Development Agreement (CRADA) with Alzeta Corporation.
- modeling (FLUENT code) of the Multi-Annular Swirl Burner topping combustor, as part of a CRADA with Westinghouse Corporation.
- testing of novel schemes for controlling combustion instabilities in lean premixed systems, and development of a theoretical understanding of these phenomena.

In addition, our plans for future work on fuel gas combustion issues will be discussed, and an update on the status of the METC syngas generator will be given.

## 5.2 Performance of Low Btu Fuel Gas Turbine Combustors

### CONTRACT INFORMATION

| | |
|---|---|
| **Contract Number** | DE-AC21-87MC23170 |
| **Contractor** | GE Environmental Services, Inc.<br>200 N. Seventh St.<br>Lebanon, PA 17042<br>(717) 274–7000 |
| **Contractor Project Manager** | Stephen Bevan |
| **Principal Investigators** | John H. Bowen, GE Corporate Research and Development<br>Alan S. Feitelberg<br>Stephen L. Hung<br>Michael A. Lacey<br>Kenneth S. Manning |
| **METC Project Manager** | Justin L. Beeson |
| **Period of Performance** | September 30, 1987 to September 30, 1995 |

**Schedule and Milestones**

**Program Schedule**

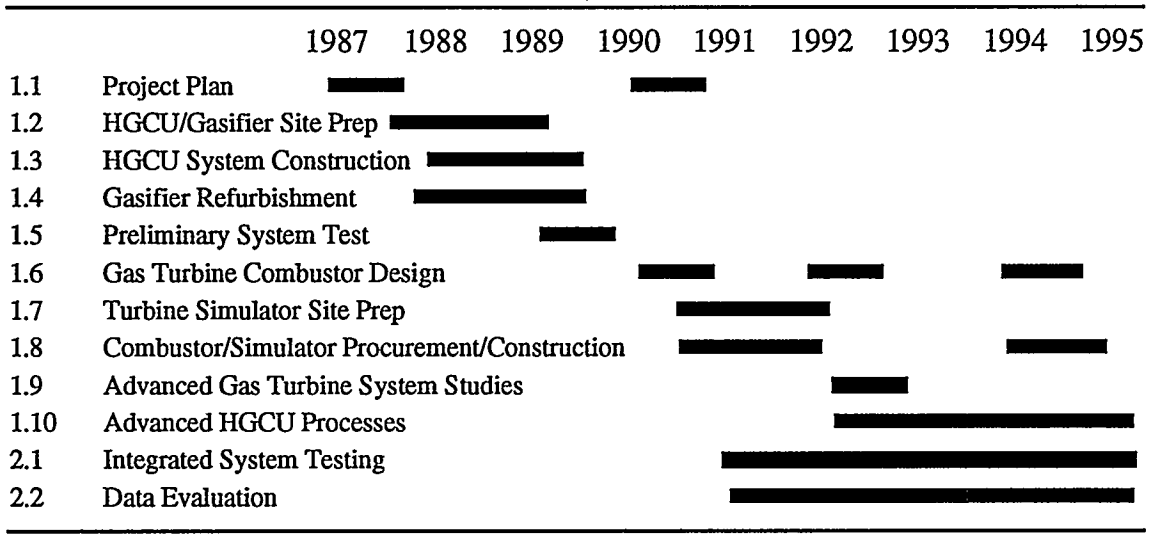

## OBJECTIVES

General Electric Company is developing and testing low Btu fuel gas turbine combustors for use in integrated gasification combined cycle (IGCC) power generation systems. Conducting low Btu fuel combustion tests in the turbine simulator located at GE Corporate Research and Development is a significant portion of this effort. The primary objective of recent turbine simulator tests has been to compare and contrast the performance of several different low Btu fuel nozzle designs. Parameters related to fuel nozzle performance include: (1) emissions of CO, $NO_x$, and unburned hydrocarbons; (2) flame stability; and (3) combustor liner and fuel nozzle temperatures. A total of five fuel nozzles, based on three distinct nozzle concepts, have been evaluated over a wide range of operating conditions.

GE is also developing and testing a rich-quench-lean (RQL) low Btu fuel gas turbine combustor. The overall objective of this work is to develop an RQL combustor with lower conversion of fuel bound nitrogen (FBN) to $NO_x$ than a conventional diffusion flame gas turbine combustor. Initial tests were conducted in RQL1, a reduced scale (0.75 lb/s total flow) combustor. Insights gathered from the successful RQL1 tests have been incorporated into the design of RQL2, a full scale rich-quench-lean gas turbine combustor now under construction.

## BACKGROUND INFORMATION

Although the low Btu gas fuel nozzle developed several years ago [1] performed reasonably well, this fuel nozzle was too large for use in large gas turbine combustor cans which typically use multiple fuel nozzles. For this reason, GE Power Generation began development of smaller low Btu gas fuel nozzles. The long term objective of this effort is to develop a single fuel nozzle concept that is suitable for use with low Btu fuel produced from any type of gasifier (air or oxygen blown) and any type of cleanup system (low or high temperature). In addition, the nozzle should be suitable for use in both relatively small combustors that use a single fuel nozzle and large combustors that use multiple fuel nozzles. The single fuel nozzle tests described in this paper complement multi-nozzle tests conducted by GE Power Generation at the Gas Turbine Development Lab in Schenectady, NY.

Depending upon the feedstock and the process conditions, the low Btu fuel produced by a gasifier and high temperature desulfurization system will contain hundreds to thousands of parts per million of FBN (primarily $NH_3$). In a conventional combustor, a significant fraction of the FBN will be converted into $NO_x$. RQL combustion can reduce the conversion of FBN to $NO_x$, because a large fraction of the FBN is converted into non-reactive $N_2$ in the fuel rich stage. Additional air is introduced in the quench stage, and the lean stage provides sufficient residence time to complete combustion.

The subscale RQL combustor described in this paper (RQL1) is a significant improvement over the reduced scale RQL combustor discussed in previous work [2, 3]. The most important design enhancement is the incorporation of a converging rich stage combustor liner, which separates the rich stage recirculation zones from the quench stage and lean stage air. Although premixing the low Btu fuel and the rich stage air would probably improve the performance of RQL1, premixing is no longer considered to be a requirement for low conversion of FBN to $NO_x$.

## PROJECT DESCRIPTION

### Turbine Simulator

The low Btu gas turbine simulator is shown in Figure 1. High temperature low Btu fuel is supplied by the pilot scale coal gasification and

hot gas cleanup (HGCU) facility at GE Corporate Research and Development in Schenectady, NY. The turbine simulator is designed to operate at full gasifier capacity, 8000 lb/hr of fuel gas produced by gasifying 1800 lb/hr of coal. The gasifier produces low Btu fuel at a pressure of 20 atm and a nominal temperature of 1000°F. A typical fuel composition (after $H_2S$ removal by the hot gas cleanup system) is given in Table 1. Details of the gasifier and HGCU system can be found in Gal *et al.* [4].

The turbine simulator includes: a low Btu gas fuel nozzle; a modified GE MS6000 combustor liner; a film cooled, first stage LM6000 nozzle assembly; and an impingement cooled transition piece (see Figure 1). A recent addition to the turbine simulator test stand is the optional ability to blend natural gas into the low Btu fuel. The added natural gas allows the turbine simulator to maintain 'F' conditions (combustor exit temperature = 2550°F) even when the gasifier is operated at 80% of capacity. Comparisons of combustor liner temperatures, fuel nozzle temperatures, and CO emissions typically show that the addition of natural gas has little effect on turbine simulator performance.

The most recent turbine simulator tests (designated as Tests 5, 6, 7A, 4A, and 7B) have focused on evaluating the performance of different low Btu fuel nozzle designs (see Table 2). The three basic nozzle concepts are shown in Figures 2, 3, and 4. Nozzle N5-40, designed for low Btu fuel combustion several years ago [1], consists of concentric slot-type axial fuel and air swirlers. Nozzle N5-15 is identical to N5-40, except the N5-15 fuel swirl angle is 15°, not 40°. The results of tests with both of these fuel nozzles were discussed by Abuaf *et al.* [5].

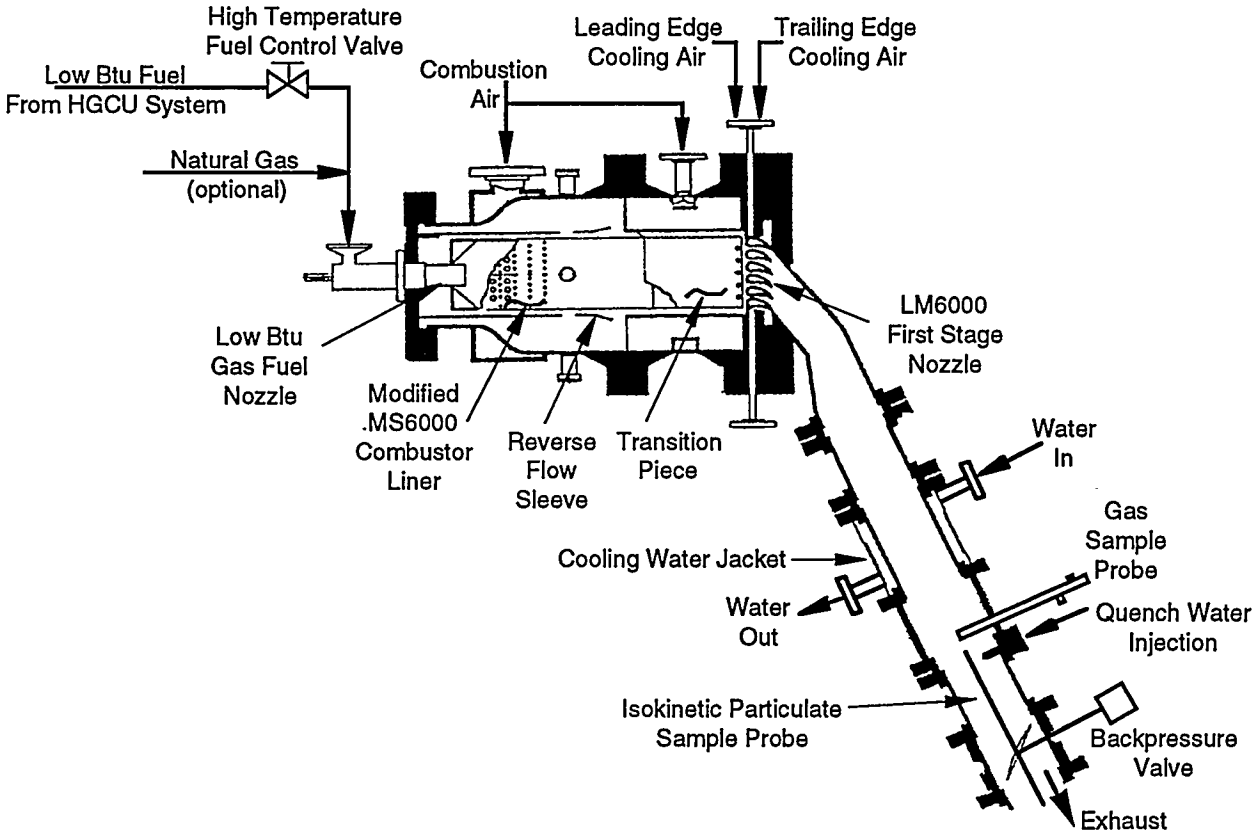


**Figure 1. The Turbine Simulator Test Stand**

Both the N7A nozzle type (Figure 3) and the N7B nozzle (Figure 4) have a smaller overall diameter than the N5 nozzle type. The N7A fuel nozzle type is best described as an axial fuel swirler and a radial air swirler. Nozzles N7A-20 and N7A-30 are identical, except for the location and angle of the fuel holes. The N7A-20 fuel swirl angle is 20°, and the fuel hole centers are located on a 2.5" diameter circle. The N7A-30 fuel swirl angle is 30°, and the the fuel hole centers are located on a 3.25" diameter circle. These changes were designed to increase the fuel/air mixing and flame stability of the N7A nozzle type.

The N7B nozzle consists of axial air and fuel swirlers and an air-cooled mixing cup. Unlike the N5 and N7A nozzle types, only one version of the N7B nozzle has been tested in the turbine simulator.

**RQL Combustor**

The RQL1 test stand is shown in Figure 5. The RQL1 combustor has a modular design, which allows for rapid evaluation of different hardware configurations. The rich and lean stages are separate components, and the air flow to each stage can be varied independently. Although both stages are impingement cooled, only the rich stage has a separate cooling air supply that is not used for combustion. The RQL1 low Btu fuel nozzle is similar in design to the N7A nozzle type, although much smaller.

Both the turbine simulator and the RQL1 combustor were fired with pilot plant fuel during Test 4A (completed November 1994). RQL1 was fired for 37 hours, during which time all of the RQL test objectives were completed. Because of the low fuel flow rate needed for the subscale RQL1 combustor, the gasifier was fueled with anthracite during the RQL1 portion of Test 4A to minimize tar deposition in the fuel line. The use of anthracite resulted in a lower than usual fuel ammonia content (see Table 2.) Following completion of the RQL1 portion of the test, the fuel

**Table 1: Typical Pilot Plant Low Btu Fuel Composition**

| Species | Mole Percent |
|---|---|
| CO | 8.6 |
| $H_2$ | 17.3 |
| $CH_4$ | 2.7 |
| $N_2$ | 30.1 |
| $CO_2$ | 12.6 |
| $H_2O$ | 28.0 |
| Ar | 0.3 |
| $NH_3$ | 0.4 |
| TOTAL | 100.0 |

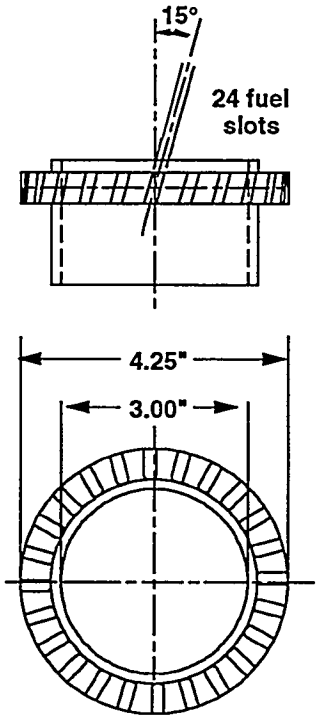


**Figure 2. Nozzle N5-15 (concentric air swirler not shown)**

line and some shared instrumentation lines were disconnected from RQL1 and connected to the turbine simulator, which was fired for a total of 25 hours.

RQL1 has been fired with both pilot plant low Btu fuel and natural gas/$N_2$ blends. The natural gas/$N_2$ tests were completed before beginning Test 4A. The main goals of the natural gas/$N_2$ tests were to: (1) check the instrumenta-

**Table 2. Recent Long Duration Tests**

| Test | Date | Firing Time (hours) | Turbine Simulator Fuel Nozzle | $NH_3$ Concentration in Low Btu Fuel (ppmv) |
|---|---|---|---|---|
| 5 | 11/93 | 41 | N5-40 | 4100 |
| 6 | 5/94 | 67 | N5-15 | 4400 |
| 7A | 8/94 | 77 | N7A-20 | 4250 |
| 4A | 11/94 | 25 (simulator)<br>37 (RQL1) | N7A-30 | 2200 (simulator)<br>1650 (RQL1) |
| 7B | 3/95 | 111 | N7B | 4600 |

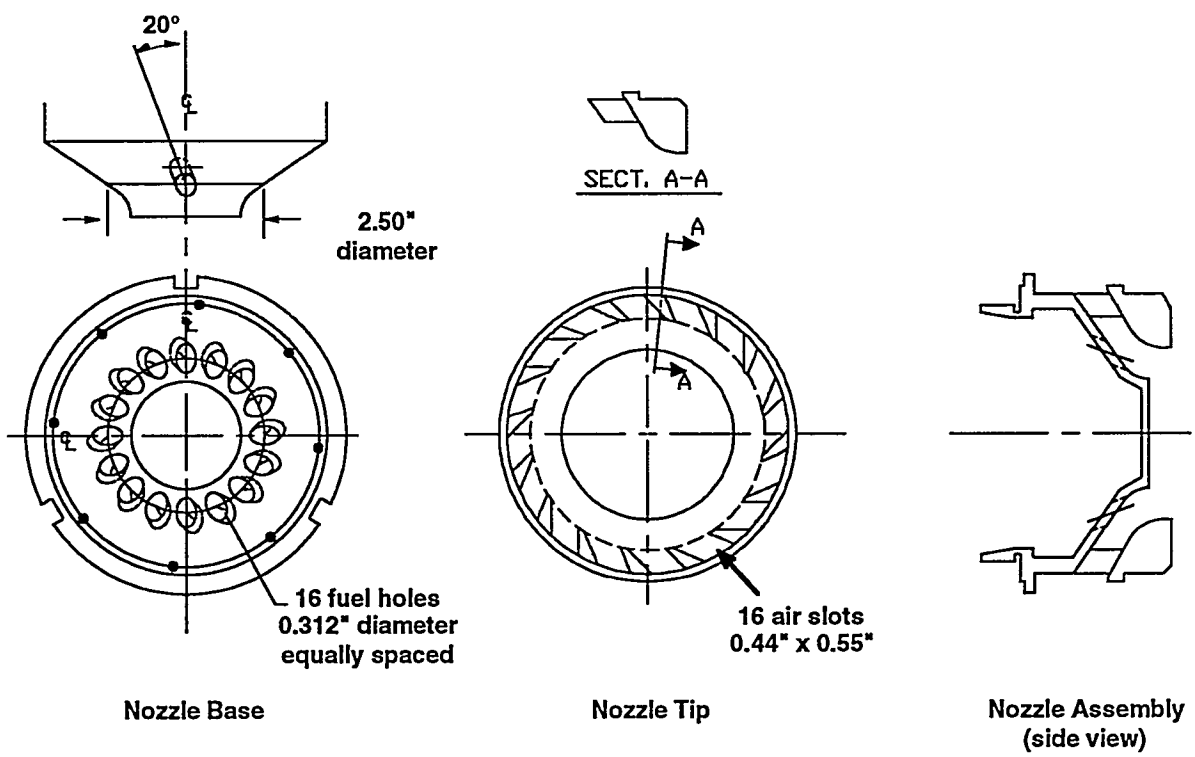


**Figure 3. Nozzle N7A-20**

tion and data acquisition software; (2) verify the effectiveness of the cooling scheme; (3) observe flame stability, dynamic behavior, and ignition characteristics; and (4) provide an opportunity for operator training. Given the limited time available during a pilot plant test, these tasks had to be completed before beginning pilot plant Test 4A. Only the results of the pilot plant test with low Btu fuel will be presented in this paper.

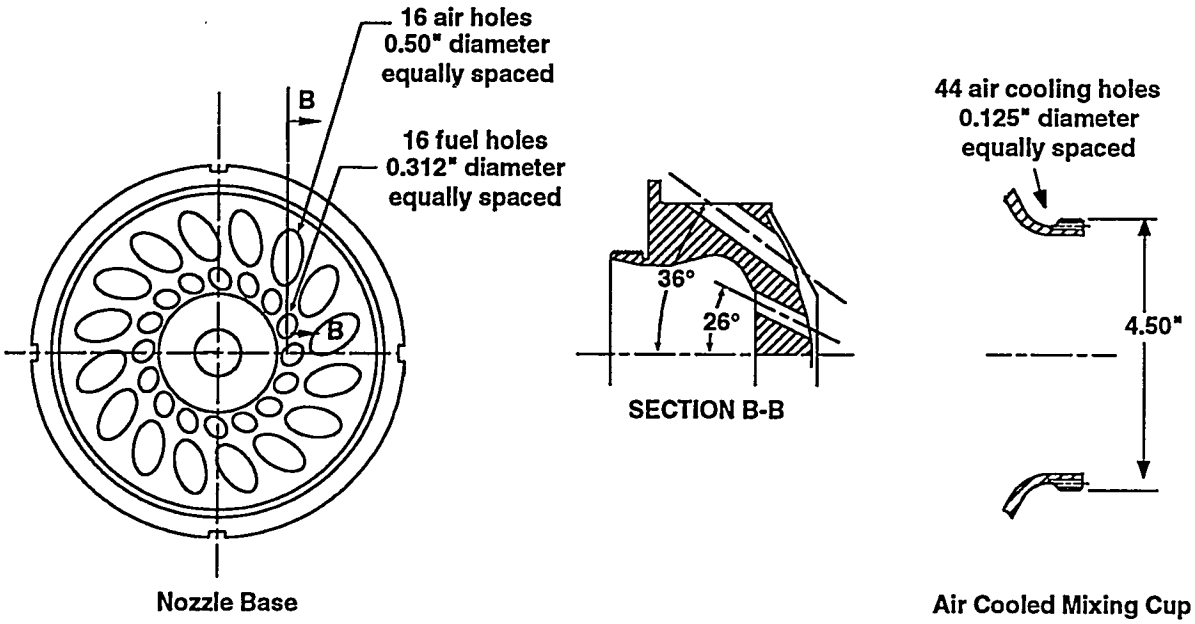


**Figure 4. Nozzle N7B**

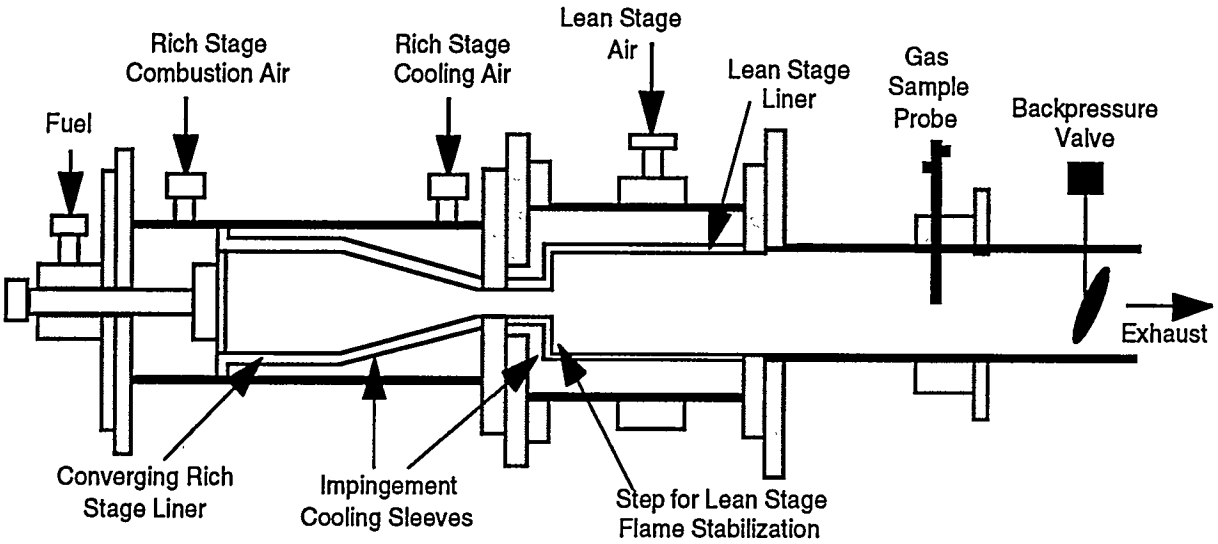


**Figure 5. RQL1 Test Stand**

## RESULTS

### Turbine Simulator

$NO_x$ emissions measured during the last 4 turbine simulator tests are shown in Figure 6 (only emissions measurements without natural gas added to the low Btu fuel are shown). Most of the $NO_x$ formed in the turbine simulator comes from $NH_3$ in the fuel. $NO_x$ emissions decrease as combustor exit temperature increases because the head end of the combustor becomes increasingly fuel rich as exit temperature increases.

A casual inspection of Figure 6 suggests that the conversion of $NH_3$ to $NO_x$ differs between fuel nozzles. However, when the variation in fuel ammonia content between tests is taken into account (see Table 2), the conversion of $NH_3$ to $NO_x$ is seen to follow a uniform trend for all of the fuel nozzles (Figure 7). Although the consistency between the nozzles is somewhat surprising, keeping the axial distribution of fuel/air ratio the same for all of the nozzles probably contributes to the observed uniformity. The overall conversion in the turbine simulator is somewhat lower than expected from a commercial installation, because the simulator operates at reduced flows, and the gas residence time in the combustor is greater than at full flow.

Although the fuel nozzles cannot be ranked based on their conversion of $NH_3$ to $NO_x$, flame stability and CO emissions vary significantly between nozzles (see Figure 8). The CO emissions shown in Figure 8 are a combination of measurements made both with and without natural gas added to the low Btu fuel (natural gas addition has almost no measurable influence on CO emissions). CO emissions were typically below 10 ppmv (on a dry, 15% $O_2$ basis) at combustor exit temperatures greater than 2100°F. CO emissions increase rapidly as the combustor exit temperature decreases and the combustor approaches blowout. For most of the fuel nozzles, blowout occurred at combustor exit temperatures below 1400°F.

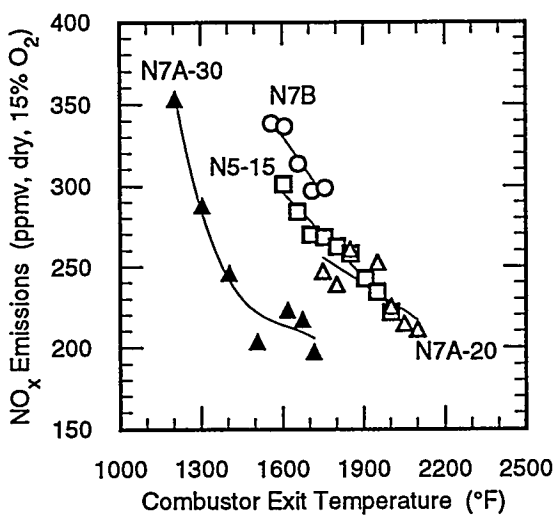


**Figure 6. Turbine Simulator $NO_x$ Emissions**

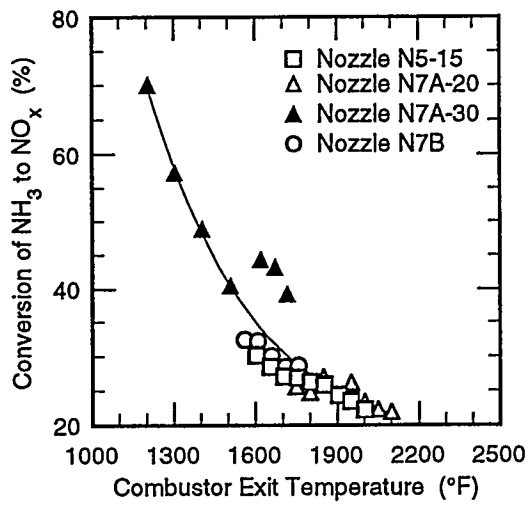


**Figure 7. Conversion of $NH_3$ to $NO_x$ in the Turbine Simulator**

Although not shown in Figure 8, nozzle N5-40 produced lower CO emissions than any of the other nozzles. This nozzle also resulted in unacceptably high cap/cowl temperatures, and as a result the cap/cowl was damaged during Test 5. The decreased fuel swirl angle of nozzle N5-15 reduced cap/cowl temperatures to acceptable levels, but resulted in unacceptably high CO emissions.

Nozzle N7A-20 improved the CO emissions over nozzle N5-15, but yielded unacceptably poor flame stability. When using Nozzle N7A-20, the combustor tended to blow out at low combustor exit temperatures ($T \leq 1750°F$) when the fuel heating value was low. (Due to the motion of the stirrer in the fixed bed gasifier, fuel heating value fluctuates sinusoidally with an amplitude of ±15% and a period of about 20 minutes.) Of the five fuel nozzles tested, only Nozzle N7A-20 exhibited this phenomenon. Nozzle N7A-30, with an increased fuel swirl angle and fuel holes relocated closer to the air swirler, had improved flame stability. However, these changes also significantly increased combustor liner temperatures (see Figure 9).

Nozzle N7B improved upon N7A-30 and had good flame stability, reasonable CO emissions (Figure 8) and very low liner temperatures (Figure 9). Nozzle N7B also performed well in multi-nozzle tests conducted at the GE Power Generation Gas Turbine Development Lab. For this reason, nozzle N7B has been selected for use in the GE MS7001FA gas turbine being supplied for the Tampa Electric Co. Polk County IGCC power plant.

Figure 10 shows unburned hydrocarbon (UHC) emissions measured during the last four turbine simulator tests. Because adding natural gas to the low Btu fuel had almost no measurable effect on UHC emissions, the data in Figure 9 are a combination of measurements made with and without natural gas added. Note that unlike CO and $NO_x$, UHC emissions have not been corrected

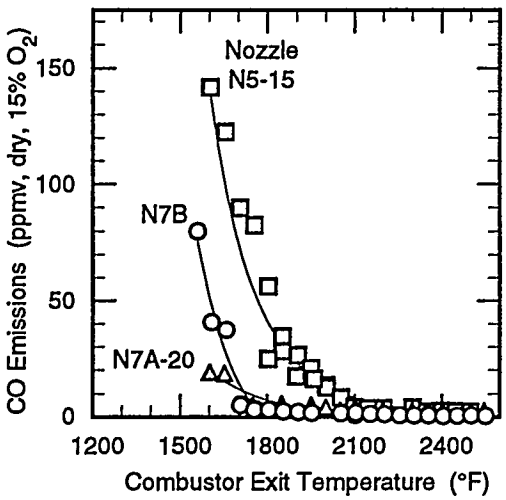


**Figure 8. Turbine Simulator CO Emissions**

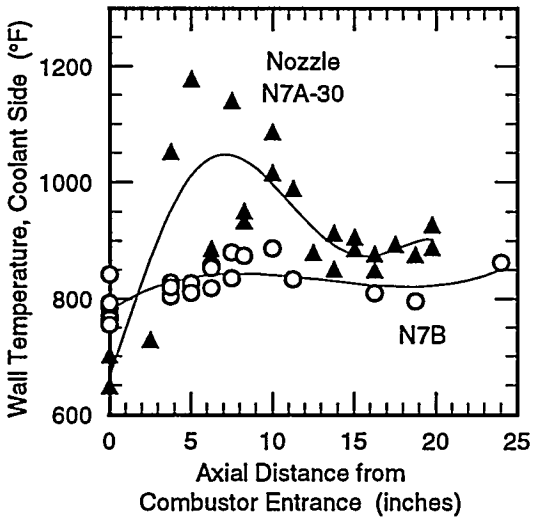


**Figure 9. Turbine Simulator Combustor Liner Temperatures at a Combustor Exit Temperature of 1750°F**

to a dry, 15% $O_2$ basis. UHC emissions, like CO emissions, tend to increase as the combustor exit temperature decreases and the combustor approaches blowout. UHC emissions were frequently at or near the detection limit of about 2 ppmv. For this reason, identifying clear differences in UHC emissions from the different fuel nozzles is difficult.

**RQL1**

Test conditions for the RQL1 portion of Test 4A are listed in Table 3. The relatively low flow rates of fuel and air resulted in lower than expected fuel and air temperatures. The low fuel $NH_3$ concentration (1650 ppmv) was not unexpected, and was a result of gasifying anthracite during the RQL1 portion of Test 4A (usually, Illinois #6 is gasified). To find the optimal operating conditions, three sets of measurements were conducted with the RQL1 combustor. In the first set of measurements, 40% of the total combustion air was sent to the rich stage, and the remaining 60% was sent to the lean stage. The air split was held constant as the fuel flow rate was varied. The resulting $NO_x$ emissions are shown as a function of combustor exit temperature in Figure 11.

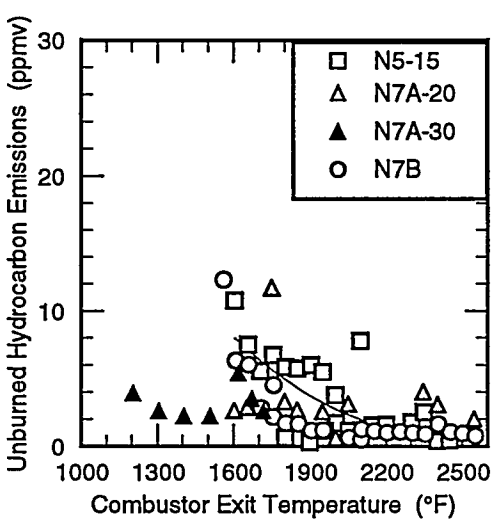


**Figure 10. Turbine Simulator Unburned Hydrocarbon Emissions**

The most striking feature of Figure 11 is the minimum in $NO_x$ emissions. This type of trend is expected in a rich-lean combustor and has been widely reported in other experimental [e.g., 6] and theoretical [e.g., 7] studies. For a fixed air split between the rich and lean stages, there is an optimum rich stage fuel/air ratio which minimizes the conversion of $NH_3$ to $NO_x$. Factors which reportedly influence the optimum fuel/air ratio include the rich stage residence time and the fuel composition.

The overall conversion of $NH_3$ to $NO_x$ is also shown in Figure 11. Since the contributions of non-FBN $NO_x$ (e.g., thermal $NO_x$ and prompt $NO_x$) cannot be separated from the total measured $NO_x$ emissions, the conversion has been calculated assuming that there is no thermal $NO_x$ for-

**Table 3. RQL1 Test Conditions**

| | |
|---|---|
| Pressure: | 10 atm |
| Rich Stage Residence Time: | 27–51 ms |
| Rich Stage Air Temperature: | 460°F |
| Lean Stage Air Temperature: | 620°F |
| Low Btu Fuel Temperature: | 520°F |
| Low Btu Fuel Composition: | 34% $N_2$ |
| | 28% $H_2O$ |
| | 14% $H_2$ |
| | 12% CO |
| | 10% $CO_2$ |
| | 1.4% $CH_4$ |
| | 1650 ppmv $NH_3$ |

mation. In other words, all of the measured $NO_x$ has been assumed to come from $NH_3$ in the fuel. Using this approach, the conversion of $NH_3$ to $NO_x$ is overestimated slightly.

The second set of measurements was conducted with 60% of the total combustion air sent to the rich stage and 40% sent to the lean stage (see Figure 12). Comparing Figures 11 and 12 shows that the minimum in $NO_x$ emissions shifted to a higher combustor exit temperature. The third set of measurements was conducted with 67% of the total combustion air sent to the rich stage and 33% sent to the lean stage (see Figure 13). The minimum in $NO_x$ emissions shifted to an even higher combustor exit temperature, about 2350°F. For a given RQL combustor configuration, the minimum in $NO_x$ emissions can be made to occur at any desired combustor exit temperature by carefully selecting the air split between the rich and lean stages.

Figure 12 shows that at the optimal rich stage fuel/air ratio, the conversion of $NH_3$ to $NO_x$ is about 15%. This conversion is a substantial improvement over a standard, diffusion flame based gas turbine combustor. At these conditions, the conversion of $NH_3$ to $NO_x$ in a diffusion flame based gas turbine combustor is expected to be about 30%.

The conversion of $NH_3$ to $NO_x$ in the RQL1 combustor has been modeled with a series network of perfectly stirred reactors (PSRs) and plug flow reactors (PFRs). The rich stage was modeled as an equivolume PSR and PFR in series. Model predictions were insensitive to the relative sizes of the rich stage PSR and PFR. The flow exiting the rich stage PFR was combined with the lean stage air in a second PSR, which fed a second PFR. Inputs to the model were the known rich stage and lean stage combustor volumes, as well as measured pressures, fuel and air flow flow rates, fuel composition, and temperatures. Since

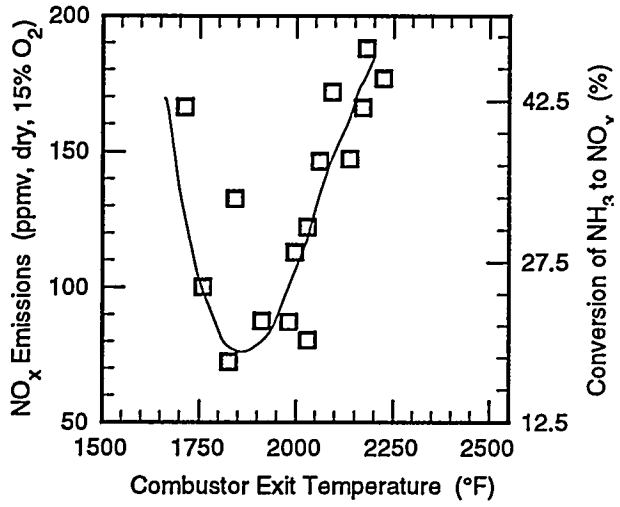


**Figure 11. RQL1 $NO_x$ Emissions at a 40% Rich / 60% Lean Combustion Air Split**

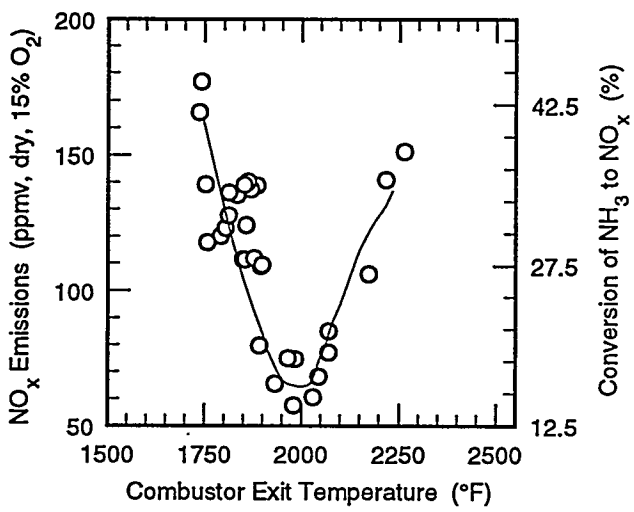


**Figure 12. RQL1 $NO_x$ Emissions at a 60% Rich / 40% Lean Combustion Air Split**

heat loss from the RQL1 combustor to the surroundings was significant, a heat removal term was included in the first PSR. The three other model reactors were assumed to be adiabatic. For each data point, the rate of heat loss from the first PSR was varied until the model predicted combustor exit temperature matched the measured exit temperature. The chemical kinetic mechanism included more than 50 species and 250 elementary reaction steps [8]. Calculations were performed using the CHEMKIN II package of subroutines and associated programs [9].

The model predictions are shown as the solid line in Figure 13 (modeling of the $NO_x$ emissions for the other air splits has not been completed). The model reproduces both the magnitude of $NO_x$ emissions and the location of the minimum fairly well. Using these types of models, key reaction pathways responsible for $NH_3$ oxidation and destruction can be identified. These type of models can also be used to perform 'what-if' calculations, and to investigate the influence of operating conditions (e.g., fuel composition, total rich stage residence time) on the performance of an RQL combustor.

RQL1 CO emissions were low under all test conditions (see Figure 14). The air split between the rich and lean stages had relatively little influence on CO emissions.

## FUTURE WORK

Fabrication and assembly of RQL2, a full scale rich-quench-lean combustor, is now underway (see Figure 15). Like RQL1, the RQL2 design includes a converging rich stage liner and a backward facing step at the entrance to the lean stage to enhance lean stage flame stabilization. The RQL2 design also allows the air flow rates to the rich and lean stages to be varied independently. RQL2 has been designed to take the place of the turbine simulator and to connect to the existing turbine simulator transition piece and LM6000 cascade. The first pilot plant test of RQL2 is tentatively scheduled for the third quarter of 1995.

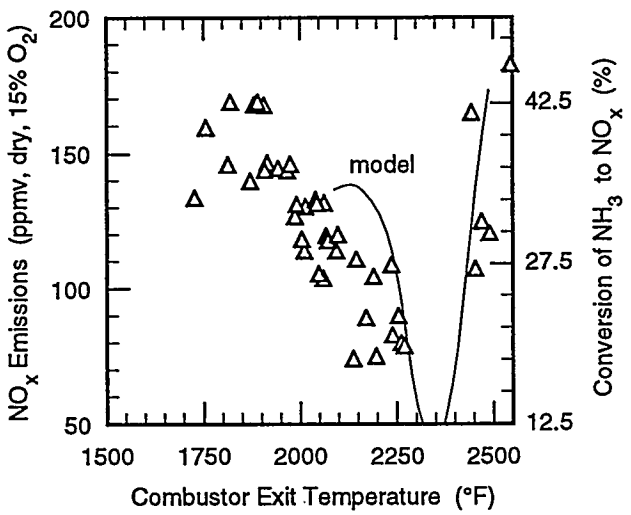


**Figure 13. RQL1 Emissions and Model Predictions at an Air Split of 67% Rich / 33% Lean**

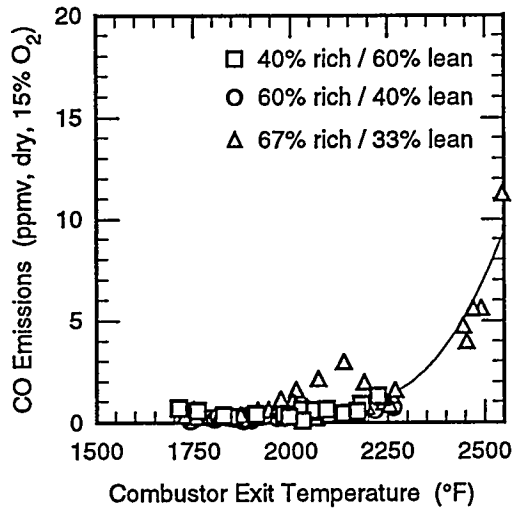


**Figure 14. RQL1 CO Emissions at Three Combustion Air Splits**

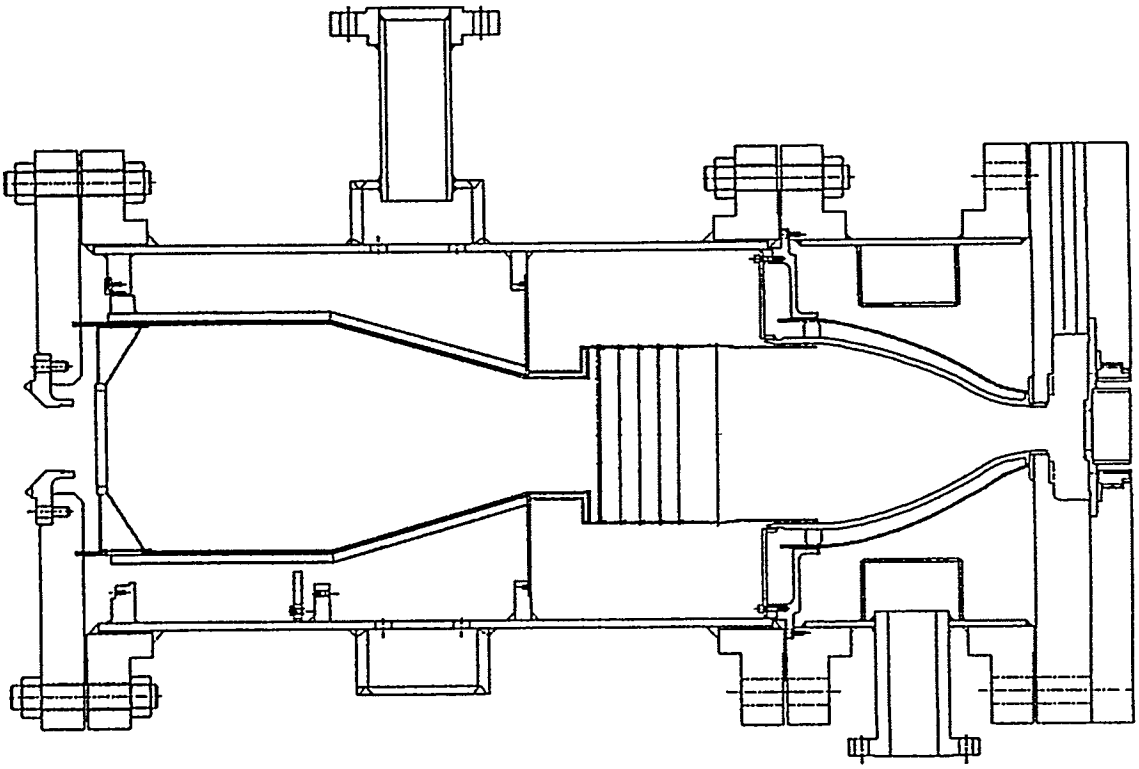

**Figure 15. RQL2 Test Stand**

## REFERENCES


1. Lawson, C. C. *Water-Cooled Components Test Program, Final Report.* 1985. DOE/MC/20192-1953. Contract DE-AC21-83MC20192.

2. Abuaf, N., A. S. Feitelberg, S. L. Hung, D. J. Najewicz, and M. S. Samuels. 1993. Combustion Tests of a Turbine Simulator Burning Low Btu Fuel and a Rich-Quench-Lean Combustor. In *Proceedings of the Coal-Fired Power Systems 93 — Advances in IGCC and PFBC Review Meeting*, 169-178. DOE/METC-93/6131. NTIS/DE93000289. Springfield, VA: National Technical Information Service.

3. Abuaf, N., A. S. Feitelberg, S. L. Hung, D. J. Najewicz, and M. S. Samuels. 1993. Combustion Tests of a Turbine Simulator Burning Low Btu Fuel From a Fixed Bed Gasifier. In *Proceedings of the Joint Contractors Meeting: FE/EE Advanced Turbine Systems Conference FE Fuel Cells and Coal-Fired Heat Engines Conference*, 199-208. DOE/METC-93/6132. NTIS/DE93011308. Springfield, VA: National Technical Information Service.

4. Gal, E., D. Najewicz, A. H. Furman, R. Ayala, and A. Feitelberg. 1994. Integrated Operation of a Pressurized Gasifier, Hot Gas Desulfurization System and Turbine Simulator. In *Proceedings of the Coal-Fired Power Systems 94 -- Advances in IGCC and PFBC Review Meeting*, 222-235. DOE/METC-94/1008. NTIS/DE94012252. Springfield, VA: National Technical Information Service.

5. Abuaf, N., A. S. Feitelberg, S. L. Hung, M. S. Samuels, and A. K. Tolpadi. 1994. Development and Testing of Low Btu Fuel Gas Turbine Combustors. In *Proceedings of the Coal-Fired Power Systems 94 -- Advances in IGCC and PFBC Review Meeting*, 280-289. DOE/METC-94/1008. NTIS/DE94012252. Springfield, VA: National Technical Information Service.

6. Nakata, T., M. Sato, T. Ninomiya, and T. Hasegawa. 1994. A Study on Low NOx Combustion in LBG-Fueled 1500°C-Class Gas Turbine. ASME Paper 94-GT-218. New York: American Society of Mechanical Engineers.

7. Heap, M. P., T. J. Tyson, J. E. Cichanowicz, R. Gershman, C. J. Kau, G. B. Martin, and W. S. Lanier. 1977. Environmental Aspects of Low Btu Gas Combustion. In *16th Symposium (International) on Combustion*, 535-542. Pittsburgh: The Combustion Institute.

8. Michaud, M. G., P. R. Westmoreland, and A. S. Feitelberg. 1992. Chemical Mechanisms of $NO_x$ Formation for Gas Turbine Conditions. In *24th Symposium (International) on Combustion*, 879-887. Pittsburgh: The Combustion Institute.

9. Kee, R. J., F. M. Rupley, and J. A. Miller. 1989. Chemkin-II: A Fortran Chemical Kinetics Package for the Analysis of Gas-Phase Chemical Kinetics. Sandia National Laboratories Report SAND89-8009.

## 5.3 Development of a Topping Combustor for Advanced Concept Pressurized Fluidized-Bed Combustion Systems

### CONTRACT INFORMATION

| | |
|---|---|
| **Contract Number** | DE-AC21-86MC21023 |
| **Contractor** | Westinghouse Electric Corporation<br>4400 Alafaya Trail<br>Orlando, Florida 32826-2399<br>(407) 281-3387 (telephone TED)<br>(407) 281-5014 (FAX) |
| **Other Funding Sources** | Cost Shared by Westinghouse, Foster-Wheeler, and Other Major Subcontractors |
| **Contractor Project Manager** | William F. Domeracki |
| **Principal Investigators** | Thomas E. Dowdy<br>Dennis Bachovchin |
| **DOE Project Manager** | Donald L. Bonk |
| **Period of Performance** | January 5, 1987 to December 31, 1994 |
| **Schedule and Milestones** | No activity planned FY95 |

**FY1994 Program Schedule**

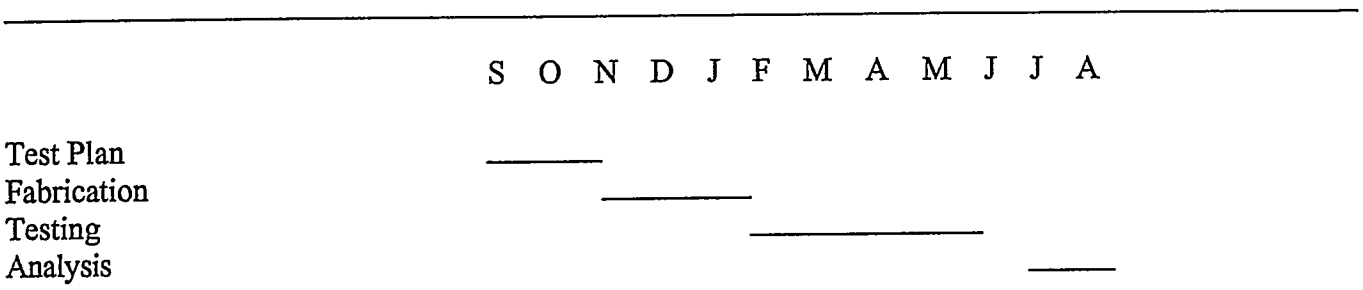


### OBJECTIVE

A project team consisting of Foster Wheeler Development Corporation, Westinghouse Electric Corporation, Gilbert/Commonwealth and the Institute of Gas Technology, are developing a Second Generation Pressurized Fluidized Bed System. Foster Wheeler is developing a carbonizer (a partial gasifier) and a pressurized fluidized bed combustor. Both these units operate at a nominal 1600°F (870°C) for optimal sulfur capture. Since this temperature is well below the

current combustion turbine combustor outlet operating temperature of 2350°F (1290°C), to reach commercialization, a topping combustor and hot gas cleanup (HGCU) equipment must be developed.

Westinghouse's efforts are focused on the development of the high temperature gas cleanup equipment and the topping combustor. This paper concentrates on the design and test of the topping combustor, which must use a low heating value syngas from the carbonizer at approximately 1600°F and 150 to 210 psi. The syngas entering the topping combustor has been previously cleaned of particulates and alkali by the hot gas cleanup (HGCU) system. It also contains significant fuel bound nitrogen present as ammonia and other compounds. The fuel-bound nitrogen is significant because it will selectively convert to NOx if the fuel is burned under the highly oxidizing conditions of standard combustion turbine combustors.

The fuel must be burned with the vitiated air produced by the pressurized fluidized bed combustor (PFBC). The vitiated air has been cleaned of particulates and alkali by the HGCU system, and has also been partially depleted in oxygen. The 1600°F (870°C) vitiated air must also be used to cool the combustor as much as possible, though a small amount of compressor discharge air at a lower temperature 700°F may be used.

The application requirements indicate that a rich-quench-lean (RQL) combustor is necessary and the multi-annular swirl burner (MASB) was selected for further development. This paper provides an update on the development and testing of this MASB combustor. Additionally, Westinghouse has been conducting computational fluid dynamic (CFD) and chemical kinetic studies to assist in the design and to help optimize the operation of the combustor. Results of these models are presented and compared to the test results.

## BACKGROUND

### Cycle Description

In a second generation PFB combined cycle, coal is fed to a pyrolyzer/carbonizer unit that operates at 1600°F to produce a low heating value fuel gas and combustible char. The char is burned in the PFB, and the 1600°F product gases, after filtration, are piped back to the combustion turbine as illustrated in Figures 1 and 2.

Before entering the gas turbine, the 1600°F (870°C) gas, still rich in oxygen, is raised to 2100°F (1150°C) or higher by burning the filtered, pyrolyzer-produced low heating value fuel gas in a topping combustion system. Since turbine inlet temperature is at least 500°F (260°C) higher than the PFB air temperature, plant efficiency is 5- to 7-percentage points higher than similar first generation PFB plants.

### The Combustion Turbine

The use of a Circulating Pressurized Fluidized Bed Combustor (CPFBC) as the primary combustion system for a combustion turbine requires transporting compressor air to the CPFBC and vitiated air/fuel gas back to the turbine. In addition, the topping combustion system must be located in the returning vitiated airflow path. The conventional fuel system and turbine center section require major changes for the applications.

The combustion zone of the Westinghouse 501 combustion turbines currently in production cannot contain a topping combustion system within the main structural pressure shell. Although the pressure casing can be enlarged both radially and longitudinally to accommodate the topping combustor system, the integrity and rigidity of the

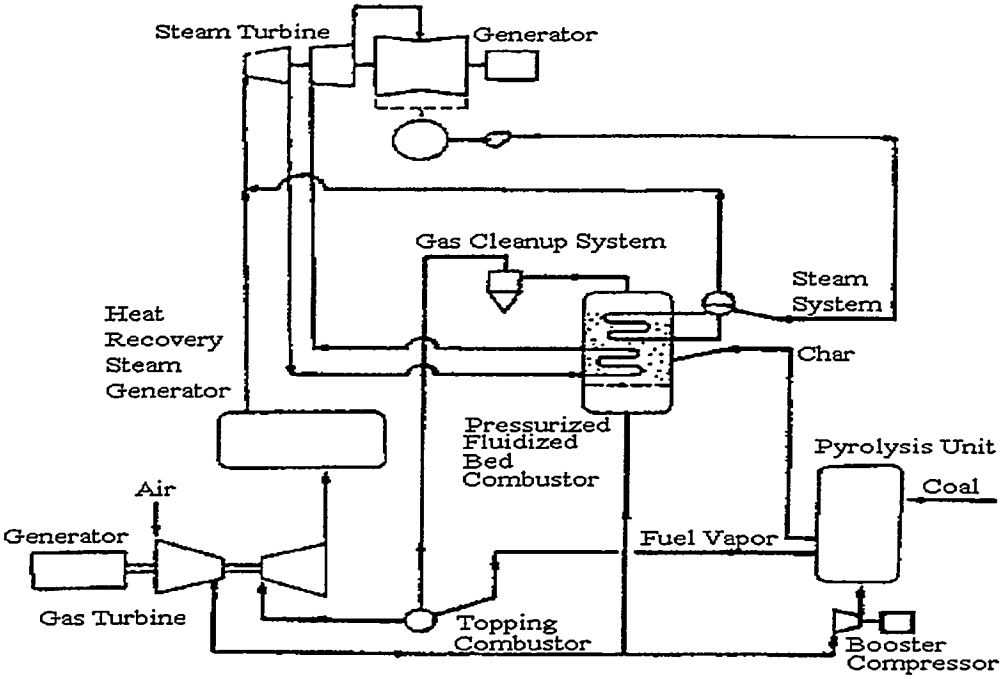


**Figure 1. Schematic Representation of a Second Generation PFB Combined Cycle**

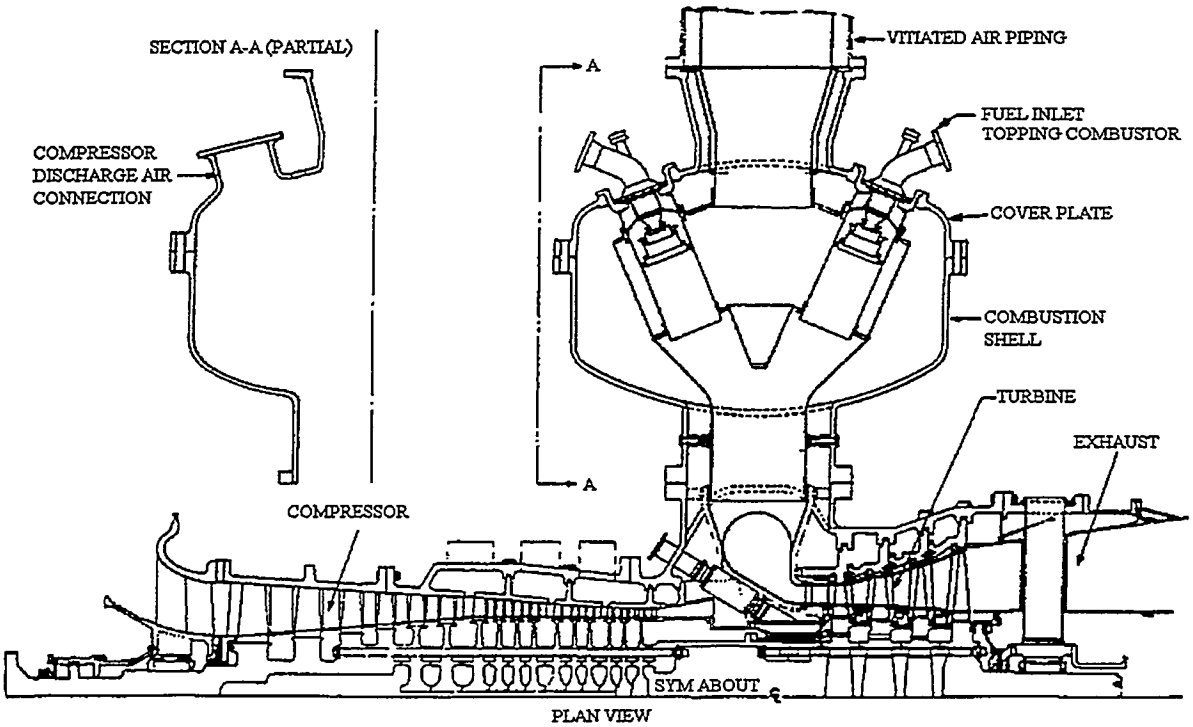


**Figure 2. Combustion Turbine Conceptual Design**

main shell would be significantly affected, possibly impacting rotor dynamics and precluding shipping the unit assembled.

One alternative configuration, which uses two topping combustor assemblies, on the side of the unit, is shown in Figure 2. The vitiated air from the CPFBC enters each of the internal plenum chambers in which the topping combustors are mounted. Fuel gas enters the assembly via the fuel nozzles at the head end of the combustor. Combustion occurs, and the products of combustion are ducted into the main shell for distribution to the first-stage turbine vanes.

Compressor discharge air leaves the main shell, flowing around the annular duct into adjacent combustion shells. The air flows around the vitiated air plenums and leaves each combustion assembly via nozzles and is ducted to the CPFBC and carbonizer. (See Figure 2.)

**Combustor Design**

Because the air entering the combustor is at 1600°F rather than the 700°F usual for gas turbines, the conventional type of combustor is not suitable. Both emissions and wall cooling problems preclude the use of the conventional design. Therefore, a combustor that will meet the requirements of utilizing the higher temperature air for both wall cooling and combustion is required.

In selecting a combustor design that will withstand the conditions expected in the topping application, the effective utilization of the 1600°F air mentioned above could satisfy the wall cooling challenge by maintaining a cooling air layer of substantial thickness. The creation of thick layers of cooling air at the leading edge of each inlet section is easily achieved if the combustor is made up of concentric annular passages. In addition to wall cooling considerations, the burner must inhibit the formation of NOx from syngas that contains fuel-bound nitrogen, have high combustion efficiency, produce an acceptable exhaust temperature pattern, exhibit good stability, and be able to light off at cold plant conditions. The Multi-Annular Swirl Burner (MASB), was chosen as the candidate to meet these requirements.

The MASB as shown in Figure 3 is designed to operate in a staged combustion mode to inhibit the formation of NOx. The details of the NOx-inhibiting process were described in a previous paper (Garland and Pillsbury, 1990). Figure 4 shows the half-scale 14" MASB.

**Test Facility**

The topping combustor tests are being conducted at the University of Tennessee Space Institute (UTSI), Tullahoma, Tennessee in the DOE Coal, Oil, or Gas-Fired Flow Facility (CFFF). This facility was designed to accommodate a variety of coal-, oil-, or gas-fired energy conversion equipment.

UTSI modified the existing facility to accommodate the topping combustor and provided all necessary ancillary systems required to conduct the test and obtain data for evaluation. Modifications included the installation of the syngas fuel system with heater, which delivers fuel from tube trailers to the combustor at 1200°F, establishing required pressure, and perform fuel blending. The fuel gas is a six component mixture of $N_2$, $H_2$, $CH_4$, CO, $H_2O$ and $NH_3$, that simulates the heating value and flammability limits of carbonizer gas.

**Test Rig**

The Westinghouse advanced combustor test rig was adapted for use at the UTSI test site. Figure 5 is a longitudinal view of the rig as configured for use in the topping combustor tests.

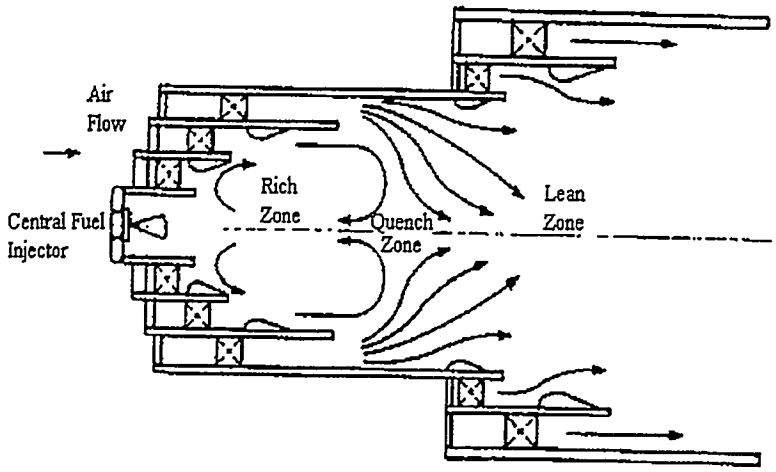


**Figure 3. Conceptual Arrangement of the Multi-Annular Swirl Burner Based on J. M. Beér's Patent Design (1989)**

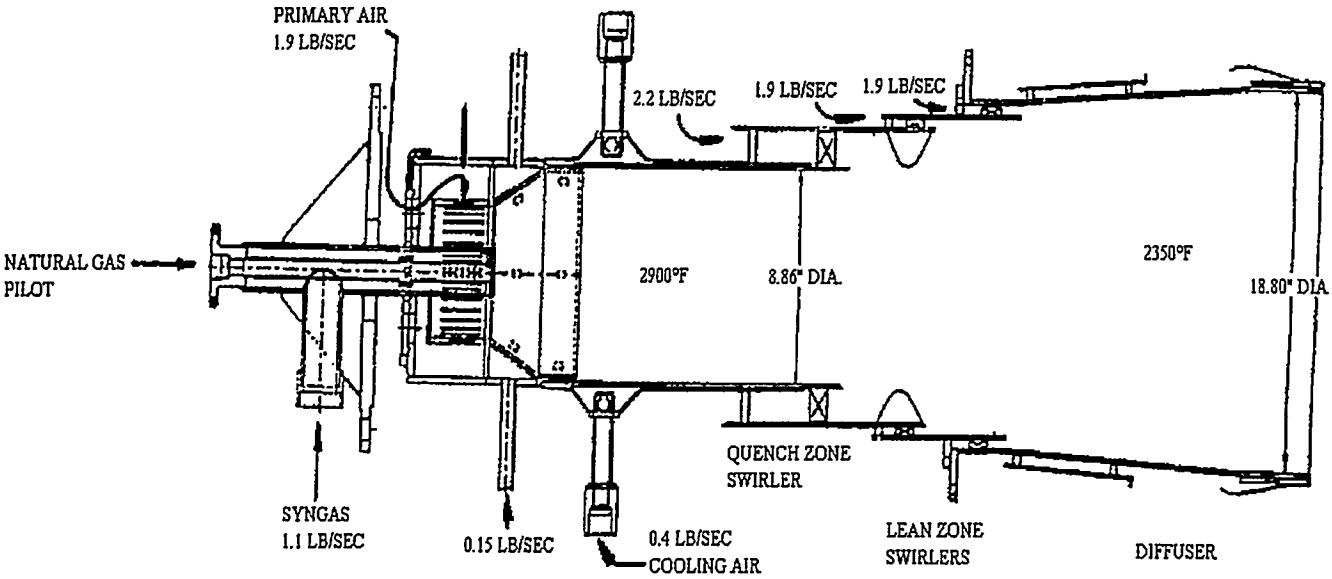


**Figure 4. Recent 14" MASB Design**

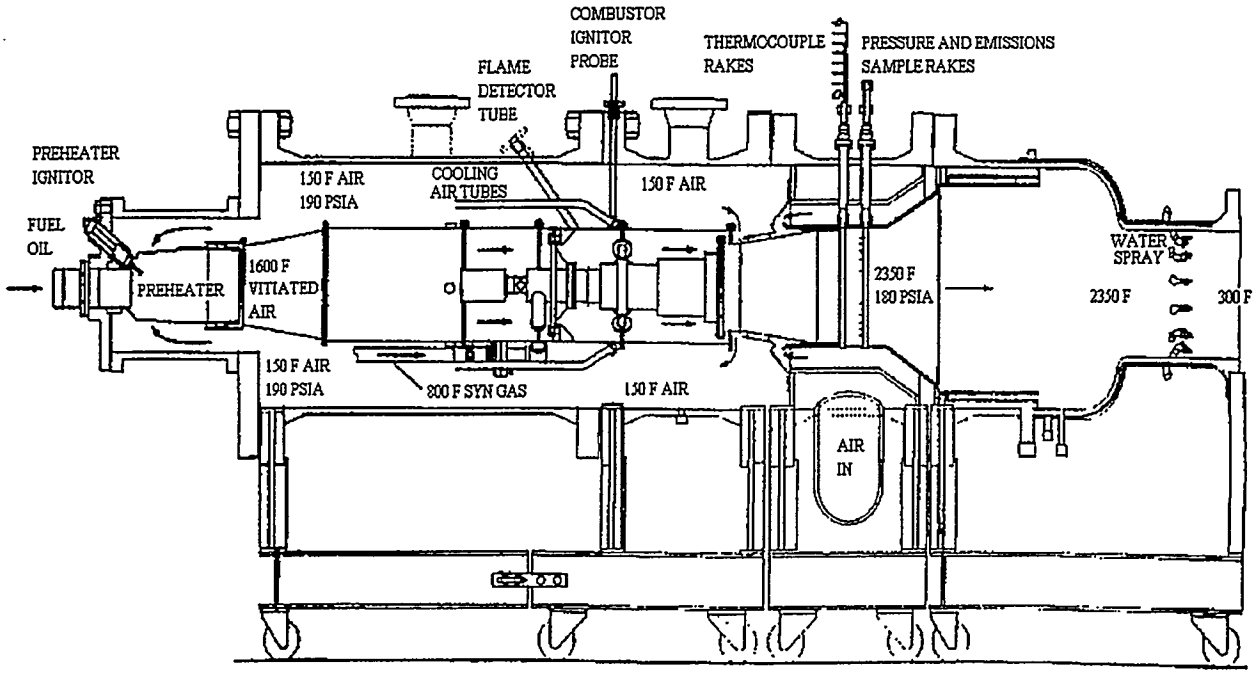


**Figure 5. Topping Combustion and Test Rig Configuration**

To simulate actual operating conditions, several modifications and auxiliary systems were required. These items provided: the supply of hot vitiated air; the supply of hot, synthesized fuel gas and/or natural gas and/or fuel oil; and, the ability to dope the fuel with ammonia when firing syngas. The ammonia allowed investigating the effects of fuel bound nitrogen on emissions.

The test facility at UTSI is capable of delivering 20 lb/s of air at 200 psia and 120°F. To raise this air to the required 1600°F temperature, a distillate oil-fired combustor, referred to as the preheater or the preburner, is placed upstream of the MASB. Directly heating the air through combustion partially depletes the oxygen in the air while adding carbon dioxide, water vapor and NOx. The vitiated air, still high in oxygen content, produced by the preheater simulates the PFB exhaust gases and makes the test conditions more realistic. The high oxygen content is important as it relates to obtaining high plant efficiency. (Garland and Robertson, 1988.)

Note on Figure 5 that the MASB is held within a series of flanged containment cylinders. In this way, the entering 120°F air comes forward to the preheater, where it burns the distillate oil, and is raised to 1600°F.

### Instrumentation and Control

Approximately 200 temperature measurements, over 50 pressure measurements, and measurements relating to flow and emissions were taken during testing.

## PROJECT DESCRIPTION

The MASB has the desired characteristics for a topping combustor for this application. Three syngas tests and one fuel oil/natural gas test were

conducted in 1990-1991 with 12" and 14" diameter MASB's at UTSI. These tests have confirmed that the MASB can be successfully cooled with 1600°F vitiated air (supplemented with a small amount (5 to 10% of total air flow) of additional cooling air at the hottest locations). The 12" combustor demonstrated that good temperature patterns could be obtained at 2100°F firing temperature, and the 14" test showed that a uniform 2350°F combustor outlet temperature could be obtained without overheating the materials of construction.

Emissions from the 12" and 14" MASB tests have shown low CO, and no soot or unburned hydrocarbons have been detected. In a "conventional" oil or natural gas fired combustion turbine combustor, Westinghouse would predict that as much as 85% of the fuel-bound nitrogen would be selectively converted to NOx. The 1990-1991 tests with the 12" and 14" MASB's have shown 20% to 30% conversion of the $NH_3$ added to the syngas to simulate fuel bound nitrogen to NOx. This is obviously a significant improvement over conventional combustors, but further improvements on the $NH_3$ conversion appear possible.

**Recent MASB Design Development**

The MASB has been designed as a combustor specifically for low-Btu, coal-derived fuel gases containing significant fuel bound nitrogen, primarily in the form of $NH_3$. Standard Dry Low-NOx combustors have focused on minimization of thermal NOx generation. The MASB must minimize thermal NOx and also must convert $NH_3$ to molecular nitrogen.

The MASB approach is to:

- employ a high-residence-time, fuel-rich zone at an optimized temperature such that $NH_3$ is converted to $N_2$ rather than to NOx.
- establish strong swirl and strong recirculation in the rich zone for flame stabilization, and to ensure that the entire rich zone is used for this purpose.
- achieve a rapid quench to fuel lean conditions to minimize the formation of thermal NOx after the rich zone.

Westinghouse together with UTSI have completed significant computer models of the system, both with computational fluid dynamic (CFD) codes and with chemical kinetics codes. Output from this analysis has been factored into the latest designs of the MASB, particularly with respect to the primary (fuel-rich) zone. CFD modeling of the redesigned configuration shown in Figure 4 shows that this new design will have significant recirculation in the primary zone.

A half scale cold flow model with similar Reynolds number and velocity profiles as the hot 18" MASB was tested to verify the flow characteristics required and expected. Axial and radial velocity measurements were made across the diameter of the unit at each of seven axial positions.

Figure 6 is a map of the resulting axial velocities. A strong donut-shaped recirculation region was confirmed in the wake of the bluff body end of the fuel swirler. This extends about one third of the way down the rich zone cylinder. Additionally, there is an absolute boundary (location C to C2) between the rich and quench zones through which no reverse flow occurs, thereby guaranteeing the existence of fuel rich combustion. Swirl was very strong (100 to 200 ft/sec tangential velocity), especially near the wall, for good stabilization, and wall cooling.

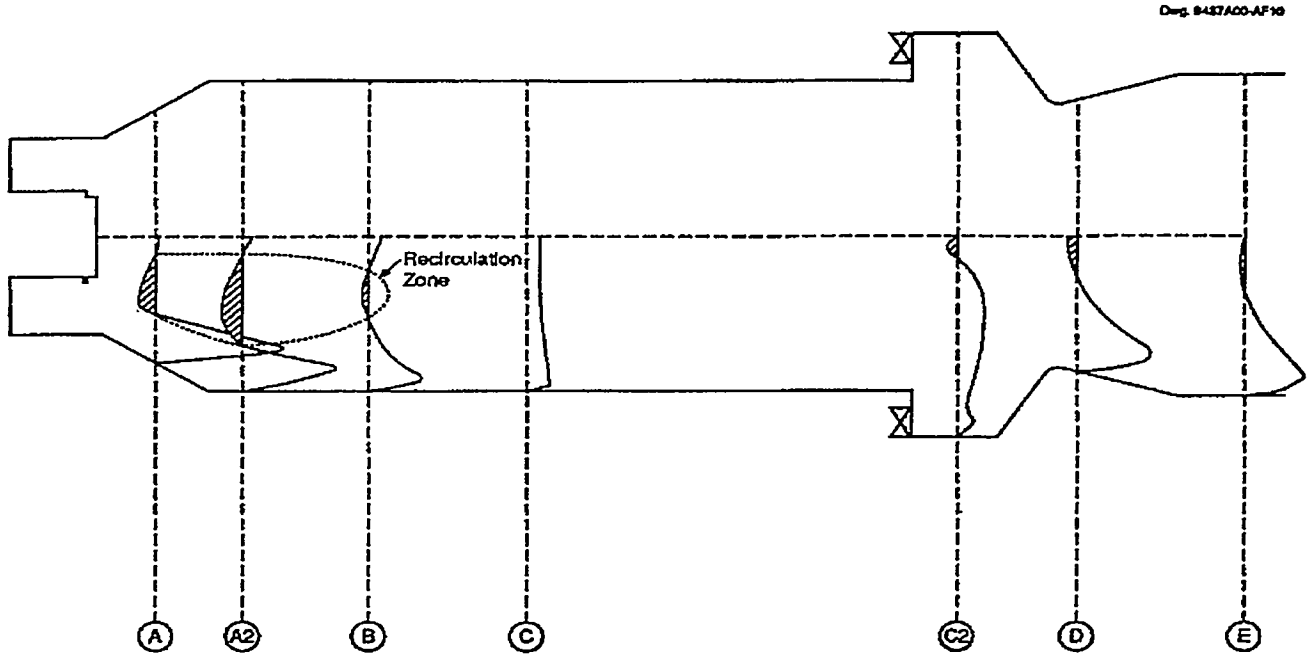


**Figure 6. Cold Flow Model Axial Velocities**

## RESULTS

These results verified CFD modeling efforts and confirmed that no additional design changes were needed prior to full size MASB testing.

Westinghouse has performed chemical kinetic studies under conditions as close as possible to those planned for the next series of tests. Basically, the equivalent of 5 milliseconds of backmixing followed by 40 miliseconds of plug flow could yield NOx levels below 20 ppm when corrected to 15% $O_2$. The CFD model and the cold flow work indicate that significant recirculation (backmixing) should occur with the redesigned fuel-rich zone.

Recently, significant MASB design improvements have been made with the objective of improving the flame pattern in the combustor, and thereby achieving improved low NOx performance. The effectiveness of these improvements is to be demonstrated in a two stage test.

The first test was conducted in June 1993 with the 14" configuration shown in Figure 4. These tests confirmed that the redesigned fuel nozzle achieved the rich zone environment control, flame stability and oxidant distribution required. The redesigned rich zone also improved upon the fuel bound nitrogen to NOx conversion rates. Results of the tests showed a conversion rate of only 9% to 10% at the 0.27% ammonia levels, surpassing our goal of 10% to 12% conversion. The detailed results of these tests were reported in a previous paper (Domeracki et al. 1994).

In the next stage, a full-scale 18" MASB was tested. Lessons learned in the 14" MASB tests were incorporated into a full-scale 18" MASB. In addition, the 18" design will have a greater rich

zone residence time for improvement of low-NOx performance, higher pressure drop downstream swirlers, and on-line oxidant flow control.

**Full Scale 18" MASB Test Results**

During the summer of 1994, the 18" MASB was successfully tested, meeting all of the following objectives:

1. Demonstrate successful scale up to full commercial size single basket design.
2. Optimize rich zone performance for lower (12% target) conversion of fuel nitrogen (as NH3) to NOx, by increasing residence time and tighter and control of equivalence ratio in the 1.2 to 1.4 range.
3. Demonstrate effectiveness and durability of mechanical design improvements, particularly as related to the quench flow deflector, swirlers, ignitor, and cooling designs.
4. Operate on-line adjustable control of the variable orifice mechanism for rich zone fuel/air ratio control.
5. Operate firing with syngas in vitiated air, and with natural gas in vitiated air.

Explore affects of variable operating parameters: fuel NH3 content, rich zone temperature, part load, vitiated air temperature, vitiated air oxygen level.

Remaining future test objectives include demonstration of operation firing natural gas in compressor (700ºF) air, and on-line fuel switching.

Natural gas firing in vitiated air was successfully demonstrated over a range of operating conditions. A stable flame was easily achieved, with no ignitor firing required. The burner proved mechanically durable, with no metal distress and wall (Haynes 230) temperatures maintained at less than 1500ºF at all conditions. Generally, the rich zone was operated at higher temperatures and lower equivalence ratio than planned, because of difficulties in operating the fuel/air ratio control mechanism (caused by pre-test preburner excessive discharge temperature). MASB exhaust temperature rakes revealed the flame to be somewhat stretched out.

The emission results in terms of NOx and CO are summarized in Table 1. Note that the burner functions as a very low NOx combustor for natural gas when the rich zone is operated rich, and then NOx results are not excessive even when operated lean. The MASB completely burns out CO in vitiated air at the levels expected in actual PFBC plant operation.

**Table 1. Natural Gas Test Results - Emissions**

Conditions:

- Vitiated air oxygen level: 12 to 18 vol% (dry)
- Vitiated air temperature: 1575 to 1700°F
- Background NOx in vitiated air: 26 to 200 ppm (dry, unnormalized)
- Pressure: 7.3 and 10 atm
- Calculated rich zone temperature: 2300 to 3460°F

Nox (dry, normalized to 15% O2):

7.3 atm results (rich zone equivalence ratio 1.05 to 1.3)

- 2 ppm MASB-generated NOx @ 12.2 vol% 02 in vitiated air
- 5 to15 ppm MASB-generated Nox @ 14.7 vol% 02 in vitiated air
- 50 to 75% reduction compared to earlier 14-inch MASB testing

10 atm results (rich zone equivalence ratio 0.85 to 1.05)

- 46 to 74 ppm MASB-generated NOx

CO (dry)

- 0 to 20 ppm exit CO when vitiated air CO < 100 ppm CO
- CO reduced by 50 to 75% when vitiated air CO > 150 ppm

Following natural gas testing, the two identified issues were solved by minor hardware modifications. 1) The fuel/air ratio control mechanism was rebuilt with more forgiving tolerances to differential thermal expansion. 2) Several backwall holes were drilled to admit a fraction of the primary air without swirl, thereby reducing flame stretch.

Note that rich zone temperatures are calculated using flow distributions and assuming uniformity without backflow from subsequent zones, and so are approximations ONLY.

Syngas testing was then successfully executed. Again a stable flame was easily achieved and controlled, without the need for ignitor firing. Apart from one thin weld crack, without test performance consequence, there was no burner damage. The fuel/air ratio control functioned properly. Rich zone equivalence ratio was controlled in the proper range. There was no flame stretch apparent.

Emissions results for the syngas tests are shown in Table 2. The MASB has now been demonstrated to generate negligible NOx additional to the PFBC background levels. This is a result of engineering the rich zone to achieve needed residence time and good recirculation. Figure 7 shows theoretical curves of NOx generation, as well as data for the 14" MASB and the current 18" MASB. Note in Figure 7 and in Table 2 that "MASB-generated NOx" is defined as the difference between the measured exit NOx, and the expected NOx exit level if 100% of the vitiated air NOx survived and no additional NOx were generated. The theoretical curves in Figure 7 were calculated using the Chemkin model with a Westinghouse data base, with the "no recirculation" line being plug flow, and the "good recirculation" line being 5 msec well mixed plus balance of residence time plug flow. (There is scatter because of the wide range of other variables in the actual testing.) The progress made is clear.

**Table 2. Syngas Test Results - Emissions**

Conditions:

- Vitiated air oxygen level: 10 to 17 vol% (dry)
- Vitiated air temperature: 1400 to 1630°F
- Background NOx in vitiated air: 20 to 130 ppm (dry, unnormalized)
- Pressure: 7.3 atm
- NH3 in syngas: 0 to 0.41 vol% 0.17 for most set points
- Calculated rich zone temperature: 2650 to 3160°F
- Calculated rich zone equivalence ratio: 0.9 to 1.5, 1.2 to 1.4 for most set points

Nox (dry, normalized to 15% O2):

- 8.3 ppm MASB-generated Nox, averaged over entire test matrix
- 5.8% conversion of NH3 to Nox, averaged over entire test matrix
- Insensitive to NH3 leve
- Low sensitivity torich zone equivalence ratio or temperature
- 50% reduction from 14" MASB results

CO (dry)

- CO reduced by 50% (Vitiated air CO always > 150 ppm)

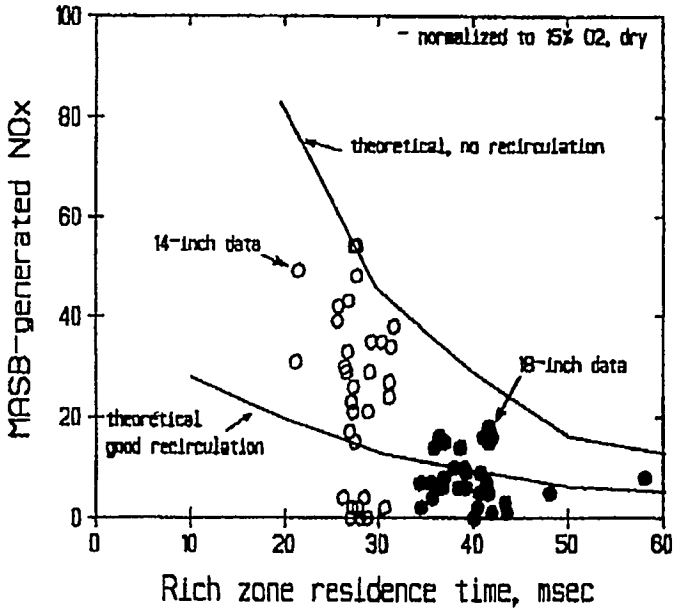


**Figure 7. MASB Performance vs. Design Basis**

## FUTURE WORK

The MASB design described in this paper will be used at the Power Systems Development Facility (PSDF) in Wilsonville, Alabama which is a DOE/Industry cost-shared facility operated by Southern Company Services.

This facility is designed to provide long-term hot gas cleanup and process testing for an advanced design Pressurized Fluidized Bed Combustion (PFBC) and Gasification system. It incorporates carbonization with a circulating fluidized bed and topping combustion developed at Foster Wheeler. The nominal 7-MW plant is being designed by Foster Wheeler and is scheduled to be in operation in 1996.

Figure 8 shows the topping combustor assembly for the PSDF. Each of the carbon steel spools is a pressure vessel. A concentric stainless steel cylinder inside each piece serves as the high temperature boundary. A layer of insulation fills the void between the concentric cylinders. The exhaust diffuser is a double-wall steel piece designed to accommodate cooling water for this region of the MASB. The inner liner of this piece is a Hastelloy alloy. The topping combustor itself is an Inconel or Hastelloy-type alloy with a diameter of about 18 in., which is commercial scale. Multiple combustors will be used in a utility-size plant incorporating Westinghouse 501 or 251 combustion turbines.

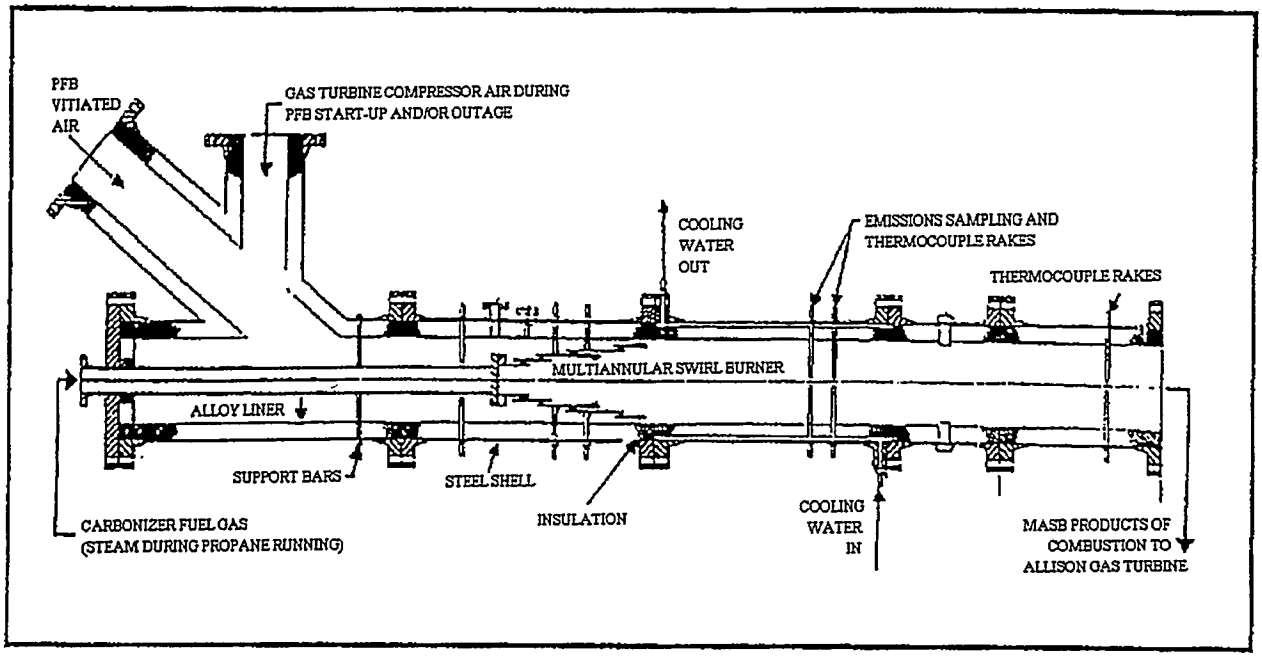


**Figure 8. Topping Combustion Assembly**

About 76,000 lb/h vitiated air enters the combustor at 1.03 MPa-a/760°C (150 psia/ 1400°F). About 1.46 kg/s (11,600 lb/h) carbonizer fuel gas, at about 1650°F, is burned in the MASB, producing an exhaust gas temperature of 2350°F--the optimum firing temperature for a utility-size plant. In a commercial plant, the 2350°F gas from the MASB is fed at full temperature to the gas turbine expander. For Wilsonville, the gas will be cooled to about

1975°F with compressor bypass air since the combustion turbine is limited to this temperature level. This advanced CPFBC facility at Wilsonville Alabama was described in detail by J. D. McClung et al. 1994.

In addition to the Wilsonville facility mentioned above, the MASB configuration will be applied at Air Products and Chemicals Four Rivers Energy Modernization Project (FREMP). This application will be the first commercial power plant using second generation pressurized fluidized bed (CPFBC) combustion technology. Air Products has been selected in the DOE Clean Coal Technology Round V to build, own and operate this combined cycle facility which will produce 66 MWe, export up to 400,000 lb/hr of steam, and be located at their chemical manufacturing facility in Calvert City, KY. The gas turbine will be a Westinghouse model 251B12 that will be modified to accommodate full air extraction and an external topping combustor with a cluster of MASB's as shown in Figure 2. This project was described in detail by J. J. Lewnard et al 1993.

## REFERENCES


Robertson, A., Garland, R., Newby, R., Patel, J., and Rubow, L., 1988, "Second-Generation PFB Combustion Plant Performance and Economics," EPRI Seminar on Fluidized Bed Combustion Technology for Utility Applications.

Garland, R., Pillsbury, P., 1990, "Status of Topping Combustor Development for Second Generation Fluidized Bed Combined Cycles," ASME paper 90-GT-30.

Domeracki, W. F., Dowdy, T. E., Bachovchin, D. M., 1994, "Topping Combustor Development for Second-Generation Pressurized Fluidized Bed Combined Cycles", Proceedings of the ASME, IGTI 1994 Gas Turbine Conference.

McClung, J. D., Quandt, M. T., Frochlich, R. D., 1994, "The Advanced CPFBC Facility at Wilsonville, AL, USA". Proceedings of the First International Conference on Combined Cycle Power Generation, Calcutta, India, 1994.

Lewnard, J. J., et al., 1993, "Commercialization of Second Generation Pressurized Circulating Fluid Bed Combustion Process". Proceedings of the Power Gen Americas Conference, Dallas, TX, 1993.

## 5.4 Development and Demonstration of a Solid Fuel-Fired Gas Turbine System

### CONTRACT INFORMATION

| | |
|---|---|
| **Cooperative Agreement** | DE-FC21-93MC30127 |
| **Contractor** | Western Research Institute<br>365 North 9th Street<br>Laramie, Wyoming 82071-3395 |
| **Contractor Project Manager** | James G. Speight |
| **Principal Investigator** | Vijay K. Sethi |
| **METC Project Manager** | Madhav Ghate |
| **Period of Performance** | March 94 to March 96 |

### ABSTRACT

Western Research Institute (WRI) and Power Generating Incorporated (PGI) are developing a solid fuel-fired gas turbine system for specialized cogeneration applications. The system is based on a patented pressurized combustor designed and tested by PGI in conjunction with McConnell Industries. The other components of the system are (a) fuel receiving, preparation, storage and feeding system, (b) gas clean-up equipment, and (c) a gas turbine generator.

A demonstration of the technical and economic viability of the integrated system is being funded by the U.S. DOE through METC and the National Renewable Energy Laboratory, and PGI. An approximately 400 kW prototype system is under construction at the WRI facilities in Laramie, Wyoming. As a part of this demonstration the integrated system, following a short shakedown period, will be operated on white wood. White wood was selected as the fuel for early tests because of its low ash (0.5 - 1.0 %), silica, and sulfur contents. The system will then be operated on coal. It is expected that the design of the coal-based system will evolve as the wood testing proceeds.

In previous similar wood-fired system development attempts, albeit at lower turbine inlet temperatures, a major technical hindrance to long-term operation of a gas turbine power system has been the degradation of the hot section of the gas turbine. Deposition, erosion, and corrosion are main issues that need to be addressed. In the wood-fired PGI system, erosion is not likely to be of concern because of the low silica and low overall ash content of the fuel and the fact that the wood ash particle size is expected to be in the range where little or no erosion would be

expected. However, because of the high alkali content of the fuel, deposition and corrosion can become major issues.

This paper will deal with the issues pertaining to the design of the prototype being constructed at the WRI premises. Preliminary thoughts on the design aspects of the plant modifications required for coal testing will also be presented.

# Poster Session B

*Filters and Sorbents*

# PB.1 Assessment of Ceramic Membrane Filters

## CONTRACT INFORMATION

**FTPA Number** ANL 49969, B&R Code AC-15

**Contractor**

Argonne National Laboratory
9700 South Cass Avenue
Argonne, IL 60439-4832
(708) 252-5979 (telephone)
(708) 252-4007 (telefax)

**Contractor Project Manager** Rajesh K. Ahluwalia

**Principal Investigators**

Rajesh K. Ahluwalia
Howard K. Geyer
Kwan H. Im
Chao Zhu
David Shelleman (Penn State University)
Richard E. Tressler (Penn State University)

**METC Project Manager** Norman Holcombe

**Period of Performance** May 1994 to May 1995

**Schedule and Milestones**

**FY95 Program Schedule**

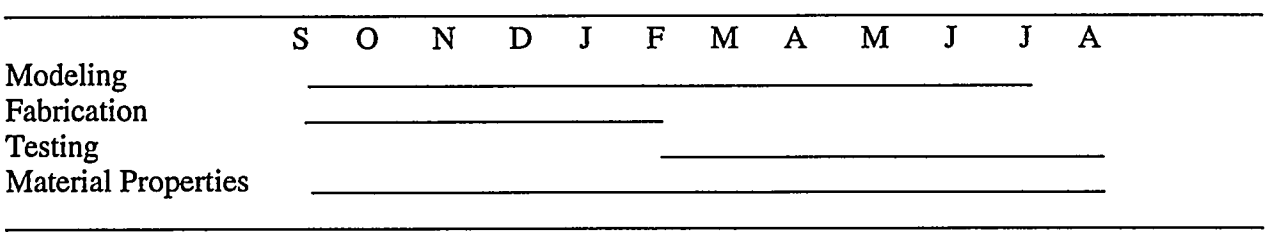


## OBJECTIVES

1. To develop analytical models for evaluating the fluid mechanics of membrane coated, dead-end ceramic filters.

2. To determine the effects of thermal and thermo-chemical aging on the material properties of emerging ceramic hot gas filters.

## BACKGROUND INFORMATION

CeraMem Corporation has been active in developing a unique, high-efficiency ceramic gas filter for removal of particulate matter from flue gas and hot gas streams. The filter is fabricated by coating a thin ceramic membrane (50 μm) on a commercially available honeycomb cordierite monolith (EX-80) with multiplicity of passageways. The membrane filter operates as a dead-end filter. This

flow configuration is achieved by modifying the monolith structure by plugging every other cell at the upstream face with a high-temperature inorganic cement. Cells which are open at the upstream face of the monolith are plugged at the downstream face. The particle laden gas is thus constrained to flow through the membrane-coated porous cell walls. The thin membrane has a pore size approximately 100-fold finer than that of the monolith support. Thus, the retention efficiency of the filter for entrained particles is determined by the membrane pore size. After the particulate matter has accumulated for a defined interval of time or to a defined pressure drop, the filter is backpulsed to dislodge the collected particulates. Whereas complete regeneration of the filter by simple backpulsing has been achieved in laboratory and field tests, some problems were recently encountered during tests at pilot scale. Subsequently, DOE requested ANL to provide assistance by developing analytical models for the backpulse cleaning operation.

The CeraMem cordierite material and the Industrial Filter and Pump Manufacturing (IFPM) Company fibrous material are at a stage of development where long term reliability issues must be addressed. For example, their tolerance to exposure to alkali-containing combustion gas, being able to absorb $Na_2O$ without serious degradation of the mechanical properties at use temperatures, must be demonstrated. Their performance must be correlated to the phase composition and microstructure, in general, of the materials after exposure.

The thermal and chemical aging at use temperature may significantly alter the thermophysical and thermomechanical properties of these materials in ways which must be documented. In fact, the values of thermal expansion coefficient, thermal conductivity, and elastic moduli as a function of temperature must be measured for the as-fired or as-received materials in addition to the thermally and chemically aged materials. These parameters determine the thermal gradients in the components during transient and steady state operating conditions, and the thermoelastic stresses which develop in the components as a result of these thermal gradients. The thermoelastic stresses can be accurately mapped in a given component if the temperature distributions are known (assumed and/or calculated) and the thermomechanical properties are known as a function of temperature and aging history. In conjunction with a knowledge of the strength distributions of the materials as a function of temperature and aging exposure, these thermoelastic stress calculations can be used to predict survival of the components in actual or simulated use.

In addition, when the details of the microstructural changes are established as a function of temperature and thermochemical aging and the properties are related in a cause-effect relationship, the microstructure can be tailored to resist the deleterious changes.

The two materials under consideration are very different structurally. The CeraMem material is rigid, monolithic material with parallel channels along the axis of the filter body, created by the "green" extrusion process. The IFPM filter is similar to the rigid candle filters except it is highly compliant, being comprised of refractory fibers loosely bonded together with an inorganic-binding agent.

The reaction of these materials to thermal transients such as pulse-cleaning is quite different. The cordierite body is 3-D mechanically coupled so the thermoelastic stresses can be determined, in principle, by knowing the thermal gradients and the thermophysical properties. The IFPM material, on the other hand, is very loosely mechanically coupled such that thermal strains can be more readily tolerated without generating destructive thermoelastic stresses. The degree of mechanical coupling in this material can be dramatically affected by thermal and chemical exposure. For example, the fibers can develop "welds" where they cross due to fluxes (such as $Na_2O$). The incorporation of very fine particulates will fill void space and tend to "rigidize" the structure. Thus,

careful analysis of the rigidity of this latter material with exposure is essential. Also, oxide fibers have been shown to be degraded (mechanically weakened) by exposure to alkali and other fluxes such as $H_2O$ which assist crystallization and grain growth at exposure temperature.

The CeraMem material will show subtle changes in microstructure (phase composition, grain size, pore size and shape) with exposure which will dramatically affect the mechanical properties, particularly strength, as has previously been demonstrated with the Coors alumina/ mullite material. Thus, careful x-ray diffraction, SEM, and chemical analyses are required to make the correlation between microstructural changes and property changes.

## PROJECT DESCRIPTION

This program utilizes combined experience, skills and facilities at three organizations: Argonne National Laboratory, Penn State University (PSU) under subcontract to ANL, and CeraMem Corp. (not funded under this initiative). ANL is responsible for analytical modeling of filtration and pulse-cleaning operations, flow-through testing, and prediction of filter response to thermal cycling under realistic service conditions. PSU is responsible for measuring properties and microstructural changes of exposed filter specimens. CeraMem is charged with the responsibility of fabricating and supplying the filters, advising ANL on its experience with pulse cleaning, and conducting exploratory or confirmatory laboratory tests as needed.

## RESULTS

### Analytical Model

In order to analyze the forward and reverse flows, models were developed for jet entrainment and mixing, fluid flow in filter passages, and venturi nozzle and diffuser. Referring to Fig. 1, it is clear that these models can be combined appropriately to represent the fluid mechanics of gas filtration and backpulse cleaning operations. Entrainment of the suction/plenum gas by the motive/ pulse gas issuing from the blow hole is modeled as a constant area, steady and adiabatic process. Flow in the filter passages is determined on the basis of a one-dimensional compressible flow in square channels with proper accounting for skin friction and mass, momentum and energy transfer across the porous walls. In order to satisfy the no-flow outlet boundary condition in the inlet channel, pressure P at entrance to the exit channel is guessed and varied. Depending on the initial guess, 3 to 40 iterations are required to satisfy the outlet boundary condition. Flow in the diverging section (area ratio >1) of the venturi is analyzed on the basis of a specified diffuser pressure recovery coefficient and in the converging section on the basis of a specified nozzle efficiency.

In the filtration mode, dirty gas enters the filter and exits through the converging-diverging venturi. For specified mass flow rate ($\dot{m}$), this flow is analyzed by executing the filter model, the nozzle model and the diffuser model. Within the filter model, P at x = 0 in the exit channel is determined iteratively such that $\dot{m}$ at x = L in the inlet channel is reduced to zero.

To analyze the pulse cleaning mode, entrainment/ejector model, diffuser model and channel model are executed sequentially. An iterative procedure is required since the suction gas pressure ($P_2$) in the ejector model is unknown. The Newton-Raphson iteration scheme is employed to determine $P_2$ such that the exit pressure from the filter model matches the specified pressure in the dirty gas plenum. Alternatively the suction gas flow rate $\dot{m}_2$ can be regarded as unknown and determined iteratively to satisfy the exit pressure constraint. An advantage of $\dot{m}_2$ iterations is that the possibility of negative entrainment can also be factored in. Note that separate iterations are still required within the channel model as in the analysis of the filtration mode.

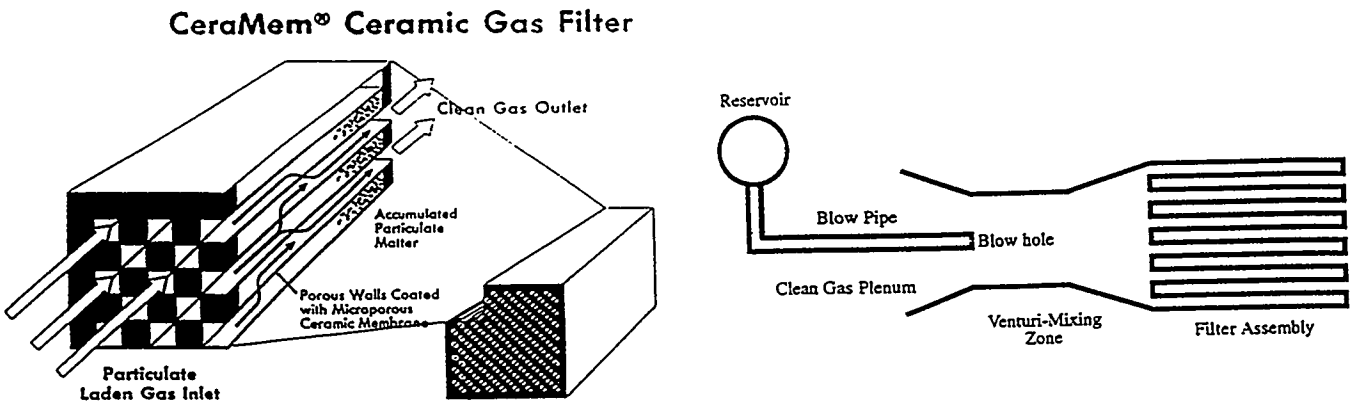


**Figure 1. Flow passage configuration. Reproduced with permission from CeraMem Corporation**

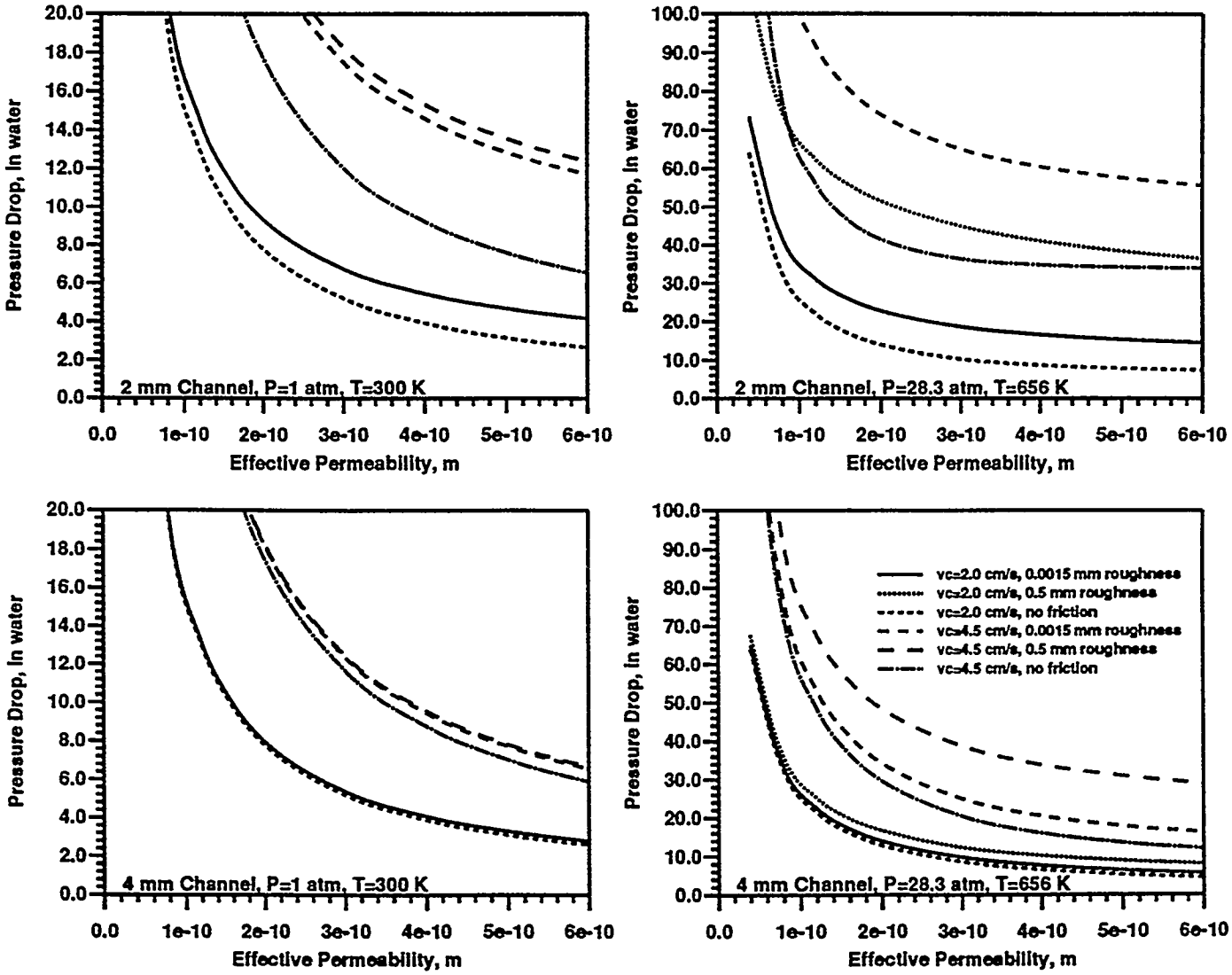


**Figure 2. Filtration pressure drop behavior as a function of channel width, face velocity, wall roughness and gas pressure. Channel length is 30.5 cm.**

## Filtration Pressure Drop

Figure 2 shows the pressure drop characteristics of 30.5-cm long membrane filters as a function of channel width (W), face velocity ($v_c$), gas pressure/ temperature, effective permeability ($K_{eff}$) and the equivalent sand grain roughness ($\varepsilon$). The medium is air for atmospheric system calculations and a reducing gas of molecular weight 21.9 g/gmole for the pressurized system. The effective permeability may be regarded as combination of in-series resistances offered by the monolith, membrane, adherent ash deposit layer, and the removable ash deposit.

**2-mm Channels.** At 2 cm/s face velocity and P = 1 atm, the flow in the channels is laminar. The observed experimental $\Delta P$ for clean channel is 1.3 kPa (6.8" $H_2O$) from which a $K_{eff}$ of 4 x $10^{-10}$ m may be inferred from Fig. 2a. The model calculations indicate that a $\Delta P$ of 3.9" $H_2O$ may be attributed to Darcy flow and 1.3" $H_2O$ to friction effects. In many applications, this filter would be pulsed at $\Delta P$ of about 1.7 kPa (6.8" $H_2O$) which corresponds to a $K_{eff}$ of 3 x $10^{-10}$ m . This implies that if ash had a specific permeability of 4.5 x $10^{-14}$ $m^2$, pulse cleaning is initiated when the cake thickness builds up to 0.038 mm.

At $v_c$ = 4.5 cm/s and P = 1 atm, the channel flow is mostly laminar and $\Delta P$ is almost independent of the wall roughness. The observed experimental $\Delta P$ for clean channels is 3.36 kPa (14.6" $H_2O$) at the above-inferred $K_{eff}$ of 4 x $10^{-10}$ m. The calculations indicate that 9.3" $H_2O$ of $\Delta P$ may be attributed to Darcy flow and 5.1" $H_2O$ to the friction effects.

At P = 28.3 atm and T = 656 K, the channel flow becomes turbulent. At 2 cm/s face velocity and $K_{eff}$ = 4 x $10^{-10}$ m, the calculated pressure drop for smooth channels is 16.6" $H_2O$ (4.13 kPa) of which 8" $H_2O$ is due to friction effects. If the walls are treated as rough, the pressure drop increases to 40" $H_2O$ at 0.5 mm equivalent sand grain roughness. At this operating point, $\Delta P$ (friction) >> $\Delta P$ (Darcy) and the flow may be regarded as friction dominated.

At $v_c$ = 4.5 cm/s and P = 28.3 atm, calculated $\Delta P$ for smooth channels is 60.6" $H_2O$ of which 25.8" $H_2O$ can be attributed to friction effects. The pressure drop becomes unacceptable, > 200" $H_2O$, if the channel walls are treated as 0.5 mm rough. Given the uncertainty over $\varepsilon$, one would not select 2-mm channels for service at 4.5 cm/s face velocity in most high-pressure applications.

**4-mm Channels.** At P = 1 atm, the channel flow is laminar. The computed pressure drop is 4.1" $H_2O$ at $v_c$ = 2 cm/s and $K_{eff}$ = 4 x $10^{-10}$ m, and 9.5" $H_2O$ at $v_c$ = 4.5 cm/s and same $K_{eff}$. More than 95% of computed $\Delta P$ occurs across the porous walls at $v_c$ = 2 cm/s and more than 90% at the higher face velocity. Thus, the friction effects are not important in 4-mm channels for service at atmospheric pressure.

At P = 28.3 atm, the channel flow is turbulent. The computed pressure drop for smooth walls is 7.7" $H_2O$ at $v_c$ = 2 cm/s and $K_{eff}$ = 4 x $10^{-10}$ m, 85% of which is due to the porous media. The pressure drop increases to 10.2" $H_2O$ if the walls are treated as 0.5 mm rough. At the higher face velocity, 4.5 cm/s, computed $\Delta P$ is 20.5" $H_2O$ for smooth walls, 33.9" $H_2O$ for 0.5-mm rough walls, and 16.1" $H_2O$ for flow without friction. Thus, friction and Darcy pressure drops become equally important at 4.5 cm/s face velocity and P = 28.3 atm.

## Pulse Cleaning of Atmospheric System

A number of parametric calculations have been performed to explore the fluid mechanics of the cleaning operation. A 15.2 cm x 15.2 cm square filter assembly is selected as reference. The assembly contains 900 4 mm x 4 mm channels, each 30.5 cm long, and blocked at alternate ends. The total filtration area is 2.2 $m^2$. For pulse cleaning, compressed air at 334 K issues from a 1.9-cm diameter blow hole into a converging-diverging venturi with 10.2 cm x 10.2 cm throat cross-section. The venturi and the blow pipe are located in a plenum containing air at 422 K and atmospheric pressure. Flow in the diverging portion of the venturi is modeled as a diffuser with

0.5 pressure recovery coefficient. When choked, the total flow rate through the blow hole is 0.37 kg/s at stagnation pressure ($P_0$) of 5.9 atm, 0.50 kg/s at $P_0$ = 7.9 atm, and 0.63 kg/s at 9.9 atm. At zero entrainment, these represent average face velocities of 15.4 cm/s, 20.7 cm/s and 25.9 cm/s.

**Role of Effective Permeability.** Figure 3 displays the computed jet entrainment ratio and the average face velocity along the clean channel as a function of effective permeablity ($\varepsilon$ = 0.5 mm). Using the filtration pressure drop data presented in Fig. 2, the results in Fig. 3 can be reinterpreted in terms of the trigger pressure drop, i.e., $\Delta P$ at which pulse cleaning is initiated. A pressure of 15.5 kPa gauge (2.25 psig) is calculated at inlet to clean channel for $P_0$ = 5.9 atm and $K_{eff} = 4 \times 10^{-10}$ m which compares favorably with 2 psig measured in some laboratory experiments. The gauge pressure increases mainly with $P_0$ and secondarily with decrease in $K_{eff}$. A higher gauge pressure of 29.6 kPa can be established at $4 \times 10^{-10}$ m effective permeability by raising $P_0$ to 9.9 atm. A nearly-uniform velocity field is established inside the clean-gas channels at low effective permeability. The velocity variation along the channel increases with $K_{eff}$ and $P_o$.

Amount of plenum gas entrained by the pulse jet is very sensitive to effective permeability. As $K_{eff}$ decreases (e.g., due to deposit buildup, sintering or low specific permeability), so does the entrainment ratio. There is a critical $K_{eff}$ at which the net entrainment is zero and below which a part of the motive gas is reflected back into the plenum. This condition must be avoided (e.g., by more frequent pulsing) because it represents under utilization of pulse gas compression energy with concomitant reduction in face velocity. Both $v_c$ and channel gauge pressure are deemed important in determining the efficacy of the pulse cleaning operation.

**Venturi Geometry.** For optimum pulse cleaning, the venturi should be deigned to maximize jet entrainment. Figure 4 quantifies the improvement in pulse cleaning with narrowing of venturi throat. For $K_{eff} = 2.4 \times 10^{-10}$ m and $P_0$ = 5.9 atm, the entrainment ratio can be increased from 0.08 at $A_{th}$ = 100 cm$^2$ to 1.02 at $A_{th}$ = 22.5 cm$^2$ with corresponding increase in channel pressure from 16.7 kPa gauge to 35.5 kPa gauge.

In general, as the venturi throat is made narrower jet entrainment increases as does the pressure generated in the channel. There is a critical throat area, 26.5 cm$^2$ for $P_0$ = 5.9 atm, below which further increase in flow kinetic energy obtained by reduction in $A_{th}$ and improvement in entrainment is not usefully converted to the pressure head. At this point, the excess pressure generated in the channel begins to level off or to even diminish slightly. For a given filter (L, W and $K_{eff}$) and pulse system ($P_0$, blow hole diameter), the critical $A_{th}$ corresponding to the maximum channel pressure, is a function of the pressure recovery coefficient. As $A_{th}$ is further reduced, a mismatch develops between the venturi flow and the filter flow in that the pressure generated at the venturi is insufficient to drive the combined motive gas and the suction gas through and across the filter assembly. Thus, a part of the combined flow has to be reflected back into the plenum. The model has not been extended into this flow regime because it clearly represents a suboptimal operating condition.

**System Optimization.** In general a reverse flow cleaning system must be designed to generate a pressure pulse of predetermined magnitude ($\Delta P$) in the clean channel. Effective permeability at which cleaning is to be initiated can be inferred from the trigger pressure. Together $K_{eff}$ and $\Delta P$ specify the required face velocity. The task is then to determine the reservoir pressure, blow hole size and venturi geometry capable of achieving the target $\Delta P$. For reasons stated earlier it is desirable to minimize compressed gas usage and maximize plenum gas entrainment. A methodology to accomplish this objective is best enumerated through an example problem.

The dimensions of the filter assembly are the same as for calculations presented in Fig. 3. Figure 5 shows that for given stagnation pressure ($P_0$) and temperature (322 K) at the blow hole , there are

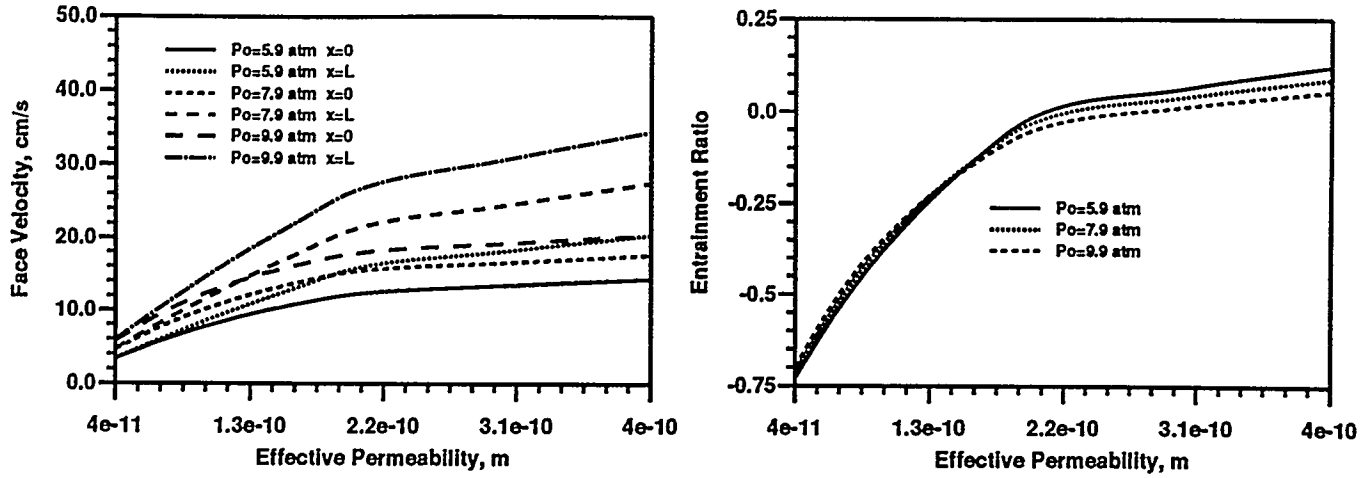


**Figure 3. Fluid mechanics of pulse cleaning operation on a 15.2X15.2X30.4-cm filter assembly attached to a 10.2 X 10.2-cm throat venturi. Compressed gas at 334 K is supplied through a 1.9-cm diameter blow hole. The exit pressure from the filter is 1 atm.**

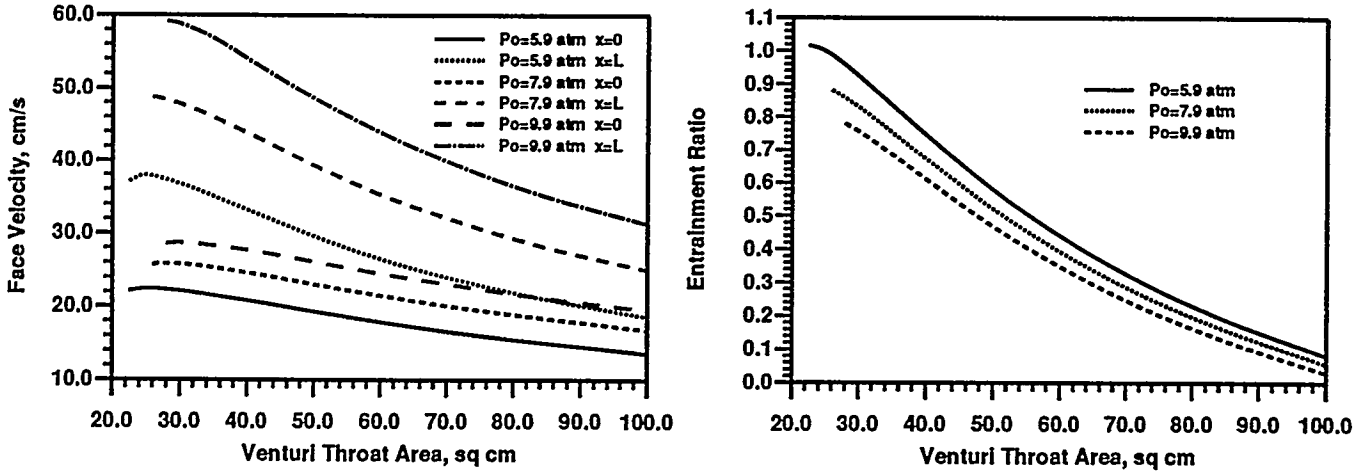


**Figure 4. Improvement in pulse cleaning with narrowing of venturi throat. Effective permeability is 2.4e-10 m.**

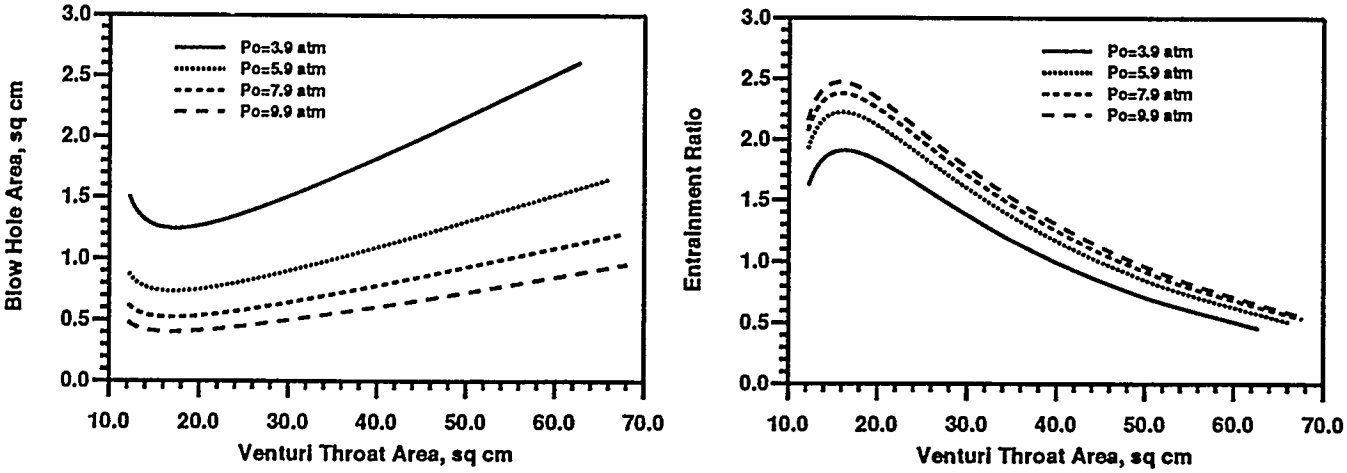


**Figure 5. Optimization of pulse cleaning system: 900 passages, L = 30.5 cm, W = 4 mm, plenum gas pressure = 1 atm, blow gas at 334 K, and 2.4e-10 m effective permeability.**

many combinations of blow hole diameter and venturi throat area that can achieve the target $\Delta P$ (14 kPa/2 psig). The optimum combination is the one that leads to the maximum flow entrainment, i.e., the smallest blow hole diameter. Note that at $P_0 = 5.9$ atm the optimum nozzle/blow hole area is one-fourth of the original design (2.8 $cm^2$ in Fig. 3), and the venturi throat area is one-sixth of the original design (104 $cm^2$). The optimum combination achieves an entrainment ratio of 2.2 compared to only 0.1 in the original design.

The combination of $P_0$, blow hole diameter and venturi throat area that minimizes compression power can also be determined from the results presented in Fig. 5. The results favor the lowest $P_0$ capable of achieving the target $\Delta P$, but other considerations such as the reservoir volume may dictate that somewhat larger $P_0$ be selected.

**Filter Performance**

A test apparatus, shown schematically in Fig. 6, has been assembled to expose ceramic filter specimens to chemical environments simulating operation of pressurized fluidized bed (PFB) and integrated gasification combined cycle (IGCC) plants. The exposed specimens are analyzed for changes in thermophysical and thermomechanical properties: thermal expansion coefficient, thermal conductivity, strength, elastic moduli and microstructure. The tests also monitor the collection efficiency of the filters and the ability of pulse reverse gas flow to regenerate the filter. The following are the nominal test conditions.

| | |
|---|---|
| Pressure: | atmospheric |
| Temperature: | 600 - 900°C |
| Superficial face velocity: | 2-4 cm/s |
| Filter specimens: | 5.08 - 15.24 cm long, 25 or 100 cpsi |
| Nominal gas flow rate: | 9-15 slm, variable $SO_2$, alkali and ash concentration |
| Test duration: | 100 - 2,000 h continuous or interrupted |

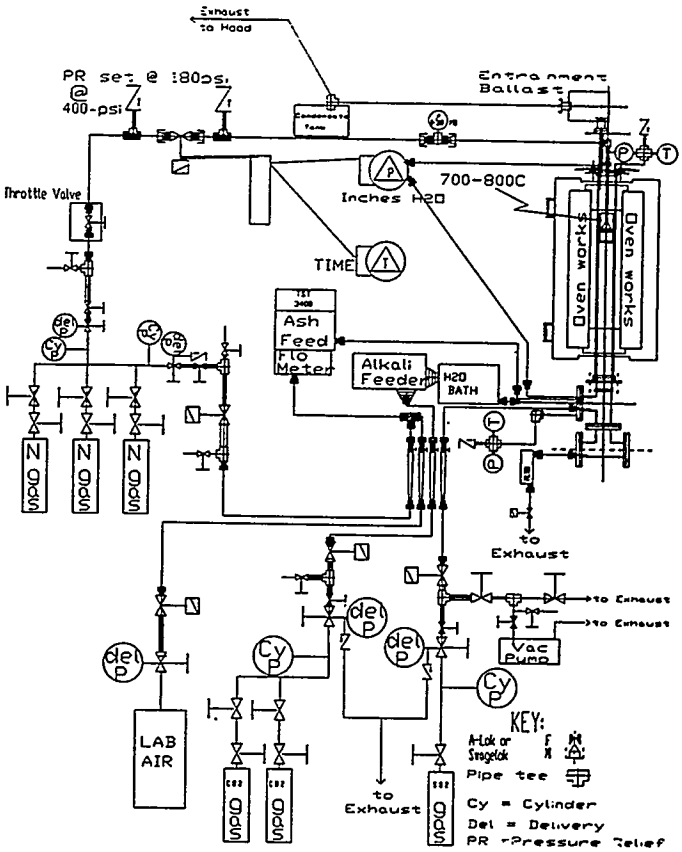


**Figure 6. Filter Exposure Apparatus**

**Gas Handling System.** Initial tests will simulate the oxidizing environment of PFB operation. A mixture of shop air, bottled $N_2$, $CO_2$ and $SO_2$, and $H_2O$ vapor at nominal volumetric composition of 17.1%, 58.8%, 13.5%, 0.01% and 10.5% respectively, is used to match the oxygen potential, $SO_2$/-$SO_3$ concentration, moisture level and $CO_2$ concentration typical of PFB environment.

**Pulse Gas System.** After exposure to the particle laden gas for a defined interval of time or to a defined pressure drop, the ceramic filter is back pulsed to dislodge the accumulated ash deposit. Nitrogen from the high-pressure line is used for back pulsing. Pulse duration and frequency are adjustable by means of a computer-controlled solenoid valve. The nominal values are 1 s duration and 4-6/h frequency.

The pulse gas from the high-pressure line is directed into a blow pipe and issues from a small blow hole of 1.25-mm diameter. It discharges into the plenum region and entrains some of the plenum gas. The resulting mixed jet enters the venturi atop the filter holder. For the conditions of the experiment, the flow is choked at the blow hole and the estimated entrainment ratio is about 1.2. A ballast tank, with a capacity of 4 filters, is connected to the upper plenum and serves as a reservoir for entrained gas. It is estimated that the maximum differential pressure generated in the venturi will be less than 3 psi.

The blow tube and the venturi section are machined from a nickel based alloy, Inconel 625. To further improve the corrosion resistance at high temperature in presence of sulfur oxides and alkali species, these are coated with alumina particles (alonized).

**Ash/Alkali Feed System.** For tests under oxidizing conditions, fly ash from Tidd plant is used. The ash has a top size of about 10 μm and is extremely cohesive. Repeated attempts to feed this ash by a fluidized-bed aerosol generator proved futile because of in-bed agglomeration leading to volcanic deposits on the distributor plate. A new feed system had to be designed in which ash is introduced into a plenum on a chain conveyor and is blasted with two jets of nitrogen which cross at an angle of 140°. The jets have a diameter of 1.6 mm, meet at a point on the conveyor and serve to suspend and deagglomerate the ash. A third jet from the bottom helps in entraining and transporting the suspended ash particles to the test chamber.

An ultrasonic nebulizer is used to feed water containing dissolved sodium chloride or sodium hydroxide sufficient to provide a concentration of 1- 10 ppmv in the gas stream.

**Gas Heating System.** Flowing gas is heated by a Lindberg/Blue M three-zone tube furnace capable of achieving a maximum temperature of 1200 °C. A concentric tube arrangement is used to contain the gases. The tubes are of ceramic (mullite) construction and are clamped at the bottom. The inner tube (8.89 cm ID, 0.9 m long) has one collar and is shorter than the outer tube (10.16 cm ID, 1.07 m long) which has two collars. The filter assembly is positioned at the top of the inner tube. The outer tube is longer to provide a plenum for the hot clean gas and to permit all connections to the metallic tubes to be made outside the furnace.

**Filtration System.** The ceramic filter specimens are provided by CeraMem Corp. The specimens to be tested are 5.08-cm or 15.24-cm in length, and may contain 25 cpsi (cells per square inch) or 100 cpsi. Four 100 cpsi, 5.08-cm long specimens can be exposed at a time. At a superficial face velocity of 2 cm/s, the expected pressure drop across a clean filter specimen at room temperature is about 4" of water. The filter holder is machined from Inconel 625 which is superior to stainless steel in high temperature strength and corrosion resistance. To further protect the surface and for life extension, the filter holder is alonized by Alon Processing.

## Material Properties

**Strength.** Strength testing as a function of temperature has been completed for the uncoated EX-80 material with 4 mm cell size. Four-point flexure tests were conducted on 2" long by 1 cell by 1 cell specimens at room temperature, 800 °C and 870 °C. All specimens were loaded using a support span of 40 mm, a load span of 20 mm and a loading rate of 0.02"/min (a strain rate of 9.64/min). Specimens tested at elevated temperatures were heated to the test temperature (800 °C or 870 °C) and held for 15 minutes for thermal equilibration prior to loading. Compared to the measured room temperature strength (9.6 ± 0.6 MPa), the uncoated EX-80 material did not exhibit a significant strength increase at 800 °C (9.7 ± 1.5 MPa), but did show a slight increase in strength at 870 °C (10.8 ± 1.3 MPa). Slight increase in strength at 870 °C may be caused by closure of microcracks.

The same procedure was followed in conducting four-point flexure tests on coated 4-mm cell size specimens. Based on the average strengths and standard deviations, the coated filter material did not exhibit a significant increase in strength, even after accounting for differences in surface area under uniform tension due to the slight difference in size. To be consistent with the uncoated filter material, the tensile surface was always the outer surface of the filter bars, which received the sanding treatment performed by CeraMem. The sanding was done to ensure a flat and uniform surface for loading the specimens. However, the sanding also removes some, if not all, of the coating, which may explain why the coated filter material did not exhibit a significant increase in strength. While the inner surface of the square cell contained the as-processed coating, the maximum tensile stress during four point flexure occurs on the outer surface (which was the surface that was sanded) within the load span.

Strength tests were also conducted on coated 2-mm cell size specimens, 2" in length and two cells by two cells wide. Table 1 gives the experimentally obtained Weibull strength distribution for both the coated and uncoated filters. Fractographic analysis using scanning electron microscopy is being performed to determine the source of some of the low strength failures for some of the strength distributions. The fracture patterns for the flexure bars of the uncoated EX-80 material show only intergranular fracture, as expected, at room and elevated temperatures. Fractures initiated from the outer surface of the bottom cell wall, which is the location of maximum tensile stress. No fractures were observed to initiate from cell walls (strut) parallel to the applied load. Thus, the expression used to calculated the strength of the flexure bars, which were based on the outer fiber strength of an open-square wall bar, are valid.

**Elastic Moduli.** Elastic moduli data as a function of temperature were obtained using an acoustic resonance technique. Specimen are suspended inside a furnace via sapphire fibers, which are glued to transducers outside the furnace. An amplifier is used to excite one of the transducers, thereby sending vibrations down the sapphire fibers, through the specimen, and back up the other sapphire fiber to the receiving transducer. The resonance spectrum is then analyzed using a fast Fourier transform computer program to identify the primary resonant frequency for the corresponding mode of vibration (longitudinal or torsional).

The longitudinal mode measurements, which yield the Young's modulus, were conducted on specimens which were 2" in length by 6 cells wide by 2 cells thick with a small, through-thickness slit (to accommodate the sapphire fiber) machined into the center strut at each end of the specimens. For the torsional mode, which yield the shear modulus, the slits were machined into the ends of the specimens (2" in length by 6 cells wide by 3 cell thick) at diagonal corners.

Specimens were heated to 950 °C at 10 °C/ minute and held for five minutes (to allow for thermal equilibrium and resonating of the specimens) at 400°, 800°, 870°, and 950 °C. The specimens were then cooled at a rate of 10 °C/ minute to 400 °C with five minute holds at 870 °C and 800 °C. The room temperature measurement was repeated after the furnace cooled. The structural stiffness of the uncoated EX-80 material (4 mm x 4 mm cell size) for the longitudinal resonance mode increased from 0.38 x $10^6$ psi at room temperature to 0.5 × $10^6$ psi at 950°C. Upon cooling the longitudinal stiffness increased to 0.52 × $10^6$ psi at 870°C and 800°C, and then returned to 0.38 × $10^6$ psi at room temperature. The torsional stiffness exhibited the same hysteresis increasing from 0.12 x $10^6$ psi at room temperature to a maximum of 0.16 x $10^6$ psi at 800°C during cooling and back to 0.12 x $10^6$ psi at room temperature. The increase in stiffness with temperature may by due to closure of microcracks during heating or some sintering (densification) at the elevated temperatures. Significant sintering probably did not occur since identical stiffnesses were measured at room temperature prior to heating and upon cooling from 950 °C. If the increase in stiffness is due to closure of microcracks, then the hysteresis observed upon cooling

**Table I. Average Strength and Weibull Parameters for Uncoated and Coated Filters Using Four Point Flexure**

| Material | Temperature (°C) | Average Strength (MPa)[1] | Weibull Modulus LR[2] | Weibull Modulus ML[3] | Weibull Characteristic† Strength (MPa) LR[2] | Weibull Characteristic† Strength (MPa) ML[3] |
|---|---|---|---|---|---|---|
| Uncoated | 20 | 9.6 (0.6)* | 17.8 | 22.3 | 5.9 | 6.5 |
| | 800 | 9.7 (1.5) | 7.4 | 8.9 | 3.2 | 3.8 |
| | 870 | 10.8 (1.3) | 8.9 | 12.7 | 4.3 | 5.7 |
| Coated 25 cpsi | 20 | 10.1 (0.4) | 27.6 | 31.2 | 7.5 | 7.8 |
| | 800 | 10.4 (1.3) | 8.3 | 12.5 | 3.8 | 5.3 |
| | 870 | 10.4 (0.9) | 13.1 | 11.8 | 5.7 | 5.3 |
| Coated 100 cpsi | 20 | 8.8 (0.8) | 13.6 | 15.2 | 4.8 | 5.1 |
| | 800 | 8.4 (0.9) | 10.7 | 10.4 | 3.8 | 3.7 |
| | 870 | 8.6 (1.5) | 6.8 | 7.4 | 2.5 | 2.8 |

† - Characteristic strength based on a unit area of surface in uniform tension.
1 - Data based on ten samples/temperature.
2 - Linear Regression
3 - Maximum Likelihood
* - One Standard Deviation based on ten samples per temperature.
Loading rate = 0.02"/min---Strain rate = 8.65-03/min for uncoated and 9.64E-03/min for coated.

**Table 2. Young's Modulus (GPa) and CTE (ppm/°C) Data**

| Material | Temperature (°C) | Young's Modulus (GPa) Heating | Young's Modulus (GPa) Cooling | CTE (ppm/°C) Heating | CTE (ppm/°C) Cooling |
|---|---|---|---|---|---|
| Uncoated 25 cpsi | 22 | 13.2 | 13.2 | -0.5 | |
| | 400 | 13.2 | 15.2 | 0.2 | 0.05 |
| | 800 | 15.5 | 17.9 | 0.5 | 0.45 |
| | 870 | 16.6 | 17.8 | 0.6 | 0.50 |
| | 950 | 17.5 | 17.5 | 0.6 | 0.55 |
| Coated 25 cpsi | 22 | 9.9 | 9.9 | -0.4 | |
| | 400 | 10.1 | 11.9 | 0.05 | -0.1 |
| | 800 | 13.4 | 15.5 | 0.37 | 0.3 |
| | 870 | 14.4 | 15.8 | 0.35 | 0.35 |
| | 950 | | | 0.40 | 0.38 |

suggests that the micro-cracks did not reopen above 800 °C and possibly until cooling below 650 °C.

Independent confirmation of the elastic modulus for the uncoated Ex-80 material was achieved at room temperature using a second acoustic resonance apparatus. This is equipped with an oscilloscope that enabled us to identify first (represented by ellipse) and half-order (represented by a figure "8") resonant frequencies and can measure frequencies less than 5,000 Hz that are typically masked by background or system noise.

To measure the modulus of the material, a single layer of the EX-80 material was machined from the 6 cell by 6 cell bar of uncoated EX-80. The final dimensions of the single layer were 51.232 mm long by 19.761 mm wide by 0.889 mm thick. Stainless steel taps were glued to the ends of the single layer plate at locations of mid-width (for flexural mode) and diagonal corners (for torsional mode). The single layer was then suspended such that the steel taps were oriented directly above transducers. A frequency generator was then turned on and the frequency was adjusted to resonate the sample.

The first and half order resonant frequencies for the flexural mode were determined to be 1211 and 606 Hz, respectively, which yielded an elastic modulus of 14.8 GPa. Likewise, the first and half order resonant frequencies for the torsional mode were determined to be 2010 and 1006 Hz, respectively, which yielded a shear modulus of 6.6 GPa. Based on the elastic and shear moduli, a Poisson's ratio of 0.12 was calculated for the uncoated EX-80 material at room temperature.

Since the first and half-order frequencies for a single layer are less than 5,000 Hz, we can not measure the resonant frequencies using the elevated temperature accoustic resonance apparatus. However, the ratio of the structural stiffness ($E^*$) to the elastic modulus of the strut ($E_s$) is related to the ratio of the thickness (t) to the length (l) of the strut (cell wall). For a honeycomb material with open-square cells, the above two ratios are directly related: $E^*/E_s = t/l$. For the uncoated EX-80 material with a 4 mm cell size, t = 0.034" and 1 = 0.17". Knowing $E^* = 2.6$ GPa (resonance technique), the room temperature elastic modulus of the strut (i.e. uncoated EX-80) was calculated to be 13 GPa , which is in very good agreement with 14.8 GPa determined using the single wall specimen. Thus, this equation can be used to determine the elastic modulus of the material from the structural stiffness measured via resonance at elevated temperature (see Table 2).

Elastic moduli measurements were performed on the coated EX-80 filters with 25 cpsi. As compared to the uncoated filters (E = 14.8 GPa), the coated filters exhibited slightly lower moduli (9.9 GPa), which is the opposite of what was expected. While measuring the structural stiffness at elevated temperatures (> 800 °C) the resonance signal decays fairly abruptly, making measurements quite difficult. In fact, the resonant signal became lost in the background noise at 950 °C and no results were recorded. This evidence suggests that the coating material acts to dampen the resonance of the material at elevated temperatures. Similar behavior has been observed for material with extensive glassy phase in the microstructure. At elevated temperatures, materials with a significant glassy phase in the microstructure prove very difficult to resonate, because the glassy phase tends to soften (viscosity decreases) and dampens the acoustic vibrations in the material.

While room temperature X-ray diffraction patterns (XRD) indicate that the coated filters contain no significant amorphous phases, heating to elevated temperatures may form an amorphous [e.g., silicate] phase(s), that could reduce the ability to resonate this material. Since the intensity of the resonant signal increases as the temperature is lowered from 950 °C, it is unlikely that any significant amorphous phase(s), if formed, remains ("freeze in") upon cooling.

**Thermal Expansion.** A dilatometer has been used to measure coefficient of thermal expansion (CTE)

for 1.5" long x 2 cells x 2 cells specimens cut from uncoated and coated 25 cpsi filters. The measurements indicate that hysteresis does occur upon heating at 1,000 °C, holding for 30 minutes, and then cooling to room temperature (see Table 2). Upon heating to 1,000 °C, the percent change in the length is not perfectly linear, but shows a slight upward curvature, which may be due to closure of microcracks. Upon cooling below 800 °C, microcracks appear to open resulting in a slight hysteresis in the expansion curve. For the uncoated sample, the results compare well with that of the manufacturer in both overall shape and values of the average CTE. In agreement with the manufacturer's data, a small discontinuity in the cooling curve occurs around 650 °C due to the opening of the micro-cracks that closed upon heating to 1,000 °C.

The coated 25 cpsi filter exhibited similar expansion behavior as the uncoated filter with the exception of an additional discontinuity in the heating curve at 800 °C. The source of this discontinuity is being investigated; however, it may be due to a phase change associated with the coating. Note that the structural stiffness measurements at elevated temperature were damped at about the same temperature. An average CTE at 800 °C of $0.35 \times 10^{-6}$/°C was measured for this sample. We will continue to perform some additional thermal expansion tests to verify the repeatability of the expansion behavior.

## FUTURE WORK

Detailed three-dimensional fluid dynamics calculations are being carried out to confirm the criteria for sizing the filter passages from considerations of Darcy pressure drop, friction pressure drop and the dynamic head. The calculations will also validate the methodology for optimizing the venturi geometry from the standpoint of minimizing pulse gas usage and controlling the thermal load imposed on the filter assembly. Work is underway to expose the filter specimens and measure changes in material properties as a function of exposure time, exposure temperature and gas environment. The resulting database will provide the capability to predict the probability of survival of commercial filters under anticipated service conditions from calculated thermoelastic stresses and measured material properties.

# PB.2 Carbon Formation and Metal Dusting in Hot-Gas Cleanup Systems of Coal Gasifiers

## CONTRACT INFORMATION

| | |
|---|---|
| **Contract Number** | DE-AC05-84OR21400<br>Field Work Proposal FEAA030 |
| **Contractor** | Oak Ridge National Laboratory<br>Metals and Ceramics Division<br>1 Bethel Valley Road; P.O. Box 2008<br>Oak Ridge, TN 37831-6156<br>615-574-5119 (telephone)<br>615-574-5118 (telefax) |
| **Other Funding Sources** | Office of Fossil Energy, Advanced Research and Technology Development Materials Program<br>Field Work Proposal FEAA028 |
| **Contractor Project Manager** | Roddie R. Judkins |
| **Principal Investigators** | Peter F. Tortorelli<br>Roddie R. Judkins<br>Jackson H. DeVan<br>Ian G. Wright |
| **METC Project Manager** | Justin L. Beeson |
| **Period of Performance** | November 1, 1994 to June 30, 1995 |

**Schedule and Milestones**

**FY 1995 Program Schedule**

| | N | D | J | F | M | A | M | J |
|---|---|---|---|---|---|---|---|---|
| Thermochemical Calculations | ——— | ——— | ——— | ——— | ——— | | | |
| Literature Review & Analysis | ——— | ——— | ——— | ——— | ——— | | | |
| Draft Report | | | | ——— | ——— | ——— | | |
| Final Report | | | | | | ——— | ——— | ——— |

## OBJECTIVES

The product gas resulting from the partial oxidation of carboniferous materials in a gasifier is typically characterized by high carbon and sulfur, but low oxygen, activities and, consequently, severe degradation of the structural and functional materials can occur. The objective of this task was to establish the potential risks of carbon deposition and metal dusting in advanced coal gasification processes by examining the current state of knowledge regarding these phenomena, making appropriate thermochemical calculations for representative coal gasifiers, and addressing possible mitigation methods.

## BACKGROUND INFORMATION

There are several possible materials/systems degradation modes that result from gasification environments with appreciable carbon activities. These processes, which are not necessarily mutually exclusive, include carbon deposition, carburization, metal dusting, and CO disintegration of refractories.

Carbon formation on solid surfaces occurs by deposition from gases in which the carbon activity ($a_c$) exceeds unity. The presence of a carbon layer can directly affect gasifier performance by restricting gas flow, particularly in the hot gas filter, creating debris (that may be deposited elsewhere in the system or that may cause erosive damage of downstream components), and/or changing the catalytic activity of surfaces.

A principal corrosion effect resulting from the formation of carbon layers is the phenomenon of metal dusting,[1-5] which can be a particularly severe form of materials degradation. Metal dusting requires a high carbon activity such that carbon deposition occurs and metastable metal carbides form. It is observed at intermediate temperatures of about 400 - 900°C (750 - 1650°F). Systematic studies of this phenomenon (see, for example, the reviews in references 2, 3, and 5) have shown that the metal dusting process occurs by a series of steps in the following order:

1. Rapid uptake of carbon into the metallic phase leading to supersaturation of carbon in the alloy.

2. Formation of metastable carbides (for steels, $Fe_3C$).

3. Decomposition of these carbides (which are stable only at $a_c > 1$) when localized deposition of carbon occurs ($a_c = 1$).

4. Development of a loosely adherent layer of filamentary carbon and fine metallic particles, which then act as catalysts for further carbon deposition.

This powdery mixture may also include oxides and carbides. The products can be carried away by the flowing gas. Pits and holes on affected surfaces can be observed in addition to general metal wastage. Carbon formation is a necessary but not sufficient condition for metal dusting - a metastable carbide (typically $Fe_3C$) must also form since it is its subsequent decomposition that leads to metal wastage. Metal dusting can be distinguished from carburization, normally seen with high-temperature alloys, which results in the formation of stable carbides on and in the solid exposed to a carbon-containing environment (even at $a_c < 1$).

Deterioration of refractories used in coal gasification vessels can occur at temperatures below about 650°C (1200°F) when these materials contain iron or iron alloys (usually castable refractories). An excellent review of this phenomenon, known as CO disintegration, can be found in ref. 6. Carbon deposition from the gas mixture is a necessary step in the process, which then leads to degradation that exhibits many of the same characteristics as metal dusting. Indeed, the basic mechanisms involved in both CO disintegration of iron-containing refractories and metal dusting are similar, although, historically, the studies of the respective phenomena appear to have been conducted independently of each other.

## PROJECT DESCRIPTION

This short-term project was begun in November, 1994 to examine issues related to the potential for carbon formation and metal dusting relevant to coal gasification systems. It was funded by the U.S. DOE Office of Fossil Energy through the Morgantown Energy Technology Center and the Advanced Research and Technology Development (AR&TD) Materials Program.

Because carbon deposition and carbide formation are at the root of many of the potential operational and materials problems in coal gasifiers, a major part of this project involved thermochemical calculations of carbon activities and stabilities of iron-containing phases for representative gasifiers and an evaluation of the implications of these results for coal gasification systems. Accordingly, this paper focuses on summarizing the conclusions from this work. Much more detail can be found in ref. 7, which also includes the results from the other parts of the project, including a review of metal dusting, discussion of materials selection considerations for hot-gas cleanup sections of coal gasification systems, and more specific recommendations for followup work.

## RESULTS

### Thermochemical Calculations

**Carbon Activities.** As discussed previously, the initiation of carbon deposition and metal dusting requires a carbon activity greater than unity. For this reason, the product gas chemistries of eight representative gasifier systems were examined with respect to the chemical activity of carbon. A principal concern is the change in carbon activity brought about by reduction in the gas temperature downstream from the outlet of the gasifier reaction vessel; such cooling may accompany filtration and sulfur removal functions. The selected systems and their nominal effluent gas compositions are listed in Tables 1 and 2. The former table presents the input data for air-blown systems and the latter, data for oxygen-blown systems.

The principal components of the product gas include CO, $CO_2$, $H_2$, $H_2O$, $CH_4$, and, in the case of air-blown gasifiers, $N_2$. Minor species include $H_2S$, $NH_3$, and COS. A series of thermochemical calculations, based on the SOLGASMIX[8] computer program, was made to examine essentially all of the possible chemical interactions among these species as a function of temperature at representative system pressures. The calculations assumed that the mole fractions of the elemental constituents (C, H, O, S, N) in the compounds composing the reference product gas do not change from point to point in the system, and therefore are constant with temperature. This assumption appears valid given the conditions of forced convective flow in a closed piping system and limited reaction of the gas with its containment system. Based on these calculations, the following generalizations can be applied to all gasifier systems and their attendant product gas compositions:

1. The equilibrium gas composition and, accordingly, the carbon activity, are determined by three principal chemical reactions:

$$2CO\,(g) = CO_2\,(g) + C\,(s) \qquad (1)$$
$$CO_2\,(g) + H_2\,(g) = H_2O\,(g) + CO\,(g) \qquad (2)$$
$$CH_4\,(g) = C\,(s) + 2H_2\,(g) \qquad (3)$$

Thus, changes in the carbon activity of the product gas as a function of temperature (at a given system pressure) are controlled by the temperature dependencies of the standard free energies of these three reactions.

2. In air-blown gasifiers, nitrogen is a diluent. At a given system pressure, the effect of nitrogen on the partial pressures of the other gas species results in both a decrease (reaction 1) and increase (reaction 3) in carbon activity. Its introduction will decrease the carbon activity through reaction 1 and increase it through reaction 3. This effect on the carbon activity is indirect since nitrogen itself is not a reactant. At the nitrogen activities associated with gasifiers, the reactions of nitrogen with carbon or hydrogen are insignificant and products such as $NH_3$ are relatively unstable.

3. Even at the $H_2S$ concentrations associated with the highest sulfur coals, the sulfur availability is too small to affect the concentration of the principal carbon- or hydrogen-containing species. Therefore, the carbon activity is unaffected by the presence of $H_2S$.

For air-blown gasifiers, the calculations indicated that the compositions of the gas exiting the gasifier reactor, that is, those shown in Table 1, are at equilibrium with respect to the exit gas temperature. The carbon activity at this point is less than unity. Typically, as the gas is cooled under equilibrium conditions, the CO and $H_2$ concentrations decrease while the $CO_2$, $H_2O$, and $CH_4$ concentrations increase, and these changes are accompanied by a significant increase in the carbon activity. The temperature at which the carbon activity reaches unity is process- and fuel-dependent, but for the air-blown gasifiers examined, it ranged from a low of 770°C (1420°F) to a high of 880°C (1620°F).

In the case of oxygen-blown gasifiers, where the initial CO content was 54 vol% or greater, calculations showed that the carbon activity of the gas was already higher than unity at the reference reactor outlet temperature. Again, cooling under equilibrium conditions resulted in a decrease in the CO and $H_2$ concentrations and an increase in $CH_4$, $CO_2$, and $H_2O$ levels, while the carbon activity remained at unit activity. In the case of the Texaco gasifier, in which the initial CO content was only 46.5 vol%, the carbon activity was more typical of an air-blown system, and unit carbon activity was not established until the temperature had dropped to 870°C (1600°F).

The formation of $CH_4$ is promoted by decreasing temperature and, in effect, $CH_4$ becomes a sink for carbon as the temperature is lowered. Accordingly,

**Table 1. Gas Composition and Pressures of Reference Air-Blown Gasifiers**

| Gas Component | Sierra Pacific (MWKellogg) | Wilsonville (Foster Wheeler) | Wilsonville (MWKellogg) | Four Rivers (Foster Wheeler) | Toms Creek |
|---|---|---|---|---|---|
| | Concentration (volume %) | | | | |
| CO | 23.89 | 18.05 | 18.43 | 16.50 | 26.0 |
| $CO_2$ | 5.44 | 8.79 | 8.10 | 9.00 | 5.0 |
| $H_2O$ | 5.50 | 9.11 | 8.07 | 9.50 | 14.0 |
| $H_2$ | 14.57 | 16.57 | 13.70 | 12.90 | 5.0 |
| $CH_4$ | 1.35 | 3.97 | 0.36 | 1.40 | 2.2 |
| $N_2$ | 48.65 | 42.68 | 51.30 | 50.50 | 47.5 |
| $H_2S$ | 0.03 | 0.05 | 0.02 | 0.04 | 0.006 |
| $NH_3$ | 0.02 | 0.32 | 0.01 | 0.19 | 0.15 |
| Ar/Other | 0.56 | 0.48 | 0.02 | | |
| Gas Pressure (bar) | 20.26 | 14.19 | 20.68 | 14.18 | 22.65 |

**Table 2. Gas Composition and Pressures of Reference Oxygen-Blown Gasifiers**

| Gas Component | Shell | Duke Energy Corp. | Texaco |
|---|---|---|---|
| | Concentration (volume %) | | |
| CO | 62.9 | 54.1 | 46.5 |
| $CO_2$ | 1.3 | 3.2 | 15.3 |
| $H_2O$ | 0.2 | 0.0 | 0.0 |
| $H_2$ | 30.8 | 27.7 | 35.9 |
| $CH_4$ | 0.035 | 7.0 | 0.0 |
| $N_2$ | 4.4 | 6.8 | 2.0 |
| $H_2S$ | 0.4 | 0.0 | 0.3 |
| Ar/Other | | | 0.1 |
| Gas Pressure (bar) | 28.58 | 22.05 | 35.13 |

reaction 3 acts to offset the increase in carbon activity with decreasing temperature resulting from reaction 1. However, without the action of an effective catalyst, reaction 3 is relatively sluggish and tends to be ineffective at temperatures below 800°C (1470°F). Accordingly, calculations of the $CH_4$ gas concentration assuming equilibrium conditions for reaction 3 can be expected to give unrealistically high $CH_4$ concentrations at lower temperatures. To examine this effect, another series of calculations was made in which reaction 3 was excluded, and the $CH_4$ concentration was assumed to remain unchanged as the product gas was cooled. An unexpected finding in these latter calculations was that excluding reaction 3 had only a small effect on the temperature at which unit carbon activity was reached, and this temperature in some cases even decreased slightly. (This result appears to be associated with the relatively high $H_2$ level in the product gases compared to $CH_4$ and the combined role of $H_2$ in reactions 2 and 3.) However, once the temperature dropped below the unit carbon activity threshold, the elimination of reaction 3 significantly increased the carbon activity (or availability of solid carbon) upon further cooling.

The central conclusion to be drawn from examination of carbon activities as a function of temperature is that, from a thermodynamic standpoint, the potential for carbon deposition will exist for all gasifier systems at some temperature below that attained in the reaction vessel. This potential arises from the relatively high CO concentration in the product gas. Based on equilibrium calculations, $H_2$ will act to offset the extent of carbon deposited through the generation of $CH_4$, but this reaction is very sluggish at the temperatures at which carbon deposition will occur. The temperature at which deposition becomes possible is directly proportional to the CO content of the gas and may increase or decrease slightly with higher $H_2$ contents.

**Iron-Based Phase Stabilities.** Because the formation of a metastable carbide ($Fe_3C$, for steels) is a necessary condition for metal dusting, determination of solid phase stabilities in different gasifier environments is an important aspect of evaluating the potential for degradation of exposed materials. Accordingly, equilibrium calculations were performed to determine the phase stability of iron-containing reaction products in contact with the product gases of air- and oxygen-blown gasifiers at 600 and 800°C (1110-1470°F), respectively. The Sierra Pacific (M. W. Kellogg) and Wilsonville (Foster Wheeler) reference gas compositions in Table 1 were arbitrarily selected from the air-blown category, while the Shell gasifier composition in Table 2 was selected from the oxygen-blown class. The phase stability relationships were initially determined under equilibrium considerations that limited the carbon activity to that of the most stable carbon-containing phase. Since $Fe_3C$ is not stable at the carbon activity of graphite ($a_c = 1$), the formation of graphite supersedes that of this carbide under equilibrium conditions. However, if the deposition of solid carbon from the product gas is relatively sluggish, such that the carbon activity of the gas can build up above that of graphite, then $Fe_3C$ formation becomes thermodynamically possible, particularly at lower temperatures. Accordingly, a second series of phase stability calculations was carried out in which solid carbon formation was suppressed. The $H_2S$ concentrations used in the calculations were those listed for the given gasifiers in Tables 1 and 2. The $H_2S$ level can vary depending on the coal source and hot-gas cleanup system and that such changes will significantly affect the relative stability of iron sulfide in the system.

When graphite was allowed to form, phase stability calculations for both air-blown gasifiers indicated that iron oxide (FeO) predominated as the most stable iron-containing phase at 800°C (1470°F), and both iron sulfide ($Fe_{0.877}S$) and iron oxide were stable phases at 600°C (1110°F). Under these same conditions, only the $Fe_{0.877}S$ phase was stable in the case of the oxygen-blown Shell gasifier. When the formation of solid carbon was suppressed but $CH_4$ formation (reaction 3) was allowed, the results for the air-blown gasifiers were unchanged - FeO and $Fe_{0.877}S$ were the principal phases at 600°C (1110°F), and FeO alone was predominant at 800°C (1470°F). However, if the reaction to form $CH_4$ was suppressed along with the one to form solid carbon, then $Fe_3C$ and $Fe_{0.877}S$ became the predominant phases at 600°C (1110°F) for both air-blown gasifiers. At 800°C (1470°F), $Fe_3C$ was the single predominant phase in the case of the Sierra Pacific gasifier, while $Fe_{0.877}S$ and FeO were predominant in the case of the Wilsonville gasifier. When the formation of graphite was suppressed in the case of the oxygen-blown Shell gasifier, the $Fe_{0.877}S$ phase remained stable and the $Fe_3C$ phase did not appear even when the $CH_4$ reaction was suppressed. Only by lowering the $H_2S$ content of the gas to below 0.20 vol% at 600°C (1110°F) and 0.32 vol% at

800°C (1470°F) could stability be conferred to the $Fe_3C$ phase, where it co-existed with $Fe_{0.877}S$. At $H_2S$ concentrations below 0.09 vol% at 600°C (1110°F) and 0.20 vol% at 800°C (1470°F), $Fe_3C$ became the sole predominant phase. Similar calculations indicated that nitrogen-containing reaction products with iron would not be expected to form under equilibrium conditions even for air-blown gasifiers. A summary of the phase stability relationships for these three gasifiers is shown in Table 3.

For the air-blown gasifiers, the appearance of the $Fe_3C$ phase coincided with the disappearance of the iron oxide phase, which was a result of the oxygen activity of the system being reduced by the relatively high carbon activity. These phase stability calculations indicate that the formation of $Fe_3C$ is precluded thermodynamically under conditions where an oxide can form, a finding that suggests that FeO should be effective in mitigating metal dusting. The sulfide reaction product in the air-blown gasifiers was found to co-exist with either the oxide or the carbide. However, in the oxygen-blown Shell gasifier, the oxide was unstable and, because of the relatively high $H_2S$ concentration (1.4 vol%), the sulfide existed to the exclusion of the carbide. It follows that at higher $H_2S$ concentrations, the sulfide can act effectively to exclude the formation of $Fe_3C$ in the same manner as an oxide, while at lower $H_2S$ levels where it co-exists with the carbide, its effectiveness as a barrier to $Fe_3C$ will depend on the relative nucleation and growth rates of the carbide vis-a-vis the sulfide. Because the reaction rate to form iron sulfide is significantly faster than that of iron oxide at 600°C (1110°F), the stability of iron sulfide in this temperature range, as shown by these calculations, could be a significant factor in inhibiting the formation of $Fe_3C$. A general conclusion from these stability calculations is that the removal of $H_2S$ by a hot-gas cleanup system may have less effect on the formation of $Fe_3C$ (and therefore on metal dusting) in the two air-blown gasifier environments, where the iron oxide phase can exist and is unaffected by the removal of sulfur, than in the Shell product gas environment, where iron sulfide provides the only significant potential barrier to $Fe_3C$ formation.

**Steam Injections.** Kinetic effects can be expected to play an important role relative to carbon deposition in gasifier systems, considering that deposition is possible only at reduced gas temperatures. (These effects, particularly those associated with $H_2S$ and $NH_3$, are discussed in a subsequent section.) In fact, on the basis of the reactions controlling carbon deposition (reactions 1-3), it appears more fruitful to approach the problem of carbon deposition in gasifiers by inhibiting the reactions kinetically rather than by attempting

**Table 3. Predominant Solid-State Phases Of Iron When Exposed To Reference Product Gas Compositions**

| Gasifier System | Temp. (°C) | Predominant Phases | | |
|---|---|---|---|---|
| | | Fully Equilibrated | Carbon Deposition Suppressed | Carbon Deposition and $CH_4$ Formation Suppressed |
| Sierra Pacific (MWKellogg) | 600 | Graphite, FeO, FeS | FeO, FeS | FeS, $Fe_3C$ |
| | 800 | Graphite, FeO | FeO | $Fe_3C$ |
| Wilsonville (Foster Wheeler) | 600 | Graphite, FeO, FeS | FeO, FeS | FeS, $Fe_3C$ |
| | 800 | FeO | FeO | FeO, FeS |
| Shell (Oxygen-blown) | 600 | Graphite, FeS | FeS | FeS* |
| | 800 | Graphite, FeS | FeS | FeS** |

* $Fe_3C$ also is stable if $H_2S < 0.2$ vol%
**$Fe_3C$ also is stable if $H_2S < 0.32$ vol%

thermodynamic fixes, that is, rather than by altering the concentrations of major gas species. An example is shown by the effect of adding steam to one of the reference air-blown product gases, namely, the Sierra Pacific reference composition (Table 1). Equilibrium calculations were made in which the concentration of steam was doubled from the initial level of 5.5 vol% to a level of 11 vol% without changing the relative concentrations of the other gases. Even such a large steam injection did not eliminate the potential for carbon deposition, although it did lower the temperature at which unit carbon activity was achieved from 850°C (1560°F) to 798°C (1468°F). Accordingly, the injection of steam would not of itself eliminate the possibility of carbon deposition, although by lowering the threshold temperature for carbon deposition it could possibly aid inhibiting techniques based on kinetic effects.

Another aspect of increasing the steam content of the product gas concerns the effect on corrosion products formed by reaction with the containment material. By increasing the oxygen potential of the gas, steam injection could promote the formation of oxide reaction products which may serve to prevent development of $Fe_3C$. Accordingly, the effect of doubling the steam content of the Sierra Pacific gasifier to 11% was also examined from the standpoint of its effect on the phase stability of iron-containing reaction products. As noted above, if the formation of solid carbon is suppressed, the predominant phases formed in the nominal Sierra Pacific product gas, containing 5.5% $H_2O$, are FeO and $Fe_{0.877}S$ at 600°C (1110°F) and FeO at 800°C (1470°F). Increasing the $H_2O$ content to 11% in this case did not change the stable ensembles at either temperature. In the case where the formation of both solid carbon and $CH_4$ (reaction 3) was suppressed, increasing the $H_2O$ content to 11% had no effect at 600°C (1110°F) but was beneficial at 800°C (1470°F). $Fe_{0.877}S$ and $Fe_3C$ were retained as the predominant phases at 600°C, while at 800°C, the $Fe_3C$ phase, predominant in the nominal atmosphere, was, in fact, supplanted by FeO. It appears that $H_2O$ additions could provide an overriding effect on iron carbide formation at higher temperatures, where the carbon activity of the gas is more moderate, but very large additions would be required at lower temperatures to offset the larger carbon activities that can accrue if solid carbon deposition and $CH_4$ production fail to keep pace with carbon-forming reactions (such as reaction 1).

## Conditions That Influence Kinetics of Carbon Deposition

As shown in a previous section, essentially all representative gasifiers operate under conditions in which carbon formation is thermodynamically possible in the hot-gas cooler and cleanup sections. However, such calculations do not take account of the kinetics of the gas equilibration or carbon deposition processes since all chemical reactions are assumed to proceed sufficiently rapidly that thermodynamic equilibrium is achieved. Typically, methods exist to increase or decrease the rates of reaction either through gas-phase modifications or by altering the surfaces on which deposition is to take place.

The poisoning effect of $H_2S$ on carbon deposition reactions has long been known.[9-11] This compound is also routinely added to gas mixtures of high carbon activity to reduce degradation that involves carbon deposition as a precursor to carburization.[2,5,12-14] It is generally assumed that the sulfide acts to reduce the catalytic activity of surfaces with respect to carbon deposition.[5] The presence of water vapor has also been reported to inhibit deposition of carbon,[15] but not necessarily catalytically. Rather, water vapor can react with the deposit to form gaseous products or shift the equilibria of reactions 1 - 3 so as to reduce CO decomposition.[15] However, as discussed above, relatively large concentrations of water vapor would be required to materially affect carbon deposition in the typical gasifier.

The formation of stable surface layers of certain types of oxides has been shown to be effective in decreasing carbon formation and/or reducing the susceptibility to metal dusting (perhaps by preventing deposition on reactive surfaces). These oxides include chromia, silica, and, possibly, alumina.[1,16,17] Other surface oxides, such as $Fe_2O_3$ and $Fe_3O_4$, and carbides can actually increase carbon formation.[3,6,18,19] In addition to oxidation effects, alloying or material selection and surface condition can also affect deposition by controlling the types of carbides that form or the phase distribution of the alloy components.[20] Surface roughness increases carbon deposition rates.[3,20] As may be expected, the surface crystallography can have an important effect (see, for example, ref. 21).

**Influence of System Operating Parameters on Carbon Deposition and Metal Dusting.**

Coal gasification processes are typically targeted to the generation of a product gas containing a relatively high concentration of CO. As discussed above, this high CO concentration essentially guarantees that a carbon activity greater than unity will be achieved on cooling the gas downstream of the gasifier reaction vessel. Calculations indicated that the prospects of drastically reducing the thermodynamic potential for carbon deposition by additions of $H_2O$ do not appear feasible, given the amounts of $H_2O$ that would be required. Hydrogen additions offer another thermodynamic avenue for reducing the carbon activity on cooling, but this would involve a radical change in the gasification process or a separate source of $H_2$. Furthermore, there is no assurance that the rate of the chemical reactions involving any of these additions (particularly $H_2$) could compete with that of the CO decomposition reaction as the gas is cooled. Thus, the operating parameter variations that appear most effective for inhibiting carbon deposition come down to the $H_2S$ and $NH_3$ levels maintained in the product gas and the rate and degree of cooling between the gasifier and the gas turbine. The oxygen activity of the product gas is another operating parameter that may be important, since it could be manipulated to maintain oxide films as carbon deposition barriers on metals otherwise susceptible to metal dusting. Alternatively, barrier surface oxides could be established by a preoxidation procedure, either by treating individual components before system assembly or by operating the gasifier in an oxidizing (combustion) mode prior to the start of gasification.

As discussed elsewhere,[7] instances of metal dusting have been reported in operating gasification systems. However, it appears that most gasifiers have not been plagued by serious metal dusting and deposition problems to date, particularly in contrast to many other chemical processes containing comparable CO concentrations. One probable reason relates to the possibility that the carbon activities in these systems are not sufficient to form $Fe_3C$ to the exclusion of oxides or sulfides of iron (see above). In addition, the relatively high $H_2S$ contents that generally exist in the product gas ahead of the filtration and sulfur removal systems should assure that there is sufficient sulfur available to inhibit carbon deposition or carbide formation over the most crucial temperature range during gas cooling. Once the gas is cooled by water quenching, the kinetics of carbon deposition would no longer be favorable, with or without $H_2S$. If $H_2S$ is the key to preventing carbon deposition, this problem would assume greater significance with the adoption of hot sulfur-removal processes in future gasifiers, since the $H_2S$ will then be removed in a temperature regime where carbon deposition and metal dusting are possible. The operating parameters that then would become critical are the temperatures of the hot-gas clean-up system and the downstream piping, and the level to which $H_2S$ has been reduced in the gas flowing through these sections.

An ideal approach for setting the $H_2S$ content in gasifiers incorporating hot sulfur-removal systems would be to maintain an $H_2S$ level that is sufficient to inhibit carbon deposition and metal dusting in piping sections ahead of the gas turbine but is too low to cause corrosion by sulfidation. Barnes et al. demonstrated that, for high-chromium Fe-Ni-Cr alloys at 1000°C (1830°F), at $H_2S$ levels up to 100 ppm, sulfur adsorption on carbides formed on the alloy surface progressively inhibited carbon pickup.[22] Higher levels of $H_2S$ also reduced internal carburization, but promoted the formation of a surface layer of chromium sulfide which led to increased corrosion.[22] Whether such a critical range of $H_2S$ exists for the present case cannot be determined on the basis of current information, but it becomes a critical consideration in establishing the desired operating parameters for future gasifiers.

The $NH_3$ concentration of the product gas is another operating parameter that is reported to affect the kinetics of carbon deposition and metal dusting.[2] However, as discussed above, $NH_3$ is relatively unstable in the given product gas chemistry and may be relatively difficult to control. As in the case of $H_2S$, the level of $NH_3$ required to inhibit carbon deposition and metal dusting is an unknown in the case of the gasifier product gas and would need to be evaluated experimentally.

There is no obvious way to escape the temperature window for carbon deposition if the product gas is maintained at the exit temperature of a hot-gas cleanup system. However, cooling the gas immediately downstream from the cleanup system would afford a way of limiting any metal dusting concerns if a low-alloy steel is used as the connecting piping to the gas turbine. The gas temperature would need to be lowered to below about 400°C (750°F) to suppress any possibility of

metal dusting of the low-alloy steel, assuming no other means of inhibition were employed.

Although of limited value in inhibiting carbon deposition (see above), steam additions, by increasing the oxygen activity of the product gas, could improve the stability of oxide films (FeO on iron or low alloy steels, $Cr_2O_3$, $Al_2O_3$, $SiO_2$ on appropriate alloys) which form on metals that otherwise might be susceptible to metal dusting. Steam additions would also decrease the temperature at which unit carbon activity is achieved in air-blown gasifiers, and such a temperature decrease could prove valuable in avoiding the operative temperature window of metal dusting for certain materials.

## FUTURE WORK

There are a number of ways to examine various operating and environmental conditions in which carbon deposition and metal dusting might be expected in the product gas streams of coal gasification processes. The initial approach is by the use of thermodynamic predictions: as demonstrated in this project, knowledge of appropriate reactions and free energies is used to calculate carbon activities and phase stabilities and therefore to determine if a driving force for carbon deposition and metal dusting exists for a given gas mixture as a function of temperature and pressure. However, because other factors, such as kinetics, effects of inhibitors, and particular material conditions, actually determine the extent to which reaction products form, such thermodynamic predictions must then be experimentally evaluated. Indeed, based on this assessment, the experimental determination of the ability of equilibrium thermodynamics and accompanying assumptions on relative reaction kinetics to accurately predict carbon-related degradation tendencies forms the most important part of any relevant test program. The thermochemical calculations described above unequivocally predict carbon deposition in certain temperature ranges for all of the examined gasifiers. More importantly, it was shown that $Fe_3C$, a necessary precursor to metal dusting damage of steels, can become stable in these gasifier environments when carbon deposition and $CH_4$ formation are sluggish, as they may well be in many gasifier systems. It is therefore important to determine experimentally the temperature and environmental conditions under which $Fe_3C$ can form and lead to degradation of the steel. The necessary steps in such a process include (1) specification of a representative gas composition, specifically one in which $Fe_3C$ is predicted to be stable over a certain temperature range and under appropriate kinetic conditions, (2) exposure of a susceptible material in these environments, and (3) post-exposure analysis to correlate the occurrence of carbon deposition and metal dusting with the different environmental conditions. In a similar manner, an experimental validation approach can be taken with respect to verifying the effects of $H_2S$ and steam injection on carbon deposition and $Fe_3C$ stability. These types of experiments would help resolve the questions associated with (admittedly limited) observations that operating experience with coal gasification plants to date has not indicated significant problems that can be associated with carbon-related degradation.

## ACKNOWLEDGMENTS

The authors thank J. L. Beeson and T. Grindley of the Morgantown Energy Technology Center and T. M. Besmann, J. R. DiStefano, and D. F. Wilson of Oak Ridge National Laboratory for their valuable comments on the work and manuscript. This research was sponsored by the Morgantown Energy Technology Center and the AR&TD Materials Program, Office of Fossil Energy, U. S. Department of Energy, under contract DE-AC05-84OR21400 with Lockheed Martin Energy Systems,.

## REFERENCES

1. R. F. Hochman and J. H. Burson III, "The Fundamentals of Metal Dusting," *API Division of Refining Proc.* 46 (1966) 331-44.

2. R. F. Hochman, "Catastrophic Deterioration of High Temperature Alloys in Carbonaceous Atmospheres," *Proc. - Electrochem. Soc.* (1976), 77-1(Proc. Symp. Prop. High Temp. Alloys, 1976), p. 715-32.

3. J. C. Nava Paz and H. J. Grabke, "Metal Dusting," *Oxid. Met.* 39 (1993) 437-56.

4. H. J. Grabke, R. Krajak, and J. C. Nava Paz, "On the Mechanism of Catastrophic Carburization:

Metal Dusting," *Corros. Sci.*, 35 (1993) 1141-50.

5. H. J. Grabke, "Metal Dusting of Low and High Alloy Steels," submitted for publication in *Corrosion*, 1995.

6. J. J. Brown, Jr., "Investigation of Carbon Monoxide Disintegration of Refractories in Coal Gasifiers," Virginia Polytechnic Institute and State University report, VPI/ME-13702-12, July 1984

7. P. F. Tortorelli, J. H. DeVan, R. R. Judkins, and I. G. Wright, "Carbon Formation and Metal Dusting in Hot-Gas Cleanup Systems of Coal Gasifiers," ORNL/TM-13014, Oak Ridge National Laboratory report, 1995.

8. T. M. Besmann, "SOLGASMIX-PV, A Computer Program to Calculate Equilibrium relationship in Complex Chemical Systems," ORNL/TM-5775, Oak Ridge National Laboratory, April 1977.

9. P. A. Lefrancois and W. B. Hoyt, "Chemical Thermodynamics of High Temperature reactions in Metal Dusting Corrosion," *Corrosion* 19 (1963) 360t - 368t.

10. T. Kalina and J. A. Kivlen, "Process of Reducing Iron Oxide Ores with Gases Containing Carbon Monoxide," U. S. Patent 3,377,156, April 1968.

11. M. J. Bennett, G. H. Chaffey, B. L. Myatt, and D. R. V. Silvester, "Inhibition by Sulfur Poisoning of the Heterogeneous Decomposition of Acetone," pp. 223-38 in Coke Formation on Metal Surfaces, L. F. Albright and R. T. K. Baker, American Chemical Society, 1982.

12. H. J. Grabke, C. B. Bracho-Troconis, and E. M. Mueller-Lorenz, " Metal Dusting of Low Alloy Steels," *Werkst. Korros.* 45 (1994) 215-21.

13. T. F. Berry, R. N. Ames, and R. B. Snow, "Influence of Impurities and Role of Iron Carbides in Deposition of Carbon from Carbon Monoxide," *J. Amer. Ceram. Soc.* 39 (1956) 308-18.

14. E. Q. Camp, C. Phillips, and L. Gross, "Corrosion of 18-8 Alloy Furnace Tubes in High-Temperature Vapor Phase Cracking Service," *Corrosion* 1 (1945) 149-60 (September).

15. V. Krebs, J. F. Mareche, G. Furdin, and D. Dumay, "Contribution to the Study of Carbon Deposition in Coke Ovens," *Fuel* 73 (1994) 1904-10.

16. H. J. Grabke, R. Krajak, and E. M. Mueller-Lorenz, "Metal Dusting of High-Temperature Alloys," *Werkst. Korros.* 44 (1993) 89-97.

17. D. E. Brown, J. T. K. Clark, A. I. Foster, J. J. McCarroll, and M. L. Sims, "Inhibition of Coke Formation in Ethylene Steam Cracking," pp. 23-44 in Coke Formation on Metal Surfaces, L. F. Albright and R. T. K. Baker, American Chemical Society, 1982.

18. R. T. K. Baker, D. J. C. Yates, and J. A. Dumesic, "Filamentous Carbon Formation over Iron Surfaces," pp. 1-22 in Coke Formation on Metal Surfaces, L. F. Albright and R. T. K. Baker, American Chemical Society, 1982.

19. W. R. Ruston, M. Warzee, J. Hennaut, and J. Waty, "The Solid Reaction Product of the Catalytic Decomposition of Carbon Monoxide on Iron at 550°C," *Carbon* 7 (1969) 47-57.

20. F. W. A. Geurts, R. G. Cnossen, A. Sacco, Jr., and R. R. Biederman, "Carbon Deposition over Transition Metal Alloys-II. Kinetics of Deposition over <FeNi> and<FeCo> Alloy Foils," *Carbon* 32 (1994) 1151-69.

21. Y. Inokuti, "Formation of Graphite on the Surface of Cold Rolled Low Carbon Steel Sheet During Annealing," *Trans. ISIJ* 15 (1975) 314-23.

22. J. Barnes, J. Corish, E. Franck, and J. F. Norton, "Influence of Sulfur on the Nature and Morphology of Carbides Formed on the Surfaces of Fe-Ni-Cr Alloys at High Temperatures," *Oxid. Met.* 24 (1985) 85-97.

## PB.3 Development of a Monolithic Ceramic Cross Flow Filter

### CONTRACT INFORMATION

| | |
|---|---|
| **Contract Number** | DE-FG02-94ER18718 |
| **Contractor** | Blasch Precision Ceramics, Inc.<br>580 Broadway<br>Albany, NY 12204<br>(518)436-1263 (telephone)<br>(518)436-0098 (telefax) |
| **Other Funding Sources** | None |
| **Contractor Project Manager** | David A. Larsen |
| **Principal Investigator** | David A. Larsen |
| **METC Project Manager** | Theodore J. McMahon |
| **Period of Performance** | August 15, 1994 to March 10, 1995 |
| **Schedule** | Phase I Completed March 10, 1995<br>Awaiting Approval of Phase II |

## OBJECTIVES

The objective of this SBIR Phase I project was to demonstrate feasibility of forming a permeable, porous ceramic material using the unique and proprietary Blasch process, to meet the permeability and other material property requirements of cross flow filters. This objective was accomplished by: (1) using this process to form and fire matrices of over 100 ceramic test compositions into test specimens, and (2) performing appropriate testing to determine feasibility for cross flow filter application.

The specific criteria considered in this project to determine if a ceramic composition is feasible for cross flow filters include:

(a) Composition must be able to be formed and fired successfully using the unique and proprietary Blasch process.

(b) Permeability must meet Westinghouse's specifications for cross flow filters. This was determined to be 1 iwg/fpm maximum by Westinghouse.

(c) Apparent porosity, according to Westinghouse, should be approximately 40-50 %.

(d) Strength property requirements, although unknown, were arbitrarily targeted at minimum of 1000 psi for both room temperature and hot (870° C) modulus of rupture (MOR).

(e) Bonding phase preferably should be a non-glassy type that will be less likely to be attacked by alkali or steam in a hot gas stream environment.

(f) Pore size, according to Westinghouse experience, should be in the approximate range of 20 microns for best filtration and to eliminate the need for a membrane filtration layer.

## BACKGROUND INFORMATION

High temperature, high pressure (HTHP) particulate control is required to protect turbine equipment and to meet environmental stack emissions standards in coal-fueled power systems. Ceramic cross flow filters were designed with a high surface area per unit volume to be a highly efficient means to remove particulates from these hot gas streams. Previously developed cross flow filters were segmented; several thin porous ceramic plates with channels formed by ribbed sections were stacked atop each other and fired, to form a "monolithic filter". This filter was not truly monolithic, however, as it experienced seam delamination while in service at operating temperature. This delamination of cross flow filters degraded the filter system's performance allowing particulates in the hot gas stream to by-pass the filter. With a sufficient amount of delamination of filter elements in a system, this leakage of particulates could lead to very costly (and perhaps catastrophic) downstream turbine damage, and failure to meet environmental stack emission standards.

Therefore, an important need has been identified for a one-piece monolithic ceramic cross flow filter, rather than the present built-up segmented filter. Current ceramic technology has proved incapable of forming a complex one-piece shape such as this, with an acceptable, permeable, porous ceramic material. Blasch Precision Ceramics has a unique proprietary injection mold ceramic forming process that has been used for many years to commercially produce complex one-piece monolithic shapes, but of a non-permeable nature.

In this SBIR Phase I project, feasibility was to be demonstrated for the development of a permeable, porous ceramic material formed using this unique Blasch process, targeted to meet the permeability and other material property requirements of cross flow filters. With this

material and process, a more reliable, effective monolithic cross flow filter could evolve in Phases II and III.

## PROJECT DESCRIPTION

### Work Plan Overview

The project objective, as stated earlier, was to demonstrate feasibility of forming a permeable, porous ceramic material using the unique and proprietary Blasch process, to meet the permeability and other material property requirements of cross flow filters. To accomplish this, the following tasks were performed:

(a) Molds were designed and fabricated for the forming of ceramic disks and plates to be used for Westinghouse disk permeability and hot modulus of rupture (MOR) testing. Molds already existed for the forming of test bars and cubes for room temperature MOR and cube permeability.

(b) A test matrix was formulated of different ceramic compositions of various particle packing schemes, different fillers (pore formers) and amounts of fillers, and firing cycles. Ceramic disks, bars, and cubes were formed and fired of each composition, using the Blasch forming process.

(c) Measurements of room temperature MOR, apparent porosity, and cube permeability were made at Blasch on the compositions in this test matrix.

(d) Measurements of disk permeability were made at Westinghouse on selected compositions in this matrix.

(e) Using earlier obtained data as a basis, adjustments were made to ceramic compositions and firing schedules to form a second refined test matrix. Test bars, cubes, plates, and disks were made and fired.

(f) Measurements of room temperature MOR, apparent porosity, and cube permeability were made at Blasch on the compositions in this refined test matrix.

(g) Measurements of disk permeability and hot MOR were made at Westinghouse on selected compositions in this refined matrix. Additionally, x-ray diffraction, scanning electron microscopic analysis, and mercury porosimetry analysis were performed by other labs on selected compositions.

### General Procedure

Matrices of various ceramic compositions were devised and each composition was formed into a full set of test specimens: bars (five 1"x1"x7.5"size), ceramic cubes (three 2"cubes), and disks (four 1.5"dia x 0.25"th).

The process used for producing these test specimens was the lab scale version of the unique and proprietary Blasch process, which includes: batching/weighing, wet batch mixing, injection of ceramic slurry into molds, solidification, removal of mold, drying, and firing.

The variables in these matrices included:

*numerous particle packing schemes
*maximum particle sizes from 20 mesh down to 325 mesh
*alumina-silica compositions
*alumina-silica-silicon carbide compositions
*various types fiber pore former additions
*ground walnut shells pore former additions
*fumed silica addition
*various rheology enhancement

additions
*firing temperatures of 2700°F or 3000°F

A total of over 100 ceramic compositions were made using these variables as the basis.

**Testing**

Each composition in these matrices was tested at Blasch as follows: room temperature modulus of rupture, apparent porosity, bulk density, and permeability. Based on the results of these initial tests, several of the ceramic compositions were submitted for further permeability testing by Westinghouse. Some promising compositions were then selected for further testing (XRD phase determination, mercury porosimetry, scanning electron microscopy to illustrate physical structure, and hot modulus of rupture at 870°C).

Initial testing was done by Blasch Precision Ceramics. Room temperature MOR was done using hydraulic force and a 3 point fixture with a 4" span, on test bars formed to 1"x1"x7.5". Apparent porosity was performed by weighing and measuring a ceramic piece, filling the pores with water, and then re-weighing the saturated specimen. Bulk density was determined by measurement of dimensions and weighing of ceramic bars. Permeability was done by ASTM standard method C577 "Standard Test Method for Permeability of Refractories". In this method, flow of nitrogen gas is measured through 2" ceramic cubes while controlling the pressure differential with a mercury or water filled manometer. The readings were translated to centidarcy units, as is explained in the ASTM standard:

$$K = (MQL/ A\Delta P) \times 100$$

where:

K = permeability, centidarcies
M = gas viscosity, cP
Q = flow rate, $cm^3/s$
L = sample length, cm
A = sample area, $cm^2$
$\Delta P$ = absolute pressure drop across the sample, atm

On chosen ceramic compositions, a second tier of permeability testing was completed on the 1.5"dia x 0.25" disks by Westinghouse. Westinghouse determines permeability by the measurement of flow of nitrogen gas through the ceramic disk at specified pressure differentials, to yield a reading in units "iwg/fpm" (inches water gage /feet per minute).

Based upon the results of this testing, ceramic compositions were chosen for XRD phase analysis, mercury porosimetry, SEM (scanning electron microscope) microstructure photos, and hot MOR testing. The XRD analyses and SEM photos were done by Washington Mills Electro Minerals in Niagara Falls, NY. Mercury porosimetry was performed by Micromeretics in Norcross, GA, using their AutoPore II 9220 equipment. Westinghouse did the hot MOR tests at 870°C, using a 4 point fixture with a 1.57" span on test bars cut to 0.25"wide x 0.08"thick cross-section.

Next, ceramic disk test specimens were made from selected ceramic compositions (independently from the original specimens) so Westinghouse could determine if the earlier permeability measurements were repeatable with new batches of specimens.

## RESULTS

**Discussion of Results**

The particle packing scheme and top end

particle size that yielded both acceptable room temperature MOR strength and permeability was 100/200 mesh top end particle size, with a particle sizing gap in the compostion. The coarser (>100/200 mesh) top end particle sizes yielded lower than acceptable room temperature (R.T.) MOR strength (<1000 psi). Finer (<100/200 mesh) top end particle sizes all yielded high room temperature MOR strengths (>2000 psi), but had unacceptably low permeabilities (<200 centidarcies). In general, mixes without a particle size gap resulted in higher R.T. MOR strengths, with unacceptably lower permeabilities. Table 1 indicates mix numbers and properties of the "selected five compositions" in these matrices (out of over 100 compositions total), based on meeting these requirements for R.T. MOR strength and permeability as measured at Blasch Precision Ceramics. All of these "selected compositions" had top end particle size of 100/200 mesh with similar particle sizing gaps, and yielded the targeted results for R.T. MOR of >1000 psi and permeability of >200 centidarcies.

The "selected compositions" designated in Table 1 are all combinations of alumina and silica based raw materials, plus pore forming additives.

The substitution of 20 wt% SiC grain for similar size tabular alumina in the particle size range of 20/100 mesh was tried in ten compositions. Some of these compositions yielded adequate R.T. MOR strength, but none had acceptable permeability. It was noteworthy that, when fired @ 3000°F, these compositions glazed, apparently due to oxidation of the SiC. Further work would be required to determine if it possible to attain the needed strength and permeability with an alumina/SiC composite.

Variations of different pore forming additives were attempted in many of the compositions. Various fiber types of pore formers were tried: both organic and inorganic. Additionally, other pore forming additions were tried, such as ground walnut shells and fumed silica. Amounts and sizes of pore forming additives were varied, as well as use of combinations of the most promising candidates. Again, the objective was to attain both acceptable R.T. MOR strength and permeability with the composition. Several of the pore forming additives yielded acceptable permeability but unacceptable R.T. MOR strength, or vice versa. The ground walnut shells were used at a relatively high concentration (>15 wt%) to attain the needed permeability, but this caused the R.T. MOR strength to plummet unacceptably to below 600 psi. Fumed silica additions even in small amounts (0.5 wt%) had a very deleterious effect on R.T. MOR (result: <300 psi).

The pore formers that showed the most promise in these matrices were fibers. These were present in each of the "selected compositions" (Table 1) as combinations of different types of fibers, and resulted in ceramic compositions with both acceptable permeability (>200 centidarcies) and R.T. MOR strength (>1000 psi).

Firing temperatures were 2700°F and 3000°F in these matrices. There seemed to be little if any difference in permeability of the same composition fired @ 2700 vs. 3000°F, as is shown in identical mixes 4-300 and 4-270 (Table 1) that were fired at these different temperatures. Although when fired lower (mix 4-270), the R.T. MOR strength was lower (1011 vs 1218 psi), there is insufficient data to determine if this is really an effect of the firing temperature. Hot MOR testing indicated that these mixes 4-300 and 4-270 had nearly identical hot MOR @ 870°C (650 vs 686 psi), based again on a limited amount of data (Table 1). XRD analyses (Table 2) showed that mix 4-300 (fired at 3000°F) had 25% mullite formation, while identical mix 4-270 (fired at 2700°F) had 20% mullite formation. Neither had any free crystalline silica detectable by XRD. Further development work would be necessary to determine if higher temperature firing yields

higher room temperature and hot MOR strengths.

The "Properties of Selected Compositions", Table 1, lists the mix numbers of the best compositions in all matrices based on attaining targeted room temperature MOR (>1000 psi) and permeability (>200 centidarcies) in measurements performed at Blasch Precision Ceramics. Other properties shown on Table 1 are Blasch measurements of apparent porosity and bulk density, as well as Westinghouse measurements of permeability and hot MOR (@ 870°C). The targets were achieved for all compositions except the Westinghouse permeability reading for one mix (#1-300) was not acceptable. The hot MOR strength measurements by Westinghouse were lower than the original arbitrary target of 1000 psi (results: 650 to 805 psi; Table 1). However, hot MOR requirements for cross flow filter application are unknown and hot strength viability can only be accurately determined by full scale filtration testing (proposed as part of Phase II).

Ceramic specimens of compositions 2-300 and 4-300 were chosen for scanning electron microscope (SEM) surface microstructure photographs. SEM photos of these compositions (Figures 4 and 5) are at 100X magnification. The 2-300 and 4-300 compositions were similar, but they contain different combinations of types of fiber pore formers. The SEM microstructures of these specimens look very similar. Both have uniform pore structure and size, and many pores in the 7 to 40 micron range.

Mercury porosimetry was performed on ceramic specimens of compositions 2-300, 4-300, and 4-270. Compositions 2-300 and 4-300 were mentioned previously; composition 4-270 was identical to 4-300, except it was fired at a lower temperature (2700 vs 3000°F). Figures 1, 2, and 3 are graphs of this porosimetry work, while Table 3 is a summary table of porosimetry data and physical properties as measured by Micromeretics, Inc. All three specimens were very similar in porosimetry characteristics. All had a majority of pores in the 7 to 40 micron diameter range, with median pore diameters as follows: Sample 2-300: 16 microns; Sample 4-300: 22.4 microns; Sample 4-270: 18.8 microns.

For the "selected compositions" designated in Table 1, another set of disk specimens for each were made (processed separately from the earlier sets) and submitted to Westinghouse for permeability testing to determine repeatability as compared to earlier specimens. This comparison is shown in Table 4. The results showed good batch to batch repeatability, although compositions 1-300 and 2-300 showed greater variability than the other compositions. It is theorized that the reason for this variability for these two compositions is either lack of consistency of one type of fiber raw material used in both of these mixes, or ineffective dispersion of these fibers into the mix. It is noteworthy that neither batch of composition 1-300 met Westinghouse's permeability specification of <1.00 iwg/fpm, while all batches of the other four compositions in this table met this specification.

Blasch's permeability readings of 200 or greater centidarcies (cd) generally correlated with acceptable Westinghouse permeability readings of <1.00 iwg/fpm. Blasch achieved permeability values of 202 to 404 centidarcies in 23 compositions. Disk specimens of these 23 compositions were submitted to Westinghouse for their permeability testing. Westinghouse found 19 to be acceptable, 2 to be marginal, and 2 to be unacceptable. One of the two determined to be unacceptable was composition 1-300, where Blasch measured permeability of 234 cd and Westinghouse's measurement was 1.36 iwg/fpm (Table 1). This may be due to non-uniformity in this batch, possibly related to the earlier mentioned lack of consistency of the specific fiber pore former raw material or ineffective dispersion of this fiber into the mix.

## Summary and Conclusion

Mullite bonded, porous, permeable alumina ceramics were made on a lab scale with the unique and proprietary Blasch injection forming process. Permeability as well as the other initial targeted property requirements for the cross flow filter were achieved. These include permeability of >200 cd (or <1 iwg/fpm) and room temperature MOR of >1000 psi. The compositions that met these requirements had the following characteristics in common:

*Alumina-silica raw material base composition
*100/200 mesh top end particle size
*Gap in particle sizing
*Small percent of fiber pore forming additions
*Firing temperature of either 2700 or 3000°F

It is concluded that it is feasible to use the unique and proprietary Blasch process to form ceramic shapes of a permeable, porous nature, targeted for use in monolithic ceramic cross flow filters.

## FUTURE WORK

The future work planned is dependent upon DOE's approval of an SBIR Phase II proposal submitted by Blasch in mid April, 1995. If this Phase II is approved, the effort would occur over a two year period commencing Summer 1995. The major objectives for this Phase II proposed work include:

1. Design (with input from Westinghouse) prototype full size monolithic ceramic cross flow filter ceramic shape to be produced using the Blasch process and permeable ceramic compositions developed in Phase I.

2. Design and build a mold system capable of forming this prototype full size monolithic ceramic cross flow filter.

3. Characterize permeable ceramic compositions to be used in prototype monolithic ceramic cross flow filters, to include room temperature permeability, particulate collection efficiency, and corrosion testing.

4. Produce prototype full size monolithic ceramic cross flow filter by upscaling the lab scale process developed in Phase I.

5. Evaluate performance of these prototype filters in filtration testing and characterize after testing (testing by Westinghouse).

## REFERENCES


1. Discussions with Ms. Mary Anne Alvin and Dr. Tom Lippert of Westinghouse Electric Corporation, Science and Technology Center, Pittsburgh.

2. Discussions/meeting with Mr. Ted McMahon, Mr. Harvey Ness, Mr. Richard Dennis, Mr. Norman Holcombe, and Mr. Thomas Keech, Jr., all of DOE METC, September 1993.

3. Discussions with Mr. Ted McMahon of DOE METC throughout Phase I, September 1994 through February 1995.

4. Lippert, T.E., Alvin, M.A., Smeltzer, E.E., Bachovchin, D.M., and Meyer, J.H., Subpilot Scale Gasifier Evaluation of Ceramic Cross Flow Filter, Final Report-February 1, 1988-December 31, 1992: DOE/MC/24021-3544. August, 1993.

5. Lippert, T.E., Smeltzer, E.E., Alvin, M.A., and Bachovchin, D.M., Long-Term Durability Testing of Ceramic Cross-Flow Filter: Final Report-September 29, 1987-December 31, 1992: DOE/MC/24022-3654. August, 1993.

6. Alvin, M.A., Lippert, T.E., and Lane, J.E., "Assessment of Porous Ceramic Materials for Hot Gas Filtration Applications", Ceramic Bulletin, Vol 70, No. 9, 1991.

7. Bosart, S.J., Cicero, D.C., Zeh, C.M., and Bedick, R.C., Gas Stream Cleanup Technology Status Report: DOE/METC--91/0273. August, 1990.

8. Ventkataraman, V.L., Rath, L.K., Martin, J.W., Bedick, R.C., Proceedings of the Eleventh Annual Gasification and Gas Stream Cleanup Systems Contractors Review Meeting, Volumes I and II: DOE/METC--91/6123. August, 1991.

9. Webb, H.A., Bedick, R.C., Geiling, D.W., Cicero, D.C., Proceedings of the Eighth Annual Coal Fueled Heat Engines and Gas Stream Cleanup Systems Contractors Review Meeting: DOE/METC--91/6122. July, 1991.

10. 1990 Annual Book of ASTM Standards; Section 15: General Products, Chemical Specialties, and End Use Products; Vol 15.01.

**Table 1. Properties of Selected Compositions**

| Mix No. | BPC Perm (cd) | Whse Perm (wg/fpm) | BPC MOR @70°F (psi) | Whse MOR @870°C (psi) | BPC App Porosity (%) | BPC Bulk Density (g/cc) |
|---|---|---|---|---|---|---|
| 1-300 | 234 | 1.36 to 1.62 | 1022 | 1583 | 41.3 | 1.99 |
| 2-300 | 202 | 0.74 to 0.96 | 1044 | 760 | 43.3 | 1.92 |
| 3-300 | 287 | 0.41 to 0.43 | 1395 | 805 | 46.6 | 1.78 |
| 4-300 | 271 | 0.43 to 0.58 | 1218 | 650 | 46.5 | 1.80 |
| 4-270 | 268 | 0.69 | 1011 | 686 | 45.6 | 1.84 |

Notes:

BPC Perm is permeability in centidarcies measured by Blasch.
Whse Perm is permeability in inches water pressure difference per feet/minute velocity measured by Westinghouse.
BPC MOR is modulus of rupture in psi at room temperature using 3 point span measured by Blasch.
Whse MOR is modulus of rupture in psi at 870°C using 4 point span measured by Westinghouse.
BPC App Porosity is apparent porosity in % measured by Blasch.
BPC Bulk Density is in g/cc measured by Blasch.

**Table 2. Semi-Quantitative XRD Analyses Results**

| Composition Number | Firing Temp(°F) | % Alumina | % Mullite | % Crystalline Silica |
|---|---|---|---|---|
| 4-300 | 3000 | 75 | 25 | 0 |
| 4-270 | 2700 | 80 | 20 | 0 |
| 2-300 | 3000 | 62 | 38 | 0 |

**Table 3. Physical Properties by Micromeretics, Inc**

| Composition Number | Bulk Density (g/cc) | Open Porosity (%) | Median Pore Diameter ($\mu$) |
|---|---|---|---|
| 4-300 | 1.78 | 47.9 | 22.4 |
| 4-270 | 1.86 | 47.5 | 18.8 |
| 2-300 | 1.96 | 45.4 | 16.0 |

**Table 4. Permeability of Different Batches**

| Composition Number | Permeability, iwg/fpm November Batch | Permeability, iwg/fpm December Batch* |
|---|---|---|
| 1-300 | 1.356, 1.346 | 1.616 ± 0.302 |
| 2-300 | 0.742, 0.761 | 0.955 ± 0.228 |
| 3-300 | 0.405, 0.430 | 0.410 ± 0.025 |
| 4-300 | 0.430, 0.581 | 0.384 ± 0.099 |
| 4-270 | NA | 0.686 ± 0.180 |

Notes:

Testing by Westinghouse.
Units iwg/fpm represent inches water gage per ft/minute velocity.
* 10 disks supplied; 5 disks randomly selected for testing. Data indicates average and ±1 standard deviation.

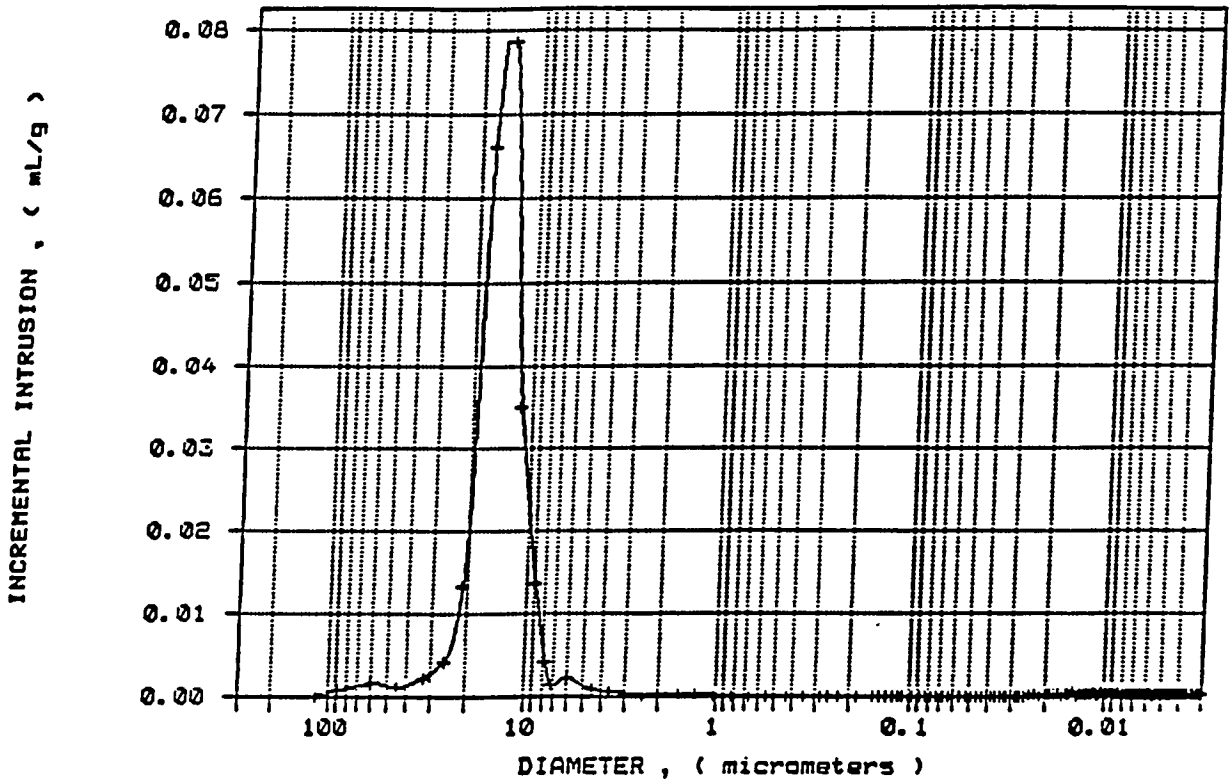


**Figure 1. Incremental Intrusion vs Pore Diameter by Mercury Porosimetry Method for Composition 2-300**

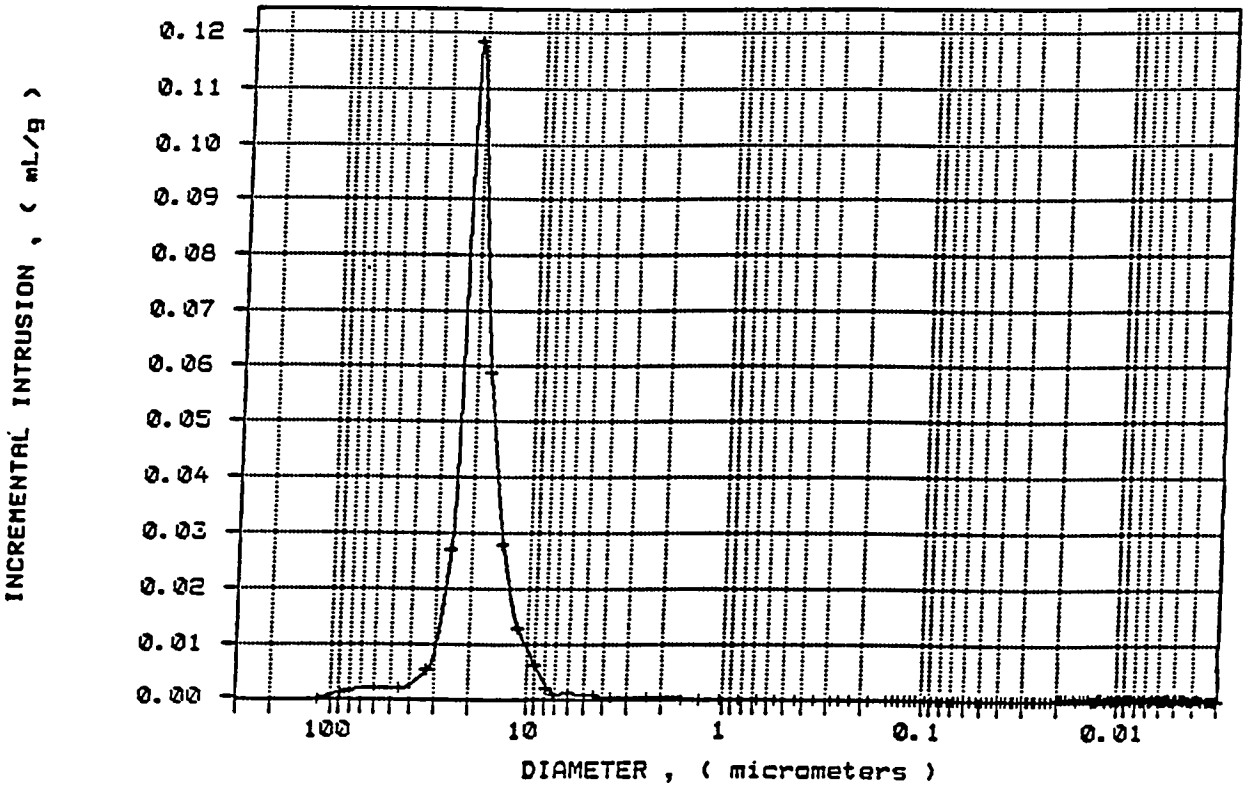


**Figure 2. Incremental Intrusion vs Pore Diameter by Mercury Porosimetry Method for Composition 4-300**

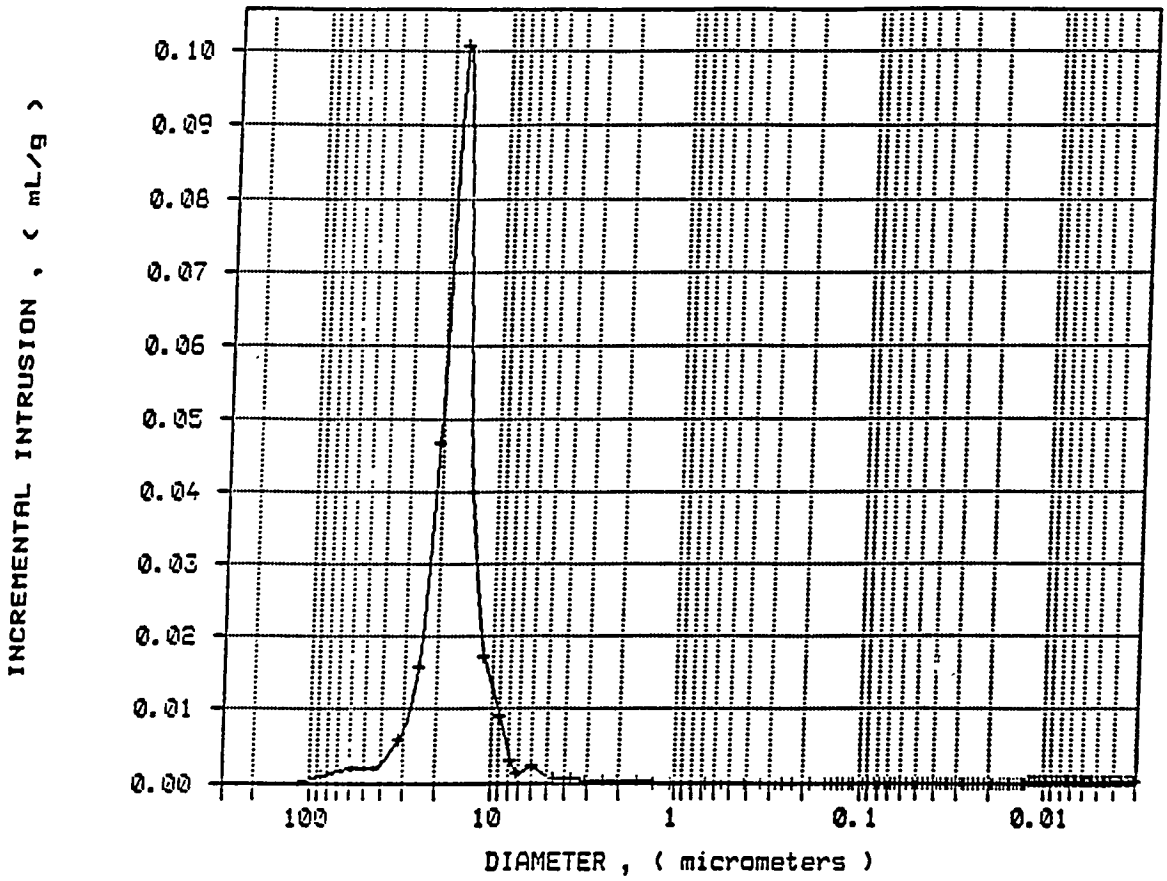


**Figure 3. Incremental Intrusion vs Pore Diameter by Mercury Porosimetry Method for Composition 4-270**

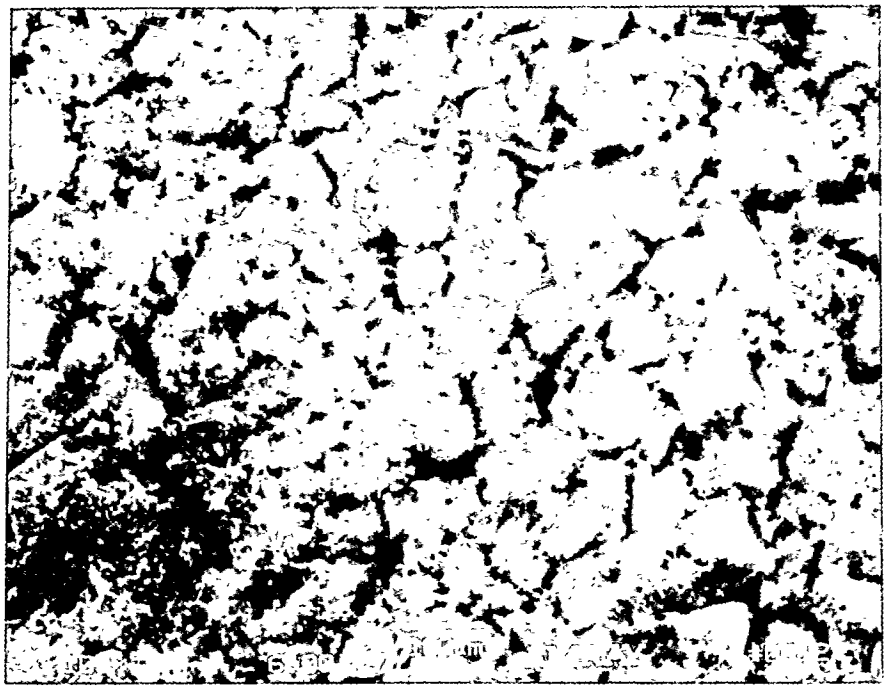

**Figure 4. SEM Microstructure of As-Formed Surface of Composition 1-300 @ 100X Magnification**

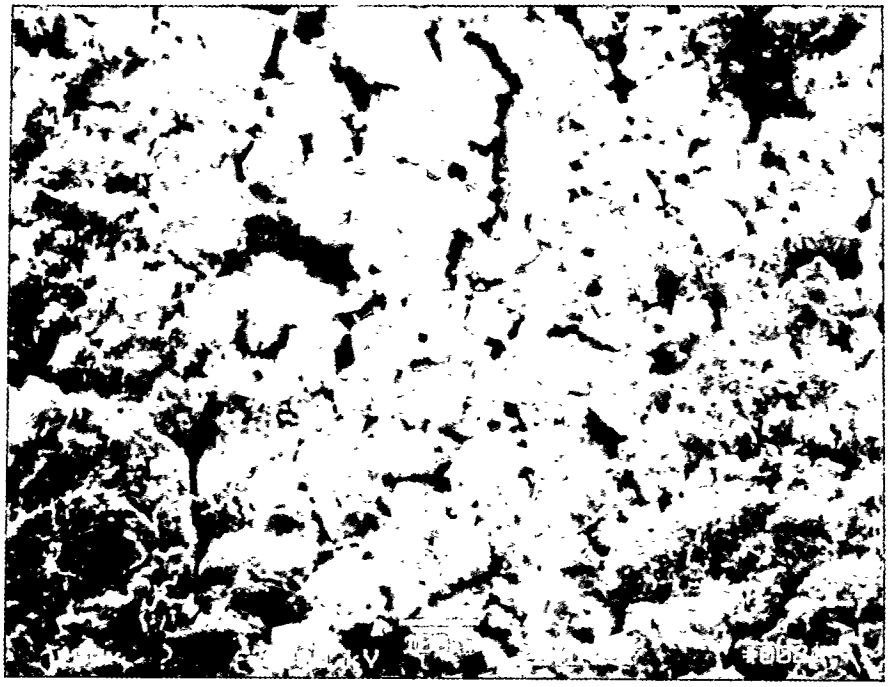

**Figure 5. SEM Microstructure of As-Formed Surface of Composition 4-300 @ 100X Magnification**

# PB.4 Properties of Ceramic Candle Filters

## CONTRACT INFORMATION

| | |
|---|---|
| **Contract Number** | DE-AC21-94MC31160 Task Order 002 |
| **Contractor** | Southern Research Institute<br>2000 Ninth Avenue South<br>Post Office Box 55305<br>Birmingham, AL 35255-5305 |
| **Contractor Project Manager** | Duane H. Pontius |
| **Principal Investigator** | H. Stuart Starrett |
| **METC Project Manager** | Ted McMahon |
| **Period of Performance** | October 1, 1994 to September 30, 1998 |

## ABSTRACT

The mechanical integrity of ceramic filter elements is a key issue for hot gas cleanup systems. To meet the demands of the advanced power systems, the filter components must sustain the thermal stresses of normal operations (pulse cleaning), of start-up and shut-down conditions, and of unanticipated process upsets such as excessive ash accumulation without catastrophic failure. They must also survive the various mechanical loads associated with handling and assembly, normal operation, and process upsets. For near-term filter systems, these elements must survive at operating temperatures of 1650°F for three years.

Property measurements and exposure to the hot gas filtration operating environment have been provided for Refractron and Schumacher clay-bonded materials and Coors alumina mullite. Results have shown that these materials are susceptible to microcracking from the thermal stress generated during pulse cleaning when the temperature drop on the I.D. of the candle is on the order of 100 to 200°F. Tensile creep tests indicated that the clay bonded materials creep at temperatures of 1400°F or greater. Neck cracks and large deformations on bowed candles removed from Tidd and Karhula have been explained by the creep test results. Degradation of mechanical properties has been measured in clay-bonded candle filters after exposure in Tidd and Karhula.

Additional materials are currently being evaluated with the goal of providing materials for continuous operation at 1600°F for three years. Four materials currently in evaluation are IF & P Fibrosic material, Dupont Lanxide silicon carbide and PRD 66 composite materials, and 3M filter material. Initial screening of the materials consists of tensile and thermal expansion measurements. These properties provide an estimate of thermal stress performance in the hot gas

cleanup environment. Tensile strength will be measured after exposure to elevated temperature to provide an indication of whether a material can survive at elevated temperatures for long times. Based on initial screening results, further testing including elevated temperature tensile, compressive, tensile creep, thermal conductivity, and microstructural evaluations will be performed. After these materials are used in a hot gas filtration environment, residual properties will also be measured.

## PB.5 Nitride-Bonded Silicon Carbide Composite Filter

### CONTRACT INFORMATION

| | |
|---|---|
| Contract Number | DE-AC21-92MC31213 |
| Contractor | Textron Specialty Materials<br>2 Industrial Ave.<br>Lowell, MA 01851<br>508-934-7519 (telephone)<br>508-934-7597 (telefax) |
| Other Funding Sources | |
| Contract Project Manager | Bruce N. Thomson |
| Principal Investigator | Stephen G. DiPietro |
| METC Project Manager | Theodore J. McMahon |
| Period of Performance | September 30, 1994 to September 30, 1997 |

Schedule and Milestones

FY 95 Program Schedule

| | O | N | D | J | F | M | A | M | J | J | A | S |
|---|---|---|---|---|---|---|---|---|---|---|---|---|
| Test Plan | ---------- | | | | | | | | | | | |
| Fabrication | | | ---------- | | | | | | | | | |
| Testing | | | | | ---------- | | | | | | | |
| Analysis | | | | | | ---------- | | | | | | |

## OBJECTIVES

The overall objective of the program is to develop and demonstrate an advanced hot gas filter, using ceramic composite technology, with enhanced durability to provide increased resistance to crack propagation and thermal fatigue, the primary modes of failure. More specifically, the objective is to modify a continuous fiber ceramic composite (CFCC) material which has already demonstrated a satisfactory level of durability in order to incorporate the required level of permeability and filtering efficiency. This material is silicon carbide (SiC) fiber reinforced nitride bonded silicon carbide (NB-SiC).

## BACKGROUND INFORMATION

It is widely recognized that porous ceramic cross flow and candle filters represent an attractive technology for the required removal of high temperature particulate in advanced coal based power systems. Significant gains have been made in recent years in demonstrating hot gas filtering media. Ceramic materials which are currently being used as cross flow filter materials include alumina/mullite, cordierite, aluminosilicate foam, cordierite-silicon nitride, and reaction bonded or sintered silicon nitride. Porous ceramic candle filters are made from clay bonded silicon carbide, alumina/mullite, clay bonded alumina, and recrystallized silicon carbide, as well as some developmental materials.

While monolithic ceramic hot gas filters are able to perform the filtration function, they do not provide adequate durability to withstand the intended operating environment for extended periods of time. In addition to the high temperature particle removal requirement, these filters are continuously subjected to thermal cycling through pulse gas cleaning or system transients during process operation and to mechanical stresses at attachment points.

An ideal solution is the application of ceramic composite technology to provide an acceptable level of material durability. The prospect of this approach is particularly attractive in light of the fact that in a separate program [Ref. 1] Textron is successfully fabricating closed end ceramic composite tubes similar in size and shape to the proposed candle filters. The composite material is nitride bonded silicon carbide (NB-SiC) with a silicon carbide reinforcing fiber. A high level of strength and toughness is provided by multidirectional fiber reinforcement.

Textron's methodology for fabricating continuous fiber ceramic composites via gas phase reaction synthesis is based on combining high performance ceramic reinforcements with silicon carbide and/or silicon nitride-containing ceramic matrices by gas phase reaction synthesis. This process, which converts metallic Si to silicon nitride via the reaction $3\ Si + 2\ N_2 = Si_3N_4$ is a net shape process that requires no pressure to effect matrix densification. Thus, complex ceramic composite parts can be made very rapidly with no restraint tooling. Additionally, no sintering aids are required to effect matrix densification, and thus matrix phase purity can be very high - consisting of mixtures which vary from combinations of $SiC + Si_3N_4$ to basically pure $Si_3N_4$ (NBSN). This is important to hot gas filters as there is a fair body of experimental evidence to suggest that the elevated temperature gaseous corrosion resistance of Si-based ceramics is strongly affected (if not dominated) by the presence of metallic impurities or sintering aids. Previous hot corrosion testing conducted by Blanchere et al[Ref 2] on silicon nitride and silicon carbide ceramics showed that high purity CVD silicon nitride exhibited the best and most predictable corrosion behavior from amongst a group of sintered and hot pressed SiC or silicon nitride

materials. Given the high degree of phase purity that can be obtained with this fabrication process, ceramic matrices based on tailorable mixtures of $Si_3N_4$ + SiC are expected to perform well in the envisioned gaseous corrosion environments.

Using a four axis McClean-Anderson filament winder, SCS-6™ silicon carbide monofilament-reinforced, non-porous tubular components have been fabricated with integral flanges and closed ends that have been up to one meter in length and 15 cm in diameter. Total fabrication times (including preform winding, binder removal and gas phase nitridation) are on the order of two to three days. The nitrided ceramic matrices normally contain 12-20% porosity and have densities in the 2.5 - 2.8 g/cc range. No dimensional alteration of the part occurs after the CFCC preform is constructed and no repeated infiltration/densification cycles are required to achieve matrix densification. This technology forms the basis of the composite filter development activity.

## PROJECT DESCRIPTION

The work is to be accomplished in two phases. The objective of the first phase is to develop and demonstrate at the coupon size level the feasibility of a hot gas filter material which will have acceptable performance and suitable manufacturing characteristics for fabricating hot gas filters. The objective of the second phase (optional) is to demonstrate the fabrication and performance of full size candle filters. This is to be accomplished by scaling up the phase one material processing approach to produce full scale filters and testing these to again validate acceptable performance. An additional part of this work will be to address quality control/quality assurance (QC/QA) issues, manufacturing cost and commercialization.

The successful accomplishment of these objectives will be demonstrated with ceramic hot gas filters which meet New Source Performance Standards and gas turbine inlet stream requirement limits of 10 ppm by weight, have a pressure drop of less than 5 inches of water at a face velocity of 10 feet per minute under standard temperature and pressure conditions, sufficient durability to resist pressure surges and thermal shock, and environmental resistance to steam and alkali. The fabrication of fifty (50) hot gas filters for pilot plant testing is an additional optional task.

During the first phase, the initial work has concentrated on establishing an acceptable level of permeability for the material. The current effort is directed toward the fabrication and testing of corrosion coupons.

## RESULTS

The primary focus to date for the fabrication of fiber reinforced hot gas filter material is to intentionally incorporate porosity into the ceramic matrix of the slurry formulations used in the modified slip casting technique used in fabrication. The technique entails addition of microspheres or microballoons to existing slurry formulations. The microspheres are fugitive and thus are removed via a burnout step. Microballoons are an attractive means to intentionally incorporate porosity in the matrix of CFCC filter materials for the following technical and economic reasons:

- A very wide variety of microballoon sizes and compositions (i.e., acrylic, glass, phenolic, etc.) are available in large quantities at reasonable cost.

- Microballoon size distributions and volume loadings in the NB SiC or NBSN slurry mixtures can be tailored to achieve different combinations of matrix strength and gas

permeability. This can be accomplished by controlling the packing density of balloon additions near or above the "percolation threshold," or the point at which microballoons just begin to contact each other.

- Microballoons can be chosen with very low residual ash contents after burnout, thus alleviating concerns about introducing contaminants that can have a deleterious effect on high temperature corrosion behavior.

- The rheological and handling characteristics of NBSiC or NBSN slurries loaded with microballoon additions are very similar to slurries which do not contain these foam-formers. This is very advantageous since Textron's proven methods for fabricating large non-porous CFCC components can directly be adapted to the manufacture of CFCC hot gas filter components.

For initial studies, nitride bonded silicon nitride (NBSN) and nitride bonded silicon carbide (NBSiC) samples were prepared which contained microballons but were unreinforced. The purpose in preparing and testing of these samples was to get insight into the range of composition which would provide acceptable permeability. The samples were cast as round disks 38mm diameter by approximately 5mm thick. Permeability tests were conducted at Westinghouse Electric Corporation Science and Technology Center.

Test results for the initial round of coupons are shown in Table 1. The range that is shown for each disc is based on testing the samples with both surfaces in the direction of the gas flow. This is generally done for two reasons; (1) to indicate whether an applied membrane has any effect on flow (which in this case, no membrane has been applied), (2) any minor chips, disc out-of-round, etc. could be easily detected when the disc is initially tested, and subsequently taken out of the holder and retested. Since the samples had variable thicknesses, the flow resistance measured was adjusted for thickness for comparison purposes (in-wg/fpm-in).

The coupon with 20 weight percent microballoons did not have sufficient structural integrity without fiber reinforcement and broke. The other samples had relatively high flow resistance, when compared to a target value of 1 in.-wg./fpm for a 0.25 inch thick disk of filter material, and a higher porosity material was therefore required.

## Table 1. Flow Resistance of Initial Filter Materials

| Composition and Weight % of Microballoons | Flow Resistance, in-wg/fpm | Thickness, in. | Adjusted Flow Resistance, in-wg/fpm-in |
|---|---|---|---|
| NBSN + ~ 8 w/o Disc 1 | 127.17-128.63 | 0.21 | 605.6-612.5 |
| Disc 2 | 123.81-126.61 | 0.18 | 687.8-703.4 |
| NBSN+~ 12 w/o Disc 1 | (a) | 0.185 | |
| Disc 2 | 61.24-70.47 | 0.307 | 199.5-229.6 |
| Disc 3 | 20.86-21.20 | 0.307 | 67.9-60.04 |
| NBSiC+~ 20 w/o Disc 1 | (b) | | |

(a) Chipped
(b) Broken

Two additional type samples were prepared; a nitride bonded silicon carbide (NBSiC) with 14 weight percent of microballoons and a pure silicon nitride (NBSN) with 10 weight percent microballoons.

The samples are identified as follows:

(A) NBSiC + approximately 14 w/o microballoons.
(B) NBSiC + approximately 14 w/o microballoons.

(C) NBSN + approximately 10 w/o microballoons.

The difference between A and B is that B has a bimodal distribution of microballoons.

The thickness of the four "A" filter discs ranged between 0.17 and 0.2 inches. One of the discs cracked apparently during delivery to Westinghouse, while the second disc had a section of material broken from its outer edge. Therefore, only two of the "A" discs were subjected to room temperature gas flow resistance measurements.

The thickness of the two "B" filter discs was approximately 0.17 inch. The one disc which remained intact was subjected to room temperature gas flow resistance measurements. The thickness of the "C" filter discs ranged from 0.22 to 0.24 inches.

All intact samples were tested twice, positioning both surfaces of each disc to the direction of the gas flow. As shown in Table 2, variation exists in the resulting gas flow resistance measurements for the three filter sample types. Both NBSiC materials (i.e., discs "A" and "B") have a measured gas flow resistance of <1 in-wg/fpm which is within the Westinghouse tolerance for a 0.25 inch thick sample disc. In contrast, however, the NBSN discs ("C" samples) which remained fully intact, have a relatively high gas flow resistance in comparison to the targeted, as manufactured resistance measurements. While the NBSiC material with 14 weight percent of microballoons has an acceptable gas flow resistance, further effort is needed to introduce porosity and/or permeability into the NBSN filter disc series and to perform duplicate experiments to verify the previous results.

The scanning electron micrographs are presented in Figures 1 through 3, illustrating the cross-sectioned morphology of the NBSiC and NBSN filter materials. The NBSiC material (Figures 1 and 2) shows interconnected porosity, whereas the NBSN material (Figure 3) is slightly below this level. The lack of gross amounts of whiskers is also evident.

## Table 2. Flow Resistance of Additional Filter Materials

| Composition and Weight % of Microballoons | Flow Resistance in-wg/fpm | Thickness, in |
|---|---|---|
| NBSiC + ~ 14 w/o Disk 1<br>Disk 2 | 0.14 - 0.21<br>0.27 - 0.38 | 0.17 - 0.20 |
| NBSiC + ~ 14 w/o | 0.13 - 0.18 | 0.17 |
| NBSN + ~ 10 w/o Disk 1<br>Disk 2<br>Disk 3 | 12.69 - 18.93<br>13.16 - 13.76<br>22.62 - 25.02 | 0.22 - 0.24 |

A second additional batch of unreinforced samples of nitride bonded silicon carbide (NBSiC) were prepared based on mixtures of microballoons and microcrystalline starch particulate with graded particle size distributions. The mixes contained four component pore former additions. These were chosen to maximize the packing efficiency of the pore formers in order to achieve the required permeability at the lowest possible weight fraction of the pore former. The purpose was to get the highest possible solids loading to minimize shrinkage during drying, and therefore the tendency towards cracking during the casting process.

Two general formulations were prepared; one at 14 weight percent pore formers and one at 16 weight percent. Both used a distribution of pore formers as shown in Table 3. The disks of these materials are being tested at Westinghouse for permeability and will be reported at a later date.

## Table 3. Pore Former Additions

| Component Description | Weight Percent |
|---|---|
| Latex microballoon with max size of 70 microns | 42 |
| Latex microballoon with max size of 40 microns | 24 |
| Latex microballoons with max size of 20-25 microns | 13 |
| Microcrystalline, roughly spherical shaped starch additive with a median size of approximately 8-10 microns | 21 |

In addition to the tests on unreinforced material, experiments were initiated to incorporate fiber reinforcement into the filter. Various approaches were tried to make flat panels which could be subsequently machined to produce flat disks for permeability, filtering efficiency and corrosion testing. These included both casting and pressure casting of the matrix into collimated arrays of SCS-6 fiber reinforcement. These attempts were only partially successful because it was difficult to achieve uniform and complete filling of the fiber array with matrix material. Since the hot gas filter configuration is tubular and the only purpose in making flat panels was to produce coupons, the decision was made to proceed directly to the fabrication of cylindrical shapes representative of candle filters. These shapes are being made by a wet filament winding approach which has proven successful in the fabrication of non-porous tubes and will be tested at Westinghouse as minicandles or sections of minicandles for permeability, filtering efficiency and corrosion behavior.

## FUTURE WORK

Future testing will validate that the material will have acceptable performance under the intended power plant operating conditions and suitable manufacturing characteristics for fabricating hot gas filters. This includes the testing of minicandles or sections of minicandles for permeability, filtering efficiency and corrosion behavior. The demonstration of the fabrication and testing of full scale hot gas filters will take place during the second phase of the work. The fabrication of fifty (50) hot gas filters for pilot plant testing is an additional optional task.

## REFERENCES


1. Continuous Fiber Ceramic Composites Program with the Department of Energy; Cooperative Agreement #DE-FC02-92 CE 41001.

2. Blanchere, etal, High Temperature Corrosion of Ceramics; (Noyes Data Corp.; 1989)

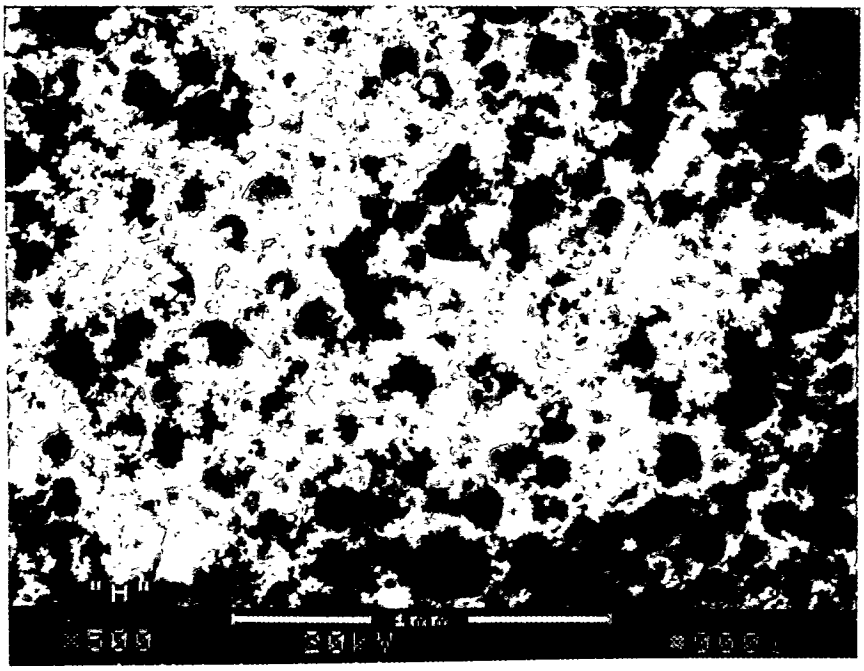


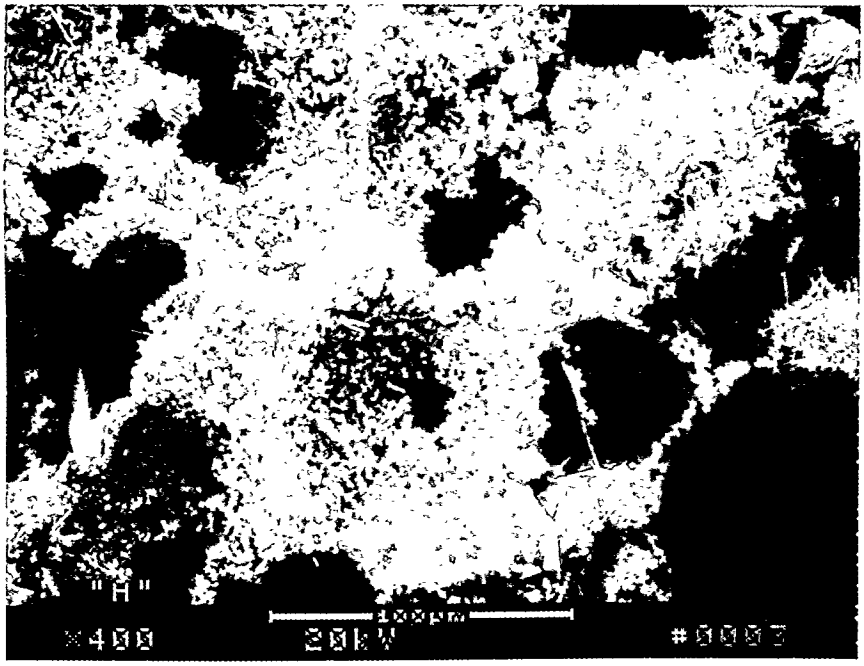


**Figure 1. NBSiC + ~ 14 w/o Microballoons**

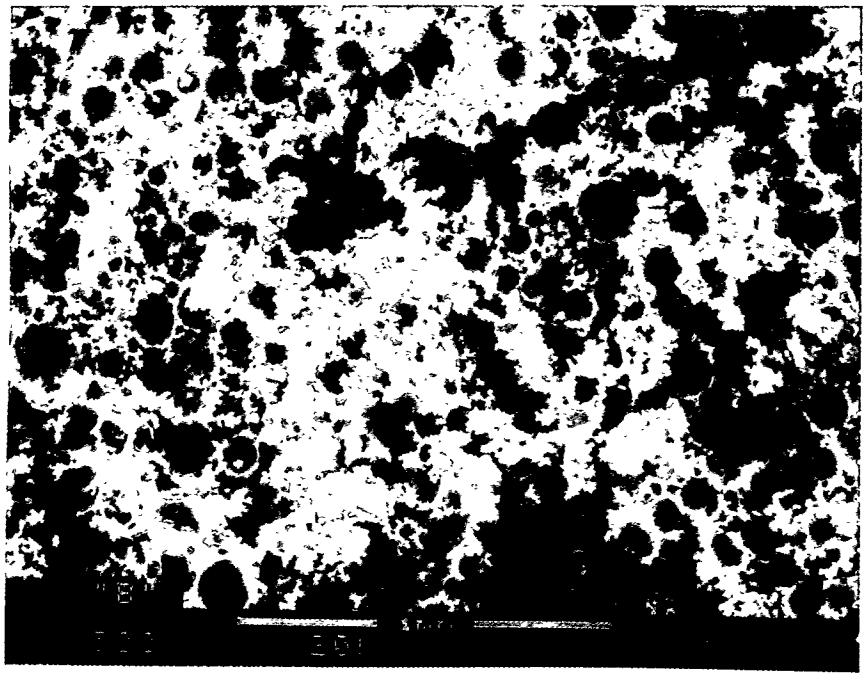

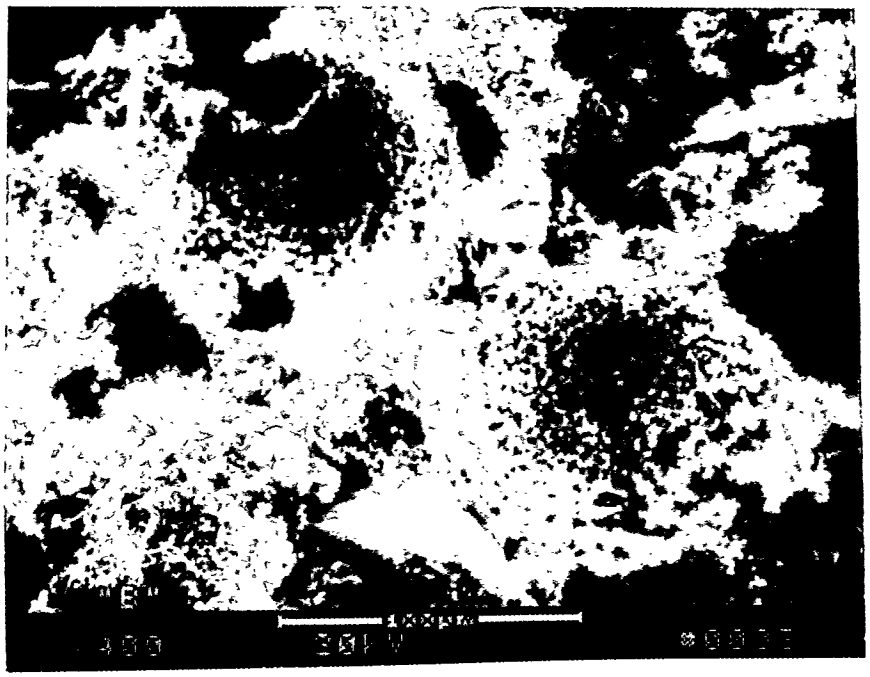

**Figure 2. NBSiC + ~ 14 w/o Bimodel Distribution of Microballoons**

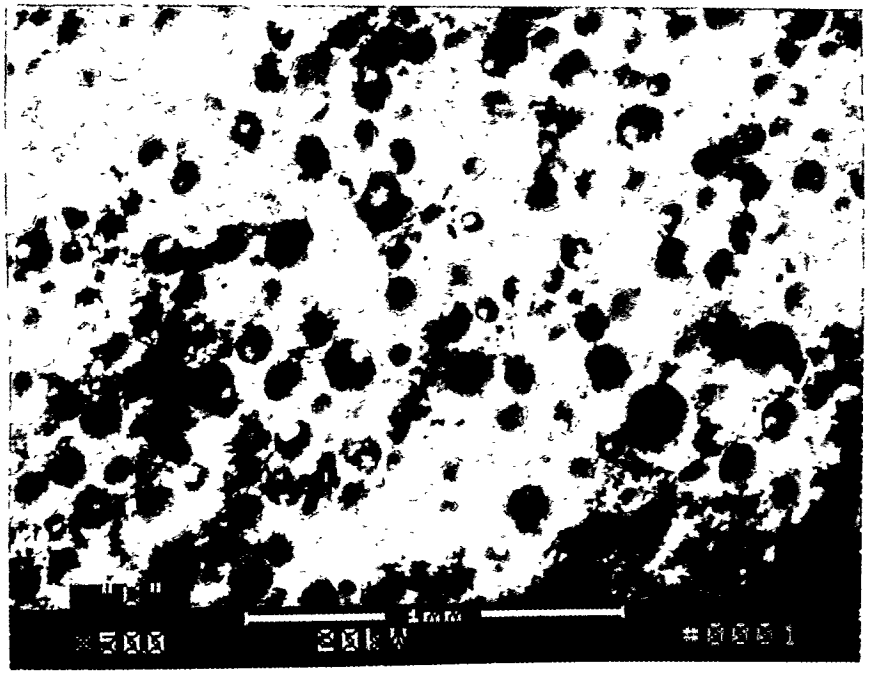


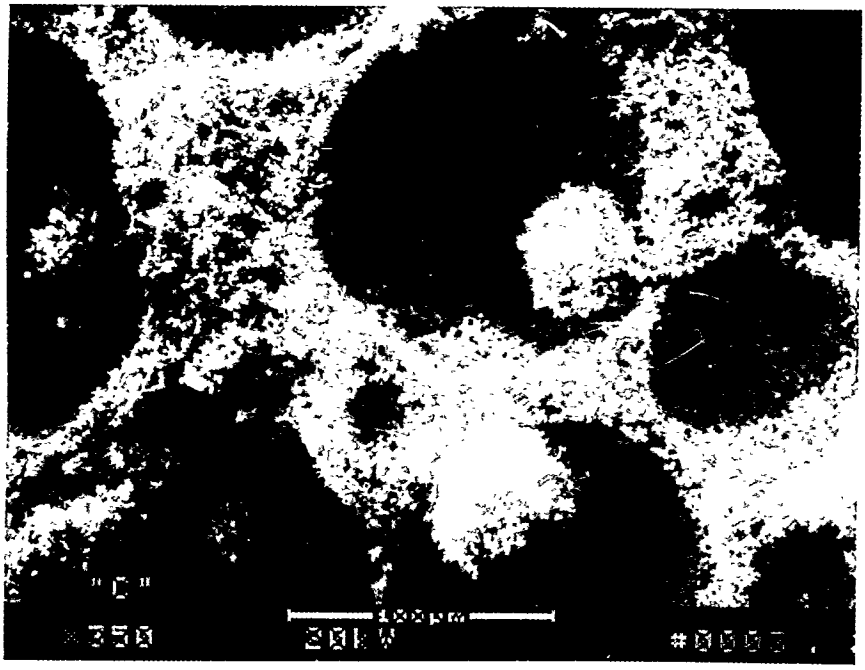


**Figure 3. 321 RBSN + ~ 10 w/o Microballoons**

## PB.6 3-D Woven, Mullite Matrix, Composite Filter

### CONTRACT INFORMATION

**Contract Number** DE-AC21-94MC31167

**Contractor**

Westinghouse Electric Corporation
Science & Technology Center
1310 Beulah Road
Pittsburgh, PA 15235-5098
(412) 256-2195
(412) 256-1267 (FAX)

**Contractor Project Manager** Jay E. Lane

**Principle Investigators**

Jay E. Lane
Carol J. Painter
Kenneth C. Radford
Jean-Francois LeCostaouec; Techniweave, Inc.

**METC Project Manager** Theodore J. McMahon

**Period of Performance** September 30, 1994 to December 30, 1995 (Phase I)

**Schedule and Milestones**

**FY95 Program Schedule**

| | O | N | D | J | F | M | A | M | J | J | A | S |
|---|---|---|---|---|---|---|---|---|---|---|---|---|
| NEPA Report | ——— | ——— | | | | | | | | | | |
| Test Plan | ——— | ——— | | | | | | | | | | |
| Develop 3D Preform | | | ——— | ——— | ——— | ——— | ——— | ——— | | | | |
| Develop Mat'l Process | | | ——— | ——— | ——— | ——— | ——— | ——— | | | | |
| Evaluate Best Material | | | | | | | | | ——— | ——— | ——— | ——— |

### OBJECTIVES

Westinghouse, with Techniweave as a major subcontractor, is conducting a three-phase program aimed at providing advanced candle filters for a 1996 pilot scale demonstration in one of the two hot gas filter systems at Southern Company Service's Wilsonville PSD Facility. The Base Program (Phases I and II) objective is to develop and demonstrate the suitability of the Westinghouse/Techniweave next generation composite candle filter for use in Pressurized Fluidized Bed Combustion (PFBC) and/or Integrated Gasification Combined Cycle (IGCC) power generation systems. The Optional Task (Phase III, Task 5) objective is to fabricate, inspect and ship to Wilsonville

50 advanced candle filters for pilot scale testing.

## BACKGROUND INFORMATION

Hot gas particulate filters are key components for the successful commercializaion of advanced coal-based power-generation systems such as Pressurized Fluidized-bed Combustion (PFBC), including second-generation PFBC, and Integrated Gasification Combined Cycles (IGCC). Current generation monolithic ceramic filters are subject to catastrophic failure because they have very low resistance to crack propagation. To overcome this problem, a damage-tolerant ceramic filter element is needed.

## PROJECT DESCRIPTION

Westinghouse and Techniweave have undertaken a three-phase progam to develop an advanced filter with damage tolerance, increased durability, increased resistance to crack propagation, and non-catastrophic metal-like failure characteristics through the use of:

- A 3D continuous fiber preform for reinforcement;
- Oxide materials, which are inherently stable in oxidizing environments and have been shown by Westinghouse under DOE Contract #DE-AC21-88MC25034, Thermal/Chemical Degradation of Ceramic Cross-Flow Filter Materials, to be more resistant to corrosive alkali species than nonoxides, such as SiC and $Si_3N_4$; and,
- Low cost sol-gel processing.

Phase I, Filter Material Development and Evaluation, activities include the laboratory-scale development, characterization, and testing of a mullite matrix 3D fiber-reinforced (Nextel 550) ceramic composite filter material. This effort focuses on meeting filter material requirements. Phase II, Prototype Filter Fabrication and Evaluation, activities include the development of a prototype filter and filter qualification testing in a simulated pressurized-bed combustion environment in the Westinghouse High-Temperature High-Pressure (HTHP) filter test facility. Phase III, Optional Pilot-Scale Filter Manufacturing, activities include the manufacture of 50 full size candle filters for pilot scale testing at Wilsonville and to implement quality assurance/quality control and non-destructive evaluation procedures developed in Phase II.

At present, only Phase I has been funded. A breakdown of the experimental activity for Phase I, Task 3 (Tasks 1 and 2 were the NEPA Report and Test Plan, respectively) follows:

Phase I

Task 3 - Development, Qualification, and Testing of Hot Gas Filter

- 3.1.1 - Develop 3D Fiber Architecture
- 3.1.2 - Develop Composite Filter Material Fabrication Process
- 3.1.3 - Fabricate and Evaluate Best Filter Material

## RESULTS

During the first half of FY95, after completing Tasks 1 and 2, efforts have been focused on experimental subtasks 3.1.1 and 3.1.2 in Task 3. A description of objectives in each subtask and a discussion of the status or resulting data in each area follows.

## 3D Fiber Architecture Development

A low cost, three-dimensional (3D) fiber architecture, that is both easy-to-manufacture and automatable, is required to produce an economical 3D preform suitable for candle filter use. Toughness in all directions, good shear properties, homogeneously distributed porosity, and surface smoothness are desirable features for selecting a preform for fabricating a ceramic matrix composite (CMC) candle filter fiber preform. A 3D fiber architecture can be designed to fulfill these requirements. Techniweave's fiber architecture design philosophy has been guided by the selection of automatic net shape weaving techniques, the generation of thin wall structures, the achievement of fiber continuity through highly stressed regions and the tailoring of the preform to the mode of matrix introduction.

Over the past five years, Techniweave has developed equipment and process technology for weaving seamless, tubular filter preforms with ceramic fibers. During an IRAD program, the use of a multilayer fabric was demonstrated for fabricating a porous mullite/mullite CMC. This technology provides the basis for the fiber architecture variations being evaluated in this program for the economical production of a fiber preform for candle filters. A generic sketch of the multi-layer fabric is presented in Figure 1.

From this baseline weave, Fig. 1, twelve fiber architectures were designed to examine the effect of fiber volume, wall thickness, fiber architecture and yarn construction on the CMC filtration characteristics and mechanical properties. The fiber orientation and yarn construction were varied to modify the sizes and distributions of porosity in the preform. The amount of fiber at the preform surface was varied to control the filtering surface smoothness and porosity.

A low cost woven preform is required. The best solution is one that will provide adequate filtration and mechanical performance while using the least amount of fiber. Thus, wall thickness was limited to 0.1 in. thick to control fiber cost and permit ease of manufacture and automation.

Initial weaving trials were conducted to establish what maximum level of fiber volume could be achieved in the warp (axial direction along the length of the filter) and fill (circumferential direction) directions without damaging the fibers. It was determined that a balanced weave could be woven with a maximum total fiber volume of 35%. The axial and circumferential loading on a candle filter in use are expected to be different. In order to be able to optimize the fiber volume in both directions, some preforms were woven with different amounts of fiber volume in the warp and fill directions.

From these initial weaving trials, eleven candidate fiber architectures were selected for fabrication into CMC panels for characterization. For each architecture, preforms are being fabricated from Nextel 550 fiber. The preforms are then infiltrated with the matrix solution to form filter material composite plates. The matrix solution is either sol-gel mullite with mullite filler powders, or sol-gel mullite without mullite filler powders.

To date, 12 plates have been fabricated from the first six architecture designs and have been shipped to Westinghouse for evaluation. These six candidate architectures

are shown in Figure 2. Two sizes were fabricated for each architecture:

1) 4 in. x 6 in. panels were made using Techniweave's baseline matrix fabrication process combining mullite sol and mullite powder infiltration. These panels were fabricated with an *in-situ* formed membrane layer. The 6 in. length of these panels is parallel to the fill direction. The warp direction, which is the 4 in. length, generally has a higher strength than the fill direction. This is of importance for those candidate architectures which have unequal fiber volume fractions in the fill and warp directions. Permeability test specimens, 41 mm diameter disks, and 4-pt bend specimens, machined according to ASTM C1161-90, were prepared for testing. Bend strength will be measured in each direction.

2) 2 in. x 2 in. plates for composite fabrication using just the mullite sol. The mullite powder is not used for the composite matrix in these samples. Thus, these samples will determine the permeability of the fiber architecture without the additional influence of the powder. Permeability test specimens have been machined from these samples.

**Permeability Test Results.** The gas flow resistance for each disc sample was measured with the Westinghouse permeability test rig. Acceptable permeability results from this test rig are gas flow resistance values < 1 in-wg/fpm at room temperature.

The samples were evaluated in this rig in two positions: a) "up" position, this is the normal expected filter material orientation where the expected external surface of the filter material is the face exposed directly to the flowing gas stream, as it would be in use, and b) "down" position, this refers to directly exposing the face of the filter material that would normally be the internal surface of the candle filter to the flowing gas stream. The intent of this evaluation is note if there are significant differences in the flow resistance through the material based on its orientation in the test rig; there should not be any differences.

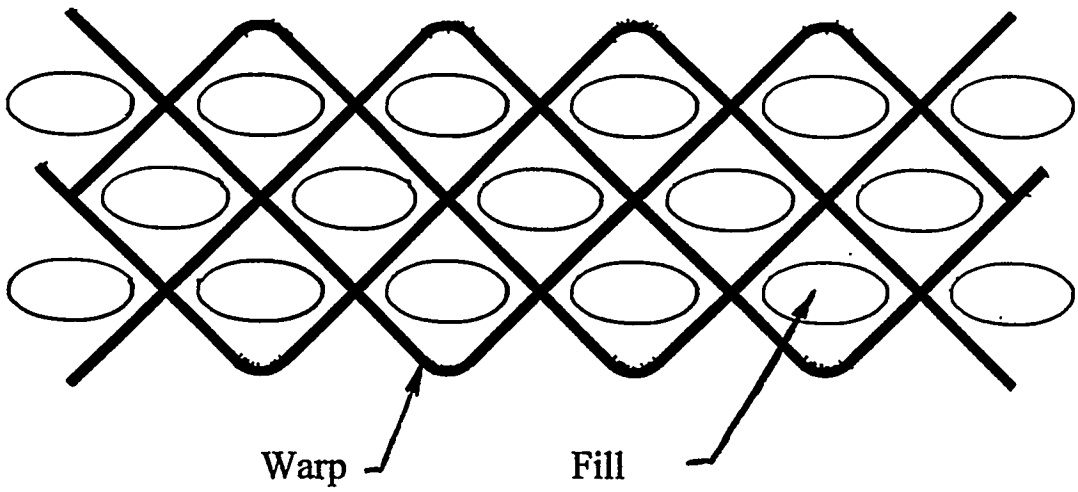


**Figure 1. Schematic of multi-layer fabric where the warp yarns provide axial and radial reinforcement while fill yarns provide hoop reinforcement.**

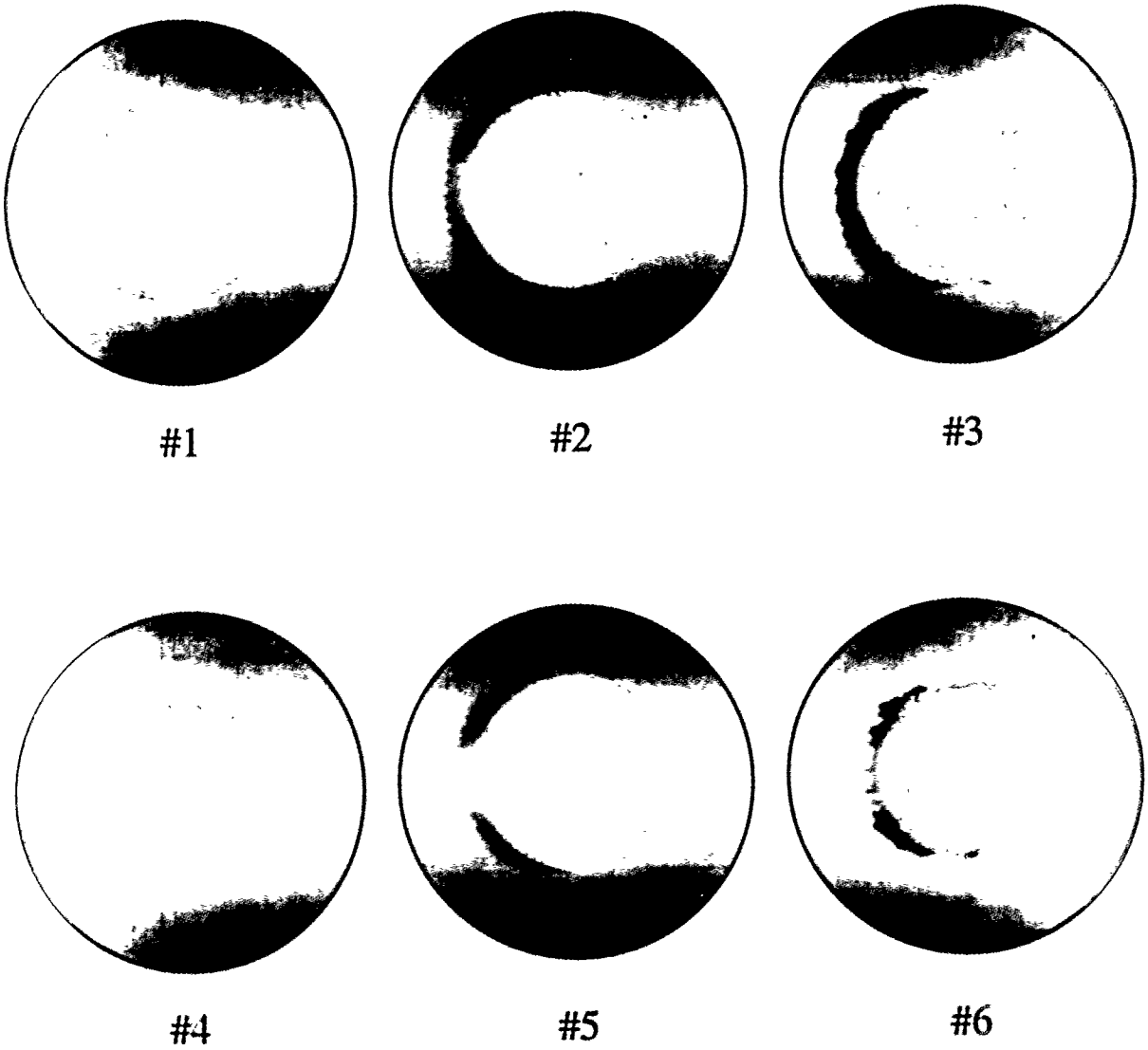


Candidate Fiber Architectures

**Figure 2. Photographs of Candidate Fiber Architectures 1-6**

During testing, six of the twelve samples had leaks at the edges or were poor fits in the test rig. These samples will be re-machined, as-needed, and edge sealed with a ceramic adhesive, then re-tested.

The data for the remaining samples is shown in Table 1. All measured architectures, in both test orientations, met the gas flow resistance requirement of < 1 in-wg/fpm at room temperature. A higher gas flow resistance was measured in the "up" position. It is hypothesized that when in this position some leak may have occurred around the periphery of the sample. Even though an attempt was made to seal the edge with Teflon tape, it is conceivable that some leak may have still occurred.

**TABLE 1. Gas Flow Resistance as a Function of Fiber Architecture**

| Architecture* | Gas Flow Resistance (in-wg/fpm at 70 °F) | |
|---|---|---|
| | Up | Down |
| 1 | 0.434 | 0.657 |
| 2 | 0.129 | 0.750 |
| 3 | 0.193 | 0.442 |
| 5 | 0.425 | 0.759 |
| 6 | 0.264 | 0.248 |
| 4 (sol only) | 0.332 | 0.622 |

*samples 1,2,3,5,& 6 were made with powder + sol

To confirm the results in Table 1, and to eliminate any potential leaks when placed in the sample holder, all samples will have their perimeters and edges sealed with a ceramic adhesive prior to being re-tested.

**Weaving Trials for Manufacturing Issues.** Separately, weaving trials of tubular sections have been initiated to determine the manufacturing issues for the tubular, closed-end, and flange sections of the candle filter. This information is one of the factors which will be used to select the best and lowest cost architecture for candle filters. Initial trials have demonstrated the feasiblity of continuously weaving tube sections with an integrated closed end.

**Develop Composite Filter Material Fabrication Process**

The objective of this effort is to optimize the matrix infiltration step and matrix sintering conditions in order to minimize the fabrication costs of ceramic hot gas filters and maintain acceptable filter performance. Our goal is to fabricate the filter material using only two matrix processing steps:

1) Infiltration of the ceramic preform with a water-based mullite sol (no mullite filler powder) to rigidize the ceramic preform and provide a protective coating on the fibers.
2) Infiltration of the ceramic preform with a water-based mullite sol with mullite filler powder added. The purpose of the filler is to create a tortuous porosity network.

Several processing variables, listed below, can influence the density/porosity, mechanical properties and performance of the ceramic hot gas filter.

- Processing method
- Mullite sol concentration
- Sol viscosity
- Particle size distribution
- Concentration of mullite filler powder added to sol
- Calcining temperature
- Sintering temperature

The evaluation of the effects of these processing variables on the matrix infiltration efficiency, filter performance and mechanical

properties have been undertaken in this subtask. A Taguchi design of experiments approach has been selected to provide a systematic analysis of the effects of the processing variables.

The intent of the Taguchi process is to identify the major effects (variables) and the most optimum values for these effects to give the desired response. In this case, the desired response is meeting the permeability specification.

Permeability is the primary response to be measured and these results will be used in the Taguchi analysis for determining the best values for the matrix processing variables. Permeability was selected because it is the most important parameter. Regardless of strength, surface condition, etc., if the candidate material does not meet the permeability requirement, it cannot be considered for filter applications.

Secondary factors being using for evaluating the results of the Taguchi test matrix are the ability to form a membrane *in-situ* and the composite density. Strength is an additional factor which will be considered in additional experiments.

Prior to conducting the first experimental design, two sets of screening studies were necessary in order to establish experimental values for the sol viscosity and mullite powder particle size distribution.

**Modification of Sol Viscosity.** Westinghouse experience indicates that a higher viscosity will help to keep ceramic filler powders in suspension and provide for a more homogeneous infiltration of the ceramic preform. Additionally, eliminating the currently required mechanical agitation to keep the powder dispersed will simplify fabrication and reduce production and capital equipment costs.

Several water-soluble polymers were evaluated in terms of their effectiveness for increasing the viscosity of the water-based mullite sol. These additives include: Carbopol by Goodyear (cross-linked polyacrylic acid polymer), Surfynol CT-324 by Air Products (pigment grind additive of proprietary composition), and Elvanol by Dupont (Polyvinyl Alcohol). Unfortunately, these products were found to be either incompatible with the water-based mullite sol or were ineffective for increasing the sol viscosity. Carbopol and Elvanol were not able to be dissolved in the Westinghouse water-based mullite sol.

Surfynol CT-324, did not completely dissolve in the water-based mullite sol, but was found to significantly improve the dispersability of the mullite powder in the sol. Concentrations in the range of 5 - 10% by mullite powder weight were found to be beneficial. The viscosity of the sol increased from 20 cp to 400-800 cp, depending on the mullite powder concentration in the sol. Unfortunately, the undissolved portions of Surfynol were in the form of large, fat-like globules. During preform infiltration, these Surfynol globules clogged the pores of the composite preform and formed a coating on the preform surface which inhibited infiltration of the mullite sol and mullite filler powder.

Vendors of dispersing and thickening agents were contacted to discuss the compatibility difficulties that were encountered. The vendors indicated that such water-soluble additives are geared towards use in systems having a pH in excess of 3. Water-based mullite sols typically have a pH less than 2. This pH difference causes a

chemical incompatibility between the additives and the sol.

Polyethylene imine and polyvinylpyrrolidone have been suggested as possible compatible additives. Polyethylene immine retains its charge in acidic conditions and hence may work in conjunction with this low pH sol. Polyvinylpyrrolidone has good solubility and chemical stability in both water and many organic solvents. These additives are under evaluation.

Other methods evaluated for either improving powder dispersion or increasing sol viscosity included: 1) The application of an "ionic" polyvinyl alcohol (PVA) coating to the surface of the mullite filler powder, prior to dispersion in the sol, as a means to improve the dispersability of the mullite powder, and 2) the use of a thermal treatment of the water-based sol to increase sol viscosity. Neither approach was successful.

**Mullite Filler Powder Particle Size Distribution.** Based on prior Westinghouse and Techniweave research, three particle size distributions were identified for the initial experimental design: 1 - 10 μm, 5 - 20 μm and 10 - 45 μm. These three desired particle sizes were not available "off-the-shelf." The three particles size distributions were obtained by classifying -200 mesh (< 70 microns) mullite powder feedstock.

Because of the additional cost of size classification of the filler powder, the test matrix was expanded to include the evaluation of the -200 mesh mullite powder. If this powder is suitable, a significant cost savings would result.

**Processing Development for Sol-Only Infiltration Step.** As previously discussed, the current objective is to fabricate filter materials using only two matrix processing steps. The first step is a sol-only infiltration to rigidize the preform and provide a protective coating on the fibers.

Westinghouse experience indicates that if the initial infiltration yields a coating which is too thick, the resulting preform will be stiff and difficult to process in subsequent steps. Furthermore, to optimize the mechanical properties of the composite filter material, it is desirable to have a thin, uniform crack-free coating with minimal bridging between fibers.

The suitability of the water-based mullite sol for forming a uniform, thin coating was evaluated by dip coating woven Nextel 550 fabric in three sol concentrations: 10, 5, and 2.5 wt%. The fabrics were then air dried, calcined at 800 °C for 1 hour and then examined using a scanning electron microscope.

The 10 wt% mullite sol resulted in a very thick and cracked coating; significant fiber bridging was observed. The 5 wt% sol also yielded a thick cracked coating. The 2.5 wt% mullite sol was found to give the most uniform crack-free mullite coating with minimal bridging. The 2.5 wt% sol was selected for use in all subsequent CMC fabrication.

**Selection of Infiltration Method.** Prior to proceeding with the initial design of experiments, the infiltration efficiency (weight gain/infiltration cycle) and permeability ratio were compared for a more conventional vacuum infiltration approach to a one-sided vacuum infiltration method. In the conventional method, the infiltrant enters the composite preform from all exposed surfaces. In the one-sided approach, vacuum was used to pull the infiltrant from one

exposed surface through the composite, see Figure 3.

Each composite was infiltrated with a 10 wt% water-based mullite sol to which 10 wt% additional mullite powder was added. The particle size of the mullite powder was 10-44 microns. The infiltration efficiency was slightly greater for the conventional vacuum infiltration process.

After 5 infiltration cycles, the immersion densities of the samples were 1.80 g/cm$^3$ and 1.68 g/cm$^3$ for the conventional and one-sided infiltrated samples, respectively. These values correspond to 58 % and 54 % of theoretical density (3.11 g/cm$^3$), respectively.

The gas flow resistance was measured for each sample. As shown in Table 2, the sample infiltrated from one-side only is within the Westinghouse filter specification for gas flow resistance (i.e., < 1 in-wg/fpm), while the conventionally infiltrated sample had a gas flow resistance exceeding the target specification.

**TABLE 2. Gas Flow Resistance as a Function of Infiltration Method**

| Infiltration Method | Gas Flow Resistance (in-wg/fpm at 70 °F) | |
|---|---|---|
| | Up | Down |
| Conventional Vacuum | 2.160 | 2.637 |
| One-Sided | 0.283 | 0.332 |

The one-sided infiltration approach was selected for all CMC fabrication. This approach is also expected to give the lowest manufacturing cost.

**Taguchi Experimental Design** The results of the screening studies for sol viscosity and mullite filler particle size distributions, as well as processing information from Techniweave, led to the formulation of the first experimental design. The variables are listed below.

- Sol Viscosity: At this time, a suitable additive or method has not been identified for increasing the sol viscosity (for the purpose of providing a uniform dispersion of mullite filler powder in the sol). Because the mullite powder can be maintained in a dispersed state through continuous agitation, this technique will be used to maintain the powder dispersion until an alternate means is identified.
- Mullite Powder Particle Size Distributions: The initially targeted distributions of 1 - 10 μm, 5 - 20 μm, and 10 - 45 mm will be utilized. Additionally, the -200 mesh mullite feedstock will also be evaluated due to the potential cost savings.
- Concentration of Mullite Filler Powder: A low, 10 wt%, and a high, 30 wt%, concentrations were selected for evaluation.
- Concentration of Mullite in Aqueous Base Sol: A low, 5 wt%, and a high, 10 wt%, concentrations were selected for evaluation.

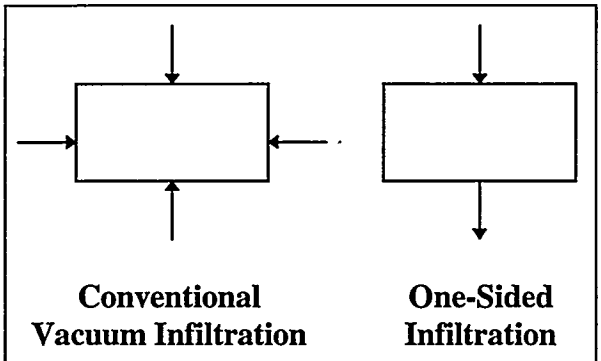


**Figure 3. Comparison of Conventional Vacuum Infiltration and One-Sided Infiltration Techniques**

- Calcining Temperature: Temperatures of 600 and 800 °C were selected.
- Sintering Temperature: Temperatures of 1050 and 1150 °C were selected.

After establishing the values of the experimental variables, a Taguchi design of experiments was set up, Table 3, to permit a systematic analysis of the variables with a minimum number of experiments. For this initial experimental design, both the calcining and sintering temperatures are being held constant at 2 and 4 hours, respectively. Only the calcining and sintering temperatures are being varied because temperature has a more significant impact on microstructure development, than does time at temperature. The times were chosen conservatively to provide sufficient time for all significant reactions to occur.

Nextel 550 preforms, using an angle interlock architecture, are being used for this test matrix. Sections of preform were first dip coated using a 2.5 wt% concentration of mullite sol. The preforms were then air dried and calcined at 800 °C for 1 hour. Permeability disks were then cut from the coated preform. The weights of each starting disk were measured.

Matrix infiltration processing of these disks is in progress. Each permeability disk is being infiltrated using the appropriate slurry composition with the one-sided infiltration method. The goal is to infiltrate until a thin, uniform membrane layer is formed on the disk surface. The infiltration efficiency of the various slurries is monitored. Upon completion of the infiltration processing, the gas flow resistance values of each disk will be measured. These data will be analyzed using standard Taguchi methods.

Thus far, the following observations about infiltration efficiency and membrane layer formation have been noted:

- The finest particle size distribution, 1-10 microns, is easily pulled through the coarse porosity network of the standard angle interlock fiber architecture. A membrane layer on the surface of the composite is unable to be formed after several infiltration cycles.
- The medium particle size distribution, 5 - 20 microns, at a loading of 10 wt%, will form a membrane layer after numerous

**TABLE 3. Design of Experiments Matrix for Filter Processing**

| Factor / Trial No. | Mullite Powder Particle Size Distribution | | | | Mullite Sol Conc. (wt%) | | Conc. of Mullite Powder in Sol (wt%) | | Calcining Temp. (°C) | | Sintering Temp. (°C) | |
|---|---|---|---|---|---|---|---|---|---|---|---|---|
| Code | 1-10 µm | 5-20 µm | 10-35 µm | -200 mesh | 5 | 10 | 10 | 30 | 600 | 800 | 1050 | 1150 |
| FD-1 | X | | | | X | | X | | X | | X | |
| FD-2 | X | | | | | X | | X | | X | | X |
| FD-3 | | X | | | X | | X | | | X | | X |
| FD-4 | | X | | | | X | | X | X | | X | |
| FD-5 | | | X | | X | | | X | X | | | X |
| FD-6 | | | X | | | X | X | | | X | X | |
| FD-7 | | | | X | X | | | X | | X | X | |
| FD-8 | | | | X | | X | X | | X | | | X |

infiltration cycles (7-15). The number of cycles required to form this layer is not practical. At a loading of 30 wt%, this particle size distribution can be used to form a membrane layer within one to two cycles.

- The use of the coarse -200 mesh powder (< 70 microns) allows a membrane to be readily formed (# of cycles is dependent on powder loading and sol concentration).
- When a film is formed, pinholes are often observed. This pinhole formation is a processing issue that is also related to the coarse surface porosity of the angle interlock architecture. It is not a characteristic of any of the particle size distributions. These pinholes do not imply a potential leak as the architecture in its own right has quite tortuous porosity and would stop any penetration of the ash. The disadvantage of pinholes is that they would be more likely to plug up with ash. Thus a large number of pinholes, if plugged with ash, would reduce the available filtering surface area.

## FUTURE WORK

The remaining candidate architectures will be woven into preform panels and used to fabricate CMCs for test and evaluation. Weaving trials will be conducted to evaluate the feasibility of continuously forming tubes with integrated flanges and closed ends. Matrix processing optimization studies will be completed with the results from the first experimental matrix being used to guide additional experiments to evaluate flexure strength as a function of the processing variables.

The results from the above will be used to select the best architecture and matrix processing approach. CMC test panels will then be fabricated using the best architecture and matrix processing technique. These panels will undergo permeability testing, 4-pt bend testing, Weibull modulus determination, and high temperature flow-through corrosion tests.

# PB.7 Hot Particulate Removal and Desulfurization Results From the METC Integrated Gasification and Hot Gas Cleanup Facility

John M. Rockey
Morgantown Energy Technology Center

## ABSTRACT

The Morgantown Energy Technology Center (METC) is conducting experimental testing using a 10-inch diameter fluid-bed gasifier (FBG) and modular hot gas cleanup rig (MGCR) to develop advanced methods for removing contaminants in hot coal gasifier gas streams for commercial development of integrated gasification combined-cycle (IGCC) power systems. The program focus is on hot gas particulate removal and desulfurization technologies that match the temperatures and pressures of the gasifier, cleanup system, and power generator.

The purpose of this poster is to present the program objectives and results of the work conducted in cooperation with industrial users and vendors to meet the vision for IGCC of reducing the capital cost per kilowatt to $1050 and increasing the plant efficiency to 52% by the year 2010.

Data relevant to the design and operation of dry particulate solids filters employing both rigid ceramic and ceramic fabric materials were tested on coal gas at conditions of commercial interest; e.g., temperatures up to 1100 °F and system pressures between 300 and 350 psia. Three LayCer™ 70/3 silicon carbide candle filters supplied by Shell Synthetic Fuels Incorporated were removed from service free from any visually detectable physical changes after 254, 525, and 868 hours of operation, respectively. Exposure for 483 hours of 3M SICONEX™ fiber-reinforced ceramic and NEXTEL™ 312 and 550 ceramic fabric materials was also obtained. One 3M ceramic composite filter was tested for 89 hours. The exposed materials were analyzed for physical property changes such as permeability, strength, and micro-structure.

Development of hot gas desulfurization technologies has centered in two areas. First is testing of regenerable mixed metal oxide sorbents that have the potential to reduce the sulfur in coal gas to less than 20 ppmv. Capabilities of commercial candidate sorbents were tested using coal gas from the FBG. Hydrogen sulfide breakthrough curves were obtained for a packed-bed material developed by METC (METC#2) and a fluidized material developed by Research Triangle Institute (Zt-4). Capacity for retention of trace contaminants (inherent in the feed coal) and changes in the physical and chemical properties of the sorbents were determined.

The second area of hot gas desulfurization technology development is in treatment of the sorbent regeneration offgas that contains $SO_2$ (2-5%). Testing of the Research Triangle

Institute (RTI) direct sulfur recovery process (DSRP) (a process in which $S0_2$ is catalytically reduced to sulfur using coal gas at temperature and pressure conditions of the regenerator) was conducted for the first time on real (versus simulated) coal gas. A total of 22 hours of DSRP testing was conducted in which $SO_2$ conversion to claus quality sulfur was up to 96% and no apparent deleterious effects of coal gas contaminants were observed.

# PB.8 Simultaneous Hot Desulfurization and Improved Filtration in Coal Utilization Processes

## CONTRACT INFORMATION

**Contract Number** DE-FG02-94ER81786

**Contractor** Industrial Filter & Pump Mfg. Co., Inc.
5900 Ogden Avenue
Cicero, IL 60650
(708)-656-7800

**Other Funding Sources**

**Contract Project Manager** Paul M. Eggerstedt

**Principal Investigator** Paul M. Eggerstedt

**METC Project Manager** Richard Dennis

**Period of Performance** August 15, 1994 to March 10, 1995

**Schedule and Milestones**

**Program Schedule**

| | 1994<br>J F M A M J J A S O N D | 1995<br>J F M A M J J A S O N D |
|---|---|---|
| **Procurement** | *** | |
| **Equipment Shakedown** | *** | |
| **$SO_2$ Testing** | **** | |
| **$H_2S$ Testing** | **** | |
| **Phase 2 Submittal / Final Report Preparation** | ****** | |

## OBJECTIVES

The primary objective of this Phase I SBIR effort was to investigate the relative effectiveness which various waste metal oxides might have in the removal of sulfur from sulfur dioxide ($SO_2$) and hydrogen sulfide ($H_2S$) gas streams, under controlled laboratory conditions. A number of waste metal oxides were tested both individually and in combination, to assess their capacity for sulfur capture in sulfur laden oxidizing and reducing

atmospheres. Additionally, inert materials such as silica sand, as well as more traditional sorbents, such as dolomite and limestone, were tested to serve as reference data. The Phase I effort also explored the overall domestic availability of the best performing waste metal oxide sorbents, taking into account their geographic distributions, intrinsic value, etc. to provide the groundwork for a low cost, highly effective sulfur sorbent which can be quickly implemented on a commercial scale for such processes as IGCC and PFBC. Finally, in that all of the sorbent samples tested were of an identical, carefully selected particle size, the data collected serve as the basis for a proposed Phase II effort, which will further utilize the waste metal sorbents as a means of increasing the permeability of the dust collected on downstream particulate control devices, such as ceramic filters.

## BACKGROUND INFORMATION

Much of America's vast coal reserves will remain unusable until technology capable of the effective, economical removal of particulate and sulfur emissions becomes more highly developed. In recent years, ceramic filtration devices have shown that particulate removal levels well within the limits of New Source Performance Standards (NSPS) can be achieved at high process temperatures, thereby enhancing the overall performance and efficiency of processes such as Integrated Gasification Combined Cycle (IGCC) and Pressurized Fluidized Bed Combustion (PFBC). Unfortunately, removal of the high levels of sulfur indigenous to much of our Nation's coal reserves has been problematic, requiring exotic (and expensive) sorbents, substantial coal feed pretreatment, or a reduction in off-gas temperature to achieve acceptable sulfur emissions.

Many researchers are aware that metal oxide sorbents can be used to effectively reduce sulfur emissions in such processes. However, because of the high cost of most metal oxides, especially such materials as zinc titanate and zinc ferrite, economic studies have shown that for such materials to be cost effective they must be used and regenerated as much as several hundred times[1] before a return on investment is realized. Unfortunately, preliminary testing of such sorbents in a pelletized bed configuration, which lends itself to such a regenerative process, have shown that the strength of the pelletized metal sorbent significantly decreases in as few as five or six regenerative cycles. In view of this, it is apparent that a "once through", non-regenerable metal oxide sorbent can be a much more attractive solution from the standpoints of capacity, overall sulfur removal efficiency, and process economics, particularly if a low cost (or no cost) source of sorbent is readily available. Moreover, in combination with ceramic filtration technology, the use of such an external sorbent becomes even more practical in that the sorbent can be introduced well upstream of the candle filter, have sufficient residence time for sulfur removal to take place, and then be easily collected on the surface of the ceramic filter, along with the ash and other particulate. By properly classifying and sizing the waste metal oxide sorbent particles, the permeability of the dust accumulating on the filter candles can be readily increased, resulting in lower pressure differentials, better pulse cleaning efficiency, and less susceptibility to candle pore "blinding".

The Phase I SBIR effort reported herein showed that significant sulfur removal capacities can be obtained using classified, spent metal oxides. Such materials are generated in tremendous volume as a result of

metal processing, smelting, and refining operations, and are generally available for little if any cost. Among the spent metal oxides tested in Phase I which exhibited a strong affinity for sulfur capture in oxidizing and reducing atmospheres were the waste oxides of tin, zinc, and iron, some of which had significantly higher capacity than a mixture of dolomite and limestone.

Phase II testing will concentrate on these three promising candidate waste materials, to verify their sorbent capacity using thermogravimetric analysis (TGA) and to determine their additional capability as a high temperature filter aid, after classifying to a specific particle size distribution. Ultimately, when utilized as a "once-through" sorbent in combination with ceramic filtration technology, these spent metal oxides will provide sulfur removal and enhanced filter performance in a cost-effective manner.

## PROJECT DESCRIPTION

The Phase I research program involved the testing and assessing of the sulfur removal capacity of waste metal oxides, under controlled laboratory conditions, by exposing a prepared bed of each waste metal oxide to sulfur dioxide ($SO_2$) and hydrogen sulfide ($H_2S$), in separate trials. The testing was performed at the Research & Development Department of Industrial Filter & Pump Mfg. Co., Inc. The waste metal oxides tested in Phase I included:

A) Iron oxide dust from a Basic Oxygen Furnace (B.O.F.) application;

B) Zinc oxide dust from a Chicago area zinc smelting operation;

C) Zinc oxide dust from a 2nd Chicago area zinc smelting operation;

D) Tin oxide dust from a Chicago area tin refiner;

E) Zinc/iron/lead oxide mixture from another local smelter.

In addition to the testing of the above waste metal oxides, test trials were performed using:

F) Nitrogen carrier gas only, without any $SO_2$ (or $H_2S$) gas or test sample;

G) Nitrogen carrier gas and $SO_2$ (or $H_2S$) only, without a test sample;

H) Nitrogen carrier gas and $SO_2$ (or $H_2S$) with an inert (silica sand) test sample;

I) Nitrogen carrier gas and $SO_2$ (or $H_2S$) with a moderately inert (diatomaceous earth) test sample;

J) Nitrogen carrier gas and $SO_2$ (or $H_2S$) with a calcium laden waste material from a cement kiln process as a test sample;

K) Nitrogen carrier gas and $SO_2$ (or $H_2S$) with a calcium laden lime waste from a sugar refining operation as a test sample;

L) Nitrogen carrier gas and $SO_2$ (or $H_2S$) with a production grade dolomite/limestone combination as a test sample.

In each of the above test scenarios, the flowrate of nitrogen carrier gas used as a diluent to the $SO_2$ (or $H_2S$) was held constant at 83 ml./min. Likewise, the $SO_2$ or $H_2S$ used

in the testing was maintained at a constant flowrate of 38 ml./min. Test sample volumes were also held constant at 50 $cm^3$, and the test temperature was maintained at 70°F in all cases. By controlling the rate of gas flow through the closed system across the 50 $cm^3$ test sample bed in a downflow fashion, then bubbling the effluent through a 500 ml. volume of analyzed collection water, a depression in the pH of the collection water would occur when the test sample bed no longer removed sulfur from the sulfur laden gas stream. By maintaining a constant system pressure from test to test, and monitoring the elapsed time required to depress the pH of the collection water to a predetermined end point, the relative sulfur removing capacity of each material tested could be observed for the test conditions cited above.

The initial test apparatus, shown in Figure 1, was used but modified to eliminate the inert dust bed and its corresponding collection water beaker, since it was felt that equivalent flow through two material beds simultaneously at the low flowrate envisioned would be virtually impossible.

Initial test trials involved only nitrogen carrier gas, without a test sample bed, and were conducted to determine the effect which pure nitrogen might have on the pH of the collection water, if any. It should be pointed out that carefully analyzed tap water was selected in favor of either demineralized or distilled water for use in the collection beaker, as the pH of these latter materials was found to be altogether too sensitive to external influences (such as $CO_2$ and other gases in the atmosphere surrounding the collection beaker, which form carbonic acid that causes pH depression).

Following the initial tests, trials involving nitrogen carrier gas and either $SO_2$ or $H_2S$, again without a test sample bed, were conducted to determine the time delay (due to piping lengths and volumes) from the onset of the test until pH depression.

Both the effect on pH of the nitrogen carrier gas as well as the "time delay" associated with the internal volume of the test apparatus were used in the final data analysis.

All tests involving sample test beds were conducted in an identical fashion. Test samples were obtained from local metal processors, and were prepared by drying at 250°F for 4 hours in an air-circulated oven, after which time the weight of the sample stabilized, indicating the removal of any moisture present. The material then underwent particle size classification using a CE Tyler Sieve Products, Inc. portable sieve shaker. Each sample material was classified and the particle fraction passing through a 140 mesh (106 micron opening) screen which was retained on a 200 mesh (75 micron opening) screen was utilized for each test specimen. This particle size is representative of that which would be used to enhance filter cake porosity in the eventual and effective use of U. S. Patent #4,865,629, which is the focus of Phase II of this research effort. By using an identical particle size fraction for each sample tested, it was hoped that the bed permeability in each sample trial would be nearly equal at constant gas flowrate conditions; also, the total available surface area exposed to the sulfur laden gas would be similar from one test to the next. Just prior to each test, the sample material was again dried in an air circulated oven to insure no moisture was retained, after which time 50 $cm^3$ of the classified sample was extracted and weighed for test purposes.

A total of five test trials involving the aforementioned test samples were performed. In evaluating the results of each of the first three sets of trials, a great deal of inconsistency was observed and it was concluded that intermittent leakage within the test apparatus was the cause of the inconsistencies in the results. The test apparatus was modified with high pressure tubing and connectors, and a "leak check" procedure, involving the pressurizing and monitoring of the apparatus static pressure, was performed prior to the actual testing of each sample in the last two test series, to insure that the results were highly accurate.

Because of the above, only the results corresponding to trials #4 and #5 were deemed accurate and are discussed in this report, to eliminate confusion with earlier inconsistent results.

## RESULTS

### $SO_2$ Trials

In the tests which involved the capture of sulfur from an $SO_2$ laden gas stream at ambient temperature, the following findings were observed:

A) Sulfur dioxide is known to dissolve in water to create a weakly acidic solution of sulfurous acid, according to the reaction below:

$$H_2O + SO_2 \rightleftharpoons H_2SO_3$$

Sulfurous acid is unstable and cannot be isolated in the anhydrous condition; all of the sulfur dioxide formed as the acid decomposes is expelled from solution by boiling. Like other diprotic acids, sulfurous acid ionizes in two steps:

$$H_2SO_3 \rightleftharpoons H^+ + HSO_3^-$$
$$HSO_3^- \rightleftharpoons H^+ + SO_3^{2-}$$

The amount of ionization is slight in both stages, but it is much less in the secondary stage than in the primary. Specifically, the ionization constants at ambient conditions for each of the above equilibrium reactions are:

$K_i\ (H_2SO_3) = 1.2 \times 10^{-2}$ moles/liter
$K_i\ (HSO_3^-) = 6.2 \times 10^{-8}$ moles/liter

Hence, although sulfurous acid is by definition a weak acid, it will readily depress the pH of tap water. For this reason, in the tests involving $SO_2$, only pH was monitored as a means of evaluating the total sulfur removal capacity of each material tested. Based on preliminary tests, an end-point pH of 5.00 was chosen for the $SO_2$ test series.

B) Of the various materials tested using $SO_2$ gas, tin oxide appeared to have a significant potential for sulfur removal. The parameters and breakthrough curve for the tin oxide/$SO_2$ test are shown in Figure 2; for comparison,the dolomite/$SO_2$ test results are shown in Figure 3.

### $H_2S$ Trials

In the tests which involved the capture of sulfur from a gas stream containing $H_2S$ at ambient temperature, the following findings were observed:

A) Hydrogen sulfide, a diprotic acid, is known to ionize in water through two

steps, the first of which yields hydrogen and hydrosulfide ions, as shown below:

$$H_2S \rightleftharpoons H^+ + HS^-$$

The expression for the ionization constant for this primary ionization of $H_2S$ is:

$$\frac{[H^+][HS^-]}{[H_2S]} = K_{H2S} = 1.0 \times 10^{-7} \text{ moles/liter}$$

The hydrosulfide ion in turn ionizes and forms hydrogen and sulfide ions, according to the following reaction:

$$HS^- \rightleftharpoons H^+ + S^{2-}$$

The expression for the ionization constant for the hydrosulfide ion is:

$$\frac{[H^+][S^{2-}]}{[HS^-]} = K_{HS-} = 1.3 \times 10^{-13} \text{ moles/liter}$$

It was noted that $K_{HS-}$ is smaller than $K_{H2S}$ by almost $10^6$ times, which means that very little of the $HS^-$ formed by the ionization of $H_2S$ actually ionizes to give hydrogen ions and sulfide ions; thus the concentration of $H^+$ and $HS^-$ are practically equal in a pure aqueous solution of $H_2S$.

Because $H_2S$ is a weaker acid than $SO_2$ when dissolved in water, and because tap water (which was purposely selected in favor of distilled or demineralized water) was used in the collection beaker, the pH depression observed upon exhaustion of the sample bed in the $H_2S$ test series would not be nearly as notable as that observed in the $SO_2$ test series.

Due to the above observation, it was decided that a pH end point value of 6.50 (rather than 5.00) would be used in the $H_2S$ test series. Additionally, total suspended solids (TSS) and total sulfites would be monitored and periodically recorded in the $H_2S$ test series to serve as two other means of validating the data.

B) Of the materials tested in an $H_2S$ laden atmosphere, zinc oxide and zinc oxide/iron oxide mixtures appear to exhibit the highest affinity for sulfur. Figures 4 and 5 show the parameters and breakthrough curves for these tests; for comparison, the dolomite/$H_2S$ test results are shown in Figure 6.

C) It should be pointed out that while copper oxide has been used as a sorbent in flue gas and fuel gas applications with a great deal of success, waste copper oxide dust from copper smelting operations often contains significant amounts of arsenic. For the safety of the research personnel involved and because of the unlikelihood that such a hazardous waste material would ever be utilized for sulfur removal, waste copper oxide materials were not evaluated in the scope of this research.

**Waste Metal Oxides: Availability**

An additional task in the Phase I undertaking involved the compilation of information[2] related to the availability, geographical location, and processes which generate the various waste materials tested in this research effort. While such information for each material tested is covered in detail in the Phase I final report, only the three best

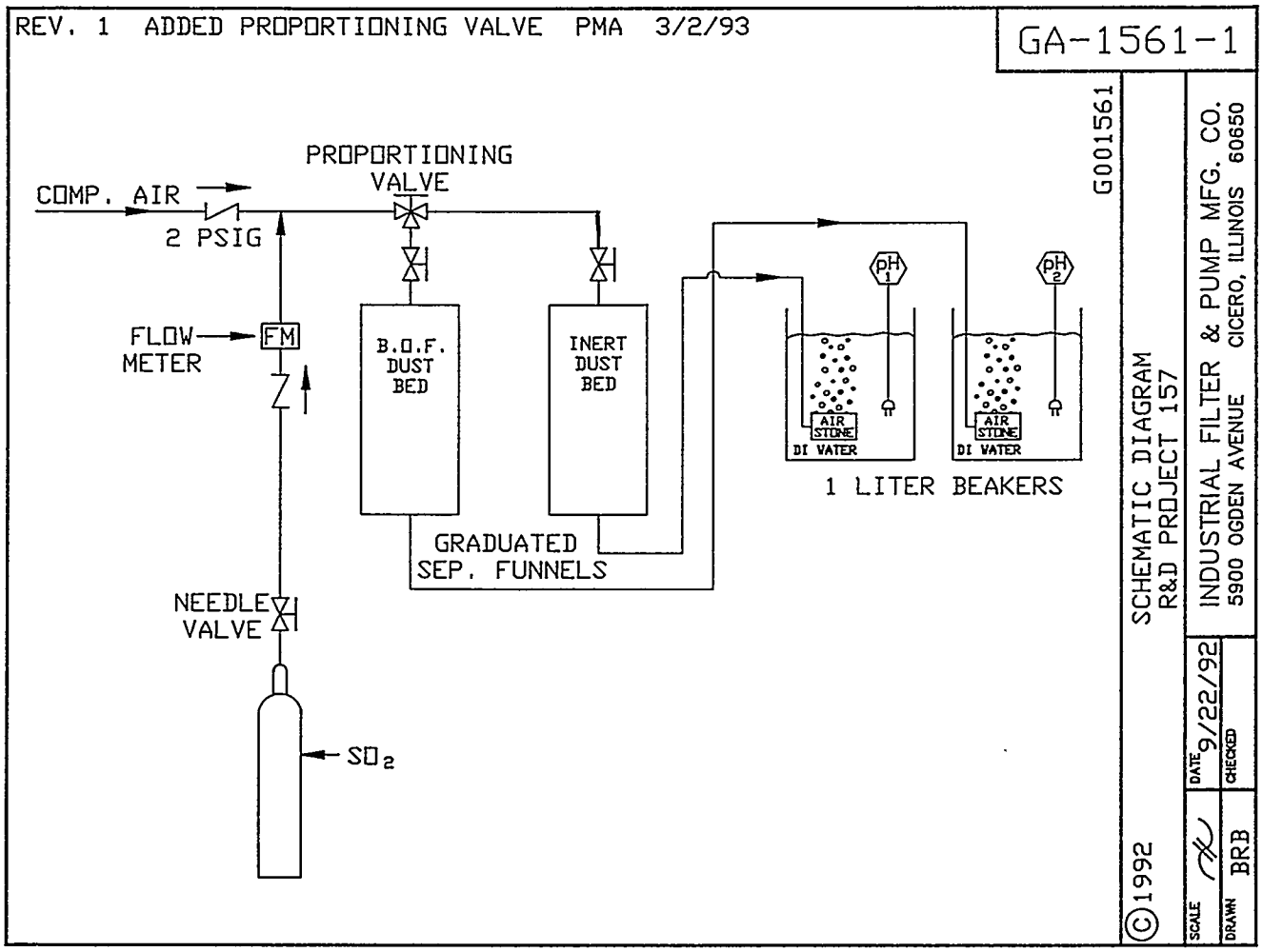


**Figure 1. Test Apparatus**

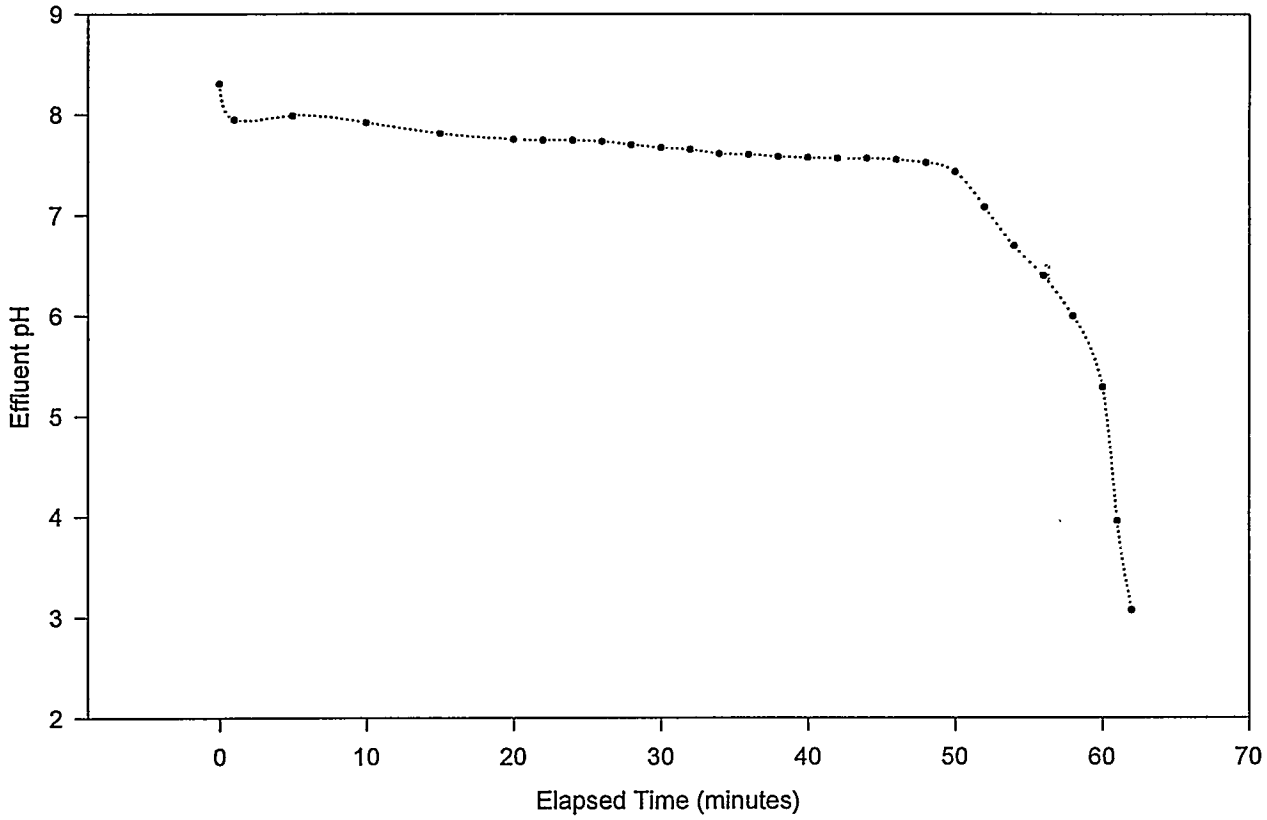


**Figure 2. $SO_2$ Adsorption Using Waste Tin Oxide Sorbent**

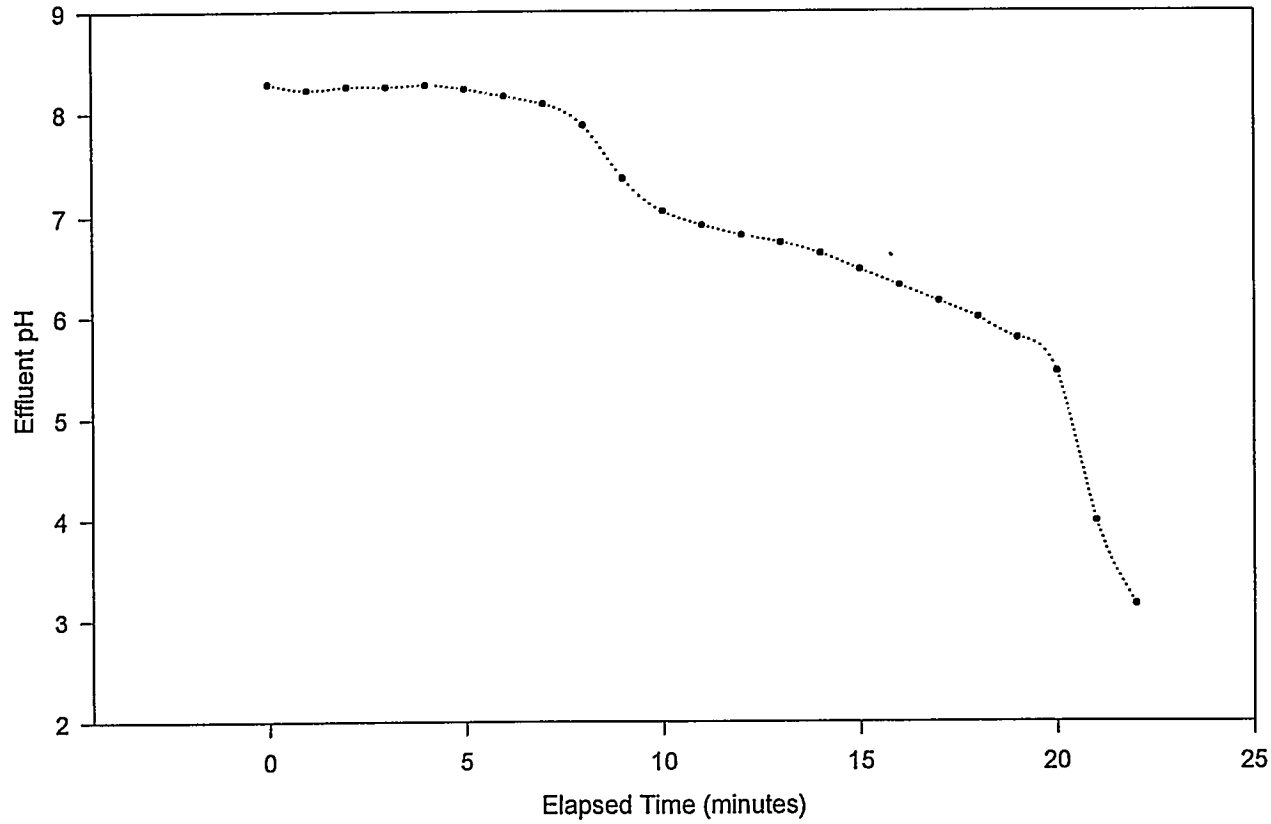


**Figure 3. $SO_2$ Adsorption Using Dolomite/Limestone Sorbent**

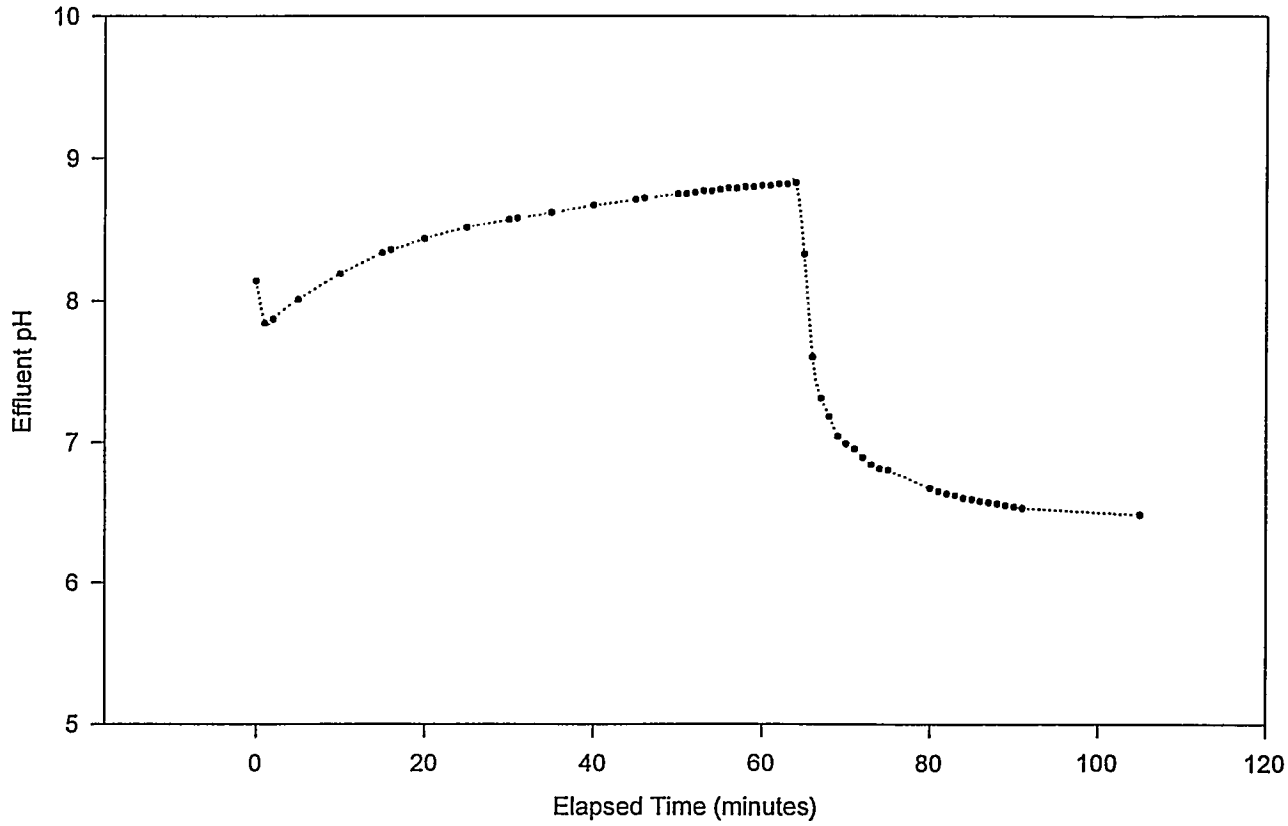


**Figure 4. $H_2S$ Adsorption Using Waste Zinc Oxide**

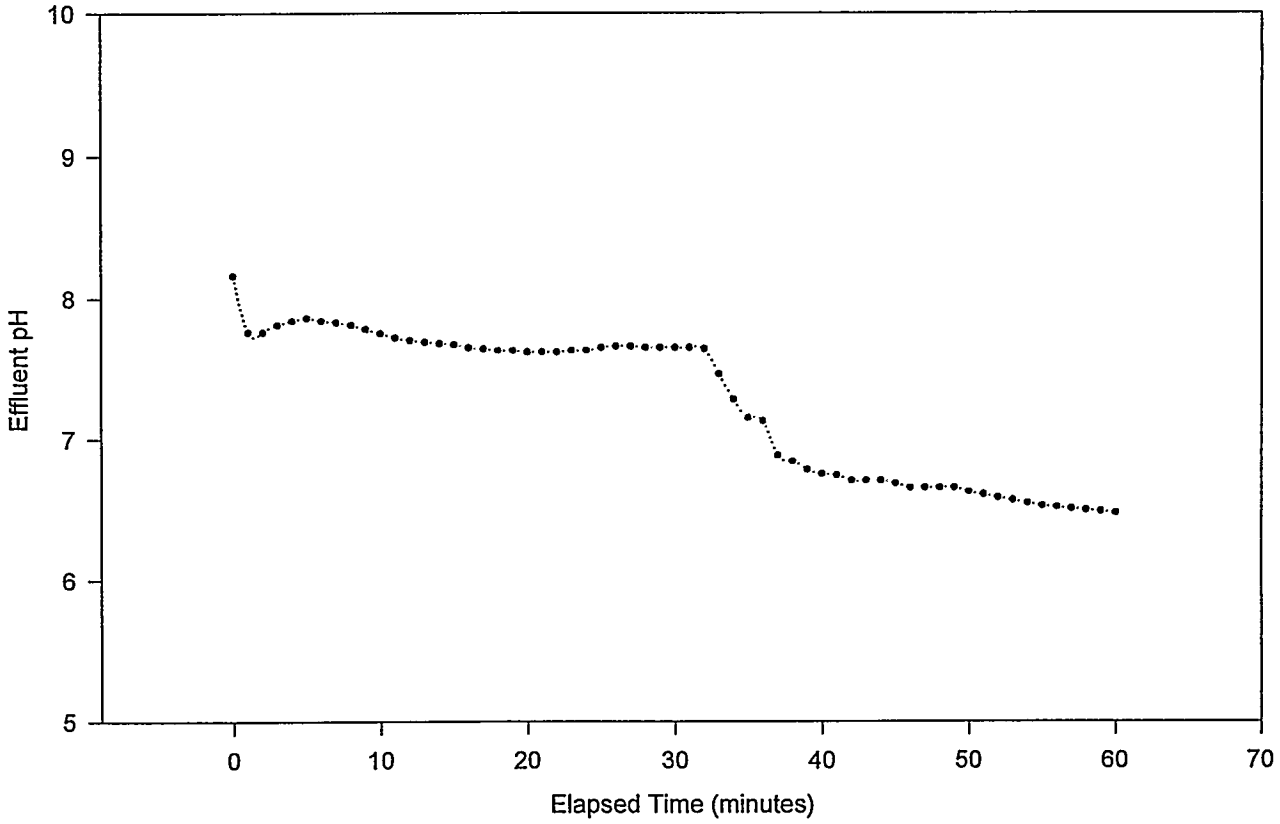


**Figure 5. $H_2S$ Adsorption Using Waste Iron Oxide/Zinc Oxide Sorbent Mixture**

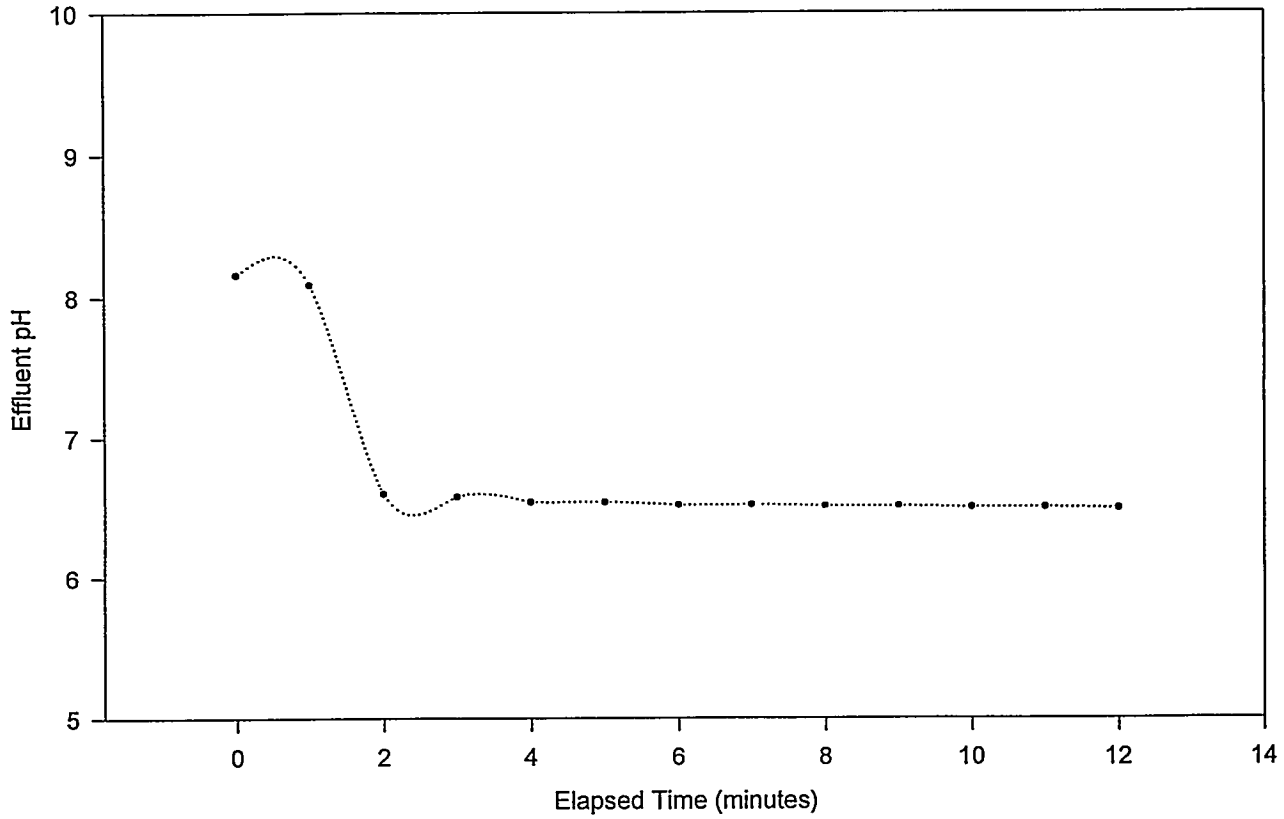


**Figure 6. $H_2S$ Adsorption Using Dolomite/Limestone Sorbent**

performing materials mentioned in the preceding section, namely the oxides of tin, zinc, and iron, appear to be the most promising; highlights of the availability and intrinsic values for these materials are given below.

**Tin**

Tin is one of the earliest metals known to humankind, and is commonly used as a protective coating or as an alloying metal with other metals. The major uses for tin are: cans and containers, 32%; electrical, 22%; construction, 10%; transportation, 11%; and other, 25%.

Waste tin oxides are readily available, since most new and old tin scrap is recycled and recovered. In 1991, an estimated 98% of the new tin scrap generated was recovered and an estimated 96% of the old tin scrap generated was recovered.

Detinning facilities are unique in the tin scrap industry, and nine plants are located across the country. Most tin scrap processing facilities are located close to the tin-using industries and to areas of high-density populations. Most are in the Midwest and Northeast. Table 1 gives statistical information on tin.

**Zinc**

Zinc is the fourth most widely used metal after iron, aluminum, and copper. More than 90% of the metal is used for galvanizing steel and for alloys; the remainder is used to produce dust, oxide, and various chemicals. In 1991, about 354,000 mt of secondary zinc valued at about $412 million, was recovered in basic forms--refined metal, alloys, dusts, and chemicals. Scrap, containing about 96,000 mt of zinc and valued at $62 million, was exported in 1991, whereas 38,000 mt of zinc in scrap, valued at $19 million, was imported.

Old zinc and brass scrap is collected at hundreds of domestic scrap yards, at more than 200 U. S. automobile and appliance shredding operations, and at numerous municipal collection centers. Tables 2 and 3 cite source and recovery data for zinc.

**Iron**

Iron is the most widely used of all the metals. Consumption of steel mill products and steel and iron castings in the United States amounts to about 100 Mmt/yr. Each year, over 50 Mmt of scrap iron and steel are recovered and recycled into new products. A major industry exists to collect such a vast amount of scrap and prepare it for recycling. Over 5,000 individual establishments, located throughout the country, purchase steel from individuals and businesses and prepare it to specification for consuming mills and foundries.

Steel production generates a number of wastes that contain ferrous or nonferrous metal residues. The USBM has developed a process to recover nickel and chromium from acid solutions used to pickle (clean) stainless steel, and currently is investigating means to remove and recycle zinc and lead from BOF dust, allowing the remaining iron to be recovered from a waste material that is normally disposed on land. A process to produce high-quality graphite from kish, a common steel plant waste, was recently developed by the USBM and is being introduced at a major steel plant. Also, investigations are underway to recover waste oils from steel plant sludge, allowing the contained iron to be recovered also.

**Table 1. Salient Tin Statistics, United States**
(Metric tons, tin content)

| | 1950 | 1960 | 1970 | 1980 | 1990 |
|---|---|---|---|---|---|
| Reported consumption | 104,464 | 80,560 | 73,829 | 53,362 | 44,363 |
| Secondary production | 33, 273 | 29,030 | 20,802 | 12,020 | 7,747 |
| Secondary production (as percent of consumption) | 32 | 36 | 28 | 21 | 17 |

**Table 2. Salient Zinc Statistics, United States**
(Thousand metric tons, zinc content)

| | 1950 | 1960 | 1970 | 1980 | 1990 |
|---|---|---|---|---|---|
| Estimated industrial consumption | 1,184 | 1,051 | 1,426 | 1,142 | 1,240 |
| Secondary production | 295 | 241 | 308 | 304 | 341 |
| Secondary production as percent of consumption | 25 | 23 | 22 | 27 | 28 |
| U. S. scrap trade | | | | | |
| Imports | 3 | 29 | 2 | 8 | 38 |
| Exports | 6 | 11 | 2 | 30 | 109 |

**Table 3. Principal Scrap Source Materials and Form of Recovery**
(Metric tons, zinc content)

| | 1950 | 1960 | 1970 | 1980 | 1990 | 1991 |
|---|---|---|---|---|---|---|
| Slab zinc | 60,166 | 61,698 | 68,450 | 29,396 | 95,708 | 124,078 |
| Brass and bronze | 146,413 | 97,452 | 148,438 | 172,040 | 148,247 | 127,009 |
| Oxide | 12,723 | 16,038 | 18,312 | 31,306 | 34,726 | 34,394 |
| Dust | 24,459 | 27,346 | 26,482 | 35,557 | 24,105 | 22,750 |
| Sulfate | 4,243 | ([1]) | 8,320 | 13,195 | 12,769 | 23,385 |
| Chloride | 11,431 | 10,881 | 9,622 | 10,944 | 7,436 | 5,311 |
| Other | 36,335 | 27,733 | 28,390 | 11,925 | 18,409 | 16,772 |
| **TOTAL** | 295,770 | 241,148 | 308,014 | 304,363 | 341,400 | 353,699 |

[1]Included in other.

**Waste Metals Oxides: Costs**

As a result of the preceding discussions on tin, zinc, and iron oxide, it becomes apparent that extremely large quantities of all three materials are and will continue to be readily available in our Nation. In many large metal processing plants, particle size fractions similar to the range tested in the Phase I effort are immediately available. In instances where such classified particles are not available, the use of "off-the-shelf" bulk handling, particle size reduction, and classification equipment can be easily used to achieve the desired particle size fraction to optimize sorbent capacity and filtration performance.

In view of the availability of all three materials, one further remaining aspect from an economic standpoint (assuming handling costs, permits, and particle size reduction and classification are similar amongst all three materials) is the intrinsic value of each material.

As of April, 1995, the intrinsic value of each of the three base metal materials is as follows:

| | |
|---|---|
| Tin (composite) | $3.94/lb. |
| Zinc (high grade) | $.54/lb. |
| Iron (steel) | $.07/lb. |

The above prices, it should be emphasized, are commodity prices for the base metals of each of the candidate waste oxides tested, and do not represent the cost of the corresponding waste metal oxides, which are much less. (In the case of iron oxide dust from BOF processing, the material is essentially free of charge, since on-site storage costs will often exceed the value of the dust). The prices do, however, provide an idea of the value of each material after it has been recycled and recovered for sale as pure metal, and are indicative of the relative value of each of the three metal oxides tested which showed significant affinity for sulfur.

By contrast, pelletized zinc ferrite or zinc titanate is significantly higher in cost. Even the most novel, fluidized zinc titanate formulations, such as "ZT-4", were reported to be $7.91/lb., as of June, 1994.[3]

Given their high affinity for sulfur compared to calcium based sorbents, overall availability, and low cost in relation to other metal oxide sorbents, the select use of waste metal oxides appears to be a most effective means of reducing sulfur in coal utilization applications.

**FUTURE WORK**

Phase I results showed that waste tin oxide appears to have a very high affinity for sulfur removal in a gas stream containing $SO_2$ gas at ambient temperature. Similarly, waste zinc oxide, as well as a mixture of zinc oxide and iron oxide wastes, have a high affinity for the removal of sulfur in a gas stream containing $H_2S$ gas at ambient temperature.

The technical objectives of future work in this area have been proposed as a Phase II SBIR effort and include:

1) A focus on the development, to commercialization, of several waste metal oxide materials which, with minimal preparation, can be used as effective sorbents for sulfur emissions control in oxidizing and reducing atmospheres, such as those encountered in PFBC and IGCC processes;

2) Further evaluation of the effect by which the use of classified waste metal oxide sorbent particles, when introduced as entrained particles into simulated ambient and high temperature gas streams containing sulfur and particulate, will serve to act as filter aids by enhancing dust cake permeability, as described in U. S. Patent No. 4,865,629 awarded to Industrial Filter & Pump Mfg. Co.;

3) Following the Phase II test efforts, recommendations will be made for the preparation of and prescribed use of these waste metal oxides for immediate commercial deployment in PFBC and IGCC processes.

As mentioned above, the goal of this project is to combine sorbent utilization with ceramic filter technology. U. S. Patent No. 4,865,629, "Control of Particle Size Distribution in Gas Filtration", assigned to Industrial Filter & Pump Mfg. Co., makes specific use of this concept. The invention relates in general to the filtration of hot gases, but more specifically to a method and apparatus for the efficient filtering of hot gases which are contaminated with a high fraction of fine particulates (such as a combustor or gasifier stream) after several stages of cyclones.

Since a waste source is used for the metal oxide sorbent, as outlined earlier, the cost effectiveness of the sorbent/filter aid concept is very attractive. By utilizing the metal oxide materials directly from the waste source, processing of the material will only include particle size classification (sieve-screening) for application of the metal oxide sorbent as a filter aid. Packaging and transportation of the metal oxide sorbent from its source (e.g., steel mill) to the utility site would be minimal, if local sources were sought.

In both the private and governmental sectors, waste metal oxide usage, as both a sorbent and high temperature filter aid, has immediate commercial application in any facility where sulfur emission is a concern. Utilities, for example, will benefit from compliance with regulations on emissions, and process performance and efficiency will increase due to the filter aid capability of the sorbent, when injected into the gas stream ahead of a ceramic filter.

Both the private sector and Federal Government will benefit from this project, in that our Nation's prevailing high sulfur content coal reserves will be utilized more fully, in a cost effective manner. Less reliance on other types and sources of our fossil fuels, more effective use of our own resources, and potential for exporting of these resources and technology all translate into increased jobs, productivity, and a cleaner environment for our country.

**REFERENCES**

1) Robin, Allen *"Integration and Testing of Hot Desulfurization and Entrained Flow Gasification for Power Generation Systems"*, U.S.D.O.E. Cooperative Agreement DE-FC21-87MC23277; excerpted from the "Proceedings of the Twelfth Annual Gasification and Gas Stream Clean-Up Systems Contractors Review Meeting", Morgantown, WV DOE/METC - 92/6128, Vol. 1, pg. 95.

2) U. S. Department of Interior Bureau of Mines Annual Reports for Tin, Zinc, and Iron (1992).

3) Gupta, R. P. and Gangwal, S. K. *"Fluidized-Bed Sorbents"*, (D.O.E. Contract No. DE-AC21- 88MC25006) excerpted from the "Proceedings of the Coal-Fired Power Systems 94 -Advances in IGCC and PFBC Review Meeting", Morgantown, WV. DOE/METC - 94/1008 Vol. 2, pg. 646.

# PB.9a Liming Efficacy and Transport in Soil of a Dry PFBC By-Product

## CONTRACT INFORMATION

| | |
|---|---|
| **Contract No.** | DE-FC21-91MC28060 |
| **Contractor** | Dravo Lime Company<br>Research Center<br>3600 Neville Road<br>Pittsburgh, PA 15225 |
| **Other Funding Sources** | Ohio Coal Development Office, CDO/D-89-35<br>Electric Power Research Institute, RP2796-02<br>American Electric Power Company, C-8276<br>Ohio Edison Company, EPRI collaborator<br>Dravo Lime Company, RF768342 |
| **Principal Investigator** | Warren A. Dick |
| **METC Project Manager** | Scott Renninger |
| **Period of Performance** | December 1, 1991 to December 31, 1995 |

## ABSTRACT

The by-products of pressurized fluidized-bed combustion (PFBC) systems are mixtures of coal ash, anhydrite ($CaSO_4$), and unspent alkaline sorbent. Because PFBC by-products are alkaline and contain large concentrations of readily soluble bases (Ca and in some cases Mg) and other essential plant nutrients such as S and K, they have potential use as soil amendments, especially in acidic soils. PFBC by-products (particularly those with large Mg contents) may cause excessively high soluble salt concentrations when applied to soil. This could be detrimental to plant growth and might also impact the release of trace elements from the coal ash component of the by-product. In field experiments on three acidic soils, the liming effectiveness of a PFBC by-product, its effects on corn and alfalfa growth, and its impacts on crop, soil, and water quality were investigated. The PFBC by-product was applied at rates from 0 to 2 times the liming requirement of the three soils (0 to 70 Mg $ha^{-1}$), and incorporated to a depth of 10 cm. Amendment with PFBC immediately increased surface (0-10 cm) soil pH (up to 7) and extractable concentrations of Ca, Mg, S, and B. Soluble Al, Mn, and Fe concentrations in the surface soil were decreased. Within 1 year of application, pH began to increase below 10 cm, and Ca, Mg, and S concentrations decreased in the surface and had leached to a depth of 60 cm. Within 2 years, increased Ca, Mg, and S were measured at depths up to 100 cm. With the exception of a small, short-lived increase in soil B, PFBC

application did not cause measurable changes in soil extractable concentrations of trace elements. Surface runoff water concentrations of Ca, Mg, and S were increased in the first year after application, however, there were no effects on trace element concentrations. Alfalfa yield was increased by PFBC amendment, but corn grain yield was not affected. Alfalfa and corn leaf tissue concentrations of Ca, Mg, and S were increased while Al, Fe, and Mn were decreased by FGD, with no evidence of any plant toxicity. Application of PFBC up to two times the lime requirement of acid soils improved production of acid-sensitive crops with no detrimental effects on soil or water quality.

# PB.9b Characterization and Laboratory Weathering Studies

## CONTRACT INFORMATION

| | |
|---|---|
| **Cooperative Agreement No.** | DE-FC21-91MC28060 |
| **Contractor** | Dravo Lime Company<br>3600 One Oliver Plaza<br>Pittsburgh, PA 15222<br>(412) 566-6000 |
| **Contract Project Manager** | Joel H. Beeghly |
| **Principal Investigator** | Dr. Warren A. Dick<br>Ohio State University<br>Department of Natural Resources<br>Wooster, Ohio |
| **METC Project Manager** | Scott Renninger |
| **Period of Performance** | December 1990 to July 1996 |
| **Title of Poster Paper** | Characterization and Laboratory Weathering Studies of PFBC By-Products |
| **Authors** | R. K. Fowler, U. I. Soto, and J. M. Bigham<br>Ohio State University |

## ABSTRACT

Characterization studies of PFBC by-products were initiated to provide baseline information need to predict the behavior and suitability of PFBC by-products for beneficial uses. The chemical composition of the by-products was dominated by Ca, Mg, S, Fe, Al, and Si. All samples were highly alkaline with paste pH values ranging from 9.9 to 12.3. All of the PFBC materials met the criteria for pollutant ceiling concentrations for land application of sewage sludge for Cd, Cr, Cu, Pb, Mo, Ni, Se, and Zn. Arsenic exceeded the concentration ceiling level in only one sample. XRD results showed that the cyclone ashes consisted primarily of dolomite, anhydrite, periclase, and calcite. PFBC bed ashes were similar in composition but contained less unspent sorbent and more anhydrite and periclase. The artificial weathering study examined water soluble ions and reaction products of two mine spoils and one cyclone ash mixed at four rates. The spoils were mixed with PFBC by-products to yield mixtures containing 0, 10, 20, and 40 weight percent by-product. Leachate composition was mostly a function of rate of application and equilibration time. In general, the addition of PFBC by-product increased pH, conductivity, and the concentrations of Ca, K, Mg, Mo,

Na, S, and Sr. The concentrations of Al, Fe, and Mn decreased. Six metals (Ag, As, Ba, Cd, Cr, and Pb) regulated by the Resource Conservation Recovery Act were below concentration levels defined for drinking water standards (Hg and Se not available). All application rates of the PFBC by-product increased the solution pH significantly. A pH of 7.8 or greater was attained in all PFBC-spoil mixtures after 132 days. Changes in solid phase composition were independent of the spoil. The final reaction products were more directly influenced by the characteristics of the PFBC by-product. There was no significant weathering of the spoil component in any of the mixtures over the 132-day period. Ca weathering reactions resulted in the precipitation of gypsum but with no further conversion of the gypsum to ettringite detected after 132 days.

# PB.10 Disposal of Fluidized-Bed Combustion Ash in an Underground Mine to Control Acid Mine Drainage and Subsidence

## CONTRACT INFORMATION

| | |
|---|---|
| **Contract Number** | DE-FC21-94MC29244 |
| **Contractor** | West Virginia University<br>National Research Center for Coal and Energy<br>P.O. Box 6064, Suite 202<br>Morgantown, WV 26506-6064<br>(304) 293-2867 ext 447<br>(304) 293-7822 |
| **Other Funding Sources** | West Virginia University and Anker Energy Corporation |
| **Contractor Project Manager** | Paul F. Ziemkiewicz, Ph.D. and D. Courtney Black |
| **Principal Investigator** | Paul F. Ziemkiewicz, Ph.D.; William J. Head, Ph.D.; Donald D. Gray, Ph.D.; Hema J. Siriwardane, Ph.D.; William A. Sack, Ph.D. |
| **METC Project Manager** | Scott Renninger |
| **Period of Performance** | Phase I February 16, 1994, to August 15, 1995 |

## ABSTRACT

This project will evaluate the technical, economic, and environmental feasibility of filling abandoned underground mine voids with alkaline, advanced coal combustion wastes (fluidized-bed combustion (FBC) ash). Both pneumatic and hydraulic injection methods will be investigated. Success will be measured in terms of technical feasibility of the approach (i.e., percent void filling), cost, environmental benefits (acid mine drainage and subsidence control) and environmental impacts (noxious ion release).

Phase I of the project is scheduled for 18 months starting in February 1994 and is concerned with the development of the grout and a series of predictive models. These models will be verified through the field phases and will allow the results to be packaged in such a way that the technology can be easily adapted to different site conditions. Phase I will also

redesign a pneumatic ejector, that was developed to stow limestone, to efficiently stow FBC ash. Bench-scale testing will verify the redesign in Phase I.

The 12-month Phase II is a small-scale field test at Anker Energy's Fairfax mine. An inactive panel will be used to evaluate flow, strength, and pressure requirements for hydraulic (grout) injection. The Phase II pneumatic injection activities will take place at an Anker Energy mine in Preston County, West Virginia. Air flow requirements, pressure requirements, stowing rate (tons per hour), and stowing efficiency (distance blown) will be determined.

Phase III is to take 26 months and will be a full-scale test at Anker's 11-acre Long Ridge mine site. The mine will be filled using both pneumatic and hydraulic injection methods.

It is expected that the FBC ash will replace what is now an acid mine pool with an alkaline solid so that the groundwater will tend to flow around rather than through the previously mined areas. The project will demonstrate whether FBC ash can be successfully disposed of in underground mines. Additionally, the project is directed towards showing that such disposal can lead to the reduction or elimination of environmental problems associated with underground mining such as acid mine drainage and subsidence.

## PB.11 Use of FBC Ash to Stabilize Dairy Barn Feedlots, Minimize Nutrient Pollution, and Develop New Utilization Outlets

### CONTRACT INFORMATION

| | |
|---|---|
| **Contract Number** | DE-AI21-94MC31205 |
| **Contractor** | USDA, Agr. Res. Ser.<br>Bldg. 004, BARC-W<br>Beltsville, MD 20705<br>301-504-5650 (telephone)<br>301-504-5062 (telefax) |
| **Other Funding Sources** | Ahlstrom Ash Development Corp. |
| **Contractor Project Manager** | Ronald F. Korcak |
| **Principle Investigators** | Ronald F. Korcak<br>William L. Stout |
| **METC Project Manager** | Jason Lewis |
| **Period of Performance** | Oct 01, 1994 to Sep 30, 1995 |

**Schedule and Milestones**

**FY95 Program Schedule**

| | S | O | N | D | J | F | M | A | M | J | J | A |
|---|---|---|---|---|---|---|---|---|---|---|---|---|
| Site Installation | | | | | | | | ——— | | | | |
| Testing | | | | | | | | | ——— | | | |
| Analysis | | | | | | | | | | ——— | | |

# Use of FBC Ash to Stabilize Dairy Barn Feedlots, Minimize Nutrient Pollution, and Develop New Utilization Outlets

## OBJECTIVES

### Objective #1-Dairy Feedlot Stabilization Demonstration

A dairy feedlot near Harrisburg, Pennsylvania will be selected for study using the following criteria: Site characteristics including slope and soil type, and proximity to a small stream in a defined watershed.

The selected feedlot will be split in half with half stabilized with FBC and the other half un-stabilized. Ten suction lysimeters or shallow sampling wells will be installed to a depth of 1 meter in each half of the feedlot. Lysimeters or wells will be sampled biweekly or after major rain events to determine water quality (nitrogen and phosphorous content) beneath the stabilized and un-stabilized areas.

Sampling will continue for one year. At the termination of the study the remainder of the feedlot will be stabilized.

### Objective #2 - Determination of nitrogen and phosphorous leaching from feces and urine through stabilized and un-stabilized feedlot cores.

Six large (0.6m diameter by 0.6m depth) undisturbed cores will be taken each from stabilized and un-stabilized feedlot areas using 0.6m diameter steel pipe (total of 12). The cores will be fitted with a bottom cap plus a collection bottle and reinstalled at an adjacent area.

Two cores each from the stabilized and un-stabilized areas will be treated with cow urine, cow feces or left untreated.

Lysimeters cores will be sampled weekly for water quality (nitrogen, phosphorous, and metals). At the termination of the experiment, one year, density and penetration measurements will be taken and chemical analyses made for nitrogen and phosphorous.

### Objective #3- Co-utilization of materials to reduce nutrient pollution potential

Samples of FBC ash, manure and straw (or bedding) will be sent to the USDA/ARS facility in Beltsville, MD in order to perform bench scale experiments under controlled conditions. Mixtures and combinations of FBC ash, manure, or straw (or bedding) will be monitored with simultaneous measurements of ammonia volatilization. After blending, the nitrogen and phosphorous content of the mixtures will be fractionated to examine the fate of these nutrients. The effect of time after blending on the fate of nitrogen and phosphorous will be examined. Moisture content and handling properties of the final materials will be evaluated.

Enhanced calcium movement into soils will be examined using PVC columns filled with soil from Beltsville. Soil columns will be surface amended with FBC ash and manure blends at ratios of 0:1, 1:1 and 1:0. Simulated rain event leaching will occur biweekly for 6 months. Leachate will be analyzed for calcium and phosphorous content. At termination, the cores will be sliced to quantify movement of calcium within the core.

### Objective #4 - Co-utilization of materials to enhance value

Bulk samples of FBC ash, manure and straw (or bedding) will be sent to the USDA/ARS facility in Beltsville, MD in order to perform small field trails with blackberries and/or sea buckthorn. Blends of FBC ash plus manure and FBC ash plus manure and straw in a 1:1:1 ratio will be compared to FBC ash alone as a soil

surface mulch.

Blackberries and/or sea buckthorn plants (species and cultivars used will depend upon availability) will be row planted and trickle irrigated. Treatment will consist of one of the 1:1:1 ratio mixes, FBC alone, or bare soil. Each treatment will be replicated four times with a minimum of 6 plants per treated row. The plots will be evaluated during the first year for plant growth, weed control via the surface mulch and nutritional status of the plants (essential elements plus metals).

## BACKGROUND INFORMATION

Using technology developed by the USDA/ARS and USDOE, the Ahlstrom Ash Development Corporation has been successfully using fluidized bed combustion (FBC) ash from the Black River Co-Gen plant in Watertown, NY as an agricultural soil amendment. This permitted land application was based primarily on the jointly derived handbook on FBC utilization (Stout, et al., 1988). During times of the year when ash cannot be spread on crop land, Ahlstrom has been using the ash as a low strength concrete to stabilize dairy barn feedlots. The stabilized feedlots provide a place for cattle to escape from muddy conditions in the spring and fall. Farmer acceptance of these stabilized feedlots is very positive. However, there is a need to provide data on the leachates from and through these barnyard pads.

## PROJECT DESCRIPTION

There are two obvious benefits to using the FBC ash to stabilize feedlots. First, ash can be used at the time of the year when fields are too wet for land spreading or there are standing crops in the fields. Second, animals on a solid surface are not subject to possible health problems caused by standing in mud and the animals are more feed efficient.

However, questions remain as to the extent of other possible benefits or detriments of the ash stabilized dairy barn feedlots.

The extent to which the ash stabilized lots keep nitrate nitrogen and water soluble phosphorous from dairy manure from reaching the ground water beneath the feedlots is unknown. Nitrogen and phosphorous in the manure retained on the feedlot surface would be available for application to cropland. Also, nitrogen would be subject to volatilization into the atmosphere. In either case, less nitrogen and phosphorous would escape to ground waters.

Soil erosion from stabilized dairy barn feedlots is anticipated to be less than that from un-stabilized feedlots. Assuming manure is removed from the feedlots on a regular basis, reduced erosion would result in less nitrogen, phosphorus, fecal coliforms, and sediment being transported to surface waters.

A possible detriment of the use of FBC ash to stabilize dairy barn feedlots would be the leaching of potentially toxic materials from the stabilized feedlots. Preliminary laboratory results indicate that leachate quality from stabilized FBC ash is not likely to be a problem under field conditions. However, field test confirmation would be desirable and would enhance the acceptance of FBC ash by regulatory agencies and the general public.

There exists some practices that could be easily adapted by the farmer, using ash stabilized feedlots, that could diminish potential nitrogen and phosphorous pollution potential and enhance the value of the field applied manure. First, spreading of straw or spent bedding material over the pad may act as an absorber of soluble nitrogen originating from the manure. The manure/straw (or bedding) mix can then be field spread. Second, intentional scrapping of the FBC pad during manure removal should result in a manure-ash mix (or manure-ash-straw mix) that will be field applied. This mix may reduce the risk of nitrogen and phosphorous pollution. The

later by reaction with the high calcium ash material. Additionally, preliminary data exist that show enhanced movement of calcium through the soil profile when soluble organic materials are present.

The above practices can be simulated on a laboratory scale. This needs to be performed prior to field demonstration.

In the future, it may be necessary to increase the distribution distance of farm derived manures as well as industrial by-products such as FBC ash. Usually, the economics of distribution is the limiting factor. One way to overcome this limitation is to enhance the value of a by-product by co-utilization of two or more by-products. The dairy barn feedlot study area would be an ideal situation to explore the potential for co-utilization of materials. Co-blending of materials as a soil amendment or pelletizing blended materials could create a product which could be distributed economically.

## RESULTS (PROGRESS)

There was a delay in initiating the project tests. This was due to the desire to wait for the Fort Drum power plant to convert to their normal coal source. This was accomplished in May of 1995. There was also a delay in obtaining permission to develop a barnyard ash pad in New York State. It was decided to move the ash pad site to Pennsylvania. Additionally, ash was delivered to Beltsville, Maryland for the crop field trials and column studies in late May of 1995.

To date the following have been performed at the Pennsylvania site under objective #1.

In April, 1995 a 6 by 15 m (20 by 50 feet) ash pad was constructed on a farm barnyard near Harrisburg, PA. The site is located on an intensively monitored agricultural watershed monitored by the USDA/ARS Pasture Systems and Watershed Management Research Laboratory. The site was chosen because of wet conditions during most of the year. Before the ash pad was constructed, the loose soil and manure was removed to a depth of 0.3 m (1 foot). Since the ash was hauled dry from Watertown, NY, the ash had to be conditioned on site. On site conditioning was accomplished by using a transit concrete mixer. The hydrated ash was poured on to the site, leveled out with a backhoe, and backfilled. The transit concrete mixer fully hydrated the ash and the result was a concrete-like product.

The following day, five suction lysimeters were installed in the ash pad by drilling to a depth just below the bottom of the pad and installing the sampling line to beyond the edge of the site. Five suction lysimeters were installed in the un-stabilized section of the barnyard and the site was ready for sampling.

In reference to objective #2, on the same day that the ash pad was constructed, six cores were constructed by pouring the conditioned ash into 0.6 m (2 foot) diameter by 0.6 m deep well casing welded to bottoms that had been drilled and fitted for sample collection. Next, six undisturbed cores of the un-stabilized barnyard were taken by driving 0.6 m diameter well casing into that portion of the barnyard with a pile driver and removing the undisturbed core. After the undisturbed soil cores were welded to the bottoms, both sets of cores were installed into the soil and were ready for treating and sampling.

The column study will consist of 16 columns manufactured from 10 cm diameter PVC pipe (schedule 40) as part of objective #3.. Each of four treatments will be replicated four times: soil alone, soil surface amended with FBC residue, soil surface amended with FBC residue plus dairy manure (1:1), and soil surface amended with FBC residue plus dairy manure plus bedding (1:1:1). To date the test plants, blackberry, have been planted at Beltsville. This planting site will be subdivided into replicated plot areas that will be treated with material combinations similar to the column amendments.

Currently, we are awaiting analysis of the dairy manure generated at the Beltsville farm site in order to determine the best ash/manure mixture to incorporate in the field and column studies.

## FUTURE WORK

If barnyard stabilization is successful, there may be other agricultural applications for FBC ash. One such application would be to provide a pavement for the bottoms of trench silos. This application would have to stand the additional weight of farm equipment and the acidity of silage.

Results from this project may provide preliminary data on the benefits derived from co-utilization of materials which could have a significant impact on the economics of FBC residue and manure utilization.

## REFERENCES

Stout, W. L., J. L. Hern, R. F. Korcak, and C. W. Carlson. 1988. Manual for applying fluidized bed combustion residue to agricultural lands, U. S. Department of Agriculture, Agricultural Research Service, ARS-74, 15 pp., Washington, DC.

# PB.12 Hot Coal Gas Desulfurization With Manganese-Based Sorbents

## CONTRACT INFORMATION

| | |
|---|---|
| **Contract Number** | DE-AC21-92MC29246 |
| **Contractor** | University of Minnesota<br>500 Pillsbury Dr., S.E.<br>Minneapolis, MN 55455-0220<br>(612) 625-6354 |
| **Contract Project Manager** | Malcolm T. Hepworth |
| **Principal Investigators** | Malcolm T. Hepworth (P.I.) & Rachid Ben-Slimane (Post Doctoral Fellow) |
| **METC Project Manager** | Venkat K. Venkataraman |
| **Period of Performance** | 9/18/92 - 9/17/94 |

## ABSTRACT

The primary major deposit of manganese in the United States which can be readily mined by an in situ process is located in the Emily district of Minnesota. The U. S. Bureau of Mines Research Centers at both the Twin Cities and Salt Lake City have developed a process for extracting and refining manganese in the form of a high-purity carbonate product. This product has been formulated into pellets by a multi-step process of drying, calcination, and induration to produce relatively high-strength formulations which are capable of being used for hot fuel gas desulfurization. These pellets, which have been developed at the University of Minnesota under joint sponsorship of the U. S. Department of Energy and the U. S. Bureau of Mines, appear superior to other, more expensive, formulations of zinc titanate and zinc ferrite which have previously been studied for multi-cycle loading (desulfurization) and regeneration (evolution of high-strength $SO_2$ and restoration of pellet reactivity). Although these other formulations have been under development for the past twelve years, their prices still exceed $7 per pound. If manganese pellets perform as predicted in fixed bed testing, and if a significant number of utilities which burn high-sulfur coals incorporate combined-cycle gasification with hot coal gas desulfurization as a viable means of increasing conversion efficiencies, then the potential market for manganese pellets may be as high as 200,000 tons per year at a price not less than $3 per pound. This paper discusses the role of manganese pellets in the desulfurization process with respect to the integrated gasification combined-cycle (IGCC) for power generation.

## OBJECTIVES

The objective of this study is to develop manganese-based sorbent pellets for the effective desulfurization of coal-derived fuel gases at high temperature (700-1200 °C). A number of formulations are prepared and screened first by testing in a thermogravimetric apparatus (TGA) in which individual pellets are weighed in mixtures of simulated fuel gases at atmospheric pressure and high temperatures, and then in a bench-scale fixed bed reactor. Sorbent screening criteria include measurement of sorbent (fresh, used, and regenerated) crush strength, chemical reactivity by thermogravimetric analysis, surface area, porosity, etc... The superior formulation is tested for long-term durability and chemical reactivity in the TGA apparatus and the bench-scale unit.

## BACKGROUND INFORMATION

The rationale for desulfurizing coal-derived fuel gases at high temperature is a result of concerns within the U. S. Department of Energy to burn coal to produce electrical power more efficiently and also to meet government regulations for sulfur emissions which have become progressively more stringent. Conventional technology of power generation is inherently inefficient and consists of reacting coal in a burner system which exchanges heat to a boiler to generate steam (essentially the Rankine Cycle). This steam then passes through a turbine to drive a generator and produce electricity.

This conventional process for power generation is shown in Figure 1. The efficiency for conversion of heat into useful electrical power ranges from 30 to 35%. In addition, a portion of this power (up to 3%) is used internally in the plant to operate environmental cleanup systems.

The sulfur in the coal is released in the form of sulfur dioxide ($SO_2$) in the flue gas. The removal of $SO_2$ from the flue gas prior to discharge into the atmosphere is essential to prevent air pollution. Conventional processes for sulfur removal are well established and require the coal gas be cooled to less than 100 °C in order to contact it with scrubbing reagents. The loss of thermal efficiency in the cooling process lowers the energy available for electrical conversion compared with the higher efficiencies which would be obtained if the coal gas were desulfurized while hot. Also, the primary scrubbing technique for sulfur removal entails the generation of gypsum which must be disposed of in increasingly expensive landfill space. For example, about one ton of limestone is required to make the lime needed to scrub the stack gas from each five tons of coal burned. A large 10,000-ton per day power plant requires 2,000 tons per day of limestone. The lime wastes from the scrubber are in the form of a watery sludge and are stored in holding ponds which are environmentally undesirable. Furthermore, although the wet limestone process and other flue gas cleaning systems help the utilities comply with new, more stringent environmental requirements, they lower plant operating efficiency and reliability, while increasing both capital and operating costs. Such limitations have been the main driving force behind technological innovations which aim at improving both the efficiency and environmental performance of power generation.

Figure 2 is a schematic diagram of an Ideal Integrated Gasification Combined Cycle (IGCC) system (the Brayton Cycle). The addition of a sorbent operating on a coal gasifier is shown in this diagram. This hot gas cleanup technique is needed to remove sulfur

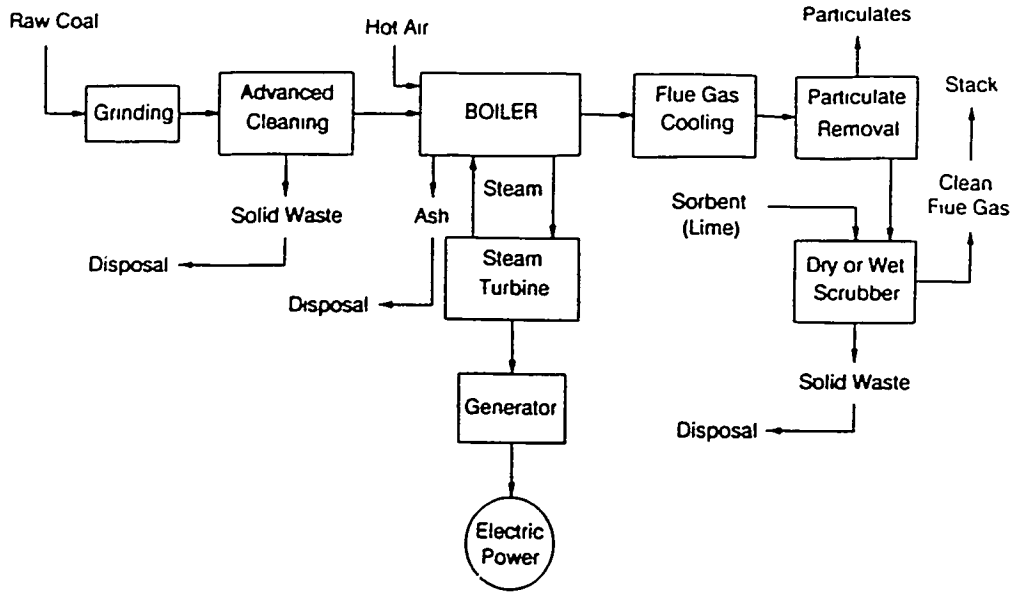


**Figure 1.** **Schematic of a Conventional Power Generation System with pre- and post-Combustion Physical and Chemical Cleaning.**

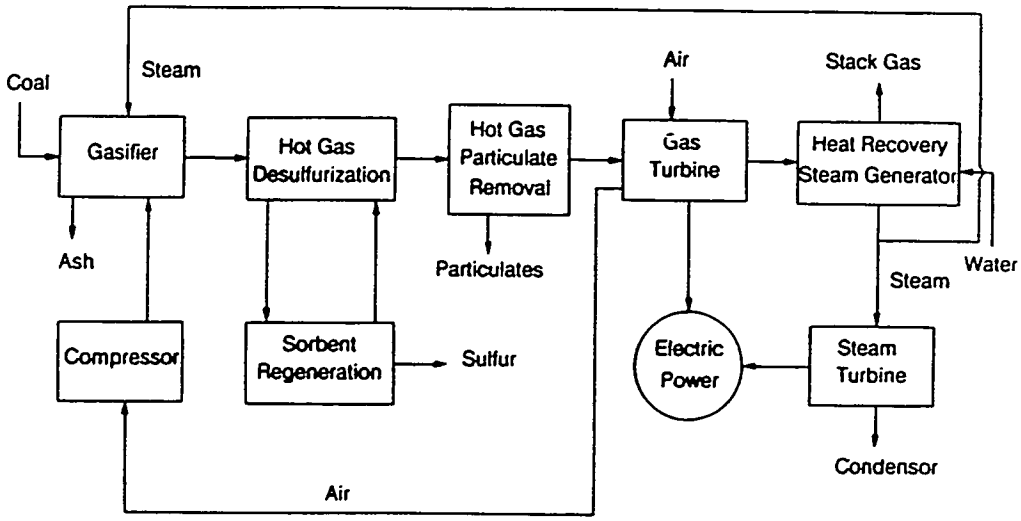


**Figure 2.** **Schematic of an Ideal Integrated Gasification Combined Cycle (IGCC) System.**

and other impurities in the fuel gas stream, mainly to meet stringent government regulations for sulfur emissions and also to protect system components from the corrosive action of $H_2S$ (the main form in which sulfur exists in the fuel gas). Hydrogen sulfide should be removed by purifying the product gas while it is still hot so that the gas can be used directly without loss of heat values. This completely eliminates the more costly, less efficient method of low-temperature, liquid-based, fuel gas scrubbing systems, and the subsequent reheat of cleaned gas which gives this design a better overall efficiency and reduces the capital costs associated with expensive heat recovery systems. In addition, since the volume of the fuel gas is significantly less than that of the flue gas stream, particularly since it is usually also at elevated pressure, the removal of sulfur-bearing species at high temperature results in considerably lower hardware costs. Also, conventional $SO_2$ scrubbing results in the formation of gypsum sludge, which requires costly management. A regenerable sorbent avoids this problem since the sulfur can be recovered as sulfur dioxide or other sulfur products. Since hot gas desulfurization is a dry process, it does not require expensive waste water treatment plants to handle process condensate from quenching processes. The desulfurizing agent (e.g. sorbent) is reusable over many sulfur capture cycles which, in turn, improves process economics and reduces the amount of solid waste generated and ultimately landfilled.

In addition to IGCC systems, the cleaned hot fuel gas may be useful in a number of applications such as the molten carbonate fuel cell (MCFC) and the pressurized fluidized-bed combustor (PFBC). Efficiencies of heat conversion to useful electrical power approaching 50 percent are feasible with IGCC systems. However, in the longer range future, power generation may be rendered more efficient by using the generated fuel gases in fuel cells for the direct conversion of heat into electricity.

Desulfurization with sorbents is essentially a process of removal of the species $H_2S$ from the gas phase. As $H_2S$ is removed, the other minority sulfur-bearing species, such as COS, equilibrate in the gas phase and also are proportionately reduced. The high temperature desulfurization can be successfully accomplished by using solid sorbents such as oxides of those metals that form stable sulfides. The effectiveness of a desulfurizing agent in treating coal gases is related to the predicted equilibrium partial pressure of sulfur which will be present in a phase combination of the reduced form of sulfide and oxide phases. A sulfur concentration limitation of approximately 150 ppmv (parts per million by volume) for IGCC systems has been established; therefore, a sorbent system capable of reducing $H_2S$ concentration from about 5000 to 150 ppmv or lower is sought.[1] The focus of much current work on hot coal-derived fuel gas desulfurization is primarily in the use of zinc ferrite and zinc titanate sorbents. The choice of zinc oxide is typically based on the thermodynamic considerations that indicated very low concentration levels of $H_2S$ in equilibrium with ZnO, ZnS, and $H_2O$ vapor.[2]

To improve the process economics further, an easily regenerable sorbent is required which would not only reduce sorbent costs but also costs associated with frequent loading and unloading of the desulfurization reactors with sorbent and disposal of the spent sorbent. Furthermore, the sulfur produced by regeneration of the sorbent should be recoverable in a form which is readily saleable, storable, or disposable. This means that the regeneration step should be flexible

and be able to produce elemental sulfur, sulfur dioxide, or sulfuric acid depending upon the demand at the location of the gasification plant.

With these restrictions in mind, research has focused almost entirely on making the zinc-based sorbents durable. However, extensive research, carried out mainly by the Morgantown Energy Technology Center (METC), casts doubt[3] that zinc ferrite or zinc titanate can be utilized even for the mild conditions associated with fixed-bed operation. Given the limited success of the zinc-based sorbents, interest has been shown in formulating and testing manganese-based sorbent pellets.

## PROJECT DESCRIPTION AND RESULTS

**Thermodynamic Arguments Supporting the Consideration of Manganese** To substantiate the potential superiority of manganese-based pellets, a systematic approach toward the evaluation of the desulfurizing power of single-metal sorbents was developed based on thermodynamic considerations.[4] This novel procedure considered several metal-based sorbents (Fe, Ni, Mg, Ca, Mn, Cu, and Zn) and singled out manganese oxide as a prime candidate sorbent capable of being utilized under a wide temperature range, irrespective of the reducing power (determined by $CO_2/CO$ ratio) of the fuel gas.

The thermodynamic feasibility of using such sorbent pellets for the removal of $H_2S$ from hot coal-derived fuel gases and the subsequent regeneration of loaded (sulfided) pellets with air was then established.[5,6] It was determined that the objective of reducing the $H_2S$ concentration in the fuel gas below 150 ppmv to satisfy the IGCC system requirement is thermodynamically feasible using a Mn-based sorbent. Although desulfurization at temperatures below 800 °C is possible, thermodynamic guidelines indicate that regeneration with air must be carried out above 900 °C to avoid sulfate formation.

**Experimental** A novel process was developed for the manufacture of Mn-based spherical pellets which have the desired physical and chemical characteristics required during the long-term cyclic sulfidation and regeneration in a high-temperature desulfurization operation. The procedures for sorbent pellet making, drying, and induration are fully documented in a patent application filed by the authors.[7]

Screening sulfidation tests on a number of formulations, consisting of a Mn-containing compound (ore or $MnCO_3$), alundum ($Al_2O_3$), and organic or inorganic binders, were carried out using $H_2S$-$H_2$ gas mixtures in a thermogravimetric apparatus (TGA, Figure 3)[5] at temperatures ranging from 700 to 1000 °C. A formulation, designated FORM4-A, was found to possess the best combination of sulfur capacity, reactivity, and strength, as shown in Figure 4 at 1000 °C. More importantly, the rate of sulfur pick-up from hot coal-derived fuel gases using Mn-based pellets compares favorably with that which is obtained using Zn-based sorbents,[1] as indicated in Figure 5.

Regeneration tests determined that for $T \geq 900$ °C, loaded pellets can be fully regenerated with air in 10 to 15 minutes, without sulfate formation, in strict accordance with thermodynamic guidelines. Repeated cycling of the leading sorbent formulation (FORM4-A) was conducted in the TGA apparatus, up to 5 consecutive cycles.[6] One important finding was that the capacity of the pellets for sulfur pickup from fuel gas and the kinetics of reduction, sulfidation, and

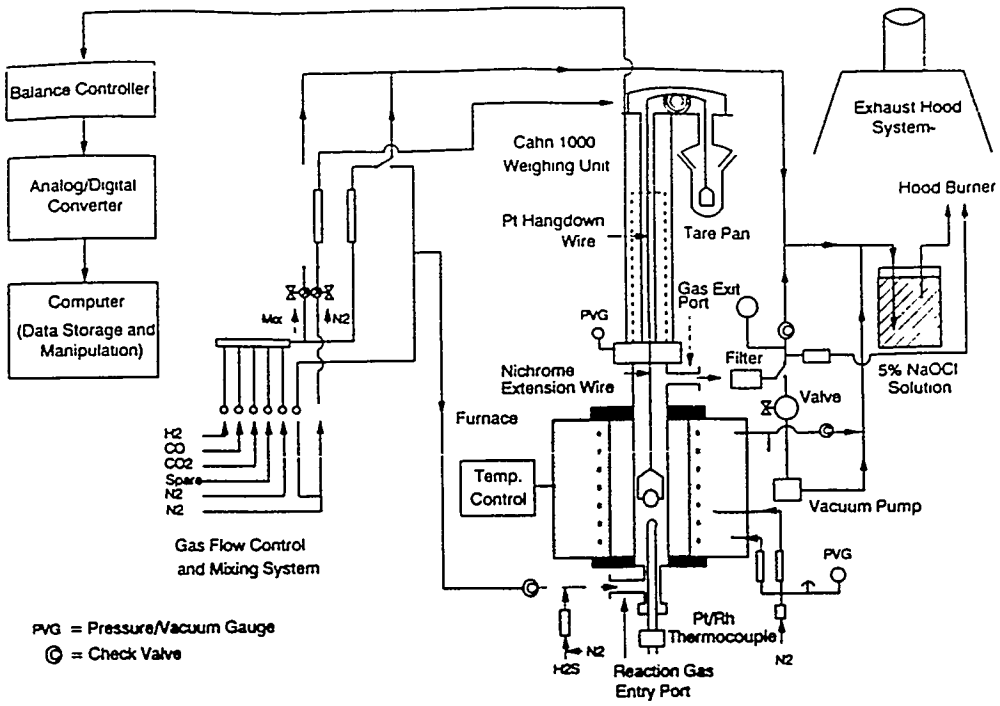


**Figure 3. Schematic of the ASTRO Thermogravimetric (TGA) Apparatus.**

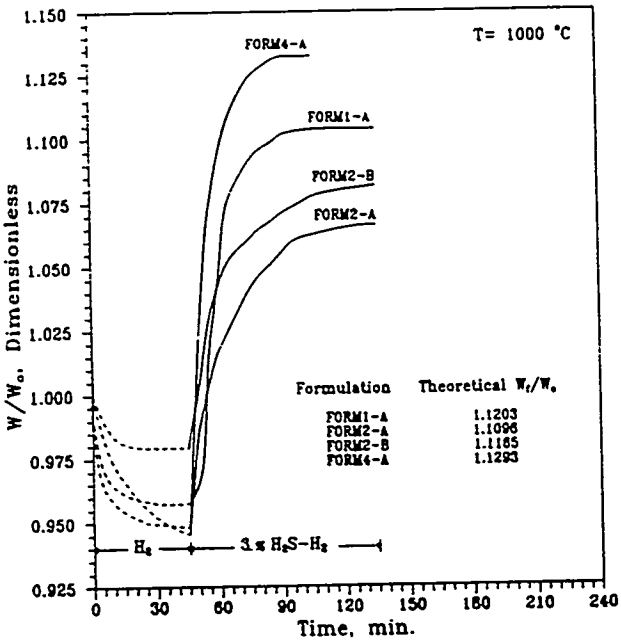


**Figure 4. Comparison between Several Formulations of Manganese-Based Pellets upon Loading with Sulfidizing Fuel Gas.**

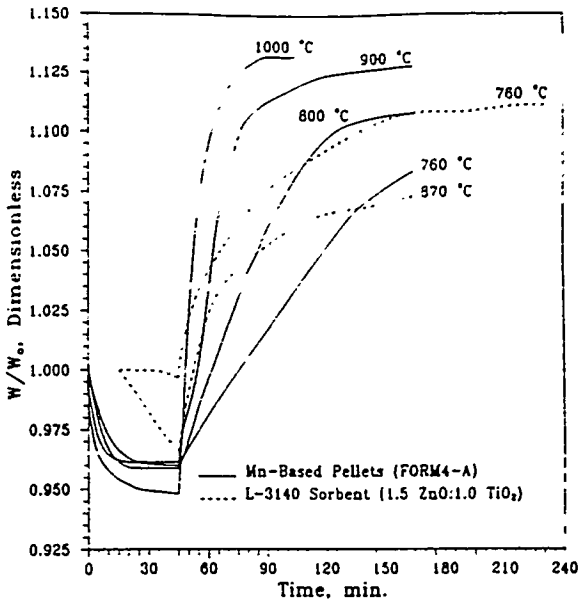


**Figure 5. Comparison between Loading Behavior of Manganese-Based Pellets (FORM4-A) and Zinc Titanate Pellets.**

regeneration reactions improved with recycling without compromising the strength. These results are reproduced in Figure 6. This desirable phenomenon was attributed to radial micro-crack formation which reduced the solid-state diffusion path within the pellet. Normally, and especially in the case of Zn-based sorbents, the onset of small cracks leads to sorbent spalling and reduced usable life due to increased "dust" loadings in an exit gas stream.[8] With the Mn-based sorbents, the presence of these small cracks apparently led to improvement in the reaction rate for sulfidation and regeneration without adversely affecting the strength.

While the results reported earlier[5,6] were obtained using thermogravimetry, the potential usefulness of Mn-based pellets may be more realistically assessed by simulating practical processes of fuel gas desulfurization, which fall into three main categories: fixed-bed, fluidized-bed, or moving-bed technology. The main focus of this paper is to report on fixed-bed testing of the leading Mn-based sorbent pellet formulation (i.e., FORM4-A). Experiments were carried out to test the long-term (up to 50 cycles) durability and regenerability of the sorbent using a simulated fuel gas (Tampella-U) for sulfidation and air for regeneration. A more thorough description of these results is provided in a recent paper published by the authors.[9]

**Experimental Results on Fixed Bed Tests**

The leading formulation, FORM4-A, is made up of 81.31% by weight manganese carbonate (containing 93-95% $MnCO_3$), 16.73% alundum (containing 96.6% $Al_2O_3$ and 2.6% $TiO_2$), and 1.96% bentonite (an inorganic binder). Upon forming pellets, they were first dried to a constant weight at 110 °C, then heated to 350 °C to allow for dissociation of the manganese carbonate. The pellets were then heated to 1250 °C and indurated for 2 hours in an air atmosphere before removal from the furnace. The average size of the pellets was 4.8 mm and they had an average strength of 23.8 N/mm of diameter (5.4 lbs/mm). The final manganese assay of the indurated pellets was 44.22% by weight, which corresponds to a theoretical sulfur capacity of 25.8%, i.e., 25.8 g S/100 g of indurated pellet.

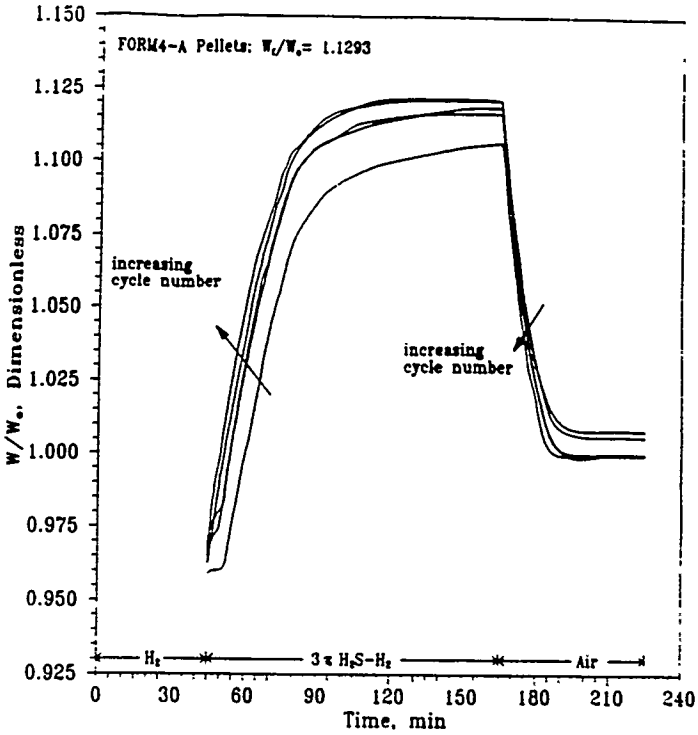


**Figure 6. Effect of Repeated Cyclical Loading and Regeneration on the Reaction Kinetics and Capacity of FORM4-A Pellets.**

The schematic diagram of the overall experimental arrangement for fixed-bed tests is shown in Figure 7. The split or two-zone furnace was positioned with respect to the bed to accomplish gas preheating and careful control of the bed temperature. Gas combinations for flows were produced via control of bottled gases through the valves and flowmeters shown in the diagram. The water content of the system was controlled by a metering pump acting on distilled water which was discharged into a heated stainless

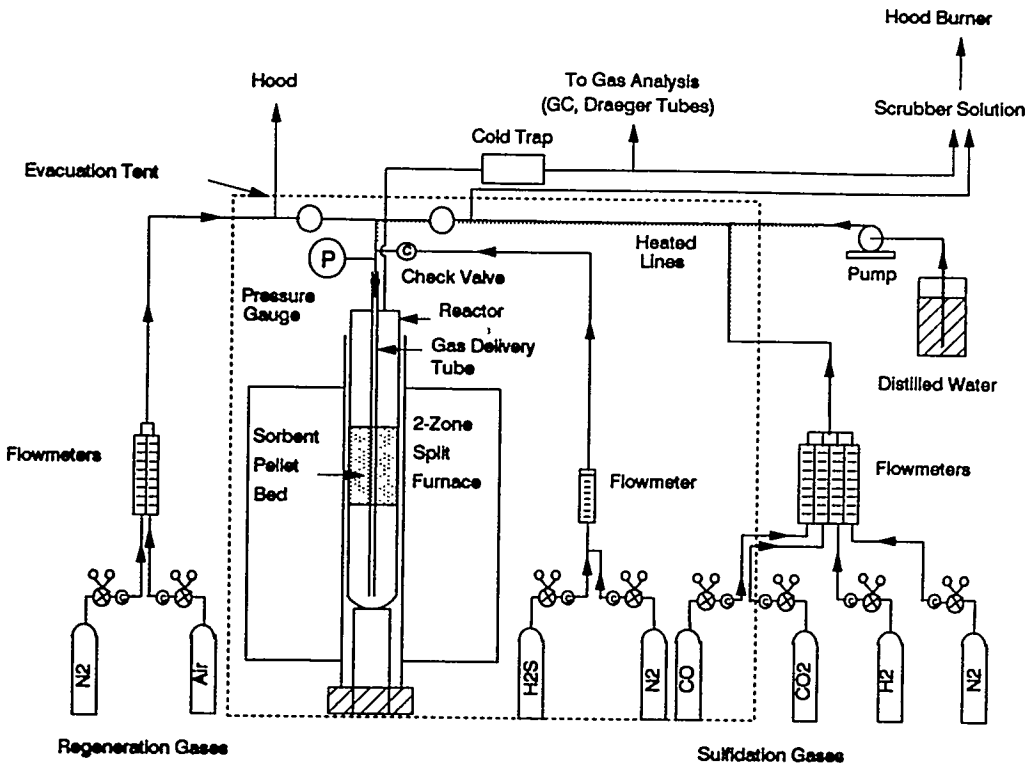


**Figure 7. Schematic of Overall Experimental Arrangement for Fixed-Bed Tests.**

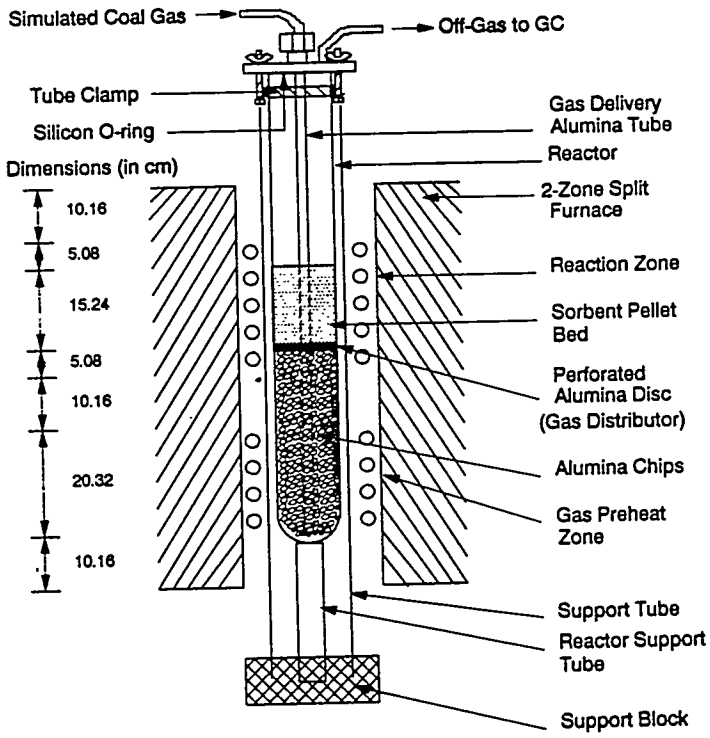


**Figure 8. Schematic Diagram of Reactor Details.**

steel tube to induce the vaporization of liquid water and provide the gas composition required for the simulation of a slightly modified form of the Tampella-U gas composition (13% $H_2$; 50% $N_2$; 24% CO; 5% $CO_2$; 5% $H_2O$; and 3% $H_2S$). The hydrogen sulfide level was about three times higher than that which would actually be produced by a gasifier to accelerate breakthrough. The hydrogen sulfide is mixed with the other gases and water vapor immediately before the introduction of the complete mixture into the reactor to minimize corrosion of system components. The reactive gas feed line was heat-traced to prevent subsequent condensation. In addition, the exhaust gas line was also heated from the top of the reactor to the cold trap to prevent any formation and subsequent freezing of elemental sulfur. Breakthrough of hydrogen sulfide gas was arbitrarily defined at a concentration of 500 ppmv in the exit gas.

The fixed-bed was made with 292.7 grams of FORM4-A pellets packed to a height of 15.24 cm (6 inches) in the 2-in (I.D.) reactor tube (Figure 8). In a typical test, the reactor was purged with nitrogen to expel air. During the purge, reactive gas flows were adjusted and routed directly to the scrubber solution. The reactive gases were then introduced into the reactor and the loading test timed. In such a fixed-bed desulfurization reactor $H_2S$ removal would first occur near the bottom of the bed where reduction of $Mn_3O_4$ to MnO and the immediate conversion of MnO to MnS occur. The majority of the unreacted pellets are then exposed to the sulfur-free reducing gas for varying times as the reaction front progressed through the bed.

At the conclusion of the sulfidation test, the bed is flushed with nitrogen in order to expel remaining combustible gases and a regeneration gas consisting of air is initiated with the product gas being periodically analyzed for $SO_2$ using detector tubes. The regeneration step is discontinued when the concentration of $SO_2$ is measured below 500 ppmv.

The breakthrough curve for sulfidation at 900 °C on the first cycle is shown in Figure 9. The concentration of $H_2S$ in the exhaust gas (on wet basis) appears to reach a steady state value of approximately 222.5 ppmv for at least the first 7 hours of the loading test. This value is close to that of the MnO/MnS equilibrium. The vertical dashed line corresponds to the theoretical time required for breakthrough and is a function of the quantity of sorbent pellets in the reactor, the loading gas flowrate or space velocity, and the equilibrium $pH_2O/pH_2S$ in the exhaust gas, i.e. reaction temperature since the amount of water vapor in the feed gas is fixed at 5% by volume. If breakthrough is arbitrarily defined at 500 ppmv in the exhaust gas, then breakthrough occurred after a total reaction time of 8 hours which corresponds to 21.12% loading or 81.86% bed utilization.

The concentration of $SO_2$ in the regeneration product gas is shown in Figure 10 as a function of reaction time. Again, the theoretical time for complete regeneration is displayed as a vertical dashed line which is a function of air flowrate, the quantity of pellets in the reactor, and temperature to a lesser extent since the reaction occurs essentially to completion. In addition, the theoretical maximum $SO_2$ concentration in the product gas (before mixing with after-burner gas) is shown in Figure 10 as a horizontal dashed line. This 13.76% value corresponds to regeneration with air and the complete consumption of oxygen in the air, and is calculated based on the stoichiometry of the overall regeneration reaction, as previously outlined in detail.[6] As can be seen in Figure

10, the breakthrough occurred rapidly when the bed was almost completely regenerated.

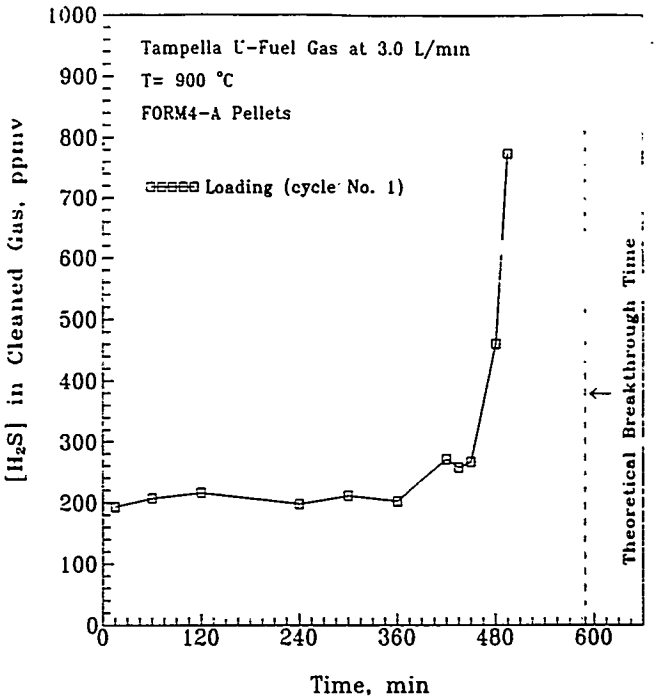


**Figure 9. Breakthrough Curve for First-Cycle Sulfidation at 900 °C.**

A relatively short series of complete sulfidation/regeneration cycles was then carried out at 900 °C to verify the sorbent as a viable candidate for a fixed-bed fuel gas desulfurization. Six consecutive cycles over a 15-day period were deemed adequate for this purpose. The results of sulfidation tests from cycles 1,2,3, and 6 are reported in Figure 11. Before breakthrough the $H_2S$ concentration in the cleaned gas approaches more closely the equilibrium value, which is an indication of an improvement in pellet reaction kinetics with increasing cyclic loading. These results are consistent with the previous results from TGA tests on individual pellets.[6]

A fifty-cycle series of tests was then completed to demonstrate the durability and regenerability of FORM4-A sorbent

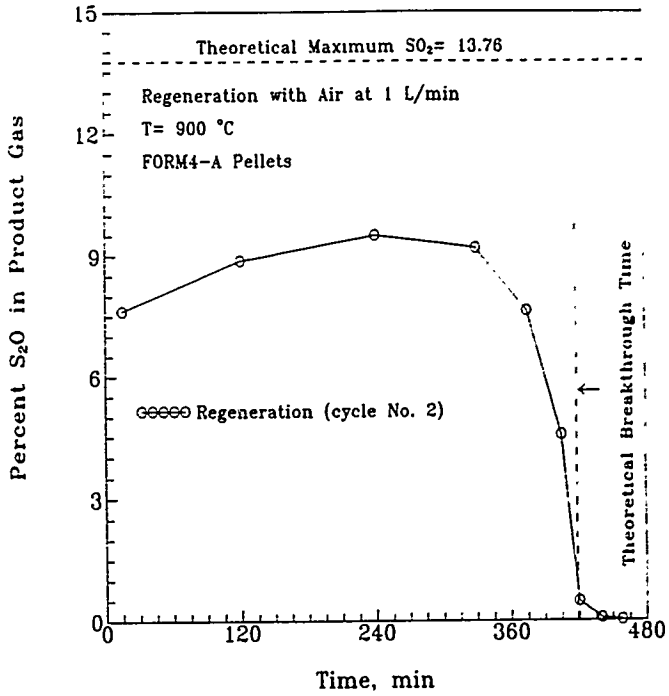


**Figure 10. Concentration of $SO_2$ in Regeneration Product Gas.**

formulation. Each sulfidation and regeneration repeated the initial run conditions. The results are reported in Figure 12 which shows the effect of cycling on the sulfur capacity of FORM4-A pellets at 900 °C upon repeated loading and regeneration. The sulfur loading capacity (defined as grams of sulfur per 100 grams of original pellet mass) shows a slight improvement with each cycle up to the fourteenth cycle. This effect is noticeable in the second cycle, but is much less pronounced in subsequent cycles. The sulfur capacity in the first eighteen cycles (except for cycle fifteen) ranged from 21.12% to 23.12%, which corresponds to approximately 90% sorbent bed utilization. This sulfur capacity is calculated using mass balances, based upon gas analyses for $H_2S$ entering and leaving the reactor. At the fifteenth cycle, a equipment failure caused that test to be aborted. Upon removing the

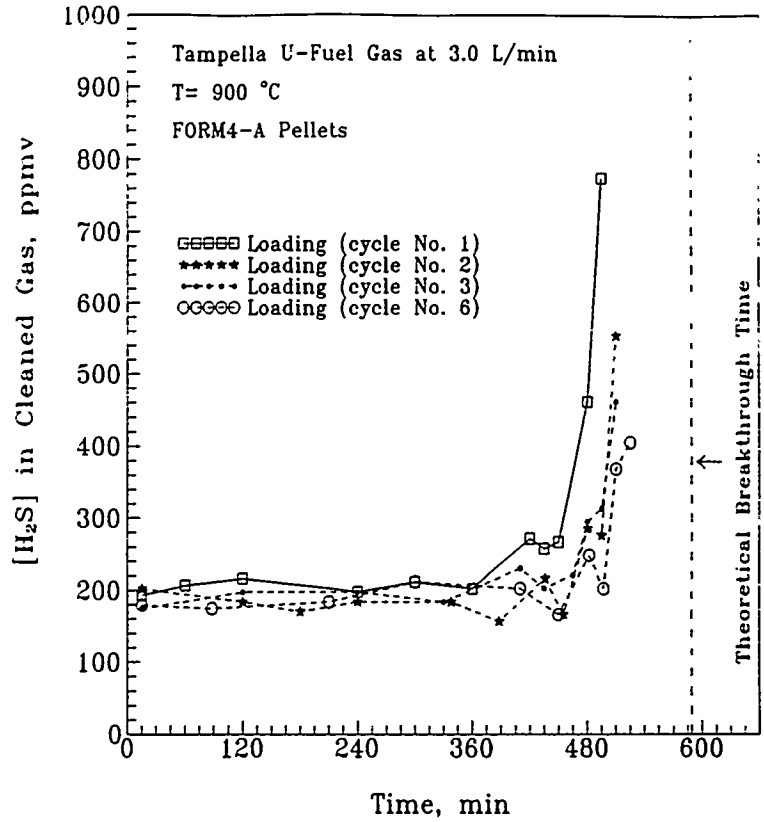


**Figure 11.** **Series of Six Loading Cycles at 900 °C to Determine Sorbent Viability for Subsequent Fixed-Bed Testing (Cycles 1, 2, 3, and 6 are shown).**

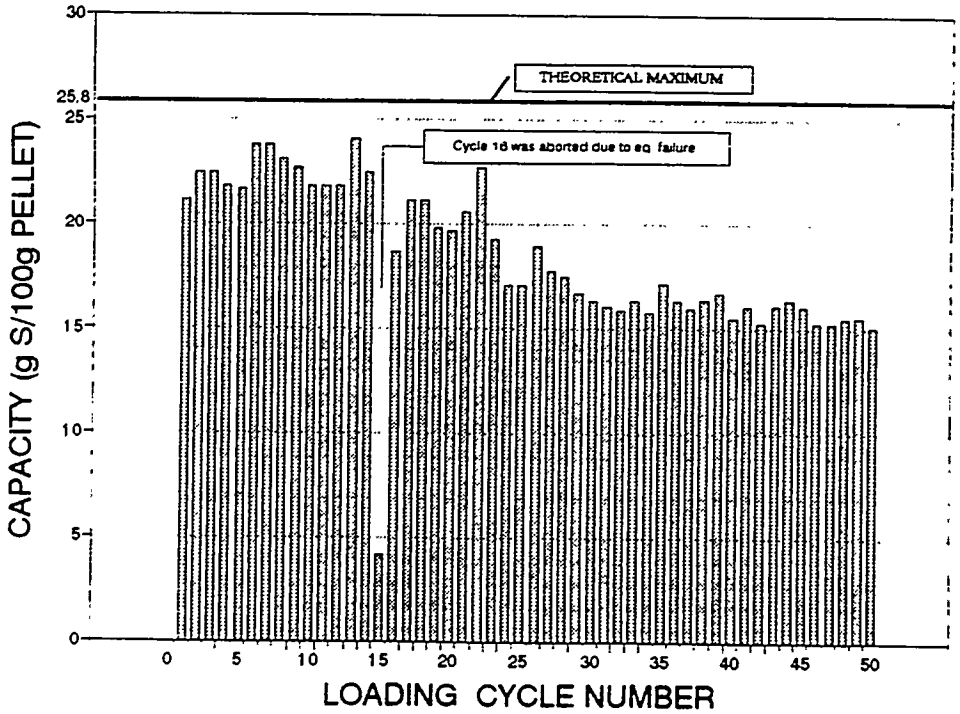


**Figure 12.** **Capacity Tests via Multicyclic Loading and Regeneration of FORM4-A Pellets.**

bed and examining the pellets, they were free-flowing and exhibited very little attrition (about 1% of their weight were in the form of fines). After the twenty-second cycle a drop off in bed performance is observed through the twenty-ninth cycle to about 17% capacity. (Studies are still in progress on this sorbent). These results can be compared with those on zinc titanate where the initial capacity on the first cycle is only 10 percent dropping to values as low as 2 percent after twenty-five cycles.[10]

**STATUS OF PROGRAM**

About five years ago, the U. S. Bureau of Mines, Twin Cities Research Center and the University of Minnesota entered into a joint program to study in situ leaching of manganese from Minnesota deposits. We decided to examine the Emily deposit since it was a high grade manganese oxide with minimal amounts of other carbonates or soluble oxides which would consume the lixiviant, sulfur dioxide. The Bureau both at Minneapolis and in Salt Lake City developed a continuous piloting process for purification of the leach solutions and the production of a pure manganese carbonate. (see Figures 13 and 14) About three years ago, the University secured funding for undertaking the use of manganese pellets as regenerable sorbents for hot fuel gas desulfurization. This application was included in the Bureau's economic overall evaluation and was found to be the most favorable candidate for development. The high manganese purity and low iron levels of their product are necessary in order to achieve the required properties of cyclic loading and regeneration.

Simultaneous with the development of the piloting process, the University continued to study pellet formulations and to engage in long term cyclic testing. The program with the Department of Energy, initially begun with support from the Morgantown Energy Technology Center has been extended for three more years by the Pittsburgh Energy Technology Center. These future studies are to examine the kinetics of loading and regeneration and also to determine if loading can proceed at lower temperatures by changes in the pellet formulation.

In the past year, the Minnesota Manganese Resources Company has shown an interest in these studies and has encouraged our efforts to develop a value-added application for in situ mined manganese. Their ore body has been the one which the Bureau was exploring with respect to leach tests on core samples to produce leach liquors for their purification pilot plant. Although the tests we reported in this paper were for reagent-grade manganese carbonate, we are planning to determine the reproducibility of the pellet formulations made with in-situ mined-product (ISMP) with respect to its: strength, effectiveness in loading and regeneration and resistance to degradation upon multiple cycle loading. Preliminary results indicate that pellets from ISMP is equivalent to the commercial grade manganese and has a potential value ranging from $3 to $7 per pound. (The latter value is that generally assigned to the zinc titanate product which is considered for use in IGCC systems).

As a final note for those of us which are more familiar with taconite pellet production, it might be useful to think of the future potential of manganese pellets in these terms:

> The manganese pellet product has the potential for one hundred times the value of taconite pellets, but will have a market demand less than one-half of

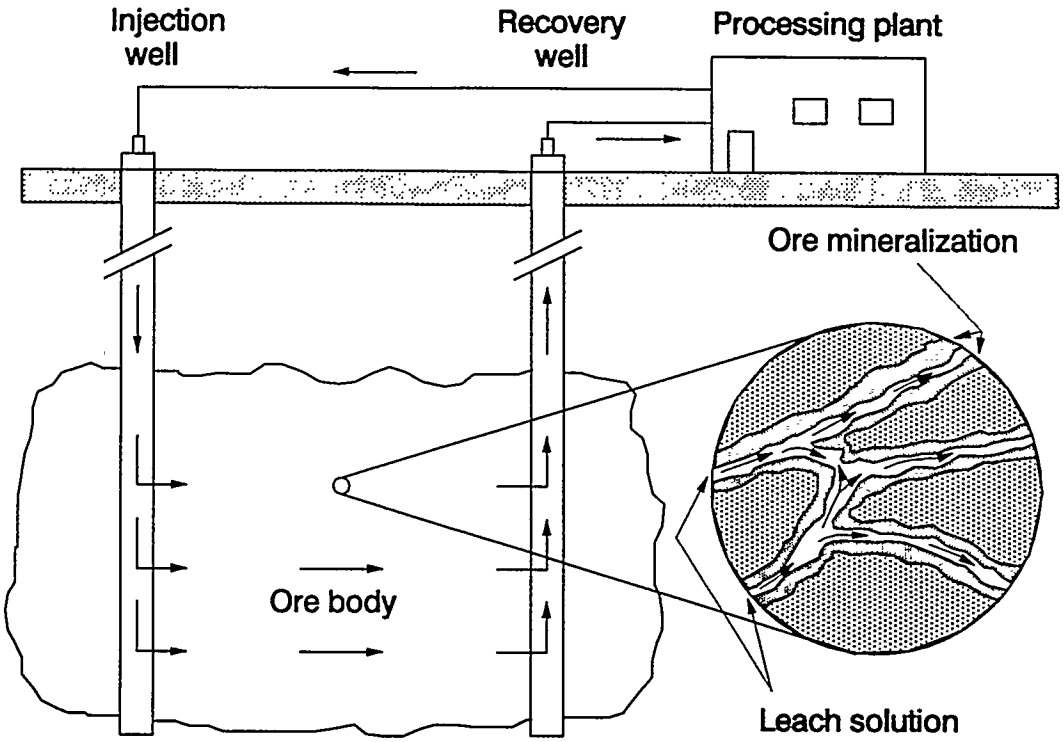


**Figure 13.** **Cross Section of an In Situ Leach Mining System in which the Core is Leached via a System of Vertical Wells.[11]**

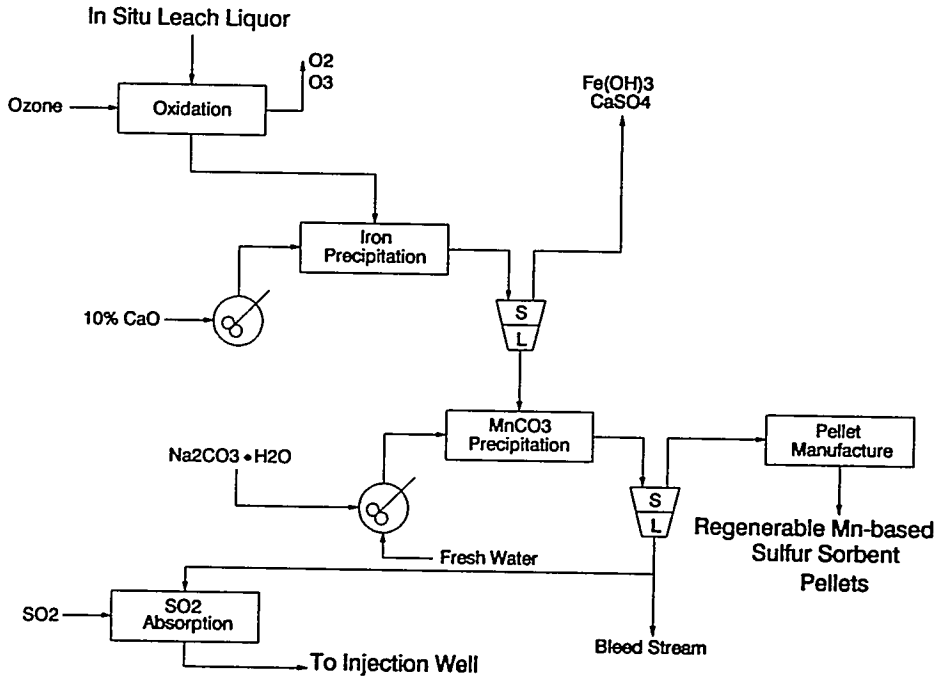


**Figure 14.** **Simplified Flow Diagram for a Manganese Carbonate Recovery Process Developed at the the Salt Lake City Research Center of the U.S. Bureau of Mines.[12]**

one percent of the taconite tonnage. This leads one to hope that if all factors are favorable, a new industry for north-central Minnesota may be in the offing: a product to improve the environment produced by a mining process with minimal impact on the environment.

What are the "ifs"? At present the requirements for this product to move forward are dependent upon the willingness of the power industry to shift to combined cycle operation and avoid gypsum sludge by use of a regenerable sorbent. Zinc titanate appears to be inferior to manganese; however, most of the research work conducted by the U.S. DOE and its contractors has been done on zinc titanate. Consequently, a body of information must be assembled to support manganese as an alternative.

**Acknowledgements** The authors express their appreciation to the Department of Energy, Morgantown Energy Technology Center, under Contract DE-AC21-92MC29246 and also the U.S. Bureau of Mines, Twin Cities Research Center, Grant USDI-BM/C0299002-Mod.3 for providing support for this study. Thanks are also extended to graduate students Kent Wagner and Rick Stuart for their help with the fixed bed work.

## REFERENCES

1. Woods M. C. et al. Reaction between $H_2S$ and Zinc-Oxide-Titanium Oxide Sorbents. 1. Single-Pellet Kinetic Studies. *I&EC RESEARCH*, 1990, pp. 1160-1167.

2. Jha, M. C.; Blandon, T.; Hepworth, M. T. Durable Zinc Ferrite Sorbent Pellets for Hot Coal Gas Desulfurization. U.S. Patent No. 4,732,888, March 22, 1988.

3. Venkataraman, V. K. Private Communication: Information on Workshop "Status and Direction of Research and Development for High Temperature Sulfur Removal Sorbents," Morgantown Energy Technology Center, January 28, 1993.

4. Hepworth, M. T.; Ben-Slimane, R.; Zhong, S. Thermodynamic Comparison of Several Sorbent Systems for Hot Coal-Derived Fuel-Gas Desulfurization. *Energy & Fuels* **1993,** 7, 602-609.

5. Ben-Slimane, R.; Hepworth, M. T. Desulfurization of Hot Coal-Derived Fuel Gases with Manganese-Based Regenerable Sorbents. 1. Loading (Sulfidation) Tests. *Energy & Fuels* **1994,** 8, 1175-1183.

6. Ben-Slimane, R.; Hepworth, M. T. Desulfurization of Hot Coal-Derived Fuel Gases with Manganese-Based Regenerable Sorbents. 2. Regeneration and Multicycle Tests. *Energy & Fuels* **1994,** 8, 1184-1191.

7. Ben-Slimane, R.; Hepworth, M. T. Regenerable Manganese-Based Sorbent Pellets and Methods of Manufacture and Use. Patent Application Filed in the U.S. Patent and Trademark Office, June 17, 1994.

8. Notestein, J. E. *Commercial Gasifier for IGCC Applications Study Report*, DOE/METC-91/6118 (DE91002051), June 1990.

9. Ben-Slimane, R.; Hepworth, M. T. Desulfurization of Hot Coal-Derived

Fuel Gases with Manganese-Based Regenerable Sorbents. 3. Fixed-Bed Testing. *Energy & Fuels* **1995**, 9, 372-378.

10. O'Donnell, J. J.; Katta, S.; Grindley, T.; Delzer, G.; Khare, G. Desulfurization of Hot Fuel Gas with Z-Sorb III Sorbent, *Proceedings of the Coal-Fired Power Systems 93 -- Advances in IGCC and PFBC Review Meeting*, 1993; Bonk, David L., Ed.; DOE/METC-93/6131; NTIS: Springfield, VA, 1993; 179-190.

11. U. S. Bureau of Mines, In Situ Leach Mining, Proceedings: Technology Transfer Seminars, Phoenix, AZ, April 4, and Salt Lake City, UT, April 6, 1989, IC 9216, p. 2.

12. Redden, L., Hepworth, M.T., Ben-Slimane, R., and Welch, G., "Recovery of Manganese Carbonate from Leach Liquor," U. S. Patent Application Serial No. 08/339,083 : Filed November 1994.

# PB.13 High-Temperature $H_2S$ Removal Using Limestones

## CONTRACT INFORMATION

| | |
|---|---|
| **FWP Number** | AA-20-15 |
| **Contractor** | Lawrence Berkeley Laboratory<br>Applied Science Division<br>Berkeley, CA 94720<br>(510) 486 5028 |
| **Contractor Project Manager** | Elton J. Cairns |
| **Principal Investigator** | Scott Lynn |
| **METC Project Manager** | Daniel C. Cicero |
| **Period of Performance** | October 1, 1994 to September 30, 1995 |

**FY 95 Program Schedule**

| | O | N | D | J | F | M | A | M | J | J | A | S |
|---|---|---|---|---|---|---|---|---|---|---|---|---|
| Test Plan | ——— | ——— | ——— | | | | | | | | | |
| Fabrication | ——— | ——— | ——— | ——— | ——— | | | | | | | |
| Testing | ——— | ——— | ——— | ——— | ——— | ——— | ——— | ——— | ——— | | | |
| Analysis | ——— | ——— | ——— | ——— | ——— | ——— | ——— | ——— | ——— | ——— | ——— | ——— |

## OBJECTIVES

This project is exploring the technical and economic feasibility of using limestone in a high-temperature process for cleaning coal gas prior to combustion in a gas turbine. In one version of the process the coal gas would pass counter-currently through a nearly-isothermal, moving bed of limestone that would serve to remove particulates (by filtration), and hydrogen sulfide (by chemisorption), and ammonia (by catalysis). Alternative process configurations include the use of limestone in a cocurrently moving bed, in a fluidized bed, or in an entrained flow sorption system. The objectives of this research have been to define the range of temperatures at which these goals can best be realized at a given pressure, to determine the effect of the magnesium content of the limestone on sulfidation kinetics and calcium utilization, to use the kinetic data to model the various types of sorption systems, and to develop a process for converting calcium sulfide to elemental sulfur and calcium carbonate.

## BACKGROUND INFORMATION

One of the most important needs in coal gasification is the development of reliable methods

of removing solid and gaseous contaminants from the coal gas at high temperatures and pressures. Gaseous contaminants include $H_2S$, $NH_3$ and volatilized alkali salts, all formed from trace components of the coal. Suspended solids are mainly fines formed during gasification. Squires *et al.* (1971) showed that cleaning the gas at high temperature and pressure offers numerous advantages, most notably higher thermal efficiency and reduced volume (hence cost) of processing vessels. Current industrial practice is to add limestone to the gasifier. This achieves moderately successful removal of $H_2S$, but requires a significant excess over the stoichiometric quantity of limestone theoretically necessary to attain close-to-equilibrium removal of $H_2S$ and produces large amounts of mixed-limestone/slag-solid waste.

Sulfur is present in two main forms in coal: pyritic and organic. Pyritic sulfur is contained as mineral inclusions inside the organic matrix of coal. However, one-half or more of the sulfur, along with some nitrogen and oxygen, is organically bound to the coal (Nowacki, 1981). In a gasification process both forms are converted to $H_2S$ because of the reducing conditions present in the gasifier.

Calcium-based sorbents for sulfur removal have been the subject of an extremely large number of publications in recent years. Swisher and Schwerdtfeger (1992) identified more than a thousand references on this topic for the 1975-1990 period, including more than 200 between 1988 and 1990. They attributed this interest in calcium compounds (mainly limestones and dolomites and their calcined forms) to their low price and their effectiveness in both reducing and oxidizing conditions to form, respectively, calcium sulfide, CaS, and calcium sulfate, $CaSO_4$. A large fraction of these papers deals with the removal of $SO_2$ from power plant flue gas. However, as the development of advanced coal gasification systems intensifies, more and more research is now directed toward $H_2S$ sorption.

Ruth *et al.* (1972) and Borgwardt and Roache (1984) showed that dolomite was an excellent $H_2S$ sorbent, whereas limestone proved to be a rather poor one. However, most interest in these sorbents was rapidly lost because of their poor regenerability by the then-favored scheme of back-reacting CaS with steam and $CO_2$ at 600 to 700 °C (Sun *et al.*, 1978; Swisher and Schwerdtfeger, 1992). In all types of dolomite the calcium atoms react quasi-completely to CaS, provided that $MgCO_3$, at least, is calcined to MgO. In the sulfation of calcium containing sorbents, by contrast, slight variations in the reaction conditions (Haji-Sulaiman *et al.*, 1990), sorbent composition (Davini *et al.*, 1992; Alvfors and Sverdberg, 1992), pore size distribution and volume (Ulerich *et al.*, 1978; Hartman *et al.*, 1978; Chang and Thodos, 1984), reactive surface area (Borgwardt and Bruce, 1986), or calcination conditions (O'Neill *et al.*, 1976) translate into sizeable variations in reactivity and sorption capacity.

Most industrial applications have been geared toward *in-situ* desulfurization, where limestone or dolomite is added to the coal charge before injection into the gasifier, avoiding the need for an additional vessel to remove the sulfur from the coal. Moreover, limestones and dolomites can catalyze the kinetics of coal gasification and tar decomposition (Leppälahti *et al.*, 1991). However, a calcium-to-sulfur molar ratio of about 2 is generally needed to achieve 90% sulfur removal (Robertson *et al.*, 1993; Swisher and Schwerdtfeger, 1992). The one-fold excess for a 1-GW power plant using 50 kg/s of Pittsburgh #8

(3 wt% sulfur) means consuming an additional 400 to 450 metric tons of limestone daily. Moreover, the resulting slag is a dirty mixture of coal ash and calcium sulfide, sulfite and/or sulfate that would require further processing before disposal. It would be advantageous to keep most of the coal ash and the spent calcium sorbent separated, especially if the sorbent is to be regenerated and recycled.

The excess of calcium results from the relatively slow rate of reaction between calcium oxide and hydrogen sulfide compared to the sorbent residence time in the gasifier. The latter cannot be freely adjusted, but is dictated by the gasifier design and may be extremely short (of the order of a second or less in the case of a Texaco gasifier). Moreover, the thermodynamic conditions encountered in the gasifier are generally not optimal. Calcium sulfate, responsible for pore closure in the sorbent, can form since oxidizing conditions are present in some parts of the gasifier. The high temperatures encountered near the combustion zone of the gasifier cause rapid sintering of CaO and CaS, which results in severe surface area reduction and pore closure. Furthermore, only near the calcination temperature of calcium carbonate can the lowest $H_2S$ level in coal gas be achieved. Finally, some of the sorbent tends to react with silica present in the coal slag rather than with the sulfur (Swisher and Schwerdtfeger, 1992).

Westinghouse Electric Corporation (Newby *et al.*, 1993) injects -325 mesh limestone particles at the exit of the gasifier. The residence time of the limestone particles thus entrained does not exceed 300 ms. About 90% sulfur removal is achieved with a Ca/S ratio of 1.7 using Pittsburgh #8 coal for temperatures up to 1600 °F (871 °C) and pressures between 12 and 34 atmospheres. However, very large quantities of fine calcium sulfide/calcium carbonate powder must be filtered from the coal gas.

Most of the studies of the reaction between dolomite and $H_2S$ were carried out under conditions at which $CaCO_3$ as well as $MgCO_3$ would partially or totally calcine (Squires *et al.*, 1971; Yen, 1979; Freund, 1981). Sulfidation of fully-calcined dolomite can be near-complete, given enough time (Squires *et al.*, 1971). Under these completely calcining conditions, the reaction kinetics appeared to be half-order with respect to $H_2S$ even with very small dolomite particles (−200 +230 mesh, or about 69 $\mu$m on average), which is characteristic of kinetics controlled by the diffusion of the reacting gas through the product layer (Fenouil and Lynn, 1995).

A separate, moving bed of millimeter-size limestone particles located after the gasifier offers several advantages over *in-situ* desulfurization and the Westinghouse entrained-flow reactor approach. Regulating the sorbent feed rate allows maximum conversion of the solid. Cooling the coal gas to the $CaCO_3$ calcination temperature ahead of the moving-bed optimizes the thermodynamic driving force of the sulfidation reaction. The moving-bed can also act as an efficient filter (Wilson *et al.*, 1993), thus reducing the duty of any additional filter located downstream rather than increasing it. The spent sorbent is relatively clean (since it is not mixed with the coal slag), which should ease regeneration of CaS. Finally, the use of a separate unit to perform the desulfurization allows easy retrofit of coal gasification systems without modification of the gasifier. We would also prefer to use limestone rather than dolomite because of its larger potential sulfur loading (0.32 g sulfur/g limestone versus 0.17 g sulfur/g dolomite).

This paper compares the kinetics and the completeness of the sulfidation of CaO and $CaCO_3$ in three different types of calcium sorbents: limestone, provided by Great Lakes Co. (Green Bay, WI), dolomitic limestone and dolomite, both provided by National Lime and Stone Co. (Findlay, OH) under the respective names Bucyrus #18 and Carry #20. The suppliers' data on the average composition of the three sorbents are given in Table 1. Since we favor the use of the sorbent in a moving bed, for which the residence time of the solid in the coal gas can be adjusted as desired, we will mainly focus on the following aspect of the sulfidation kinetics of CaO and $CaCO_3$: the possibility of achieving 100% conversion of $CaCO_3$ (CaO) to CaS in a "reasonable" amount of time, for millimeter-size particles under conditions that are encountered in a typical hot coal gas, at temperatures below and above the calcination temperature of calcium carbonate.

## PROJECT DESCRIPTION

The experimental apparatus, a quartz reactor, is shown in Figure 1. The reactor was placed in an electric furnace that produced a quite uniform temperature profile in the region of the sample. The experimental techniques, together with the analytical methods, are described by Fenouil and Lynn (1995). All experiments were performed with 18-35 mesh samples (Tyler Standard, which corresponds to particle diameters of 0.417 mm to 1.00 mm). The mass-average radius of the stones was measured at 0.40 mm. The composition of the gas feed was estimated by allowing for equilibrium at the temperature of the reaction (*e.g.*, at 915 °C it was: $H_2S$ (900 ppm), $CO_2$ (24.7%), $H_2$ (2.1%), $H_2O$ (8.5%), CO (8.5%) and $N_2$ (56.1%)). With this gas composition, the thermal decomposition of $H_2S$ was limited to well below 10%, producing primarily COS. The total gas flow past the sample was maintained at about 6.25 ml(STP)/s to ensure negligible external heat- and mass-transfer limitations on the reaction kinetics. Furthermore, at 915 °C $MgCO_3$ and $CaCO_3$ calcined completely in a few minutes.

The total quantity of calcium in the samples was kept the same in all experiments, approximately $2.0\times10^{-3}$ mole. The sample size was 0.20 g for limestone, 0.25 g for dolomitic limestone, and 0.275 g for half-calcined dolomite. We chose to operate with low $H_2S$ concentrations both to increase the contrast between the reaction rates of different sorbents and because of our interest in the reaction kinetics when the driving force is small. Any reaction that occurs with 900 ppm of $H_2S$, will *a fortiori* also take place with higher $H_2S$ concentrations.

## RESULTS

**A. Fully Calcined Sorbents** Figure 2 shows an example of the way the temperature and gas composition affect the equilibrium $H_2S$ level that can be achieved using CaO or $CaCO_3$ as sorbents. It is highly beneficial to operate near but somewhat above the calcination temperature; as will be seen below, only dolomite is an effective sorbent below the calcination temperature.

*i) Absorption of $H_2S$ by Lime* As has been reported in detail elsewhere (Fenouil and Lynn, 1995), after limestone has been calcined it can be sulfided to nearly 100% of its theoretical CaS capacity. As is seen in Figure 3, the rate of sulfidation is nearly independent of temperature. The data in Figure 3 are for two separate conditions: a) the pellets are initially limestone but the temperature is high enough so that the rate of calcination is fast relative to the rate of sulfidation; or b) the pellets are initially calcined, then

cooled and exposed to a gas free of $CO_2$ so that $CaCO_3$ cannot re-form.

*ii) Chemical Attrition of the Sorbents* Dolomite and dolomitic limestone samples exposed to our simulated coal gas at 915 °C produced some fine particles because of the rapid calcination of the $MgCO_3$. However, the quantity of these fine particles remained well below 1% of the total weight of sample. When dolomite was exposed to the same conditions we found that 1% or more of the total weight of solids was very rapidly pulverized. Curran *et al.* (1974) found similar results when they tested various dolomites.

*iii) Sulfidation Kinetics* Table 2 compiles the fractional sulfidation of $CaCO_3$ in samples of each of the three sorbents for two exposure durations. In samples of the three sorbents exposed to a 1% $H_2S$ concentration at the same temperature for two hours the $CaCO_3$ was completely converted to CaS. It is clear that a higher $MgCO_3$ content has two major effects: it increases the reactivity of the sorbent with $H_2S$ but also increases sorbent pulverization, resulting in a severe increase in "dust". Increased reactivity results from the increase in porosity and structural stability provided by MgO in the sorbent. However, the flash calcination of rapidly heated $MgCO_3$ releases $CO_2$ that bursts parts of the sorbent into fine pieces. High-magnesium dolomites are thus undesirable if one wants to limit the loading of dust in the coal gas. Dolomitic limestones, which have a smaller fraction of $MgCO_3$, may prove to have the optimal combination of reactivity and sulfur capacity.

**B. Half-Calcined Sorbents** The following experiments measure the effect of magnesium carbonate present with the calcium carbonate on the sorbent performance at temperatures below calcination. Samples of the three sorbents were exposed to the following gas mixture for varying periods of time at 760, 710 and 610 °C: $N_2$ (52%), $CO_2$ (35%), $H_2$ (5%), CO and $H_2O$ (4%), and $H_2S$ (1000 and 8000 ppm).

*i) Dolomite* It was found that at both 710 °C and 760 °C $CaCO_3$ was directly converted to CaS at a rate only slightly slower than at 915 °C (Table 2) with the same dolomite when the calcium carbonate was calcined to CaO before reacting with $H_2S$ (Figure 4). Moreover, almost complete conversion was obtained after about 16 hours at 760 °C with 1000 ppm $H_2S$ and 2 hours with 8000 ppm. This shows that dolomite can be used to remove $H_2S$ efficiently below the calcination temperature of $CaCO_3$, which is impractical with limestone. (Of course, the equilibrium limitation shown in Fig. 1 still obtains at the lower temperatures.) As the reaction temperature is dropped to 610 °C the sulfidation rate decreases significantly, reflecting both the lower reactivity of $H_2S$ with $CaCO_3$ and the decrease in the calcination rate of $MgCO_3$.

*ii) Dolomitic Limestone* The results for dolomitic limestone (Figure 5) are qualitatively very similar to those obtained with dolomite. The key difference is that complete conversion of the calcium carbonate is no longer possible. Instead, a plateau is reached at about 40% conversion regardless of the temperature or concentration of $H_2S$ in the gas (Fenouil and Lynn, 1995). Consequently, dolomitic limestone, or at least the kind of dolomitic limestone used in this work, does not seem to be a useful sorbent of $H_2S$ for temperatures below the calcination temperature of calcium carbonate. SEM and EDAX pictures of the dolomitic limestone reveal that it is actually a heterogeneous mixture of dolomite and calcium carbonate with domain sizes varying between a fraction of a micron to few hundred microns for each of the constituents. EDAX pictures of

sulfided samples also show that significant amounts of sulfur are present only where magnesium atoms are concentrated (*i.e.* in the dolomitic part of the sorbent) (Fenouil, 1995). This is consistent with the previous observations that the calcium atoms in dolomite completely react with $H_2S$, whereas only 10 to 20% of the calcium atoms in limestone react to form CaS. The average chemical composition of the dolomitic limestone used in this work reveals that there are almost exactly 4 calcium atoms per magnesium atoms, suggesting $[MgCO_3\text{-}CaCO_3]_1 \bullet [CaCO_3]_3$ as a global formula for the sorbent. Out of 4 moles of calcium, the one mole associated with the dolomite regions, plus 10 to 20% of the three moles associated with the limestone regions react to form CaS to yield an overall conversion of 33 to 40%. Dolomitic limestones with higher (or lower) Mg/Ca ratios would be expected to show correspondingly higher (or lower) sulfidations when exposed to $H_2S$ at temperatures below the calcination temperature of $CaCO_3$.

*iii) Limestone* Experiments with limestone particles exposed to the same simulated coal gas as the dolomite and dolomitic limestone samples for temperatures ranging from 760 to 610 °C confirmed previously published results (Fenouil *et al.*, 1994) that a plateau in the conversion of $CaCO_3$ to CaS is rapidly reached at all temperatures. At 760°C under 1000 ppm of $H_2S$ the conversion stays limited to about 10% CaS, with no incremental conversion between 6 and 14 hours of exposure. At 610 °C under 8000 ppm of $H_2S$, only 17% conversion was achieved after 25 hours of exposure. The presence of $MgCO_3$ (MgO) is essential to achieve complete, and moderately rapid, $CaCO_3$ sulfidation.

## C. Design of Sorption Systems

Analysis of the data for sorption of $H_2S$ by large calcined limestone pellets above 700 °C showed that the kinetics is fit very well by either the Unreacted Shrinking Core Model or the Grain Model (Fenouil and Lynn, 1995). Differential equations based on both models were solved analytically to determine the concentration profiles in several sorption systems (moving, packed, and fluidized beds and entrained-flow). The behavior of these reactors can be expressed as a function of only 4 parameters: the size of the sorbent pellet and the Péclet, Sherwood (or Biot), and Damköhler numbers. These general equations were then applied to the lime(stone)/$H_2S$ systems. Using limestone particles with diameters of the order of 100 $\mu$m for entrained-flow, and with diameters of the order of one millimeter for the other configurations, it was found that $H_2S$ could be removed from the hot coal gas to near its equilibrium value with more than 75% sorbent utilization and with reasonable bed depth (about one meter, or 1 s. contact time for entrained-flow) when the reactor temperature is maintained 25 to 50 °C above the calcination temperature of the calcium carbonate.

Figures 6 and 7 show the concentration profiles for countercurrent and cocurrent moving beds, respectively. The term Z is the dimensionless ratio of the bed length to the particle radius. Pe'' is a modified Péclet number, which characterizes the effects of particle radius, grain radius, particle porosity, and the diffusivity of the gas in the porous solid and in the CaS product layer. It has a value of the order of 500 to 1000 at 35 bar total pressure. A typical value of the modified Sherwood number (Sh'') is of the order of 100 (Fenouil, 1995). As would be expected, countercurrent flow of gas and solids is the more efficient since the gas is contacted with the most reactive pellets when its $H_2S$ content is most dilute. These equations, combined with the

kinetic data for the $CaCO_3/H_2S$ and $CaO/H_2S$ systems, provide a practical way to design and scale-up the reactor configurations considered in this work. Furthermore, the equations can be combined with kinetic data for other sorbents, such as zinc ferrite, to model their use in these sorption systems.

## CONCLUSIONS

i) For temperatures slightly *above* the calcination temperature of $CaCO_3$ (about 900 °C under 1 bar of $CO_2$), complete conversion of $CaCO_3$ to CaS by $H_2S$ is achievable for all three sorbents. The reaction rate increases as the magnesium-to-calcium ratio increases in the sorbent. However, chemical attrition of the sorbent also increases as more magnesium is present and is responsible for the formation of a relatively large quantity of fine powder. Limestone, which has the best sulfur loading, should thus be the sorbent of choice, but dolomitic limestone and dolomite can also be used.

ii) For temperatures *below* the calcination temperature of $CaCO_3$, limestone and dolomitic limestone are not effective $H_2S$ sorbents. Dolomite is the only tested sorbent that could be completely sulfided. At any temperature above 700 °C, the rate of dolomite sulfidation is quite comparable to the rates of either of the other two sorbents when they are used above the calcination temperature of calcium carbonate. However, it is still necessary to operate near the calcination temperature for $CaCO_3$ to achieve maximum $H_2S$ removal from the coal gas.

**Acknowledgment.** The authors would like to thank the Great Lakes Corporation and James Welshimer from National Lime and Stone Company for their samples.

## FUTURE WORK

There are two advantages to using a separate sorption system, compared to mixing the limestone with the coal in the gasifier. First, because the sorption can occur near the optimal temperature, a significantly higher Ca/S ratio can be achieved. Second, the CaS can be kept relatively clean, which facilitates treating the CaS to obtain elemental sulfur and $CaCO_3$. The latter can be formed into pellets and recycled to the sorption system, fed as an anti-caking agent and catalyst to the gasifier, or discarded as a non-hazardous waste. Reacting solid CaS with $CO_2$ and steam is an unsatisfactory method of regeneration because the resultant $CaCO_3$ loses capacity for $H_2S$ after repeated recycling (Sun *et al.*, Swisher and Schwerdtfeger, 1992).

CaS is only sparingly soluble in water, whereas $Ca(HS)_2$ is highly soluble. It is difficult to obtain a satisfactory reaction between $CO_2$ and CaS in an aqueous slurry because a layer of $CaCO_3$ coats the particles of CaS and slows the reaction. The preferred approach is first to dissolve the CaS with $H_2S$:

$$CaS + H_2S \rightarrow Ca(HS)_2$$

and then to precipitate $CaCO_3$ from the aqueous solution:

$$Ca(HS)_2 + CO_2 + H_2O \rightarrow CaCO_3 + 2\ H_2S$$

The $H_2S$ would be recovered as a gas containing no more than 10% $CO_2$ and converted into elemental sulfur by known technology. There are two problems with this reaction system: First, a slurry of CaS in water dissolves very slowly when $H_2S$ is bubbled into it because the solubility of $H_2S$ in water is very low. Second, the rate of

reaction between $CO_2$ and $Ca(HS)_2$ has a low rate since $CO_2$ is rather sparingly soluble and the kinetics of the hydration of $CO_2$ is also slow. A patent application has been filed for a process that solves these problems: it greatly facilitates both reaction steps, prevents the formation of a carbonate coating on the CaS particles, and also aids in the recovery of a relatively pure stream of $H_2S$.

## REFERENCES


Alvfors, P.; Svedberg, G.; "Modelling of the Simultaneous Calcination, Sintering and Sulphation of Limestone and Dolomite". *Chem. Eng. Sci.*, 1992, **47**(8), 1903-1912.

Borgwardt, R.H.; Bruce, K.R.; "Effect of Specific Surface Area on the Reactivity of CaO with $SO_2$", *AIChE Journal*, 1986, **32**(2), 239-246.

Borgwardt, R.H.; Roache, N.F., "Reaction of $H_2S$ and Sulfur with Limestone Particles". *Ind. Eng. Chem. Process Des. Dev.*, 1984, **23**, 742-748.

Chang, E.Y.; Thodos, G.; "Complex Nature of the Sulfation Reaction of Limestones and Dolomites". *AIChE Journal*, 1984, **30(3)**, 450-457.

Davini, P.; DeMichele, G.; Ghetti, P.; "An Investigation of the Influence of Sodium Chloride on the Desulphurization Properties of Limestone". *Fuel*, 1992, **71**, 831-834.

Fenouil, L.A.; "Kinetic and Structural Studies of the Sulfidation of Large Particles of Lime and Limestone in Coal Gas". PhD Dissertation, University of California at Berkeley, 1995.

Fenouil, L.A.; Lynn, S.; "Study of Calcium-Based Sorbents for High-Temperature $H_2S$ Removal". Accepted for publication in *Ind. Eng. Chem. Res.*, 1995.

Fenouil, L.A.; Towler, G.P.; Lynn, S.; "Removal of $H_2S$ from Coal-Gas Using Limestone: Kinetic Considerations". *Ind. Eng. Chem. Res.*, 1994, **33**(2), 265-272.

Freund, H.; "Kinetics of Limestone/Dolomite with $H_2S$ under Rich Combustion Conditions". *Combustion Science and Technology*, 1981, **26**, 83-88.

Haji-Sulaiman, M.Z.; Scaroni, A.W.; Yavuzkurt, S.,; "Optimum Sulfation Temperature for Sorbents Used in Fluidized Bed Coal Combustion". *Fuel Processing Technology*, 1990, **25**, 227-240.

Hartman, M.; Pata, J.; Coughlin, R.W.; "Influence of Porosity of Calcium Carbonates on their Reactivity with Sulfur Dioxide". *Ind. Eng. Chem. Process Des. Dev.*, 1978, **17(4)**, 411-419.

Leppälahti, J., Simell, P., Kurkela, E.; "Catalytic Conversion of Nitrogen Compounds in Gasification Gas", *Fuel Processing Technology*, 1991, **29**, 43-56.

Newby, R.A., Alvin, M.A., Bachovchin, D.M., Smeltzer, E.E.; Integrated Low Emissions Cleanup System for Multi-Contaminant Control, Proceedings of the Coal-Fired Power Systems 93--Advances in IGCC and PFBC Review Meeting. DOE/METC-93/6131. DE93000289, 1993.

Newton, G.H., Harrison, D.J., Silcox, G.D, Pershing, D.W., *Environ. Progress*, 1986, **5**(2), 140-145.

Nowacki, P., *Coal Gasification Processes*, Noyes Data Corp., Park Ridge, New Jersey, U.S.A., 1981.

O'Neill, E.P.; Keairns, D.L.; Kittle, W.F.; "A Thermogravimetric Study of the Sulfation of Limestone and Dolomite-The Effect of Calcination Conditions". *Thermochimica Acta*, 1976, **14**, 209-220.

Robertson, A., and 13 others, "Second-Generation PFBC Systems Research and Development – Phase 2: Best Efficiency in Light of Current Data", Proceedings of the Coal-Fired Power Systems 93 - - Advances in IGCC and PFBC Review Meeting. DOE/METC - 93/6131. DE93000289, 1993.

Ruth, L.A.; Squires, A.M.; Graff, R.A.; "Desulfurization of Fuels with Half-Calcined Dolomite: First Kinetic Data". *Environmental Science and Technology*, 1972, **6**(12), 1009-1114.

Squires, A.M.; Graff, R.A; Pell, M.; "Desulfurization of Fuel with Calcined Dolomite. I. Introduction and First Kinetic Results". *Chem. Eng. Prog. Symp. Series*, 1971, **67(115)**, 23-34.

Sun, C.C.; O'Neill, E.P.; Keairns, D.L.; "The Sulfidation and Regeneration of Half-Calcined Dolomite". *Thermochimica Acta*, 1978, **26**, 283-296.

Swisher, J.H.; Schwerdtfeger,K.; "Review of Metals and Binary Oxides as Sorbents for Removing Sulfur from Coal-Derived Gases". *Journal of Materials Engineering and Performance*, 1992, **1(3)**, 399-408.

Ulerich, N.H.; O'Neill, E.P.; Keairns, D.L.; "A Thermogravimetric Study of the Effect of Pore Volume-Pore Size Distribution on the Sulfation of calcined Limestone". *Thermochimica Acta*, 1978, **26**, 269-282.

Wilson, K.B.; Haas, J.C.; Eshelman, M.B.; Applications of Moving Granular-Bed Filters to Advanced Systems, Proceedings of the Coal-Fired Power Systems 93-- Advances in IGCC and PFBC Review Meeting. DOE/METC-93/6131. DE-93000289, 1993.

Yen, J.H., "Kinetic and Structural Studies in the Sulfidation of Dolomite", PhD Dissertation, Department of Chemical Engineering, Carnegie-Mellon University, 1979.

**Table 1: Average composition of the three sorbents (wt% basis)**

| | $CaCO_3$ | $MgCO_3$ | $SiO_2$ | $Fe_2O_3$ | S | $Al_2O_3$ |
|---|---|---|---|---|---|---|
| Limestone | 97.8 | 1.63 | 0.28 | 0.15 | 0.065 | 0.13 |
| Dolomitic Lime-stone | 80 | 17 | 2.5 | 0.2 | 0.1 | --- |
| Dolomite | 54.5 | 45.0 | 0.3 | 0.07 | 0.03 | 0.08 |

**Table 2: Conversion of $CaCO_3$ to CaS with time for three sorbents (900 ppm $H_2S$ at 915°C)**

| Time (min) | Limestone | Dolomitic Lime-stone | Dolomite |
|---|---|---|---|
| 240 | 18 ± 5% | 21 ± 5% | 35 ± 5% |
| 360 | 23 ± 5% | 30 ± 5% | 55 ± 5% |

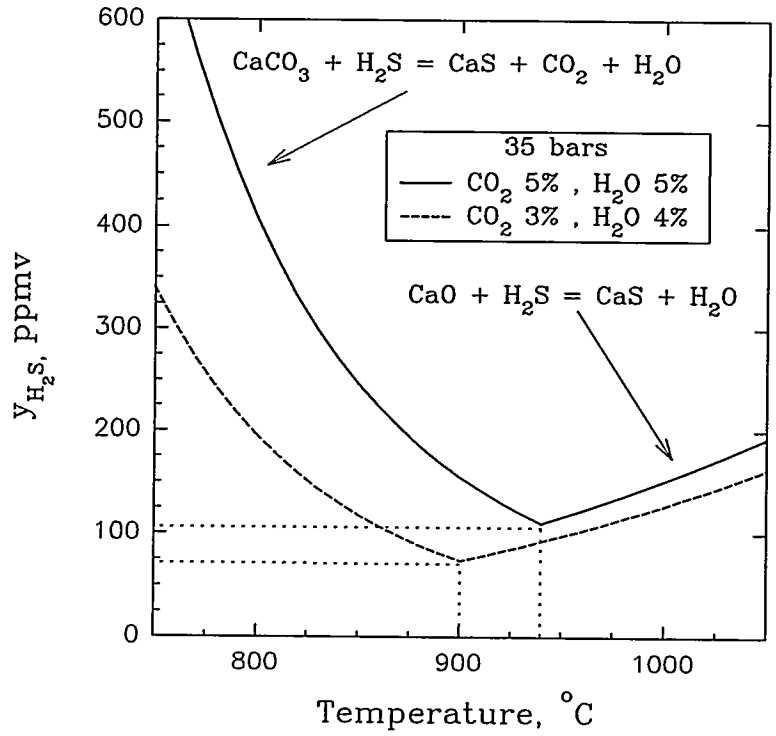


**Figure 1: Effect of Temperature, $CO_2$ and $H_2O$ on $H_2S$ Sorption from Coal Gas**

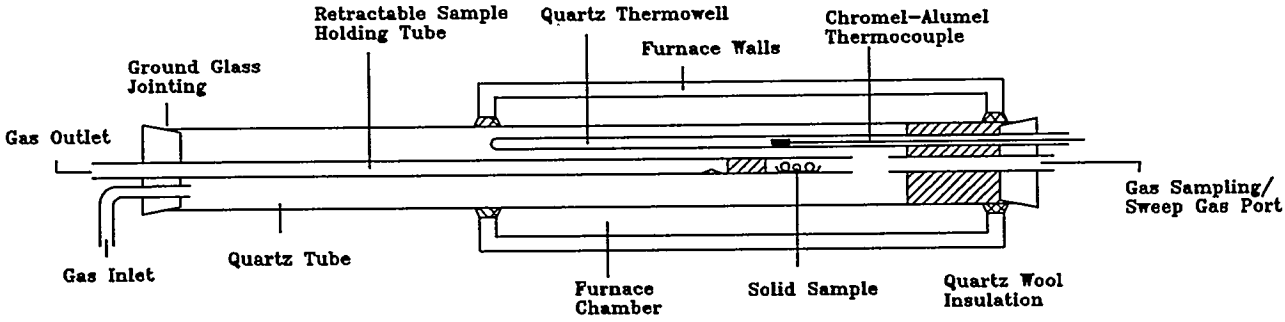


**Figure 2: Differential Tube Reactor.**

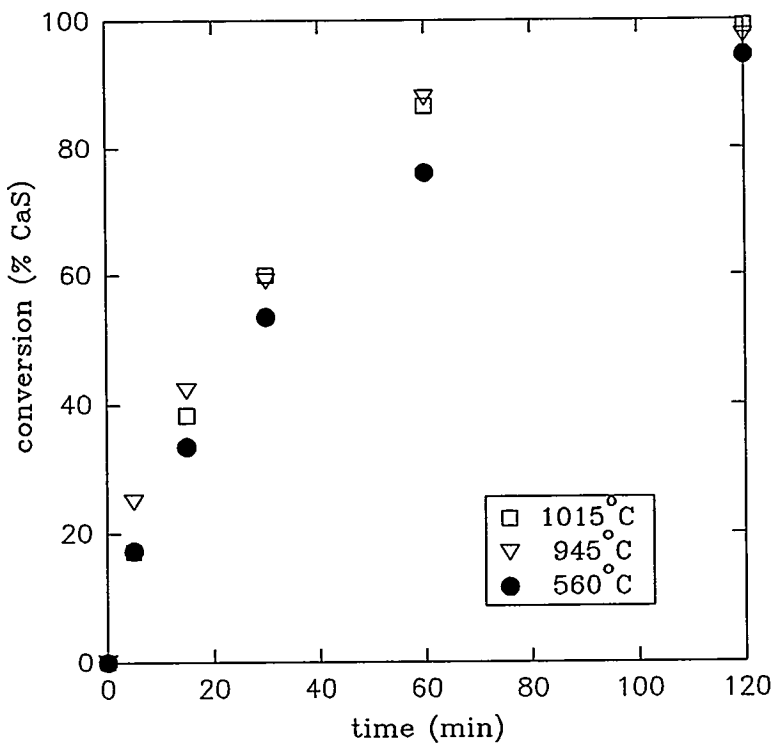


**Figure 3: Effect of Temperature on Lime Conversion**
**1015 °C: 87.5% $CO_2$; 5.25% CO & $H_2O$; 0.7% $H_2$; 1.3% $H_2S$ (no precalcination)**
**945 °C: 88% $CO_2$; 4.75% CO & $H_2O$; 0.8% $H_2$; 1.7% $H_2S$ (no precalcination)**
**560 °C: 93.3% $N_2$; 5.0% $H_2$; 1.7% $H_2S$ (precalcined for 30 min. under $N_2$ at 865 °C)**

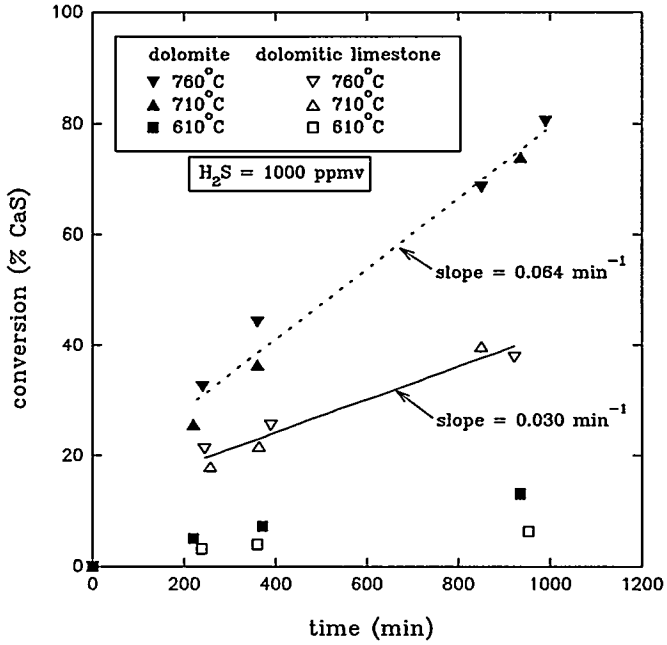


**Figure 4: Conversion Data for Dolomite and Dolomitic Limestone for Low Levels of $H_2S$**

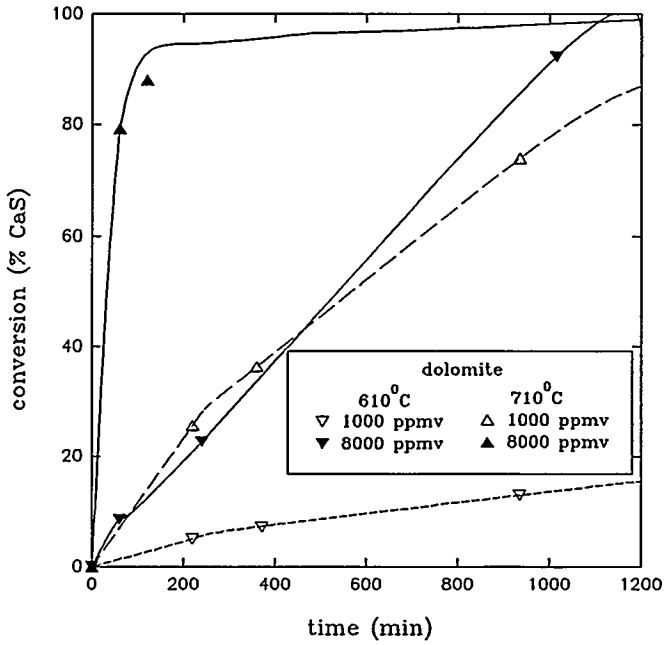


**Figure 5: Comparison of the Sulfidation Kinetics of Dolomite under 1000 and 8000 ppm $H_2S$ at 610 °C and 710 °C**

PB.14

# A Long Life ZnO - $TiO_2$ Sorbent

## CONTRACT INFORMATION

| | |
|---|---|
| **Contract Number** | DE-FG03-94ER84881 |
| **Contractor** | TDA Research, Inc.<br>12345 West 52nd Avenue<br>Wheat Ridge, Colorado 80033<br>(303) 422-7819 |
| **Contractor Project Manager** | Michael E. Karpuk |
| **Principal Investigator** | Robert J. Copeland<br>Mike Cesario<br>Margarita Dubovik<br>Dan Feinberg<br>Brian Windecker |
| **METC Project Manager** | Ronald Staubly |
| **Period of Performance** | August 1994 - April 1995 |

**Schedule and Milestones**

**FY95 Program Schedule**

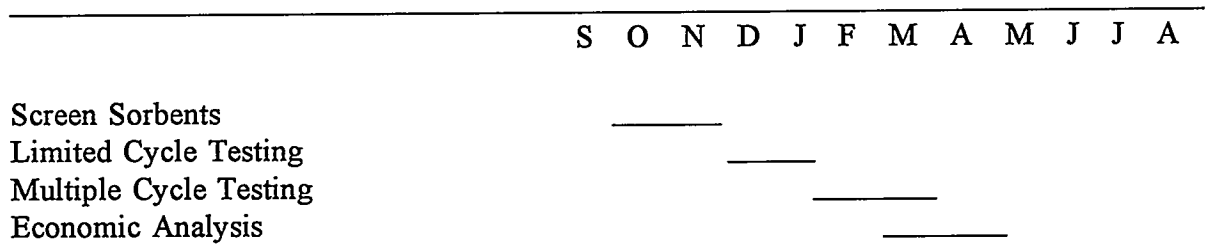


## OBJECTIVES

The objective of this Phase I SBIR was to develop and test a long life ZnO-$TiO_2$ sorbent for hot gas cleanup. Specifically, we measured the sulfur loading at space velocities typically used for absorption of $H_2S$ and regenerated the sorbent with diluted air containing $SO_2$ for multiple cycles. Based on the experimental results, we prepare a conceptual design of the sorbent fabrication system, and estimated the cost of producing the sorbent and the cost of sulfur removal.

## BACKGROUND INFORMATION

Combined cycles (combinations of a gas turbine and a steam bottoming cycle) are the most efficient power generation technology, while coal is the lowest cost fuel. Therefore, the combination of Coal Gasifiers and Combined Cycles is predicted to be the lowest cost source of baseload electric power in the next decade. Indeed, there are now six Coal Gasification Combined Cycles (GCCs) with a total value of over 1.5 billion dollars under construction as part of the DOE Clean Coal Program, and over half of this investment is contributed by industry.

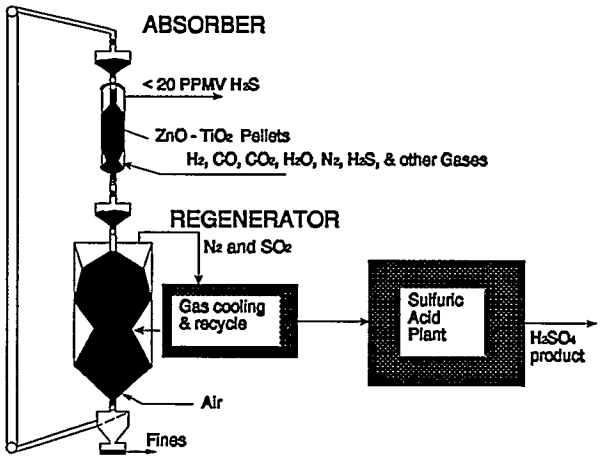


**Figure 1. Moving Bed Reactor System**

In a GCC, the sulfur and particulates are removed from the gasifier gases before they enter the turbine combuster. While $H_2S$ (and $COS/CS_2$) can be removed effectively by cooling hot gases down to near room temperature and scrubbing them with an aqueous amine solution, removing the $H_2S$ without cooling the gases (*i.e.*, hot gas cleanup) is more advantageous.

The leading hot gas sulfur absorbent uses a regenerable zinc oxide (ZnO) based sorbent, zinc titanate ($Zn_2TiO_4$ and/or $ZnTiO_3$), to remove the $H_2S$ and other sulfur compounds from the hot coal gases. The zinc absorbs $H_2S$, forming ZnS, ZnS is then regenerated with oxygen (air), releasing the sulfur as a concentrated stream of $SO_2$. The $SO_2$ can be converted into sulfuric acid, sulfur, or reacted with calcium carbonate to form calcium sulfate (gypsum). A schematic of a moving bed system with the production of sulfuric acid from the $SO_2$ is shown in Figure 1.

ZnO has a high affinity for $H_2S$ and produces a very clean gas stream. Unfortunately, the life of many ZnO based sorbents is very limited, especially in fixed and moving bed reactors. The molar volumes of the ZnS is 50% greater than that of ZnO. During regeneration some zinc sulfate can form, which can occupy more than 250% of the volume of the original ZnO. Prior to returning to the absorber, the zinc sulfate is decomposed and returns the sorbent to its originally oxide form. Thus, the zinc atoms move substantially during absorption (to ZnS), to regeneration (to ZnO and some $ZnO*2ZnSO_4$), and finally back to the oxide (ZnO). This repeated expansion and contraction of the sorbent as it is cycled causes many sorbents to spall (*i.e.*, break into small pieces), which eventually destroys the sorbent (Jung *et al.* 1992)(Mei *et al.* 1993). Because of the high sorbent loss rate, fresh sorbent must be continually added to the process. This continual replacement increases the cost of sulfur removal; substantial cost reductions could be achieved by making a more durable sorbent.

Recent developments in hot gas cleanup sorbents have reduced the spalling of the sorbent. Ayala *et al.* (1994) present data on both Z-Sorb and an improved zinc titanate. Z-Sorb, a product of Phillips Petroleum Company, performs well but is currently expensive. Similarly the zinc titanates are also expensive. These high costs are in part due to the high costs associated with small scale production but there may be factors in their production that require high costs. For example, several of Phillips' patents (*e.g.*, Khare 1994, Khare 1993, and Kidd *et al.* 1993) require the use

of an aqueous acid solution (*e.g.*, nitric acid or acetic acid), which is later decomposed. Since the acids are lost in manufacture and the production equipment may be inherently expensive to handle acidic mixtures, Z-Sorb may be unavoidably expensive. What is needed is a low cost sorbent that contains a large amount of active and accessible chemical sorbent and also has a long life.

## PROJECT DESCRIPTION

In order to make a sorbent pellet that can hold large amounts of sorbent without being destroyed by the absorption-regeneration process, TDA has developed a new sorbent structure. This sorbent structure: 1) is very strong, 2) allows the sorbent to expand and contract freely without disrupting the pellet structure, 3) allows the $H_2S$ to diffuse quickly into the interior of the pellet, and 4) can contain very large amounts of sorbent without spalling.

TDA's process to produce the sorbent is also inherently low in cost and can achieve high loadings of the chemically active material. The sorbent is formed by mixed metal oxide techniques (*i.e.*, all of the ingredients are mixed at ambient temperature and fired only once), yet the sorbent has the high strength and long life typical of a catalyst support. In addition, the sorbent fabrication process does not require the use of an expensive decomposable salt.

### Sorbent Preparation and Screening

TDA prepared small quantities of sorbents with many different compositions in order to identify the preferred firing conditions and starting materials. First we screened our raw materials by producing small batches of either chemical sorbent only or inert support only. Several sources of ZnO and titania were evaluated and tested to determine their crush strength, porosity, and surface area. From this matrix, we selected one source of zinc oxide and one titania. To minimize the loss of surface area in the sorbent we required that the sorbent be fired at a temperatures of 900°C (1652°F) or less.

Then we produced sorbents with varying ZnO contents. We exposed these samples to 1% $H_2S$ for 6 hours using simulated Texaco gasifier gases. We measured the sulfur content by chemical analysis after the first absorption and eliminated those compositions that had low sulfur loadings. We prepared a larger quantity of five different sorbents and cycled them through 8 absorption and regeneration cycles. We measured the sulfur content, pore volume, and crush strength of the initial material, and then remeasured these properties after the 1$^{st}$ regeneration, after the 3$^{rd}$ absorption, after the 8$^{th}$ absorption, and after the 8$^{th}$ regeneration.

From these tests we selected three formulations for further evaluation. We then described the sorbent preparation methods to Norton Chemical Process Products Corporation (Norton). Norton is one of the world's leading producers of ceramic products and catalyst supports. Under contract with TDA, Norton then prepared larger batches of sorbents. Norton extruded > 1 kg samples of the most promising formulations using techniques that are representative of commercial practice. Table I presents the properties of these extrudates.

TDA measured the resistance to spalling of the extrudates prepared at Norton (*i.e.*, by exposing them to 5% $SO_2$, 20% $O_2$ at 760°C for two hours). None of the extrudates spalled. The extrudate with the highest zinc oxide content (*i.e.*, TMZ-6) was selected and tested to determine its breakthrough characteristics with multiple cycling. TMZ-6II, the second batch of the same formulation, is made in the same manner as TMZ-6; but TMZ-6II has a slightly lower ZnO content.

**Table I. Norton Produced Extrudates**

| Extrudate | Crush: lb/mm | Pore volume cc/g | ZnO (wt.) |
|---|---|---|---|
| NXTZ-1 | 1.0 | 0.28 | 41% |
| NXTZ-2 | 2.9 | 0.28 | 33% |
| NXTZ-3 | 2.1 | 0.32 | 33% |
| NXTZ-4 | 0.5 | 0.33 | 40% |
| TMZ-5 | 2.4 | 0.21 | 49% |
| TMZ-6<br>TMZ-6II | 1.1<br>1.3 | 0.26<br>0.27 | 48%<br>44% |

## RESULTS

### Breakthrough Testing

Each of the absorption half cycles was conducted with 1% $H_2S$ and simulated Texaco gasifier gases entering the reactor at 538°C (1,000°F). The breakthrough data were measured until the exit gas stream exceeded 500 ppmv $H_2S$. The absorption was then continued for 2 more hours with 1% $H_2S$ and then the sorbent was exposed to 6% $H_2S$ at a lower space velocity (SV). The later stages fully loaded all of the sorbent in the reactor with sulfur, thereby exposing the sorbent to the most damaging conditions. Two sets of regeneration cycles were carried out as follows:

TMZ-6 Mild regenerations (only $N_2$ diluted air in the inlet), and

TMZ-6II Regenerations with $SO_2$ added to the inlet (*i.e.*, $\leq$ 5% $SO_2$ and $\leq$ 20% $O_2$ gases with temperatures to 760°C, 1400°F).

During the regenerations we raised the sorbent bed to 600°C and flowed diluted air for about 6 hours to oxidize the zinc sulfide to zinc oxide. We then increased the $O_2$ concentration in stages, finally flowing only air through the reactor at 700°C (TMZ-6). During the second series (*i.e.*, with TMZ-6II), $SO_2$ was added to the inlet air throughout the regeneration for all cycles. During the final regeneration we exposed the sorbent to 5% $SO_2$, 20% $O_2$ for 2 hours with the reactor at 760°C. This is a very severe test because the addition of $SO_2$ produces large quantities of zinc sulfate in the sorbent, *i.e.* sulfation. Following the sulfation, we then purged the reactor with $N_2$ at 760°C for 2 hours to decompose the sulfate and to return the sorbent to its original oxide form. We then compared the used and fresh sorbents in the same (*i.e.*, ZnO) chemical state.

**Table II. Fresh & Cycled TMZ-6 Properties**

| Property | Fresh | 20 cycles |
|---|---|---|
| Crush Strength | 1.1 lb/mm | 1.7 lb/mm |
| Pore Volume | 0.26 ml/g | 0.31 ml/g |
| Wetability | 0.15 cc/g | 0.13 cc/g |
| Bulk Density | 1.3 g/cc | 1.3 g/cc |
| Surface Area | 2.5 $m^2/g$ | 2.8 $m^2/g$ |
| Sulfur (wt.) | 0.00% | 0.14% |

**Testing of TMZ-6.** Table II presents the measured properties of the TMZ-6 sorbent before and after a 20 cycle test. There is very little change in the characteristics of the sorbent over the 20 cycles. The crush strength was slightly increased. The porosity and surface area were also slightly improved. The overall bulk density of the sorbent bed was unchanged and the sorbent

retained little sulfur upon regeneration after 20 cycles. Perhaps most importantly, we measured the mass of the sorbent added to and removed from the reactor after the tests; the loss rate was less than 0.1% per cycle.

Figure 2 presents the breakthrough characteristics for TMZ-6 through 20 cycles. Although the sorbent removes $H_2S$ effectively, a background level at 100 ppm(v) $H_2S$ was measured in our tests. This background is present because our tests used a stainless steel reactor that had been previously used and contain significant quantities of iron oxide, which reacted to FeS during absorptions. The FeS produced elemental sulfur by reaction with $SO_2$. Due to the sulfur contamination in the stainless steel reactor, we were not able to measure the actual equilibrium concentration at the reactor outlet. Based on previous work, the zinc oxide/titanates will remove the $H_2S$ down to about 20 ppmv. The breakthrough data also show that the sorbent remained active throughout the 20 cycles. The data show some scatter in the breakthrough time, which was due to experimental difficulties that produced incomplete regeneration in some cases.

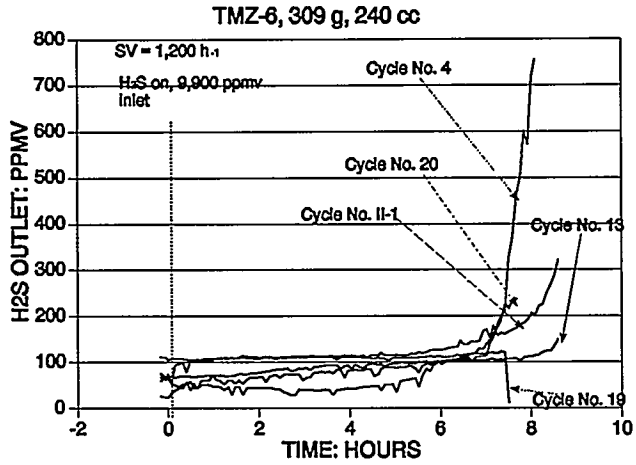


**Figure 2. Cycling Of TMZ-6**

**Testing of TMZ-6II.** Table III presents the measured properties of the TMZ-6II sorbent before and after 3 cycles. Samples were removed after the 3rd absorption (*i.e.*, noted as ZnS) and after the 3rd regeneration (*i.e.*, noted as ZnO). These test results indicate that there were only minimal changes in the characteristics of the sorbent. Again the sorbent crush strength slightly improved and the porosity also increased. The sulfided form of the sorbent was substantially stronger than the oxide form and it also had a higher surface area.

**Table III. TMZ-6II Before & After Cycling**

| Property | Fresh | 3rd Cycle |
|---|---|---|
| Crush Strength lb/mm | 1.3 | 1.6 (ZnO)<br>2.8 (ZnS) |
| Pore Volume: cc/g | 0.27 | 0.27 (ZnO) |
| Wetability: cc/g<br>ZnO<br>ZnS | 0.18 | 0.18<br>0.08 |
| 3rd Regen.<br>3rd Absorption | Sulfur (wt.) | 0.01%<br>16.1% |
| Bulk Density | 1.3 g/cc | 1.3 g/cc |
| Surface Area ZnO<br>ZnS | 2.3 $m^2/g$ | 1.5 $m^2/g$<br>3.9 $m^2/g$ |

During the time before 0 hours we were flowing $H_2$, $H_2O$, CO, and $CO_2$ but no $H_2S$. The high level of $H_2S$ was released by the reductive regeneration of zinc sulfate, which was formed during the regeneration with $SO_2$ and $O_2$. This large peak was not seen with the first series (*i.e.*, TMZ-6, Figure 2), since the regeneration conditions were less severe.

The breakthrough curves for TMZ-6II are similar to those obtained in the first series (TMZ-6). The breakthrough data in Figure 3

showed an increase in breakthrough time with cycling. The longest time occurred in cycle No. II-2 but cycle No. II-3 was also longer than the initial material. However, since the level of sulfur contamination in the reactor was unknown, we can only conclude that the sorbent remained active; additional work would be needed to establish the extent to which the activity is affected with cycling.

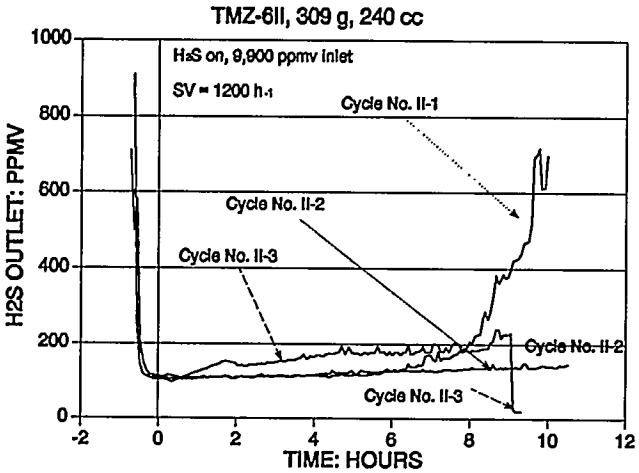


**Figure 3. Breakthrough With TMZ-6II**

## Comparison to Other Sorbents

We compared our sorbent to other sorbents currently being developed for hot gas cleanup. Table IV presents a comparison of the sulfur loading in the sorbent for TMZ-6, a United Catalyst Incorporated (UCI) zinc titanate, and Z-Sorb B, produced by the Phillips Petroleum Corporation.

The theoretical maximum sulfur loading is lower in our sorbent, due to a lower ZnO content. The fraction of the sorbent that is converted to ZnS in our sorbent is significantly higher in our sorbent than in zinc titanate, but approximately equal to that of Z-Sorb. The bulk density of our sorbent bed is less than zinc titanate but higher than Z-Sorb. The net sulfur loading per unit volume of the bed (*i.e.*, which determines the size of the absorber and sorbent cycling rate) is significantly higher for TMZ-6 than the competing sorbents.

**Table IV. Comparison Of Sorbents**

| | TDA TMZ-6 | UCI L-4103 B2 | Phillips Z-SORB |
|---|---|---|---|
| Sulfur Capacity (#/100 #) | 19 | 25 | 20 |
| % Total S | 16 * | 6.0 - 8.9 | 10.6 - 16.2 |
| % Sulfur Capacity | 90 | 27 - 40 | 58 - 88 |
| lb per $ft^3$ | 80 | 107 | 60 |
| lb S per $ft^3$ of Bed | 13.8 | ≈ 9 (7.3 - 10.7) | ≈ 9 (7.0 - 10.7) |

measured at end of 20th absorption.

We estimated the cost of producing our sorbents. The cost is very sensitive to the annual production quantity. We estimated the costs for a dedicated plant that produces 60 tons/year of sorbent (*e.g.*, the requirements of a CCT demonstration plant). With a two year payback on the capital, the estimated costs were $9/lb for TMZ-6. However, if the production quantity were 600 tons/year, the costs would drop substantially, to about $3.40/lb.

Table V presents the economics of hot gas cleanup using several different zinc oxide based sorbents. In this case we have assumed the same life for all of the sorbents. We assume the cost for zinc titanate to be $3.20/lb assuming the same cost for ZT-4 (Gangwal and Gupta 1994). Although Z-Sorb currently sells for a significantly

higher price, we assumed a cost of $5/lb in large scale production. Hot gas cleanup using TMZ-6, a sorbent developed and tested in Phase I, is significantly less than other systems developed to date.

**Table V. Sorbent Replacement Costs**

| Cost Element | TDA TMZ-6 | UCI L-4103 B2 Zinc titanate [1] | Phillips Z-Sorb B [1] |
|---|---|---|---|
| Sulfur: wt.% | 16 | 7.5 | 13 |
| Loss Rate: %/cycle | 0.1 | 0.1 | 0.1 |
| Cost: $/ton sorbent | 6,800 | 6,400 [2] | 10,000 [3] |
| Cost of Sorbent Replacement | $43 per ton sulfur | $85 per ton sulfur | $77 per ton sulfur |

1 Ayala and Gupta (1994)
2 Gangwal and Gupta (1994), $3.20/lb for ZT-4 in large scale production.
3 $12/lb to $15/lb currently; TDA assumed $5/lb for large scale production.

Given that we are still early in our development, the cost/performance of our sorbents is anticipated to be further improved by the work to be done in a recently granted Phase II. For example, if we are able to produce a commercial sorbent with the zinc oxide content and cost of TMZ-6, we could reduce the sorbent replacement cost by 25%. In addition, the higher loading of sorbent could potentially reduce the capital cost of the power plant, saving an additional 10% in equivalent sorbent replacement costs. Potentially, we can reduce the equivalent cost for sorbent replacement to less than $40 per ton of sulfur (or about half that of current sorbents).

## FUTURE WORK

TDA produced several different sorbent formulations with different zinc oxide contents, and different strengths and pore volumes. One sorbent formulation was selected for multiple cycle tests, and the measured properties of the sorbent improved slightly over the 20 cycle test (TMZ-6). The initial selection was a sorbent that has a high sulfur loading capacity. The sorbent is resistant to spalling and retained its reactivity, porosity, and crush strength with cycling.

TDA compared the performance of our sorbents to that of other sorbents. We found that TMZ-6 has a 30% higher sulfur content per unit volume and similar costs to other hot gas cleanup sorbents. However, additional work will be needed to develop and demonstrate that these improvements can be achieved in larger scale and for more cycles.

We will be improving the properties of the $ZnO$-$TiO_2$ sorbent in a recently awarded Phase II. A number of multiple cycle breakthrough tests will be conducted to determine the impact of cycling on different methods of forming the

sorbent. Finally, after an improved sorbent formulation has been developed and proven, a revised production cost analysis will be conducted and the economics of hot gas cleanup calculated and compared to that achieved with other sorbents.

## REFERENCES


Ayala, R.E., T. Chuck, E. Gal, and R.P. Gupta (1994). Development of Sorbents for High Temperature Desulfurization in Moving-Bed Systems," in *Proceedings of the Coal-Fired Power Systems 94 -- Advances in IGCC and PFBC Review Meeting*, Bonk, sponsored by U.S., Department of Energy, Morgantown Energy Technology Center: Morgantown, West Virginia, Report No. DOE/METC-94/1008, (CONF-9406131).

Gangwal, S.K. and R.P. Gupta (1994). "Fluidized-Bed Sorbents," in *Proceedings of the Coal-Fired Power Systems 94 -- Advances in IGCC and PFBC Review Meeting*, editor H.M. McDaniel, R.K. Staubly, and V.K. Venkataraman, sponsored by U.S., Department of Energy, Morgantown Energy Technology Center: Morgantown, West Virginia, Report No. DOE/METC-94/1008 (CONF-9406131).

Jung, D.Y., J.S. Kassman, T.F. Leininger, J.K. Wolfenbarger, and P.P. Yang (1992). "Integration and Testing of Hot Desulfurization and Entrained Flow Gasification for Power Generation Systems," presented at the *Twelfth Annual Gasification and Gas Stream Cleanup Systems Contractors Review Meeting*, Morgantown, West Virginia: Morgantown Energy Technology Center, U.S. Department of Energy, September 15-17.

Khare, G.P. (1993). *Absorption of Hydrogen Sulfide and Absorbent Composition therefor*, United States patent Number 5,244,641.

Khare, G.P. (1994). *Absorption of Hydrogen Sulfide and Absorbent Composition therefor*, United States patent Number 5,306,685.

Kidd, D.R., G.A. Delzere, D.H. Kubicek, and P.F. Schubert (1993). *Selective Removal of Hydrogen Sulfide over a Zinc Oxide and Silica Absorbing Composition*, United States patent Number 5,248,489.

Mei, J.S., L. Gasper-Galvin, C.E. Everitit, and S. Katta (1993). "Fixed-Bed Testing of a Molybdenum-Promoted Zinc Titanate Sorbent for Hot Gas Desulfurization," in *Proceedings of the Coal-Fired Power Systems 93 -- Advances in IGCC and PFBC Review Meeting*, editor D.L. Bonk, sponsored by U.S., Department of Energy, Morgantown Energy Technology Center: Morgantown, West Virginia, Report No. DOE/METC=93/6131 (CONF-9306148).

## PB.15 Development of Advanced Hot-Gas Desulfurization Sorbents

### CONTRACT INFORMATION

| | |
|---|---|
| Contact Number | DE-FG21-94MC31393 |
| Contractor | Hampton University<br>Department of engineering<br>Hampton, VA 23668<br>(804) 727-5288 |
| Contractor Project Manager | K. Jothimurugesan |
| Principal Investigators | K. Jothimurugesan<br>Adeyinka A. Adeyiga<br>Santosh K. Gangwal ( RTI) |
| DOE Project Officer | Kamalendu Das |
| Period of Performance | October 1, 1994 to September 30, 1995 |

Schedule and Milestones

FY 1994 Program Schedule

| | O | N | D | J | F | M | A | M | J | J | A | S |
|---|---|---|---|---|---|---|---|---|---|---|---|---|
| Test Plan | | | | | | | | | | | | |
| Sorbent Preparation | | | | | | | | | | | | |
| Sorbent Screening | | | | | | | | | | | | |

### OBJECTIVES

The objective of this study is to develop hot-gas cleanup sorbents for relatively lower temperature application, with emphasis on the temperature range from 343-538°C (650-1000°F). A number of formulations will be prepared and screened for testing in a 1/2-inch fixed bed reactor at high pressure (1 to 20 atm) and high temperatures using simulated coal-derived fuel-gases. Screening criteria will include, chemical reactivity, stability, and regenerability over the temperature range of 343°C (650°F) to 538°C (1000°F). Each formulation will be tested for up to 5 cycles of absorption and regeneration. To prevent sulfation, catalyst additives will be investigated, which would promote a lower ignition of the regeneration. Selected superior formulation will be tested for long term (up to least 30 cycles) durability and chemical reactivity in the reactor.

## BACKGROUND INFORMATION

Advanced high-efficiency integrated gasification combined cycle (IGCC) power systems are being developed to produce power from coal under the U.S. Department of Energy's (DOE's) multibillion dollar Clean Coal Technology (CCT) Program (Gangwal et al., 1993). In these advanced systems, coal is gasified to produce a gas at high temperature and high pressure (HTHP) conditions. The hot gas is cleaned of contaminants, primarily particulates and sulfur gases such as hydrogen sulfide ($H_2S$) and burned in a combustion turbine. IGCC systems are capable of higher thermal efficiency and lower gaseous, liquid, and solid discharges than conventional pulverized-coal-fired power plants. Hot gas cleanup offers the potentially key advantages of higher plant thermal efficiencies and lower costs due to the elimination of fuel gas cooling and associated heat exchangers.

Sorbents based on zinc oxide are currently the leading candidates and are being developed for moving-, and fluidized-bed reactor applications. Zinc oxide based sorbents can effectively reduce the $H_2S$ in coal gas to 10 ppm levels. Most of the hot-gas desulfurization research has focused on the development of mixed-metal oxide sorbents for application at 538°C (1000°F) to 760 °C (1400°F).

This project aims to develop hot-gas cleanup sorbents for relatively lower temperature applications, 343°C (650°F) to 538°C (1000°F) with emphasis on the temperature range from 400 to 500°C. There are a number of reasons for development of sorbents suitable for this temperature range. Recent economic evaluations (Novem, 1991: Leininger et al., 1992; Rutkowski et al., 1993) have indicated that the thermal efficiency of IGCC systems increases rapidly with the temperature of hot-gas cleanup up to 350°C and then very slowly as the temperature is increased further. This suggests that the temperature severity of the hot-gas cleanup devices can be reduced without significant loss of thermal efficiency. Another important reason to reduce hot-gas cleanup severity is to reduce the operating temperatures and temperature swings of on-off valves and vessels for cyclic fixed-bed desulfurization/regeneration systems, lock-hopper valves for moving-bed applications, and the turbine load control valves. Finally, the current plans in Europe call for hot-gas desulfurization system operation at 350-600 °C. Also iron-oxide process development studies in Japan have concentrated on a temperature range of 400-600 °C. Thus development of suitable advanced sorbents in this temperature range is necessary to remain in the forefront in hot-gas cleanup technology.

## PROJECT DESCRIPTION

### Sorbent Preparation and Characterization

A highly promising method was recently developed under this contract to prepare suitable sorbents. Zinc oxide based sorbents was prepared using this proprietary technique. The following analytical techniques was used to characterize the fresh, sulfided and regenerated sorbents

1. X-ray Diffraction (XRD) for crystalline phase.
2. Surface area measurement will be based on the standard BET method.
3. Hg-porosimetry for pore volume, bulk density, average pore diameter and pore size distribution determination.
4. Atomic Absorption (AA) Spectrometry for elemental composition analysis.

### Experimental Setup

The sorbents were evaluated with respect to their sulfidation-regeneration performance, in a packed-bed microreactor. The set-up is shown schematically in Figure 1.

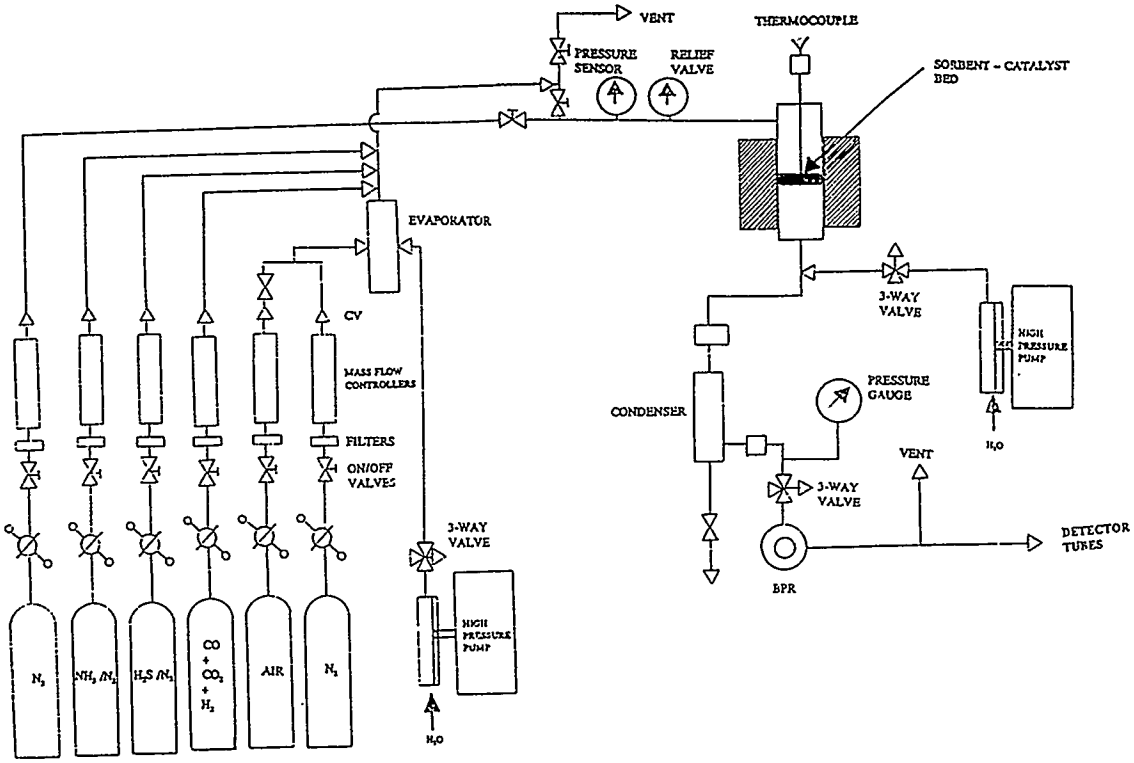


Figure 1. Schematic of the Reactor System for Sulfidation and Regeneration Studies

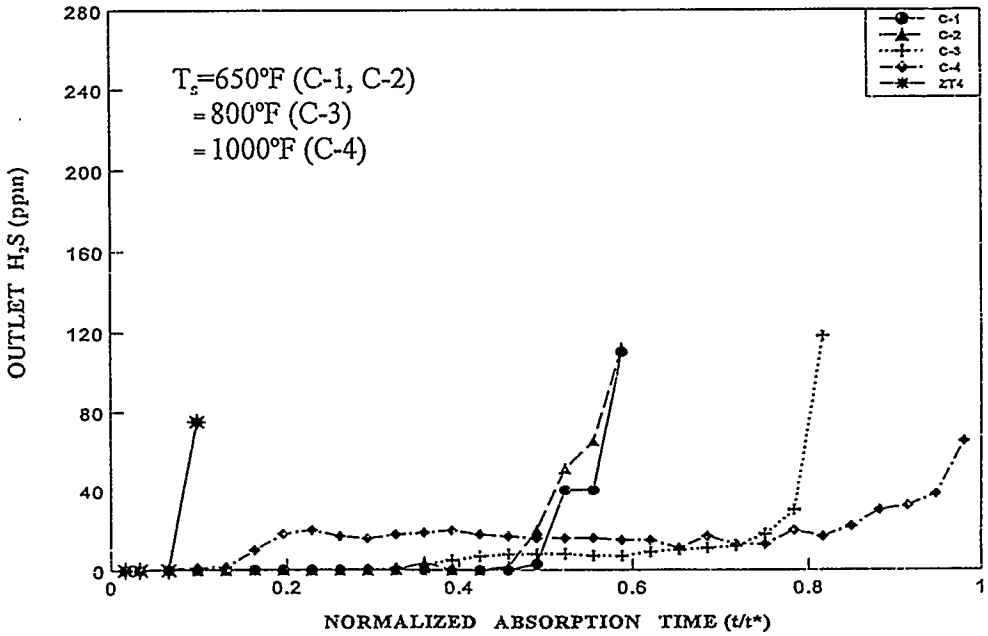


Figure 2. $H_2S$ Breakthrough Curves in Successive Sulfidation Cycles of Sorbent MCRH-1

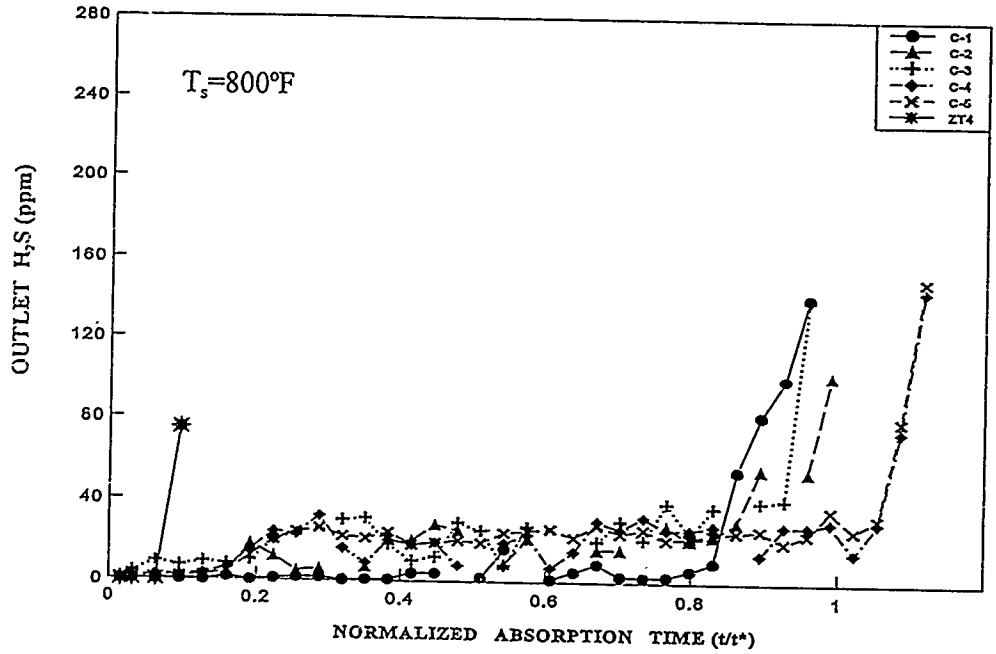


Figure 3. $H_2S$ Breakthrough Curves in Successive Sulfidation Cycles of Sorbent MCRH-10

This system includes a feed gas supply section in which the simulated coal gas components, supplied from standard high-pressure cylinders equipped with pressure regulators, are mixed and metered by a battery of electronic mass flow controllers. Steam is added to the mixed dry gas by vaporizing liquid water injected into the gas stream at a controlled rate by a high pressure metering pump. The pressure inside the reactor is controlled by a back pressure regulator and measured by an electronic pressure sensor. The bed temperature is measured by a chromel-alumel thermocouple. The product gas is passed through ice traps to condense water, and then analyzed for $H_2S$, and $SO_2$ by Matheson gas detector tubes.

## TEST RESULTS

The ZnO-based sorbent (MCRH-1) was evaluated in a sulfidation gas mixture containing (in mole%): $H_2$=10%, CO=15%, $CO_2$=5%, $H_2S$=1%, $H_2O$=15% and bal $N_2$. Figure 2 show the $H_2S$ breakthrough profiles as a function of normalized time. In tests with the MCRH-1 sorbent conducted at 800°F , the sorbent conversion at breakthrough was 80 percent. In fact, the $H_2S$ level remained at 0 ppm until 17 percent sorbent conversion and then gradually increased to ~5 ppm when conversion reached 80 percent. The sorbent conversion at 650 and 1000°F was 60 and 100 percent respectively. Under the same conditions, at 800°F ZT-4 (currently the leading sorbent) conversion was less than 10%.

Figure 3 show the $H_2S$ breakthrough profiles for a another ZnO-based sorbent(MCRH-10) as a function of normalized time. Complete (100%) sorbent conversion was observed at breakthrough at 800°F and the pre-breakthrough $H_2S$ level was below 35 ppm.

## FUTURE WORK

Various formulations of sorbents with

catalyst additives will be prepared and investigated for their ability to be regenerated at lower temperature.

## PUBLICATION/PRESENTATION

K. Jothimurugesan, A.A. Adeyiga and S.K. Gangwal "Development of Advanced Hot-Gas Desulfurization Sorbents" Project Review Meeting, DOE/METC, February 24, 1994

K. Jothimurugesan, A.A. Adeyiga and S.K. Gangwal "Development of Advanced Hot-Gas Desulfurization Sorbents" 1995 Annual AIChE Meeting, November-17,Miami Beach, FL. Abstract submitted

## REFERENCES

Gangwal, S.K., Gupta,R., and McMichael., W.J."Sulfur Control Options For igccSystems", Proceedings of UNDEERC Low-Rank Fuels Symposium, St.Louis, MO, 1993.

Leininger,T., et al., "Integration and Testing of Hot Desulfurization and Entrained Flow Gasification for Power Generation Systems," Proceedings of the 12th Annual Gasification and Gas Stream Cleanup Contractor's Review Meeting, Vol.1, DE93000228,p.95, 1992.

NOVEM. System Study high temperature gas cleaning at IGCC systems.Netherlands Agency for Energy and the Environment, 1991.

Rutkowski,M., et al., "IGCC Database and Hot Gas Cleanup Systems Studies," Proceedings of the Coal-Fired Power Systems 93-Advances in IGCC and PFBC Review Meeting,DOE/METC-93/6131(DE93000289), p.359, 1993.

PB.16

# Advanced Low-Temperature Sorbents

## CONTRACT INFORMATION

| | |
|---|---|
| **Contract Number** | DE-AC21-94MC31089 |
| **Contractor** | GE Corporate Research and Development<br>P.O. Box 8<br>Schenectady, NY 12301<br>(518) 387-5850 (telephone)<br>(518) 387-7258 (telefax) |
| **Contractor Project Manager** | Raúl E. Ayala |
| **Principal Investigators** | Raúl E. Ayala, GE Corporate R&D<br>Venkat S. Venkataramani, GE Corporate R&D<br>Javad Abbasian, Institute of Gas Technology<br>Andy H. Hill, Institute of Gas Technology |
| **METC Project Manager** | Daniel C. Cicero |
| **Period of Performance** | September 30, 1994 to February 27, 1997 |

**Schedule and Milestones**

**FY95 Program Schedule**

| | O | N | D | J | F | M | A | M | J | J | A | S | |
|---|---|---|---|---|---|---|---|---|---|---|---|---|---|
| Task 1 – NEPA Report | — | | | | | | | | | | | | |
| Task 2 – Sorbent Preparation | | — | — | — | — | — | — | — | — | | | | |
| Task 3 – Provision of Bench Unit | | | | | | | | — | — | | | | |
| Task 4 – Bench Testing | | | | | | | | | | — | — | — | |
| Task 5 – Sorbent Cost Assessment | | | | | | | | | | | | | →FY'96 |
| Task 6 – Topical Report | | | | | | | | | | | | | →FY'96 |
| Task 7 – Market Plan | | | | | | | | | | | | | →FY'96 |
| Task 8 – Long-Term Testing (option) | | | | | | | | | | | | | →FY'96 |

## OBJECTIVES

The objective of the proposed program is to develop regenerable sorbents to remove hydrogen sulfide from coal-derived fuel gases in the temperature range 343 to 538 °C (650 to 1000 °F) using the fixed-, moving-, and fluidized-bed reactor modes. Sorbent materials should be prepared in bench-scale quantities for screening and characterization of physical properties, mechanical durability, and chemical reactivity. A cost assessment and a market plan for large-scale fabrication of the sorbents is to be

developed. Under a Contract Option, a long-term bench-scale test (at least 100 cycles) will be conducted to demonstrate durability and reactivity of the sorbents.

## BACKGROUND INFORMATION

A number of promising technologies are currently being optimized for coal-based power generation, including the Integrated-Gasification Combined Cycle (IGCC) system. If IGCC is to be used successfully for power generation, an economic and efficient way must be found to remove the contaminants, particularly sulfur species, found in coal gas. Except for the hot gas desulfurization system, all major components of IGCC are commercially available or have been shown to meet system requirements [Corman, 1986]. Over the last two decades, the U.S. Department of Energy/Morgantown Energy Technology Center (DOE/METC) has sponsored development of various configurations of high-temperature desulfurization systems [Bossart et al., 1990] including fixed-bed, moving-bed, transport-bed, and fluidized-bed systems. Because of their mode of operation and requirements for sorbent manufacturing, the fixed-bed systems can generally use the same materials as moving-bed configurations, i.e., pelletized or extruded sorbents, while fluidized-bed (circulating or bubbling configurations) and transport reactor configurations use materials generally described as agglomerated or granulated.

### Moving-bed systems

Moving-bed systems are under development at GE [Bevan et al., 1994]. Although the sorbent materials move slowly between the absorber and regenerator vessels, the level of deterioration at process conditions requires the material to be mechanically durable. Sorbent formulations prepared for moving-bed systems must have mechanical durability and exhibit satisfactory desulfurization kinetics at 538 °C (1000 °F) [Ayala et al., 1994]; however, larger-scale demonstration systems such as the Tampa Electric Co.'s Polk Station will operate at lower temperatures, close to 482 °C (800-900 °F). Hence, development of sorbents with reactivity in this middle temperature range of 343 to 538 °C (650-1000 °F) is important for moving-bed systems.

### Fluidized-Bed Systems

Although the fixed-bed approach using metal oxides has been shown to reduce the $H_2S$ content of the cleaned gas to very low levels, the operation is not continuous, it suffers from operational problems, and requires large-scale high temperature valves. To overcome these problems, US DOE has also sponsored fluidized-bed hot gas desulfurization research in recent years. The fluidized-bed approach offers advantages because of its ability to control the reactor temperature during the highly exothermic regeneration step.

The key characteristic of concern in the fluidized-bed application is maintenance of the physical integrity of the sorbent during the chemical transformations associated with absorption-regeneration. Testing appears to verify that excessive attrition results primarily from the changes in composition during transformation and not from mechanical forces. The extreme temperature and severe chemical conditions of air-steam regeneration is deleterious to many inorganic support materials and sorbent compounds. A sorbent suitable for fluidized-bed application must, therefore, have both good thermodynamic equilibrium and initial chemical reactivity in the range of 343-538 °C, as well as acceptable long-term physical and

chemical durability with a reasonable cost of production.

## PROJECT DESCRIPTION

The technical work is directed at developing regenerable desulfurization sorbents in the temperature range 343 to 538 °C (650 to 1000 °F). The proposed program is divided into eight tasks:

In Task 1, the information required for preparation of a NEPA report by DOE will be provided. In Task 2, several sorbents suitable for fixed-, moving-, and fluidized-bed applications will be fabricated. Three classes of materials will be used: zinc-based materials (e.g., zinc titanates), advanced metal oxide (non-zinc) materials, and proprietary materials. Selection will be based on thermodynamic and laboratory evaluation of powder materials. GE-CRD, IGT, and Prof. M. Flytzani-Stephanopoulos (consultant, Tufts University) will be responsible for identifying and screening the chemical compositions of the sorbents. Pelletization (for moving/fixed beds) and granulation (for fluidized beds) will then be conducted on the promising materials using suitable binders and pore formers. Standard techniques (extrusion and calcination) as well as novel techniques (solution precipitation or sol/gel formation) will be used to modify the morphology of the formed materials. GE-CRD will focus on moving/fixed-bed applications, while IGT will focus on fluidized-bed applications. Commercial sorbent and catalyst developers will pelletize or agglomerate the final formulations for bench testing according to recommendations by GE-CRD and IGT. In Task 3, the moving/fixed-bed bench reactor at GE-CRD and the fluidized-bed reactor at IGT will be refurbished for use. In Task 4, the eight most promising sorbents that passed screening under Task 2 will be tested for ten cycles of absorption and regeneration each in the GE-CRD moving/fixed-bed bench reactor and IGT fluidized-bed reactor, and the properties of the used materials will be compared against those of the fresh sorbents. In Task 5, a sorbent cost assessment will be performed to determine costs and sensitivity of costs for raw materials, fabrication, disposal, or recycle. In Task 6, a Topical Report will be prepared summarizing the results obtained in the program. In Task 7, a Market Plan will be developed jointly with the commercial sorbent manufacturers and users to develop a strategy for commercialization, teaming/licensing approaches, and benefits to IGCC technologies.

Finally as an optional task, Task 8 will test a minimum of two formulations, one for moving/fixed-bed systems and the other for fluidized-bed systems for long-term (at least 100 cycles) durability and chemical reactivity in the corresponding bench-scale reactor configurations.

## RESULTS

### Literature review results

The research and development for high-temperature desulfurization of fuel gases has been sponsored primarily by the Morgantown Energy Technology Center (METC) of the United States Department of Energy (U.S. DOE). Over the last decade a number of studies have been reported on high-temperature $H_2S$ removal, primarily using various transition metal oxides as regenerable sorbents [Grindley and Steinfeld, 1981; Jalan and Wu, 1980].

The sorbent most intensively studied is iron oxide, which yields equilibrium $H_2S$ concentrations in the few hundred ppm range for a composition representative of low-Btu coal-derived gas and temperatures of above 500 °C. While the sulfidation kinetics of iron oxide are very good [Tamhankar et al., 1981], this sorbent

cannot be used for single-stage coal gas desulfurization to reduce the $H_2S$ content of the fuel gas down to a few ppm of sulfur.

Zinc oxide was originally used as a non-regenerable sorbent in "guard beds" protecting catalyst beds from trace sulfur impurities. More recently, zinc oxide has also been investigated as a regenerable sorbent [Lew and Flytzani Stephanopoulos, 1989; Westmoreland et al., 1977]. The thermodynamic equilibrium for sulfidation of ZnO is quite favorable, yielding desulfurization down to a few ppm $H_2S$. The sulfidation kinetics of ZnO, however, are much slower [Westmoreland et al., 1977] compared to those of iron oxide, and the regenerability of ZnO is restricted by the loss of surface area at high temperatures and the formation of zinc sulfate at low regeneration temperatures. Reduction to metal and sulfidation take place simultaneously when the hot fuel gas contacts the sorbent.

Until the early 1980's most of the elements in the periodic table were being considered on an empirical basis for use as sorbents for sulfur removal. Westmoreland and Harrison [Westmoreland and Harrison, 1976] did a systematic thermodynamic analysis of 28 elements and arrived at 11 useful elements (i.e., Fe, Zn, Mo, Mn, V, Ca, Sr, Ba, Cu, and W) to be considered in the temperature range of 400 to 1200 °C. Jalan and coworkers [Jalan, 1983] studied some of these metals for desulfurization capabilities at 650 °F. Even under adverse conditions of interference from coke formation and water gas shift reactions, these candidates were attractive for desulfurization to low levels. Other researchers have studied many other pure metal oxides, and their review will be postponed because of space limitations.

Work on zinc titanates such as $ZnTiO_3$, $Zn_2TiO_4$, and $Zn_2Ti_3O_8$ [Lew et al., 1989; Flytzani-Stephanopoulos, 1987] has shown that titanium oxide is a better alternative to iron oxide additives in terms of the higher stability of the titanates over the ferrite compounds of zinc, and their similar sulfidation equilibria. However, resistance to attrition is still an issue. With zinc titanates, the sulfidation temperature has been shown to extend to 700 °C and sintering of the ZnO was greatly reduced, depending on the Zn:Ti ratio chosen. Although zinc titanate has also shown better attrition resistance than zinc ferrite in pilot tests, this sorbent also suffers gradual loss of reactivity in long-term cyclic operation, resulting in high fresh sorbent makeup rate to maintain the desired level of desulfurization. Other mixed-metal oxides such as copper-based and cobalt-based sorbents have also been investigated [Abbasian et al, 1992]; however, the research has been limited to laboratory-scale equipment.

Thus far, the temperatures of interest have been mostly above 500 °C (932 °F) with emphasis in the range 538–700 °C (1000–1302 °F). This temperature range was chosen because higher coal gas temperatures to the turbine inlet resulted in higher overall efficiency for the IGCC system. However, recent economic studies indicate that very high coal gas temperatures also carry significant penalties in terms of costs of the materials of construction and choice of alloys needed to withstand temperature, pressure, and corrosion requirements of the coal gas. A reasonable compromise between cycle efficiency and capital and operating costs appears to be now in the range of 343–538 °C (650–1000 °F) [Droog et al., 1992]. In addition, the stringent requirement for sulfur removal efficiency at temperatures above 538 °C (1000 °F) limits the choice of the sorbents to a few metal oxides (based on thermodynamic equilibrium) that have been shown to have other limitations as described earlier. The thermodynamic equilibria of many

metal oxides significantly improve as the temperature decreases, making many metal oxide sorbents suitable for hot gas cleanup application in the temperature range of 343 to 538 °C (650 to 1000 °F). On the negative side, the intrinsic rate of reaction decreases exponentially with temperature, so much slower desulfurization kinetics will be anticipated below 538 °C (1000 °F).

Although the initial chemical reactivities of the sorbents generally decrease with decreasing temperature, the lower thermal stresses incurred can lead to better sorbent reactivity after a large number of cycles, reducing the sorbent replacement cost. In addition, issues such as zinc evaporation are no longer a problem when going to absorption temperatures below 1000 °F. In general, the benefit to be gained by lower temperature application to 343 to 538 °C (650–1000 °F) may outweigh the slight loss of efficiency due to lower temperature application, resulting in lower overall cost of electricity. The investigation to be undertaken in this program must include selection of the appropriate material that can offer good thermodynamic equilibrium and initial chemical reactivity, as well as acceptable long-term physical and chemical durability with reasonable cost of production.

Copper-based sorbents were recently evaluated at IGT for their application at temperatures of 650-850 °C [Abbasian et al, 1992]. Two "promising" copper-based sorbents were identified in this program for further development. $H_2S$ breakthrough curves for these sorbents typically indicated very low $H_2S$ pre-breakthrough levels, ranging from less than less than 1 to about 10 ppmv, which are significantly lower than those predicted for the elemental Cu-$H_2S$ equilibrium (implying that the copper in the compound oxide was not completely reduced to elemental copper by the fuel gas during sulfidation reaction). These results and the fact that the thermodynamic equilibria of many metal oxides improve as the temperature decreases, suggest that copper-, or other metal oxide-based sorbents may also have a potential for hot gas cleanup application at the lower temperatures of interest in this program. Although the initial chemical reactivities of metal oxide sorbents generally decrease with decreasing temperature, the lower thermal stress incurred at lower temperatures can lead to better sorbent reactivity after a large number of cycles, reducing the sorbent replacement cost.

## Thermodynamic calculations

The thermodynamic $H_2S$ equilibrium concentration in simulated fuel gases (U-GAS and Texaco) for a number of potential metal oxides were determined at elevated temperatures (i.e. 350-550 °C) and pressure (20 bar). The metal oxides considered for this analysis included copper, zinc, iron, nickel, tin, cobalt, molybdenum, manganese, and tungsten. The number of moles of the fuel gas and the solid oxides were selected to correspond to 50% sorbent conversion during sulfidation. Based on the available data, certain restrictions were imposed on formation of a number of species, to better simulate the actual environment. The results of these analyses are presented in Figures 1 and 2 for U-GAS and Texaco fuel gases respectively, indicating that the calculated $H_2S$ equilibrium is not significantly affected by the fuel gas composition, if one allows for water-gas-shift reaction equilibration. Furthermore, because of the lower temperature range (i.e. 350-550 °C), a large number of metal oxides are capable of reducing the $H_2S$ level of the fuel gases to below 20 ppmv for IGCC application. It should be noted that the $H_2S$ equilibrium for copper oxide is the lowest (e.g. below 0.1ppmv) if reduction to metallic copper is prevented,

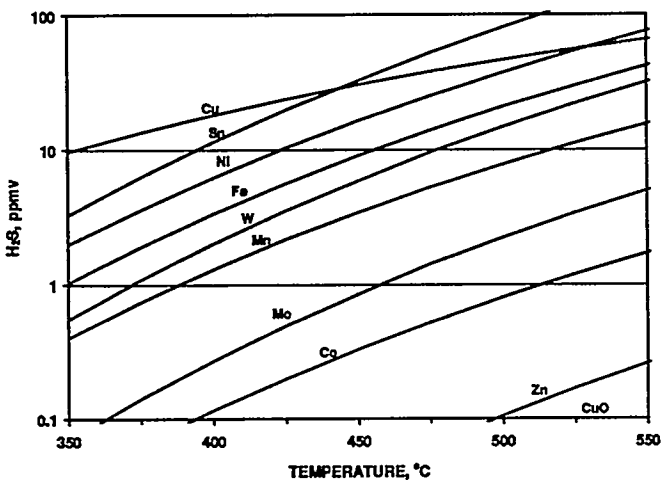


**Figure 1.- H2S equilibrium concentration in fuel gas with various oxides (U-GAS)**

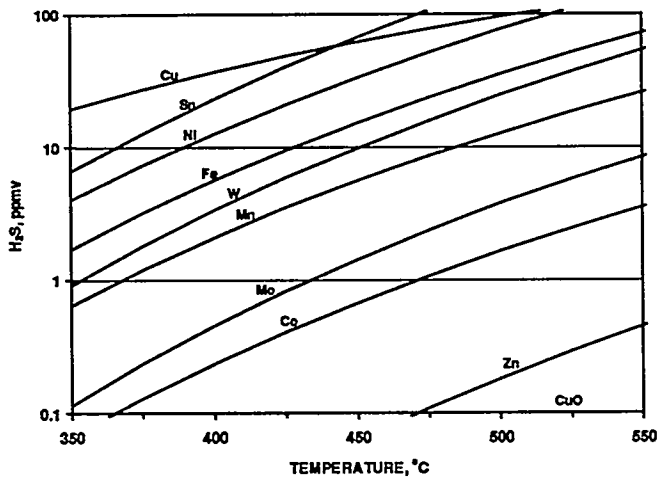


**Figure 2.- Equilibrium Concentration In Fuel Gas With Various Oxides (Texaco)**

while in the reduced form, metallic copper is still acceptable candidate.

Phase stability diagrams for reducing gas atmospheres (i.e., coal gases) and oxidizing gas atmospheres (i.e., regeneration gases) have been constructed using algorithms that predict the stability of chemical species based on minimization of the Gibbs free energy of the system. The phase stability of metals under regeneration gases containing $SO_2$ and $O_2$ is important because spalling and pellet deterioration occurs more often as a result of metal sulfate formation. Figure 3 shows the stability of copper and molybdenum as a function of the log partial pressure of $O_2$ and $SO_2$. For gas compositions containing approximately 0.02 atm of $O_2$ and 0.5 to 0.1 atm $SO_2$, (typical of atmospheric regeneration gases in the moving-bed system) the thermodynamically stable phase of copper is copper sulfate, while the thermodynamically stable form of molybdenum is the oxide. For most pure oxides, including zinc oxide, the metal sulfate is the stable form under oxidizing gas conditions at temperatures around 500-700 °C, depending on $SO_2$ and $O_2$ concentration. Of course, thermodynamic predictions do not take into account the rate of approach to equilibrium (i.e., kinetic rates) and hence experimental data is still needed to confirm the extent of formation of the predicted species. Nevertheless, thermodynamics allows the investigator to determine if formation of certain compounds is favored.

## Selection of metal oxides process

Early thermodynamic analysis by Westmoreland and Harrison in 1976 set the stage for desulfurization candidates in the range of 400 to 1200 °C (752 to 2182 °F). With the new requirements of lower temperatures (343 to 538 °C), an update of the thermodynamic analysis was made to redefine the applicability of the various metal oxides to desulfurization in temperature regime of interest. Furthermore, the sorbent evaluation considered process-specific requirements for fixed/moving-bed and fluidized-bed configurations.

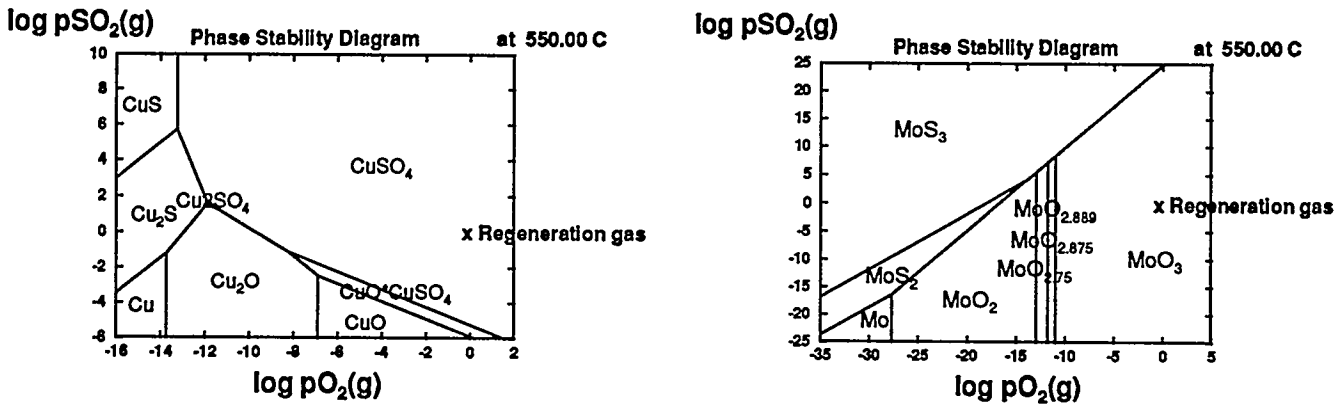


**Figure 3.- Phase stability diagrams for Cu-S-O (left) and Mo-S-O (right) systems**

Process requirements were taken as a basis for determining metal oxides suitability for high-temperature desulfurization.

1. Rate of desulfurization and stability of the sulfide under reducing gas conditions

2. Potential for detrimental secondary reactions on the solid under reducing coal gases (e.g., metal carbides, reduction to zero-oxidation state, formation of chlorides from HCl)

3. Rate of regeneration and production of sulfur dioxide or elemental sulfur under oxidizing gas conditions.

4. Potential for detrimental secondary reactions on the solid under oxidizing gases (e.g., sulfates) and hydrothermal stability during regeneration.

Taking previous experimental data and thermodynamic predictions into consideration, four metals (Zn, Fe, Ce, Cu) were selected as primary desulfurization species, four other metals (Mo, Co, Cu, Fe, as secondary species (i.e., additives) for desulfurization, and three metal species (Ti, Zr, Ce) were selected as support and structure stabilizers. Combinations of these metal species will be tested in the laboratory and pelletization/agglomeration feasibility will be evaluated at commercial vendors.

## Preliminary Sorbent Evaluation

The work on the preliminary sorbent evaluation focused on the determination of the sulfidation reactivity and effective capacity of metal oxide compounds in the temperature range of 350-500 °C to identify potential candidate sorbents for evaluation of other important characteristics such as sorbent regenerability and mechanical durability in multicycle operation.

The work performed included fixed-bed desulfurization testing of two copper-chromite sorbents and one zinc titanate sorbent. As mentioned above, these sorbents were shown to be highly efficient desulfurization sorbents at higher temperatures (550-850°C). The copper-chromite sorbents used in these tests contain about 10% (CuCr-1) to 25 % (CuCr-2) copper and have an average particle size of about 550 micron. The zinc titanate sorbent tested (UCI-4) has an average particle size of about 260 micron.

The sulfidation tests were carried out in a quartz fixed-bed reactor system at about one atmosphere pressure using a simulated coal derived-fuel gas mixture containing 0.5 vol% $H_2S$ at a space velocity of 2000 $hr^{-1}$. Sulfided sorbents were regenerated by using nitrogen-air mixtures at temperatures of 650-750 °C. The product gas was analyzed for $H_2S$ and $SO_2$ by a dedicated gas chromatograph.

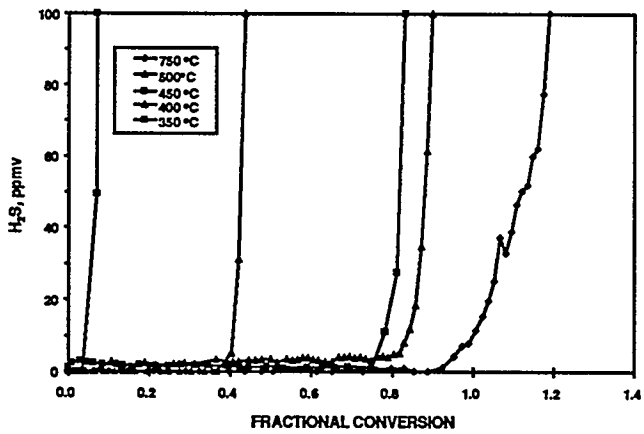


**Figure 4.- H2S Breakthrough Curves For Copper Chromite Sorbent (CuCr-1)**

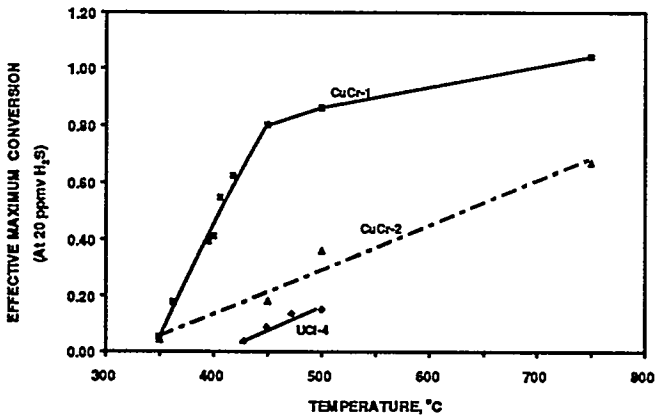


**Figure 5.- Effect of temperature on effective maximum conversion**

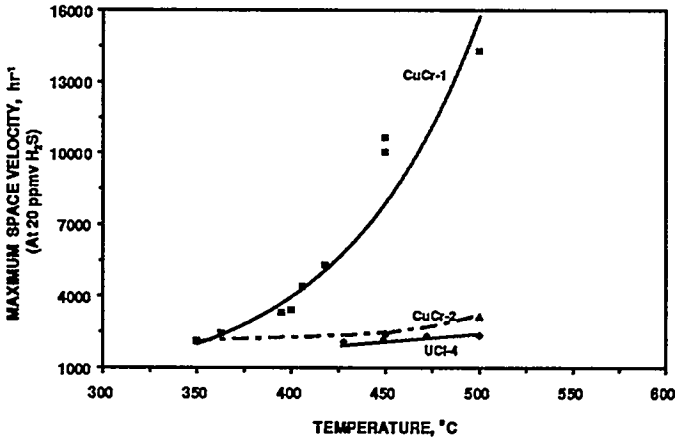


**Figure 6.- Effect of temperature on maximum space velocity**

The results of the sulfidation reactivity testing indicate that:

- All three mixed metal oxide compounds can reduce the $H_2S$ content of the coal-derived fuel gas to below 20 ppmv in the desired temperature range; specifically, copper chromite can reduce the $H_2S$ exit gas concentration to less than 5 ppmv (Figure 4), corresponding generally to the CuO-$H_2S$ equilibrium.
- The reactivity of the copper chromite sorbents is generally higher than that of the zinc titanate sorbent tested.
- High levels of copper dispersion significantly improve copper chromite sulfidation reactivity up to very high effective maximum conversion levels of 85% (Figure 5), and allow the use of increased space velocities above 15,000 $hr^{-1}$ (Figure 6).

## FUTURE WORK

The matrix of powder formulations selected was falls generally into three classes:

1. Modified zinc titanate and zinc-based formulations

2. Other novel (i.e.non-zinc) compositions

3. Optimization of proprietary existing formulations.

The composite and compound approaches to exploit the product and synergistic properties of the constituting components will also be focused upon. For example, the beneficial effects of small amounts of additives such as $MoO_3$ or CuO on the $ZnO$-$TiO_2$ system should be further explored by proper thermodynamic study of the CuO and $MoO_3$ doped compounds of $ZnO$-$TiO_2$. Spalling due to sulfate formation is a problem because the sorbent pore morphology is not fully compatible with (1) the thermodynamics of desulfurization and (2) the preparation technique used to fabricate the sorbent, both in moving-bed pellets and in fluidized-bed sorbent granules.

Chemical composition screening of powders is independent of the final reactor configuration. Further screening of the compositions will be based on the material cost and ceramic fabricability into useful sorbent morphologies at reasonable costs for the desired reactor applications. In the next step, pelletization of powders for moving beds and granulation for fluidized beds will be conducted jointly with commercial sorbent vendors. This step is extremely important to identify potential problems in the production of sorbents in commercial quantities at reasonable costs.

**Moving-bed systems**

Characterization techniques for pelletized formulations will be performed using the following techniques:

- Chemical reactivity on single pellets by thermogravimetric analysis (TGA)
- Attrition resistance before and after desulfurization testing by the modified ASTM D-4058-81 test.
- Crush strength by dead-weight load testing
- Long-term mechanical and chemical durability by the 10-cycle bench-scale tests

Characterization of moving-bed sorbents will be performed before and after bench testing to compare sorbent performance and/or degradation as a function of time.

**Fluidized-bed systems**

Based on the superior sulfidation performance of the chromium-rich copper chromite in the sulfidation reactivity tests, this sorbent will be evaluated for other important characteristics, such as sorbent regenerability and mechanical durability, in multicycle sulfidation-regeneration tests. Secondary components, such as Fe, Mo, or Co, will be added to enhance desulfurization reactivity, chemical stability, porosity and/or maintain mechanical durability as needed.

The kinetic and thermodynamic benefits of using pure copper oxide, as well as iron oxide, for desulfurization will also be examined.

Copper and iron oxide sorbents, stabilized against reduction and sintering by using inert support/dispersant materials, are expected to be more reactive and possibly lead to even lower thermodynamic equilibrium $H_2S$ levels than the respective mixed metal oxide compounds.

Two materials, titania and zirconia, have been identified as potential candidates to have the proper chemical and physical properties needed for a regenerable metal oxide sorbent. Pure metal oxide supported sorbents containing different amounts of uncombined copper and iron oxide with zirconia and titania will be prepared in a granular form using a similar technique used for producing the highly dispersed, porous copper-chromite sorbents. The sulfidation reactivity and capacity of these supported sorbents will also be determined.

The most reactive and mechanically durable sorbent/additive combination will then be produced in a form and quantity suitable for fluidized-bed testing in the bench-scale desulfurization test unit.

## REFERENCES


Abbasian, J., A. H. Hill, and J. R. Wangerow, "Development of Novel Copper Based Sorbent for Hot Gas Cleanup," Final Technical Report, September 1, 19909-August 31, 1992, prepared by Institute of Gas Technology for Center for Research on Sulfur in Coal.

Bossart, S.J., D.C. Cicero, C.M. Zeh, and R.C. Bedick. 1990. Gas Stream Cleanup. Technology Status Report. DOE/METC-91/0273. NTIS/DE91002037. Springfield, Va.: National Technical Information Service.

Corman, J.C. 1986. *System Analysis of Simplified IGCC Plants,* Topical Report. U.S. Dept of Energy, DOE/ET/14928-2233.

Droog, H.A., A. Delwel, and R. Assink. Comparison of High Temperature Gas Treatment Options with Low Temperature Gas Treatment in IGCC's Following Entrained Flow Gasification. Paper presented by Comprimo at 1992 EPRI Conference.

Flytzani-Stephanopoulos, M. et al., Final Report to DOE, DOE/MC22193-2582, October 1987.

Grindley, T. and G. Steinfeld, "Development and Testing of Regenerable Hot Coal Gas Desulfurization Sorbents," Final Report No. DOE/MC/16545-1125, 1981.

Jalan, V. (Giner, Inc.), Final Report, DOE/MC/16021-1486, 1983

Lew, S., "High-Temperature Regenerative $H_2S$ Removal by $ZnO$-$TiO_2$ Systems," M.S. Thesis, Massachusetts Institute of Technology, January 1987.

Lew, S., K. Jothimurugesan, and Flytzani-Stephanopoulos, M., Ind. Eng. Chem. Res. 28, 535 (1989).

Westmoreland, P.W., and D. P. Harrison. 1976. Evaluation of Candidate Solids for High-Temperature Desulfurization of Low-Btu Gases. *Env. Sci. Tech.*, 10, 659 (1976).

Westmoreland, P. R., Gibson, J. B. and Harrison, D. P., Env. Sci. Tech. 11 (5), 488-491 (1977).

## PB.17 Spectral Methods Applied to Fluidized Bed Combustors

### CONTRACT INFORMATION

| | |
|---|---|
| **Contract Number** | **DE-FC21-91MC28081** |
| **Contractor** | Iowa State University<br>209 Beardshear Hall<br>Ames, Iowa 50011<br>(515) 294-8733 (telephone)<br>(515) 294-3261 (telefax) |
| **Other Funding Sources** | Iowa State Electric Power Research Institute<br>Ahlstrom Pyropower, Inc. |
| **Contract Project Manager** | Robert C. Brown |
| **Principal Investigator**<br>**Research Assistants** | Robert C. Brown<br>Thomas S. Raines<br>Theodore D. Thiede |
| **METC Project Manager** | Wu K. Lan |
| **Period of Performance** | September 30, 1991 to December 1, 1995 |

**Schedule and Milestones**

**FY95 Program Schedule**

| | S | O | N | D | J | F | M | A | M | J | J | A |
|---|---|---|---|---|---|---|---|---|---|---|---|---|
| Select coals and sorbents | XXXXXXX | | | | | | | | | | | |
| Transient testing of coal | | | XXXXXXXXXXX | | | | | | | | | |
| Transient testing of sorbents | | | | | XXXXXXXXXXX | | | | | | | |
| Analysis of coal transient data | | | | | | XXXXXXXXXXXX | | | | | | |
| Analysis of sorbent transient data | | | | | | | XXXXXXXXXXXXX | | | | | |
| Final Report | | | | | | | | | | | XXXX | |

## OBJECTIVES

The goal of this research is to characterize coals and sorbents during the normal operation of an industrial-scale circulating fluidized bed (CFB) boiler. The method determines coal or sorbent properties based on the analysis of transient $CO_2$ or $SO_2$ emissions from the boiler. Fourier Transform Infrared (FTIR) spectroscopy is used to qualitatively and quantitatively analyze the gaseous products of combustion. Spectral analysis applied to the transient response of $CO_2$ and $SO_2$ resulting from introduction of a batch of coal or limestone into the boiler yields characteristic time constants from which combustion or sorbent models are developed. The method is non-intrusive and is performed under realistic combustion conditions.

## BACKGROUND INFORMATION

References [1] and [2] describe the theoretical aspects of this coal combustion research and the development of combustion models. From the relations given for devolatilization and char burning rates in these references, it can be shown that the $CO_2$ profile resulting from introduction of a batch of coal into a fluidized bed combustor has a fast exponential decay in the devolatilization region and, for time less than the char time constant $\tau_c$, a slower exponential decay in the char burnout region.

The calcination and sulfation processes resulting from introduction of a batch of limestone into a fluidized bed boiler are quite complex. Calcination results in the release of $CO_2$ from the limestone, while sulfation results in the decrease of $SO_2$ due to reaction with the calcined limestone. Calcination and sulfation models have been developed [3], but are not as mature as the coal combustion models. Refinement of calcination and sulfation models is ongoing.

### Spectral Analysis

Taking the Fourier transform of time series data was developed as a means of finding the hidden periodicities of that data [4]. The modulus-squared of a Fourier transform of a finite data set, called the periodogram, is a statistic which is representative of a zero-mean data series. Plotting the periodogram (with the steady state background level removed and beginning at the time of the devolatilization peak) versus frequency on a log-log plot, called a Bode plot, gives a plot where the two cornering frequencies correspond to the reciprocal of the devolatilization and char time constants. This methodology resolves weak signals in a noisy steady-state background.

The combustion process is characteristic of two first-order processes acting in parallel (devolatilization and char burning). Figure 1 is an example of frequency domain analysis (Bode plot) of the signal from a $CO_2$ non-dispersive infrared analyzer (NDIR) when a 5 gram sample of 10x14 mesh Indiana bituminous coal is batched into a laboratory combustor. The low-frequency cut-off gives $\tau_c$ equal to 27.0 s, which is within 13% of the time-domain value. The high-frequency cut-off gives devolatilization time constant $\tau_v$ equal to 2.94 s, in excellent agreement with the value from the time-domain analysis. This spectral analysis method, while providing good results, is sensitive to the duration of the data set. If a long enough data set is not acquired, the analysis will provide a plot which gives clear, but erroneously low, cornering frequencies.

### FTIR Theory

Fourier Transform Infrared (FTIR) spectroscopy is a tool which has long been used by analytical chemists, but its use is expanding as capabilities increase and ease of use is improved. Infrared spectroscopy can directly monitor the vibrations of the functional groups which

characterize molecular structure and govern the course of chemical reactions [5]. The "mid-IR" region of the electro-magnetic spectrum between 2.5 μm and 25 μm (normally expressed as wavenumber, 4000 - 400 $cm^{-1}$) is attractive because it includes the frequencies corresponding to the fundamental vibrations of virtually all of the functional groups of organic molecules. This region has meaningful, well understood absorption bands often adjacent to weakly absorbing regions. This is particularly true for the gases being considered: $CO_2$, CO, $SO_2$, NO, $NO_2$, and $N_2O$. Quantitative calibrations in the mid-IR are usually straightforward and robust. However, simple diatomic molecules, such as $N_2$ and $O_2$, are invisible to infrared radiation and cannot be detected with an FTIR.

The heart of the FTIR is a Michelson interferometer which consists of a beam splitter, compensating plate, and a pair of mirrors [5, 6]. By mechanically varying the linear position of one of the mirrors, the path length between the two arms is altered, giving rise to a time dependent variation in optical intensity, called the interferogram. If the optical source is a broad band infrared spectrum, the interferogram will correspond to the superposition of an infinite number of sine waves having different periods (but a common zero point which occurs when the lengths of the two arms are equal).

A digital computer is used to perform a Fourier transformation of the interferogram, yielding a composite spectrum of the source, the instrument, and any sample in the optical path. This is the basis of all modern rapid-scan FTIR spectrometers.

Water vapor is strongly absorbing in the mid-IR region and its bands overlap the bands of a number of other gases (particularly NO, $NO_2$, and $SO_2$) and can obscure their features. However, it can easily be dealt with by removing it from the sample gas stream or subtracting out a pure water vapor spectrum from the spectrum of interest. Water vapor has been subtracted out of the spectra presented in this paper.

Chemical species are identified through spectral structure and the wavenumber regions in which those features exist. For example, the CO spectrum consists of a series of fine lines between 2250 and 2050 $cm^{-1}$, while $SO_2$ has a predominant smooth double hump between 1400 and 1300 $cm^{-1}$ with a sharp spike at 1355 $cm^{-1}$ in addition to smaller, less distinct regions about 1150 and 2400 $cm^{-1}$ (Fig. 2).

Quantification involves identifying a region of interest for each gas and taking spectra of the gases at a number of concentrations spanning the range of concentrations to be measured. A partial least squares approach based on Beer's Law and using Nicolet's Quantir software were used to develop quantification methods for $CO_2$, $SO_2$, CO, NO, $NO_2$, and $N_2O$.

## PROJECT DESCRIPTION

An FTIR was chosen for this project because of its ability to detect and quantify multiple gas species with a single instrument. By developing new quantification methods, quantification of additional gases can be simply, quickly, and inexpensively accomplished. Conventional gas analysis equipment requires a separate instrument for each gas. Since the presence of unburned hydrocarbons, or other interfering gases, was unknown at the beginning of the project, the FTIR provided the ability to identify and deal with any such gases.

The rationale for choosing an FTIR spectrometer was to provide simultaneous, rapid quantification and analysis of a minimum of 6 gaseous combustion products with a single piece of equipment, encompassing the ability to interface with a personal computer for data processing and analysis. The system can detect and quantify the previously mentioned gases in the concentration ranges expected in the boiler flue gas with a small

volume (275 ml) gas cell at one second intervals. The small volume cell permits rapid gas exchange providing the ability to accurately detect fast transients of gas concentration . Inability to detect trace amounts of slightly absorbing gases (specifically $H_2S$ and HCl), lower resolution, and increased lower detection limits are compromises resulting from use of the small-volume, short path length gas cell. Post-processing converts the transient sample spectra to concentrations of the gas species. Spectral analysis is performed on this quantified concentration data.

Experimental apparatus and methods used in the laboratory are described in [1]. A number of experiments similar to those described in [1] were run using the FTIR instead of the NDIR instruments for training, establishing operating parameters for the FTIR, and verifying comparability of the FTIR and reference [1] results.

Figure 3 is a schematic of the Ahlstrom Pyropower circulating fluidized bed boiler (CFB) installed at the Iowa State University power plant. At full load each of the two CFB boilers is rated at 170,000 lb/hr steam flow, 420 psig, 750$^{o}$F, 250,000 lb/hr coal flow rate, and 8,070 lb/hr limestone flow rate. The bed material is limestone and ash. Normal operating condition is about 60% full load.

The gas sample is drawn from the hot cyclone outlet (at approximately 1600$^{o}$F and 1/2" $H_2O$ vacuum) by a vacuum pump through about 20 ft. of 3/8" stainless steel tubing, three Balston 0.1 micron in-line filters in series to remove fly ash, a Permapure membrane dryer to remove water vapor, and then through the cell. The cell is maintained at 600 mm Hg. pressure and 180$^{o}$F.

A batch of about 25 pounds of double screened coal is injected into the boiler through a hopper installed on the end of the coal drag conveyor that dumps into the lower part of the bed opposite the loop seal. With a quick opening slide gate valve, the batch can be dumped into the boiler in less than two seconds, simulating an impulse input.

The FTIR system is set to record at 2 wavenumber resolution and 2 scans per spectrum giving approximately 1 second sampling intervals. Two to three minutes of steady state background are recorded before dumping the coal batch to verify the background steady state condition.

## RESULTS

### Laboratory Results

Figure 4 shows a typical FTIR $CO_2$ profile of a 5g batch of 14x16 Kentucky coal batch test . The devolatilization and char time constants calculated using FTIR data were within experimental error of those presented in [1], calculated from NDIR instrumentation. This confirmed the FTIR would provide experimentally consistent results.

Figure 2 is an FTIR spectrum of a gas sample of the above test at the devolatilization peak. The presence of the light hydrocarbons (methane and acetylene) could not have been identified using the NDIR and chemiluminescence instruments. This indicates that local oxygen starvation and incomplete combustion occurred. The methane spectrum overlapping $SO_2$ can alter the $SO_2$ quantification, but can be subtracted out.

### Power Plant Results

Figure 5 is the $CO_2$ profile resulting from dumping a 25 lb batch of 16x18 sieve size Illinois wash coal into the CFB boiler. The +/- .3% fluctuations about the mean in the steady state background are true fluctuations in the $CO_2$ emissions, and not a result of instrument or flow noise in the sampling system. These fluctuations, due to variations in coal feed rate and coal particle fragmentation hamper calculation of char time

constants. The overall profile is similar to that seen in the laboratory testing, and is anticipated from combustion theory.

However, there are significant, and as of yet unexplained, differences from the laboratory test $CO_2$ profiles in the bubbling fluidized bed combustor. The $CO_2$ profile peaks sharply, before decaying to essentially background levels, rises slightly, flattens and begins a slow decay to background level. The sharp peak is clearly associated with devolatilization whereas the second peak is thought to be due to slow char combustion. This indicates char burnout does not begin until after devolatilization is complete, in contradiction to [1] which showed that devolatilization and char burnout occurred simultaneously. The maximum $CO_2$ level of the char burnout is much less than that seen in the lab results for similar sized particles. Particle fragmentation and slow heating of the char are potential explanations. Further investigation into this phenomenon is planned.

Devolatilization time constants calculated for the samples run in the CFB are within experimental range of error of those from lab tests. The char time constants are more difficult to calculate, and correlation with laboratory data has not yet been achieved due to the different profile. These observations are based on a very limited number of samples and cannot be considered conclusive.

The spectrum at the devolatilization peak, Fig. 6, shows $CO_2$, CO, $SO_2$, NO, acetylene, and methane with potentially trace amounts of $N_2O$. The presence of CO, acetylene, and methane during the devolatilization phase indicates that incomplete combustion occurs in this phase, at least near the batched particles. Methane and acetylene would not have been detected with conventional boiler instruments. The interpretation of these results are the subject of continuing research.

Due to the very recent completion of these CFB boiler tests, the results of spectral analysis applied to this data has not been completed.

## FUTURE WORK

- Determine impact of the industrial-scale CFB boiler on combustion dynamics in comparison to the laboratory scale bubbling bed combustor, particularly as relates to the devolatilization and char $CO_2$ profile differences.
- Determine variation of $\tau_v$ and $\tau_c$ with initial particle diameter and compare to laboratory results.
- Test two different coal types provided by Pyropower.
- Determine calcination and sulfation rate constants in the CFB .
- Refine calcination and sulfation models.
- Refine spectral analysis methods for the FTIR data.

## REFERENCES


1. Christofides, N.J., and Brown, R. *Combustion and Flame* 94:449-461 (1993).

2. Junk, K., and Brown, R. C. *Combustion and Flame* 95:219-228 (1993).

3. Christofides, N. and Brown, R. C. *Proceedings of the Tenth Annual International Pittsburgh Coal Conference*, 1993.

4. Brillinger, D. R. *TIME SERIES Data Analysis and Theory*, Holden-Day, Inc., San Francisco, 1981.

5. Doyle, W. M. *Process control and quality* 2:11-41 (1992).

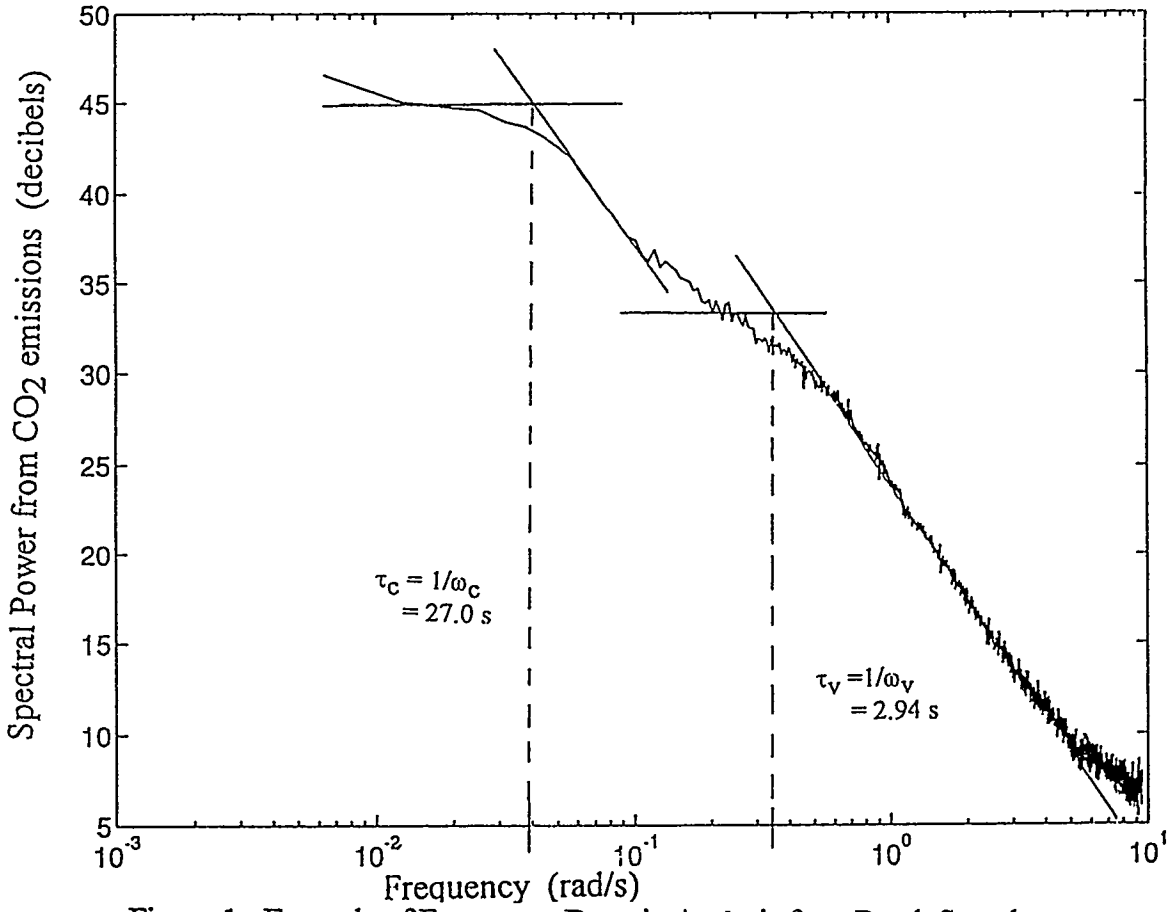


Figure 1. Example of Frequency-Domain Analysis for a Batch Sample

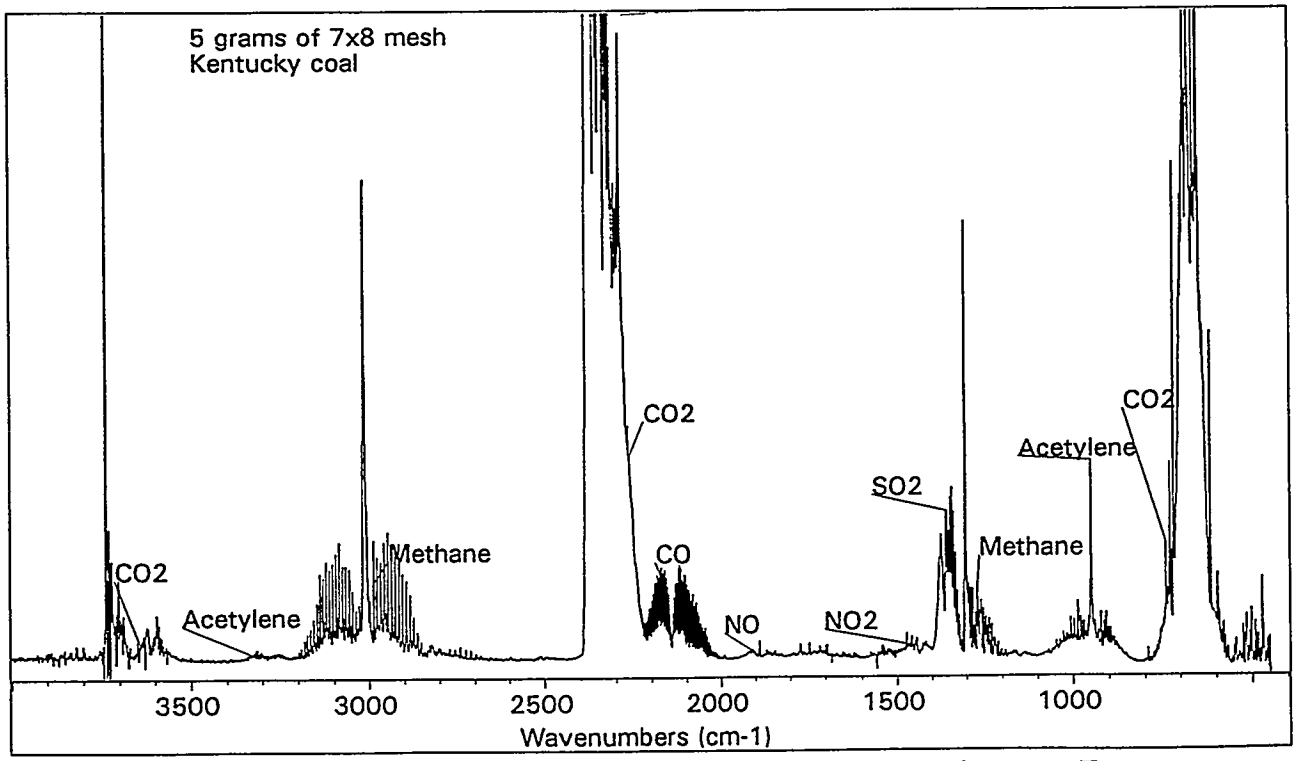


Figure 2. Example Spectrum of Devolatilization Peak From Laboratory Test

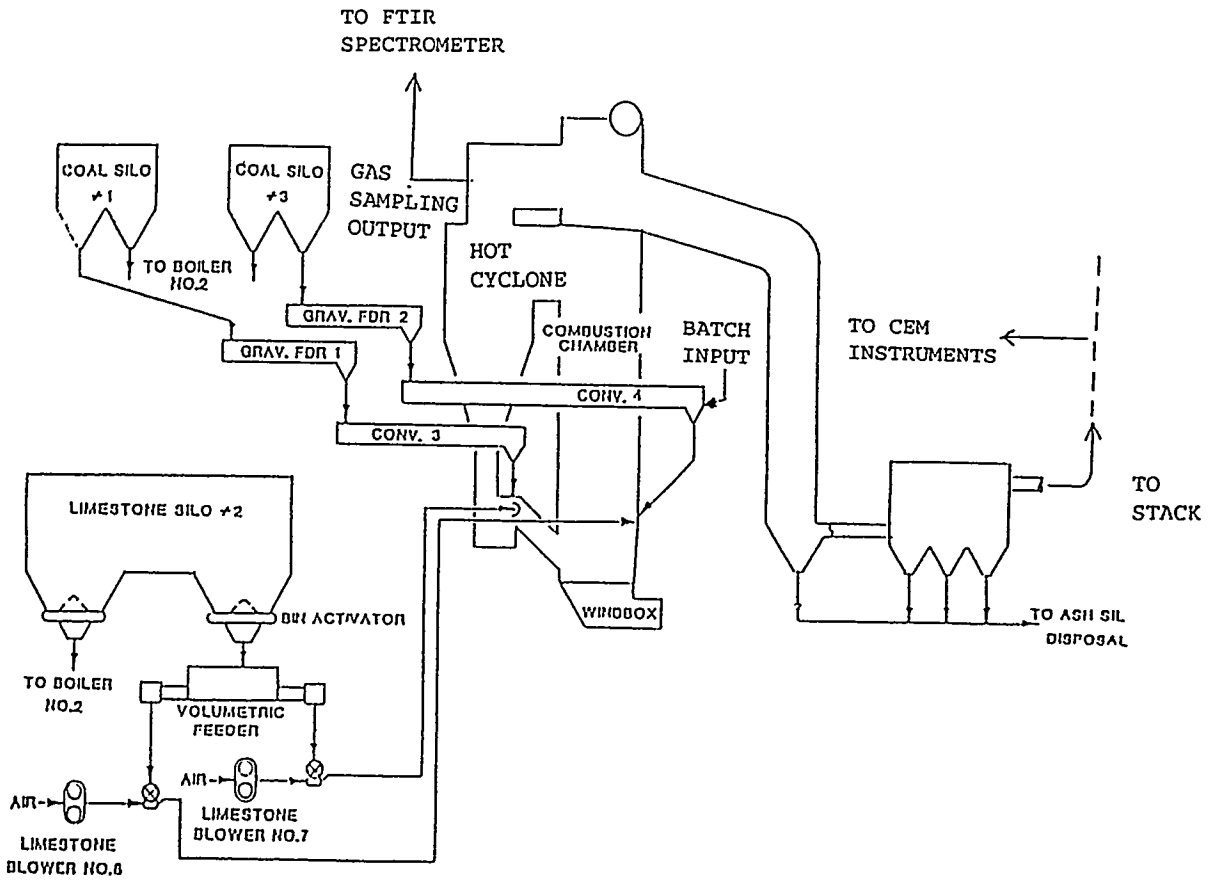


Figure 3. Instrumentation of the Pyropower Boiler at ISU Physical Plant

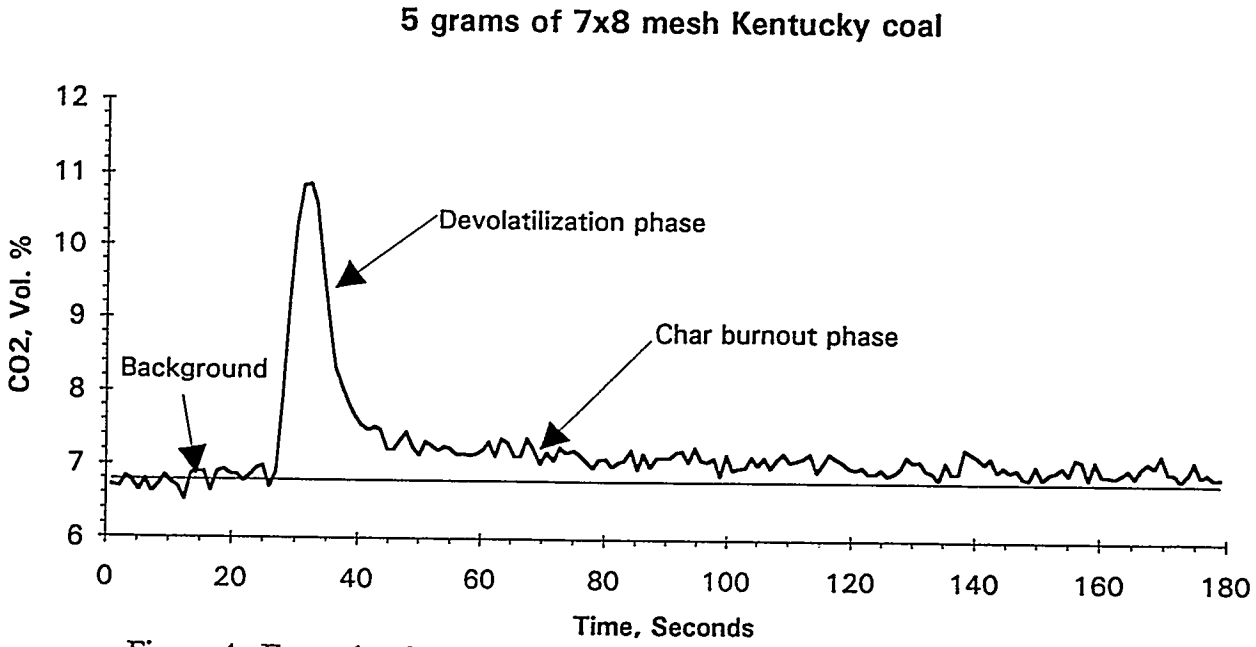


Figure 4. Example of $CO_2$ Profile from Laboratory Bubbling Bed Combustor

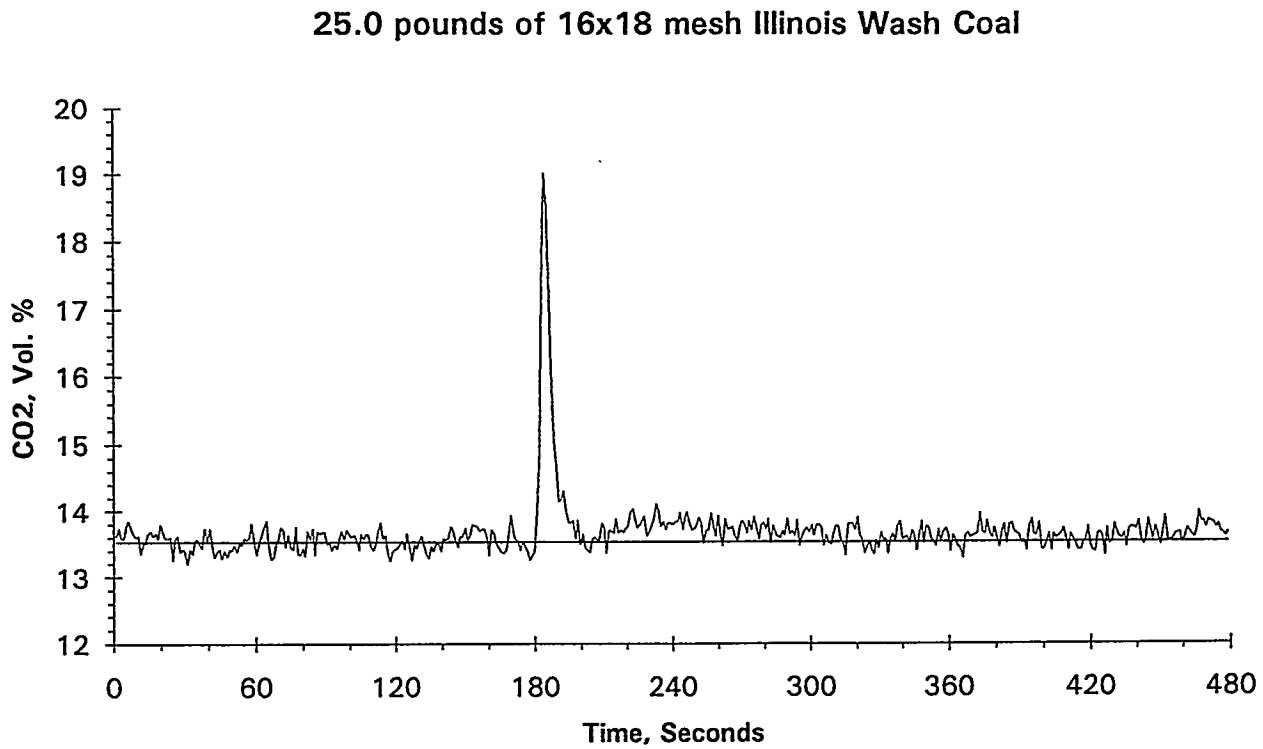


Figure 5. Example of $CO_2$ Profile from ISU Circulating Fluidized Bed Boiler

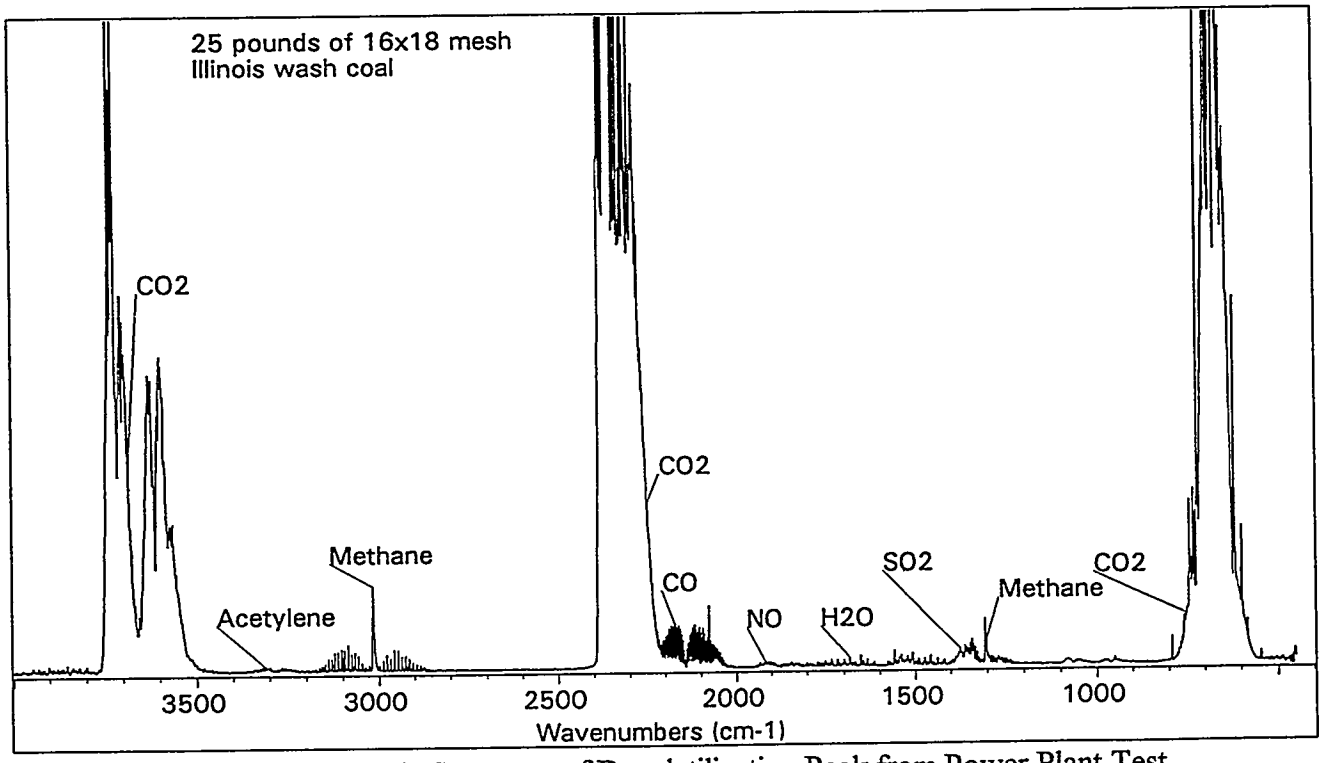


Figure 6. Example Spectrum of Devolatilization Peak from Power Plant Test

## PB.18 Fossil Fuel Conversion - Measurement And Modeling

### CONTRACT INFORMATION

**Contract Number:** DE-AC21-93MC30040


**Contractor:** Advanced Fuel Research, Inc.
87 Church Street
(203) 528-9806 (phone)
(203) 528-0648 (fax)

**Subcontractor:**
Brigham Young University
(801) 378-4326 (phone)
(801) 378-3831 (fax)

**Contractor Project Manager:** Peter R. Solomon — L. Douglas Smoot

**Principal Investigators:** Michael A. Serio, David G. Hamblen — B. Scott Brewster, Predrag T. Radulovic

**METC Project Manager:** Norman T. Holcombe


**Period of Performance:** September 14, 1993 to September 13, 1996

**FY95 Program Schedule**

| | | S | O | N | D | J | F | M | A | M | J | J | A |
|---|---|---|---|---|---|---|---|---|---|---|---|---|---|
| 2. | Gasification Processes | | | | | | | | | | | | |
| 3. | Gas Phase Combustion | | | | | | | | | | | | |
| 4. | Fluidized-Bed Systems | | | | | | | | | | | | |
| 5. | Applications | | | | | | | | | | | | |

### OBJECTIVES

The main objective of this program is to understand the chemical and physical mechanisms in coal conversion processes and incorporate this knowledge in computer-aided reactor engineering technology for the purposes of development, evaluation, design, scale up, simulation, control and feedstock evaluation in advanced coal conversion devices. To accomplish this objective, this program will: 1) provide critical data on the physical and chemical processes in fossil fuel gasifiers and combustors; 2) further develop a set of comprehensive codes; and 3) apply these codes to model various types of combustors and gasifiers (fixed-bed, transport reactor, and fluidized-bed for coal and gas turbines for natural gas).

## BACKGROUND INFORMATION

To expand the utilization of coal, it is necessary to reduce the technical and economic risks inherent in using a feedstock which is highly variable and which sometimes exhibits unexpected and unwanted behavior. Reducing the risks can be achieved by establishing the technology to predict a coal's behavior in a process. This program is creating this predictive capability by merging technology developed at Advanced Fuel Research, Inc. (AFR) in predicting coal devolatilization behavior with technology developed at Brigham Young University (BYU) in comprehensive computer codes for modeling of entrained-bed and fixed-bed reactors and technology developed at the U.S. DOE-METC in comprehensive computer codes for fluidized-bed reactors. These advanced technologies will be further developed to provide: 1) a fixed-bed model capable of predicting combustion and gasification of large coal particles, 2) a transport reactor model, 3) a model for lean premixed combustion of natural gas, and 4) an improved fluidized-bed code with an advanced coal devolatilization chemistry submodel.

## PROJECT DESCRIPTION

The program consists of five tasks: 1) Preparation of a Research Plan, 2) Modeling of Gasification Processes, 3) Modeling of Gas Phase Combustion, 4) Modeling of Fluidized Bed Systems, and 5) Applications. This paper describes the work performed during the second year of the contract.

## RESULTS

**Devolatilization of Large Coal Particles (AFR)** - Fluidized-bed coal combustion and gasification systems normally use comparatively large size coal particles of several millimeters in diameter. Due to heat and/or mass transport limitations, such large coal particles have slower devolatilization rates compared to micron-sized particles used in pulverized coal combustion. This section reports the progress in developing a large coal particle devolatilization model (LCPD) for fixed-bed and fluidized-bed coal combustion and gasification. The model combines a heat transfer model with a general coal devolatilization model FG-DVC [1-3] which was developed for pulverized coal particles.

Coal particles are considered to be spherical in the model. The particle size is assumed to remain unchanged during the devolatilization, since two counteracting processes, weight loss and swelling, lead to negligible size changes for mm-size coal particles in fluidized beds [4]. This assumption implies that the coal particle density will decrease with time due to weight loss. The devolatilization is assumed to be thermally neutral in accordance with most of the data which indicate relatively small effects [5]. The mass transport is modeled by an existing mechanism in FG-DVC. The key components in the model are 1) a heat transfer submodel; 2) a coal devolatilization submodel, FG-DVC; 3) a coal physical property (thermal conductivity and specific heat) submodel by Merrick [5,]; and 4) a correlation for convective heat transfer from gas to the particle reported by Kunii and Levenspiel [7] and Kothari [8].

Model predictions are being compared with experimental data in the literature for model verification. Morris and Keairns [4] studied three American coals at high pressure (10 atm) in a laboratory small scale fluidized bed facility with inert fluidizing gas. They reported 50% and 95% methane devolatilization times corrected for in-bed gas dispersion time for an Indiana coal. Fig. 1 compares the model predictions with data on the variation of the methane devolatilization time with mean particle size. The model predicts quite well the 50% methane devolatilization time. The slight

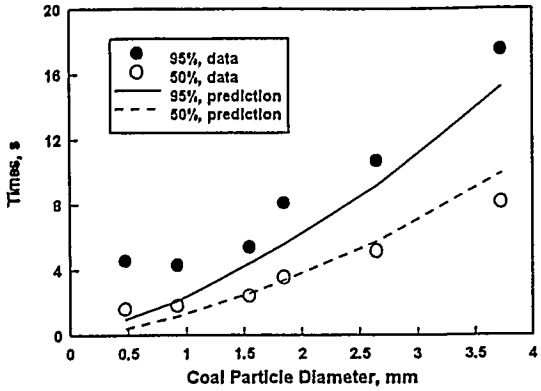


**Fig. 1. Predicted and Measured [4] $CH_4$ Devolatilization Times as a Function of Particle Size.**

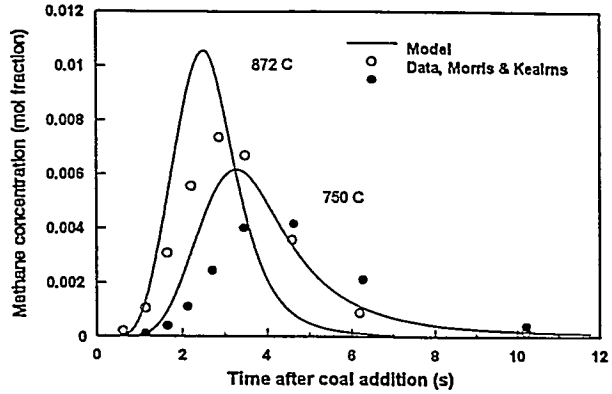


**Fig. 2. Comparison of Predicted In-Bed $CH_4$ Concentration with Measured $CH_4$ Off-Gas Concentration [4] for 1.55 mm Coal Particles at 872°C in Fluidized Bed.**

under-prediction of the 95% time is believed to be caused by the fact that coal particles used in the experiment had a range of particle sizes, which is not accurately described by an arithmetic mean particle size. This is more clearly shown when the methane concentration in bed is predicted and compared with the uncorrected off-gas data in Fig. 2. The time lag between the predicted and measured curves could arise from gas dispersion between the bed and the outlet. However, the contribution from larger particles in the size range could also lead to longer devolatilization times. Morris and Keairns [4] measured the dispersion time with a tracer method, and showed that the minimum dispersion time is 3 seconds. Since their off-gas data in Fig. 2 indicate that methane starts to be collected at the outlet as early as 1 second after coal addition, it is not clear how this information can be used to correct the off-gas data to derive the in-bed concentration. Given these uncertainties, the model predicts well both the evolution rate and the ultimate yield of methane of the large particles.

It appears that the heat transfer to coal particles in fixed and fluidized beds is difficult to model. Many investigators have reported correlations to calculate the Nusselt number from the particle Reynolds number. Gunn [9] pointed out that these values have several orders of magnitude difference at the same Reynolds number. Further work is needed to clarify this uncertainty.

**Transport Reactor Modeling (AFR)** - Significant progress has been made in developing a computational fluid dynamics (CFD) model for coal combustion and gasification in transport reactors (or circulating fluidized beds, CFBs). This work is being done using the BYU entrained-bed model (PCGC-2) as the framework. Since CFBs have much higher solid loadings than entrained beds, for which PCGC-2 was developed, major modifications have been made in the Lagrangian particle trajectory submodel. A stochastic particle turbulence dispersion model is used to model the particle dispersion. This modification is necessary because of the extensive gas-solid interactions in CFBs. Numerical modifications have also been made in the gas-phase aerodynamics model to handle the substantial interphase momentum exchange and pressure variations. This approach has been successful in cold flow modeling of CFBs. Model verification is being carried out based on a large set of experimental data from cold particle-laden flow data collected at the CCNY circulating fluidized-bed facility. Additional data are available from CFB research, which has been very active in the past decade. Fig. 3 illustrates a comparison of measurements and model predictions for the radial profile of void fraction at the 1/2 height of the CCNY reactor. The

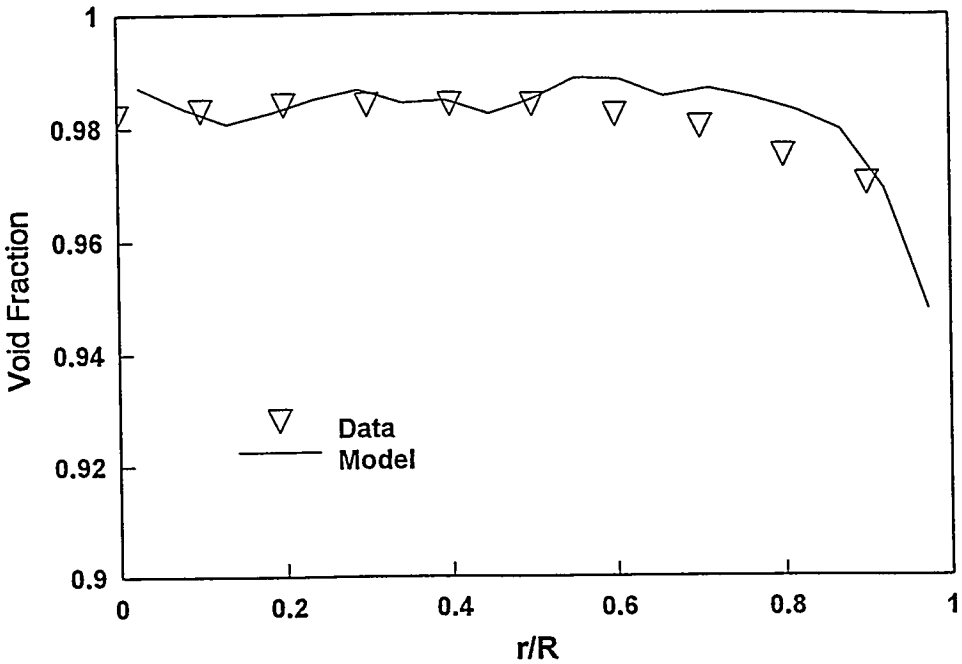


**Fig. 3. Comparison of Calculated and Measured Void Fraction Distribution in a Transport Reactor.**

comparison is surprisingly good. The model also predicts correctly the axial pressure drop and the particle velocity profile with downward flow near the reactor wall. The shape of the gas velocity profile is predicted but the discrepancy in the magnitude indicates a need for further investigation. It is planned to carry out systematic verification of the model with various flow conditions and to extend it to predict data for coal combustion and gasification.

The experimental work reported in the literature has revealed a unique gas-particle two-phase flow structure in CFBs. There is a dilute core coupled with a dense annulus. The masses (both gas and solids) in the core are rapidly transported upward while the annulus flow is slow but significantly downward-moving. There is no consensus on what causes this unique flow structure. Our calculations indicate that the turbulence structure plays an important role. Experimental observations have shown the intensive mass exchange between the core and the annulus. Such exchange is undoubtedly driven by the turbulence, since the average radial gas velocity is very low. Our calculations show two important phenomena. 1) When the turbulence is not homogeneous in the radial direction, solid particles tend to segregate in regions with low turbulence intensity. And 2) if the turbulence intensity in the core is high enough, particles will concentrate near the reactor wall.

This conclusion calls for a careful reconsideration of turbulence models. In addition, gas-particle turbulence interactions, particle-particle interactions, and particle-wall interactions may need to be further considered in the model.

**Fluidized-Bed Model (AFR) -** A reduced version of the FG-DVC model (FGDVC-RES) has been developed as a submodel for an existing fluidized-bed code, MFIX, developed at METC. FGDVC-RES employs only one ordinary differential equation to model the total devolatilization weight

loss, while coal dependent information (elemental compositions of char, tar and gas, rates and yields of char, tar and gas species) is provided through their correlations to the total weight loss. These correlations are given by a pre-calculation with the standard FG-DVC model based on the knowledge of nominal reactor conditions (pressure, temperature heating rate). This approach allows CFD codes to use FG-DVC as a submodel (in this case, MFIX) without the formidable computation burden of calculating the detailed devolatilization rates while retaining the predictive capability of the standard FG-DVC model. A version of FGDVC-RES is currently being integrated with MFIX at METC and will also be integrated at BYU with the fixed-bed code (FBED-1) under development there (see below).

**Nitrogen Evolution from Small and Large Coal Particles (AFR)** - Three bituminous coals were studied in this part of the project: Mettiki #2, Mapco #2, and Consol #2. Their proximate and ultimate analyses are given below (wt.% daf; ash and volatile matter on a dry basis; oxygen by difference):

| Coal | Ash | VM | C | H | N | S | O |
|---|---|---|---|---|---|---|---|
| Mettiki | 13.8 | 18.8 | 89.6 | 4.8 | 1.4 | 2.0 | 2.3 |
| Mapco | 8.3 | 37.8 | 83.2 | 5.4 | 1.5 | .78 | 9.1 |
| Consol | 11.2 | 35.8 | 84.8 | 5.6 | 1.5 | 2.0 | 6.1 |

These coals are being considered for use in the METC Gasification Product Improvement Facilities (GPIF). Experiments were carried out in a TG-FTIR system (thermogravimetric analysis combined with Fourier-transform infrared analysis of volatile products) using the procedure described in a previous publication [10]. In a typical experiment, a coal sample is placed in a flow of helium and heated at 30 K/min to 1173 K. Then the sample is held at the final temperature for three minutes. During this temperature excursion, weight loss is continuously monitored, and infrared spectra of the released gases are obtained once every forty-one seconds. To study the effect of particle size on the release of ammonia ($NH_3$) and hydrogen cyanide (HCN), samples with two particle diameters, $d_p$, were prepared for TG-FTIR testing: $d_p < 0.150$ mm; and $d_p \approx 5$ mm. In each run, the sample size was approximately the same ($m_s$ = 57-59 mg).

A strong influence of particle size on volatile-nitrogen evolution has been observed for all three coals. In Fig. 4, HCN and $NH_3$ evolution curves are shown as thick lines for the particle-size range 0-150 mm. As in the previous study of nitrogen release [11], a bimodal $NH_3$ evolution pattern can be seen. This is attributable to the primary and secondary ammonia release (the low- and high-temperature $NH_3$ peaks, respectively). According to the proposed model, coal-bound nitrogen (coal-N) is first released as HCN and (primary) ammonia, and this stage is followed by HCN reaction with char-hydrogen to form secondary ammonia as a product (Fig. 5).

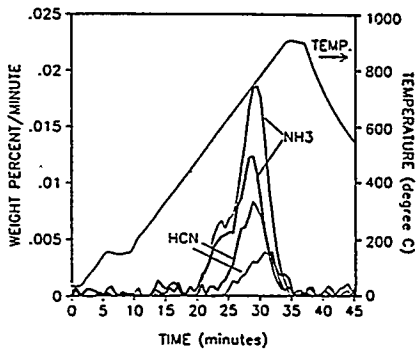


**Fig. 4. Nitrogen Evolution Patterns During Pyrolysis of Mettiki Coal. Thick Lines: $d_p < 0.150$ mm; Thin Lines: $d_p \approx 5$ mm.**

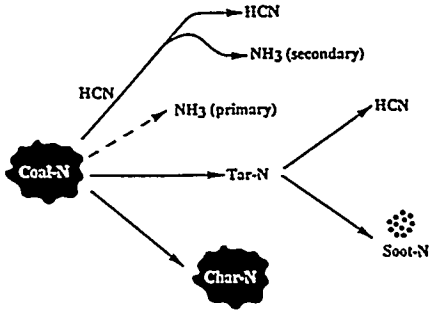


**Fig. 5. Nitrogen Evolution From Coal During Pyrolysis.**

If this mechanism is correct, then an increase in the particle size, and thus also in gas residence time within the particle, would lead to an increase in secondary-$NH_3$ release at the expense of the HCN peak. The primary ammonia peak should remain unchanged, or only weakly affected, as the amount of primary ammonia formation should not depend on the gas diffusion path length within the particle. This is precisely what is seen in Fig. 4, where the large-particle evolution curves are shown as thin lines. It should also be noted that the release of secondary-$NH_3$ and HCN occurs at the same time, which is in agreement with the proposed mechanism. The heterogeneous HCN-to-$NH_3$ conversion scheme is offered as an alternative to the gas-phase HCN hydrogenation mechanism suggested by Baumann and Möller [12]. If the HCN-to-$NH_3$ conversion were indeed a gas-phase reaction involving molecular hydrogen, then it would be difficult to justify the particle-size dependence, unless $H_2$ evolution happens to be particle size dependent. The collected data certainly provide strong evidence in favor of the heterogeneous scheme. Nitrogen evolution curves similar to those shown in Fig. 4 were also obtained in the case of Mapco and Consol coals.

**Modeling of hydrogen cyanide and ammonia release during coal pyrolysis** - The objective of this work is to demonstrate the potential of the FG-DVC model for predictive modeling of HCN and $NH_3$ release during coal pyrolysis. The FG-DVC model combines a functional group (FG) model for gas evolution and a statistical depolymerization, vaporization and cross-linking (DVC) model for tar formation. The model has been developed at Advanced Fuel Research, Inc., and described in several publications [1-3].

The nitrogen-evolution modeling is based on the following assumptions:

- Both HCN and $NH_3$ can be formed as primary coal pyrolysis products. The original coal-N is divided into inventories that potentially produce HCN, $NH_3$, and char-N.
- $NH_3$ is additionally produced by a secondary reaction between HCN and char-surface hydrogen. The time scale of this reaction is governed by the gas residence time within a particle, which is evaluated by a gas transport subroutine.
- Primary HCN and $NH_3$ formation mechanisms follow first-order kinetics with distributed activation energies. The secondary $NH_3$ formation from HCN is assumed to be first order in HCN and second order in surface hydrogen.
- As pyrolysis progresses, tar-N evolves from HCN, $NH_3$, and char-N producing inventories.
- The sizes of the HCN- and $NH_3$-producing inventories, as well as the kinetic parameters for nitrogen evolution, are determined by a laboratory TG-FTIR experiment.
- Tar-cracking reactions are neglected, except for the initial stage, which is treated using the same kinetics as those for coal pyrolysis.
- Frequency factors for all pyrolytic reactions are assumed to be of order $10^{12}$-$10^{14}$ $s^{-1}$ [13].

The input to the model is: (1) coal elemental analysis; and (2) low heating rate pyrolysis data collected for a given coal in a TG-FTIR experiment. The latter data are used to

determine the kinetic parameters for nitrogen evolution during pyrolysis.

Modeling of fluidized-bed pyrolysis data has been attempted in this study. Four Australian bituminous coals were used, and their elemental compositions are shown in the table below (wt.% daf; ash and VM dry basis; oxygen by difference). The fluidized-bed pyrolyzer and experimental conditions have been described elsewhere [13,14].

| Coal | Ash | VM | C | H | N | S | O |
|---|---|---|---|---|---|---|---|
| A | 12.1 | 39.8 | 83.6 | 5.4 | 1.9 | 1.1 | 8.1 |
| B | 13.6 | 23.8 | 87.4 | 4.6 | 1.7 | .32 | 5.9 |
| C | 11.2 | 20.3 | 88.5 | 4.7 | 1.8 | .48 | 4.5 |
| D | 13.0 | 16.0 | 88.7 | 4.6 | 2.0 | .57 | 4.2 |

HCN and $NH_3$ yields for coal B are plotted as a function of temperature in Fig. 6. It can be seen that the HCN evolution increases with temperature, whereas $NH_3$ yields exhibit a maximum at about 1050 K. It should be noted that the model accurately predicts both trends. The maximum in $NH_3$ yields can be qualitatively explained by a decrease in HCN residence time within the particle at elevated temperatures. As temperature increases, so does the rate of evolution of HCN and other species. Since transport rates within the particle increase with the volume of gases evolved, HCN is more rapidly shuttled out of the particle. As a consequence, the reduced HCN residence time leads to smaller quantities of secondary $NH_3$. The reason for the slight underprediction of $NH_3$ release near the maximum is believed to be related to inaccuracies in estimating the gas residence time within the particle. Work on improving the sub-model describing gas diffusion through the porous particle is under way.

Results for coals A, C, and D are similar to those shown in Fig. 6, except that the model underpredicts HCN yields at higher temperatures for coal A. This is due to the tar cracking reactions, which are not accounted for by the model. Tar formation is more important in the case of the more volatile coal A than for the higher-rank coals B, C, and D.

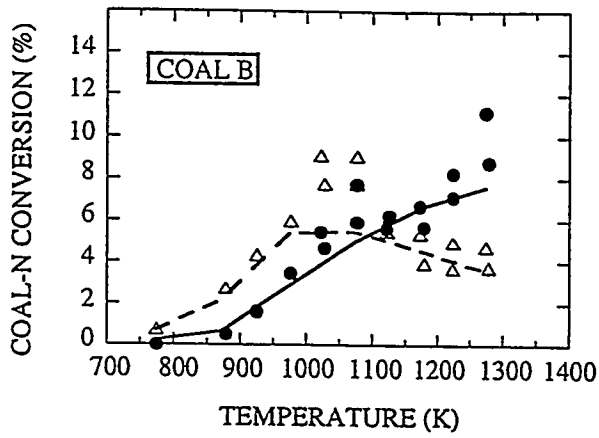


**Fig. 6. HCN (•) and $NH_3$ (Δ) Yields in Fluidized-Bed Pyrolysis of Coal B. Solid and Dotted Lines are Model Predictions for HCN and $NH_3$, Respectively.**

**Oxidation Rates for Large Coal Particles at High Pressures (BYU)** - Fixed-and fluidized-bed combustion and gasification processes are typically done with large coal particles at high pressures but the previously available fixed-bed codes use kinetic rates derived from small particle experiments at atmospheric pressure. Thus, work was conducted to measure kinetic rates for large coal particles at high pressures.

In a previous project, a unique experimental facility was constructed to obtain oxidation rates of large particles at high temperatures and high pressures. It consists of a cantilever beam balance insert for the BYU High Pressure Controlled Profile (HPCP) reactor. The balance unit measures the mass loss of the particles as they oxidize in the HPCP reactor. It includes a force transducer, a ceramic cantilever beam, and a platinum wire-mesh sample basket. The basket is secured to the cantilever beam and

extends into the reactor tube through one of the optical access ports of the HPCP reactor. This facility permits measurements of the oxidation and gasification rates of char particles at pressures up to 17 atm and temperatures up to 1700 K. It was successfully demonstrated by measuring the effects of pressure on oxidation rates of mm-sized Utah bituminous and North Dakota lignite char particles.

During the past year, the facility was overhauled and a new round of experiments was begun. The experiments are being conducted with Consol #2, Mapco #2, and Mettiki #2 coals. As discussed above, these coals are to be used for the PyGas™ gasifier under the DOE/METC Gasification Product Improvement Facility (GPIF) project. Parametric experiments were performed by measuring mass loss and gas temperature versus time for coal samples of 0.1, 0.2, and 0.3 grams, at temperatures of 900, 1050, and 1200 K, and Reynolds numbers of 63, 126, and 252 all at atmospheric pressure. This resulted in 39 runs; 20 additional runs at the average values of the parameters were also performed to check the reproducibility of the experiment. The results are still being analyzed but the following statements can be made at present. The experiments ran typically for 15 minutes and could be divided into devolatilization, oxidation, and decay zones. The devolatilization zone had the greatest mass loss rate while the oxidation zone had the greatest mass loss. The cube root of mass declined linearly with time for all coals as shown in Figure 7 and as previously observed. This is consistent with a thick ash layer model. Ash layers formed and usually remained in place around the char particles. Additional parametric experiments will be performed at higher pressures such as 5 and possibly 10 atmospheres. The experimental results will be analyzed and correlated and, based on these results, a new model of large coal particle oxidation at high pressures will be developed.

**Advanced Fixed-Bed Model Development and Evaluation (BYU)** - Some coals such as caking coals, cannot be readily gasified in traditional fixed-beds. Therefore, novel configurations have been proposed to gasify caking coals. One such complex configuration is a high-pressure, air-blown, dry-ash, staged gasifier of the PyGas™ gasification process, which is under development for the DOE/METC Gasification Product Improvement Facility (GPIF) project. Another such complex configuration is used in the DOE Clean Coal Technology's (CCT) ENCOAL mild coal gasification process. There is a need for a general, advanced, computer model that can be used as a reliable design and analysis tool capable of simulating both traditional and emerging novel configurations such as the staged gasifier of the GPIF project and the rotary fixed beds of the ENCOAL project.

The overall approach in developing such a model is to improve and extend the comprehensive, one-dimensional fixed-bed code (FBED-1) developed previously to (1) include provisions for countercurrent, cocurrent and possible crosscurrent flows as well as for the additions and withdrawals of gases at multiple locations in the bed, (2) incorporate the advanced submodels being developed in other projects for coal devolatilization, oxidation, and gasification processes for large coal particles in fixed beds, (3) incorporate an efficient and robust numerical method appropriate for stiff, non-linear problems and (4) evaluate the advanced fixed-bed code by comparing its predictions with the experimental data for temperature, pressure, and composition profiles in fixed beds available from the literature and from the developers.

Accomplishments this year include additional sensitivity analysis of the FBED-1 model to study the effects of the devolatilization

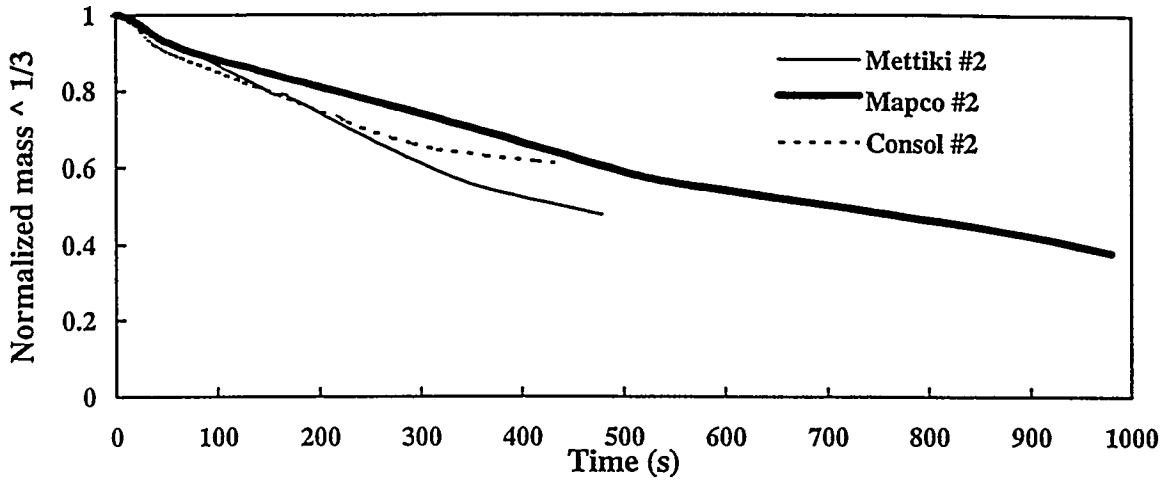


**Fig. 7. Cube Root of Normalized Mass Loss vs. Time For Coal Sample of 0.2g at 900K, 126 Re, and 1 atm.**

submodels, the oxidation and gasification submodels, and the gas phase chemistry options. Based on this analysis, the recommended options for the FBED-1 model are: the FG-DVC submodel for devolatilization, the Shell Progressive (SP) submodel for oxidation and gasification, and a partial chemical equilibrium option for the gas phase. The partial equilibrium option involves keeping tar non-reactive and gases non-reactive below a switch temperature, although both are kept in thermal equilibrium. Also, the fixed-bed model, FBED-1, was extended to handle a cocurrent flow pattern. Modifications were made to allow for additions and withdrawals of gases at multiple locations in the bed, but the preliminary results indicated a need for full kinetic treatment of gas phase chemistry, which is now under consideration. Also, under consideration is a reduced version of the FG-DVC devolatilization submodel, FG-DVC-RES, which is computationally more efficient than the standard version, FG-DVC.

The modified FBED-1 code with the cocurrent flow option was successfully used to simulate the PyGas™ staged gasifier using preliminary input data proposed by CRSS, Inc. and again using more recent design geometry and input data. The geometry of the gasifier required separate simulation of five flow regions, with the results of one region being used as the input for the following region. The simulations were done for the all-rank oxidation and gasification kinetics at atmospheric pressure, for the Pittsburgh #8 kinetics at atmospheric pressure, and for the Pittsburgh #8 kinetics at 41 atm. Simulation results for the latter case, which show detailed profiles for both cocurrent and countercurrent sections of the gasifier, are displayed in Figure 8.

Additional improvements will be made in the FBED-1 model to improve its industrial utility as a design and analysis tool. These improvements will include incorporation of a large particle devolatilization version of FG-DVC called LCPD (see above) and a large particle oxidation submodel being developed under this project. A robust solution method suitable for stiff, non-linear problems of fixed-bed systems will be implemented. The model will be evaluated by comparison with experimental data and by application to gasifiers of interest such as the PyGas™ gasifier.

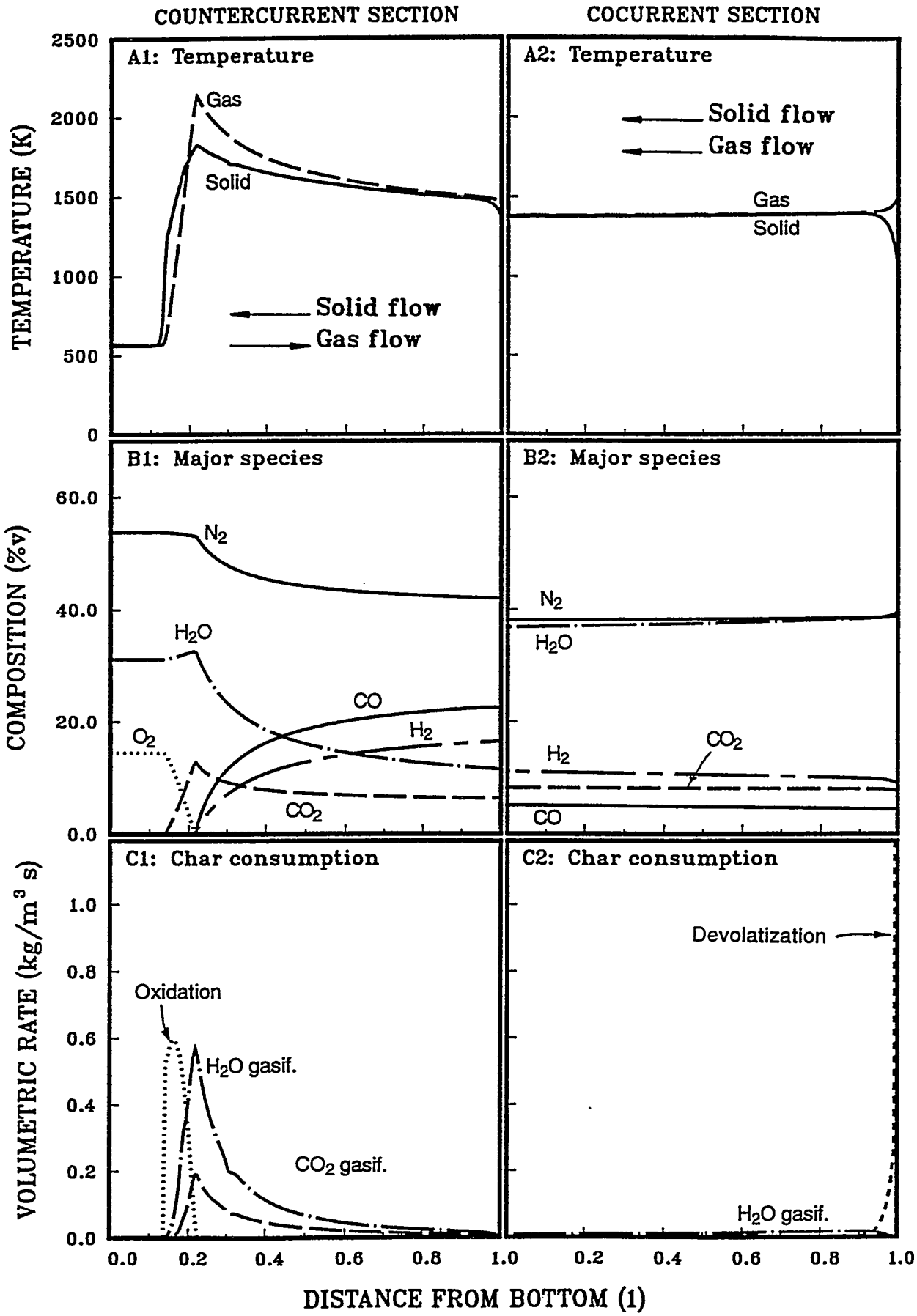


**Fig. 8. FBED-1 Predictions for the PyGas Gasifier for the Pittsburgh #8 Kinetics at 41 atm.**

**Application of ACERC Combustion and Gasification Codes and AFR Diagnostic Capabilities to Systems of Interest to METC (BYU/AFR)** - The Hague coal combustor is a part of the Kennebunk Test Facility, an externally-fired, combined cycle demonstration facility being built by Hague International under funding from the DOE Morgantown Energy Technology Center. The Hague coal combustor is a two-stage, down-fired combustor. A collar divides the first stage from the second and also provides access ports for the second stage air. The first stage operates fuel-rich to reduce $NO_x$ emissions. To complete combustion, the remaining combustion air is added in the second stage. Successful operation of the downstream units, the slag screen and the ceramic heat exchanger, depends strongly on the performance of the combustor.

The performance of the combustor was predicted by a three-dimensional, coal combustion code, PCGC-3. The gas flow is solved in the Eulerian framework, using a finite-difference formulation of the Navier-Stokes equations coupled with the energy conservation equation. The particle transport is solved separately in the Lagrangian framework, and the two phases are coupled through various source terms. The turbulent, Reynolds stresses are approximated by an effective eddy viscosity. The conservation equations are closed by the Prandtl mixing length model, the standard k-ε model, or the nonlinear k-ε model. The gas phase reactions are assumed to be fast and limited by turbulent mixing rates only. Thus, the reaction rates are calculated using locally instantaneous equilibrium based on the degree of mixing of the relevant species. The extent of mixing between inlet gas streams is described by a conserved scalar variable, mixture fraction. The fluctuations of the mixture fraction are modeled by a probability density function. Particle reactions such as drying, devolatilization, oxidation, and gasification are included. Devolatilization is modeled by a single-step or a two-step model. Oxidation and gasification rates are determined from Arrhenius-type expressions. Radiative heat transfer between gases, particles, and walls is modeled by a discrete-ordinates method. Formation of thermal and fuel $NO_x$ is included. The Zel'dovich mechanism is used for the thermal NOx and global reaction rates based on the de Soëte rates were used for the fuel $NO_x$. Formation and capture of $SO_x$ species by a sorbent can also be modeled if needed.

The simulations were conducted using the following options and parameters: the standard k-ε turbulence model, the single-step devolatilization model, the oxidation model, and the devolatilization and oxidation rate constants for a hvAb coal such as Pittsburgh #8. The computational grid was constructed of 86,240 cells (110 x 28 x 28). The mass balance closure was within 0.01% and the energy balance closure within 4.79%. The gas velocity vectors in an axial section through the center line are shown in Figure 9. These first results are preliminary in nature.

Additional simulations will be performed to yield better convergence and to confirm grid size independence. Simulations will also be performed to investigate the effects of coal kinetic rates, inlet conditions such as flow rate and swirl of primary and secondary air, boundary conditions such as wall temperature, and design elements. The specific, devolatilization and oxidation rates of coal fired at the Kennebunk Test Facility will be measured by AFR and BYU and used in the new computations.

**Submodel for Lean Premixed Combustion of Natural Gas in Industrial Gas Turbines (BYU)** - A submodel for lean, premixed combustion (LPC) of natural gas in industrial gas turbines is being developed for implementation into a general, comprehensive gas turbine combustion model being developed under independent funding. The submodel must incorporate finite-rate chemistry

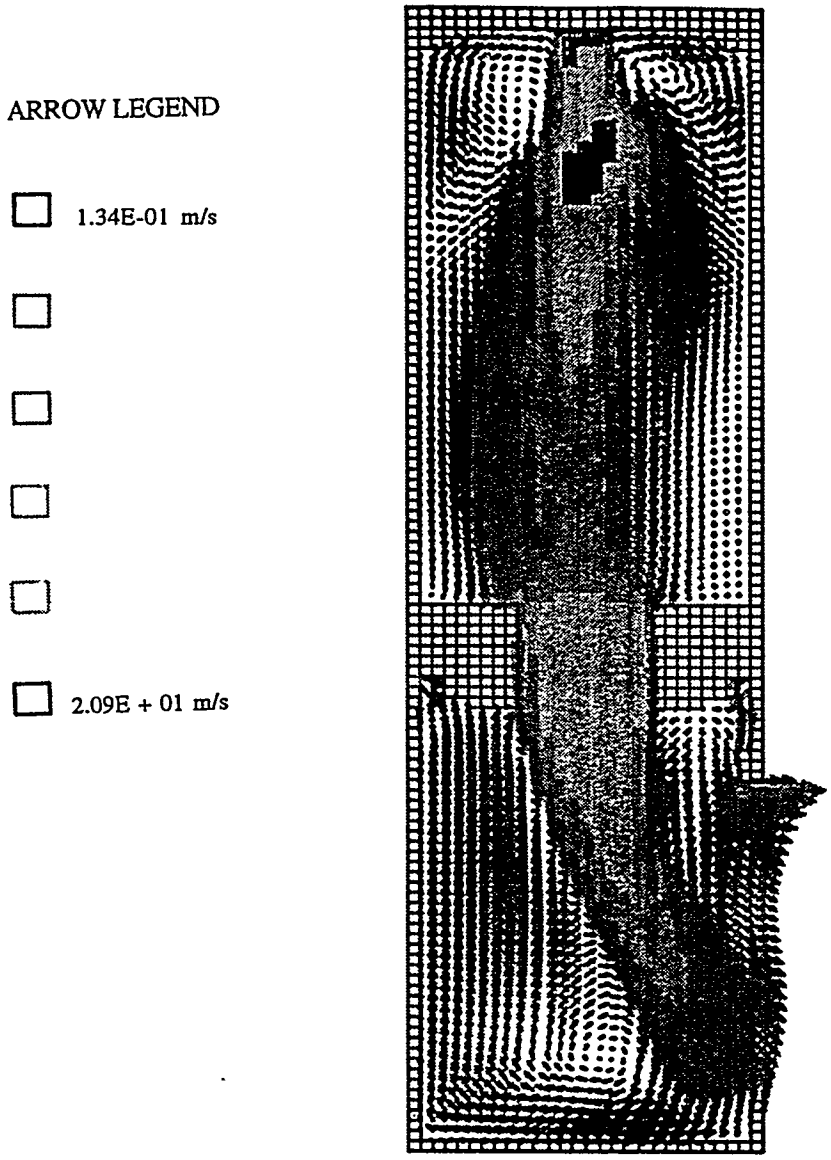


**Fig. 9. PCGC-3 Prediction of the Gas Velocity Field for the Hague Coal Combustor at the Axial Section Through the Center Line.**

and predict $NO_x$ and CO emissions at conditions approaching fuel-lean blowout (0.4 to 0.6 stoichiometric ratio in the primary zone). Proper accounting for the effects of chemistry/turbulence interactions is important. The Monte Carlo probability density function (pdf) method [15] has been selected as a basis for the submodel.

A partially-stirred reactor (PaSR) model has been used to investigate the pdf method and to help evaluate reduced kinetic schemes. In the PaSR [16], there is a finite rate, given by a mixing frequency, at which the reactive fluids are mixed on a molecular level, as well as a finite rate at which they react after being mixed. Both the mixing and reaction time scales are important in the PaSR. Chemical mechanisms of varying complexity for $CH_4$-air have been tested with the PaSR model at conditions typical of gas turbines. Figures 10a and b show lean premixed $CH_4$-air combustion (equivalence ratio = 0.378, pressure = 30 atm, inlet temperature = 1200 K) predictions of mean temperature and CO mass fraction, respectively.

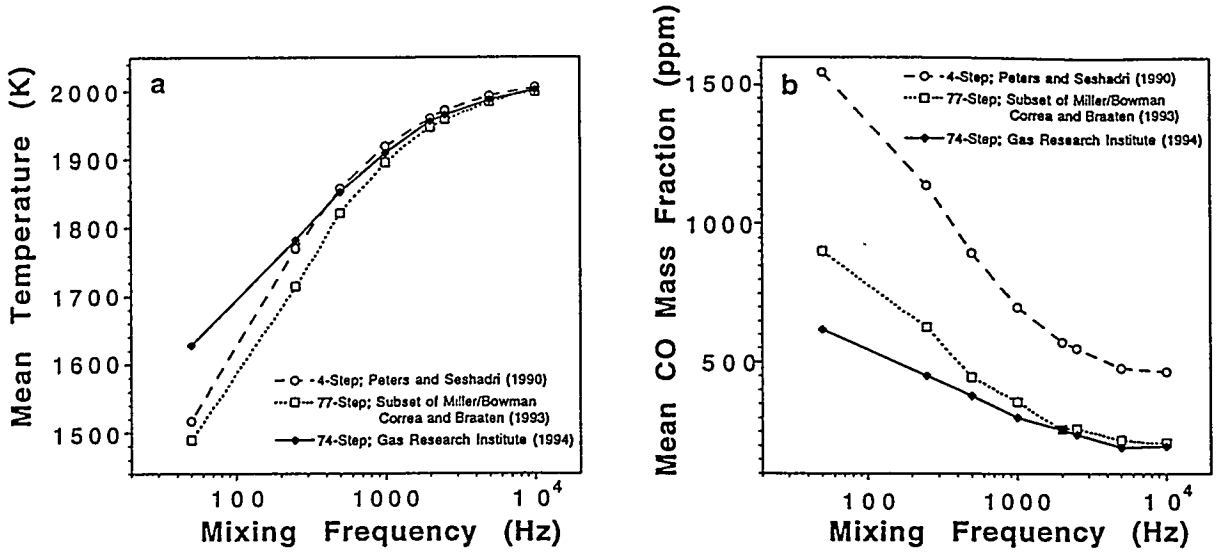


**Fig. 10. (a) Predicted Mean Temperature and (b) CO Mass Fraction vs Mixing Frequency for Reduced and Detailed Chemical Mechanisms.**

A velocity-scalar pdf submodel [17] has been tested and is being incorporated into an existing combustion flow code. The velocity-scalar pdf method is more accurate than the scalar-only pdf method and avoids the assumption of gradient diffusion. The chemistry was modeled with a single reaction progress variable, using Model A from the work of Chen and Kollmann [18]. Figure 11 shows scatterplots of particle position for non-premixed, adiabatic combustion of hydrogen and oxygen. The two-dimensional, axisymmetric jet enters at the left, and the flow is from left to right. The bottom edge of the figure represents the centerline of the reactor, and the outside wall is at a radial location of 0.2 m. There is a recirculation zone in the upper left corner. Each dot represents a pdf fluid "particle." Approximately 108,000 fluid particles were used in the calculation. A 20 x 20 grid was used in the flow code. Only one out of every five particles is shown.

During the next year, the submodel will be refined and extended to three dimensions. The model will be tested with kinetic schemes for LPC provided by independent work, and the submodel will also be incorporated into an unstructured flow code and applied to gas turbine configurations.

## FUTURE WORK

Work during the next year will include: completion of verification of the FGDVC-RES model for fixed and fluidized beds; 2) completion of the large coal particle devolatilization (LCPD) version of the FG-DVC model; 3) completion of the CFB model development; 4) completion of the integration of FGDVC-RES with the MFIX model; 5) complete development of nitrogen devolatilization submodel; 6) complete development of large particle oxidation model; 7) complete integration of advanced submodels for large particles (oxidation, devolatilization) and improved numerical methods into FBED-1; 8) continue refinements of solution technique for LPC codes; 9) completion of case applications; 10) delivery of computer models to METC.

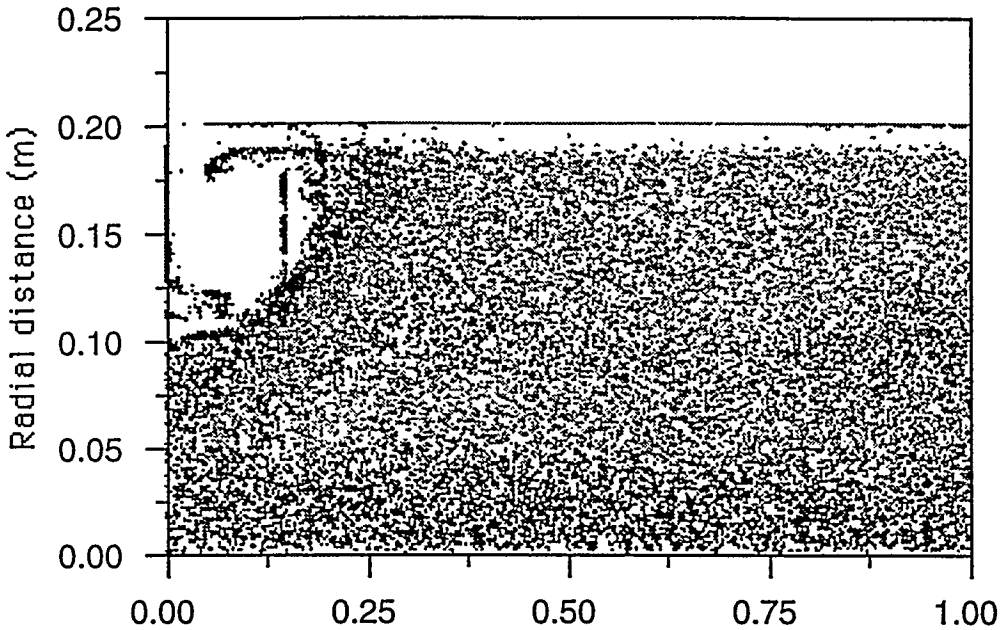


**Fig. 11. Scatterplot of Instantaneous Particle Position for Velocity-Scalar pdf Simulations of Non-Premixed Combustion of Hydrogen and Oxygen.**

## REFERENCES


1. Solomon, P.R., Hamblen, D.G., Carangelo, R.M., Serio, M.A., and Deshpande, G.V., Energy & Fuels, 2, 405 (1988).

2. Solomon, P.R., Hamblen, D.G., Serio, M.A., and Yu, Z-Z., and Charpenay S.C., Fuel, 72, 469 (1993).

3. Solomon, P.R., Hamblen, D.G., Yu Z-Z., and Serio, M.A., Fuel, 69, 754 (1990).

4. Morris, J.P., Keairns, D.L., Fuel, 58, 465 (1979).

5. Merrick, D., Fuel, 62, 540 (1983).

6. Merrick, D., Coal Science and Chemistry, A. Volborth (Ed.), p307, Elsevier, Amsterdam, 1987.

7. Kunii, D., and Levenspiel, O, Fluidization Engineering, Wiley, New York, 1968.

8. Kothari, A.K., M. S. Thesis, Illinois Institute of Technology, Chicago, 1967.

9. Gunn, D.J., Int. Heat Mass Transfer, 21, 467 (1978).

10. Whelan, J.K., Solomon, P.R., Deshpande, G.V., Carangelo, R.M., *Energy & Fuels* 2:65 (1988).

11. Bassilakis, R., Zhao, Y., Solomon, P.R., and Serio, M.A., *Energy & Fuels* 7, 710 (1993).

12. Baumann, H. and Möller, P., *Erdöl, Erdgas und Kohle* 44(1):29 (1991).

13. Wójtowicz, M.A., Zhao, Y., Serio, M.A., Bassilakis, R., Solomon, P.R. and Nelson, P.F., "Modeling of hydrogen cyanide and ammonia release during coal pyrolysis," to be presented at the 8th Int. Conf. on Coal Science, Oviedo, Spain, 10–15 Sept., 1995.

14. Tyler, R.J., *Fuel* 58:680 (1979).

15. PDF2DS [Computer Program]. Stephen B. Pope, developer. Version 0.0. Ithaca, NY: BEAM Technologies Inc.; 1975.

16. Chen, J. -Y., "Stochastic Modeling of Partially Stirred Reactors," Western States Section of the Combustion Institute, Spring Meeting, Paper No. WSS 93-071, (1993).

17. Pope, S. B., "PDF Methods for Turbulent Reactive Flows," Progress in Energy and Combustion Science, Vol. 11, pp. 119-192, (1985).

18. Chen, J. -Y; Kollmann, W. Chemical models for pdf modeling of hydrogen-air nonpremixed turbulent flames. Comb. Flame. 1990; 79: 75-99.

# PB.19 Development of Methods to Predict Agglomeration and Deposition in FBCs

## CONTRACT INFORMATION

| | |
|---|---|
| **Contract Number** | DE-FC21-93MC30098 |
| **Contractor** | Energy & Environmental Research Center<br>University of North Dakota<br>PO Box 9018<br>Grand Forks, ND 58202-9018<br>(701) 777-5000<br>(701) 777-5181 fax |
| **Other Funding Sources** | Ahlstrom Pyropower<br>Electric Power Research Institute<br>North Dakota Industrial Commission<br>Northern States Power Company |
| **Contract Project Manager** | Michael D. Mann |
| **Principal Investigators** | Ann K. Henderson<br>Michael L. Swanson<br>Thomas A. Erickson |
| **METC Project Manager** | Arthur Hall |
| **Period of Performance** | January 1, 1993, to December 31, 1995 |

## OBJECTIVES

This 3-year; multiclient program is providing the information needed to determine the behavior of inorganic components in FBC units using advanced methods of analysis coupled with bench-scale combustion experiments. The major objectives of the program are as follows:

- To develop further our advanced ash and deposit characterization techniques to quantify the effects of the liquid-phase components in terms of agglomerate formation and ash deposits
- To determine the mechanisms of inorganic transformations that lead to bed agglomeration and ash deposition in FBC systems
- To develop a better means to predict the behavior of inorganic components as a function of coal composition, bed material characteristics, and combustion conditions

## BACKGROUND INFORMATION

The successful design and operation of advanced combustion systems requires the ability to control and mitigate ash-related problems. The major ash-related problems are slag flow control, slag attack on the refractory, ash deposition on heat-transfer surfaces, bed agglomeration, corrosion and erosion of equipment materials, and emissions control. These problems are the result of physical and chemical interactions of the fuels, bed materials, and system components. The interactions that take place and ultimately control ash behavior in fluidized-bed combustion (FBC) systems are controlled by the abundance and association of the inorganic components in coal and by the system conditions. Because of the complexity of the materials and processes involved, the design and operations engineer often lacks the information needed to predict ash behavior and reduce ash-related problems.

Even though the FBC operates at a relatively low temperature, a number of potential ash-related problems exist. For example, deposition on in-bed superheater tubes and supports has been noted for several bubbling FBCs. The amount of deposition is quite variable and dependent upon fuel type. A 40°F loss in superheat temperature over a 4-month period at the Montana–Dakota Utilities (MDU) Heskett Station is one example.

In-bed agglomeration, also noted, has been responsible for unscheduled shutdowns. Agglomeration of this extent limits the range of fuels that can be burned in the FBC.

Deposition in the convective pass has also been noted by bubbling-bed FBC users. This deposition results in loss in steam temperature. Knowing the propensity of certain coal ashes to deposit in the convective section is important for the design of tube spacing and sootblower coverage and schedule.

Similar problems have been identified in circulating fluidized-bed combustion (CFBC) applications. Again, deposition in the convective pass results in a loss in steam temperature. Knowing deposition rates and deposit strengths will be important for designing tube spacing and sootblower coverage and schedule. Another problem inherent to certain fuels in the CFBC is deposition in the cyclone and other cooled surfaces. Some deposits can fall down, plugging drains and loop seals. The deposits can also serve as sites for alkali corrosion.

Agglomeration in the loop seal and bed of the CFBC is responsible for unscheduled shutdowns. As in the bubbling bed, the CFBC requires high bed turnover rates or limitations on bed material selection for control of agglomeration. These problems limit the range of fuels that can be burned in the CFBC.

## PROJECT DESCRIPTION

This is a multifaceted program designed to further our understanding of ash-related problems in FBCs. The major tasks include enhancement of analytical techniques, analyses of material from full-scale FBCs, bench-scale reactor development, applied fundamental chemistry and physics, and development and verification of predictive techniques and mitigating measures.

Samples from full-scale units will be analyzed in detail with scanning electron microscopy. The information collected will allow detailed analyses of the fuel causing agglomeration or deposition problems; identify the coating and bonding material causing the agglomeration and deposition; indicate the mineral species contributing to strength development; provide data for developing a model to predict agglomeration and deposition; and ensure validity and relevance of bench-scale tests.

The bench-scale fluidized-bed reactor will be used to perform combustion tests to determine the effect on agglomeration of operating conditions, bed material, sorbents, and additives. The information collected will provide an extensive database of fuel, bed, and sorbent properties and operating conditions for model development. This task should result in information to use to predict agglomeration and provide a device for studying mitigating measures.

Samples from the full-scale units and the bench-scale reactor will be used to 1) determine the physical and chemical processes that result in the partitioning of ash components in FBCs and 2) to better understand the physical and chemical interactions of ash components upon cooling, sintering, and deposition. The information collected during this task will identify specific processes and conditions responsible for operational problems and provide input to the development of predictive techniques and mitigating measures for FBCs.

A computer model currently available to predict deposition in pulverized coal (pc)-fired units will be adapted for FBC use. The ultimate model would be an empirical algorithm to predict the rates of fines generation, sticky particle generation, elutriation, deposition on in-bed tubes and supports, agglomeration and defluidization, deposition on walls, and deposition on convective pass tubes. It is desirable to be able to predict these rates as a function of firing mode, velocity, bed type and size distribution, fuel type and size, sorbent, and oxygen concentration.

## RESULTS

### Fluidized-Bed Agglomeration

The detailed analyses of agglomerate, deposit, and bed material samples from the Montana–Dakota Utilities (MDU) Heskett Station and the Tidd pressurized fluidized-bed combustor (PFBC) provided the information required to develop mechanisms of formation for FBC agglomeration and deposition. The proposed mechanism is shown in Figure 1. Bed material agglomerates can typically be classified into four distinctly different categories. One type of agglomerate forms from relatively small bed particles that stick together, forming larger masses of bed material. In this case, coal ash reacting with bed material forms the substance that acts as the "glue" in agglomeration. These ash-related interactions occur under normal atmospheric FBC operating conditions and include the formation of low melting points between sodium-, potassium-, calcium-, and sulfate-rich components and possibly some solid–solid reactions. These agglomerates have a solid core and resemble raspberries.

The second type of agglomeration appears as hollow "eggs." These can be drained out of the bed with spent-bed material in mild cases, but will cause defluidization and a forced shutdown in severe cases. These agglomerates form around burning coal particles. After the coal burns out, a hollow egg-shaped agglomerate remains. Agglomerates ranging from about ½ in. to 3 in. in diameter have been noted by EERC personnel from various units.

A third type of agglomeration is the result of localized hot spots of bed material, where temperatures in the FBC can exceed the typical 1700°F limit. Temperatures capable of melting various ash species can be attained even during relatively stable operation of the FBC. This type of agglomerate appears as a sintered mass with obvious signs that melting had occurred. This type of agglomerate is typical of localized zones of poor fluidization, such those that may exist during start-up or turndown of a multicell unit. Agglomerates of this type are also formed when defluidization occurs because of other

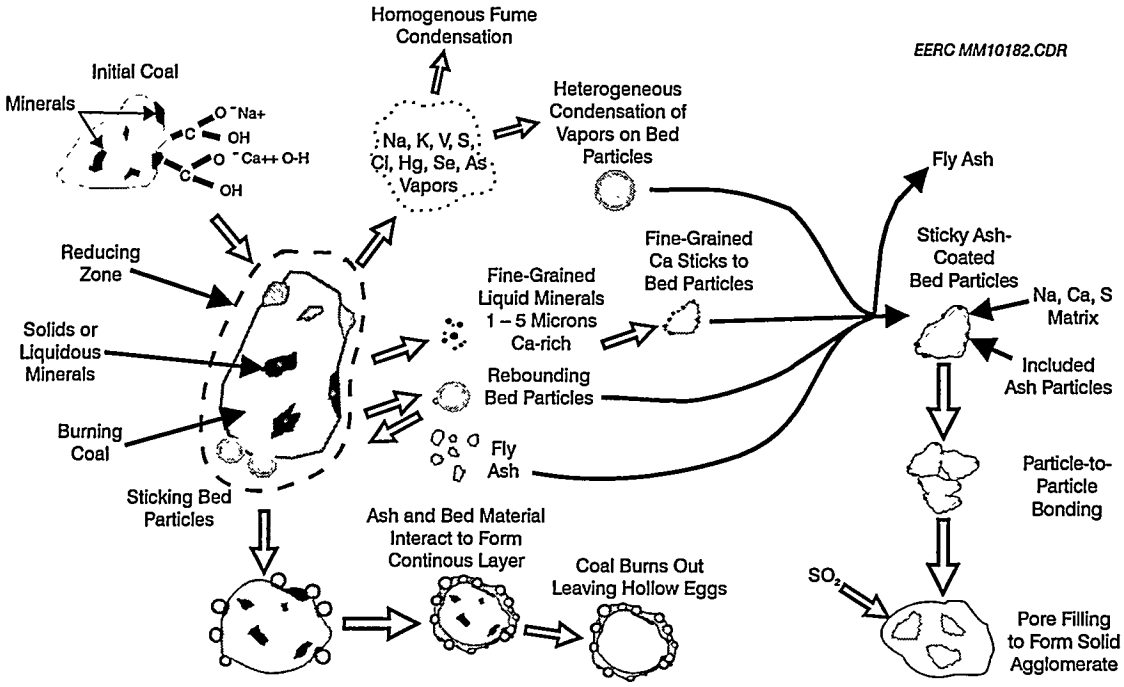


**Figure 1. Pictorial Reproduction of the Mechanisms of Ash Formation and Bed Material Agglomeration in Fluidized-Bed Combustion**

mechanisms, and local temperatures increase as a result of the poor fluidization.

A fourth type of agglomerate consists mainly of sintered fly ash, with some fine sorbent material intermixed. This type of agglomerate is very fine-grained and dense. Typically these agglomerates are much weaker and can be broken up more easily than can the other three types of agglomerates. These sintered fly ash agglomerates are more commonly found in loop seals or other areas of low or stagnant flow.

The primary components of the fuel that are typically associated with agglomeration are the alkaline-earth elements, specifically, organically bound or water-associated sodium or potassium. Other elements that have been associated with agglomeration in atmospheric systems at normal operating temperatures (<1700°F) include iron, vanadium, and calcium. Higher operating temperatures and pressures can also cause certain silicon and aluminum compounds to participate in the agglomeration mechanisms.

## Factors Enhancing Agglomerate Formation

Egg-type agglomerates will form if conditions within the bed promote melting of the fuel ash. Therefore, agglomeration is enhanced by the mineral content of the fuel. The size and composition of the minerals in the fuel must be known to determine whether agglomerates may be a problem with a particular fuel.

Agglomeration is enhanced by local reducing zones, since the liquidus temperature of the mixture is lower for reducing than for oxidizing

zones. The viscosity is also lower in the reducing zones, making sinter formation easier.

Agglomeration becomes more severe when the melting temperatures of the various mineral phases are approached. Therefore, higher temperature, especially at the surface of the burning coal particle, will enhance agglomeration.

As pressure increases, even for a fixed bed temperature, the temperature of the burning coal particle increases. This increase in temperature is caused by the high reaction rates related to the higher partial pressure of oxygen.

The propensity to agglomerate increases with the presence of a fluxing agent. Sodium and calcium are good fluxing agents, lowering the melting point of certain silicate-based clays. The ability of the calcium to flux increases as the particle size decreases because of the increased surface area.

**Ash Formation and Boiler Tube Fouling**

The ash formation and fouling mechanism for boiler tube deposition is shown in Figure 2. This mechanism shows that the combustion of the initial coal particles again results in the formation of vapor-phase species (such as Na, K, S) and the formation of fine-grained liquid droplets (as calcium-rich oxides and sulfates) and fly ash particles. The fouling mechanism is initiated by the condensation of alkaline salts from the vapor phase on the surface of the tube to form a concentrated alkali sulfate layer. This layer increases in thickness until the reduced heat transfer allows the 1- to 5-micron inorganic Ca-rich droplets to impact the condensed alkali sulfate layer, where sintering of the calcium sulfate bonds the fine-grained ash to the tube surface. As the sintering of the deposit continues, a thicker, more dense deposit develops in which other ash species can become trapped on the captive surface of the deposit. Thus, coals with more organically bound cations of sodium and calcium show higher deposition rates than coals with no alkalis or clay-associated alkalis. The presence of certain aluminosilicates in the coal ash has been shown to react with some of the alkali elements, thereby reducing the alkali-induced deposition.

**Bench-Scale Testing**

A fluidized-bed reactor (FBR) has been constructed to simulate the bed chemistry, ash interactions, and emissions from a fluidized-bed combustor under closely controlled conditions. This reactor is used for sorbent characterization, gaseous emissions including trace elements, agglomeration, and hot-gas cleanup testing in a cost-effective manner over a wide range of operational conditions. The 55-in.-tall reactor, constructed of 3-in. Schedule 80 pipe, is externally heated with three ceramic heaters. A hot cyclone collects the ash and bed material that are carried out of the reactor. The preheated fluidizing gas can be a mixture of air and nitrogen or just air; in addition, one additional gas such as carbon dioxide, carbon monoxide, sulfur dioxide, or a nitrogen oxide can be added to result in a fuel gas similar to that generated in a full-scale fluidized-bed combustor. Preheated gas at temperatures up to 1000°F is supplied at the bottom of the reactor through a 1-in. Schedule 40 pipe. The fluidizing gas is supplied at sufficiently high velocities to prevent the sized bed material from dropping out during operation. A schematic of the bench-scale FBR is shown in Figure 3.

Table 1 shows the operating conditions and duration of the tests performed on the FBR. The fuel for each test was sized to −1/8-in., and sand was used as a start-up bed material for all but Test KR2-1995, which used Gabbro bed material. Superficial gas velocity was approximately 6 ft/s

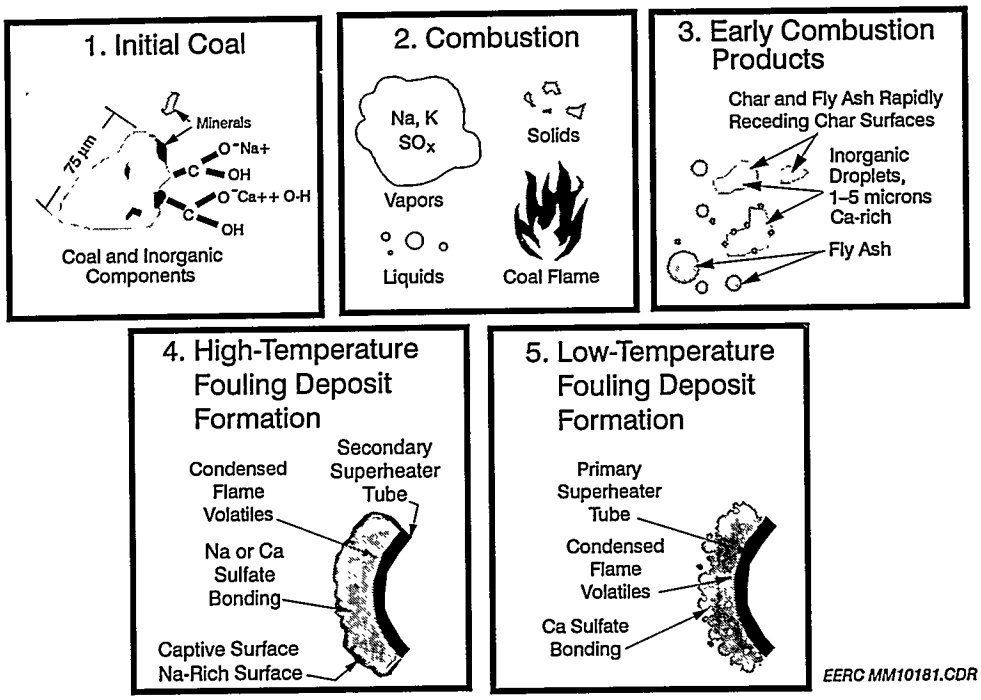


**Figure 2. Ash Formation and Fouling in Fluidized-Bed Combustion**

for all tests except KR1-0295, which had a velocity of 11 ft/s. Standard test length was 16 hr; bed material and fly ash samples were collected every 4 hours. These samples were analyzed with x-ray fluorescence (XRF) to determine the change in bed chemistry over time and scanning electron microscopy (SEM) to examine the coating on bed material particles and sticking between particles.

## FUTURE WORK

Work on this project will continue through December 1995. Funding continues from Ahlstrom Pyropower, EPRI, Northern States Power Company, and the North Dakota Lignite Research Council. Funding through the new DOE–EERC Jointly Sponsored Research Program is also in place for the final year of the project. It is hoped that at the end of this 3-year project, an accurate method will have been developed to predict the propensity for fouling and agglomeration, along with methods to reduce or eliminate these ash-related problems.

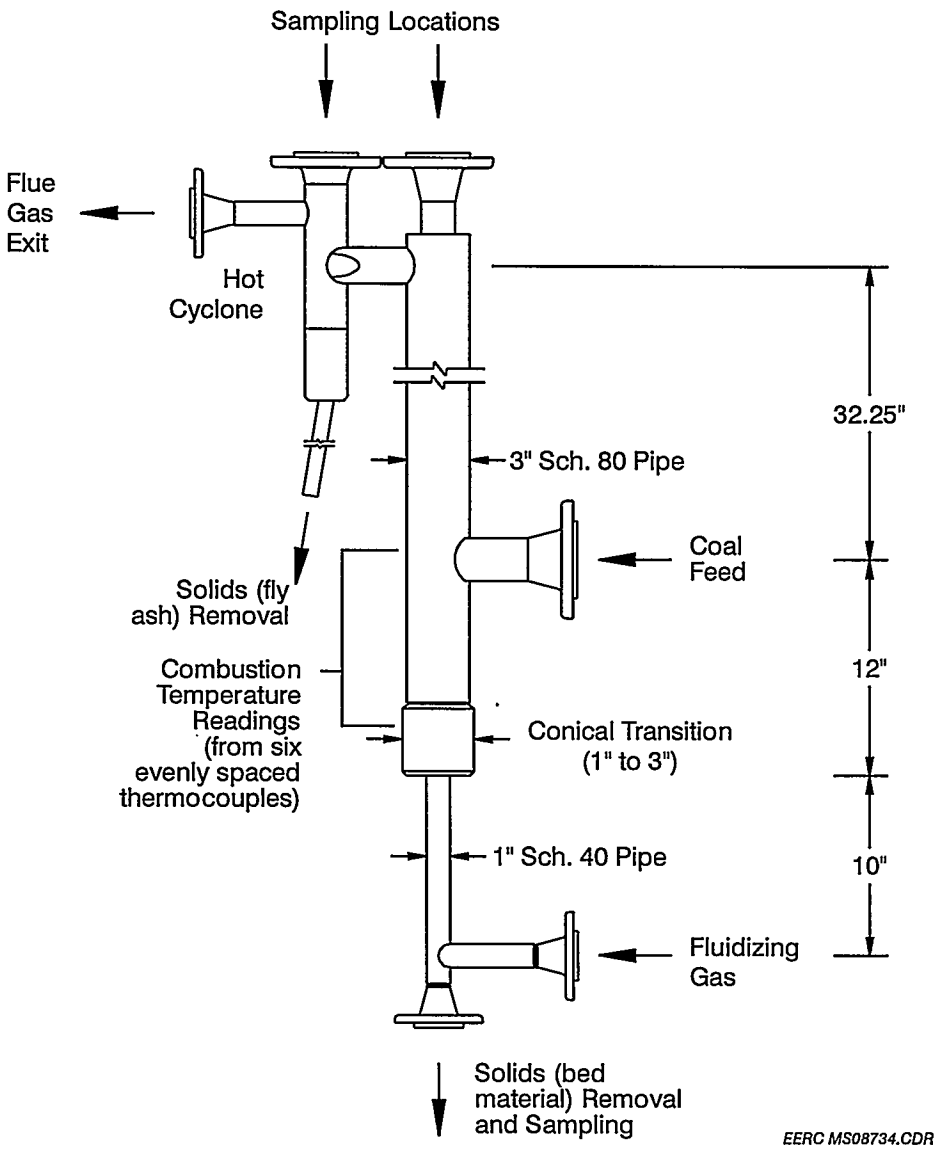


**Figure 3. Side View of FBR**

## Table 1. Operating Conditions and Results of Bench-Scale Testing

| Test Number | Bed Temp., °F | Excess Air, % | Bed Material | Results |
|---|---|---|---|---|
| KR1-0195 | 1500 | 30 | Washed sand | Ran 16 hr. |
| KR1-0295 | 1700 | 30 | No. 30 Red Flint sand | Ran 15 hr; air flow rate unknown. Trouble with reactor heaters. |
| KR1-0395 | 1600 | 15 | No. 30 Red Flint sand | Temps unstable; defluidized after 5 hr. |
| KR1-0495 | 1700 | 2.5 | No. 30 Red Flint sand | Defluidized after 3 hr. |
| KR1-0595 | 1500 | 2.5 | No. 30 Red Flint sand | Ran 16 hr. |
| KR1-0695[1] | 1700 | 30 | No. 30 Red Flint sand | Ran 8.5 hr, until coal supply ran out. |
| KR2-0795[2] | 1500 | 30 | No. 30 Red Flint sand | Defluidized after 40 min. |
| KR2-1095[2] | 1500 | 30 | No. 30 Red Flint sand | Defluidized after 1 hr. |
| KR2-1295[3] | 1500 | 30 | No. 30 Red Flint sand | Ran 16 hr. |
| B1-1395 | 1500 | 30 | No. 30 Red Flint sand | Ran 113 hr. |
| KR2-1495 | 1600 | 15 | No. 30 Red Flint sand | Defluidized after 1.85 hr; tried again and ran 50 min. |
| KR2-1595 | 1700 | 30 | No. 30 Red Flint sand | Defluidized after 2.95 hr. |
| KR2-1695[4] | 1700 | 30 | No. 30 Red Flint sand | Defluidized after 3.33 hr. |
| KR2-1795[4] | 1500 | 30 | No. 30 Red Flint sand | Defluidized after 6.28 hr. |
| KR2-1895[5] | 1500 | 30 | No. 30 Red Flint sand | Defluidized after 0.93 hr; tried again and ran 2.38 hr. |
| KR2-1995 | 1500 | 30 | −10 +20 mesh gabbro | Defluidized after 9.52 hr. |

[1] Repeat of KR1-0295, using air instead of water cooling.
[2] Repeat of KR1-0195, using air instead of water cooling and using Red Flint sand as bed material.
[3] Included kaolin addition at the rate of 0.093 lb kaolin/lb fuel.
[4] Added 2000 ppm $SO_2$ with combustion gas.
[5] Added Plum Run dolomite at the rate of 125 g/3200 g coal.

# PB.20 Evaluation of Options for $CO_2$ Capture/Utilization/Disposal

## CONTRACT INFORMATION

| | |
|---|---|
| **Contract No.** | DE-92MC29220 |
| **Contractor** | Argonne National Laboratory<br>9700 S. Cass<br>Argonne, IL 60439<br>(708) 252-7723 |
| **Contractor Project Manager** | David K. Schmalzer |
| **Principal Investigator** | Richard D. Doctor |
| **METC Project Manager** | Richard A. Johnson |
| **Period of Performance** | June 1, 1993 to June 1, 1995 |

## ABSTRACT

The project objective is to develop engineering evaluations of technologies for the capture, use, and disposal of carbon dioxide ($CO_2$). This project emphasizes $CO_2$-capture technologies combined with integrated gasification combined-cycle (IGCC) power systems. Complementary evaluations address $CO_2$ transportation, $CO_2$ use, and options for the long-term sequestration of unused $CO_2$. Commercially available $CO_2$-capture technology is providing a performance and economic baseline against which to compare innovative technologies. The intent is to provide the $CO_2$ budget, or an "equivalent $CO_2$" budget associated with each of the individual energy-cycle steps in addition to process design capital and operating costs. The value used for the "equivalent $CO_2$" budget is 1 kg $CO_2$/kWhe. The base case is a 458-MW (Gross) IGCC system using an $O_2$-blown Kellogg-Rust-Westinghouse (KRW) agglomerating fluidized bed gasifier, Illinois #6 bituminous coal feed and low-pressure glycol sulfur removal followed by a Claus/SCOT treatment to produce a salable product. Mining, feed preparation and conversion result in a net electric power production for the entire energy cycle of 411-MW with a 0.801 kg/kWhe $CO_2$ release rate. For comparison, the gasifier output was taken through water-gas shift and then to either low-pressure glycol or chilled methanol for $H_2S$ recovery; low-pressure glycol or membranes for $CO_2$ recovery; and finally either a combustion turbine or fuel cell as the topping cycle. $CO_2$ recovery was set at 80% for all cases so that the membrane system could be compared with the glycol on a consistent basis. The combustion turbine was then fed a high hydrogen content fuel. From the IGCC plant, a 500-km pipeline took the $CO_2$ to geological sequestering. For the optimal case, the net electric power projection was reduced by 73-MW with a 0.277-kg/kWhe $CO_2$ release rate (when make-up power was considered).

## PB.21 Hot-Gas Filter Ash Characterization

### CONTRACT INFORMATION

| | |
|---|---|
| **Contract Number** | RP3910-01 |
| **Contractor** | Energy & Environmental Research Center<br>University of North Dakota<br>PO Box 9018<br>Grand Forks, ND 58202-9018<br>(701) 777-5000 (telephone)<br>(701) 777-5181 (fax) |
| **Other Funding Sources** | Electric Power Research Institute (EPRI) Consortium |
| **Contractor Project Manager** | John P. Hurley |
| **Principal Investigators** | John P. Hurley<br>Tina M. Strobel<br>Bruce A. Dockter |
| **METC Project Manager** | Norman T. Holcombe |
| **Period of Performance** | May 1, 1994, through April 30, 1997 |

**Schedule and Milestones**

**FY95 Program Schedule**

| | S | O | N | D | J | F | M | A | M | J | J | A |
|---|---|---|---|---|---|---|---|---|---|---|---|---|
| Task 1 – Field Sampling and Archive Sample Analysis | | | | | | | | | | | | |
| Task 2 – Laboratory-Scale Testing | | | | | | | | | | | | |
| Task 3 – Bench-Scale Testing | | | | | | | | | | | | |
| Task 4 – Computer Modeling | | | | | | | | | | | | |

## OBJECTIVES

One of the key difficulties in the development of advanced pressurized fluidized-bed combustion (PFBC) and integrated gasification combined-cycle (IGCC) systems is the need to remove particulates from the gas stream at high temperatures and pressures. For over ten years, both U.S. Department of Energy (DOE) Morgantown Energy Technology Center (METC) and Electric Power Research Institute (EPRI) have been sponsoring research devoted to solving problems in pilot- and commercial-scale PFBCs and IGCCs and their associated hot-gas cleanup systems. This research has revealed numerous cases of ash cake buildup on filter elements that has been difficult to remove using on-line jet pulsing. The objectives of this research are to 1) determine the mechanisms by which a difficult-to-clean ash is formed and how it blinds or bridges hot-gas filters, 2) develop a method to determine the rate of blinding or bridging based on analyses of the feed coal and sorbent and on the operating conditions, and 3) provide suggestions for ways to prevent filter blinding and bridging by the troublesome ash.

## BACKGROUND INFORMATION

Large-scale hot-gas filter testing has revealed numerous cases of cake buildup on filter elements that has been difficult, if not impossible, to remove. At times, the cake can bridge between candle filters, leading to high filter failure rates. It is speculated that chemical as well as physical effects are playing a role in helping to bond the ash to the filter or to itself. These factors include particle-size and composition distribution, particle shape, gas condensation, the aerodynamics of deposition, and system temperature. The Energy & Environmental Research Center (EERC) is working with EPRI and a consortium of companies in partnership with DOE METC to perform the research necessary to determine the relative importance of these factors in causing hot-gas cleanup filters to be blinded by ash or to develop deposits that can bridge the filters and cause them to fail. The primary deliverable will be a graphics-driven computer model that can be used to predict and control the problems based on data from the analyses of coal and sorbent, as well as system operating parameters.

## PROJECT DESCRIPTION

This research is examining ashes from large-scale filters, ashes originally from large-scale PFBCs or gasifiers which have been reentrained in a laboratory-scale rig and deposited on filters in simulated filtration environments, and newly generated ashes from small pilot- or bench-scale facilities where parametric evaluations will be employed. The problem is being defined through full-scale sampling. Parametric testing will be done at the lab, bench, and pilot scale to determine the factors leading to the problem. Finally, the data will be used to develop a user-friendly computer model to help predict the occurrence of the problem, choose appropriate fuels or operating conditions, or design the system to reduce the blinding and bridging problems. Solutions predicted by the model will be tested on the bench scale.

Four tasks are being performed:

- Task 1 – Field Sampling and Archive Sample Analysis
- Task 2 – Laboratory-Scale Testing
- Task 3 – Bench-Scale Testing
- Task 4 – Computer Modeling

The initial stages of the project have focused on determining chemical, mineralogical, and

physical characteristics of archive and on-line PFBC and IGCC coal, sorbent, bed ash, cyclone ash, and filter samples. To date, filter fines collected from four runs of the Grimethorpe PFBC, and coal, sorbent, bed ash, cyclone ash, and filter fines collected from three test series of the Tidd PFBC were characterized using several standard and advanced analytical techniques. The filter fine samples represent ashes of varying cleanability from both systems. Standard analytical techniques included x-ray fluorescence (XRF) for bulk chemistry and x-ray diffraction (XRD) for mineralogy, and advanced analytical techniques included a developmental scanning electron microscopy (SEM) technique to determine particle-size and composition distributions of sub- and supermicron ash on a particle-by-particle basis. Scanning auger electron spectroscopy was used to determine surface chemistry of the ash particles.

## RESULTS

### Task 1 – Field Sampling and Archive Sample Analysis

The objectives of Task 1 are to determine the mechanisms by which difficult-to-clean ash is formed and how it blinds or bridges hot-gas filters. The analyses of many samples from various systems and operating conditions are necessary to fully characterize ash-bridging mechanisms, such as initial stickiness of ash and long-term sintering processes. The two sources for samples are on-line field sampling during the project and analyses of archive samples collected by project sponsors. To date, we have been able to acquire samples from several test series of the Tidd PFBC and four archive samples from the Grimethorpe PFBC. We have also received two samples each from the Filter Development Rig and the Gas Utilization Facility Filter from British Coal.

**Tidd PFBC.** The American Electric Power Service Corporation (AEP) and Ohio Power Company donated filter ash samples from several test series of the Westinghouse advanced particle filter (APF) assembly at the Tidd PFBC Demonstration Plant (1). The samples were collected by METC and Southern Research Institute (SRI) in May and October 1994. Filter fines were collected in February 1995 by AEP and sent to the EERC. AEP has also provided the EERC with archived coal, coal slurry, sorbent, bed ash, and cyclone ash for some of these tests at Tidd.

The APF experienced ash bridging and pressure drop increases during the first test series (May 1994 samples) while firing a Pittsburgh No. 8 coal and a Plum Run Greenfield dolomite. There was buildup of ash on all filters. During the next test series, July through November 1994, some filter candles appeared clean, with some ash cake on others. Testing at Tidd during 1995 has shown less ash buildup on filters because of complete spoiling of the cyclone (P11) upstream of the APF (the P11 cyclone was only partially spoiled during testing in 1994). A summary of the operation of the Tidd PFBC and APF are shown in Table 1. Chemical and mineralogical characterization were performed on the samples from these test series at the Tidd PFBC.

*Bulk Chemistry and Mineralogy.* Proximate analyses indicate differences in moisture and volatile contents for the Tidd filter ash samples. The May and October 1994 samples were collected from residual filter cakes, whereas the February 1995 sample was from the APF ash hopper. The May 1994 ash contains up to 3 wt% moisture, whereas the other two ashes contain less than 0.5 wt% moisture. The higher moisture in

**Table 1. Operating Conditions at the Tidd PFBC**

| Parameter: | May 1994 | October 1994 | February 1995 |
|---|---|---|---|
| Coal | Pittsburgh No. 8 | Pittsburgh No. 8 | Pittsburgh No. 8 |
| Sorbent | Dolomite | Dolomite and Limestone | Dolomite |
| Bed Temperature, °C (°F) | 818 (1504) | 855 (1571) | 861 (1581) |
| Cyclone Inlet Temp., °C (°F) | 748 (1378) | 793 (1385) | 799 (1471) |
| APF Inlet Temp., °C (°F) | 727 (1340) | 760 (1400) | 802 (1475) |
| APF Pressure, psig | 129 | 129 | 137 |
| Upstream P11 Cyclone | Partially spoiled | Partially spoiled | Completely spoiled |

the May 1994 APF ashes may be related to conditions during operation or the presence of moisture during off-line sampling of the APF. The higher volatile matter content in the February 1995 ash is related to a higher carbonate content of this ash. The source of carbonate is the sorbent that was carried over from the bed to the APF. The carbonate was not calcined or sulfated in the APF.

Figure 1 shows the averaged XRF results for the three Tidd filter ash samples collected in May 1994, October 1994, and February 1995. The February 1995 ash contains less $SiO_2$, $Al_2O_3$, and $SO_3$ and more CaO and MgO than the other two ashes. XRD results also show that the mineralogy of the ashes differs. The May and October 1994 ashes contain calcium magnesium sulfate and anhydrite and the major phases, whereas only anhydrite is a major phase in the February 1995 ash. The February ash also contains minor amounts of carbonate phases, such as calcite and dolomite, whereas the other two ashes contain no carbonates. The presence of the carbonates and $CO_2$ indicates that the February 1995 filter ash is relatively fresh and that the sorbent has not all calcined or sulfated. According to engineers at Tidd, the cyclone upstream of the APF was completely spoiled during all of the 1995 testing, therefore much larger particles were entering the filter vessel. These larger particles are not as easily sulfated because of the lower surface area-to-volume ratio as smaller, submicron particles. These results may indicate that the submicron sulfur-containing ash plays a role in ash bridging as the prevalence of this type of ash in the 1994 samples was accompanied by more dust buildup on the filters than testing in 1995.

Samples of coal, sorbent, and cyclone and bed ash were analyzed for runs occurring in the same time frame as the collection of the APF ashes. Complete sample sets were available for all except the May 1994 test. Bulk chemistries of these samples are illustrated in Figures 2 through 4. The usefulness of the bulk chemistries is to determine mineral and chemical interactions occurring from the bed to the APF that may influence behavior of the ash in the APF. For all of the three tests, Pittsburgh No. 8 coal was the fuel injected as a slurry, with

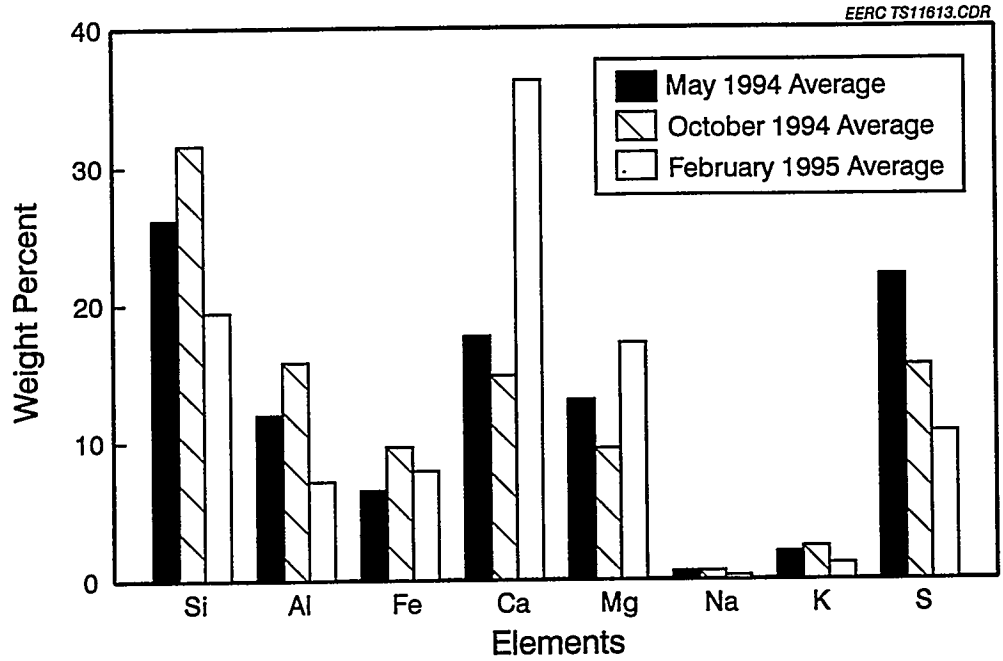


**Figure 1. Averaged XRF Results for the APF Tidd Ashes from May 1994, October 1994, and February 1995**

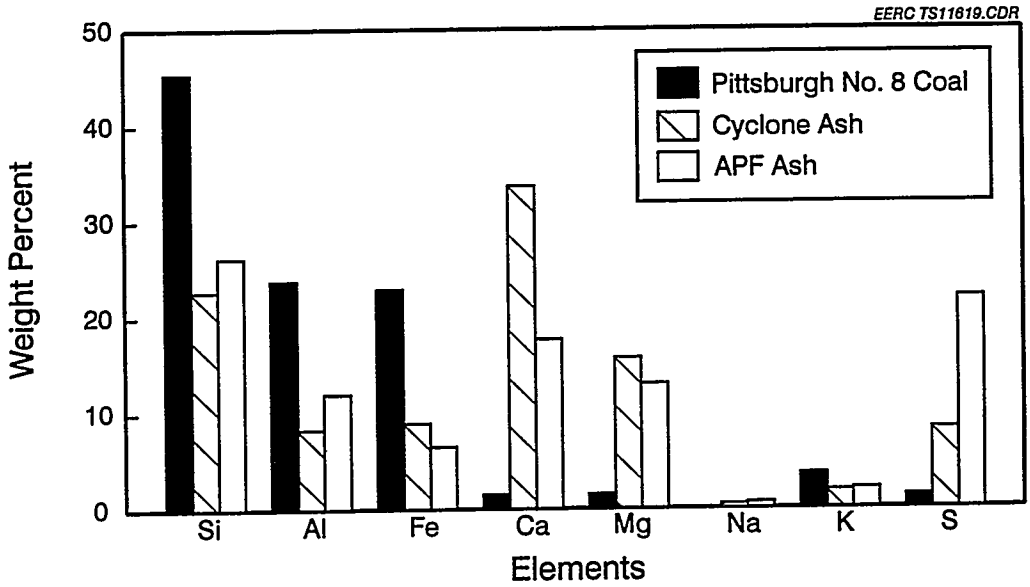


**Figure 2. XRF Results for the Tidd Samples from Test No. 51 Conducted in May 1994**

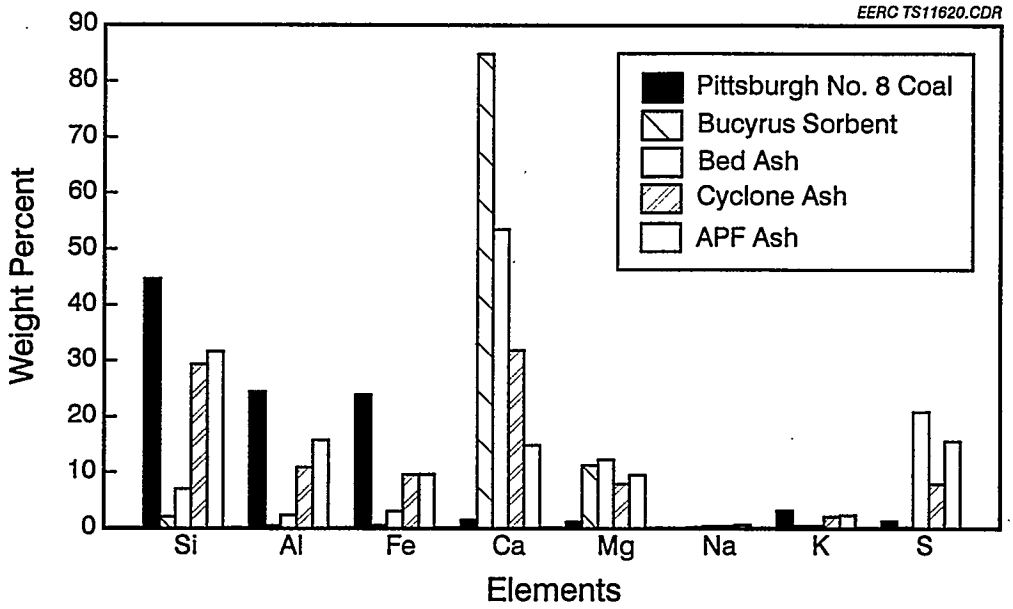


**Figure 3. XRF Results for the Tidd Samples from Test No. 78 Conducted in October 1994**

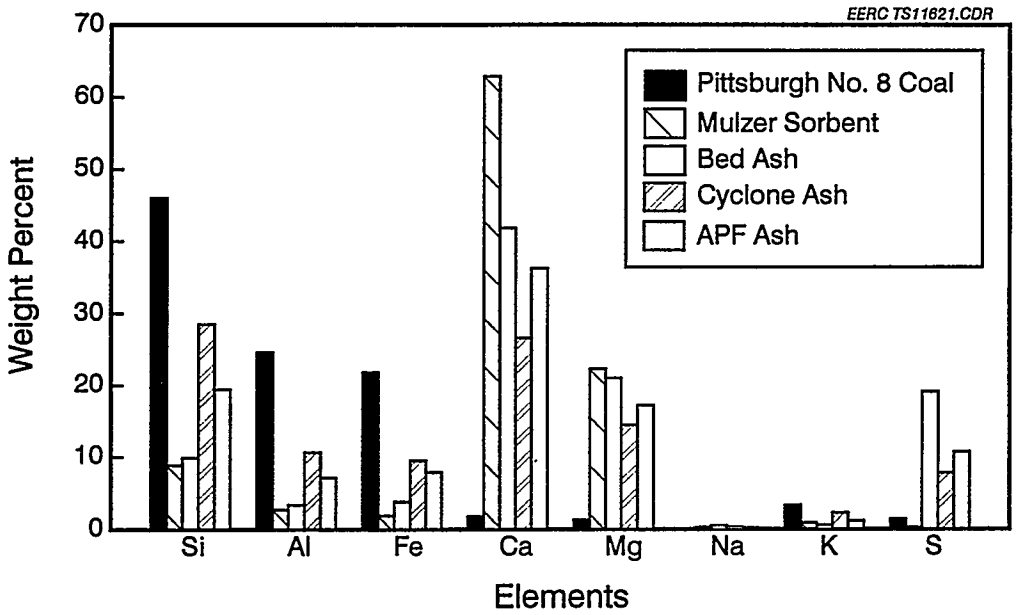


**Figure 4. XRF Results for the Tidd Samples from Test No. 87 Conducted in February 1995**

paste moistures ranging from 24 to 28 wt%. The sorbents used were dolomites in Tests No. 51 (May 1994) and No. 87 (February 1995), and limestone in Test No. 78 (October 1994).

Results for Test No. 51 show that the APF ash contains greater amounts of $SO_3$ and less CaO and MgO than the cyclone ash (Figure 2). Test No. 78 shows a trend of decreasing CaO and increasing $SiO_2$ from the bed ash to the APF ash (Figure 3). The results for Test No. 87 show that there is preferential removal of aluminosilicate-rich particles before the APF, and the APF ash is enriched in calcium magnesium sulfate-rich particles (Figure 4). Results from XRD may be able to confirm these interpretations. The bulk compositions of the coal from the three tests were identical.

*Fine Particle Analysis.* An automated SEM technique to determine the chemical composition distribution, size distribution, and shape of submicron particles is being developed under this project. Other researchers have used similar automated SEM techniques to characterize aerosol particles from 0.1 to 2.0 $\mu$m collected on filters and coal ash from 1.0 to 100.0 $\mu$m (2–4). Because of the submicron size of the APF ashes and the differing compositions when compared to aerosols and coal particles, modifications of these techniques were needed to develop a fine particle technique (FPT) for analyzing submicron coal ash.

The technique involves dispersing particles of ash on a vitreous carbon substrate using an organic solvent. The dispersion of the particles is necessary to avoid interaction of the x-ray beam with particles adjacent to the particle of interest. The carbon substrate is used instead of mounting the ash in an epoxy plug to avoid the analysis of ash particles which may be below the particle of interest. The x-ray beam scans across the sample locating, sizing, and analyzing up to 3000 particles per sample. These data are then reduced using a program called "Finepart," which categorizes the particles into phase groups based on chemistry. "Finepart" is a modification of "Partchar," which is used to reduce the data from a computer-controlled SEM analysis of coal or fly ash (3). Both programs were developed at the EERC. Originally, Finepart classified the raw data into 33 chemical composition categories for the ash particles ranging between 0.1 to 16 μm in average diameter. The program is being altered to characterize ash particles ranging from 0.1 to 100.0 μm in diameter to better characterize PFBC ashes.

*FPT Analytical Results.* The Tidd APF ashes from May and October 1994 were analyzed using the FPT. The results are given in Tables 2 and 3 and compared with XRF results. The samples were collected from the top and bottom plenums of the APF. The elemental determinations are within acceptable analytical error of ±10% except for the Si weight percent for the bottom B cake in October 1994. Further examination shows that the FPT seems to overestimate the Si when compared to the XRF results. Since the FPT analysis of the May and October samples only analyzed particles less than 16.0 μm, there may have been a tendency for particles composed of similar elements to form agglomerates which are larger than 16.0 μm and were not analyzed. Also, there may be an inordinate number of Si particles present that are smaller than 16.0 μm.

In a PFBC, the size of the fly ash particles determine their collection efficiency and ability to form difficult-to-clean cakes. The size distributions using FPT for particles ranging from 0.1 to 16.0 μm for the averaged May and October 1994 samples and for the February

**Table 2. Comparison of Analytical Techniques for the Tidd APF Ashes Collected in May 1994**

| | Top B | | Bottom B | |
|---|---|---|---|---|
| | FPT | XRF | FPT | XRF |
| Na | 0.1 | 0.6 | 0.2 | 0.6 |
| Mg | 6.3 | 13.3 | 4.9 | 12.8 |
| Al | 8.1 | 11.5 | 15.8 | 12.6 |
| Si | 34.0 | 25.4 | 33.5 | 26.6 |
| P | 0.6 | 0.3 | 0.6 | 0.5 |
| S | 29.3 | 21.1 | 26.4 | 20.8 |
| K | 3.4 | 1.9 | 3.1 | 2.0 |
| Ca | 15.9 | 18.7 | 12.7 | 16.9 |
| Fe | 1.2 | 6.5 | 1.7 | 6.5 |
| Ti | 1.1 | 0.7 | 1.1 | 0.7 |

**Table 3. Comparison of Analytical Techniques for the Tidd APF Ashes Collected in October 1994**

| | Top B | | Bottom B | |
|---|---|---|---|---|
| | FPT | XRF | FPT | XRF |
| Na | 0.1 | 0.6 | 0.3 | 0.6 |
| Mg | 1.6 | 9.0 | 8.4 | 10.0 |
| Al | 24,7 | 16.4 | 22.3 | 15.2 |
| Si | 49.1 | 32.7 | 39.3 | 30.7 |
| P | 0.5 | 0.2 | 1.0 | 0.2 |
| S | 10.2 | 15.3 | 12.8 | 14.3 |
| K | 4.2 | 2.4 | 4.7 | 2.2 |
| Ca | 4.9 | 12.8 | 8.1 | 16.4 |
| Fe | 3.7 | 9.7 | 2.0 | 9.7 |
| Ti | 0.9 | 0.8 | 1.0 | 0.7 |

1995 sample are shown in Figure 5. The FPT results indicate that the May and October 1994 particle-size distributions are smaller than the February 1995 sample. The larger particle-size distribution in the February 1995 sample may be due to complete spoiling of the cyclone upstream of the APF, which allowed larger ash particles to enter the filter vessel. The difference in the size distributions may also be related to the location of the samples; the 1994 samples are residual filter cakes whereas the February 1995 sample is from the APF hopper. Smaller particles may preferentially deposit on the filter cakes.

Figure 6 shows the comparison of the mineral composition for the 0.1- to 16.0-μm particles for the May and October 1994 samples and for the February 1995 filter ash sample. It should be noted that the February 1995 APF ash contained a large percentage of particles in the greater than 16.0-$\mu$m size range. Therefore, future FPT results will concentrate on the size range from 0.1 to 100.0 $\mu$m. For the smaller size range (0.1 to 16.0 $\mu$m), the amount of quartz was similar for the three samples, while the relative percentages of the other mineral classifications varied. The February 1995 sample contains less gypsum/Al-silicate and other Al-silicate phases such as kaolinite and montmorillonite than the 1994 ash samples. The presence of larger particles in this ash may have prevented sulfation, as larger particles are not as easily sulfated as smaller particles because of the lower surface area-to-volume ratio. Thus these results indicate that spoiling of the cyclone upstream of the APF resulted in larger particles entering the APF, and these larger particles possibly experienced less sulfation and less ash bridging.

*SEM Morphology*. The three Tidd APF ashes were also examined by SEM morphology. The objective of the SEM examination was to determine differences in the chemical and physical nature of the February 1995 ash and the May and October 1994 ashes and how these differences relate to ash bridging. Calcium- and sulfur-rich particles were found in the May and October 1994 ashes, and many of these particles were agglomerated (Figure 7). The necks between the particles were composed either of sulfate-rich or silicate-rich material. Surface analyses of the ashes also indicated calcium- and sulfur-rich areas in these neck areas, as well as segregation of calcium- and magnesium-rich areas in the bulk ash. Further analyses are needed to determine if this segregation is related to ash-bridging mechanisms.

SEM morphology of the February 1995 APF ash indicated less particle agglomeration. The main phases determined by SEM/energy-dispersive XRF included calcium magnesium sulfate, dolomite and calcite, quartz, hematite, and partially sulfated carbonate phases. Some dolomite grains were rimmed with sulfate, indicating only minor sulfation (Figure 8). Cross-sectioning the ash reveals some FPT limitations: coatings on particles are difficult to evaluate. Other phases present included aluminosilicates with Ca, Fe, and Mg as minor constituents. Some of the aluminosilicates also contained Fe and K. Sintered and agglomerated particles were not as prevalent as in the May and October 1994 samples, and most of the particles were angular in shape.

*Summary*. Changes in ash behavior in the Tidd APF are related to system operation, such as complete spoiling of the P11 cyclone upstream of the APF. When the cyclone was completely spoiled during the February 1995 testing, much larger ash particles entered the APF. These larger particles differed in composition from the APF ash samples

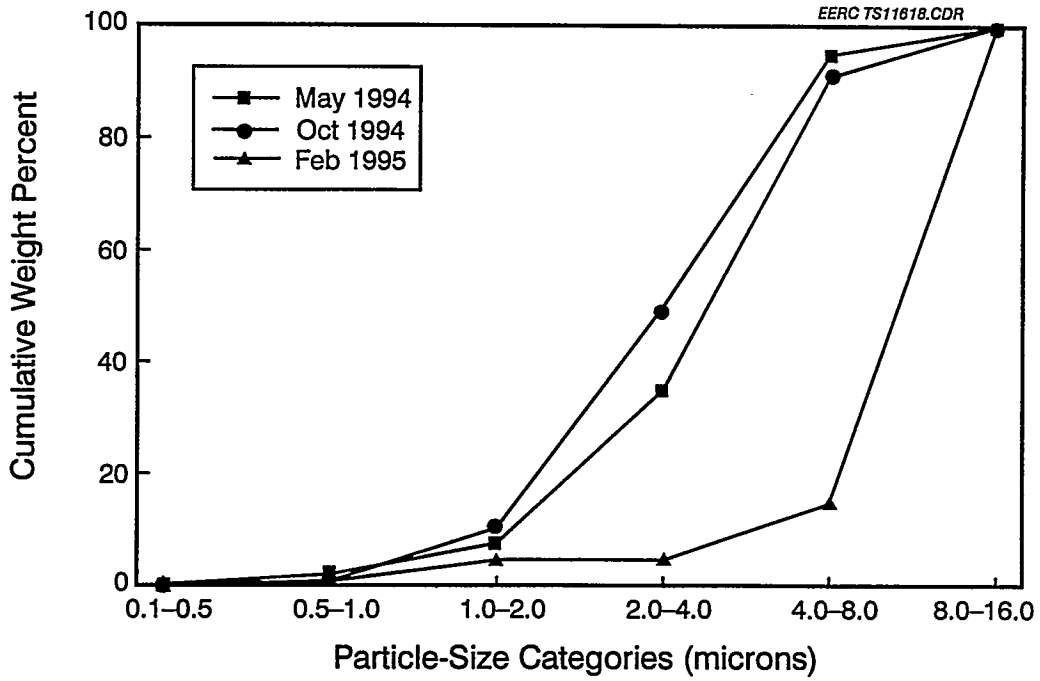


**Figure 5. Particle-Size Distribution (cumulative weight percent) for the Averaged May and October 1994 and for the February 1995 Samples from the Tidd PFBC for the 0.1- to 16.0- μm Particles**

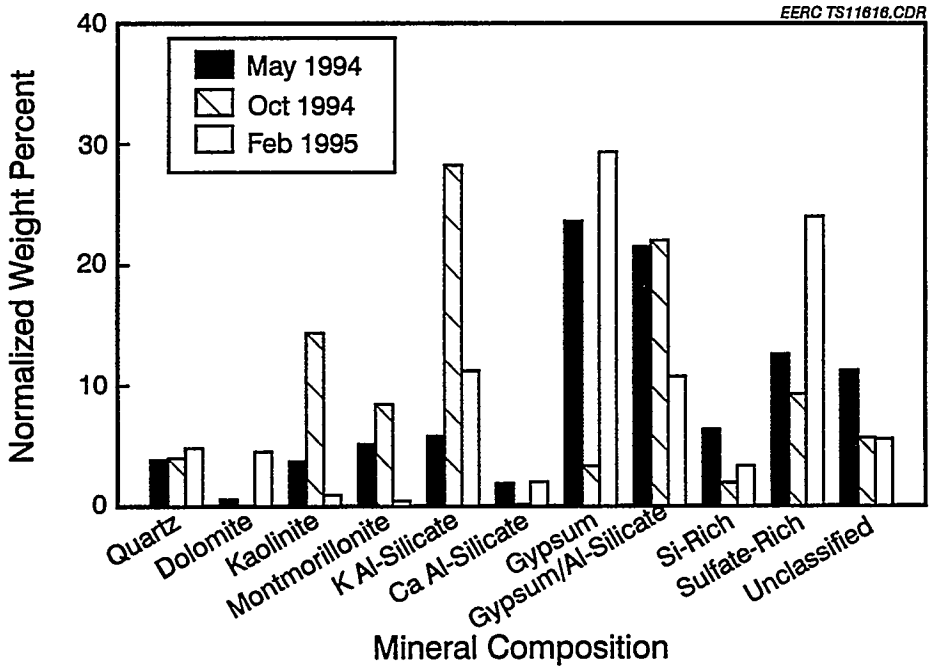


**Figure 6. Composition Distribution for the Averaged May and October 1994 and February 1995 Samples for the Tidd PFBC for the 0.1- to 16.0- μm Particles (normalized weight percent)**

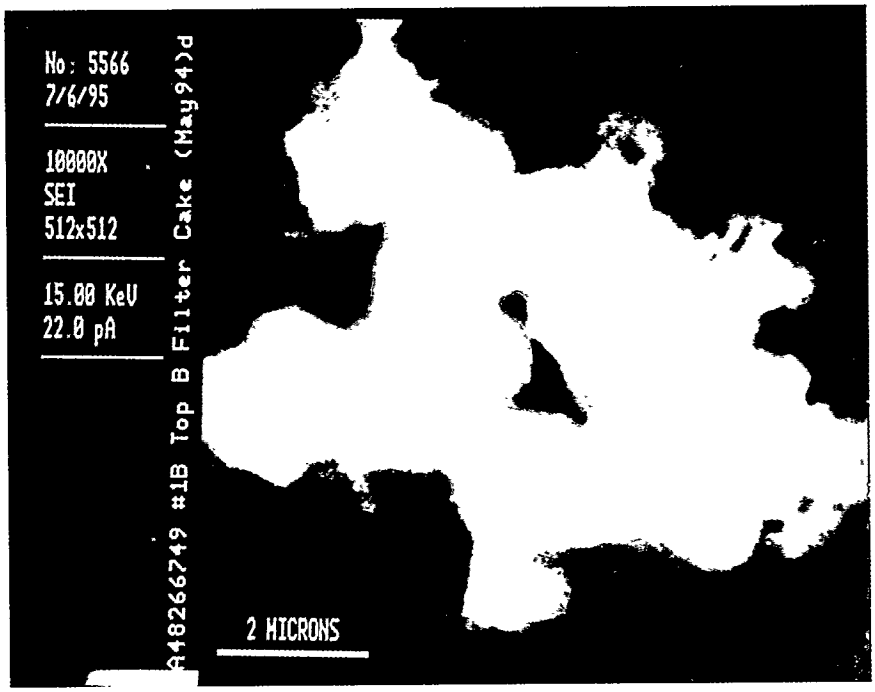


**Figure 7. SEM Photo Showing an Agglomerated Particle from the May 1994 Tidd APF Ash**

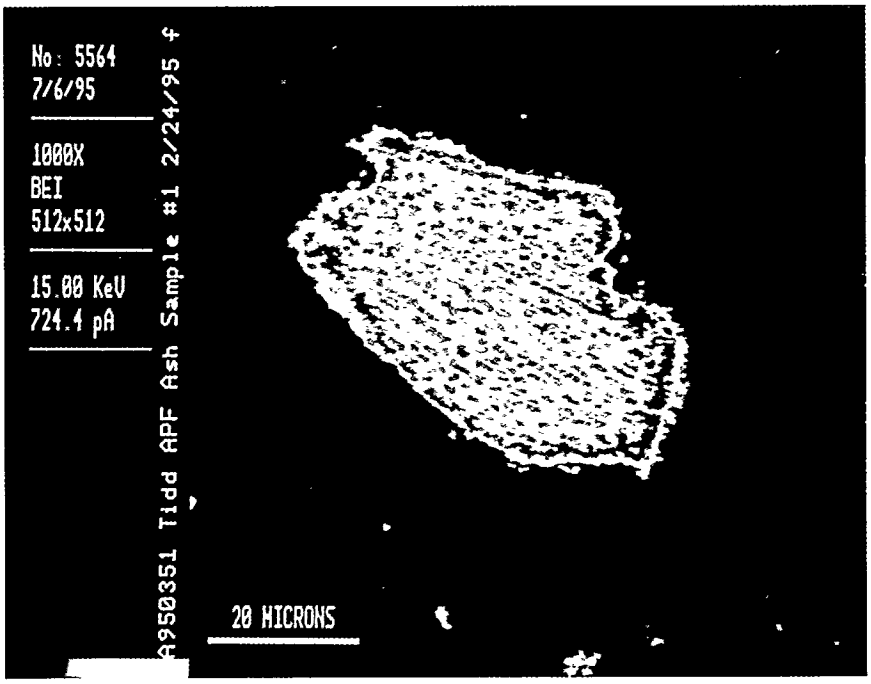


**Figure 8. SEM Photo Showing a Dolomite Grain with a Rim of Sulfate from the Tidd APF Ash Collected in February 1995.**

collected in May and October 1994. The main differences included higher carbonate, Ca, and Mg concentrations. The February APF ash had experienced less sulfation, probably due to the lower surface area-to-volume ratio of the larger particles. Smaller particles are more easily sulfated because of higher surface area-to-volume ratios. Also, smaller particles tend to be more sticky because of the greater influence of factors such as Van der Waals forces. Therefore, the particle and composition distributions and the degree of sulfation of the APF ash may have an influence on ash stickiness and bridging. Further examination of the other samples, such as the cyclone and bed ashes, may also give more insight into the APF ash formation and behavior.

**Grimethorpe PFBC**

Four samples from the Grimethorpe PFBC archives were sent by British Coal's Coal Technology Development Division and PowerGen. The samples are filter fines from the EPRI filter during four runs at Grimethorpe between 1991 to 1992, and the run conditions are indicated in Table 4. Pressure drop across the filters during Runs 155 and 159 were relatively high because of the presence of difficult-to-clean ash on the filters. Runs 160 and 161, which used a dolomite sorbent, resulted in less problematic ash (5).

The samples were analyzed for bulk chemistry and mineralogy and will be analyzed by FPT. The objective of the analyses is to determine how the particle-size and composition distributions affect the ash behavior in the filter vessel. The bulk chemistries of the samples show reduced silica and alumina contents for Runs 159 through 161, which is probably a result of using partly clean coal (Figure 9). Unfortunately, the bulk chemistries do not show major differences between the difficult-to-clean ashes (Runs 155 and 159) and the less problematic ashes (Runs 160 and 161), indicating that more detailed analyses, such as FPT, are needed.

**Task 2 – Laboratory-Scale Testing**

**High-Temperature Tensile Strength Testing**. The measurement of the tensile strength of powder deposits is useful for determining the magnitude of the cohesive forces that cause powders to agglomerate. Several procedures exist for determining tensile strengths of powder beds; however, available techniques allow for measurement of tensile strength only at ambient conditions. For this project, construction is under way for a testing apparatus for measuring tensile strength of ash at temperatures to 900°C under simulated PFBC and IGCC conditions.

**Cake Sintering Tests**. To determine long-term interactions between the ash and filter materials that lead to the formation of a conditioning layer of ash that remains on the filter after pulse cleaning, cylinders of filter material will be coated with ash collected from the field and sintered while allowing gas to flow through the ash cake and filter cylinder. The sintering tests will be performed in a large laboratory sintering reactor that was built under another project. The hot-gas reaction furnace (HGRF) consists of an alloy retort 9" in diameter and 6 feet long with a 48" heated length. End caps on the HGRF have ports to allow for the introduction and exhaust of gases, and measurement of pressure, temperature, and relative humidity. Shakedown runs of the HGRF have been completed, and plans are to coat filters with Tidd and Grimethorpe PFBC ashes for 500-hour exposures in a simulated PFBC atmosphere of 15% $CO_2$, 15% $H_2O$,

**Table 4. Run Conditions for the Grimethorpe Filter Samples**

| Sample | Fuel | Sorbent | Filter Inlet Temperature °C (°F) | Pressure Drop (mbar) |
|---|---|---|---|---|
| Run 155 | ROM Kiveton Park | Middleton limestone | 798 (1468) | 360 |
| Run 159 | Partly cleaned Kiveton Park | Middleton limestone | 819 (1506) | 300 |
| Run 160 | Partly cleaned Kiveton Park | Cadeby dolomite | 828 (1522) | <20 |
| Run 161 | Partly cleaned Kiveton Park | Cadeby dolomite | 840 (1544) | <20 |

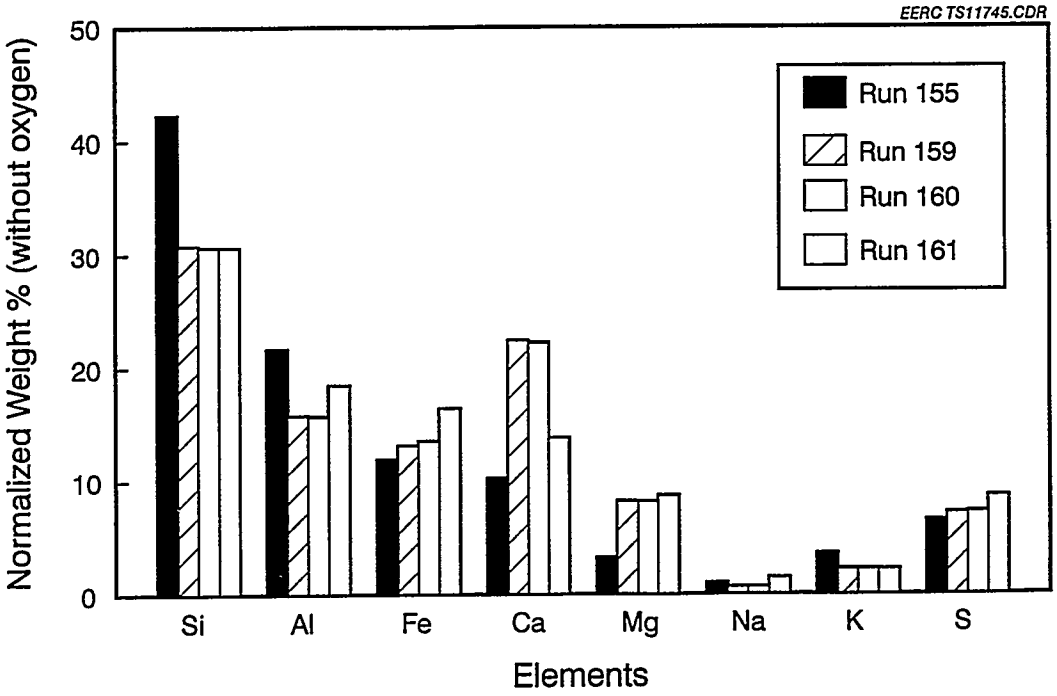


**Figure 9. XRF Results for the Grimethorpe Filter Ashes**

3% $O_2$, 0.5% $SO_2$, and 0.05% HCl in a balance of nitrogen. The gas stream will also be laden with 10 ppm of NaCl in solution with the water. The objective of the lab-scale sintering tests is to determine the rates and mechanisms of ash sintering and ash filter interactions as functions of system conditions, ash properties, and time.

**Task 3 – Bench-Scale Testing**

The objective of this task will be to determine the factors affecting the final particle-size and composition distribution of the ash and to determine the ash-related factors affecting the efficiency of pulse-jet cleaning of the filter. Two bench-scale facilities will be used for parametric testing under pressurized gasification or fluidized-bed combustion conditions. The first is the 4-lb/hr continuous fluid-bed reactor (CFBR), and the second is the 7–15-lb/hr pressurized fluidized-bed reactor (PFBR). The reactors will be used for the generation of ash under realistic operating conditions so that the factors affecting the chemical and physical properties of the ash can be determined. Tests of up to 100 hr each will be performed on three filter types under both combustion and gasification conditions. Combustion tests will be performed under conditions simulating the Tidd PFBC, and gasification tests will be performed under conditions simulating the British Coal gasifier and the Demkolec Shell gasifier.

**Task 4 – Computer Modeling**

The objective of this task is to develop a technique to predict a priori the ability to clean the filter cake for a given fuel, bed material, and operating condition. In this task, data collected during the first three tasks will be correlated and the best set of predictive criteria developed. Testing and analytical data will be used to modify existing computer algorithms and create new ones that will be tied together into a user-friendly computer model, which can be used to predict the approximate rate of filter blinding and bridging for a given fuel, bed material, and set of operating conditions.

## FUTURE WORK

Near-term work will include continued characterization of the Grimethorpe and Tidd samples and development of the FPT. Work will begin on determining high-temperature tensile strength of both the Tidd and Grimethorpe ashes in the laboratory. Also, long-term laboratory sintering tests will be performed. Cylinders of filter material will be coated with ashes collected from both the Tidd PFBC and the Grimethorpe PFBC and sintered under simulated PFBC environments to determine the long-term interactions between the ash and filter leading to the formation of a difficult-to-remove ash layer. Bench-scale activities will commence by Fall 1995. In the long term, we intend to collect and analyze ashes from hot-gas filter test facilities all over the world.

## REFERENCES


1. Hafer, D.R.; Mudd, M.J.; Bauer, D.A.; Stogran, H.K. "AEP's Tidd PFBC Demonstration Plant: Start-Up and Operating Experience," *In* Proceedings of the Application of Fluidized-Bed Combustion for Power Generation; Cambridge, MA, Sept. 23–25, 1992; pp 19-1 to 19-17.

2. Anderson, J.R.; Aggett, F.J.; Buseck, P.R.; Germani, M.S.; Shattuck, T.W. "Chemistry

of Individual Aerosol Particles from Chandler, Arizona, An Arid Urban Environment," *Environ. Sci. & Technol.* **1992**, *22*, 811–818.

3. Jones, M.L.; Kalmanovitch, D.P.; Steadman, E.N.; Zygarlicke, C.J.; Benson, S.A. "Application of SEM Techniques to the Characterization of Coal and Coal Ash Products," In *Advances in Coal Spectroscopy*; Meuzelaar, M.L.C., Ed.; Plenum Publishing Co.: New York, 1989.

4. Katrinak, K.A.; Brekke, D.W.; Hurley, J.P. "Freeze-Dried Dispersions for Automated Scanning Electron Microscope Analysis of Individual Submicron Airborne Particulates," *In* Proceedings for the 50th Annual Meeting of the Electron Microscopy Society of America; San Francisco Press, Inc.: San Francisco, 1992; pp 408–409.

5. Lowe, T.M.; Oakey, J.E. "Evaluation of Filter Materials Exposed in the EPRI Filter During the Grimethorpe Topping Cycle Project," EPRI Specific Task Report prepared under Contract RP1336-08 Amendment No. 5, in press.

This cover stock is 30% post-consumer waste
and 30% pre-consumer waste, and is recyclable.